Preparation of egg-shell magnetic membrane modified for preconcentration of Cu (II) and Tl (I) prior to determination by FAAS

Matin Naghizadeh[*1, 2], **Mohammad Ali Taher** [1], **Ali-Mohammad Tamaddon** [3, 4]

[1]Department of Chemistry, Shahid Bahonar University of Kerman, Kerman, Iran
[2]Young Researchers Society, Shahid Bahonar University of Kerman, Kerman, Iran
[3]Center for Nanotechnology in Drug Delivery, Shiraz University of Medical Sciences, Shiraz, Iran
[4]Department of Pharmaceutics, School of Pharmacy, Shiraz University of Medical Sciences, Shiraz, Iran

*Corresponding author: E-mail address: matin.naghizadeh@yahoo.com

Summary: Eggshell membrane modified by Fe_3O_4 magnetite were prepared and used as an adsorbent for simultaneous extraction and preconcentration of copper and thallium ions via magnetic solid phase extraction (MSPE) method. After adsorption, these ions were desorbed with hydrochloric acid followed with specific determination by flame atomic absorption (FAAS). The prepared Surface modification of eggshell membrane with doped Fe_3O_4 magnetite nanoparticles was investigate with Fourier transform infrared spectroscopy (FT-IR). The effect of various parameters, such as pH, type and concentration of acid, effect of the adsorbent amount and effect of ultrasonication time were optimized. As a result, it is hoped to use the method for extraction and preconcentration of metal ions in real samples used effectively. The proposed method permitted a large enrichment factor (about 200). The relative standard deviation of the method was ± 1.78 % (for ten replicate determinations of 2.0 $\mu g\ mL^{-1}$ of Cu (II) and Tl (I) and the limit of detection was 1.2 $\mu g\ mL^{-1}$ and 1.7 $\mu g\ mL^{-1}$. The results showed that Fe_3O_4@egg-shell membrane could be employed as an effective material for preconcentration and their determination of Cu (II) and Tl (I) from aqueous solutions.

Keywords: Heavy metal, Magnetic nanocomposites, Magnetic adsorbent.

Introduction: Hen egg is the most popular food in the world. Eggshell membrane principally includes of fibrous proteins such as collagen type I. nevertheless, eggshell membranes have also been explained to contain glycosaminoglycan, such as dermatan sulfate, sulfated glycoproteins, and glucosamine [1-2]. It is worth mentioning that recently pertinent attentions have been assigned to the application of biomaterials as sorbent media for performing sample pretreatment. Biological cells and natural bio mass has been described for the separation and preconcentration of nanoparticle sulfur and arsenic [3]. The eggshell membrane (ESM) is natural biomaterials with an intricate lattice network of stable, microporous, water insoluble fibers and a very high surface area. In this study, a facile and totally green method to in situ synthesizes Fe_3O_4 nanoparticles on ESM. Here, we successfully prepared an adsorbent based on a magnetically doped eggshell membrane. Then, this a green adsorbent was applied in MSPE for preconcentration of Cu (II) and Tl (I) simultaneously prior to flame atomic absorption spectrometric (FAAS) determination.

Methods and Experimental: The concentration of metal ions was determined by flame atomic absorption spectrometry (FAAS) using a Varian model SpectAA220 apparatus (Australia). The instrumental settings of the manufacturer were followed. FT-IR spectra (4000-450 cm^{-1}) in KBr were recorded on a Bruker, Tensor 27, and FT-IR spectrometer. The pH values were controlled with a pH/mV meter (Metrohm-827) supplied with a combined electrode. A Sonorex digitec model DT 225 H with 35 KHz Ultrasonicator was used to disperse the nanoparticles in solution. Magnetic stirrer Hot plate and Mechanical stirrer (2000 rpm) was used to homogenize.

Preparation of Fe_3O_4 magnetite doped eggshell membrane: Firstly, the broken fresh eggshell was incubated in diluted 1% acetic acid at 22 ºC for 1 h. Afterward the EM was easily separated and cut

into small pieces (1 cm^2) and was cleaned with a copious amount of twice distilled water. This is used as the substrate and membrane. Then, the preparation of Fe$_3$O$_4$ magnetic doped eggshell membrane was based on dissolving FeCl$_3$.6H$_2$O (11.68 g) and FeCl$_2$.4H$_2$O (4.30 g) in 200 mL deionized water. This solution was stirred with a magnetic stirrer (2000 rpm) at 50 ºC for 1 h. Nitrogen gas was continually bubbled through this solution to expel oxygen. Then, the EM was immersed in solution following that, 10 mL of 25% NH$_3$ was rapidly added to the solution. After that, the color of the bulk suspension changed from orange to black quickly by adsorption was on it. Iron oxides will be adsorption on eggshell membrane. The magnetite eggshell membrane (MESM) was collected by a magnet after washing numerous times by deionized water and then with ethanol because ethanol is a polar solvent with a low boiling point and to wash impurities. Finally, they were dried in an oven at 50 ºC for 12 h.

Extraction and desorption procedure: MSPE was carried out as follows. A portion of 2 mL sample solutions containing Cu (II) and Tl (I) was transferred into a 100 mL glass flask and the pH was adjusted to 7.0 using HCl and NaOH solutions. Then, 0.025 g of the synthesized MESM was added and the mixture was ultrasonicated for 3 min. In this step, the analytes were adsorbed on the adsorbent. Cu (II) and Tl (I) ions are trapped and training within the membrane, causing the Vander Waals bonding. Then, a piece of a magnet was placed outside the flask to collect adsorbent and the supernatant was decanted directly. In desorption step, 2.0 mL HCl (0.3 mol/L) was supplement as eluent and ultrasonicated for 3 min. subsequently, the magnet was used again to collect the MESM, and the eluent was transferred to a test tube for consequent FAAS analysis.

Results and Discussion: Fe$_3$O$_4$ nanoparticles show the absorption peak at 576 cm^{-1} which corresponding to the Fe–O vibration in Peak at 3411 cm^{-1} which corresponding to -OH and –NH$_2$ stretching vibrations. 3051, 2923 and 2886 cm^{-1} which was attributed to the C-H asymmetric stretching vibration in =C-H and =CH$_2$. 1652 cm^{-1} related to C=O stretching mode assigned as amide I vibration. 1443, 1103 and 630 cm^{-1} related to C=C, CO and C-S stretching vibrations respectively. There was a most significant peak at 1413 cm^{-1} which was attributed to the carbonate in the basic ingredient of eggshells. And the other two strong peaks at about 874 cm^{-1} and 711cm^{-1} were assigned to the out-plane deformation modes and in-plane deformation of calcium carbonate, respectively.

To demonstrate that the method allowed an efficient extraction of trace amount of Cu (II) and Tl (I), the extraction and elution procedure was optimized to achieve quantitative recovery. The effect of various parameters, such as pH, type and concentration of acid, effect of the adsorbent amount and effect of ultrasonication time were optimized.

Conclusion: Magnetite eggshell membrane with good saturation magnetization has been successfully prepared and used as a novel and effective adsorbent for simultaneous extraction and preconcentration of copper and thallium ions from aqueous solutions prior to the determination by FAAS. It is a very fast extraction method, because of high surface area of the adsorbent and fast magnetic separation. Ease of operation, minimal sample preparation, lower solvent and reagent consumption, high selectivity and sensitivity are other advantages. Furthermore, to some extent, the developed methodologies here widen the application areas of eggshell wastes and reduce environmental pressures and contamination. Furthermore, the combination of MSPE with the as-prepared nanoadsorbent with FAAS offers significant analytical performance.

References

[1] R. Mohammad-Rezaei, H. Razmi, S. Dehgan-Reyhan. Colloids and Surfaces B: Biointerfaces, **2014**, 118: 188-193.

[2] S. Jain, A.K. Anal. LWT-Food Science and Technology, **2016**, 69: 295-302.

[3] A. Guijarro-Aldaco, V. Hernández-Montoya, A. Bonilla-Petriciolet, M.A. Montes-Morán, D.I. Mendoza-Castillo. Industrial & Engineering Chemistry Research, **2011**, 50: 9354-9362.

The Inhibitory Effect of Allopurinol on Mild Steel (st 37) Corrosion in Sulfuric Acid Solution

Narjes Karamnejad*, Seyed Mohammad A. Hosseini, Mehdi Shahidi Zandi and Mohammad J. Bahrami
Department of Chemistry, Shahid Bahonar University of Kerman, Kerman, Iran
Email address: *karamnejad.n@gmail.com*

****

Introduction: One of the most common forms of corrosion is mild steel corrosion in the acidic solution. Most commercial inhibitors are toxic and replacing them with environmentally friendly inhibitors is necessary [1]. Pharmaceutical compounds offer possibilities for corrosion inhibition due to the presence of hetero atoms like nitrogen, sulphur and oxygen in their structure. In this study the inhibitory effect of allopurinol in sulfuric acid has been studied on carbon steel st37.

Methods and Experiments: Experiments are performed on carbon steel st37 in a 0.5 M sulfuric acid solution by adding different concentrations of the inhibitor. Electronic impedance spectroscopy experiments are performed to evaluate the inhibition efficiency and the performance of the inhibitor. To study the absorption mechanisms, electrochemical impedance spectroscopy [2] has been performed.

Results and Discussion: Figure 1 shows Nyquist plots obtained from EIS experiments. As it can be observed in this figure, Nyquist plots diameter increases by adding Allopurinol up to concentration of 300 ppm to the 0.5 M sulfuric acid which represents the increase of the charge transfer resistance. The results obtained from the Nyquist plots are given in table 1. It can be observed that an increase in the Allopurinol concentration leads to an increase in the charge transfer resistance and the inhibition efficiency. It can also be observed that the double layer capacity has been reduced which is due to adsorption of the inhibitor on the surface of metal.
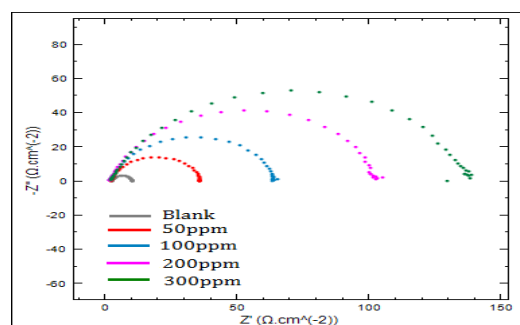

Figure 1: Nyquist plots without and with Allopurinol for various concentrations

Table 1: Results obtained from Nyquist plots

C(ppm)	C_{dl} (μF/cm^2)	R_t (Ω cm^2)	IE(%)
Blank	6.4×10^{-3}	7.86	-
50	3.4×10^{-4}	34.4	77.15
100	1×10^{-4}	63.5	87.62
200	3.9×10^{-5}	103	92.37
300	2.3×10^{-5}	138	94.30

The effect of temperature on different corrosion parameters such as corrosion rate values, corrosion potential, surface coating and inhibition percentage in temperature range of 25-55 °C in the absence and the presence of the inhibitor with optimum concentration in the sulfuric acid solution have been investigated. These results are given in table 2.

Table 2: The effect of temperature on different corrosion parameters

T(°C)	i_{corr} (μA cm^{-2}) without inhibitor	i_{corr} (μA cm^{-2}) with inhibitor	E_{corr} (mV) without inhibitor	E_{corr} (mV) with inhibitor	IE(%)
25	1543.8	78.31	-499.70	-480.90	95
35	3003.3	169.06	-506.54	-480.45	95.4
45	2642.4	526.60	-499.90	-478.30	80.1
55	17064	897.72	-492.03	-472.84	94.7

Conclusion: By increasing the inhibitor concentration, corrosion rate decreases and the corrosion inhibition percentage increases. The temperature rise results in increasing of the corrosion rate and does not have significant influence on the corrosion potential value. In addition, the temperature rise does not lead to remarkable charge corrosion inhibition efficiency. The present investigation reveals that Allopurinol is a proper inhibitor for preventing the corrosion of the Carbon steel in sulfuric acid solution.

References

[1] A.S. Fouda, A. S.; Motawee, M. S.; Megahid, H. S.; Abdul Mageed, H. A., IJCPS, 2015, 3(7), 1808–1817.

[2] Pathak, R. K.; Pratiksha Mishra, P., IJSR, 2016, 5(4), 671-677.

Synthesis and Investigation of New Organic Dyes in Dye-Sensitized Solar Cells

Mozhgan Hosseinnezhad[a*]**, Shohre Rouhani**[a, b]

[a] Department of Organic Colorants, Institute for Color Science and Technology, P.O. Box 16656118481, Tehran, Iran

[b] Center of Excellence for Color Science and Technology, Institute for Color Science and Technology, P.O. Box 16656118481, Tehran, Iran.

E-mail address: hosseinnezhad-mo@icrc.ac.ir

****

Introduction: Dye-sensitized solar cells (DSSCs) have been investigated extensively as topic of research in the field of renewable energy resources [1]. Inorganic dye molecules are commonly utilized in DSSCs but, metal free organic dyes that is environmentally friendly and easily synthesized have been utilized in DSSCs in 1993 [2]. Several type dyes such as coumarin dyes, polyene dyes, hemicyanine dyes, thiophene based dyes and indoline dyes have been prepared for DSSCs application. A donor-π-conjugation-linkage-acceptor (D-π-A) structures are basic concept for design and synthesis organic photosensitizers [3]. Substitution of an electron donor group at the photosensitizer molecule with amino group lead to a large bathochromic shift in both absorption and emission wavelength and generation of fluorescent dye [2]. Moreover, fluorescent dyes possess good photo response in the visible region and have applied as sensitizers in DSSCs [4]. In this study, we synthesis a new organic dye contain cyanoacrylic acid as the fundamental electron acceptor group. The spectrophotometric and photovoltaic properties of the organic dye were also examined. The synthesis route for the organic dye is given in Figure 1.
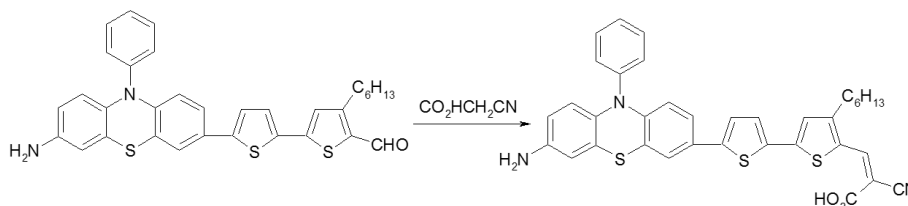

Figure 1. Synthesis route of organic dye

Experimental: 8 mmol starting compound and 14 mmol cyanoacetic acid were dissolved in 20 mL Acetonitrile and 10 mmol of piperidine was added to mixture. The reaction mixture was refluxed for 6 h. After each reaction was complete, it was cooled to room temperature. The resultant precipitate was filtered and purified by silica gel column chromatography using ethylacetate: methanol=10:1. Fluorometric and spectrophotometric analysis were investigated. Electrochemical measurements of the synthesized dye was carried out in solution in acetonitrile. The oxidation potential (E_{ox}) was measured using three small-sized electrodes [5]. Dye sensitized solar cell was fabricated in similar ways described in the literature [3].

Results and discussion: The all organic dyes were prepared as schematically shown in Figure 1. The organic dyes were synthesized by Knoevenagel reaction in the presence of piperidine. Yield=83%; mp=256-258 °C, FTIR (KBr) (Cm^{-1}): 3428: NH str., 2989: CH str., 1465, 1599:

C=C str. Ar., 1711: C=O str.; ^{1}HNMR (500 MHz, CDCl$_3$, δ/ppm): 0.92-0.98 (3H, CH$_3$), 1.01-1.07 (m, 6H, 3CH$_2$), 1.11-1.17 (m, 4H), 1.82-1.88 (dd, 4H, 2CH$_2$), 5.33 (s, 2H, NH$_2$), 6.77-6.81 (d, 3H, J=7.5 Hz), 6.88 (t, 4H), 7.15 (s, 1H), 7.22 (s, 2H), 7.29-7.34 (d, 2H, J=6.9 Hz), 9.26 (s, 1H, CO$_2$H). The UV-Visible absorption of the organic dyes in chloroform are shown in Figure 2 and the wavelength of maximum absorption (λ$_{max}$), the molar extinction coefficients (ε$_{max}$) and λ$_{max}$ of the corresponding dyes adsorbed on TiO$_2$ films are listed in Table 1. The synthesized organic dyes show good light harvesting abilities due to suitable molar extinction coefficients [1]. The formation of aggregation dye on TiO$_2$ substrate reduced electron transfer, thus anti-aggregation agents commonly used in DSSCs [2]. The fluorescent properties of synthesized dyes measured in Chloroform are also reported in Table 1 and showed in Figure 2. The oxidation potential (E$_{ox}$) of synthesized dyes was measured in acetonitrile by cyclic voltammetry to estimate the possibility of electron injection and dye regeneration. The E$_{pa}$, and E$_{red}$ level of organic dye was +0.91 V and −1.26 V, respectively. The J-V curves of DSSCs based on organic are presented in Figure 2 and summarized in Table 1. Indoline dyes in dye-sensitized solar cells devices have good conversion efficiency. All synthesized dye show similar IPCE ranged from 75-80% due to similar absorption spectra and energy level.

Table 1. Spectroscopy and photovoltaic properties of organic dye

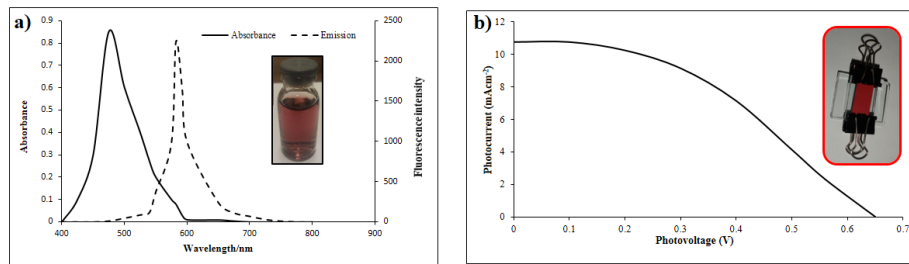| λ$_{max}$ (nm) in solution	ε (M^{-1}cm^{-1})	λ$_{max}$ (nm) on TiO$_2$	λ$_F$ (nm)	V$_{OC}$ (V)	J$_{SC}$ (mA.cm^{-2})	FF (%)	η (%)
462	41578	476	589	0.65	10.73	0.67	4.67

Figure 2. a) Absorbance and fluorescence spectra and b) J-V curve of organic dye

Conclusion: A new organic dye were synthesized by employing cyanoacrylic acid as the electron acceptor group. The absorbance and emission of organic dye are 462nm and 589 nm, respectively. Thus, electron injection and dye regeneration are permissible and all dyes are suitable for use in DSSCs device. Finally, DSSCs was prepared by employing new organic dye as photosensitizer and power conversion efficiency of 4.67% was achieved for organic dye.

Reference

[1] S. Rouhani; M. Hosseinnezhad. *Progress in Color Colorants and Coatings*, **2015**, 8, 259-265.
[2] X. Ren; S. Jiang; M. Cha; G. Zhou; Z. Wang. *Chemical Materials*, **2012**, 24, 3493-3499.
[3] M. Hosseinnezhad; S. Moradian; K. Gharanjig, Dyes and Pigments, **2015**, 123, 147-153.
[4] M. Hosseinnezhad; S. Moradian; K. Gharanjig. *Opto-electronic Review*, **2015**, 23, 126-130.
[5] S. Kushwaha; L. ahadur. *Journal of Luminescence*, **2015**, 161, 426-430.

Solid-phase synthesis of linear carnosine peptide analogue using Wang resin

M. Gholibeikian[a] , A. Bamoniri[a*], M.H. HoushdarTehrani[b], B.F. Mirjalili[c]

[a]Department of Org. Chem., Faculty of Chem., University of Kashan, Kashan, I.R. Iran.

[b]Department of Pharm. Chem., School of Pharm., Shahid Beheshti University of Med. Sci., Tehran, I.R. Iran.

[c]Department of Chem., College of Sci., Yazd University, Yazd, I.R. Iran.

Email address: bamoniri@kashanu.ac.ir

****

Introduction:

L-Carnosine, a dipeptide consisting of two amino acid residues, β-alanine and L-histidine, was discovered by Gulevich and Amiradzibi from Liebig's meat extract[1].Although, many physiological observations have been made and there are good experimental evidences for carnosine's ability to scavenge reactive oxygen species or its buffering capacities, there are many open questions on how carnosine exhibits its manifold functions at the molecular level. That is especially for its antineoplastic activity in mice which was already demonstrated and confirmed by Renner and Horii [2,3]. A further interesting observation with regard to a therapeutic value of carnosine was made by Holliday and Mc Farland[4]. They demonstrated that carnosine has an inhibitory effect on cultured neoplastic cells. We have investigated the effect of carnosine and its analogue on human cancer cell lines including, HepG2, HT-29 and A549 in this work.

Methods/Experimentals:

General procedure for the synthesis of pentapeptide analogue of carnosine

The protected first amino acid (2 mmol) was attached to resin with N,N-di isopropyl ethyl amine (1mL) in anhydrous di methyl formamide for 2h. The resin-bound protected-amino acid was treated with 10% piperazine for 30 min and the resin was washed with di methyl formamide (4 × 20 mL). Then, a solution of protected second amino acid (2 mmol), coupling reagent (2 mmol), and N,N-di isopropyl ethyl amine (0.5 mL) were added to the resin for 2h at room temperature. Other amino acids were added in the same way. Penta peptide analogue of carnosine was prepared (Scheme 1).

β-alanine-His-Pro-β-alanine-His
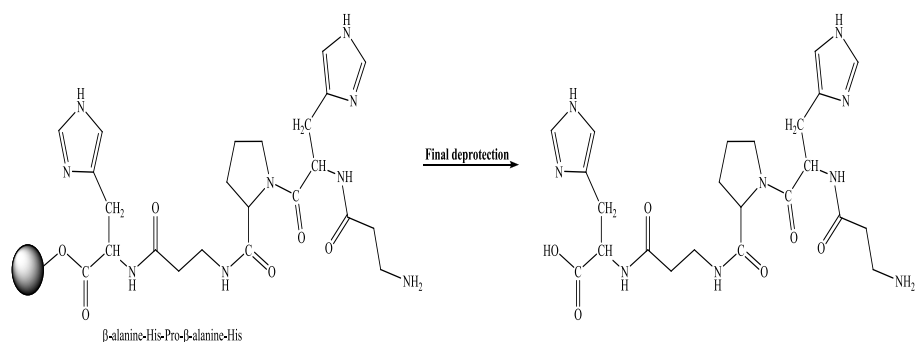
Scheme 1

Results and Discussion:

By the above mentioned method, penta peptide analogue of carnosine was prepared and the cell activity was analyzed by MTT method which is based on the conversion of orange MTT to purple formazan crystals by mitochondrial succinate dehydrogenase enzyme in living cells. After multi steps treatment, special plates were incubated for 30 min and the optical densities were read at 570 nm with a reference wavelength of 630 nm. 5-fluorouracil as the positive control and dimethyl sulfoxide as the solvent was also used. IC_{50} values for linear carnosine analogue were recorded 12.82±0.06 in HepG2 cell line, 9.12±0.05 in HT-29 cell line and 9.95±0.13 in A549 cell line respectively.

Conclusion:

Linear peptide has been successfully synthesized by solid phase methodology with Fmoc/t-Bu. Carnosine analogue have sufficient activity and good toxicity against, HepG2, HT-29 and A-549 cell lines with mean IC_{50} values ranging from 9 to 13 μg/ml, in comparison to standard drug 5-fluorouracil (5-FU).The anti cancer activity of penta peptide analogue of carnosine was examined in vitro and showed significant anti-cancer activity against cancer cells such as HepG$_2$, HT-29 and A549.

References

[1]- Gulewitsch W; Amiradžibi S. *Berichte deutsch. Chem. Gesellschaft*, **1900**, 33 (2), 1902-3
[2]- Renner C ;Zemitzsch N; Fuchs B. *Mol Cancer*, **2010**, 6, 2-9.
[3]- Shen J; Fujisaki Y; Yoshida K; Nagai K. *Neurosci Lett.*, **2012**, 510, 1–5.
[4]- Holliday R ; McFarland G. *British J. Cancer*, **1996**, 73 (8), 966-7.

Selective oxidation of alcohols with H_2O_2 catalyzed by zinc polyoxometalate immobilized on MCM-41 modified with ionic liquid

Robabeh Hajian,* Freshteh Jafari

Chemistry Department, Yazd University, Yazd 89195-741, Iran (E-mail: rhajian@yazd.ac.ir)
****

Introduction: Catalytic oxidation of alcohols to carbonyl compounds is a crucial transformation in organic chemistry, with both in industrial level and research [1]. The supported ionic liquid phase technology is an essential, new approach to acquire liquid containing solid materials that do not evaporate, made through surface modification of a porous solid by dispersing a thin film of ionic liquid onto it [2]. Supported ionic liquid catalyst is a concept that combines the advantages of ionic liquids and heterogeneous support materials [3]. Herein, Keggin-type polyoxometalate [(n-C_4H_9)$_5$$PW_{11}$$ZnO_{39}$] was immobilized on the imidazolium functionalized MCM-41 by electrostatic interaction.

Methods / Experimental: The ionic liquid support and polyoxometalate were prepared according to the literature [4,5]. To study the catalytic activity of the system, alcohol (0.5 mmol) and [PW_{11}Zn@Im-MCM-41] (50 mg, 0.003 mmol) in 3 mL CH_3CN were introduced into a 25 mL round-bottom flask equipped with a magnetic stirrer. H_2O_2 (5 mmol, 30%) was added to this mixture and refluxed. The progress of the reactions was monitored by GC.

Results and Discussion: The catalytic activity of the supported PW_{11}Zn cluster was tested in the oxidation of benzyl alcohol to benzaldehyde with hydrogen peroxide. In the presence of [PW_{11}Zn@Im-MCM-41] alcohols were converted to their corresponding aldehydes with 100% selectivity. The oxidation of the benzyl alcohol afforded benzaldehyde with an excellent yield of 95%. The electronic nature and the position of the substituent showed little effect on the reaction process. Substituted benzyl alcohol with donating and drawing groups such as NO_2, Cl, OH, OMe, and t-Bu gave the desired products with yields of 60-85%. The results also showed that the oxidation of linear aliphatic alcohols (for example 1-octanol) is much more difficult than that for benzylic and cyclic alcohols. For cinnamyl alcohol the corresponding aldehyde was produced without oxidation of C=C double bond. To assess lengthy cycle stability and reusability of [PW_{11}Zn@Im-MCM-41], oxidation of benzyl alcohol was selected as model reaction, and recycling experiments were carried out with a single sample of the catalyst. After each experiment, the catalyst was removed by simple filtration, washed with acetonitrile and *n*-hexane, dried at room temperature and reused. The catalyst was sequentially reused several times.

Conclusion: In this work, [(n-C_4H_9)$_4$N]$_5$PW$_{11}$ZnO$_{39}$].3H$_2$O was immobilized on ionic liquid-modified MCM-41-Im. The Zinc containing polyoxometalate was efficient in the oxidation of alcohols with H$_2$O$_2$ as an oxidant, producing the corresponding aldehydes in excellent selectivity. The major advantages of ionic liquid-supported catalyst were its high catalytic activity reusability.

References

[1] Sheldon, R. "*Metal-catalyzed oxidations of organic compounds: mechanistic principles and synthetic methodology including biochemical processes*"; Elsevier, **2012**.

[2] Fehrmann, R.; Riisager, A.; Haumann, M. "*Supported ionic liquids: fundamentals and applications*"; John Wiley & Sons, **2013**.

[3] Mehnert, C. P.; Cook, R. A.; Dispenziere, N. C.; Afeworki, M. *J. Am. Chem. Soc.* **2002**, *124*, 12932-12933.

[4] Hajian, R.; Tangestaninejad, S.; Moghadam, M.; Mirkhani, V.; Mohammadpoor-Baltork, I.; Khosropour, A. R. *J. Coord. Chem.* **2011**, *64*, 4134-4144.

[5] C.M. Tourne, G.F. Tourne, S.A. Malik, T.J.R. Weakley. *J. Inorg. Nucl. Chem.* **1970**, *32*, 3875-3890.

HEALTH RISK ASSESSMENT OF THRIHALOMETANS IN DRINKING WATER DISTRIBUTION SYSTEM OF TEHRAN CITY, IRAN

Giti Kashi[a, *], Maryam Moradian[b,*],

[a, b] *Department of Environmental Health, Islamic Azad University, Tehran Medical Sciences *2Branch,*

Khaghani St. Shariati Ave, Tehran State, Postal code: 19395/1495, Iran

Water Purification Research Center of, Tehran Medical Sciences Branch, Islamic Azad University, Tehran, Iran

Email address of the corresponding author: g.kashi@yahoo.com

****

Introduction:
Chlorination process, the most common method of drinking water chemical disinfection, has been applied for microbial pollutants inactivation leads to formation of trihalomethanes (THMs). The most harmful organic compounds in drinking water are considered as disinfection byproducts (DBPs). THMs as a main sub-group of DBPs are carcinogenic for persons [1]. Effective factors on the optimal performance of chlorination are: chlorine dosage, bromides concentration, contact time, natural organic matter (NOM), pH, residual chlorine, and temperature. The aim of this study is to investigate the concentration of THMs in drinking water distribution system of Tehran city, Iran and compared with national standard.

Methods or Experimental: In this analytical study to sample, cluster random sampling is used. We examine the THMs concentration of 17 drinking water distribution systems in Tehran city during winter season in the year of 2016 by using gas chromatography coupled electron capture detector(5710 method) [2]. We compare the results with national standard values of drinking water and draw distribution of THMs concentrations in drinking water distribution system of Tehran city. For health risk assessment, the average daily dose and hazard quotient(HQ)are computed.

Results and Discussion: The chloroform (TCM), bromodichloromethane (BDCM), Dibromocholoromethane (DBCM), and Bromoform (BCM) average of 17 samples are 9.1±0.81 (8.14-10.55) µg/l, 8.07±0.9 (6.92-9.52) µg/l, 7.25±0.92 (6.2-9.23) µg/l, and 1.27±0.37 (0.75-1.9) µg/l, respectively. The average water temperature (Tem), pH, and residual chlorine (RCl) concentration are 19.05±4.95 (12-27)℃, 7.39±0.25 (7.0-7.8), and 0.79±0.49 (0.0-1.5) mg/l, respectively. This study indicates that an increase in Tem, pH, and RCl leads to enhancing THMs concentration [3]. Daily dose (D_i) of TCM, BDCM, DBCM, and BCM that may be leads to exposing consumer are 2.78, 2.44, 2.43, and 0.5 µg/kg/d, respectively. The hazard quotient (HQ) of TCM, BDCM, DBCM, and BCM are 0.278, 0.122, 0.1215, and 0.025, respectively. The hazard index (HI) is 0.5465. The incremental lifetime cancer risk (ILCR) of TCM, BDCM, DBCM, and BCM are $53.0×10^{-6}$, $46.5×10^{-6}$, $46.4×10^{-6}$, and $9.5×10^{-6}$, respectively. The oral route is the most important route of hazardous exposure to human health. Findings show that residents living in distinct 18 and 2 have the high and low cancer risk due to the THMs exposure via water exposure pathway, especially due to TCM, respectively. TCM is grouped as group B_2 of probable human carcinogen.

Conclusion: It is concluded that the state authorities to give more attentions in producing TCM problem compared with BCM, BDCM, and DBCM. The TCM, BDCM, DBCM, and

BCM range of 17 samples are lower than the national standard and the drinking water consumers are not at risk of exposure to them. HQ and HI higher than 1 lead to enhancing the health risk of TCM, BDCM, DBCM, and BCM heavy metals.

Keywords: "Drinking water distribution system," "gas chromatography coupled electron capture detector (GC-ECD)," "Tehran," "Trihalomethanes (THMs),"

References

[1] H. Bujar, D.; Vezi, D.; , Ismaili, M.; Shabani, A.; Abduli, Sh. *World Journal of Applied Environmental Chemistry*, **2012**, *vol. 1*, No. 2, 42-52.

[2] HAPA., AWWA., WEF (2012). Standard methods for the examination of water and wastewater, 22st ed. American Water Work Association. Washington DC: APHA.

[3] H. Bujar, D.; A. Reka, A.; Jashari, A.; Ismaili, M.; Shabani. A., Durmishi, A.; *International Journal of Advanced Research in Chemical Science*, **2016**, *vol. 3*, No. 6, X-X.

Packed in-tube solid phase microextraction sorbent for ultra-trace determination of $^\Delta$9-Tetrahydrocannabinol in biological samples and cannabis leaves

Hamid Asiabi, Yadollah Yamini, Maryam Shamsayei

Department of Chemistry, Tarbiat Modares University, P.O. Box 14115-175, Tehran, Iran

Asiabihamid@yahoo.com

Introduction: Cannabis is the most common illegal drug-producing plant in the world. The cannabis products (marijuana, hashish, hashish oil, etc.) can be obtained from leaves, flowers, seeds and stem of hemp, and consumed in a variety of ways, such as smoking, vaporizing, preparing cannabis tea and using it in baked products. $^\Delta$9-Tetrahydrocannabinol (THC) is the major psychoactive constituent of cannabis, with bioavailability of ~25% via the smoked route, and a plasma terminal half-life of ~4 days. The oral dose of THC (20 mg) affect on mood, memory, motor coordination, cognitive ability, sensorium and self-perception, and may produce behavioral effects, including feelings of euphoria and relaxation, lack of concentration and hallucinations. Consequently, sensitive and specific analytical methods for the determination of THC in cannabis plant at different time of plant life is essential. In-tube solid-phase microextraction (IT-SPME), using an open tubular fused-silica capillary with an inner surface coating as the SPME device, was initially introduced by Eisert and Pawliszyn in 1997 to solve the intractable problems existing in the traditional SPME mode, such as poor extraction efficiency and the difficulty for on-line operation. IT-SPME is an ideal sample preparation technique because it is fast to operate, easy to automate, solvent-free, and inexpensive. In the present work, a new nano-structured sorbent consisting of Co/Cr LDH with nitrate interlayer anion, was synthesized. Then, a simple packed IT-SPME method using ternary Co/Cr (NO_3)-LDH sorbent was developed for the extraction and pre-concentration of trace amounts of THC from cannabis leaves.

Methods / Experimentals: Cannabis seeds were planted and in different times sampling was occurred from cannabis leaves. Then, the cannabis leaves were air-dried at room temperature for 5 days until a constant weight was achieved and then they were grinded to fine powder. Then 15 mg of the power was placed in a screw cap glass test tube and 1.5 mL of methanol was added to it and placed in the ultrasonic water bath for 30 min at 32 ◦C. After that, the solution was centrifuged for 15 min at 4000 rpm to separate the fine solid particles of leaves from the solution. Finally for increasing preconcentration factors and decreasing matrices effects, back extraction was occurred by packed IT-SPME method. So, methanol solution was removed by a pipette and placed into extraction vessel and diluted with ultra-pure water (pH = 10.0) to 30.0 mL, and then for filtered through a 0.45-µm pore filter prior to packed IT-SPME.

Results and Discussion: To evaluate the performance of the proposed method linear dynamic ranges (LDR), limits of quantification (LOQ), limits of detection (LOD), intra- and inter-assay precision (RSD %) were calculated under the optimized conditions. Calibration curve was found to be linear in the range of 0.09-500 ng mL^{-1} with coefficients of determination of 0.9999, 0.9991 in water sample. The LODs, based on a signal-to-noise ratio (S/N) of 3, were 0.02 ng mL^{-1} in water sample.

Conclusion: The synthesized sorbent has remarkable advantages including the ease of synthesis, good chemical stability, being green, low memory effect, and low cost in comparison with the conventional sorbent. Besides, shorter sample analysis time, more accurate quantification, and satisfactory reproducibility were achieved by packed IT-SPME-HPLC, which are favorable for routine analysis of the THC in various matrices.

References: [1] M. Pellegrini, E. Marchei, R. Pacifici, S. Pichini, Journal of pharmaceutical and biomedical analysis, 36 (2005) 939-946.

[2] Y. Hu, C. Song, G. Li, Journal of Chromatography A, 1263 (2012) 21-27.

[3] S.-W. Zhang, J. Xing, L.-S. Cai, C.-Y. Wu, Analytical and bioanalytical chemistry, 395 (2009) 479-487.

Determination of Brilliant Green and Basic Fuchsin in Binary Mixture Using CPE- Scanometry Method

Foroogh Ebrahimi, Ardeshir Shokrollahi*
Department of Chemistry, Yasouj University, Yasouj
E-mail address: ashokrollahi@mail.yu.ac.ir

Introduction: The extensive use of dyes often brings pollution problems in the form of colored wastewater and discharge into water bodies [1]. Most analytical methods developed for simultaneous analysis of components, are complex and time consuming [2]. In this work, cloud point extraction-scanometry, as a facile and sensitive method, has been used for simultaneous preconcentration and determination of brilliant green (BG) and basic fuchsin (BF). CPE is an attractive technique that reduces consumption, exposure to a solvent, disposal costs, and extraction time [3]. The solution scanometric method is based on scanning of solution in Plexiglas$^®$ cells and the application of the RGB color model in color monitor [4].

Experimental: An aliquot of 15 mL of a solution containing 0.50 mg L^{-1} of BG and BF, 0.27% (w/v) Triton X-114 was adjusted to pH 4.00. Then, the mixture was heated at 35 °C. After phases separation, the surfactant rich phase was diluted with ethanol and were determined by solution scanometric method [5]. In this work the effective intensities of the red and green values were chosen for BG and BF respectively.

Effective intensity$_R$ = -log (R$_{sample}$ / R$_{blank}$)

Effective intensity$_G$ = -log (G$_{sample}$ / G$_{blank}$)

Results and discussion: In order to achieve a high extraction recovery, the influence of analytical parameters including the pH (Fig.1), Triton X-114 concentration, time of centrifugation, electrolyte and equilibration temperature and time were investigated and optimum conditions were established by one at a time method. Under optimum conditions the calibration curves were linear in the concentration ranges of 0.025-1.000 and 0.050-2.500 mg L^{-1} with limits of detection (LOD) of 0.008 and 0.019 mg L^{-1} for BG and BF, respectively (Fig.2). The precision (RSD, %) for six replicate determinations of the analytes was 1.93% for BG and 1.30% for BF. The preconcentration factor was 30. The enrichment factors (EF) based on the slope ratio of calibration curves with and without preconcentration, were

obtained 34.46 and 15.91 for BG and BF, respectively. In order to evaluate the selectivity of the proposed method the effects of some interfering ions and dyes were investigated. It was found that most common ions and organic compounds do not interfere in the determination of BG and BF. Finally, the proposed method was applied for the determination of these dyes in several real water samples and the method was validated by recovery studies. The recovery values were in the range 91.20-108.00%.
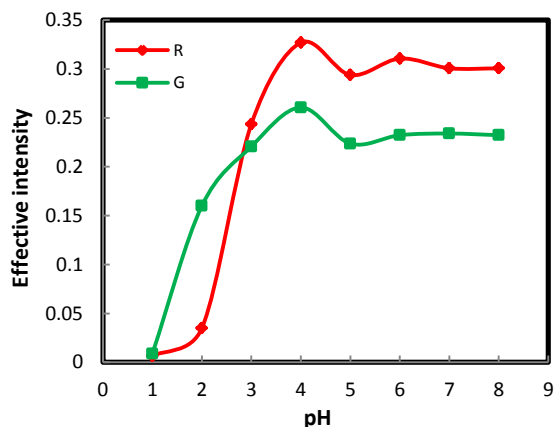

Figure 1. Effect of pH on the CPE of mixture of BG and BF
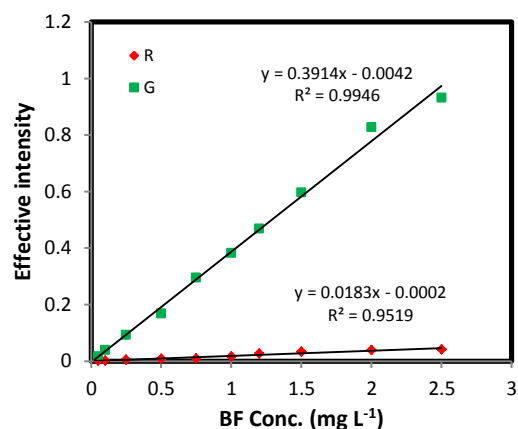
Figure 2. Calibration graph of BF

Conclusions: In this work, we have proposed the use of cloud point extraction as an alternative method for the preconcentration of brilliant green and basic fuchsin as a prior step for their determination by solution scanometry. This method offers novelty, facility, high speed, sensitivity, low cost and safety. It has good enrichment factor, low LOD and can be successfully applied to the determination of BG and BF in real samples with low errors and high recoveries.

References

[1] Zhang, L.; Zhou, X.; Guo, X.; Song, X.; Liu, X. J. Mol. Catal. A: Chem., **2011**, 335, 31-37.

[2] Xian, Y.; Wu, Y.; Guo, X.; Lu, Y.; Luo, H.; Luo, D.; Chen, Y. Anal. Methods, **2013**, 5, 1965-1974.

[3] Gouda, A. A.; Amin, A. S. Spectrochim. Acta Part A, **2014**, 120, 88-96.

[4] Shokrollahi, A.; Abbaspour, A.; Ardekani, Z. A.; Malekhosseini, Z.; Alizadeh, A. Anal. Methods, **2012**, 4, 502-507.

[5] Shokrollahi, A.; Behrooj Pili, H. Current Anal. Chem., **2016**, Inpress.

Thermal Degradation Kinetics of a Tryptophan-Cured Epoxy-Based Nanocomposite

Ahmad Motahari[a*], Abdollah Omrani[a] , Abbas Ali Rostami[a], Morteza Ehsani[b]

[a]*Faculty of Chemistry, University of Mazandaran, P. O. Box 453, Babolsar, Iran*

[b]*Iran Polymer and Petrochemical Institute, P. O. Box 14965-115, Tehran, Iran*

Email: motahari@umz.ac.ir

Introduction

Study on the thermal degradation of epoxy systems is of great interest due to the widespread use of these materials as structural adhesives, coatings, matrices in reinforced composites [1]. It is very important to know about the long-term behavior of high-performance composites for their applications in high temperature environments. In this regard, the degradation study of these composites is very crucial. It is of highly desirable to use green and biocompatible materials, such as amino acids, instead of toxic curing agents, such as polyamines, polyamides and anhydrides [2].

Methods

Diglycidyl ether of bisphenol-A with a molar ratio of 2:1 with respect to tryptophan was dissolved in acetone. Then, the appropriate amount of tryptophan, 1 wt% of 2,4,5-triphenylimidazole, and 5 wt% of silica nanoparticle were added to this solution. After stirring well, the mixture was further homogenized by ultrasonic treatment. The samples were placed in a vacuum oven at 150 °C for 60 min and then 165 °C for 30 min. Thermal stability of the samples was examined at four different heating rates.

Results and Discussion

TGA data at different heating rates are listed in Table 1.

Table 1. TGA data of the thermal degradation at different heating rates.

β (°C/min)	$T_{initial}$ (°C)	T_{max} (°C)	$W_{residual}$ (%)
Neat epoxy			
5	223	348	12.2
10	248	361	12.8
15	258	368	12.5
20	278	374	12.2
Nanocomposite			
5	219	348	13.0
10	276	361	12.1
15	250	366	13.1
20	243	371	13.5

The advanced isoconversional method [3] was used to obtain different activation energies as a function of the extent of degradation (Fig. 1).
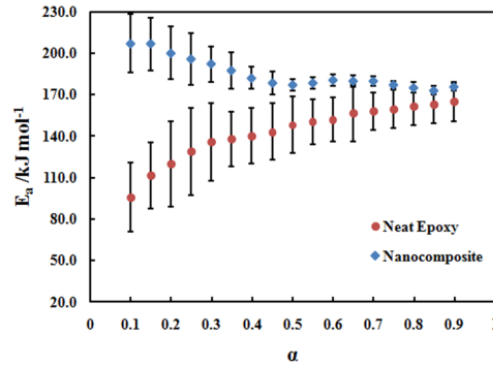
Fig. 1. Variation of effective activation energy E_a with conversion α during the thermal degradation using advanced isoconversional method.

In order to find a kinetic function, the master curve plots of $Z(\alpha)$ versus α were used according to the Criado method [4]. The average of activation energies in the range of $0.45 \leq \alpha \leq 0.85$, which were constant within the range of error bars, were applied. The experimental data of $Z(\alpha)$ for both the neat epoxy and nanocomposite agreed with an $F1$ master curve. By knowing the values of the activation energies and the kinetic model, the pre-exponential factor for the Kissinger equation can be calculated. Therefore, the rate of the solid-state degradation process was modeled by Eqs. (1) and (2) for the neat epoxy and nanocomposite, respectively as:

$$\frac{d\alpha}{dt} = 2.62 \times 10^{12} exp(\frac{-154700}{RT})(1-\alpha) \tag{1}$$

$$\frac{d\alpha}{dt} = 2.50 \times 10^{14} exp(\frac{-177700}{RT})(1-\alpha) \tag{2}$$

The rate constants are listed in Table 2. The rate constant for the nanocomposite is lower than that of the neat epoxy at the same temperature.

Table 2. Rate constants and time predictions at $\alpha = 0.5$ for three different temperatures.

Temperature /°C	200	250	300
k /min^{-1}			
Neat epoxy	2.16E-5	9.27E-4	2.07E-2
Nanocomposite	5.93E-6	4.46E-4	1.58E-2

Conclusion

The kinetic analysis showed that the degradation rate of the epoxy nanocomposite was lower than that of the neat epoxy, and therefore, adding silica nanoparticle to the epoxy system could improve the thermal stability.

References

[1] E. M. Petrie. *Epoxy Adhesive Formulations*, McGraw-Hill, New York, **2006**.

[2] T. Fishback; C. McMillin; M. Farona. *Biomed. Mater. Eng.*, **1992**, *2*, 83-87.

[3] S. Vyazovkin; N. Sbirrazzuoli. *Macromol. Rapid Commun.*, **2006**, *27*, 1515-1532.

[4] J.M. Criado; J. Malek; A. Ortega. *Thermochim. Acta*, **1989**, *147*, 377-385.

Liquid-phase selective oxidation of toluene to benzaldehyde by O_2 and H_2O_2 with mesoporous KIT-6-VPO catalyst

Masoume Rezaei, Alireza Najafi Chermahini*, Hossein A. Dabbagh

Department of Chemistry, Isfahan University of Technology, 84154-83111 Isfahan, Iran.

E-mail: anajafi@cc.iut.ac.ir; najafy@gmail.com.

Introduction: Toluene is a typical aromatic hydrocarbon with three primary C-H bonds and can be oxidized to several oxygenates such as benzyl alcohol, benzaldehyde, benzoic acid, and benzoate [1, 2]. Among these products, benzaldehyde is the most desirable due to its enormous importance in our life [3]. It is used in the synthesis of other organic compounds, manufacture of dyes, solvents and flame retardants [4]. The present study is to adopt KIT-6 as a support material for VPO dispersion and to investigate the physicochemical property of VPO particles on KIT-6 the liquid phase catalytic oxidation of toluene using environmentally oxidants (O_2 or H_2O_2).

Experimentals: The synthesis of mesoporous KIT-6 was performed according to the literature procedure reported elsewhere [5]. In order to VPO-functionalized on KIT-6, V_2O_5 was suspended in a mixture of 2-butanol/benzyl alcohol and stirred under reflux for 5 h, after which KIT-6 materials was introduced in suitable amounts. Then, phosphoric acid was added drop wise. After 6 h, the suspension was filtered and dried at 393 K for 24 h. The dried precursor was heated to 773 K for 3 h.

Results and Discussion: To evaluation of effect of active sites that contribute to conversion and selective oxidation of toluene to benzaldehyde, three types of same family of VPO nanocatalysts supported on KIT-6 mesoporous material were synthesized and characterized.

In this study, we have developed ordered mesoporous KIT-6 catalysts containing different amounts of vanadium for selective oxidation of toluene. Based on TEM and elemental mapping analysis (Fig. 1) it is evidenced a uniform and highly dispersed nanoparticles of VPO containing catalyst successfully constructed.

The results show amount of V in the fresh **(0.4)KIT-6-VPO** catalyst is 17% but after 5 recycles the V amount decrease to 10%, while the catalytic activity is remain good. In general, oxidation of toluene by molecular oxygen and in atmospheric pressure did not show desired toluene conversion yields. However, toluene oxidation with **(0.4)KIT-6-VPO** and by the H_2O_2 as the oxidant (Fig. 2), offers about 17.76 % conversion and 69.24 % selectivity for benzaldehyde.
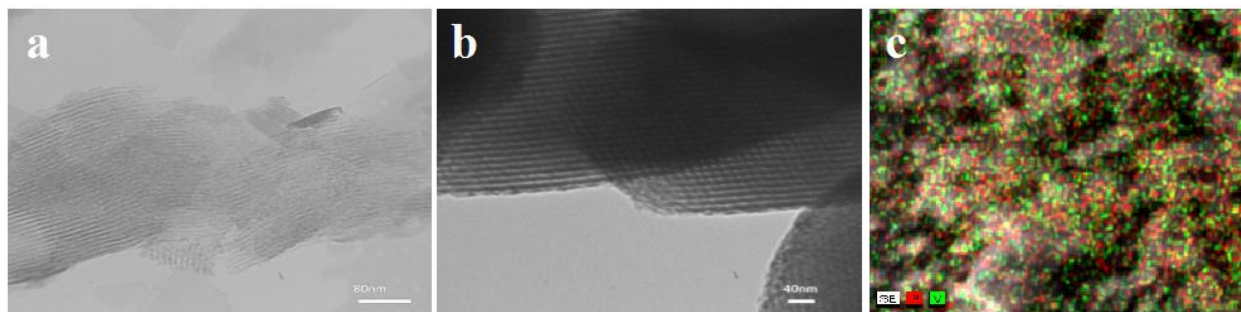

Fig. 1. TEM images of (a) **(0.4)KIT-6-VPO**, (b) KIT-6, (c) Elements distribution maps recorded.
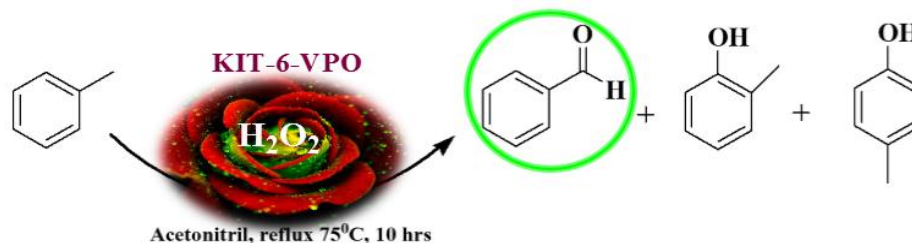
Fig. 2. Oxidation of toluene to benzaldehyde

Conclusion: Highly ordered like KIT-6 silica materials containing different amounts of vanadium have been synthesized. Under the optimum reaction conditions the prepared catalysts showed good conversion of toluene 17.76 % and 69.24 selectivity for benzaldehyde using aqueous 35 % H_2O_2. Finally, the catalyst can be easily reused several times without any significant loss of its activity, indicating its heterogeneous nature.

References:

[1] Y. Wang, H. Li, J. Yao, X. Wang, M. Antonietti, *Chemical Science,* **2011**, *2*, 446-450.

[2] A. Martin, U. Bentrup, G.-U. Wolf, *Applied Catalysis A: General*, **2002**, *227*, 131-142.

[3] L. Kesavan, R. Tiruvalam, M.H. Ab Rahim, M.I. bin Saiman, D.I. Enache, R.L. Jenkins, N. Dimitratos, J.A. Lopez-Sanchez, S.H. Taylor, D.W. Knight, *Science*, **2011**, *331*, 195-199.

[4] L. Ma, F. Su, W. Guo, S. Zhang, Y. Guo, J. Hu, *Microporous Mesoporous Materials*, **2013**, *169*, 16-24.

[5] M. Choi, F. Kleitz, D. Liu, H.Y. Lee, W.-S. Ahn, R. Ryoo, *Journal of the American Chemical Society*, **2005**, *127*, 1924-1932.

Preparation and microstructure of Nano crystalline nickel oxide powder

Shahrzad mohseni maybodi [a,*] **masoud madani** [b]

[a] **Department of chemistry, maybod branch,Islamic Azad university, maybod ,Iran**

[b] **Department of chemistry ,varamin(pishva) branch , Islamic Azad university ,varamin. ,Iran**

[a]**sh.mohseni۱۷@yahoo.com**

Introduction:

Various methods such as sol–gel [۱,۲], chemical precipitation [۳,٤], microwave assisted method and anodic arc plasma technique (AAPM) [٥] have been developed to produce NiO nanocrystalline powder [٦]. Sonochemical methods have recently been acknowledged as a promising route for preparation of various nanocrystalline materials including metallic and ceramic particles [۷].

Methods/Experimentals:

Nanocrystalline NiO powder was produced through sonochemical route by gradual drop-wise addition of ۰.۱ M sodium hydroxide (NaOH) to ۰.۱ M nickel nitrate $Ni(NO_3)_2$ solution and vigorous stirring and adjust the pH۷.۲. The light-green solution was irradiated subsequently with ۲۰ kHz ultrasound (MISONIX Inc. S-٤۰۰۰, USA) wave for ٦۰ min. The obtained gel was then dried at ۸۰ °C by leaving it in an oven overnight. The conversion temperature of $Ni(OH)_2$ to NiO was determined by thermal analysis. The oven-dried cake was heated at ۳۲۰ °C for ۱ h to form nanocrystalline NiO particles.

Results and discussion:

Microstructural parameters of the NiO powder were calculated via Rietveld refinement method. The obtained data are given in Table ۱. A comparison between the mean crystallite sizes of the nanocrystalline NiO particles prepared by a sonochemical method
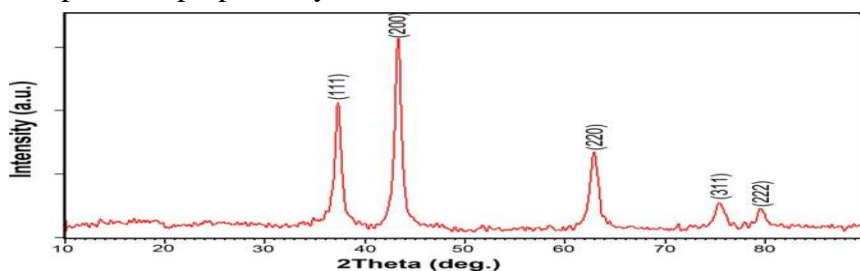

Fig. ۱. X-ray diffraction pattern of sonochemically synthesized nickel oxide powder after annealing at ۳۲۰ °C for ۱ h.

Table ۱:Microstructural parameters of nanocrystalline NiO powder obtained via sonochemical rout calculated by Rietveld refinement method.

Parameters	Value
Cell length (a)	٤.۱۷٥A
Crystal size	۱۸ nm
Micro strain	۰.۲۰٪

Fig. ۲ shows the STA (TG/DTA) curve of nickel hydroxide. As it can be observed in this figure, there are two endothermic reactions in DTA curve of $Ni(OH)_2$ powder during heating from room temperature up to ٦۰۰ °C. On the other hand, slope changes occurring around ۲٦٥ °C in TG graph reveals two weight losses correspond-ing to two H_2O dissociation reactions:

$$Ni(OH)_2\chi H_2O \rightarrow Ni(OH)_2 + \chi H_2O \text{ (۱)} \qquad Ni(OH)_2 \rightarrow NiO + H_2O \text{(۲)}$$
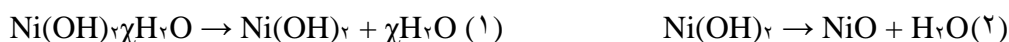
As shown in Fig. ۲, the reactions start at about ۲۲۰ °C and finish at about ۳۱۰ °C. Accordingly, the least temperature was chosen for heat treatment of the as-synthesized powder in order to suppress the intense grain growth at high temperatures. The oven-dried cake was heated hence at ۳۲۰ °C for ۱ h to form nanocrystalline NiO particles.
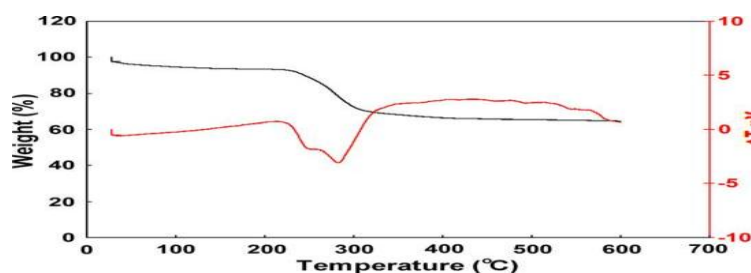

Fig. ۲. STA (TG/DTA) graphs of nickel hydroxide; (۱) held at ۳۰ °C for ۱ min,
(۲) heated at a rate of ۱۰ °C/min from ۳۰ °C to ٦۰۰ °C and (۳) held at ٦۰۰ °C for ۱۰ min.

TEM micrograph of the powder Fig۳a exhibits nanocrystalline NiO grains having an average dimension of ~۲۰ nm. Morphology of this powder is cubic which can be ascribed to the cubic NaCl structure of NiO. From Fig. ۳b, it is obvious that the primary nanocrystalline particles agglomerate to larger particles due to collisions caused by ultrasonic shock waves and electromagnetic interactions.

Fig۴a depicts the FTIR spectrum of the dried green gel after sonochemical treatment (hydrated Ni(OH)۲) in the range of mid-IR. The broad absorption peak located at ۳۳۸۰ cm^{-1} is related to the O–H stretching vibration of interlayer water molecules and H-bound of OH group. The IR spectrum of the final product is shown in Fig. ۴b.
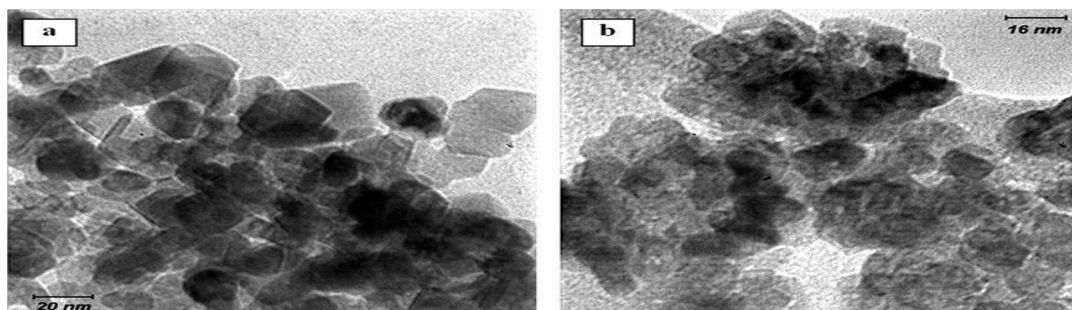

Fig. ۳. Transmission electron micrograph of (a) well-dispersed and (b) agglomerated nanocrystalline NiO powder.

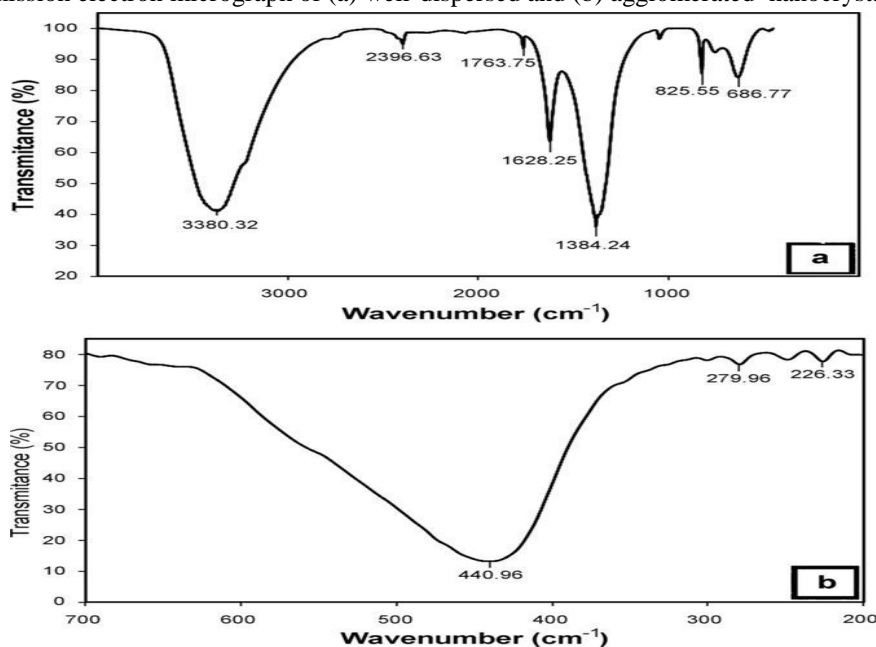**Fig. ۴.** The FT-IR spectra of sonochemically synthesized powder (a) before and (b) after annealing step.

Conclusion:

Wide band gap nanocrystalline nickel oxide particles with the mean crystallite size of ~۲۰ nm were synthesized by a novel sonochemical approach. Morphology of the prepared powder was found in cubic shape according to the TEM micrographs which was attributed to the NaCl-like structure of NiO. Ultrasonic irradiation resulted in cavitation phenomenon and led to decrease in crystal-lite size of the NiO particles. Nickel oxide powder synthesized in this work was a non-stoichiometric nanocrystalline compound discoloring from green to black.

References:

[۱] M. Ghosh, K. Biswas, A. Sundaresan, C.N.R. Rao, Journal of Materials Chemistry ۱۶ (۲۰۰۶) ۱۰۶–۱۱۱.

[۲] Y. Wu, Y. He, T. Wu, T. Chen, W. Weng, H. Wan, , Materials Letters ۶۱ (۲۰۰۷) ۳۱۷۴–۳۱۷۸.

[۳] J. Bahadur, D. Sen, S. Mazumder, S. Ramanathan, Journal of Solid State Chemistry ۱۸۱ (۲۰۰۸) ۱۲۲۷–۱۲۳۵.

[۴] Y. Bahari Molla Mahaleh, S.K. Sadrnezhaad, D. Hosseini, Journal of Nanomaterials ۱ (۲۰۰۸) ۱–۴.

[۵]H. Qiao, Z. Wei, H. Yang, L. Zhu, X. Yan, Journal of Nanomaterials ۱ (۲۰۰۹) ۱–۵.

[۶]E.A. Souza, J.G.S. Duque, L. Kubota, C.T. Meneses, Journal of Physics and Chemistry of Solids ۶۸ (۲۰۰۷) ۵۹۴–۵۹۹.

[۷]M. Mazloumi, S. Zanganeh, A. Kajbafvala, P. Ghariniyat, S. Taghavi, A. Lak, M. Mohajerani, S.K. Sadrnezhaad, Ultrasonics Sonochemistry ۱۶ (۲۰۰۹) ۱۱–۱۴.

Polypyrrole--silver nanoparticles hollow fiber solid phase microextraction coupled with high performance liquid chromatography for the determination of parabens in water and fruit juice samples

Mahnaz Nozohour Yazdi[a], Yadollah Yamini[a*], Hamid Asiabi[a]

[a] *Department of Chemistry, Faculty of Sciences, Tarbiat Modares University, P.O. Box 14115-175, Tehran, Iran*

E-mail: yyamini@modares.ac.ir (Y. Yamani).

****

Introduction: Parabens are a family of alkyl esters of *p*-hydroxybenzoic acid including methyl, ethyl and propyl paraben. They are widely used as preservatives in cosmetics, personal care products (PCP) and foodstuffs. Their popularity is based on their broad spectrum of action against numerous microorganisms, non- volatility and good stability [1]. As personal care products, parabens are continuously released into the environment through urban wastewater [2]. Therefore, the development of simple, rapid and accurate methods for the determination of parabens is highly desirable to monitor them.

Methods/Experimental: In order to resolve SPME drawbacks such as low thermal and chemical stability of SPME fiber, memory effect, fragility, limited coating lifetime, damaging at extreme pH and low selectivity for the target analytes, hollow fiber solid-phase microextraction (HF-SPME), as an alternative miniaturized sample preparation was used [3]. In this method, composite of PPY-Ag NPs was used as a new sorbent due to their high reactivity, large surface to volume ratio, high adsorption capacity and the ease of synthetic procedure [4].

Results and discussion: Several factors affecting the extraction efficiency of the parabens were optimized. The optimized experimental conditions were pH, 9; ionic strength, 0%; extraction time, 35 min; desorption time, 5 min; eluent type, acetonitrile; desorption volume, 1.5 mL; and stirring rate, 500 rpm. Under the optimal conditions, calibration curves were found to be linear in the range of 0.07–50 µg L^{-1}, 0.09–50 µg L^{-1}, and 0.1–50 µg L^{-1} for PP, EP, and MP in water samples, respectively. The LODs, based on a signal-to-noise ratio (S/N) of 3, were 0.02, 0.03, and 0.04 µg L^{-1} for PP, EP, and MP, respectively. The intra- and inter-assay precisions (RSD%, n = 3) were in the range of 5.9–7.0% and 4.4–5.7% at three concentration levels of 2, 10, and 20 µg L^{-1}, respectively. The extraction recoveries for the spiked samples were in the acceptable range of 80.3–90.2%. The validated method was successfully applied for analysis of methyl-, ethyl-, and propyl parabens in some water, beer, and juice samples.

Conclusion: The sorbent of PPY-Ag NPs for HF-SPME was successfully developed for the determination of parabens in water and fruit juice samples. The synthesized coating has remarkable advantageous such as higher specific surface area and sorption capacity, high extraction efficiency, good mechanical strength, ecofriendly and repeatability. Under the optimized condition, the proposed method provided low detection limit, good linear dynamic range and acceptable precision in comparison with other methods.

References:

[1] Usama Alshana, Nusret Ertas, Nilgun G. Goger. *Food Chemistry*, **2015**, *181*, 1–8.

[2] Hamid Asiabi, Yadollah Yamini, Shahram Seidi, Ali Esrafili, Fatemeh Rezaei. *Journal of Chromatography A*, **2015**, *1397*, 19-26.

[3] Amene Zendegi-Shiraz, Ali Sarafraz-Yazdi, Zarrin Es'haghi. *Journal of Separation Science*, **2016**, *39*, 3137-3144.

[4] Habib Bagheri, Solmaz Banihashemi, Samaneh Jelvani. *Journal of Chromatography A*, **2016**, *1460*, 1-8.

Polyvinyl pyridine/cerium oxide nanocomposite as a solid phase microextraction coating for determination of phthalate esters

Mahsa Nazraz, Yadollah Yamini*, Hatam Amanzadeh

Department of Chemistry, Tarbiat Modares University, Tehran, Iran

yyamini@modares.ac.ir

****

Introduction: phthalate esters (PEs) are typically utilized as plasticizers in many products, such as pesticides, plastics, paints, cosmetics and food industry [1,2]. These compounds are not chemically bounded to polymer chains [3]. So, PEs are easily released from the polymer, during manufacturing, under thermal or mechanical stress. This phenomenon may induce adverse on human health, specifically on the liver, kidney, and testicles [4]. Thus, great deal of attentions is paid to water samples as environmental pollutants. Therefore, simple, sensitive, and reliable analytical methods for evaluating and monitoring trace amounts of PEs in different water samples must be developed for human health protection and environmental control.

Methods / Experimentals: Head-space solid phase microextraction (HS-SPME) technique followed by gas chromatography-flame ionization detection (GC-FID) was developed for determination of PEs in water samples. The method started with electropolymerization of polyvinyl pyridine / cerium oxide nanocomposite (PVP/CeO_2) as a coating fiber for HS-SPME; then target analytes were extracted on PVP/CeO_2 coating fiber. The effects of important parameters on the extraction efficiency of the analytes were investigated. Under optimal extraction conditions, figures of merit of the method was determined and analysis of the analytes in the real samples were evaluated.

Results and discussion: The effect of different parameterson the extraction efficiency of the plasticizers were evaluated by one variable at a time method. The results showed that at extraction temperature of 90 ˚C, extraction time of 30 min, ionic strength of 30% w/v of NaCl salt, stirring rate of 1000 rpm, desorption temperature of 280 ˚C, and desorption time of 5 min the best results for extraction of PEs from water samples were obtained. Under optimal extraction conditions, the extraction recoveries ranged from 80 to 96%, and relative standard deviation, for analysis in intra-day, ranged from 7.4 to 9.5% and 6.9 to 8.6% at two concentration spiked levels of 25 and 50 µg L^{-1} respectively (n=5). Also, relative standard deviation for three days analysis ranged from 8.1 to 10.3% and 6.4 to 8.0% for two concentration spiked levels of 25 and 50 µg L^{-1} respectively. Detection limits were in the range of 0.2 to 2 µg L^{-1} for the four PEs.

Conclusion: For preconcentration and determining four PEs in water samples, a new fiber based on PVP/CeO_2 was established as a solid phase microextraction coating. Compared with the other methods, the proposed method was superior as it facilitated simultaneous extraction, preconcentration, and determination in one step with rapidity, simplicity, reliability, and low cost. The results of recovery and coefficient of variation indicated the method is accurate and precise for routine analysis.

References

[1]   Cai, Y. Q.; Jiang, G. B.; Liu, J. F. Anal. Chim. Acta, **2003**, 494, 149−156.

[2]   Cao, X. L. Compr. Rev. Food Sci. Food Saf, **2010**, 9, 21−43.

[3]   Insuan, W.; Khawmodjod, P.; Whitlow, H. J. Anal. Chem., **2016**, 64, 3287-3292.

[4]   Liang, P.; Xu, J.; Li, Q. Anal. Chim.Acta, **2008**, 609, 53−58.

Fast photopolymerization of composite of nanomolecularly imprinted polymer-nano TiO₂ by LED lamp and its application for photodegradation of Tartrazine in water media

Naghmeh Arabzadeh[a*], Parsa haroonian[b]

a) *Department of Chemistry, Amirkabir University of Technology*

b) *Department of Chemistry, yasouj University*

Email address: sarina2480@yahoo.com

Introduction:

One of the major concerns in the world today is water pollution [1-2]. Water-soluble dyes are Commonly used as coloring agents in a variety of products; even at very low concentrations they are highly visible. These dyes are considered as non oxidizable by conventional physical and biological treatments because of their complex molecular structure and the large size of their molecules. Thus, their decolorization is one of the necessary processes in wastewater treatment. In this research a new composite of nanomolecularly imprinted polymer (MIP) – nanophotocatalyst (TiO2) for tartrazine with high-efficiency were synthesized by photo polymerization in aqueous medium as a green method.

Experimental:

In a typical preparation, Tartrazine as the template and acryl amide as the functional monomer were dissolved in 40ml of distilled water. N, N´-methylene-bis-acrylamide as a cross linking agent, and TiO2 as a photocatalyst and initiator were added to the mixture and then was dispersed by sonication. After sonication the Pyrex glass was sealed under N2 atmosphere. Afterwards, the glass tube was put under the UV LED lap for 60 min to complete the polymerization.

Result and discussion:

A measure of tartrazine in aqueous solution was investigated in batch experiments. 1mg of nanocomposite particles was added into a 10ml aqueous solution of tartrazine, which its concentration was $3 \times 10{-5}$ M. The pH of all solutions was adjusted at two with HCl as the best pH for photodegradation of tartrazine. The mixture was stirred continuously at 25°C for 1–5 h under UV-C radiation, and then centrifuged. Afterwards the concentration of free tartrazine was determined by UV–Vis spectrophotometer. The instrument response was periodically checked with the known tartrazine standard solution.

The synthesized nanocomposite was characterized by SEM, TEM and FT-IR. The effects of pH, time, and composite dosage were studied.

The FT-IR spectra of non-washed and washed MIP nanocomposite nanocomposite were studied at 4,000–400 cm−1. Similar characteristic peaks indicate the similarity between the backbone structures of the different nanocomposites. A strong peak at ~1,650 which was observed in the FT-IR spectra of the nonwashed and washed MIP nanocomposite which is attributed to the vibration mode of C=O group. A sharp peak at 1,114.54 cm−1 shown in non-washed MIP nanocomposite is because of the −SO3H of tartrazine, which has disappeared in washed MIP nanocomposite

Conclusion:

As it is known removing hazardous tartrazine from the water environment is so important. In this research, high efficiency nanocomposite of nanoMIP-nanophotocatalyst was synthesized for tartrazine by fast and simple photopolymerization method by LED lamp. The MIP nanocomposite revealed high affinity to template and photodegrade the color of solution completely under UV radiation. The synthesis of nanocomposite was carried out in water, which is a green solvent.

References

[1] X. Luo, Y. Zhan, X. Tu, et.al, J. Chromatoger A, 1218(2011) 1115-1121.

[2] X. Shen, L. Zhu, G. Liu,H. Yu, H.Tang, J.Environ. Sci, Technol, 42 (2008) 1687-1692.

Preparation of stabilized ionic liquid on the SBA-15 and evaluation its catalytic property in oxidation of sulfides

Fereshteh Hosseini Eshbala*, Alireza Sedrpoushan, Farajollah Mohanazadeh

Institute of Industrial Chemistry, Iranian research Organization for Science and Technology, Tehran, Iran
Feresh_Hosseini@yahoo.com

Introduction: The selective oxidation of sulfides has been a challenge for many years and is a useful transformation in organic chemistry [1,2]. Unfortunately, most of the methods for this transformation, use toxic reagents or complex reaction procedures are accompanied with overoxidation of sulfoxides. In this way, when a homogeneous catalyst is used, require the separation of the catalyst, and consequently, a chromatographic procedure for the recovery is invariably inevitable [3]. To deliver more viable "green" methods for sulfoxidation reactions, several strategies aiming immobilization of tungsten-based catalyst into/onto inorganic supports and organic–inorganic hybrid materials, with the hope of improving the recyclability of the employed catalyst systems have subsequently been developed [4].

Methods/ Experimentals: This paper describes a simple procedure for the synthesis and application of SBA-15/Im/WO$_4^=$ as a novel nano catalyst in oxidation of sulfides by 30% H$_2$O$_2$ as green oxidant under neutral aqueous reaction conditions. In a conical flask, H$_2$O$_2$ (1.5 mmol) and SBA-15/Im/WO$_4^{2-}$ (0.08 mol %) were added to a solution of sulfide (1 mmol) and water and the mixture was stirred magnetically at room temperature for 8 hours. Furtheremore, in order to testify the recyclability of the catalyst, it is recovered and efficiency reused in 5 succeeding reaction cycles without any significant loss.

Results and Discussion: Herein, we report the application of (1-octyl-1H-imidazol-3-ium)WO$_4^=$ immobilization on mesoporous SBA-15 as a heterogeneous catalyst in sulfides oxidation. First, the preparation of SBA-15/IL was performed then was allowed to react with Na$_2$WO$_4$ to replace some chloride ions with tungstate ions by ionexchange. Comparison of the low angle XRD patterns of SBA-15/OcIm, SBA-15/OcIm/WO$_4^=$, and parent SBA-15 indicates that the ordered mesoporous structure of the material was not damaged even after immobilization of WO$_4^=$ in SBA-15 matrix. In particular, the results for N$_2$ adsorption–desorption provide useful information on the textural properties and mesoscopic quality of the presented materials. In addition, upon modification the surface area and pore volume decreased obviously. Additionally, the structural elucidation of SBA-15/OcIm and SBA-15/OcIm/WO$_4^=$ was performed in some details using TEM technique. The thermogravimetric analysis (TGA) of the WO$_4^=$@SBA-15/IL catalyst was performed at temperatures that ranged from 40 to 700°C under an argon flow. Finally, the amounts of loaded tungstate ions in the catalyst were found to be 4.24 % using ICP-OES. After the initial characterization of the prepared hybrid material (SBA-15/OcIm/WO$_4^=$), its catalytic activity was studied in the oxidation of sulfides to the corresponding sulfoxides or sulfones with aqueous 30 % H$_2$O$_2$ as terminal green oxidant.
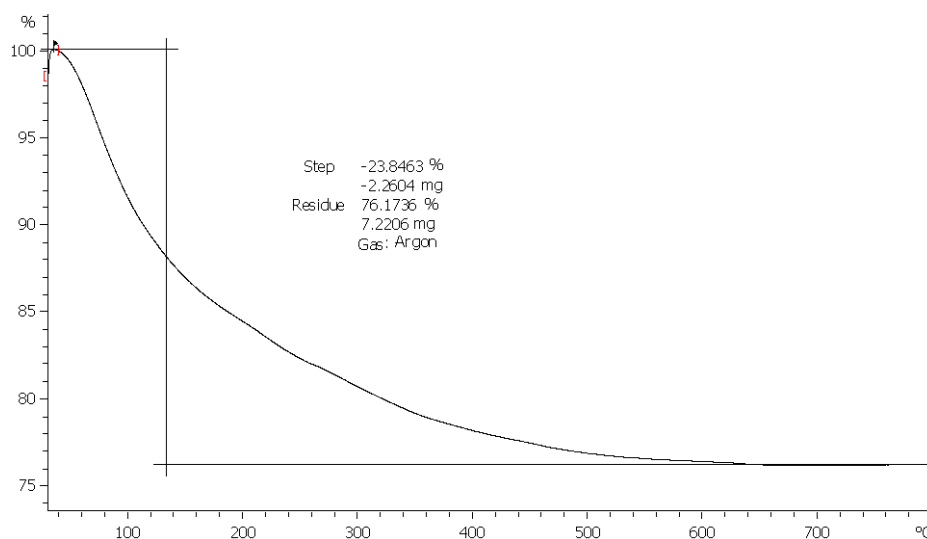
Fig. 1 TGA thermograms of SBA-15/OcIm/WO$_4^=$.

Conclusion: In summary, we have reported the successful synthesis of a novel catalyst from commercially available starting materials with potential catalytic application in the selective oxidation of organic sulfides under feasible conditions. Our studies showed that various aliphatic or aromatic sulfides comprising readily oxidizable groups are converted into the sulfoxide. The use of green solvent, very short reaction time with excellent yields and recyclability of the catalyst make this protocol highly advantageous.
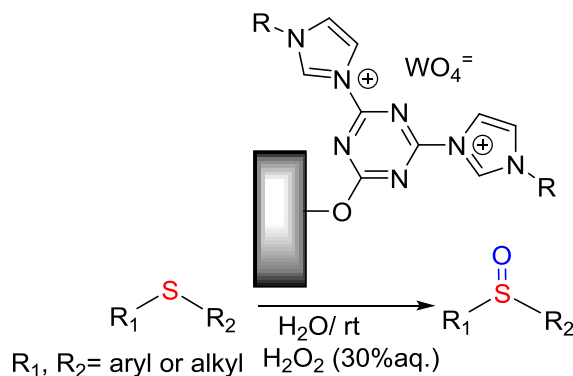
References

[1] J. N. Moorthy; K. Scnapati; K. N. Parida. *J. Org. Chem.*, **2010**, *75*, 8416.

[2] B. Maleki; S. Hemmati; A. Sedrpoushan; S. S. Ashrafi; H. Veisi. *RSC Adv.*, **2014**, 4, 40505.

[3] R. Noyori; M. Aoki; K. Sato. *Chem. Commun.*, **2003**, 1977.

[4] X. Shi, W. Ma, H. Ou, X. Han, C. Lu, Y. Chen, J. Wei, J. Braz. *Chem. Soc*. **2012**, 23, 1536.

Synthesis of polythiophene/ layered double hydroxide nanocomposite coating for electrochemically control fiber-in-tube solid phase microextraction

Maryam Shamsayei, Yadollah Yamini[*], Hamid Asiabi

Department of Chemistry, Tarbiat Modares University

yyamini@modares.ac.ir

Introduction:

Since in-tube solid phase microextraction (IT-SPME) has been widely applied to the extraction of analytes in biological, food, environmental, forensic, and pharmaceutical samples [1]. After presentation IT-SPME method, was introduced a novel miniaturized sample preparation method based on fiber-in-tube solid phase microextraction (FIT-SPME) method [2]. In this method wires were packed into a micro-diameter tube to get a fiber-in-tube device.

Among different types of sorbents used for the extraction of organic analytes, conducting polymers, particularly polythiophene (PTh) and its derivatives have attracted a great attention due to their multi functional properties such as large surface area, the ability to establish π–π interactions, polar functional groups and excellent chemical, mechanical, and thermal stability [3].

Experimental:

In the present study, the applicability of polythiophene/ layered double hydroxide coating in FIT-SPME combined with HPLC-UV was investigated for extraction of ultra-trace amounts of perphenazine and chlorpromazine in biological samples. In order to optimize the extraction efficiency of perphenazine and chlorpromazine by FIT-SPME seven variables including, extraction voltage, desorption voltage, pH of sample solution, extracting flow rate, desorption flow rate, extraction time and desorption time should be considered. Then, a nanostructured layered double hydroxide /polythiophene coating was prepared on the inner surface of stainless steel tube and surface of stainless steel wires.

Results and Discussion:

A schematic diagram of the complete assembly and operation mode of the instrument are shown in Fig. 1 [4]. The coated SS wires inside SS tube was mounted on valve 1 (V_1) in the location where the loop was originally positioned. Both V_1 and valve 2 (V_2) were initially set at the load position (red arrows). The effluent of V_1 was poured again into sample compartment after passing through the coated SS wire inside SS tube. In other words, this procedure was carried out in a circulating path. Also, the HPLC mobile phase was directly driven by HPLC pump through the analytical column at the flow rate of 1.0 mL min^{-1} to obtain a stable baseline for chromatographic separation.

After extraction for a given period of time, V_1 was directed to inject position, pump A was turned off while pump B was turned on to flow the desorption solvent (0.1 mol L^{-1} NaCl in methanol) through the tube at a flow rate of 2.7 mL min^{-1}. The effluent of desorption solvent was circulated as same as the extraction procedure to reach the maximum desorption efficiency (blue arrows). Finally, after a given desorption time interval, pump B was turned off, so that desorption elution was located into the HPLC loop, V_1 was returned to the load position while V_2 was directed to the inject position. Then, the extracted analytes was transferred into the loop of V_2 were eluted by the mobile phase into the HPLC column for further analysis.
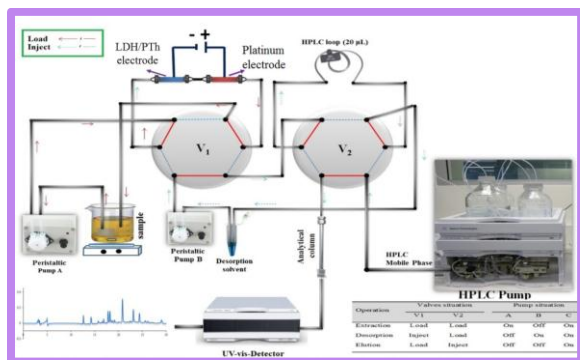
Conclusion:

A steel based FIT-SPME device with high extraction efficiency and selectivity was developed based on the combination of extraction effect of steel SPME fibers and steel SPME tube. Moreover, in this study, a new nanostructured coating consisting of LDH-PTh was synthesized on the surface of steel wire and internal surface of steel tube and used as sorbents for FIT-SPME method. LDH-PTh composite coating also showed an excellent extraction efficiency for cationic analytes. Under the optimized extraction and desorption conditions, the proposed FIT-SPME–HPLC method showed higher extraction efficiency and lower LODs compared with the previous reported methods.

References:

[1] C.L. Arthur, J. Pawliszyn, Solid phase microextraction with thermal desorption using fused silica optical fibers, Anal. Chem. 62 (1990) 2145–2148.

[2] Saito and K. Jinno, Miniaturized sample preparation combined with liquid phase separations, J. Chromatogr. A, 1000 (2003) 53-64.

[3] H. Asiabi, Y. Yamini, S. Seidi, A. Esrafili, F. Rezaei, Electroplating of nanostructured polyaniline–polypyrrole composite coating in a stainless-steel tube for on-line in-tube solid phase microextraction, J. Chromatogr. A 1397 (2015) 19–26.

[4] H. Asiabi, Y. Yamini, F. Rezaei, S. Seidi, Nanostructured polypyrrole for automated and electrochemically controlled in-tube solid-phase microextraction of cationic nitrogen compounds, Microchim. Acta 182 (2015)1941-1948.

Bagasse nano-catalytic conversion to biofuel in a mixed supercritical/subcritical medium

Mohammad Barati[*1], Gholamhossein Kahid Baseri[2]
[1]Faculty of Chemistry, University of Kashan, Kashan, Iran
[2] Graduate Faculty of Environment, University of Tehran, Tehran, Iran
barati.m@kashanu.ac.ir

1- Introduction

Plant biomasses conversion to fuels and chemicals has been investigated widely. Chemical and biochemical treatments were performed to extract chemicals with high energy values. Pyrolysis, hydrothermal treatments such as steam reforming as well as sub, near and supercritical water gasification and liquefaction have been performed to convert biomass to chemicals, fuels and fuel additives [1, 2]. The processes produce CO, CO_2, CH_4 and H_2 as gaseous products. Supercritical water gasification has shown a promising biomass hydrothermal treatment to produce H_2 rich gas products. Alcohols and ethers are other products that can be produced from near-critical water liquefaction of biomass [3-8].

2- Methods / Experimental

Conversion of Iranian bagasse to gaseous and liquid fuels was carried out in a basic and reducing medium of subcritical water and supercritical methanol with 80%wt and 20%wt, respectively. The process was performed in a bomb 200 mL reactor in presence of Cu /γAl$_2$O$_3$-MgO catalysts. The catalysts were promoted with different percentages of K and the effects of Cu and K loadings on quality and quantity of biofuel products were investigated. The catalysts were prepared with 20wt% of Cu and 1, 2.5, 5, 7.5 and 10wt% of K. They were shown in the text with Cu20, Cu20-K1, Cu20-K2.5, Cu20-K5, Cu20-K7 and Cu20-K10, respectively.

2-1- Catalyst characterization

The catalysts' Characterization results were reported on table 2 and figures 1 and 2.

Table 2: Textural properties of catalysts.

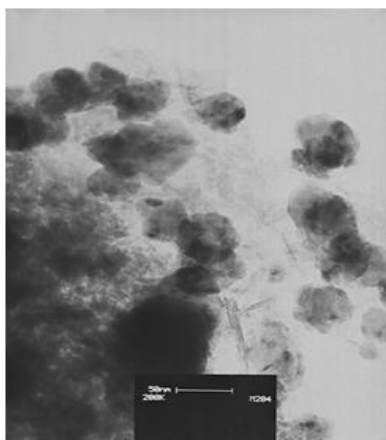| Sample	S_{BET} (m^2.g^{-1})	Pore volume (mL.g^{-1})	Average pore diameter (A)
Cu20	151.98	0.39	99.58
Cu20-K1	150.14	0.3855	99.18
Cu20-K2.5	146.21	0.3532	94.12
Cu20-K5	138.59	0.2907	87.85
Cu20-K7.5	126.64	0.2081	82.35
Cu20-K10	113.07	0.1577	77.93

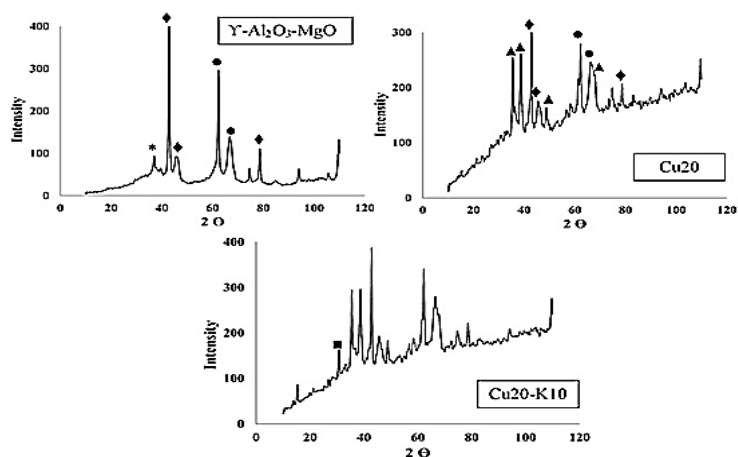
Figure 1: TEM micrograph of Cu20-K2.5.

Figure 2: XRD patterns of support, Cu20 and Cu20-K10.

3- Results and discussion

Gaseous product compositions were analyzed using GC-TCD. Results indicated CO, CO_2, H_2, CH_4 and some other light hydrocarbons. Figure 3 shows gaseous product amounts of the process in presence of catalysts. Gas production decreased with addition of potassium from 1 to 5 percent. Potassium addition blocks Cu active sites and can partially prevent biomass gasification and methanol reforming. However, excess addition in potassium percentage caused mild increasing in CO, CO_2 and light hydrocarbons production. Hydrogen production had a little different behavior among others. It totally decreased with addition and increasing of potassium percentage. Decelerating MeOH reforming and bagasse gasification reactions are reasons for this
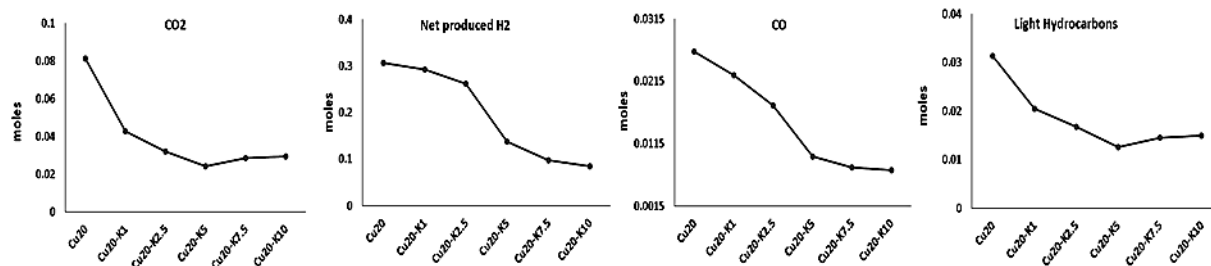
behavior.

Figure 3: Gaseous product amounts of the process.

The liquid products were analyzed using GC-MS. Figure 4 compares carbon moles in liquid and gaseous products with converted carbon of methanol, bagasse and total carbon conversion. Total
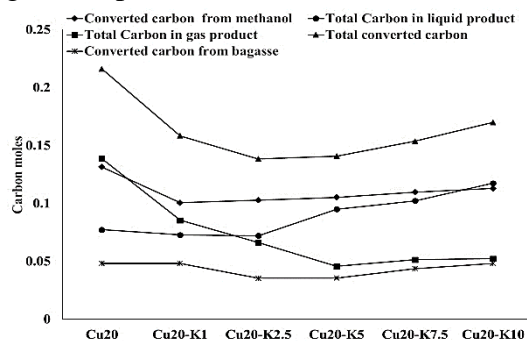

converted carbon decreased from Cu20 to Cu20-K2.5. It can be related to sudden decreasing in gas species amounts that was discussed in previous section. Also there was an increasing in carbon moles of liquid product. Potassium gives catalyst oxygenates molecularly adsorption tendency which proceeds alcohol and ether production mechanism compare to hydrocarbon one. Supercritical methanol also has an important role while solvolysis of bagasse.

Figure 4: Carbon balance for the processes.

4- Conclusion

Potassium makes catalyst sites more active to adsorb oxygenates, molecularly. So, conversion of $CnH_{2n-2-x}(OR)_x$, CH_3OH and CO that are responsible for alcohols and ethers production become easier. Supercritical methanol/subcritical water medium in presence of potassium promoted $Cu/\gamma\text{-}Al_2O_3\text{-}MgO$ catalysts for liquefaction of bagasse shows promising selective method for obtaining alcohols and ethers. Non-converted methanol can be recycled to process and the products easily and with no expensive treatments can be used.

5- References

[1] L. Zhang, B. Xiao, Z. Hu, S. Liu, G. Cheng, P. He, L. Sun, Waste Management, 34 (2014) 180-184.
[2] L. Lemee, D. Kpogbemabou, L. Pinard, R. Beauchet, J. Laduranty, Bioresource Technology, 117 (2012) 234–241.
[3] P. Azadi, H. Foroughi, T. Dai, F. Azadi, R. Farnood, Fuel, 117 (2014) 1223-1230.
[4] M. Barati, M. Babatabar, A. Tavasoli, A. K.Dalai, U. Das, Fuel Processing Technology, 123 (2014) 140–148.
[5] S. Xiu, A. Shahbazi, V. Shirley, M. R. Mims, C. W. Wallace, Journal of Analytical and Applied Pyrolysis, 87 (2010) 194–198.
[6] S. N. Reddy, S. Nanda, A. K. Dalai, J. A. Kozinski, International Journal of hydrogen Energy, 39 (2014) 6912–6926.
[7] Md. N. Uddin, W.M.A. W. Daud, H. F. Abbas, Renewable and Sustainable Energy Reviews, 27 (2013) 204-224.

[8] N. Sudasinghe, J. R. Cort, R. Hallen, M. Olarte, A. Schmidt, T. Schaub, Fuel, 137 (2014) 60–69.

Why not inspiring from Nature?!

Caffeine-H$_2$SO$_4$: A Novel Bioinspired Dual Acidic catalyst for the one-pot preparation of 2H-indazolo[2,1-*b*]phthalazine-triones

Seyyed Jafar Saghanezhad [a,*]

[a] ACECR-Production Technology Research Institute, Ahvaz, Iran

Corresponding Author Tel: (+98) 61-33364400, Email: jafar_saghanezhad@yahoo.com

Introduction

Quite recently organic chemists have been more interested in multi-component reactions (MCRs) due to their simplicity, high yield of the products, one-pot synthesis and eco-friendly reaction conditions [1]. Due to the great potential of MCRs in designing novel organic reactions [2], different strategies have been devised including solvent-free conditions [3], application of homogeneous or heterogeneous catalysts [4], or performing reaction in unconventional solvents [5].

Results and Discussion

Caffeine- H$_2$SO$_4$ was easily prepared by addition of conc. H$_2$SO$_4$ to a solution of caffeine in CH$_2$Cl$_2$ and subsequent stirring for 24 h. Caffeine-H$_2$SO$_4$ is introduced as a novel bio-inspired acidic catalyst for the preparation of 2H-indazolo[2,1-*b*]phthalazine-triones as a sample reaction.

Experimental

Typical procedure for the preparation of 2H-indazolo[2,1-b]phthalazine-trione: A mixture of dimedone (0.14 g, 1 mmol), phthalhydrazide (0.16 g, 1 mmol), aromatic aldehyde (1.1 mmol), and Caffeine-H$_2$SO$_4$ (0.01 g, 3.4 mol%) was heated at 100$^\text{o}$C. Completion of the reaction was indicated by TLC [TLC acetone/n-hexane (3:10)]. After completion of the reaction, the mixture was washed with water and the crude product was recrystallized in hot ethanol to afford the pure product.

Conclusion

In conclusion, Caffeine-H_2SO_4 has been applied as a novel bioinspired dual acidic catalyst in the one-pot preparation of 2H-indazolo[2,1-*b*]phthalazine-triones. This catalyst has been characterized by FT-IR, ^{1}H NMR, ^{13}C NMR and TGA. According to the obtained results including time, yield and recyclability, Caffeine-H_2SO_4 could be considered as an efficient catalyst for this reaction and other organic transformations.

References

[1] A. Dömling, I. Ugi, Angew. Chem. Int. Ed., **39**(18), 3168 (2000)

[2] B. Ganem, Acc. Chem. Res. **42**(3), 463 (2009)

[3] M. S.Singh, S. Chowdhury, RSC Adv. **2**, 4547 (2012)

[4] M. J. Climent, A. Corma, S. Iborra, RSC Adv. **2**, 16 (2012)

[5] Y. Gu, Green Chem. **14**, 2091 (2012)
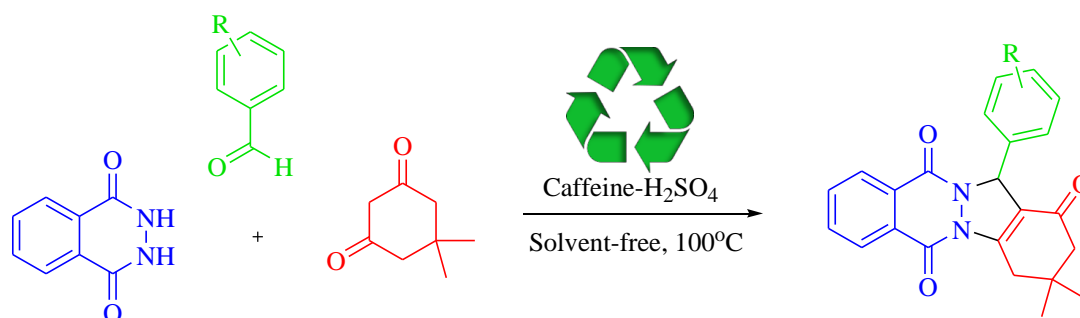
One-pot preparation of 2H-indazolo[2,1-*b*]phthalazine-triones

Fe$_3$O$_4$ nanoparticles-supported as a heterogeneous catalyst for the synthesis of propargylamines derivatives

Atefeh Shouli, Soheil Sayyahi*

Department of Chemistry, Mahshahr Branch, Islamic Azad University, Mahshahr, Iran

Email:sayyahi.soheil@gmail.com

Abstract

The recovery of expensive catalysts after catalytic reaction and reusing it without losing its activity is an important factor for sustainable process management [1, 2]. The difficulty of separating homogeneous catalysts from reaction medium consumedly restricts their applications in industry, especially in the drug and pharmaceutical industry owing to the issue of metal contamination in the case of metal-catalyzed synthesis [3]. Surface functionalization of nano-magnetic nanoparticles is a well-designed way to bridge the gap between heterogeneous and homogeneous catalysis [4]. Since such catalysts work under quasi-homogeneous conditions, their performance is usually very good and exhibit high selectivity, activity, and stability. The catalysts can be easily separated by magnetic decantation and reused in many cases [5, 6]. In this paper and in continuation of our attempts to introduced new magnetically recoverable nanocatalyst systems for organic reactions [7-9], we report our results on the synthesis, and characterization of Cu-based magnetic nanoparticles and their catalytic application in propargylamine synthesis.
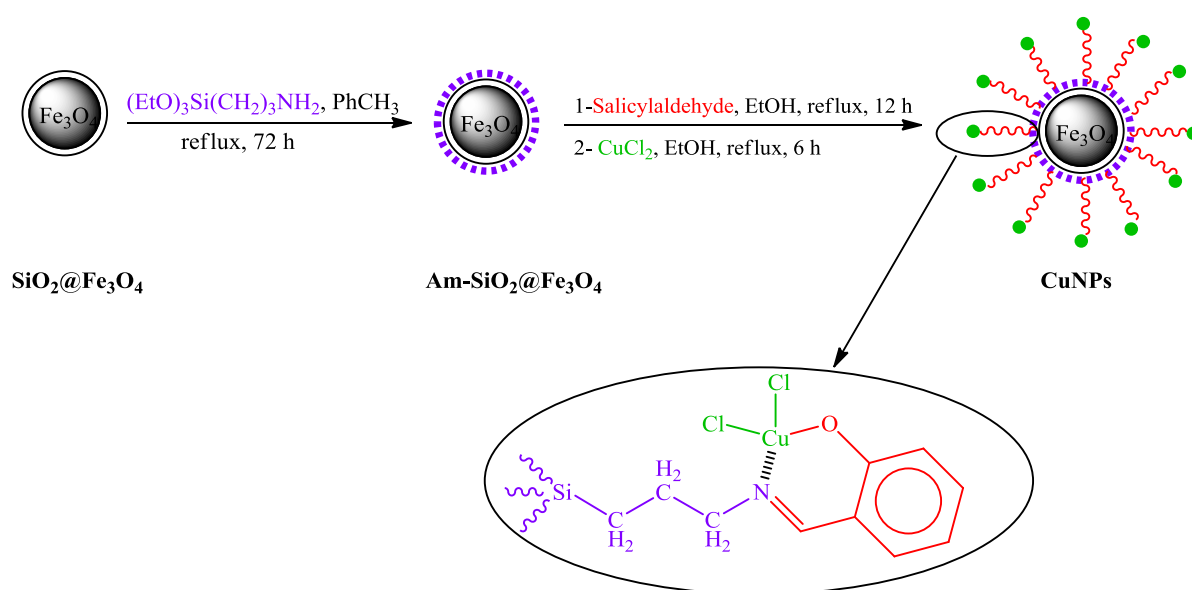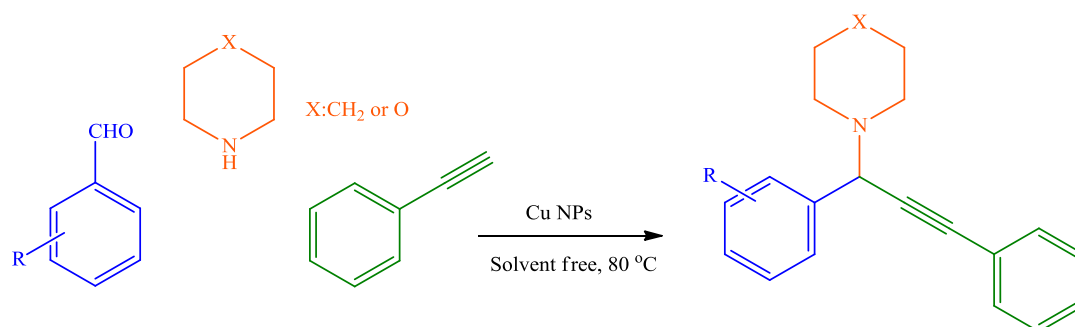
Figure 1. Synthesis of propargylamines catalyzed by Cu(II)-imine ligand@SiO$_2$@Fe$_3$O$_4$

Keywords: Magnetic nanoparticle; Propargylamines; Cu catalysts

References

[1] S. Shylesh, V. Schünemann, W.R. Thiel, Magnetically Separable Nanocatalysts: Bridges between Homogeneous and Heterogeneous Catalysis, Angew. Chem., Int. Ed., 49 (2010) 3428-3459.
[2] R.B.N. Baig, R.S. Varma, Magnetically retrievable catalysts for organic synthesis, Chemical Communications, 49 (2013) 752-770.
[3] D. Wang, D. Astruc, Fast-Growing Field of Magnetically Recyclable Nanocatalysts, Chemical Reviews, 114 (2014) 6949-6985.
[4] M.B. Gawande, P.S. Branco, R.S. Varma, Nano-magnetite (Fe$_3$O$_4$) as a support for recyclable catalysts in the development of sustainable methodologies, Chem. Soc. Rev., 42 (2013) 3371-3393.
[5] R. Mrowczynski, A. Nan, J. Liebscher, Magnetic nanoparticle-supported organocatalysts - an efficient way of recycling and reuse, RSC Advances, 4 (2014) 5927-5952.
[6] V. Polshettiwar, R. Luque, A. Fihri, H. Zhu, M. Bouhrara, J.-M. Basset, Magnetically Recoverable Nanocatalysts, Chemical Reviews, 111 (2011) 3036-3075.
[7] S. Sayyahi, S. Mozafari, S.J. Saghanezhad, Fe$_3$O$_4$ nanoparticle-bonded β-cyclodextrin as an efficient and magnetically retrievable catalyst for the preparation of β-azido alcohols and β-hydroxy thiocyanate, Res. Chem. Intermed., 42 (2016) 511-518.
[8] A. Amini, S. Sayyahi, S.J. Saghanezhad, N. Taheri, Integration of aqueous biphasic with magnetically recyclable systems: Polyethylene glycol-grafted Fe$_3$O$_4$ nanoparticles catalyzed phenacyl synthesis in water, Catal. Commun., 78 (2016) 11-16.
[9] F.K. Olia, S. Sayyahi, N. Taheri, An Fe$_3$O$_4$ nanoparticle-supported Mn (II)-azo Schiff complex acts as a heterogeneous catalyst in alcoholysis of epoxides, C. R. Chim. (2016) DOI; org/10.1016/j.crci.2016.06.007

Nano-*gama*-Al$_2$O$_3$.SbCl$_5$; an efficient and heterogeneous solid acid for the synthesis of *N*-nitrosoamines at room temperature

Sepideh Saleh[a], Abdolhamid Bamoniri[a,*], BiBi Fatemeh Mirjalili[b]

[a]*Departement of Org. Chem., Faculty of Chem., University of Kashan, Kashan, I. R. Iran*
[b]*Department of Chem., College of Sci., Yazd University, Yazd, I. R. Iran*

E-mail address: bamoniri@kashanu.ac.ir

Introduction

Nitroso compounds and their reactions have been studied extensively. Their pharmaceutical applications have been studied. Many of their uses for the treatment of cardiovascular and central nervous system diseases, and diseases related to immunity and physiological disorders have been reported [1]. The most general reagent is nitrous acid, generated from sodium nitrite and mineral acid in water or in mixed alcohol / water solvents. Other nitrosating agents such as sodium nitrite and oxalic acid two hydrate [2], tungstate sulfuric acid [3], silica sulfuric acid [4] have been used.

Herein, we wish to report a convenient method for *N*-nitrosation of secondary amines, using Nano-γ-Al$_2$O$_3$.SbCl$_5$ under solvent free conditions at room temperature by grinding.

Methods / Experimentals

Chemicals were purchased from Merck Chemicals Company. The nitrosation products were characterized by comparison of their spectral (IR, ^{1}HNMR, ^{13}CNMR), TLC and physical data with the authentic samples. Secondary amine (1 mmol), NaNO$_2$ (1.5 mmol) and nano-γ-Al$_2$O$_3$.SbCl$_5$ (0.2 g) were ground in a mortar with a pestle for a few minutes to obtain a homogeneous mixture. After complete conversion as indicated by TLC, 10 ml dichloromethane were gradually added to the mixture, and this solution, was stirred at room temperature. Then reaction mixture was filtered and washed with 4 ml dichloromethane. Then anhydrous Na$_2$SO$_4$ was added to the filtrate and was filtered after 10 min. The solvent was evaporated and the *N*-nitroso compound was obtained. For further purification, flash chromatography on silica gel [*n*-hexane: ethylacetate 80:20] provide highly pure products (Scheme 1).

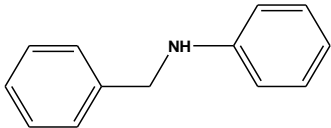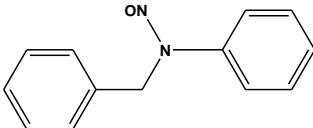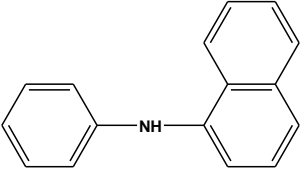$$R_1R_2NH \xrightarrow[\text{Nano-}\textit{gama}\text{-Al}_2\text{O}_3.\text{SbCl}_5, \text{ rt}]{\text{NaNO}_2} R_1R_2NNO$$
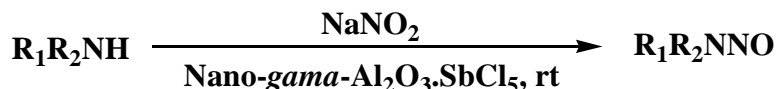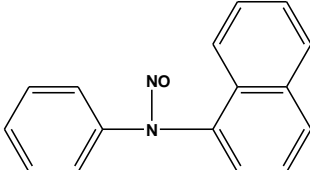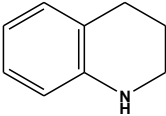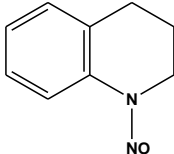
Scheme 1

Results and Discussion

General procedure for the synthesis of N-nitrosation of secondary amines

Different kinds of secondary amines was subjected to nitrosation reaction in the presence of nano-γ-Al$_2$O$_3$.SbCl$_5$ and NaNO$_2$. The nitrosation reactions were performed under mild and completely heterogeneous conditions at room temperature and take place with excellent to moderate yields (Table 1). The nitroso amines can be obtained by filtration and evaporation of the solvent. A reaction of phenyl benzyl amine as a model substrate with sodium nitrite was

carried out at 25°C. The best result based on yield and time of the reaction was obtained with 0.25g of nano-γ-Al$_2$O$_3$.SbCl$_5$.

Table 1. *N*-Nitrosation of secondary amines with NaNO$_2$ in the presence of nano-γ-Al$_2$O$_3$.SbCl$_5$ at room temperature

Entry	Amine	Time (min)	Product	Yield (%)
1		2.5		90
2		3		70
3		2		90

The results have shown that aliphatic amines were reacted effectively under heterogeneous conditions, since the nitrogen atom of aliphatic amines has more basic and nucleophilic character than that of aromatic amines.

Conclusions

A highly effective methodology for the synthesis of *N*-nitrosoamine compounds was developed at room temperature in solvent free conditions. The advantages of this procedure are mild reaction conditions, simple work-up procedure, cheapness and the availability of the reagents, chemoselectivity and high yields.

References

[1]. Iranpoor, N; Firouzabadi, H; Nowrouzi, N. *Tetrahedron Lett.* **2008**, *49*, 4242–4244.

[2]. Zolfigol, M. A. *Synth. Commun.* **1999**, *29*, 905-910.

[3]. Karami, B; Montazerozohori, M; Habibi, M. H. *Bull. Korean Chem. Soc.* **2005**, *26*, 1125-1128.

[4]. Zolfigol, M. A. Bamoniri, A. *Synlett.* **2002**, 1621–1624.

Transfer of Calibration Models between Different Analytical Methods Based on Projection concept

Mahdieh Ghaffari[a], Hamid Abdollahi[a,*]

Faculty of Chemistry, Institute for Advanced Studies in Basic Sciences, Zanjan, Iran

m.ghaffari@iasbs.ac.ir

Introduction: The problem of calibration transfer is well-known in analytical chemistry. It appears every time when one wants to use calibration model developed for one analytical instrument with the data obtained by another instrument. Direct application of a calibration model to the data from another instrument is normally not possible. To perform calibration transfer techniques such as Direct Standardization (DS), it is necessary to measure representative samples in the instruments involved. Nevertheless, something like volatilization of the compounds present in the samples may cause changes in their composition over time.

Methods / Experimental: This approach is based on the conversion of analytical signals from one instrument (Slave) into the format of another instrument (Master). The proposed algorithm can be summarizing as below:

$$A_1 = D_1\, C_{h,1}^+ \qquad A_2 = D_2\, C_{h,1}^+ \qquad C_{x,2} = D_{x,2} A_2^+ \qquad D_{x,1} = C_{x,2} A_1$$

First step is projection of D_1 and D_2 into $C_{h,1}\ and\ C_{h,2}$, respectively. D_1 and D_2 are data matrices belong to golden samples of master and slave instruments. In all calibration methods composition of samples in D_1 and D_2 must be exactly similar. One of the advantages of this new approach is possibility of accurate calibration transfer in dissimilar golden samples. $C_{h,1}$ and $C_{h,2}$ are s by nc matrices, which s is number of samples and nc is number of components. In these matrices all columns except concentration of analyte has filled with synthetic vectors which are orthonormal. Next step is projection of $D_{x,2}$, which we plan to use for prediction with calibration model from the first instrument into A_2 . Finally we compute corrected response matrix, $D_{x,1}$ which can be further used with the model from the first instrument.

Results and Discussion: The performance of the suggested method, which is based on the correction of second instrument's responses, was tested with simulated data and real data set. The real data set was calibration models for quantification of moisture and oil in corn samples by two dissimilar NIR instruments. The RMSEP values obtained for the primary instrument, without the use of transfer techniques for moisture and oil were 0.749% and 0.853% respectively. After calibration transfer with 20 samples the RMSEP values for moisture and oil change to 0.140% and 0.252%, respectively.

Conclusion: In this paper, a calibration transfer method based on projection concept is proposed. After a successful calibration transfer, the data from the slave analyzer can be predicted with a model built from the master analyzer.

References:

[1]. R. N. Feudale, N. A. Woody, H. Tan, Chemometrics and Intelligent Laboratory Systems, 2002, 64, 181-192.

Design&Construction of "Micronized and nanosized Powder Production Machine

Parviz AhmadiAvval[a],*, Fathollah Pourfayaz[b], Zahra Sheybanifard[c]

a Chemical Processes Design Research Group, ACECR, Faculty of Engineering, University of Tehran, Tehran, Iran

b *Department of Renewable Energies, Faculty of New Science and Technologies,* University of Tehran, Tehran, Iran

c Chemical Processes Design Research Group, ACECR, Faculty of Engineering, University of Tehran, Tehran, Iran

Email address pchemco@gmail.com

****

Introduction: In most cases, particle size reduction is required in order to use of solid materials in chemical reactions and formulations. Grinding or reducing the size of solid particles according to the type of material is usually performed by using various methods such as Ball mill, Cutting, End Hummer and etc [1-3]. Over the years, Chemical Processes Design Research Group, ACECR has been succeeding to create technical knowledge of materials for the petrochemical industry. In order to convert some of these materials into micronized powder, cooling process, grinding and sifting are used but because of waste time and high cost, therefore it is essential designing efficient method for producing micronized/ nanosized powders.

Methods/Experimental: A solid organic compound with melting point about 120°C is converted into micronized/nanosized powders with a device that is schematically shown in Fig 1. The effect of some parameters such as fluid viscosity, fluid temperature and air pressure of the spray nozzle head has been examined.
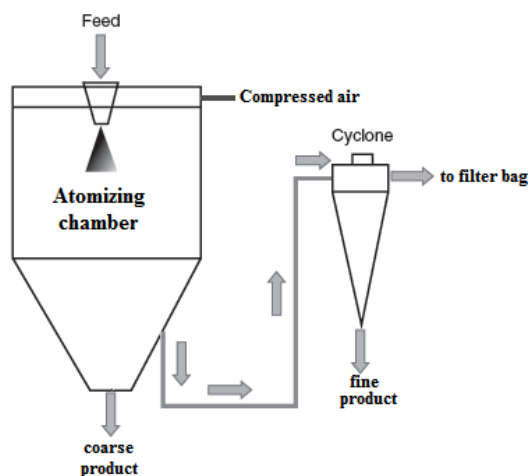

Figure 1. Schematic of a micronized powder machine.

Results and Discussion: In the former method, several stages are utilized in order to have micronized powder: Initially, the materials are cooled and solidified in the trays. Afterward,

these materials are placed in a fridge and are cooled to a temperature of -20°C. In the final stage, the solid is converted into powder by a mill. In the proposed method, the hot liquid in the reactor is sprayed by suitable nozzles and micronized/nanosized powders are produced and finally collected by two steps: in a chamber and a cyclone (Figure 1). According to the results, Fluid temperature changes don't have a directly affect on performance of a nozzle and particles size. In fact, the temperature will affect on viscosity and density of the fluid and therefore affect the performance of the nozzle and particles size. Generally, by increasing temperature of the fluid the particles size is reduced but by increasing viscosity of the fluid, the high pressure is needed for spraying and then the particles size is increased. Also, increasing air pressure of the spray nozzle head can be caused a decrease in particles size. In Figure 2, the generation of drops while the fluid is passed from the nozzle is shown. In addition, the results show that the particle size distribution is about 50 nm to 100µm.
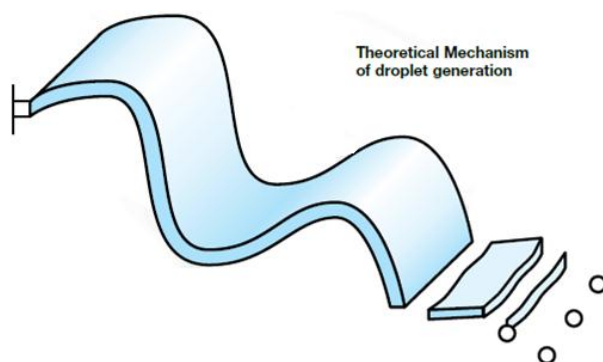

Figure 2: The schematic of the formation of drops while spraying process.

Conclusion: By doing some laboratory tests it was found that it is possible to emulate from systems such as spray dryer, designing new machine to have micronized/ nanosized powders in a shorter time and consumption lower cost with high quality products. By this method several operational steps of the powder production is removed.

References

[1] Lisa J. Grahama, Rebecca Taillona, Jim Mullina, Trevor Wigleb, *Computers and Chemical Engineering*, **2010**, 34, 1041-1048.

[2] Abdulrahman Bahrami, Farshid Ghorbani, Hossien Mahjub, Farideh Golbabei, Mohsan Aliabadi, *Industrial Health*, **2009**, 47, 436–442.

[3] Khosro Adibkia, Mohamad Barzegar-Jalali, Yusef Javadzadeh, Hossein Maheri-Esfanjani, *Pharmaceutical Sciences*, **2012**, 18,119- 132.

A simple and fast Fe_3O_4 magnetic nanoparticles-based dispersion solid phase extraction of Aflatoxins in nut coupled with high-performance liquid chromatography

Rouhollah Karami-Osboo [a]* and M. Mirabolfathy [a]
a Mycotoxins Research Laboratory, Iranian Research Institute of Plant Protection, Agricultural Research Education and Extension Organization (AREEO), Tehran, Iran.
Email address: karamiosboo@gmail.com

****

Introduction: Aflatoxins (AFs), the second metabolites of Aspergillus fungi, are probably the most intensively researched mycotoxins in food [1].They could occur before and after harvest in cereals and nuts. AFs are known to be mutagenic, teratogenic, carcinogenic and immunosuppressive compounds [2]. In the past decades, several sample preparation methods, such as solid phase extraction columns particularly C18 and immunoaffinity columns followed by HPLC have been developed for cleanup and extraction of AFs from food and feed. These methods are time consumer, relatively expensive, and have low stability against organic solvents and pH [3]. In the present research, we used Fe3O4 MNPs as cleanup materials along with microlitere amounts of chloroform as the extractant for extraction of AFs from pistachio nuts. Simultaneous purification and extraction made sample pre-treatment simple and quick.

Methods / Experimentals: Twenty grams of pistachio paste were extracted with 100 mL of methanol-water (80-20 v/v) and then, in order to obtain high extraction efficiency, important factors which may influence the performance of clean up and extraction, such as amount of nanoparticles (MNPs), volume of extraction solvent, and salt addition, were evaluated. Optimization was accomplished on real extracted samples, under different experimental conditions, and extraction recovery was applied to assess the effect of different parameters. Under optimized conditions, the LODs, LOQs, repeatability (RSD, %) and recovery, in different levels of spiked samples were evaluated (table. 1).

Results and Discussion: The experimental results indicated that; when 1 mL of methanolic pistachio extract diluted in 1 mL deionized Water, maximum extraction efficiency was observed at 0.05 mg of MNPs, 250 µL of chloroform as an extraction solvent and 0.1 g NaCl. Results showed that there are no significant differences between the proposed method and conventional laboratories method (IAC). Duo to the small particle size and high specific surface area of MNPs, the time of the cleanup process can significantly decrease and a small amount of MNPs are needed to obtain acceptable results. The extraction solvent has a crucial role to clean up and concentrate AFs in pistachio extract. In this research, same as many research chloroform had higher extraction capacity for the AFs [4]. By increasing the ionic strength of aqueous phase, up to 0.1 g of sodium chloride, the extraction recovery was increased; but after that by increasing the ionic strength the solubility of AFs ions in the aqueous phase was increased and the affinity of AFs in the organic phase reduced.

Conclusion: In summary, the proposed Fe3O4-based MSPE method has multifaceted advantages: first, Fe_3O_4 MNPs do not need any functionalization and the preparation of unmodified Fe_3O_4 MNPs is facile, low-cost and accessible to numerous labs; second, compared to the IAC (Immunoaffinity column clean up), which consist of several preparation steps and demand expensive reagents, the Fe3O4-based MSPE assay for AFs developed here offers the advantage of easy automation and high throughout; third, the Fe3O4 MNPs

adsorbent could remove the potential matrix interference and chloroform could preconcentrate the four aflatoxins rapidly and effectively, thus making this method very suitable for the determination of trace amounts of AFs by the disperse SPE-HPLC. We believe the method developed here presents a promising technique for the estimation of AFs in nut samples and monitoring the amount of AFs in nut.

Table 1. The recovery, LODs and LOQs results of MNPs method in three different spike levels.

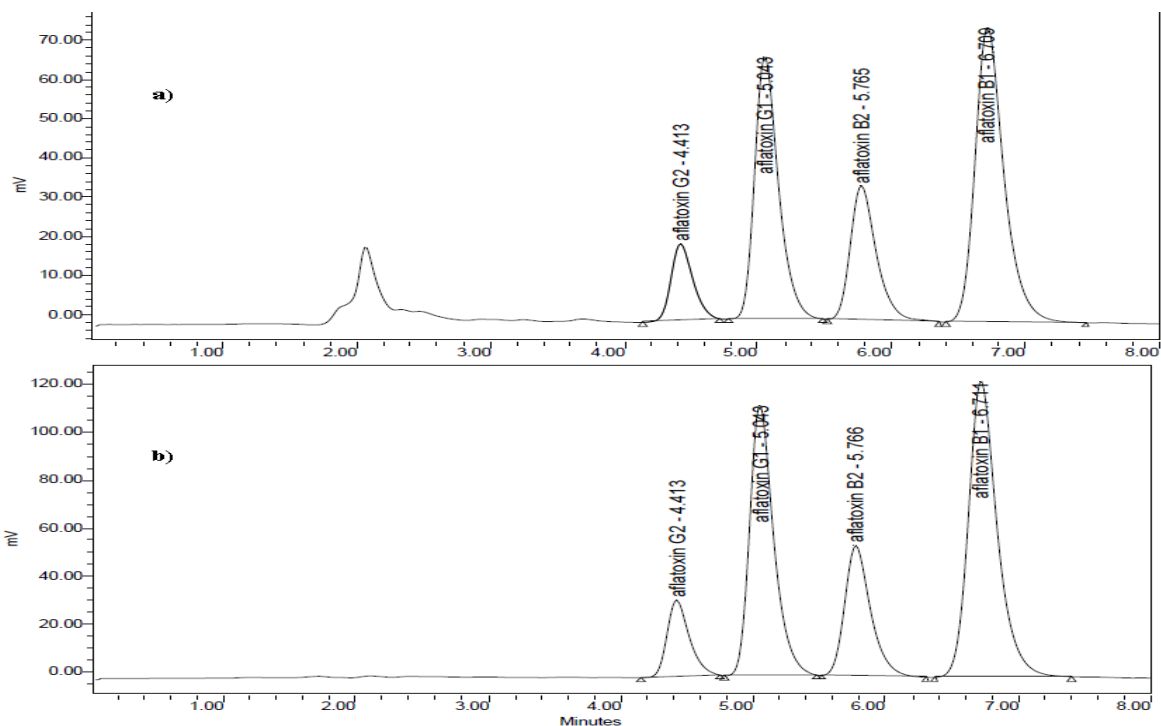|	LOD (ng/g)	LOQ (ng/ g)	Mean value ± standard deviation (n = 3), Spike 5 ng/ g	Mean value ± standard deviation (n = 3), Spike 15 ng/ g	Mean value ± standard deviation (n = 3), Spike 30 ng/ g
aflatoxin G_2	0.06	0.2	107.5±10.2	81.6±4.1	78.1±6.5
aflatoxin G_1	0.35	1	105.8±7.6	80.0±3.5	76.0±6.7
aflatoxin B_2	0.06	0.2	109.0±5.9	84.3±2.6	80.3±7.2
aflatoxin B_1	0.35	1	114.7±3.2	82.9±3.3	78.5±7.1

Fig.1. HPLC-FLD chromatograms of (A) spiked samples at 5 ng/g AFs and (B) AFs standards 3.6 ng/ml.

References
[1].Karami-Osboo, R, M. Mirabolfathy, R. Kamran, M.S.Boushehri, S Sarkari. Food Control, 2012. vol. 23: 271-274.
[2]. IARC.2002. IARC Monographs on the Evaluation of Carcinogenic Risks.240-247.
[3]. Stroka, J., Ankle, E., Jorissen, U., Gilbert, J.,. J. AOAC Int. 2000.83, 320–340.
[4]. Karami-Osboo, R, Maham, M., Miri, R. Shojaee Ali Abadi, M.H., M. Mirabolfathy. K. Javidnia. Food Analytical Methods, 2013. 6 (1), 176-180.

A density functional theory (DFT) study on the tautomerism of 2-amino-6-methyl pyrimidine-4-one: Solvation effects and NBO analysis

Seyedhossein Hosseini[1], **Elahe Jalali**[2]

[1]Chemistry Department, Science Faculty, farhangian branch, University, Gonbad Iran
[2]Chemistry Department, Science Faculty, Damghan branch, Islamic Azad University, Damghan, Iran

ABSTRACT

A Density Functional Theory (DFT) study is used to calculate structural data of tautomers of 2-Amino-6-methyl pyrimidine-4-one (AMPO) in the gas phase and selected solvents (benzene (non-polar solvent), tetrahydrofuran (THF) (polar aprotic solvent) and methanol (protic solvent), Dimethyl sulfoxide (DMSO) (polar aprotic solvent) and water (protic solvent)) by using PC model. All tautomers are optimized at the B3LYP/6-31++G(d,p). The results show that the tautomer AMPO1 is more stable than the other tautomers especially in water.

Keywords: DFT study, NBO analysis, Pyrimidine, Tautomerism, PC model.

INTRODUCTION

Amino–imino tautomerization processes facilitated by intermolecular proton transfer in heterocycles have been the subject of a number of studies [1-2]. These processes are relevant to many areas of biological chemistry and have been invoked in mechanisms of radiation-induced damage in DNA [3]. The physical–chemical properties of the aminopyridine and their biochemical importance have received considerable attention from both experimental and theoretical approaches [4-5], due to the understanding for many fundamental biochemical processes.

Tautomerism as one of the possible mechanism of mutation in DNA, has extended area for studies. Therefor different theoretical and experimental studies were performed on this process [6]. Nucleic acids are polymer molecules composed of different kinds of bases, such as pyrimidine [7].

EXPERIMENTAL SECTION

Quantum Chemical Calculation

All these calculations were carried out on a Pentium V personal computer by means of GAUSSIAN03 program package [8] and for our computations. First, all compound's structures were drawn using Gauss View 03 [9] and optimized in semi. To characterize all the optimized geometries the vibrational frequencies for all the conformers have been done at B3LYP levels. The stationary structures are confirmed by ascertaining that all ground states

---

have only real frequencies. The tautomers were also optimized in solvents according to the polarisable continuum method of Tomasi and co-workers, which exploits the generating polyhedra procedure [6] to build the cavity in the polarizable continuum medium, where the solute is accommodated.

RESULTS AND DISCUSSION

Gas phase

Structures and numbering of 2-Amino-6-methyl pyrimidine-4-one (AMPO) are depicted in figure 1 and the results of energy comparisons of six tautomers in the gas phase and different solvents are given. In the gas phase AMPO6 form is more stable than the other forms. The major difference between AMPO6 and the other forms in gas phase was found for AMPO3 with 25.08 kcal mol^{-1}. The order of stability of all the tautomers in the gas phase is AMPO6 > AMPO4> AMPO1> AMPO2> AMPO5>AMPO3.
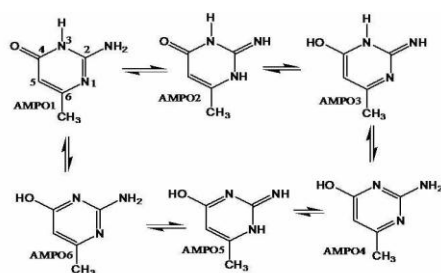

Figure 1. Tautomeric forms of AMPO and numbering of AMPO ring

CONCLUSION

In this work a DFT study is used to calculate structural data of tautomers of 2-Amino-6-methyl pyrimidine-4-one (AMPO) in gas phase and selected solvents from non-polar to polar aprotic. In the gas phase AMPO6 form was more stable than the other tautomers. In the solution the stability of some tautomers is deferent than gas phase and stability of tautomers were affected by deferent solvents. Also the dipole moments of all compounds are affected by solvent. With increase of the polarity of solvents the dipole moments of all tautomers were increased and the charges on all six positions were affected by solvents. In addition with increase of dielectric constant a variation was found.

REFERENCES

[1] PR Cantor; PR Schimel, Biophysical Chemistry, vol. 2, W.H. Freeman, San Francisco, CA, 1980.

[2] PT Chou; ML Martinez, .J. Phys. Chem., 1992, 96(4), 2018-2019.

[3] MJ Nowak; L Lapinski; H Rostkowska; A Les; L Adamowicz, J. Phys. Chem. A., 1990, 94(19), 7406-7414.

[4] H Ishikawa; K Iwata; H Hamaguchi, J. Phys. Chem. A., 2002, 106(10), 2305-2312.

[5] F Hung; W Hu ; T Li; C Cheng; P Chou, J. Phys. Chem. A., 2003, 107(18), 3244-3253.

[6] JS Kwiatkowskri; RJ Barlett; Person, J. Am. Chem. Soc.,1988, 110(8), 2353-2358

[7] JD Watson; FHC Crick, Nature.,1953, 171(4356), 964-965.

[8] MJ Frisch; GW Trucks, Gaussian 03, Revision C02, Wallingford CT, 2004.

[9] R Dennington; T Keith; J Millam; K Eppinnett; WL Hovell; R Gilliland, GaussView, Version 309, Semichem, Shawnee Mission, KS, 2003.

Preparation and characterization of Fe-Mg oxide Nanoparticles based on Nano Alumina prepared by the co-precipitation method and the study of the effect of different drying condition on their structures

Ali Karimianfard *[1] , Ahad Zare [1]

[1] Department of Chemistry, Islamic Azad University Marvdasht branch, Fars, Iran

*Corresponding author: E-mail address: ali_karimianfard@yahoo.com

Abstract: In this research, Fe-Mg oxide Nanoparticles based on Nano Alumina were synthesized by co-precipitation method in various times and different temperatures of drying conditions. The purpose of this research was the investigation of drying conditions on morphology and size of Fe-Mg oxide Nanoparticles. The results show that the products were crystallized and particles size ranged from 28-82 nm. Samples synthesized by changing the drying temperature between 100-180°C and the time of 6-12 hours. FESEM, XRD and EDS analysis were employed to characterize the obtained products. The results show that the best particles were obtained in 12 hours and 120°C of drying condition.

Keywords: Temperature and time, Drying condition, Nano Alumina, Fe-Mg oxide, FESEM, XRD, EDS, Co-precipitation.

Introduction: Spinel ferrite Nanoparticles are constituted by a general formula $A^{2+}Fe_2^{3+}O_4$, where A^{2+} has been replaced by suitable divalent metal ions such as Co, Cu, Mg, Zn, Mn and Ni etc [1]. Spinel ferrite Nanoparticles are prepared using various methods. Among these methods co-precipitation method is widely used for the preparation of ferrites for its overriding advantages such as ease of preparation, composition flexibility, homogeneity of particle size, etc [2]. Spinel ferrites have the chemical formula MFe_2O_4 in which M can be any divalent metal cation. In spinel ferrite, oxygen forms an FCC-lattice with divalent cations at tetrahedral (A) and/or octahedral (B) sites. Magnesium ferrite ($MgFe_2O_4$) has an inverse spinel structure with the preference of Mg^{2+} cations mainly on octahedral sites [3]. Spinel ferrites have been widely investigated due to their under lying applications on high-density magnetic recording, microwave devices, magnetic fluids, etc [4]. The aim of the present work is to study the role of different preparation conditions in the change of morphology, structure and magnetic properties of spinel iron oxide Nanoparticles obtained by the co-precipitation technique. This method has advantage such as easy preparation, low cost, enough digestion to form the final structure suitable, control of particle size and shape, magnetic separation in order to obtain different particle size, pH control, maintenance of the oxidation state, sample preparation at different temperature [5].

Methods or Experimental: First, 0.5M solutions of Iron (III) nitrate and Magnesium (II) nitrate were made. 6g Nano Alumina weighted and dissolved into 20ml water and a thick white solution obtained. Since Nano Alumina is the base of this experiment, prepared Iron (III) nitrate and Magnesium (II) nitrate should be added to that. Beaker placed in a warm bath of water when the temperature was 60-70°C and a magnet added for stirring. In this step, titration with sodium carbonate, which is a precipitator, begun. pH of mixture was acidic until by adding sodium carbonate it raised to 9 and color of solution turned into brick red. Beaker hold for 4 hours to reactants fully react and aging take place. A sample acquired from 4 hour aged solution and dehydrated by filter paper, Buchner funnel and vacuum pump, and sediment washed by distilled water in order to ions get removed and a dry sediment

with the least impurity achieved. After washing, sediment divided into 8 crucibles to be prepared for drying. Four samples were dried in fixed temperature of 120°C and variable times of 6, 8, 10, and 12 hours, and other four samples were dried in fixed time of 6 hours and variable temperatures of 100, 140, 160 and 180 $^{\circ}$C. Then all samples were calcined at 600°C for 2 hours in furnace. For investigating phase detection, determining size of Nanoparticles and crystals and morphology of Nanoparticles, EDS, XRD and FESEM tests performed respectively.

Results and Discussion: Images of FESEM analysis show that particles are in Nano scale, and Nanoparticles generated appropriately. In the first batch of four samples (i.e. A_1-A_4) particles seen as light spots that demonstrated Nanoparticles placed on surface of sample and cohesion and dark spots were seen less. In the second batch of four samples (i.e. A_5-A_8) particles are not appropriately crystalline and agglomerated, and dark spots suggest that particles are at depth and probably need more temperature or time to migrate to surface and cohesion to be decreased. In these four samples, increasing time of drying caused a decline in size of Nanoparticles but particles distribution was not suitable. Images from surface of Nanoparticles in sample A_4, they were 54-82 nm in size and spherical in morphology. All of obtained EDS images from samples demonstrated that four elements of Iron, Magnesium, Oxygen and Aluminum are present at the samples, and there is no type of impurities. In all of samples, except A_4, Aluminum and Oxygen have the highest weight percent. Also in all of samples, Aluminum has the peak with highest intensity and Magnesium has lowest weight percent. Obtained pattern from XRD analysis demonstrate that crystals are broken an many spots and are in form of single crystal. There is no significant phase change in samples, and phases ate almost same, but in three samples of A_5, A_7, A_8 increase in crystal size is significant. Using debye-scherrer relation, crystal size in A_4 sample obtained 6.53 nm. Available phases in this sample are MgO, $MgFe_2O_4$, Fe^+ which most of phases observed in this sample and the largest pick corresponds to $MgFe_2O_4$ spinel structure. Also crystal structure of all samples are reported cubic.

Conclusion: Results suggest that because of magnetic properties and synthetic conditions, Iron-Magnesium Nanoparticles agglomerated in some points, particularly in drying with fixed time, which this can be because of their chemical nature or short time of drying, but all of Nanoparticles are Nano sized. All of expected metallic elements such as Iron, Magnesium, Aluminum as well as Oxygen which are indicator of metal oxidation present in all of samples with different amounts and expected metallic oxides and also Nanocomposites formed in most of samples. At long times of drying in fixed temperature, particles being seen better but in samples that are dried in fixed time, particles are agglomerated. If time of reaction or aging become shorter and time of drying become longer, better Nanoparticles form, and agglomeration decreases. According to analysis, best sample is A_4, which is synthesized in drying temperature of 120°C.

References:
[1] T. Vigneswari; P. Raji. Molecular Structure, **2016**, 1127, 515–521.
[2] Ch.Srinivas; B.V.Tirupanyam; S.S. Meena. Magnetism and Magnetic Materials, **2016**, 407, 135–141.
[3] S. Rahman; K.Nadeem; M.Anis-ur-Rehman. Ceramics International, **2013**, 39, 5235–5239.
[4] Y. Zhang; Z. Yang; D. Yin. Magnetism and Magnetic Materials, **2010**, 322, 3470–3475.
[5] J.C. Aphesteguy; G.V. Kurlyandskaya; J.P. de Celis. Materials Chemistry and Physics, **2015**, 161, 243–249.

Synthesis, Characterization and DFT Calculations of Schiff Bases Derived from 2-Aminophenol and Benzaldehyde Derivatives and their Oxovanadium (IV) Complexes

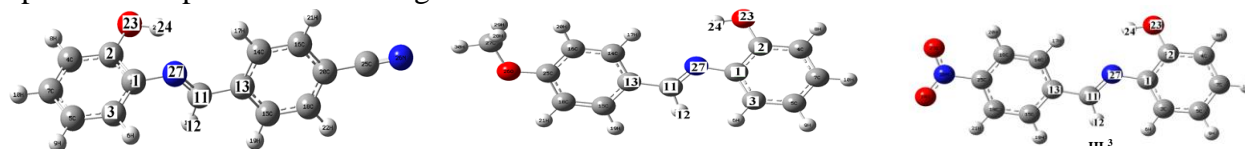**Khosro Mohammad*** and **Soghra Marzooghsavadi**
Chemistry Department, Faculty of Sciences, Persian Gulf University, Bushehr 75169, I.R. Iran
khmohammadi@pgu.ac.ir, khmohammadi@yahoo.com

Introduction: Schiff base ligands are used in variety range of applications such as anti-corrosion [1], anti-cancerous [2], anti-HIV [3], anti-bacterial and anti-fungal materials [4] and DNA cleavage.[5] Furthermore, their industrial potential make them good choice for catalysis [6], drug design [7], and chemical sensor [8]. They were usually formed by the condensation reaction between an aldehyde and an amine to eliminate water and formation the imine group which plays a key role in Schiff base ligands. The chelating centers (nitrogen, oxygen and etc.) to metal ion have the potential of biological activities. [9] The complexation with transition metal ions improves their stability.

Experimental: The Schiff base ligands (L^n) were prepared, by dropwise adding hot ethanolic solution of 2-aminophenol (1 mmol) to the benzaldehyde derivatives (1 mmol) in hot ethanol and refluxed. The progress of the reaction and purity the product was checked by TLC test. The obtained precipitation was filtered, washed with n-hexane and water. The oxovanadium(IV) complexes were prepared, by dropwise adding hot ethanolic solution of vanadium acetylacetonate (0.5 mmol) to the ligand (1 mmol) in hot ethanol and refluxed. Complete geometrical optimizations of the investigated molecules were performed using the B3LYP at 6-311+G(d,p)/LANL2DZ basis sets with the Gaussian 09W software package 16 and Gauss view visualization program.

Results and Discussion: The experimental and calculated NMR and FTIR data of the ligands and the complexes are reported in following Tables.
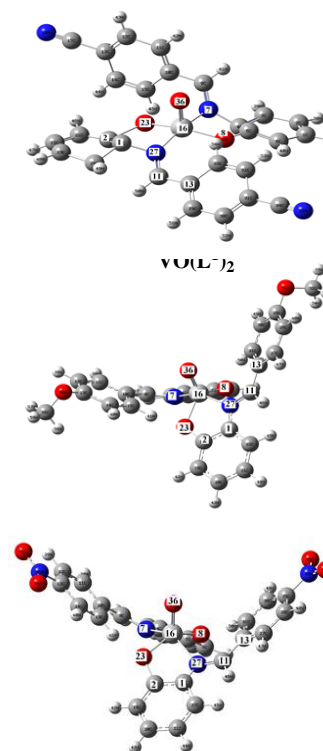

atoms	δ_{exp} (ppm)			δ_{Cal} (ppm) B3LYP/6-311+G(d,p)		
	HL^{1a}	HL^{2b}	HL^{3b}	HL^1	HL^2	HL^3
H_1	7.37	7.16	7.30	7.20	7.58	7.75
H_2	6.97	6.82	6.86	7.02	7.05	7.08
H_3	7.30	7.04	7.14	7.09	7.33	7.46
H_4	7.08	6.88	6.93	7.05	7.16	7.20
H_5	7.18	-	-	7.63	-	-
H_6	8.77	8.61	8.89	9.07	8.88	9.07
$H_{8,8'}$	7.82	7.97	8.29	7.93-7.69	7.70-8.66	7.99-8.06
$H_{9,9'}$	7.06	7.06	8.35	7.10-7.08	7.16-7.19	7.93-8.69
OCH_3		3.83			3.85-4.14	

[a] $CDCl_3$, [b] DMSO-d6

atoms	δ_{exp} (ppm)			δ_{Cal} (ppm) B3LYP/6-311+G (d,p)		
	HL^{1a}	HL^{2b}	HL^{3b}	HL^1	HL^2	HL^3
C_2	153	151	152	161	159	161
C_{11}	154	158	157	158	160	157
C_{20}	115	162	149	117	170	156
C_{25}	116	-	-	118	-	-
C_{27}	-	55	-	-	55	-
$C_{13}-C_{18}$	120-134	127-131	124-137	130-146	114-139	129-149
C_1-C_7	120-134	114-138	116-142	118-139	117-141	119-139

[a] $CDCl_3$ Solvent, [b] DMSO-d_6 Solvent,

atoms	ν_{exp} (cm^{-1})						ν_{cal} (cm^{-1}) B3LYP/6-311+G(d,p)					
	HL^1	HL^2	HL^3	VO(L^1)$_2$	VO(L^2)$_2$	VO(L^3)$_2$	HL^1	HL^2	HL^3	VO(L^1)$_2$	VO(L^2)$_2$	VO(L^3)$_2$
ν_{OH}	3408	3335	3367	-	-	-	3545	3531	3545	-	-	-
ν_{CH}	3000	2920	3085	3000	3063	3049	2934	2919	2937	3126	3008	3020
$\nu_{C=N}$	1624	1594	1589	1586	1584	1587	1617	1619	1615	1588	1588	1591
ν_{C-N}	1287	1250	1244	-	-	-	1235	1229	1234	-	-	-
ν_{C-O}	1246	1157	1230	1193	1188	1193	1272	1236	1230	1193	1195	1193
$\nu_{C\equiv N}$	2224	-	-	2224	-	-	2249	-	-	2138	-	-
ν_{sNO2}	-	-	1520	-	-	1522	-	-	1520	-	-	1535
ν_{asNO2}	-	-	1343	-	-	1344	-	-	1316	-	-	1383
$\nu_{V=O}$	-	-	-	990	970	975	-	-	-	990	998	995

The calculated electronic properties by DFT method of the complexes are reported in following Table.

Electronic properties/Complexes	VOL$^1_2$	VOL$^2_2$	VOL$^3_2$
E_{HOMO}(ev)	-6.4416	-5.3890	-6.3450
E_{LUMO}(ev)	-3.0657	-2.3199	-3.7247
E_{L-H}(ev) Δ	3.3759	3.0691	2.6203
Electronegativity(χ)	4.7537	3.8545	5.0348
hardness (η)	1.6879	1.5345	1.3101
Softness (S)	0.2962	0.3258	0.3816
electrophilicity(ω)	-6.6938	-4.8407	-9.6744
dipole moment(μ)(debye)	6.3208	3.4365	7.9795

Conclusion: New NO donor Schiff base ligands and their oxovanadium(IV) complexes with the general formula [VOL$_2$] were prepared by using reflux methods and characterized by spectral methods. Also, DFT calculations were applied successfully to predict the structural geometry and confirm the IR and NMR data. Finally, the frontier molecular orbitals (HOMO and LUMO), ionization potential energy (I), electron affinity (A), electrophilicity (ω), electronegativity (χ), hardness (η) and softness (S) of the compounds were investigated. The stability of the compounds is as following: [VO(L^1)$_2$] > [VO (L^2)$_2$] > [VO (L^3)$_2$]. The trend of dipole moment of the complexes is following: [VO(L^2)$_2$] < [VO(L^1)$_2$] < [VO(L^3)$_2$]

References

[1] H. H. Eissa, *BAOJ Chem.* **2015**, *1(1)*, 1-9.
[2] N. Suleiman Gwaram and P. Hassandarvish, *App. Pharm. Sci.* **2014,** *4(10)*, 75-80.
[3] M. C. Mandewale, B. R. Thorat and R. S. Yamgar, *Der Pharm. Chem.* **2015**, *7(5),* 207-215.
[4] N. S. A. Kader, A. L. El-Ansary, Tarek. A. El-Tayeb and M. M. F. Elnagdi, *J. Photochem. Photobiol. A: Chem.* **2016,** *321*, 223-237.
[5] T. A. Khan, H. Zafar, S. N. Khan and A. U. Khan, *Synth. React. Inorg. Met. Org. Chem. Nano-Met. Chem.* **2014,** *44*, 1175-1183.
[6] D. K. Sandhya, *J. Chem. Pharm. Res.* **2014,** *6*, 746-750.
[7] X. Zhang, C. Liao, J. Cao, L. Yang, and Q. Li, *J. Comput. Theor. Nanosci.* **2015,** *12,* 2745-2750.
[8] L. M. Mesquita, V. Andre, C. V. Esteves, T. Palmeira, M. N. Berberan-Santos, P. Mateus and R. Delgado, *Inorg. Chem.* **2016,** *55(5)*, 2212-2219.
[9] P. A. Vigato and S. Tamburini, *Coord. Chem. Rev.* **2004,** *248*, 1717-2128.

Densities, Viscosities, and Refractive Indices for Binary and Ternary Mixtures of Acetone + Chloroform + Methanol at Temperatures from 298.15 to 313.15 K

M.Hamzehloo[*a] and <u>M.Doost Mohammadi</u> [a]

[a] University of Tehran, college of science, school of chemistry, Department of physical chemistry, Tehran, Iran

Email: mhamzehlo@khayam.ut.ac.ir

Introduction

Thermodynamic and transport properties are essential in process design and operation. Density and viscosity of the multicomponent mixtures are required in many chemical engineering calculations involving fluid flow, heat, and mass transfer. [1] The experimental data of excess thermodynamic properties of the liquid mixtures provide useful information about molecular interactions. Excess molar volumes (V^E), deviations in the viscosity ($\Delta\eta$), and deviations in the refractive index (Δn_D) for the mixtures were derived from the experimental data. The experimental results are considered to talk about the strength of intermolecular interactions between the components of the systems.

Experimental

Chemicals are supplied by Merck with purity higher than 99% .The mixtures were prepared by weighing pure liquids into stoppered bottles to prevent evaporation and reducing possible errors in mole fraction calculation. The densities were measured with digital densitometer and viscosities were measured with an Ubbelohde viscometer. The apparatus was frequently calibrated by known pure liquid viscosity and density. The uncertainty in the mole fraction is estimated to be lower than $\pm 10^{-4}$.

Results and discussions

Dynamic viscosities and viscosity deviations were calculated from the following equation:

$$\frac{\eta}{\eta_0} = \frac{\rho}{\rho_0} \times \frac{t}{t_0} \qquad\qquad \Delta\eta = \eta_{mix} - \sum_{i=1}^{N} x_i \eta_i$$

where η_0, ρ_0 and t_0 refers to viscosity, density and efflux time of pure water respectively.

The excess molar volumes (V^E) were calculated from density data by:

$$V^E = \sum_{i=1}^{N} x_i M_i \left(\frac{1}{\rho} - \frac{1}{\rho_i} \right)$$

The mixing functions V^E, $\Delta\eta$, and Δn_D were represented mathematically by the Redlich-Kister [2] equation for correlating the experimental data:

$$\Delta Q_{ij} = x_i x_j \sum_{i=1}^{N} A_k (x_j - x_i)^k$$

Derived data (V^E, $\Delta\eta$, Δn_D) for the ternary system were correlated, respectively, using the equation:

$$\Delta Q_{123} = \Delta Q_{bin} + x_1 x_2 x_3 \Delta_{123}$$

$$\Delta Q_{bin} = \sum_{i=1}^{3} \sum_{j>i}^{3} \Delta Q_{ij}$$

where ΔQ_{123} refers to V^E, $\Delta\eta$ and Δn_D for the ternary mixtures. The ternary contribution term Δ_{123} was correlated using the expression suggested by Cibulka [3]:

$$\Delta_{123} = B_0 + B_1 x_1 + B_2 x_2$$

where the ternary parameters B_0, B_1, and B_2 were determined with an optimization algorithm similar to that for the binary parameters.
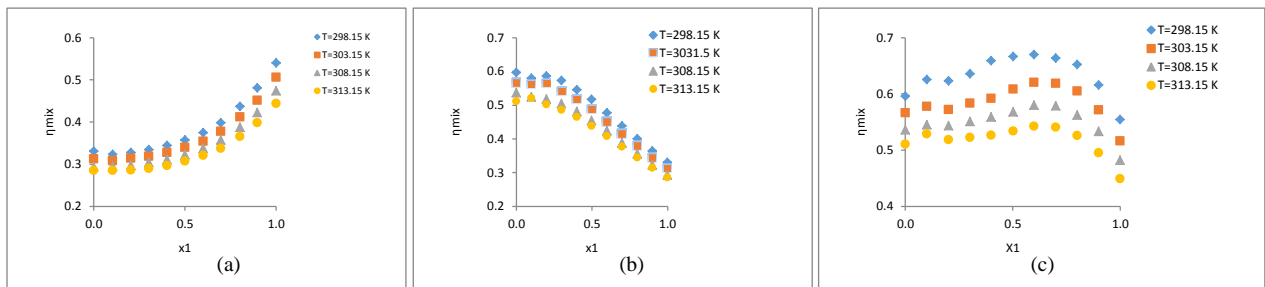
Figure1. Experimental viscosities for binary systems: a) methanol (1) +acetone (2), b) acetone (1) +chloroform (2) and c) methanol (1) +chloroform (2) at different temperatures.

Conclusion

Densities, viscosities, refractive indices and derived properties for binary and ternary mixtures consist of Acetone, Chloroform and Methanol were measured at temperatures from 298.15 to 313.15 K in the whole range of mole fractions. The measured data and calculated values of all systems are in good agreement with literature and Redlich-Kister and the Cibulka equations.

References

[1] Alvarez, E.; Sanjurjo, B.; Cancela, A.; Navaza, J. M. Mass Transfer and Influence of Physical Properties of Solutions in a Bubble Column. Chem. Eng. Res. Des. 2000, 78, 889–893

[2] Redlich; O. J. Kister. A. T. Algebraic representation of thermodynamic properties and the classification of solutions. Ind. Eng. Chem. 1948, 40, 345-348.

[3] Cibulka, I. Estimation of excess volume and density of ternary liquid mixtures of non-electrolytes from binary data. Collect. Czech, Chem.Commun. 1982, 47, 1414-1419.

Study of propane dehydrogenation over Pt-Sn/Al$_2$O$_3$ catalyst using temperature-programmed reaction technique

F. Tahriri Zangeneh*, S. Sahebdelfar

National Petrochemical Company, Petrochemical Research and Technology Company, P.O. Box 14358-84711, Tehran, Iran

Email: tahriri_zangeneh@yahoo.com

Introduction: Propane dehydrogenation has received much attention because of increasing demand for propylene. Well-dispersed Pt catalysts show good performance due to small proportion of low-coordination number sites favoring C-C bond cleavage [1]. However, rapid catalyst deactivation by coke formation is a major problem [2]. One method to achieve constant conversion over a deactivating catalyst is to constantly increase the reaction temperature to compensate catalyst deactivation [3]. This strategy, however, could be limited by promoting side reactions at higher temperatures which reduce the selectivity. In this work the applicability of temperature-programmed strategy in propane dehydrogenation over a Pt-based catalyst is studied.

Experimental: Commercial Pt–Sn/γ-Al$_2$O$_3$ catalyst with trade name DP-803 was supplied by Procatalyse Company. Catalyst test runs were performed in a fixed–bed quartz reactor (ID =15 mm) under atmospheric pressure using a mixture of propane and hydrogen (H$_2$/HC=0.6) as the feed with a WHSV=2h^{-1}. A step-wise temperature-time program beginning from 600 °C to 650 °C was used to compensate catalyst deactivation such that the initial propane conversion was maintained. The reactor effluent was analyzed with an online gas chromatograph.

Results and discussion: Figure 1 shows the temperature variation and corresponding propane conversion with time. A fairly constant propane conversion is observed. A careful look at Fig. 1b reveals that within each step, the conversion showed a small "exponential" decay with time which was compensated by the temperature rise in the next step. Higher temperatures increase the reaction rate both due to kinetic effects (i.e., Arrhenius law) and thermodynamic effects (by increasing equilibrium conversion, Fig. 1b) for this equilibrium limited reaction.
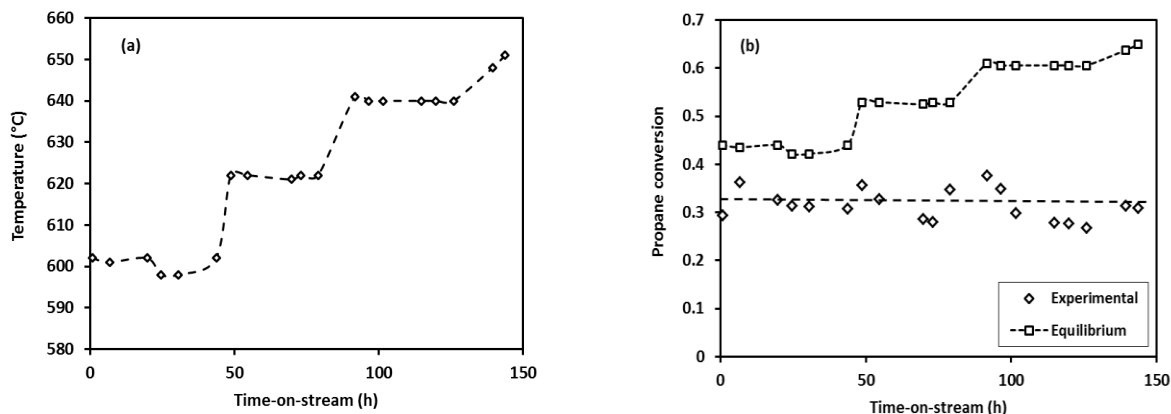

Figure 1. Plots of (a) temperature and (b) propane conversion versus reaction time.

Figure 2 shows the selectivity to propylene and to by-products resulted from side reactions versus time (or temperature). During test run, selectivity to ethylene increased significantly from ca. 0.01 to 0.25 after 150 h, or 50 °C temperature rise, implying the ever-increasing role of non-catalytic thermal cracking. Meanwhile, ethane selectivity as a measure of propane hydrogenolysis decreased from 0.1 to 0.06. The overall effect was a decrease of propylene selectivity from 0.85 to 0.45 which is too large to be acceptable. This illustrated that temperature-time trajectory is not appropriate for dehydrogenation of lower paraffins and sequential catalyst regeneration appears more satisfactory.
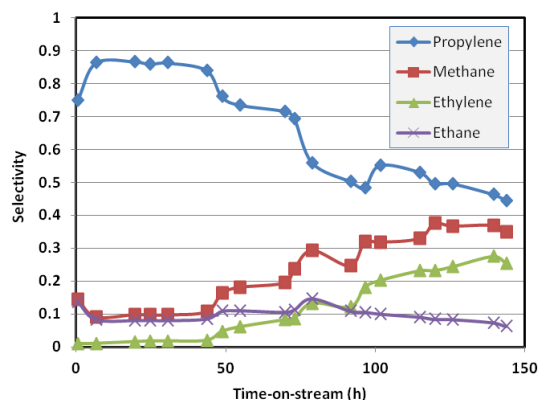
Figure 2.Selectivity of products versus reaction time.

Conclusions: The dehydrogenation of propane over Pt-Sn/Al$_2$O$_3$ catalyst was studied by temperature-programmed reaction from 600 to 650 °C. Although the temperature-time programmed strategy could maintain a constant propane conversion over the deactivating Pt-Sn/Al$_2$O$_3$ catalyst, the selectivity to propylene was adversely affected. The main cause of selectivity loss was found to be propane cracking which is the thermodynamically more favorable reaction and could occur thermally at higher reaction temperatures.

References

[1] F. Tahriri Zangeneh , A. Taeb, K. Gholivand, S. Sahebdelfar, *Applied Surface Science*, **2015**, *357*,172–178.

[2] S. Luo, S. He, X. Li, J. Li, W. Bi, *Fuel Processing Technology*, **2015**, *129*,156–161.

[3] H.S. Fogler, *Elements of Chemical Reaction Engineering*, 4th ed., **2006**, Prentice-Hall, New Jersey, 707-757.

Synthesis and Properties of Novel Poly(urethane-imide)s Nanocomposites

Baharak Pooladian and **Mir Mohammad Alavi Nikje***

Department of Chemistry, Faculty of Science, Imam Khomeini International University, Qazvin, Iran

Email address:drmm.alavi@gmail.com

Introduction:

Polyurethane (PU) is a versatile polymer and can be easily prepared by a simple polyaddition reaction of polyol, isocyanate. Polyurethanes (PUs) are one of the important classes of polymeric materials which have various applications such as coatings, adhesives, construction, foams, and rubbers [1, 2]. Unfortunately, the conventional PU is known to exhibit poor heat resistance that limits their applications. For example, their mechanical properties rapidly deteriorate above 80-90 °C and thermal degradation takes place at temperatures above 200 °C [3]. Because of the poor heat resistance of polyurethanes, their applications were limited. Attempts to improve the thermal stability of polyurethane have been made over a long period. The most accepted approach for the improvement of thermal stability of PUs is a chemical modification in the structure by introducing thermally stable heterocyclic polymers such as azomethine [4], urea [5], diacetylene [6], and polyimide [7].

Polyimides (PI) are the most important members of heterocyclic polymers with remarkable heat resistance and excellent mechanical, electrical, chemical and durability properties [8]. Poly (urethane-imide) (PUI) is a new polymeric material; it has the excellent properties of both polyurethane and polyimide, such as good mechanical properties, thermal stability, high mechanical strength, electrical insulating properties, chemical resistance, hydrolysis resistance, radiation resistance, abrasion resistance and biological compatibility, etc [9].

Experimental:

In this paper, we would like to report a new method for the synthesis of –NCO terminated poly (urethane-imide) (PUI) nanocomposites, which was prepared from diisocyanate, polyol and dianhydride by using Fe_3O_4 nanoparticle.

Results and Discussion:

The thermal stability of the polymer was investigated by TGA. The TGA of PU and PUI is shown in figure 1. It can be seen that all of PUI has two stages during the thermal degradation process. The first decomposition stage starts at roughly 380 °C, indicating the decomposition of the most thermally labile urethane component. The second stage corresponding to the decomposition and carbonization of the imide components occurs above 480 °C in each TGA curve. The degradation temperature was comparatively low in polyurethane without imide content. Therefore, an increase of imide content could increase thermal stability of PUI.
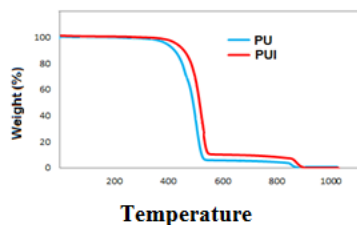

Figure 1. TGA curves of PU and PUI

Conclusion:

A series of PUI nanocomposite films have been prepared in this research. In this report, isocyanate-terminated PUI, which combines the advantages of polyurethane and dianhydride, was successfully synthesized and characterized. By inserting the nanoparticle inorganic compounds, the properties of polymers improve and hence this has a lot of applications depending upon the inorganic material present in the polymers. The results of thermogravimetric analysis and magnetic properties analysis showed that the thermal stability and magnetic properties of PUI film were increased by dispersion of NPs in the PUI matrix having a super paramagnetic property.

References:

[1]. G. Gorrasi; M. Tortora; V. Vittoria, *J. Polym. Sci. Polym. Phys*., **2005**, *43*, 2454-2467.

[2]. M. M. Alavi Nikje; R. Akbar; R. Ghavidel; M. Vakili, *Cellular Polym*., **2015**, *34***,** 137-155.

[3]. H. J. Farbis. *Advances in Urethane Science and Technology*, Technomic Publishing Co., Inc, Westport, CT, **1979**

[4]. I. Kaya; A. Avci, *Mater. Chem. Phys.,* **2012**, *133*, 269-277.

[5]. N .Yui, K. Nojima, K. Sanui; N. Ogata, *Polym. J.*, **1985**, *17*, 969-975.

[6]. M. F. Rubner, *Macromolecules*, **1986**, *19*, 2114-2128.

[7]. G. Maier, *Prog. Polym. Sci.,* **2001**, *26*, 3-65.

[9]. Q. Tang; R. Yang; J. He, *Ind. Eng. Chem. Res*. 2014, *53*, 9714-9720.

Synthesis of pyrimido[4,5-*d*]pyrimidine derivatives using natural catalyst in green media

Osman Shahnavazi, Enayatollah Sheikhhosseini*

Department of Chemistry, Kerman Branch, Islamic Azad University, Kerman, Iran,

Email address: sheikhhosseiny@gmail.com

.

****

Introduction: Multi-component reactions (MCRs) are significant tools for the rapid and efficient synthesis of a wide variety of organic molecules. These reactions have been investigated extensively in organic and diversity-oriented synthesis; primarily due to their ability to generate complex molecular functionality from simple starting materials via one-pot reactions. MCRs leading to interesting heterocyclic compounds are particularly important for the preparation of diverse chemical libraries of 'drug-like' molecules [1-3]. Pyrimidines and fused pyrimidine derivatives represent a class of annulated uracils with biological significance because of their close association with purines and pteridine systems [4]. In addition, they have been used as effective antitumor agents, herbicide antidotes and diuretics [5-6].

Methods / Experimentals: A mixture of urea or thiourea (2.2 mmol), substituted benzaldehydes (2 mmol) and barbituric acid (2 mmol) and chromite ore in water (8-10 mL) was heated at reflux for 1-2 h in order to synthesize pyrimido[4, 5-d]pyrimidine derivatives. Progress of the reaction was monitored by TLC. Upon completion of the reaction, the reaction mixture was filtered off immediately, washed with DMSO and the precipitates were collected by addition of cool water.

Results and Discussion: The natural chromite ore catalyst that used in this work was obtained in the southern Kerman region (Iran). To optimize the conditions, three component reaction of benzaldehyde, uria and barbituric acid in the presence of chromite ore as heterogeneous catalyst was selected as the model. It was found to be a good catalyst for preparation of pyrimido[4, 5-d]pyrimidine derivatives (Scheme 1). The attempts for evaluation of different solvents in preparing product in model reaction showed that carrying out the reaction in H_2O as media had satisfactory results.

Afterward, a variety of aldehydes to check the viability of this protocol in obtaining a library

of pyrano-pyrimidinone derivatives were used.
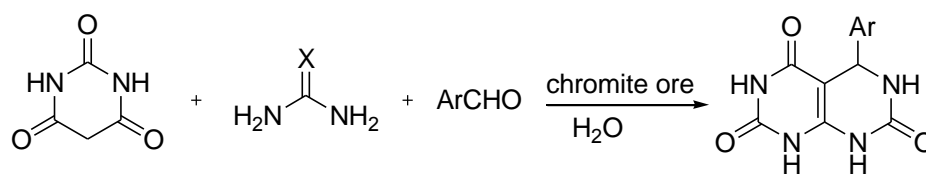
Scheme 1. Synthesis of pyrimido[4, 5-d]pyrimidine derivatives in the presence of chromite ore

Conclusion: An efficient synthesis of pyrimido[4, 5-d]pyrimidine derivatives is achieved via an one-pot tree-component reaction of aromatic aldehydes, barbituric acid and urea in the presence of chromate ore as natural catalyst. The use of water as the reaction medium makes the process environmentally and eco-friendly benign.

References

[1] Domling, A. *Chem. Rev*., **2006**. *106*, 17-89.

[2] Ramazani, A.; Kazemizadeh, A.R. *Curr. Org. Chem*., **2011**, *15*, 3986-4020.

[3] Domling, A.; Ugi, I. *Angew. Chem., Int. Ed*., **2000**, *39*, 3168-3210.

[4] Clercq, E.D.; Beraaerts, R. *J. Biol. Chem*. **1987**, *262*, 14905 – 14911.

[5] Parajapati, D.; Thakur, A.J. *Tetrahedron Lett.,* **2005**, *46*, 1433-1436.

[6] Gohain, M.; Prajapati, D.; Gogoi, B.J.; Sandhu, J.S. *Synlett***., 2004**, 1179-1182.

One-pot, four-component synthesis of novel spiroindoloquinazoline derivatives

Maryam Beyrati,[a] Alireza Hasaninejad,[*a]

[a]Department of Chemistry, Faculty of Sciences, Persian Gulf University, Bushehr, 7516913817, Iran.

E mail address: a_hasaninejad@yahoo.com

Introduction: Multi-component reactions (MCRs) have attracted great attention having an undeniable status in biological and medicinal chemistry as well as modern organic synthesis [1, 2]. Derivatives of quinazolinone are important class of six-membered nitrogen-containing heterocyclic systems that have been intensively studied [3] Tryptanthrin consists of indole and quinazoline core structure is an active ingredient and its derivatives are a pharmacologically important class of heterocyclic compounds [4]. To further the synthesis of this class of compounds, a synthetic route for the preparation of a novel class of spiroindoloquinazolines from the reaction of isatoic anhydride, isatin, malononitrile and enolizable carbonyl compound under classical condition (refluxing in acetonitrile) has been developed (Scheme 1).
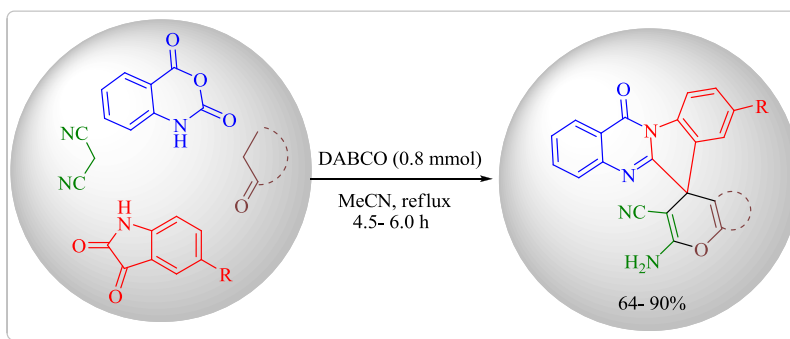
Scheme 1

Experimental: DABCO was added to a stirred mixture of isatoic anhydride, isatin derivative in MeCN and the reaction mixture was refluxed to complete the formation of related tryptanthrin. Subsequently, malononitrile and cyclic ketone were added to this reaction mixture and reacted under reflux conditions for the appropriate amount of time. After completion of the reaction, the

reaction mixture was cooled to room temperature. Then, the precipitated product was filtered and washed with cooled acetonitrile to afford the pure products.

Results and Discussion: To study the effect of reagent loading on the synthesis of spiroindoloquinazolines, the condensation reaction of isatoic anhydride, isatin, malononitrile, and dimedone was chosen as a model reaction. Subsequently, the scope and efficiency of these conditions were tested on the components in a two-step procedure. First, tryptanthrin derivatives were obtained from the condensation reaction of isatoic anhydride and isatin derivatives. These intermediates were treated with malono derivatives and carbonyl compounds to afford spiroindoloquinazoline derivatives as the desired products.

Conclusion: In conclusion, we have reported a highly efficient method for the synthesis of spiroindoloquinazoline derivatives *via* a one-pot, two-step, four-component condensation reaction using DABCO as an inexpensive, eco-friendly, highly reactive and non-toxic reagent under conventional heating.

References:
(1) Hasaninejad, A.; Zare, A.; Shekouhy, M. *Tetrahedron* **2011,** 67, (2), 390-400.
(2) Maryamabadi, A. Hasaninejad, A.; Nouroozi, N.; Mohebbi, G.; Asghari, B. *Bioorg. Med. Chem.* **2016,** 24,, 1408-1417.
(3) Sharma, M.; Chauhan, K.; Shivahare, R.; Vishwakarma, P.; Suthar, M. K.; Sharma, A.; Gupta, S.; Saxena, J. K.; Lal, J.; Chandra, P. *J. Med. Chem.* **2013,** 56, (11), 4374-4392.
(4) Phadtare, S. B.; Shankarling, G. S. *Green Chem.***2010,** 12, (3), 458-462.

Thermo-Responsive Poly(*N*-isopropylacrylamide–*b*–ionic liquid)/Pd Nanoparticles *via* RAFT Polymerization as a Novel Smart Catalyst in Suzuki Coupling Reaction

Zahra Amini harandi and Soheil Ghasemi*

Department of Chemistry, Faculty of Sciences, Shiraz University, Shiraz, Iran
Email address: ghasemis@shirazu.ac.ir

Introduction

Controlled radical polymerization (CRP) can be employed for the preparation of well-defined polymer structures such as block copolymers [1]. Common CRP methods include atom transfer radical polymerization, nitroxide-mediated polymerization and reversible addition-fragmentation chain transfer (RAFT) polymerization [2]. Block copolymers are one of the most important polymeric materials because of their exceptional properties due to the microphase separation [3].

Smart materials are being able to responses to proper stimuli such as temperature, pH, light, etc. [4]. Among these substances, temperature-responsive polymers such as poly(*N*-isopropylacrylamide) (PNIPAM) have attained much attention recently [5].

The Pd-catalyzed Suzuki reaction of aryl halides with boronic acids has proved to be a versatile reaction in the synthesis of biaryls and in many areas of organic synthesis [6].

Methods

Initially, NIPAM as monomer, AIBN as initiator and 2-(dodecylthiocarbonothioylthio)-2-methylpropionic acid as chain transfer agent (CTA) in dry 1,4-dioxane were used for the preparation of PNIPAM by RAFT technique. Freeze-pump-thaw cycle is used to degas the mixture. Then, PNIPAM is used as macro-CTA in order to produce PNIPAM-*b*-polyvinylpyridine. Afterward, PNIPAM–*b*–PIL is synthesized through the reaction of this block copolymer with 1,3-propanesultone. Finally, PNIPAM–*b*–PIL supported Pd nanoparticles (PdNPs) is prepared through the reaction of PNIPAM–*b*–PIL with Pd(OAc)$_2$ and subsequent reaction with NaBH$_4$.

Results and Discussion

In the present study, the synthesis and characterization of thermo-responsive PNIPAM–*b*–PIL/PdNPs based on modified vinylpyridine type ionic liquid *via* RAFT polymerization is reported as illustrated in Scheme 1. The catalyst was characterized by IR, NMR, ICP, UV–Vis spectrophotometer, X–ray diffraction, SEM, EDX and TEM techniques. Figure 1 depicted the XRD pattern, SEM image and EDX of the catalyst.
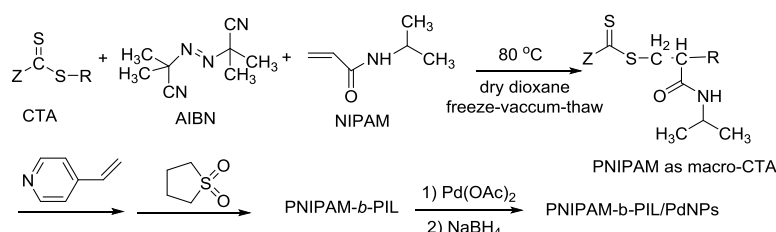
Scheme 1: preparation of PNIPAM–*b*–PIL/PdNPs

This efficient thermo-responsive catalyst with the cloud point i.e. around 38 °C was used in Suzuki reaction. The results are presented in Table 1. The strength and dramatic improvement in this work is related to the extremely reusability of the catalyst up to 11 times, using water as a green reaction media and different catalytic behaviors below and above its lower critical solution temperature (LCST).
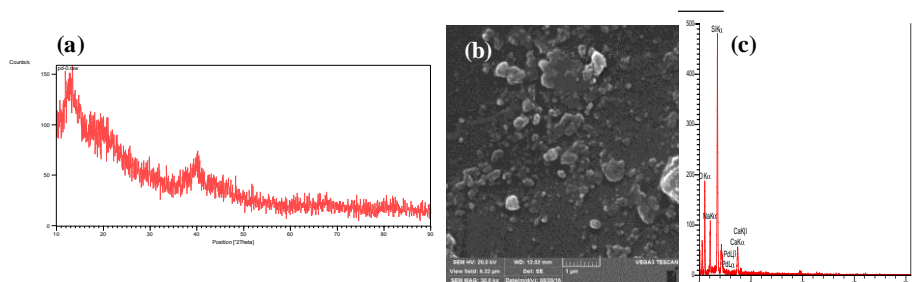
Figure 1: XRD pattern, SEM image and EDX of the Pd catalyst

Table 1: Suzuki reaction of phenylboronic acid with aryl halides using PNIPAM–*b*–PIL/PdNPs [a]

Entry	Aryl halides	Time (h)	Yield [b]%
1		20	98
2		90	98
3		40	99
4		20	98

[a] Molar ratio of the reagents ArX: Phenylboronic acid: Et$_3$N: Pd catalyst = 1.0: 1.2: 2.0: 0.001. Reaction conditions: H$_2$O, 80 $^\circ$C; [b] Isolated yields.

Conclusion

Novel thermo-responsive catalyst based on PNIPAM–*b*–PIL/PdNPs was prepared and characterized. High efficiency and stability of this catalytic system was shown for Suzuki coupling reactions in aqueous environment. The catalyst was highly recyclable and showed low leaching.

References

[1] G. Moad, E. Rizzardo, SH. Thang, *Acc Chem. Res.* **2008**, *41*, 1133-1142.
[2] K. Matyjaszewski, Controlled/living radical polymerization: progress in ATRP, NMP, and RAFT, *American Chemical Society*, Washington DC, **2000**.
[3] D.P. Rodrigues, J.R.C. Costa, N. Rocha, J.R. Góis, A.C. Serra, J.F.J. Coelho, Colloids Surf. B **2016**, *145*, 447-453.
[4] M.R. Aguilar, J.S. Roman, *Smart polymers and their application*, Woodhead Publishing, Cambridge, UK, **2014**.
[5] J. Zhang, Z. Cui, R. Field, M.G. Moloney, S. Rimmer, H. Ye, *Eur. Polym. J.* **2015**, *67*, 346-364.
[6] A. Gniewek, *J. Organomet. Chem.* **2016**, *823*, 90-96.

Ni(II) and Cu(II) Schiff Base Complexes Immobilized on Mesoporous Silica Nanoparticles: Synthesis, Characterization and Antibacterial Activity

Leila Tahmasbi [a], **Tahereh Sedaghat** [a,*], **Hossein Motamedi** [b], **Mohammad kooti** [a]

[a] Department of Chemistry, College of Sciences, Shahid Chamran University of Ahvaz, Ahvaz, Iran

[b]Department of Biology, College of Sciences, Shahid Chamran University of Ahvaz, Ahvaz, Iran

Email address: tsedaghat@scu.ac.ir

****

Introduction: Porous materials are classified into microporous (lower 2 nm), mesoporous (2-50 nm) and macroporous (50-100 nm) [1]. Mesoporous silica materials were synthesized in 1990s by Mobil scientist [2]. Mesoporous materials are applied for catalysis, enzyme immobilization, drug delivery and removal of pollutant [3-6]. In this research work, MSNs (Mesoporous silica nanoparticles) with particle size under 100 nm were synthesized and functionalized by a Schiff base and its complexes on the surface of mesopore channels. New synthesized composites were characterized by different methods and evaluated for antibacterial activity.

Experimental: MSNs were synthesized by stirring CTAB and TEOS (sol-gel method). After extraction of surfactant, APTS functionalized nanoparticles obtain by refluxing. Schiff base is supported on APTS-MSN by condensation with salicylaldehyde in a refluxing solution. Then Ni(II)/Cu(II) acetate salt was added and final functionalized nanoparticles were filtered. Antibacterial activity was evaluated against gram positive (*S.aureus*) and gram negative bacteria (*E.coli*) using Muller Hinton broth culture media and the absorption of solutions was recorded by microplate reader.

Results and Discussion: FE-SEM and TEM images of MSN, MSN-L, MSN-CuL$_2$ and MSN-NiL$_2$ showed spherical morphology and particle size under 100 nm (Fig. 1). Low angle XRD indexed four peaks for MSN and one peak for functionalized MSNs because of irregular arrangement of functional groups. BET and BJH analyzes showed high surface area (789m^2/g) for MSN whereas it was decreased for MSN-L, MSN-CuL$_2$ and MSN-NiL$_2$. All composites showed same pore diameter about 2.42 nm. EDX analysis confirms the elements in the structure of composites. FT-IR spectroscopy of MSN showed the bonds assigned to O-H of silanol (1634 and 3463cm^{-1}) and Si-O-Si (1084, 807 and 495 cm^{-1}). The spectra of MSN-AP and MSN-L show bands assigned to CH$_2$ (1556-1471cm^{-1}) and imine group (1640cm^{-1}), respectively. Thermogravimetric analysis of nanocomposites was also investigated. Antibacterial activity evaluation for MSN-NiL$_2$ showed bacteriocidal effect against *S.aureus* and for other compounds an inhibitory activity against *E.coli* and *S.aureus* was observed.

Conclusion: New functionalized nanoparticles were synthesized and characterized by FT-IR, TEM, FE-SEM, EDX, BET and TGA. The results showed spherical morphology and particle size under 100 nm. These nanocomposites exhibit good antibacterial activity.
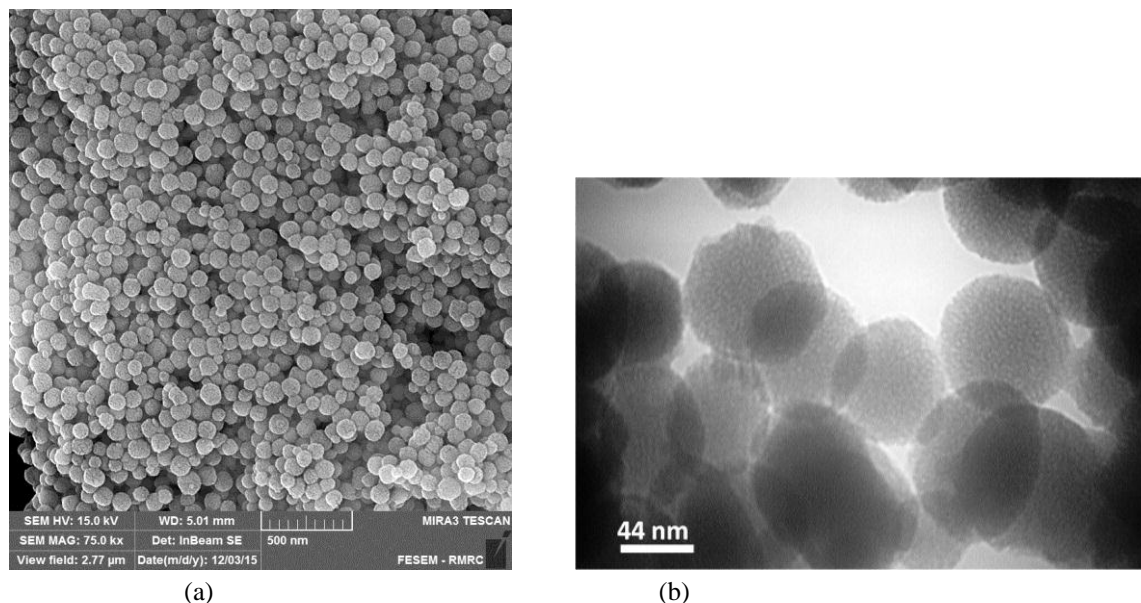

(a)   (b)

Fig. 1: (a) FE-SEM image of MSN-CuL$_2$ and (b) TEM image of MSN-CuL$_2$

(1) Linares, N.; Silvestre-Albero, A. M.; Serrano, E.; Silvestre-Albero, J.; Garcia-Martinez, J. *Chemical Society Reviews,* **2014**, *43*, 7681-7717.

(2) Hoffmann, F.; Cornelius, M.; Morell, J.; Fröba, M. *Angewandte Chemie International Edition,* **2006**, *45*, 3216-3251.

(3) Asefa, T.; Tao, Z. *Chemical Research in Toxicology,* **2012**, *25*, 2265-2284.

(4) Lin, Q.; Huang, Q.; Li, C.; Bao, C.; Liu, Z.; Li, F.; Zhu, L. *Journal of the American Chemical Society,* **2010**, *132*, 10645-10647.

(5) Nale, D. B.; Rana, S.; Parida, K.; Bhanage, B. M. *Applied Catalysis A: General,* **2014**, *469*, 340-349.

(6) Pogorilyi, R.; Zub, Y. L.; Beganskienė, A.; Kareiva, A. *Chemija,* **2014**, *25*, 75-81.

Quantitative analysis of Glycyrrhizic Acid in licorice products by using multivariate image analysis-thin layer chromatography (MIA-TLC)

Bahram hemmateenejad, __Mohammad Ali Rezaei*__

__mohamadalire@gmail.com__

Introduction

This paper has presented the ability of multivariate image analysis-thin layer chromatography (MIA-TLC) for measurement of glycyrrhizic acid (GA) in extracted licorice products and some drugs which contained it. In this chromatography system, silica gel was used as stationary phase and a mixture of water containing 1 % acetic acid and acetonitrile containing 1 % acetic acid (8:2 v/v) was used as the mobile phase. To determine GA, some parameters including solvent composition, RGB spaces and homemade software parameters were optimized. The image was recorded with digital camera in a dark cabinet and converted to 3D chromatograms by homemade software. In optimum condition, the calibration curve was linear in the range of 200.0 to 1000.0 $\mu g.ml^{-1}$ with the detection limit of 147.9 $\mu g.ml^{-1}$. Standard addition method was used to determine unknown concentration of GA in the licorice products. In comparison with previous instrumental methods such as HPLC, this method showed reliable results and also has more advantages including inexpensive analytical instruments and can determine one or multiple samples in lesser time.

Methods

All of materials were performed with analytical grade reagents. Acetonitrile, water, acetic acid and TLC plates (silica gel 60 F254, 20*20 cm) were obtained from Merck Company (German). Standard Glycyrrhizic acid was provided from Merck Company. In this study, home-made licorice extract and commercial CGA(crude Glycyrrhizic acid) were used. Glycyrrhizic acid solutions with different concentration range of 100ppm-1000ppm were prepared by solvent including same percentage of acetonitrile and water (both of them containing 1% of acetic acid). A SONY-H5 camera was used to record images. Digital micropipette was used for spotting samples on the TLC plates (Brand, Germany).

Results

Optimization of MIA-TLC system for GA analysis

Optimization of imaging system is a critical step for taking the high quality and reproducible images. A dark cabinet was used to avoid fluctuations of light such as sun or artificial light. However, two UV lamps (λ=254 nm) were used which were located on the top of the cabinet near the digital camera, to make the spots visible.

Effect of camera mode

The employed camera had different modes with special characteristic for imaging. At the auto adjustment mode, the spots were not visualized under UV light and at some modes images were highly noisy and not appropriate for MIA. In this work, the best results were obtained by using a mode called "twilight" that was useful for shooting without flashing in low light decreasing blur.

Effect of distance between camera and TLC plates

Another parameter that should be optimized was the distance between camera and TLC plates. At large distances, the spots seemed dark and their multivariate resolution was not straightforward. On the contrary, the spots were laminated by the light of the UV lamps at very close distances. Also, the resolution was decreased significantly and the background was highly affected by the instability in the light of lamps. The result of a trial revealed that the best image quality can be obtained when plates were set at 10 cm away from camera and light source.

Conclusion

In this study, a simple MIA-TLC method was reported as a suitable method for Quantitative determination of GA in licorice samples. The combination of acetonitril and water was used as mobile phase and TLC sheet was utilized as stationary phase. The best result was obtained when the volume ratio of mixture of solvents A and B was equal to 8:2 (v/v). The calibration curve reveal that the determination was linear in the range of 200-1000 $\mu g\ mL^{-1}$ with a detection limit of 147.9 $\mu g\ mL^{-1}$. In comparison with usual methods for GA analysis such as HPLC, the

proposed method was simple, inexpensive because of the cost of equipment, portable and no need for an expert operator and the volume of solvent which consumed in this study was decreased significantly.

References

Bahram hemmateenejad

Mohammad ali rezaei

Synthesis and regioselective determination of new derivatives of pyrimido[4,5-d]thiazolo[3,2-a]pyrimidine

Yasaman Etemadi, <u>Ali Shiri</u>, * **Hossein Eshghi**

Department of Chemistry, Faculty of Science, Ferdowsi University of Mashhad, Mashhad, Iran.

*E-mail address: alishiri@um.ac.ir

Introduction

Fused heterocycles containing thiazolopyrimidine and pyrimidopyrimidine have been greatly investigated in several medicinal activities.[1] General synthetic methods for the synthesis of thiazolopyrimidines involve the reaction of 4,6-dichloro-5-aminopyrimidine with isothiocyanates[2] or the reaction of ethyl-4-(3-methoxyphenyl)-6-methyl-2-thioxo-1,2,3,4-tetrahydropyrimidine-5-carboxylate with bromomalononitrile in the presence of strong base.[3] The synthesis of pyrimidopyrimidine as the other significant heterocyclic moiety has been reported via a one-pot three component heterocyclization of 5-aminopyrimidine with formamide.[4] Also, reaction of 9-cyanopurines with O-benzylhydroxylamine resulted in the formation of pyrimidopyrimidines.[5,6] Recently, a method for the synthesis of aromatic 4-acylhydrazido-8-arylamino pyrimidopyrimidine derivatives has been published.[7]

Methods and Experimental

In the mixture of 2-chloro-4-methyl-7,8-dihydro-5*H*-pyrimido[4,5-*d*]thiazolo[3,2-*a*]pyrimidine 3 and Et$_3$N in dry ethanol, the appropriate alkyl halide was added and the solution was heated under reflux. After the completion of the reaction, monitored by TLC, the solvent was evaporated under reduced pressure, water was added and the solution was filtered off.

Results and discussion

Compound **1** reacted with 4,5-dihydrothiazol-2-amine **2** as a binucleophile in CHCl$_3$ to give 2-chloro-4-methyl-7,8-dihydro-5H-pyrimido[4,5-*d*]thiazolo[3,2-*a*]pyrimidine **3**. The formation of compound **3** proceed through a combined nucleophilic substitution and an addition-elimination reaction involving the nitrogen atoms in 4,5-dihydrothiazol-2-amine followed by elimination of two molecules of HCl.
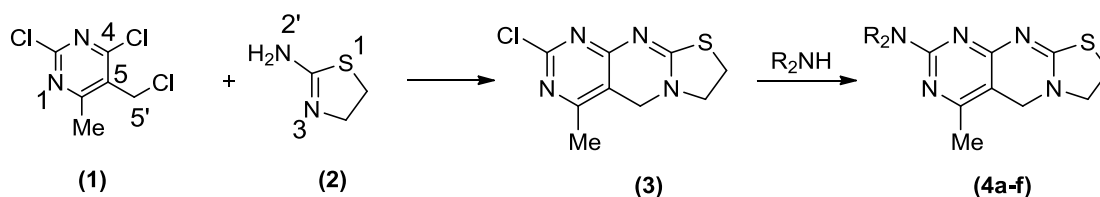
Since there are two different nitrogen atoms on reactant **2** which are candidates to act as nucleophile, two regioisomers are supposed to produce as well. To shed light and dispel this ambiguity, condensed Fukui indices were computed. The results revealed more electrophilicity on C-5′ in **1** and more nucleophilicity on N-3 in **2**. Therefore, condensed Fukui calculations suggest that compound **3** is formed in the way that endocyclic nitrogen of compound **2** was first reacted with exocyclic carbon of compound **1** to obtain C$_{(sp3)}$-N bond in the depicted structure of compound **3**.

Further investigation was carried out via nucleophilic substitution of the 2-Cl substituent with various secondary amines to produce substituted derivatives **4a-f** of the new heterocyclic ring

in good to excellent yields. All the physical, chemical and spectral data were in agreement with the newly proposed structures.

Conclusion

The objective of the present study was to synthesize and assign the regiochemistry of heterocyclization of new pyrimido[4,5-*d*]thiazolo[3,2-*a*]pyrimidine derivatives. Further structural confirmations were also made using two-dimensional COSY and NOESY techniques. The newly synthesized compounds were conducted to exhibit essentially equipotent antibacterial activity against some pathogenic bacteria. Results are suggesting pyrimido[4,5-*d*]thiazolo[3,2-*a*]pyrimidine derivatives emerge as valuable compounds with great potential to be used as antibacterial.

References

1. S. Fatima, A. Sharma, R. Saxena, R. Tripathi, S. K. Shukla, S. K. Pandey, R. Tripathi and R. P. Tripathi, *Eur. J. Med. Chem.*, **2012**, *55*, 195–204.
2. J. Liu, R. J. Patch, C. Schubert, M. R., *J. Org. Chem.*, **2005**, *70*, 10194-10197.
3. H. Nagarajaiah, I. A. M. Khazi and N. S. Begum, *J. Chem. Sci.*, **2015**, *127*, 467-479.
4. F. F. Wong, Y.-Y. Huang and C.-H. Chang, *J. Org. Chem.*, **2012**, *77*, 8492-8500.
5. A. Ribeiro, M. A. Carvalho and M. F. Proença, *Eur. J. Org. Chem.*, **2009**, 4867-4872.
6. A. H. Bacelar, M. A. Carvalho and M. F. Proença, *Eur. J. Med. Chem.*, **2010**, *45*, 3234-3239.
7. A. Rocha, A. H. Bacelar, J. Fernandes, M. F. Proenca and M. A. Carvalho, *Synlett*, **2014**, *25*, 343-348.

The relationship between ionic structure and bulk properties in alicyclic ammonium ionic liquids as lithium battery electrolytes

H. Sadeghian[a] and L. Maftoon-Azad[b,*]

Introduction:

The structural-property relations of four ionic liquids which are widely used in Lithium metal batteries as electrolytes[1], $[RmPyrr]^+$, $[RmPiP]^+$, , $[Rmm_\square pip]^+$ and $[RmAzp]^+$ cations, with $R=MeOCH_2CH_2^-$ and NTf_2^- anion are investigated. Key to this analysis is the charge lever moment (CLM) [2]. This is calculated and after evaluation of the basis set and method effects, its correlations with bulk properties such as viscosity, ion conductivity, density and glass transition temperature is investigated. The correlations between CLM and other QSPR indexes such as charge distribution, dipole moment, HOMO and LUMO energies and gaps and also ion pair and ion metal binding energies is also investigated.

Theory:

By using the center of charge approximation, the force applied by an electric field E on an ion of charge Q is, to first order, $Q\vec{E}$ and the torque will be:

$$\tau_i = \overrightarrow{L_{q,\imath}} \times \left(Q\vec{E} \right) \tag{8}$$

Where

$$\vec{L}_{q,i} = \vec{L}_q - \left(L_q \cdot \vec{R}_i \right)\vec{R}_i \tag{9}$$

and $\mathcal{R}_i$ is the shortest vector from this point to the ith axis. The charge lever moment will be defined as:

$$Z_i = Q\frac{|\overrightarrow{L_{q,\imath}}|}{I_i} = Q\frac{|\vec{L}_q \times \vec{R}_i|}{I_i} \tag{11}$$

Each ion possesses three CLMs that contain detailed information about the distribution of charge and mass in the ion.

Result and Discussion:

The Gaussian09 program [3] is used in the framework of DFT [4] at B3LYP [5] level of theory with 6-311++G (d, p) basis set [6]. Charge distribution is calculated by CHELPG algorithm.

We repeated the calculation with 8 different basis sets to seek for the best correlation between the CLM and bulk properties. The results are tabulated in table 1.

	D95	STO-3G	3-21G	6-21G	6-31G	6-31G(d,p)	6-31+G	6-31++G	6-31+ +G(d,p)
Pyr	0.0028	0.0026	0.0025	0.0025	0.0027	0.0024	0.0029	0.0028	0.0026
Pip	0.0019	0.0016	0.0017	0.0017	0.0019	0.0016	0.0021	0.002	0.0017
Azep	0.0019	0.0018	0.0017	0.0017	0.0018	0.0017	0.0019	0.0018	0.0017
mBPip	0.0013	0.0013	0.0012	0.0012	0.0013	0.0012	0.0014	0.0014	0.0013

The CLMs calculated with each basis set are not very different from each other. The viscosities of [RmPyrr], [RmPip] and [Rmm_βPip] are compared, all basis sets represent linear correlations with R-squared values near 1. Density, glass transition temperature and internal energy correlate with CLM for all cations with the best trend for 6-311++G basis set with R- squared factor equal to 0.9914. The next question is " Does CLM variate linearly with the shape and size of the rings?" in isolated free cations this quantity represents a good linear trend with R^2=0.838. Presence of the NtF$_2$ anion disturbs this trend dramatically but Li makes it more linear (R^2=0.9178). The presence of NtF2 declines the value of CLM, enormously. CLM exhibited a very good correlation with HOMO energies and this quantity increased with decreasing HOMO and IPBE energies. For the dipole moment, the trend for isolated free cations is excellent and R^2 is almost 1.

Conclusion

The CLM for four ionic liquids is calculated and its relations with bulk and molecular properties is investigated. It is understood this quantity is very well correlated with thermophysical and transport properties of these liquids such as viscosity, ion conductivity, density, internal energy, glass transition temperature and also ionic properties such as dipole moment, HOMO energy, IPBE and DOS. Also it is elucidated that the kind of basis se does not affect the value of CLM.

References:

1. Puga, A. Chemistry Today, 31 (2) 2013, 12-17.

2. Kobrak, M. N. J. Chem. Phys. 129, 124507 (2008).

3. Gaussian 09, Revision D.01, M. J. Frisch, G. W. Trucks, H. B. Schlegel, G. E. Scuseria, M. A. Robb, J. R. Cheeseman, G. Scalmani, V. Barone, B. Mennucci, G. A. Petersson et al., Gaussian, Inc., Wallingford CT, 2009.

4. W. Kohn, L. J. Sham, *Phys. Rev*. 1965, 140, A1133; P. Hohenberg, W. Kohn, *Phys. Rev*. 1964, 136, B864.

5. E. Engel, R. M. Dreizler, 'Density Functional Theory, An Advanced Course', Springer-Verlag, Berlin, Heidelberg, 2011.

6. J. B. Foresman, A. E. Frisch, 'Exploring chemistry with electronic structure methods, 2nd edn.' Gaussian Inc, Pittsburgh,PA, 1996.

Utilization of Magnetic Graphene Oxide as both Catalyst and Adsorbent for Oxidation-Extraction Desulfurization of Kerosene, Diesel and Gasoline

Mazaher Ahmadi, Tayyebeh Madrakian*, Abbas Afkhami
Faculty of Chemistry, Bu-Ali Sina University, Hamedan, Iran
Madrakian@basu.ac.ir, Madrakian@gmail.com
****

Introduction: Daily consumption of liquid fuels for energy production purposes has led to release various contaminants into the atmosphere. Sulfur oxides and sulfate particulate matters are one important family of toxic compounds which are subjected to the health regulations. In the crude oil refining process, the presence of sulfur compounds leads to deactivation of catalyst materials and also cause pipeline corrosion. On the other hand, the presence of these compounds in fuel leads to the emission of sulfur oxide gasses to the atmosphere which further cause acid rain and also impacts human health [1, 2]. Therefore, desulfurization is a critical issue environmentally and economically which needs high attention.

Methods/Experimental: Magnetic graphene oxide (MGO) has been used as both the catalyst for oxidation-extraction desulfurization (OEDS) and the adsorbent for magnetic solid-phase extraction/preconcentration of the oxidized sulfur compounds prior to ICP-OES measurements. Hydrogen peroxide and concentrated nitric acid were used as the oxidant and protonating agent, respectively. Different parameters which could affect desulfurization and extraction efficiencies were optimized using a multivariate experimental design.

Results and Discussion: The results showed that under the optimized condition (the nanocatalyst amount, 20 mg; agitation time, 33 min; HNO_3 and H_2O_2 volumes, 50 and 500 µL, respectively) removal efficiencies more than 97% were achievable using the proposed method. Also, sensitive determination of total sulfur concentration in kerosene, diesel and gasoline in the concentration range of 0.5 to 5.0 mg kg^{-1} with the detection and quantification limits of 0.15 and 0.5 mg kg^{-1}, respectively, under the optimized condition (optimized condition of desulfurization experiments and elution using 200 µL of methanol for 6.6 min) using the proposed method in combination with inductively coupled plasma optical emission spectrometry was achievable. The outstanding features of the proposed method for desulfurization are: MGO acts as both the adsorbent and the catalyst; the reaction is performed at room temperature unlike other previously developed methods which used relatively high temperatures; the reaction time is reasonable; the used chemicals are commercially available and the catalyst synthesis procedure is simple; and the catalyst is magnetically removable and there is no need to high-speed centrifugation or filtration. Furthermore, the proposed method acts as a MSPE step for preconcentration of the oxidized sulfur compounds and facilitated the ICP-OES measurements by improving the sensitivity and suppressing plasma overloading and extinction problems.

Conclusion: The results of this study showed that the application of MGO as both the adsorbent and the catalyst of the oxidation process in OEDS could provide a cost-effective and efficient method not only for desulfurization purposes but also for determination of total sulfur concentration in liquid fuel matrixes as the sample preparation step.

References
[1] V. Chandra Srivastava. *RSC Advances*, **2012**, *2*,759-783.
[2] M. Feng. *Recent Patents on Chemical Engineering*, **2010**, *3*, 30-37.

Electrocatalytic Activity of Nd_2O_3 Nanoparticles (application for quercetin detecting)

Zohreh Moradi[a]*, Meisam Noroozifar[a] , Mozhgan Khorasani Motlagh[a], Alireza Rezvani[a]

[a]Department of chemistry, Sistan and Baluchestan university,Zahedan, Iran
*Moradi.chem@yahoo.com

Introduction

Quercetin(3,3′,4′,5,7-pentahydroxyl-flavone) is present in man's daily diet (onions, tea, apples, red wine, etc) that has many pharmacological properties including anticancer, antioxidant, neurological, hepatoprotective, cardiovascular, antiviral, antimicrobial agent[1,2]. A simple, sensitive, fast and economical method for the determination of quercetin in crude drugs or plants can be electrochemical procedure based on modified carbon paste electrode. A novel graphite paste electrode (GPE) modified with the Nd_2O_3 nanoparticles for determination of quercetin is investigaed in aqueous media. The electrochemical response characteristics of the novel modified GPE/Nd_2O_3 were investigated by cyclic voltammetry(CV) and different pulse voltammetry (DPV) technique.

Materials and method

To give Nd_2O_3 nanoparticles, the as-synthesized Nd-o-phthalate complexes powders obtained with 1:3 molar ratio of metal salt to ligand were heated at 600 °C for 2 h. The GPE/Nd_2O_3 nanoparticles was prepared by hand mixing of Nd_2O_3 and graphite powder by a mortar and pestle. Paraffin oil was blended with the mixture and was ground and this wetted paste was packed into the end of a glass pipe and the copper wire was embedded into the carbon paste for electrical contact.

Results and Discussion

Fig.1(a, b) shows the FESEM image and EDS analysis of Nd_2O_3 nanoparticles obtained from the precursor complex. Fig. 2(A, B) depicts CV and DPV for the electrochemical oxidation of quercetin (66.2 µM) on the surfaces of GPE and Nd_2O_3/GPE electrode, Based on this figure the oxidation peak current of quercetin is very weak on the surface of GPE but this peak is sharp and well demonestrated on surface of Nd_2O_3/GPE. Thus, according to these observations modified graphite paste electrode can be used to determine the electrochemical quercetin. A series of DPVs was recorded at different concentrations of quercetin at optimum pH at the surface of Nd_2O_3/GPE (Fig. 2C). The DPV of increasing concentration of quercetin at pH 3 at the surface of Nd_2O_3/GPE was investigated and it is found that the response of the Nd_2O_3/GPE to quercetin was increased with increasing quercetin concentration. (Fig. 2D). Two linear relationship were observed between peak current versus quercetin concentration, in the concentration range of 0.67-8.32 µM and 10 to 66.2 µM with slopes of 1.528 and 0.421 µA µM^{-1} for Nd_2O_3/GPE.The detection limit calculated from the analytical graph was estimated to be about 2.94 µM (S/N = 3) based on the first linear segment.
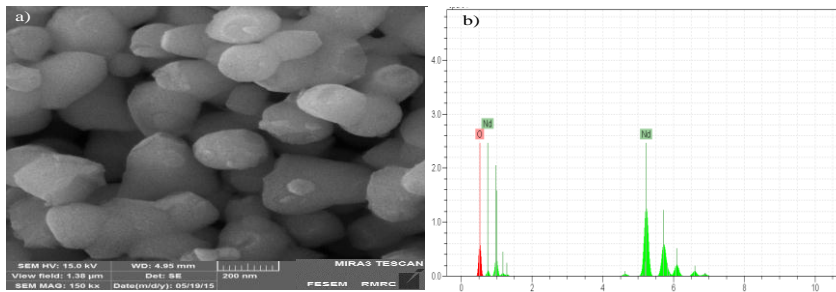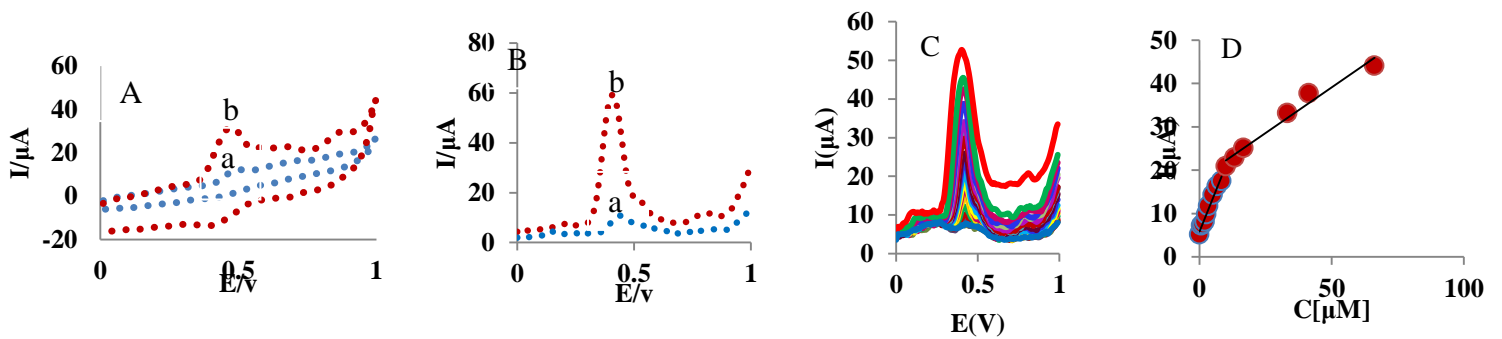
Fig.1(a, b)

Fig.2(A, B, C, D)

Conclusions

The role of as-obtained Nd_2O_3 nanoparticles in electrocatalytic process for quercetin detecting as an important antioxidant agent investigated with fabrication of Nd_2O_3/GPE using cyclic voltammetry and different pulse voltammetry techniques. Under optimized conditions, the peak current is linear to quercetin concentration in the ranges of 0.67-8.32 µM and 10 to 66.2 µM, respectively and the DPV response showed a limit of detection (LoD) of 2.94µM (S/N = 3).

References

[1]. J. Manokaran, R. Muruganantham, A. Muthukrishnaraj, N. Balasubramanian, „*Electrochimica Acta* 168 (2015) 16-24.

[2]. G.-R. Xua, S. Kim, , *Electroanalysis*,18(2006) 1786-1792.

Synthesis of (1,3,4-oxadiazol-2-yl) ethyl(methyl)carbamothioate derivatives with different substitutions in the 5 position of the ring

Akram. Fallah[*], **Farajollah. Mohanazadeh**

Institute of Industrial Chemistry, Iranian Research Organization for Science and Technology, Tehran, Iran
fallahakram8463@gmail.com
****

Introduction

Nitrogen containing heterocyclic molecules such as 1,3,4-oxadiazole derivatives have played a major role in the pharmaceutical chemistry. The number of so many synthetic heterocyclic compounds with oxadiazole nucleus used for antibacterial, antifungal, analgesic and anti-inflammatory activities. Derivatives of 1,3,4-oxadiazole with suitable substitution at 2,5-position have already been reported to have possible biological activities. 1,3,4-oxadiazole derivatives act as anticonvulsant and diuretics. These observations and our interest in the pharmaceutical chemistry of heterocyclic compounds promoted us to have synthesized different derivatives of 1,3,4-oxadiazole with different substituent at 2 and 5-positions[1,2].

Methods

As a model reaction to optimize conditions:
5-phenyl-1,3,4-oxadiazole-2-thiol: to a solution of benzohydrazide (1) (1gr, 7.3mmol) in EtOH 95% (10ml), KOH (0.41gr, 7.3mmol) followed by CS_2 (0.84ml, 11mmol) was added and then the mixture was heated under reflux for 4h.

The solvent was evaporated under reduced pressure and the remaining residue was quenched with water and was acidified with HCl 37% and then the precipitate was filtered, washed with cold water , dried and recrystallized from distillation water to afford the 5-phenyl-1,3,4-oxadiazole-2-thiol (2) (1.1gr, 86%) as a brown solid, MP: 197-199^{0}C[3]

(5-phenyl-1,3,4-oxadiazol-2-yl) ethyl(methyl)carbamothioate: to a solution of 5-phenyl-1,3,4-oxadiazole-2-thiol (1.1gr, 6.2mmol) in DMF (10ml) was added NaOMe (0.33gr, 6.2mmol) and this mixture was stirred until all the 5-phenyl-1,3,4-oxadiazole-2-thiol was dissolved. It was then added N-ethyl-N-methylcarbamoyl chloride (1.13ml, 9.3mmol) while the temperature of the solution was not exceeded of 30^{0}C. After adding it completely, the mixture was refluxed 4h. in the following, the mixture was cooled and distilled water was added drop wise to the solution. The precipitated product was filtered off and dried to give (5-phenyl-1,3,4-oxadiazol-2-yl) ethyl(methyl)carbamothioate (3) (1.49gr, 91%) as a white solid, MP: 44-46^{0}C, ^{1}HNMR(CDCl$_3$,300 M Hz), 8.07 (d, 2H) , 7.5 (3H), 3.43 (q, 2H), 3.07 (d, 3H), 1.27 (d, 3H).
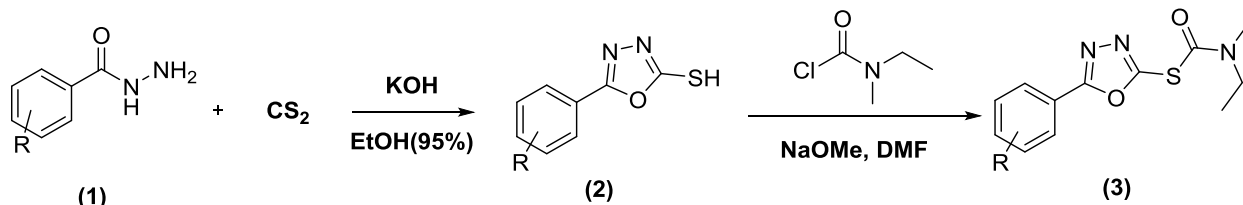
R: H, OH, NO$_2$, NH$_2$, Br

Results and discussion

The compounds were synthesized according to the sequence shown in the above. we designed a series of conformationally restricted analogues by including the N-ethyl-N-methyl-carbamoyl chloride in different 1,3,4-oxadiazolic systems. the compounds synthesized in the project have good yield value.

Conclusion

These studies have been largely focused on incorporating carbamoyl moiety into substituted oxadiazoles. This protocol provides a simple approach for the preparation of 1,3,4- oxadiazole derivatives. A series of functional groups survived the reaction conditions to give the corresponding products in excellent yields. Further investigations are ongoing in our laboratory to extend the scope of these novel reactions.

References

 [1] Singh, A.K; M. Lohani, M; Parthsarthy. R; Iranian Journal of Pharmaceutical Research (2013), 12 (2): 319-323

[2] Pei, L; Li, S; Man-Ni, G; Xia, Y; Wei, X; Bioorganic and Medicinal Chemistry Letters; vol. 25; nb. 3; (2015); p. 481 – 484.

[3] Xu, Y; Shuo, Z; Yuanqiang, W; Zemei, G; Tetrahedron; vol. 68; nb. 38; (2012); p. 7978 – 7983.

Evaluation the performance of cellulose acetate dialysis membranes modified with Polyethyleneimine and nano silica particles

Nooredin Goudarzian[1]*, Fatemeh Mojoudi[2] and Saeideh Bakhshandeh[1]

[1] Department of Applied Chemistry, Shiraz Branch, Islamic Azad University, Shiraz, Iran ; [2] Department of Environment, Faculty of Natural Resources, College of Agriculture & Natural Resources, University of Tehran, Karaj, Iran.

Corresponding author*: Ngoudarzian@iaushiraz.ac.ir

1. Introduction

The properties of a membrane can be controlled by membrane material and membrane structure. The most important properties of membrane in terms of separation performance are selectivity, permeability and yield. Currently, most commercial membranes are made from polymers. Solvent and non-solvent liquids, type and concentration of the polymer, temperature and reaction times influence physical membrane characteristics. The desirable characteristics of an ideal dialysis membrane are durability, low cost, high tensile stretch, high efficiency, Transparency, extenuation, and high mechanical strength. Off all materials for manufacturing dialysis membrane, Cellulose acetate (CA) are extensively used due to its biocompatibility, good desalting, good toughness and cost effective properties. Cellulose acetate as a natural substance is highly comparable to other synthetic polymer materials as well as high attractive in fabricating hemodialysis membrane [1].

2. Experimental

2.1. Preparation of membranes: Three types of dialysis membrane (CA, CA-nanoSiO$_2$, polyethyleneimine [PEI] and CA-PEI) were prepared with following method. Dope solution was prepared by dissolving 20 wt.% of cellulose acetate into a mixture of acetic acid/ PEI and nano-silicon solution under continuous stirring at 70°C to completely dissolve any compounds in reaction mixture and obtain a clear and transparent solution. The resultant polymer solution was sonicated and then allowed to cool down finally the solution was degassed with an ultrasound bath.

2.2. Membrane Casting: Prepared solution was poured onto a glass plate and casted using a casting knife with the same gap thickness of 50 μm. The solution films were immediately dipped in a distilled water coagulation bath at ambient temperature. With immersing cast film into the water, precipitation initiates and a thin polymeric membrane film was separated out from the glass. As the final stage, the membrane was rinsed in glycol to remove excess acetic acid and kept in DI water until use.

2.3. Membrane testing: The performance of the dialysis membranes were tested by stock solution of Urea, KCl, NaCl and it was evaluated in terms of blood clearance. The urea concentration of the sample was measured using Urea Nitrogen Rate Reagent Set. Blood packs containing anticoagulant was provided from Hospital Muslemin, Shiraz, Iran. After dialysis test, the amount of urea and creatinine were obtained using Auto analyzer Alpha-Classic. Samples were assayed using kits from

Randox (Antrim, UK) to control the measurement accuracy. Auto analyzer shows chemical composition of blood on the graph. Flame photometry was used to detect metal ions (Na^+ and K^+).

3. Results and discussion

Dialysis membranes play vital role in the treatment of patients with acute disturbance in kidney function. In this study, three different types of dialysis membrane based on cellulose acetate as the polymer were fabricated by addition of polyethyleneimine (PEI) and nano silica particles as the additives in the casting solution via phase inversion process. Pure water was used as the coagulation medium. The main objective of this study was to investigate the performances of the obtained membranes in terms of inefficient solute and negligible middle molecule removal. The synthesized membranes were characterized by the Fourier transform infrared (FTIR) technique. Moreover, the morphological studies of the best membrane in terms of separation performance were also characterized using scanning electron microscopy (SEM) and transmission electron microscopy (TEM). SEM and TEM images (a,b,c) illustrated that the addition of PEI promotes macrovoid formation and membrane forms finger like structure. According to the results, the membrane with both additives showed the best properties and its percentage removal were 53, 36.3, 70 and 80% for clearance of sodium (Na), potassium (K), and blood urea nitrogen (BUN) and creatinine (Cr) in Blood samples respectively. In conclusion, addition of small amount of PEI and nano silica particles to the dialysis membrane structure remarkably enhanced the membrane efficiency exhibited by the high solute clearance.
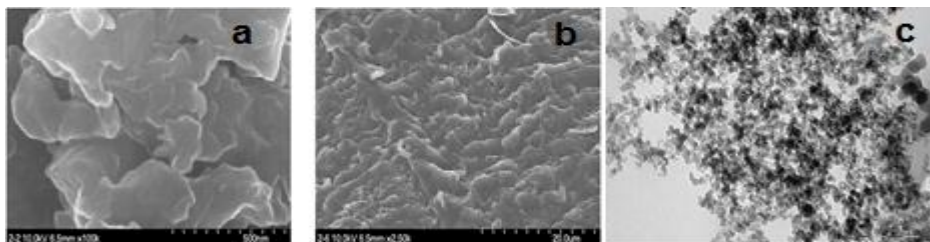
4. CONCLUSION

To prepare asymmetric dialysis membranes, phase inversion process via immersion precipitation was used. The effect of PEI and SIO_2 nanoparticles as the additives has been investigated on the performance of membranes in terms of solute removal. The membrane prepared with both additives showed the best results. All of obtained results demonstrate that the performance of CA-SIO$_2$-PEI membrane improved remarkably due to addition of PEI and SiO_2 nanoparticles compared to CA-PEI and CA membranes. Thus, PEI and SIO_2 nanoparticles can be used as the proper additives for dialysis membrane.

References: 1- C. Algieri, E. Drioli, L. Guzzo, and L. Donato, *Sensors*., **2014**, 14, 13863.

2- M. Wojcik, M. Hauser, W. Li, S. Moon, K. Xu, *Nat. Commun*., **2015**,6, 124.

Preparation of Cellulose-TiO$_2$ Nanocomposite by Click Reaction

Mahmood Tajbakhsh,[a],* Zari Fallah,[b] Hossein Nasr Isfahani,[b] Hamed Tashakkorian,[c] Abdoliman Amouei[c]

[a]Faculty of Chemistry, University of Mazandaran, Babolsar, Iran. **Email address:** tajbaksh@umz.ac.ir
[b]School of Chemistry, Shahrood University of Technology, Shahrood, Iran. **Email address**: fallah.zari@yahoo.com
[c]Cellular and Molecular Biology Research Center, Babol University of Medical Sciences, Babol, Iran.

Background:

The synthesis of organic-inorganic hybrid material using biopolymers such as cellulose have attracted a great interest in recent years [1]. Among nanoparticles, TiO$_2$ due to the nontoxicity, stability, and availability have found much attention [2]. The immobilization of highly functionalized cellulose onto solid support surfaces via click chemistry affords a facile approach to useful composite materials [3]. In fact, cellulose is at the heart of our study that aims to graft cellulose derivatives onto modified TiO$_2$ nanoparticles via click reaction.

Methods:

The objectives of this work are as follows: (1) synthesize of pure anatase TiO$_2$ nanoparticle via sol-gel method, (2) modification of TiO$_2$ nanoparticles with silane coupling agent, (3) insertion of cross linker with terminal alkyne group to the modified TiO$_2$ nanoparticles, (4) tosylation of cellulose, (5) azidation of cellulose, and (6) click rection between cellulose azide and alkyne terminated TiO$_2$ nanoparticles.

Results:

The synthesized bionanocomposite (Cell-Com) was characterized using FTIR, XRD, FESEM, EDX, AFM and BET analysis. The FESEM images of microcrystalline cellulose, TiO$_2$ and Cell-Com are shown below:
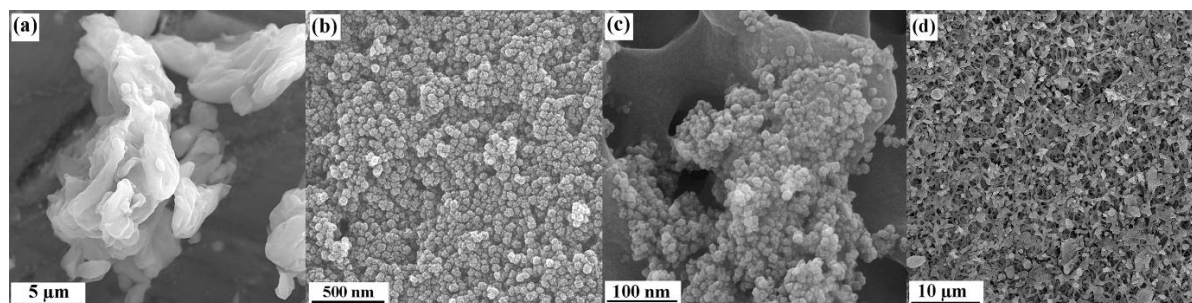
FESEM images of (a) microcrystalline cellulose, (b) TiO$_2$, and (c and d) Cell-Com.

Conclusion:

The Cell-Com consists of modified microcrystalline cellulose grafted onto the surface of modified TiO$_2$ nanoparticles was successfully prepared by click reaction. The analysis of Cell-Com exhibited that the surface-to-volume ratio was high with many active sites. The structure of obtained Cell-Com was discussed in detail according to analysis data. Application of the Cell-Com in the adsorption of heavy metals and pigments is under investigation and will be reported in due-course.

Keywords: TiO$_2$, Cellulose, Composite, Click reaction

References:

[1] Li Y., Cao L., Li L., Yang C, *J. Hazard. Mater.*, ٢٠١٥, ٢٨٩, ١٤٠-١٤٨.
[2] Shahadat M., Teng T., Rafatullah M., Arshad M, *Colloids Surf. B*, ٢٠١٥, ١٢٦, ١٢١-١٣٧.
[3] Liang L., Astruc D, *Coord. Chem. Rev.*, ٢٠١١, ٢٥٥, ٢٩٣٣-٢٩٤٥.

Synthesis and characterization of Zinc(II) and Nickel(II) complexes with Hpala ligand

Alireza Gorji[a] , Mina Avazpour[b,*], Bahare Bagherpour[c]

[a] Department of chemistry, Yazd University, Yazd

(email*:* minaavazpour@gmail.com)

Introduction

The development of new solid-state structures, which involve the self-assembly of molecules in to well-defined supramolecules has been a hot topic for several years [1]. Among these supramolecular structures, coordination polymers occupy alarge portion of the literature [2]. Reasons for the ongoing interest in this field are potential applications of coordination polymers as functional materials as well as the continuing discovery of ever new topological types of networks [3]. It is known that organic ligands play very important roles in determining the structures of the risulting coordination polymer [4]. Amino acids are good chelating agent and can coordinate to transition metals through their amino or carboxylic groups [5]. In this work reports the synthasis [Zn(pala)NCS]n **(1)**, [Ni(pala)SCN]n **(2)** coordination polymers with N-(2-pyridilmethyl)-L-alanine (Hpala).ligand.

Method /Experimentals

The ligand Hpala hase been synthesized by the published procedure [6]. All the complexes have been synthesized by a similar procedure as described here.To a methanolic solution (30 mL) of the ligand (0.003 mol), equivalent amount of the appropriate metal salts (0.003 mol) and KSCN (0.003 mol) were added, the mixture was stirred for 30 min and filtered. The filtrate was evaporated at room temperature to obtain products. water solvent used for crystallization and tiny needle crystals were obtained after two weeks.

Results and discussion

Reaction of the Hpala ligand with acetate salts of Zn(II) and Ni(II) and KSCN in 1:1:1 M ratio resulted products of [Zn(pala)NCS] and [Ni(pala)SCN] . The correlatin between the structural parameter and spectroscopic properties have been characterized by FT-IR, UV-Vis, and presented certain and proposed structers. The compounds selected IR data, (KBr, cm-1): ν(NH) near 3100, ν(CN)SCN 2110, ν(CN)NCS 2096, ν(CO$_2$) near 1600. The solid-state structure of (**1**) was solved by signal crystal X-ray difraction techeniques. An ORTEP diagram of (**1**) showing the local coordination environment of Zn(II) along with numbering scheme is presented in fig 1. All the potential binding sites of the pala ligand have utilized in the compound. The Zn(II) center hase square pyramidal geometry, while three coordination sites are from the ligand, other two coordination sites are occupied by thiocyanate and an oxygen atom. of carboxylate groups . the bonding between Zn(II) and neighboring carboxiylat oxygen atom ,O(2) generate 1D zig-zag polymer as shown in fig 2. The Polymer (1) has a intramoleculr hydrogen bond that is between the O (1) from a unit with H2N2 from adjacent unit (2.316 Å).
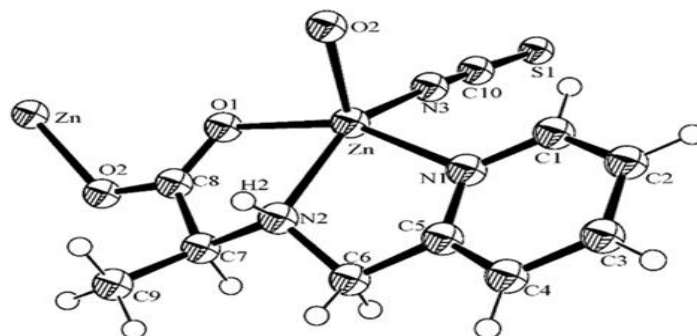
Fig 1. An ORTER drawing of [Zn(pala)NCS]

Fig 2. A portion of the 1D coordination polymeric structure of 1

Conclusion

The pala ligand is conformationally flexible ligand and optically active. The polymers 1 and 2 containing optically active pala ligand can be classified as chiral coordination polymrrs. Acording to the data from IR, UV-Vis, CHN and X-ray diffraction Compound (1) is coordination polymer with [Zn(pala)NCS] monomer. In this monomer zinc located in square pyramidal stracture and in the polymer carboxylate oxygen is bridge.

References

[1] O.R. Evans, W. Lin, Acc. *Chem. Res*. 35 **(2002)** 511**.**

[2] Ye, B.-H.; Tong, M.-L.; Chen, X.-M. *Coord. Chem. Rev.* **2005**, *249*, 545

[3] Fromm, K. M. *Coord. Chem. Rev.* **2008**, *252*, 856.

[4] Wen, M.; Munakata, M.; Suenaga, Y.; Kuroda-Sowa, T.; Maekawa, M.; Yan, S. G. *Inorg. Chim. Acta* **2001**, *322*, 133.

[5] Asemave, K.; Yiase, S.; Adejo, S. *Int. J. Sci. Technol.* **2012**, *2*, 242.

[6] X. Wang, J.J. Vittal, *Inorg. Chem*. 42 **(2003)** 5135

New Heteroleptic Complexes of Zn(II) with a N(4)-phenylthiosemicarbazone and Heterocyclic Bases as Secondary Ligands: Synthesis, Spectroscopic Investigation, Thermal Analysis and Antibacterial Activity

Mohammad Azarkish[a], Ali Reza Akbari[a], Tahereh Sedaghat[b*]

[a]Department of Chemistry, College of Sciences, Payame Noor University (PNU), 19395-4697 Tehran, Iran

[b]Department of Chemistry, College of Sciences, Shahid Chamran University of Ahvaz, Ahvaz, Iran

E-mail: tsedaghat@scu.ac.ir

****

Introduction: Heteroleptic complexes have received considerable attention due to their applications in industrial and medicinal fields [1-3]. An increasing number of studies approach to heteroleptic complexes involving bioligands. Thiosemicarbazones (TSCs) as sulfur containing Schiff bases are an interesting class of NS/NSO chelating bioligands and attract much attention due to their simple preparation, excellent complexation, variety of coordination modes and useful pharmacological properties [4-6]. We report herein the synthesis, characterization and antibacterial activity evaluation of Zn(II) heteroleptic complexes, [ZnL(MeImd)] (**1**) and [Zn_2L_2(4,4´-bipy)] (**2**), with a thiosemicarbazone (H_2L) as main ligand and 2-methylimidazole or 4,4´-bipyridine as secondary ligands.

Experimental: H_2L were prepared by condensation of N(4)-phenythiosemicarbazide with 2-hydroxynaphthaldehyde. Then the complexes were synthesized by reaction of Zn(II) acetate with thiosemicarbazone in presence of 2-methylimidazole or 4,4´-bipyridine as auxiliary ligands. The complexes were characterized by elemental analysis, FT-IR and ^1H and ^{13}CNMR spectroscopy. Thermal behavior of complexes has been investigated by themogravimetric analysis, TG/DTG-DSC. The *in vitro* antibacterial activity of ligand and complexes has been evaluated by paper-disc diffusion method.

Results and Discussion: In **t**he IR spectra of complexes ν(C=N) band is shifted to lower energies compared with the free thiosemicarbazone shows coordination of the imine nitrogen to metal. ^1H and ^{13}CNMR spectra of complexes indicate both signals of thiosemicarbazone and secondary ligand confirms the formation of ternary complexes. In ^1H NMR spectra the absence of both phenolic and hydrazinic protons signals suggests tautomerism deprotonation of the SH and OH groups and coordination of dianionic ligand to metal center *via* the phenolic oxygen and thiolate sulfur atoms. The complexes show better antibacterial activity in comparison to the

individual thiosemoicarbazone ligand. On the basis of thermal analysis data, the complexes have been found to be thermally stable.

Conclusion: In the complexes thiosemicarbazone acts as a tridentate dianionic ligand and coordinates *via* the thiol group, imine nitrogen, and phenolic oxygen. Coordination sphere of complexes are completed by by nitrogen atom of the auxiliary ligand. Coordination number of complexes is four. Complex **2** is binuclear with 4, 4′-bipy acts as a bridging ligand. The complexes are thermally stable and exhibit good antibacterial activity.

References:

[1] M.d.S. de P. Silva; I.C.N. Diógenes; I.M.M. de Carvalho; K.P.S. Zanoni; R.C. Amaral; N.Y.M. Iha. *J. Photochem. Photobio. A*, **2016**, *314*, 75-80.

[2] M. Ganeshpandian; S. Ramakrishnan; M. Palaniandavar; E. Suresh; A. Riyasdeen; M.A. Akbarsha. *J. Inorg. Biochem.*, **2014**, *140*, 202-212.

[3] P. Zhao; Q. Wei; J. Dong; F. Ding; J. Li, L. Li. *J. Coord. Chem.*, **2016**, *69*, 2437-2453.

[4] T.S. Lobana; R. Sharma; G. Bawa; S. Khanna. *Coord. Chem. Rev.*, **2009**, *253*, 977-1055.

[5] Z.-Y. Ma; J. Shao; W.-G. Bao; Z.-Y. Qiang; J.-Y. Xu. *J. Coord. Chem.*, **2015**, *68*, 277-294.

[6] M. Khandani; T. Sedaghat; N. Erfani; M.R. Haghshenas; H.R. Khavasi. *J. Mol. Struct.,* **2013**, *1037,* 136-143.

Ozone molecule adsorption onto single-walled (8,0) BC_2NNT_S nanotube : A DFT approach

V. Moeini[*,a], S.H.Rahimi[b], [c]A.H.Masoudi Gazi[c]

[a]*Department of Chemistry, Payame Noor University, P.O. Box 19395-3697, Tehran, Iran*

Email address : v_moeini@yahoo.com

Introduction: Carbon nanotubes (CNTs) are allotropes of carbon with a cylindrical nanostructure. These cylindrical carbon molecules have unusual properties, which are valuable for nanotechnology, electronics, optics and other fields of materials science and technology[1]. For the hexagonal compound BxCyNz nanostructures, the BC2N was believed to be one of the most stable stoichiometries, which the synthesis of BC2N was first reported in 1995 [2]. The BxCyNz nanotube scan be synthesized by using several different techniques, such as chemical vapor deposition, arch discharge and pyrolysis[3]. Nanotubes have been shown to be effective, though non-specific, sensors for low concentrations of gases such as NO_2, NH_3, and ozone, as well as several proteins[4]. Ozone interaction with carbon nanotubes has been studied experimentally and theoretically[5].

Method: The pristine (8,0) zigzag BC2NNTs model is made up of 16 boron,16 nitiride and 32 carbon atoms that were saturated by 32 hydrogen atoms which are in initial and end part of nanotube. In this work, all the quantum chemical calculations were performed via the Gaussian-09 software package at the level of density functional theory (DFT) using the B3LYP method and 6-31G(d) basis set[6]. GaussSum program was used to obtain density of states (DOS) results and charge transfer between the nanotubes and the adsorbed ozone molecule was calculated by using natural bond orbitals (NBO) analysis.

Results and Discussion: In this work, we considered the structural and electrical properties N1, N2, N3 models three for adsorption of O3 molecule on the surface nanotubes (Figures 1). The calculated indicate that the (N1) configuration is energetically stable relative to the separated N2 and N3 configuration, and it can be seen that the total electronic energies of the (N1) model was lower in comparison N2 and other model (Table 1). The large negative adsorption energy of final optimization geometries is related to the N1 model. Therefore in the relaxed structures of N1 configuration, O3 molecule located above BC2NNT surface with O nearby the C atoms and H atom which lead to the formation of six member two ring. Also the dipole moment increases to 3.652 Debye upon ozone molecule adsorption onto the tube in comparison pristine. The calculated charges obtained by both Mulliken and NBO indicate that the charges for the C_{37}, H_{72}, H_{83} atoms are positive and C_{22}, O_{98}, O_{99} atoms are negative. Also intermolecular interactions are of closed-shell. The calculations to optimization of systems indicate that compared with the pristine nanotube without O_3 adsorption the bond lengths of O_3 adsorbed on pristine nanotube system were changed. The calculated electronic properties shown that with the adsorption of O3 on the pristine N1, N2 and N3 model the Egap and global hardness significantly decreased respectively. Also with adsorption ozone the values of charge transfer (ΔN) increases. The calculated NBO indicate N1 model has $\sum E^2$ highest energy value and can make the structure more stable than the other models.
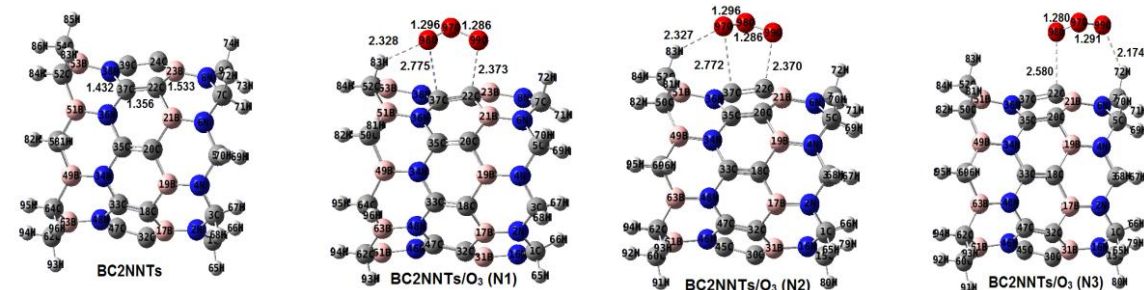
Figure 5. The optimized structures of Ozone adsorption on the BC2NNTs, of the model N1, N2 and N3 (Distance in Å)

Table1. Calculated total electronic energies E_{Total}(a.u), adsorption energies E_{ad} (kcal.mol^{-1}) with and without BSSE correction, *BSSE* (kcal.mol^{-1}) and dipole moment(Debye) of the N1, N2, N3 models.

Property	System				
	O_3	Pristine	N1	N2	N3
E_{ad}	-	-	-6.935	-6.933	-6.162
E_{ad}+BSSE	-	-	-2.857	-2.847	-3.091
BSSE	-	-	4.077	4.085	3.070
Dipole moment	0.614	1.875	3.644	3.652	2.997
E_{Total}	-225.4064536	-2513.1685653	-2738.5860713	-2738.5860683	-2738.5848394

Conclusion: The purpose of this study is determination the most stability of geometric structure of the adsorption of ozone molecule onto single-walled BC2NNT is investigated. The obtained results show that adsorption energy is negative and exothermic. Therefore, in N1 model, when the O3 molecule approach to two of C atoms, the most stable structure is achieved. Also the DOS plot clearly shows that the BC2NNT/O3 is a semiconductor. Therefore in N1 model the interaction occur between the lone pair orbitals of oxygen as donors and σ* orbitals as acceptors.

References

[1] Gullapalli S.; Wong M.S. (2011), *"Nanotechnology: A Guide to Nano-Objects"* (PDF), Chemical Engineering Progress, 107 (5): 28–32.

[2] Z. Weng-Sieh; K. Cherrey; N. Chopra; X. Blase; Y. Miyamoto; A. Rubio; M. Cohen; S. Louie; A. Zettl and R. Gronsky. *Phys. Rev. B*, 51, 11229 (1995).

[3] X.D. Bai; J. Yu; S. Liu and E.G. Wang. *Chem. Phys, Lett*., 325, 485 (2000).

[4] Bradley K; Briman M; Star A; Gruner G. *Nano Letters*, 2004, *4*, 253.

[5] Mawhinney D. B.; Naumenko V; Kuznetsova A; Yates J. T; Liu J; Smalley R. E. *J. Am. Chem*, *Soc* 2000, *122*, 2383.

[6] A.D. Becke. Density functional thermochemistry. III. The role of exact exchange, The Journal of Chemical Physics, 98 (1993) 5648-5652.

Title: Preparation and investigation of novel pyrrolidinium bonded stationary phase for reverse-phase high-performance liquid chromatography

Kourosh Tabar Heydar, <u>Elahe Naghdi</u>*

Chemistry and Chemical Engineering Research Center of Iran, Tehran, Iran

Email address of the corresponding author: enaqdi@yahoo.com

Introduction

Undoubtedly, one of the important factors in a desirable analysis by Chromatography is selecting suitable and capable stationary phase for compounds separation of sample. So, synthesis and preparation of novel stationary phase carried as a field of chromatography science. The surface confined ionic liquid (SCIL) stationary phase is one of the latest phases. The first application of SCIL in liquid chromatography was reported by Liu's research group in 2004 [1].

Ionic liquids (ILs) are organic molten salts formed by bulky dissymmetrical organic cations and various anions which are liquids at ambient temperature. They show specific physicochemical properties that make them more versatile and useful to applications in various areas of chemical fields. For example, they can be used electrochemical studies [2] and liquid-liquid extractions [3], running electrolytes [4] and electrolyte additives in capillary electrophoresis (CE) [5] and stationary phases in GC and HPLC.

Based on these considerations, a derivative of *N*-pyrrolidinium was covalently immobilized on the surface of silica particles to prepare a new stationary phase. Then was characterized and evaluated.

Experimental

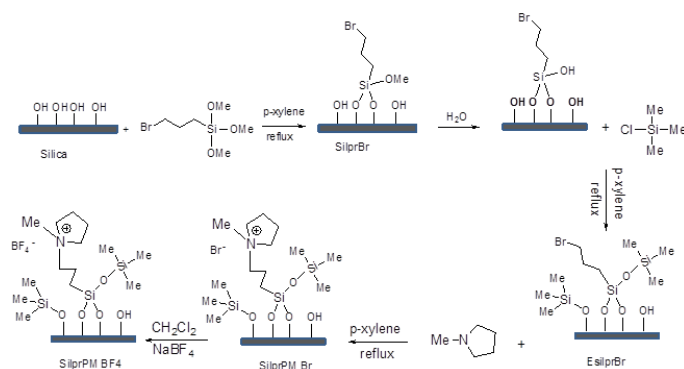A schematic diagram of the preparation of new stationary phase is outlined in Fig.1.

Fig.1. The preparation scheme of stationary phase

The modified particles were characterized by Fourier Transform Infrared (FT-IR), thermogravimetric analysis (TGA) and elemental analysis. The surface modification procedure rendered particles with a surface coverage of 1.14 µmol/m^2 for new phase.

Results

A 125 mm × 4.6 mm HPLC column was packed with stationary phase and was tested under reversed phase conditions. Aromatic, alkyl benzenes, acidic and basic compounds were separated successfully, as shown in Fig. 2 and 3.
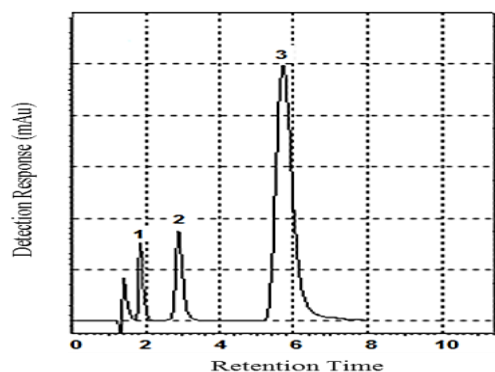

Fig 2. Separation aromatic compounds on SilprPM BF$_4$
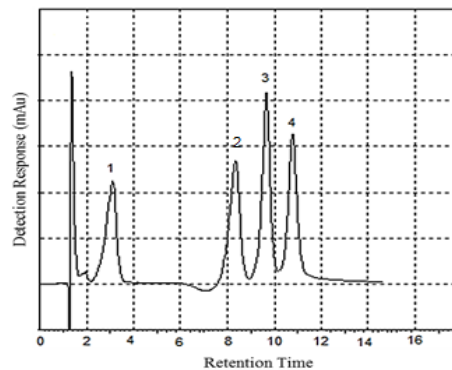
Fig. 3. Separation alkyl benzenes on SilprPM BF$_4$

Conclusions

Aromatic, alkyl benzenes, acidic and basic compounds were separated successfully on SiprMP BF4 stationary phases. The column showed multiple retention mechanisms, such as anion-exchange, hydrophobic interaction, ion–dipole interaction and electrostatic interaction. Potentially, the new stationary phase can be used to separate many compounds while small quantity of organic solvent is used at separations, so that the acidic and basic solutes are separated using only buffer solution.

References

1. Liu, S.J; Zhou, F; Xiao, X.H; Zhao, L., Liu, X; Jiang, S.X. *Chinese Chemical Letters*, **2004**, *15*, 1060-1062.
2. Lagrost, C; Carrie, D; Vaultier, M; Hapiot, P. *The Journal of Physical Chemistr,* **2003**, *A107*, 745-752.
3. Carda–Broch, S; Berthod, A; Armstrong, D. *Analytical and bioanalytical chemistry,* **2003**, *375*, 191-199.
4. Yanes, E.G; Gratz, S.R; Baldwin, M.J; Robison, S.E; Stalcup, A.M. *Analytical chemistry*, **2001**, *73*, 3838-3844.
5. He, L; Zhang, W; Zhao, L. Liu, X; Jiang, S. *Journal of Chromatography A*. **2003**, *1007*, 39-45.

An Efficient, Solvent-Free Synthesis of Linear β-Dicarbonyl Compounds: Acetoacetylation with Diketene-Acetone Adduct

Mohammad Bagher Teimouri,* <u>Zahra Mokhtare</u>

Faculty of Chemistry, Kharazmi University, Mofateh Ave., Tehran, Iran

E-mail: mbteimouri@yahoo.com

Introduction: Linear β-dicarbonyl compounds constitute important synthetic intermediates, incorporating multiple functionalities that can be involved either as nucleophilic or electrophilic species in a large variety of synthetic transformations [1]. β-ketoesters, β-ketothioesters and β-ketoamids are also excellent starting materials for the synthesis of heterocyclic compounds such as dihydropyridines (Hantzsch), pyrroles (Knorr), dihydropyrimidines (Biginelli), indoles (Nenitzescu), quinolines (Combes, Conrad–Limpach, Friedländer, Knorr), often through multicomponent strategies [2].

Results and Discussion:

The acetoacetylation of nucleophiles is a prosaic but extremely important reaction as acetoacetates are widely used synthetic intermediates in both laboratory and industrial preparations. Most of these acetoacetylations are effected with diketene [4], a highly reactive, lachrymatory, and toxic reagent.

β-ketoesters and amides were synthesized from acetoacetate derivatives with catalyst in organic solvents at high tempretures and long time [5]. Also β-ketothioesrers were synthesized in such a conditions [6,7]. Thermolysis [8] and photolysis [9] of 1,3-dioxinone provide acetylketene through a retro-hetero-Diels–Alder reaction and this intermediate can be trapped by nucleophiles such as alcohols, thiols and amines to give their acetoacetylation products [10]. Herein, the synthesis of linear β-dicarbonyl compounds from 2,2,6-trimethyl-4*H*-1,3-dioxin-4-one and various nucleophiles (alcohols, thiols and amines) in neat conditions and short reaction time with good to excellent yields, is reported.

Diketene-acetone adduct **1** and above-mentioned nucleophiles **2** and catalytic amount of sodium acetate were heated to 120 °C for 10-15 min under solvent-free conditions to form the corresponding linear 1,3-dicarbonyl compounds **3** in quantitative yields (**Scheme 1**). The reaction sequence begins with a retro-Diels–Alder reaction of **1** known to occur upon heating above 80 °C. The generated active intermediate acetylketene **4** undergoes nucleophilic attack by the alcohols, thiols or amines to form the 1,3-dicarbonyl compound derivatives (**Scheme 2**).
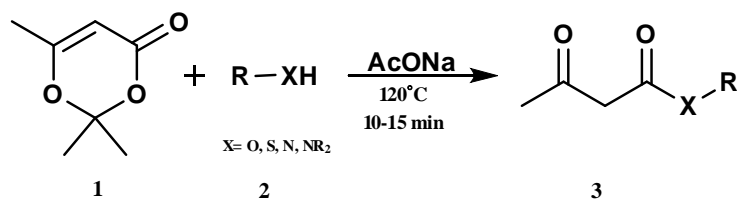
Scheme 1: Synthesis of linear β-dicarbonyl compounds from diketene-acetone adduct and various nucleophiles under solvent-free conditions.
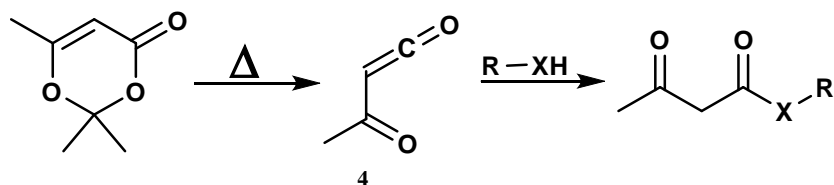
Scheme 2: A reasonable reaction mechanism for the synthesis of linear β-dicarbonyl compounds.

In order to obtain higher yields, we optimized the molar ratio of reactants (nucleophile/diketen-acetone adduct). Acetone as the sole by-product evaporated during the reaction course. All products were known compounds and were identified by using ^{1}H NMR spectra.

Conclusion:

In summary, a rapid, solvent-free green synthetic methodology that allows for quantitative synthesis of linear β-dicarbonyl compounds that is superior to other known methods is reported herein. The main advantages of this methodology with respect to the other methods are: (i) the reaction is simple to perform; (ii) the yields are good to high; (iii) there is no need for any other solvent; (iv) the reaction completes within a short period of time.

1. Liéby-Muller, F; Simon, C; Constantieux, T; Rodriguez, J. *QSAR Comb. Sci*., **2006,** *25*, 432-438.
2. Sridharan, V; Ruiz, M; Menéndez, J. *Synthesis,* **2010**, *6*, 1053-1057.
3. Wilson, S. R.; Price, M. F. *J. Org. Chem.,* **1984**, *49,* 722-727.
4. Jesus, G. M.; Francisca, R; Vicente, G. *Tetrahedron Lett.,* **1993**, 34, 6141-6142.
5. Ines, D. S. M.; Soares, B. U. E.; Marcos, D. P. *Tetrahedron Lett*, **2005**, 46, 2705 – 2708.
6. Hasegawa, T; Iwasaki, K; Yoshihara, T. *Bull. Chem. Soc. Jpn.,* **1984**, 57, 3343 – 3344.
7. Hasegawa, T; Shimizu, T; Iwasaki, K; Oguchi, S. *Bull. Chem. Soc. Jpn.,* 1983, 56, 1869 – 1870.
8. Rok, Z; Miha, T; Ljubo, G. *J. Heterocyclic.Chem.*, **1991**, 28, 1731-1735.
9. Chiang, Y; Guo, H.-X; Kresge, A. J.; Tee, O. S. *J. Am. Chem. Soc.*, **1996**, 118, 3386-3391.
10. Benetti, S; Romagnoli, R. *Chem. Rev.*, **1995**, 95, 1065-1114.

Synthesis and Characterization of New Di-nuclear Organotin(IV) Complexes with a Bis-hydrazone Containing Diphenylamine

Maryam Yousefi , Tahereh Sedaghat*

Department of Chemistry, College of Sciences, Shahid Chamran University of Ahvaz, Ahvaz, Iran

Email address: tsedaghat@scu.ac.ir

****

Introduction: In the field of hydrazone chemistry, a special place is held by bis-acyl-/aroyl-hydrazones. They have several bonding sites, with unique coordination properties capable of forming mononuclear and polynuclear complexes [1]. Organotin(IV) complexes of dihydrazones have received attention in recent years and among them only a few are binuclear [2-5]. In view of chemical properties, biological significance, industrial importance, and structural variety of organotin(IV) compounds [6,7], it has been considered worthwhile to synthesize organotin(IV) complexes with bis-acylhydrazones and to investigate their biological and structural features. Herein we have reported synthesis and characterization of dinuclear organotin(IV) complexes with a bis-hydrazone.

Experimental: 2-(4-methyl carbonyl)phenylaminobenzoic acid methyl ester was obtained through esterification of 2,4'-diphentylamine dicarboxylic acid. Then dihydrazide was prepared by reaction hydrazine hydrate. Finally bis-hydrazone (H_4L) were synthesized by condensation of dihydrazide with 2-hydroxynaphthaldehyde. Then the organotin(IV) complexes, R_4Sn_2L, have been synthesized by reaction of R_2SnCl_2 (R = Me or Ph) with H_4L in the presence of triethylamine in 1:2:4 ratio. All compounds were investigated by elemental analysis, FT-IR, ^{1}H and ^{119}Sn NMR spectroscopy.

Results and Discussion: The FT-IR spectrum of ligand, shows $\nu(C=O)$ and $\nu(C=N)$ at 1639 and 1625 cm^{-1}, respectively. The absence of $\nu(C=O)$ in complexes confirms the ligand coordinates with tin in the enol form. The $\nu(C=N)$ band is shifted to a lower energy (1615 cm$^{-1)}$ indicates that the imine nitrogen atom is involved in coordination. The appearance of new bands in the IR spectra of the synthesized complexes assigned to $\nu(Sn-N)$ and $\nu(Sn-O)$ supports the bonding of nitrogen and oxygen to the tin atom. In the ^{1}H NMR spectra of the complexes, the absence of signals attributed to acidic protons, –NH-N= and Ar-OH, suggests the complete deprotonation of ligand. Appearance of two resonances for the imine protons accompanied by satellites due to $^3J(^{119}Sn-H)$ coupling shows the two imine nitrogen atoms are chemically

different and both are coordinated to tin(IV) centers. Also two signals flanked by satellites appear for Me_2Sn moiety. Appearance of two sharp signals in the ^{119}SnNMR spectra confirms two different environments for tin centers in dinuclear complexes. Both [119]Sn resonances appear significantly at lower frequencies than that of the original $SnPh_2Cl_2$ (-32 ppm) and $SnMe_2Cl_2$ (+137 ppm) which is in agreement with the coordination number of five for both tin atoms in binuclear complex.

Conclusion: The synthesized bis-dihdrazone, H_4L, has four ionizable protons and can potentially act as ligand with two different ONO tridentate domain. This ligand is completely deprotonated and bonded to two diorganotin(IV) moieties. The complexes are binuclear with coordination number of five for both tin and different environment around tin centers.

References:

[1] Stadler, A. M.; Harrowfield, J. *Inorg. Chim. Acta*. **2009**, *362*, 4298-4314.

[2] Yin, H.; Cui, J.; Qiao, Y. *Polyhedron*. **2008**, *27*, 2157-2166

[3] Sedaghat, T.; Aminian, M.; Bruno, G.; Amiri Rudbari, H. *J. Organomet. Chem*. **2013**, *737*, 26-31.

[4] Dey, D. K.; Dey, S. P.; Karan, N. K.; Lyčka, A.; Rosair, G. M. *J. Organomet. Chem*. **2014**, *749*, 320-326.

[5] Sedaghat, T.; Aminian, M.; Amiri Rudbari, H.; Bruno, G. *J. Organomet. Chem*. **2014**, *754*, 26-31.

[6]. *Tin Chemistry: Fundamentals, Frontiers, and Applications*, Eds.; Davies, A. G.; Gielen, M.; Pannell, K.H.; Tiekink, R.E.T. John Wiley, London, **2008**.

[7]. Tarassoli, A.; Sedaghat, T. *Organometallic Chemistry Research Perspectives*, Ed.: R. P Irwin, Nova Publishers, New York, **2007**, Chapter 7.

Synthesis and Investigation of a Novel Seven Coordinate Organotin(IV) Complex

Tahereh Sedaghat[a,*], Zeinab Ansari-Asl[a], Abbas Tarassoli[a], Hadi Amiri Rudbari[b]

[a] *Department of Chemistry, Faculty of Science, Shahid Chamran University of Ahvaz, Ahvaz, Iran*

[b] *Department of Chemistry, Faculty of Science, University of Isfahan, Isfahan, Iran*

****

Introduction: Organotin(IV) compounds containing electronegative atoms show Lewis acidic character and the tin(IV) can increase its coordination number from four to five or six or rarely seven by addition of donor ligands [1-3]. The study of organotin complexes with hydrazones continues to be of interest owing to their remarkable chemical and structural characteristics and potential pharmacological applications [4, 5]. During the last few years, metal complexes with water-soluble ionic hydrazones derived from Girard's reagents represent an interesting research subject [6, 7]. In this research, We reports a novel organotin(IV) complex with an ionic hydrazone, (BrH$_2$SalGP)Cl.

Experimental: The hydrazone ligand, (BrH$_2$SalGP)Cl, was prepared by condensation of Girard-P with 5-bromo-2-hydroxybenzaldehyde. Then The organotin(IV) complex was synthesized by reaction of Ph$_2$SnCl$_2$ with (5-BrH$_2$SalGP)Cl in the presence of triethylamine. The synthesized complex was investigated by elemental analysis, FT-IR, ^{1}H and ^{119}Sn NMR spectroscopy. Recrystallization in dimethyl sulfoxide in presence of a trace acetate ion gives yellow needle single crystals suitable for X-ray crystallography.

Results and Discussion: In the IR spectrum of complex the ν(C=N) band appeared at 1620 cm^{-1} in the spectra of ligands is shifted towards lower frequency (1606 cm^{-1}) indicating coordination of the azomethine nitrogen to the tin. In the ^{1}HNMR spectra of complex the absence of signals assigned to two acidic hydrogens suggests deprotonation and coordination of phenolic and enolic oxygens to tin. In addition, the proton of CH=N gave resonance signal in the down field region with ^{3}J(^{119}Sn-^{1}H) coupling constant value of 31 Hz due to the coordination of nitrogen with tin(IV). The ^{119}Sn{^{1}H}NMR spectrum of complex shows one sharp singlet at -465.33 ppm. This chemical shift is significantly at lower frequency than those of the original SnPh$_2$Cl$_2$ (-32 ppm) indicates an increasing in coordination number of tin. The molecular structure of synthesized complex is shown in Figure 1. The hydrazone coordinates *via* the nitrogen from the imine and the two oxygen atoms from the phenolate and enolate. The coordination sphere is completed by two phenyl and one bidentate acetate groups. Therefore the tin environment is seven coordinate

with a distorted pentagonal bipyramidal geometry and phenyl groups are in axial positions.
Conclusion: In this research, we have synthesized and characterized a diorganotin(IV) complex with ionic Schiff base derived from Girard-P reagent. On the basis of spectroscopic and structural data the hydrazone behaves as ONO tridentate dibasic ligand and coordinates though phenolate and enolate oxygens and imine nitrogen. This complex is structurally interesting because the coordination number of tin(IV) is seven.

Keywords: Organotin(IV), Schiff Base, Girard-P, Crystal Structure

Fig. 1. Crystal structure of organotin(IV) complex

References

1. C. Ma; Q. Wang; R. Zhang. *Heteroat. Chem.* **2008**, *19*, 583-591.

2. T. Sedaghat; M. Naseh; H. R. Khavasi; H. Motamedi. *Polyhedron,* 2012, *33*, 435-440.

3. A. Ramirez-Jimenez; E. Gomez; S. Hernandez. *J. Organomet. Chem.* **2009**, *694*, 2965-2975.

4. S. Alexander; V. Udayakumar; V. Gayathri. *J. Mol. Catal. A: Chem.* **2009**, *314*, 21-27.

5. S. Hazra; A. Paul; G. Sharma; B. Koch, B; M.F.C. Guedes da Silva; A.J.L. Pombeiro. *J. Inorg. Biochem*. **2016** (in press).

6. O. V. Palamarciuc; P. N. Bourosh; M. D. Revenco; J. Lipkowski; Y. A. Simonov; R. Clérac. *Inorg. Chim. Acta* **2010**, *363*, 2561-2566.

7. L. S.Vojinovic-Jesic; V. I. Cesljevic; G. A. Bogdanovic; V. M. Leovac; K. Meszaros Szecsenyi; V. Divjakovic; M. D. Joksovic. *Inorg. Chem. Commun*. **2010**, *13*, 1085-1088.

One-Pot Synthesis of 1,3,4-Thiadiazoles Using Vilsmeier Reagent as a Versatile Cyclodehydration Agent

Maaroof Zarei

Department of Chemistry, Faculty of Sciences, University of Hormozgan, Bandar Abbas 71961, Iran

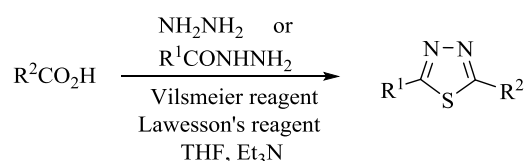E-mail: mzarei@hormozgan.ac.ir, maaroof1357@yahoo.com

****

Introduction: Thiadiazole is a five membered heterocyclic ring which is an efficient lead compound for preparation of potent bioactive agents. 1,3,4-Thiadiazoles exhibit a broad spectrum of biological activities such as antimicrobial, anti-inflammatory, anticancer, antituberculosis, antiparasitic, anticonvulsants, antioxidant, herbicidal and insecticidal [1]. 1,3,4-Thiadiazoles are generally prepared by conversion of diacylhydrazines to thiahydrazines and then cyclization of thiahydrazines. Lawesson's reagent and P_2S_5 are usualy used for thionation of diacylhydrazines and source of sulphur [2]. The cyclization step has been carried out using $POCl_3$, PCl_5, $FeCl_3$ and sulfuric acid [3]. While some of these reagents are expensive, highly toxic and need an excess of reagent or require to high temperature and harsh condition.

Vilsmeier reagent has been identified as a formylating agent and it has been used in the synthesis of esters, amides, acid chlorides, β-sultams and β-lactams [4,5]. Hence, based on the aforementioned, utilizing of Vilsmeier reagent for the synthesis of 1,3,4-thiadiazoles is reported.

Methods / Experimentals: General procedure for one-pot synthesis of 1,3,4-thiadiazoles. Hydrazine hydrate (0.2 mmol) or acylhydrazines (1.0 mmol) was added to a solution of carboxylic acid (1.0 mmol), Vilsmeier reagent (1.0 mmol) and Et_3N (3.0 mmol) in dry THF (20 mL) at room temperature. After 2 hours Vilsmeier reagent (1.0 mmol), Et_3N (2.0 mmol) and Lawesson's reagent (1.0 mmol) was added and the mixture was stirred at room temperature 13 hours. Saturated $NaHCO_3$ (20 mL) was added and the mixture was extracted with EtOAc (3×20 mL). The organic layer was washed with brine (20 mL), dried (Na_2SO_4), filtered and the solvent was

removed under reduced pressure to give the crude products. The crude residues were purified by crystallization from 95% ethanol.

Results and Discussion: After the optimization reaction condition, Vilsmeier reagent (2.0 mmol) and Et$_3$N (5.0 mmol) in the presence of 1.0 mmol Lawesson's reagent in dry THF at room temperature for 15 hours was founded the best condition. Then 10 symmetrical 1,3,4-thiadiazoles and 12 asymmetrical 1,3,4-thiadiazoles were synthesized by this method.

$$R^2CO_2H \quad \xrightarrow[\substack{\text{Vilsmeier reagent} \\ \text{Lawesson's reagent} \\ \text{THF, Et}_3\text{N}}]{\substack{\text{NH}_2\text{NH}_2 \quad \text{or} \\ R^1\text{CONHNH}_2}} \quad R^1 \underset{S}{\overset{N-N}{\diagdown\diagup}} R^2$$

The yields were satisfactory in all cases and all products were confirmed by spectral data. The IR spectra showed C=N peak at 1607-1624 cm^{-1}. Also, the ^{13}C NMR spectra showed the C=N peaks at 157.0-164.5 ppm.

Conclusion: In summary, a simple method for one-pot transformation of various carboxylic acids to 1,3,4-thiadiazoles using Vilsmeier reagent in the presence of Lawesson's reagent has been developed. The yield of cyclodehydrothionation was good to excellent, and starting materials were readily available. An aqueous work up and simple crystallisation was sufficient to obtain pure products because Vilsmeier reagent produces water-soluble by-products.

References

[1] J. Boström, A. Hogner, A. Llinàs, E. Wellner, A. T. Plowright, *J. Med. Chem.*, **2012**, *55*, 1817-1830.

[2] A. M. Sridhara, K. R. V. Reddy, J. Keshavayya, P. S. K. Goud, B. C. Somashekar, P. Bose, S. K. Peethambar, S. K. Gaddam, *Eur. J. Med. Chem.*, **2010**, *45*, 4983-4989.

[3] H. Khalilullah, M. J. Ahsan, M. Hedaitullah, S. Khan, B. Ahmed, *Mini. Rev. Med. Chem.*, **2012**, *12*, 789-901.

[4] A. Jarrahpour, M. Zarei, *Tetrahedron,* **2009**, *65*, 2927-2934.

[5] M. Zarei, M. Mohamadzadeh, *Tetrahedron*, **2011**, *67*, 5832-5840.

Efficient One-pot synthesis of 1,2,3 triazoles from terminal Alkyne and alkyl halide in water, using three metal ferrite as nano catalyst

Marzieh Ahangarpour[a], Firouz Matloubi moghaddam [a, *], Raheleh Pourkaveh[a]

[a] Laboratory of Organic Synthesis and Natural Products, Department of Chemistry,

Sharif University of Technology, Azadi Street, PO Box 111559516 Tehran, Iran

[*] E-mail Address: matloubi@sharif.edu

Introduction:

1,2,3Triazoles are important parts of 5-membered novel heterocyclic components having miscellaneous applications in agricultural components, corrosion inhibition, optical brightening [1], and also show wide range of biological activities such as antihistaminic, analgesic, anticancer, antimicrobial [2]. Due to the use of these compounds in pharmaceutical field, it is essential to remove the metal catalyst from the product. An interesting idea is using a catalyst that is easily collected from the final product with the help of the external magnet and it can be used in the next cycle reaction [3-4]. In this regard Our research group meditated using a qualified catalyst has a magnetic effect. Rolf Huisgen who was developed the triazole synthesis reactions [5]. One of the biggest complications facing with, was requirement of high temperature reaction. Furthermore, uncatalyzed Huisgen reaction suffers from a main drawback limiting its scope; that is, low regioselectivity in the approaching mode of alkyne to azide [6]. Our research group designed a catalytic system based on spinel ferrites which can catalyze the reaction in mild and green condition. The reaction yields were excellent for most of alkyl halides as a precursor.

Methods/ Experimental:

A glass tube was charged with sodium ascorbate (30 mg, 10 mol%), phenyl acetylene (0.5 mmol, 0.055 mmol), benzylbromide (0.5 mmol, 0.06 mL), sodium azide (0.5 mmol, 0.032 g), catalyst (5mol%) and H_2O (2 mL). The reaction mixture was stirred at room temperature for 90 minutes and the completion of the reaction was monitored by TLC (EtOAc/ n-hexane, 25:75). In each case, after completion, the product was worked up and purified. according to the following procedure: The mixture was diluted with ethyl acetate and water. The organic layer was washed with brine, dried over $MgSO_4$ and concentrated under reduced pressure using a rotary evaporator. The residue was purified by recrystallization from ethyl acetate/ n-hexane. In order to reuse the catalyst, the nanomagnetic catalyst was collected using an external magnet, washed with methanol and dried overnight to be ready for the next run.

Results and Discussions:

Initially, the optimized reaction conditions were determined in the reaction between sodium azide, phenyl acetylene and benzylbromide as model substrates using various types of solvents at different temperatures and in the presence of various concentrations of catalyst. The results are listed in Table 1. In order to meet the green chemistry principles, the reaction was also conducted in water as a green solvent. Having these optimized reaction conditions in hand, the scope of the reaction between alkynes and alkyl halides was explored in the presence of sodium ascorbate and sodium azide. According to the results, different alkyl halides can participate effectively in this reaction under the defined conditions. In all cases, the rate of reactions for alkyl chlorides is lower than that of alkyl bromides. After the first run, isolated yield of the reaction was measured exactly; then, the catalysts were separated by using a magnet, washed twice with methanol and dried at room temperature overnight. These recovered nanoparticles were reused in another run under the same reaction condition. This process was repeated 10 times and each time the isolated yield was calculated exactly. As is shown in Fig. 1 no significant decrease in reaction yield was observed after repeated cycles of the reaction.
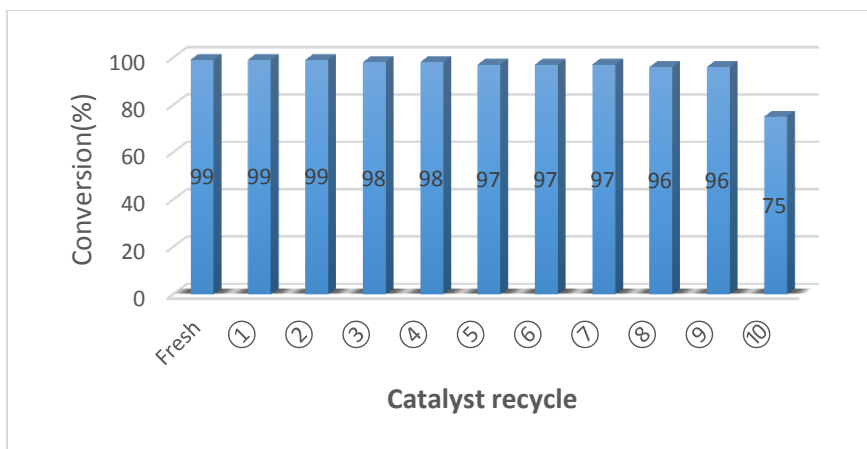
Fig. 1: recycling of catalyst for the Huisgen reaction of phenyl acetylene and benzyl bromide.

Entry	Solvent	Temp(°C)	Time(min)	Catalyst amount(mol%)	Yield(%)
1	EtOH	80	75	10	90
2	H2O	80	75	10	100
3	PEG	80	75	10	30
4	DMSO	80	75	10	30
5	TOL	80	75	10	88
6	DMF	80	75	10	30
7	H2O	100	75	10	100
8	H2O	50	75	10	100
9	H2O	room temperature	75	10	100
10	H2O	room temperature	45	10	100
11	H2O	room temperature	45	5	100

table 1: screening the reaction conditions for Huigsen reaction

Conclusion:

Application of nano $CoCuFe_2O_4$ in the 1,3-dipolar cycloaddition of phenyl acetylene to azides was examined. This catalyst can catalyze the desired reactions with excellent yields. Furthermore, due to its magnetic characteristic, separation of the catalyst is easy using an external magnetic field; it can be totally removed from the reaction medium and reused in another run. Total removal of the catalyst from the reaction media makes it possible to use the procedure in pharmaceuticals, drug discovery approaches and other sensitive synthetic procedures. Some of the main advantages of the procedure include mild reaction conditions (low reaction temperature, minimal workup and purification), very high functional group tolerance, and water tolerant nature of the reaction.

References:

[1] Fan, W. Q.; Katritzky, A. R. In *comprehensive heterocyclic chemistry II*, **1996**, *4*, 1

[2] Palhagen, S.; Canger, R.; Henriksen, O.; Van Parys, J. A.; Riviere, M. E.; Karolchyc, M. A. *Epilepsy Res.* **2001**, *43*, 115.

[3] Harmand, L.; Lescure, M. H.; Candelon, N.; Duttine, M.; Lastecoveres, D.; Vincent, J. M. *Tetrahedron Lett.* **2012**, *53*, 1417

[4] Basset, J.M.; Choplin, A. *J. Mol. Catal.* **1993**, *21*, 95.

[5] R. Huisgen, *Angew. Chem.* **1963**, *75*, 604-637

[6] A. R. Katritzky, S. K. Singh, *J. Org. Chem.,* **2002**, *67*, 9077

Synthesis, characterization, DNA binding and cytotoxicity of New water soluble Zn(II) complex

Neda Nasrollahi, Zahra Asadi[*a]

Department of Chemistry, Faculty of Sciences, Shiraz University, Shiraz 71454, Iran

1. Introduction

One important step toward rational drug design is studying the interaction of small molecules with DNA which is the subject of interest in many research fields such as biochemistry, medicinal chemistry, life science, cancer therapy and etc [1]. Mechanism of interactions between drug molecules and DNA is still relatively little known and it is necessary to introduce more simple methods for investigating the mechanism of interaction. By understanding the mechanism of interaction, designing of new DNA-targeted drugs and the screening of these in vitro will be possible [2].

2. Experimental

New water soluble Schiff base zinc (II) complex: [N,N′-bis{5-[(triphenylphosphoniumchloride)-methyl]salicylidine}-1,3-diamino-2-propanol]Zn(II) perchlorate was synthesized using template method and characterized by elemental analysis, FT-IR, ^{1}HNMR and UV–Vis spectroscopy.

2.1. DNA-binding measurements

Interaction of Zn(II) complex with FS-DNA was studied by absorption spectroscopy, fluorescence spectroscopy, viscosity measurement, and molecular docking. Tris-HCl-NaCl buffer solution (1 mM Tris, 5 mM NaCl, pH 7.4) was used for FS-DNA binding experiments. Cell viability assay on HepG2 (heptoma cell line) performed by MTT method.

3. Results and discussion

With increasing the concentration of DNA in the solution of the complex, a new band was growing, and two isosbestic points were appearing about 342 and 436 nm. Furthermore, the complex showed a strong hypochromism with a red-shift and hyperchromism with blue shift in absorption spectra (Fig.1). This observation suggested that new species was generated after interaction of complex with DNA.

The intrinsic binding constant, K_b, obtained for the complex was 9×10^5 M^{-1}. Both fluorescence quenching and enhancing for the complex can describe the mixed modes of

---

* Corresponding author. E-mail address: zasadi@shirazu.ac.ir
Tel: +98 713 6137118; Fax: +98 713 646 0788

electrostatic and intercalation interaction for it (Fig.2). The relative viscosity of DNA increased with increasing the complex concentration, indicative an intercalation mode of binding. The energy minimized docked poses obtained for compound suggested that complex was located in the minor grooves of DNA (Fig.3). The anticancer activities of compound toward human HepG2 cancer cell line have been examined by using MTT assay. It is found that the complex exhibit cytotoxic activities.

4. Conclusions

DNA-binding measurements show that the complex can bind to DNA strongly. Result of UV-Vis absorption and emission spectra show that the complex can bind with DNA by the mixed modes. DNA binding ability and the anticancer activities may possibly be tuned through varying of factors in this compound, which is useful for the design and synthesis of new drugs.
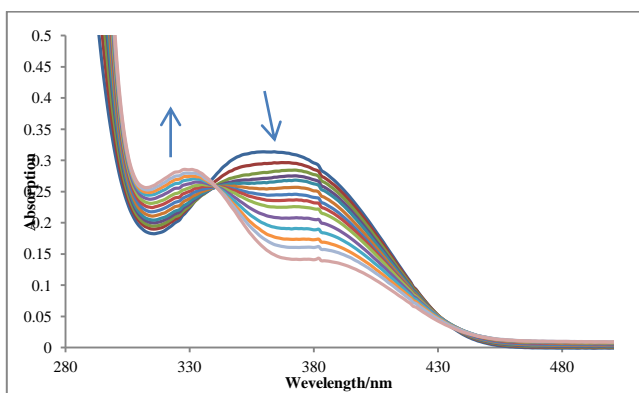
Fig. 1 Spectrophotometric titration L_1 of the complex with CT-DNA in Tris–HCl buffer
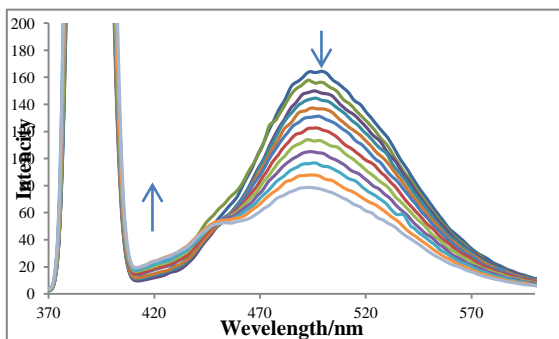
Fig. 2 Fluorescence titration of the complex at 526 nm, with DNA
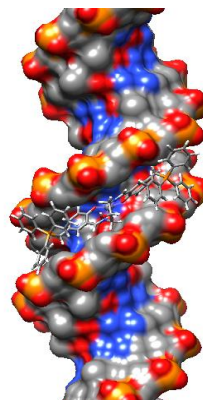
Fig. 3 model of docking of the complex

References:
[1] S.U. Rehman, T. Sarwar, M.A. Husain, H.M. Ishqi, M. Tabish, *Arch. Biochem. Biophys.* , **2015** , 576, 49-60.

.

[2] R. Hajian, N. Shams, M. Mohagheghian, *J. Braz. Chem. Soc.*, **2009**, 20, 1399-1405.

Covalently anchored 2-amino ethyl-3-propyl imidazolium bromide on SBA-15: Synthesis, Characterization and Antibacterial Activity

Mina Jafari Nasab [a], **Ali Reza Kiasat** [a,*], **Hossein Motamedi** [b]

[a] *Department of Chemistry, College of Science, Shahid Chamran University of Ahvaz, Ahvaz, Iran*
[b] *Department of Biology, College of Science, Shahid Chamran University of Ahvaz, Ahvaz, Iran*
Email address: akiasat@scu.ac.ir

****

Introduction: Recently numerous scientists have focused their interest on the modification of SBA-15 with various organo functional groups in order to render them suitable for specific applications. SBA-15 usually possess exclusive properties such as high surface area, large pore size, excellent (chemical and thermal) stability [1-5].

Antibiotic resistance is a major concern in treatment of infectors disease that can lead to life threatening infections. This resistance can be classified as innate and acquired. In innate resistance, bacteria due to structural and physiological properties don't respond to antibiotic. So, finding new approaches to overcome this type resistance can be useful for control of their infections.

Experimentals: The SBA-Cl was initially synthesized by the direct incorporation of chloropropyl groups through co-condensation of TEOS and CPTMS precursors in the presence of Pluronic P123 triblock copolymer as template. Afterwards, SBA-Im-NH$_2$ was synthesized by nucleophilic substitution reaction of SBA-Cl with imidazole and then quaternization with 2-bromo ethylamine hydrobromide. Antibacterial activity was evaluated with Streptomycin and Gentamycin. Briefly, a lawn culture was prepared from clostridium tetani and clostridium botulinum and the prepared discs and also Streptomycin and Gentamycin discs were placed on this culture.

Results and Discussion: The structure of the resulting hybrid nanocomposite, SBA-IM-NH$_2$, was comprehensively characterized by TEM, FT-IR, XRD, TGA, CHNS and BET analysis.

The size and morphology of the SBA-IM-NH$_2$ nanocomposite was characterized by TEM and SEM images (Fig 1). The TEM images of organocatalyst indicate the mesoporous structure and orderly pore arrangement, with an average diameter of approximate 30 nm. It can be clearly seen that the samples keep the unique pore structure.

The FT-IR spectra of nanocomposite in the range of 400-4000 cm^{-1} were shown peaks at 1220, 1078, 804, and 470 cm^{-1} that related to stretching, bending and vibration modes of Si-O-Si. In addition, the FT-IR spectra of the SBA-IM-NH$_2$ exhibited two new peaks

display at 1560, 1645 cm^{-1} which were assigned to C=C, C=N bands of the imidazole rings, respectively. The graft of organic units to SBA-15 was also confirmed by CHN analysis.
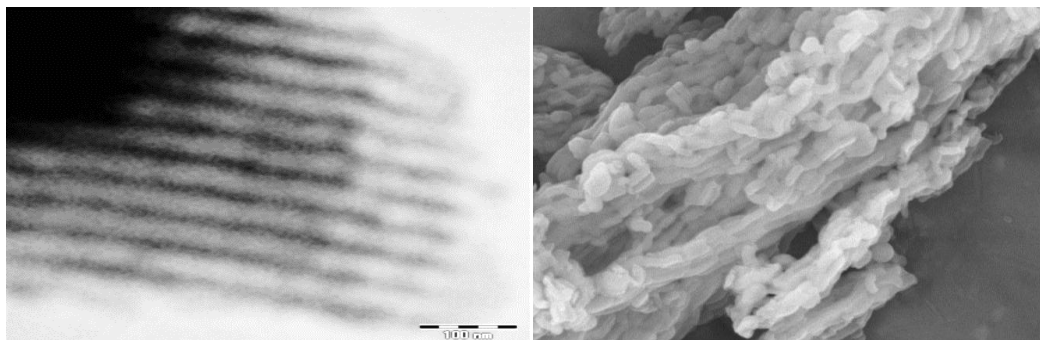

Fig. 1 The TEM, SEM images of SBA-IM-NH$_2$

Antibacterial activities of the nanocomposite was studied along with two standard antibacterial drugs gentamycin and streptomycin. Finally, the growth inhibition zone around disc was measured and recorded. The results revealed that conjugation of nanocomposite with gentamicin and streptomycin caused resistance break in case of clostridium tetani and increasing the inhibitory effect of gentamicin and streptomycin in clostridium botulinum.

Conclusion: In the present study highly ordered mesoporous SBA-15 having Brønsted basic ionic liquid pore channels was synthesized via surfactant-templated sol-gel methodology and post modification process. By this nanocomposite, it will be possible to increase intracellular concentration in bacterial cytoplasm and through this not only more inhibitory effect of antibiotic will be obtained but also, undesirable side effects of antibiotics will also be diminished.

References
[1] K. Bahrami, M.M. Khodaei, P. Fattahpour, *Catal. Sci. Technol.,* **2011**, 1, 389-393.
[2] R.V. Grieken, J.A. Melero, G. Morales, *J. Mol. Catal. A,* **2006**, 256, 29-36.
[3] A. Vinu, K. Z. Hossain, K. Ariga, J. Nanosci. Nanotechnol, 2005, 5, 347.
[4] S. Jin Bæ, S. W. Kim, T. Hyeon, *Chem. Commun*, **2000**, 1, 31-32.
[5] T. Salesch, S. Bachmann, S. Brugger, *Adv. Funct Mater,* **2002**, 2, 134-142.

The Synthesis of pyranopyrazole derivatives catalyzed by boric acid under aqueous conditions

Ahmad Reza Moosavi-Zare,* Hamid Goudarziafshar, Hadis Afshar-Hezarkhani, Mohammad Mahdi Rezaei

Sayyed Jamaleddin Asadabadi University, Asadabad, 6541835583, I. R. Iran.

Pyranopyrazoles are an interesting class of heterocyclic compounds; they have been applied as fungicidal [1], bactericidal [2], vasodilatory [3], and anticancer [4]. They have used as pharmaceutical ingredients and biodegradable agrochemicals [5]. Additionally, pyrano[2,3-c]pyrazoles have been acted as potential insecticidal [6] and molluscicidal agents. [7] Several catalysts have been introduced for this transformation. But, considerable attention has been concentrated on the development of new methods for the preparation of these important compounds. In the presented work, we have used boric acid for the synthesis of pyranopyrazole derivatives by the one-pot multi-component condensation of arylaldehydes with ethyl acetoacetate, malononitrile and hydrazine hydrate using boric acid under aqueous conditions (Scheme 1).
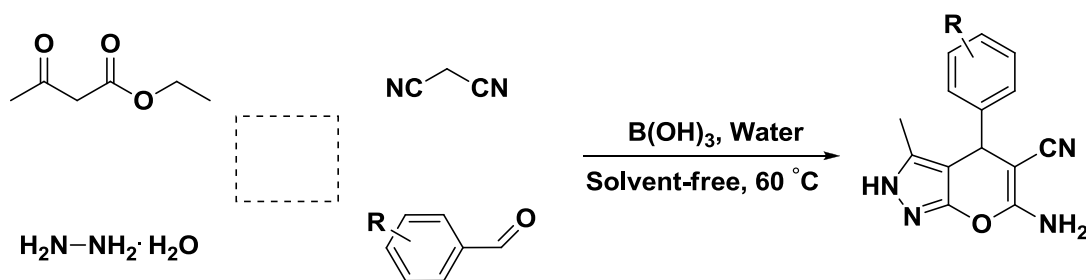
Scheme 1. The preparation of pyranopyrazole derivatives catalyzed by boric acid.

Experimental:

Procedure for the synthesis of pyranopyrazoles.

A mixture of aromatic aldehyde (2 mmol), malononitrile (2 mmol), ethyl acetoacetate (2 mmol) hydrazine hydrate (2.5 mmol), boric acid (10 mol%) and a few drops of water was added in a 25 mL round-bottomed flask connected to a reflux condenser, and stirred at 60 ℃. After completion of the reaction, the solid residue (crude product) was triturated by a mixture of ethanol and water (9/1) to obtain the pure product.

Results and discussion:

To investigate the efficacy and generality of boric acid in the synthesis of pyranopyrazoles, various arylaldehydes (including benzaldehyde, and arylaldehydes aldehydes possessing electron-releasing substituents, electron-withdrawing substituents and halogens on their aromatic ring) were reacted with hydrazine hydrate, ethyl acetoacetate and malononitrile using boric acid aqueous solution system under the optimal reaction conditions to obtain the desired products in high yields and in short reaction times.

Conclusion: In this work, we have reported the preparation of pyranopyrazoles using boric acid, at 50 °C under aqueous conditions.

References:

[1] A. Feurer, J. Luithle, S. Wirtz, G. Koenig, J. Stasch, E. Stahl, R. Schreiber, F. Wunder, D. Lang, PCT Int. Aool. Wo 2004009589, Baye Healtheare Ag, Germany.

[2] M. N. Nasr, M. M. Gineinah, *Arch. Pharm. Med. Chem*. **2002**, *335*, 289-295.

[3] V. K. Ahluwalia, A. Dahiya and V. Garg, *Indian J. Chem*. **1997**, *36B*, 88-90.

[4] A. B. Atar, J. T. Kim, K. T. Lim, Y. T. Jeong, *Synth. Commun*. **2014**, *44*, 2679-2691.

[5] H. Junek, H. Aigner, *Chem. Ber*, **1973**, *106*, 914-921.

[6] E. S. El-Tamany, F. A. El-Shahed, B. H. Mohamed, *J. Serb. Chem. Soc*. **1999**, *64*, 9-18.

[7] F. M. Abdelrazek, P. Metz, N. H. Metwally, S. F. El-Mahrouky, Arch. Pharm. **339**, 456 (2006).

Rapid and efficient synthesis of 4-[(tri fluorine methyl)-2, 6-di nitro phenyl amino]-4, 3-di hydro-6-methyl-3-thioxo-1, 2, 4-Triazine-5-ones derivatives by Nano MgO under microwave irradiation

Milad Taheri [a,*], **Razieh Mohebat** [a]

Departments of Chemistry, Islamic Azad University, Yazd Branch, 89195-155, Yazd, Iran.

* Corresponding author. E-mail addresses: milad.taheri@iauyazd.ac.ir
****

Abstract

In this research work, 4-[(tri fluorine methyl)-2,6-di nitro phenyl amino]-4,3-di hydro-6-methyl-3-thioxo-1,2,4-Triazine-5-one was produced from the reaction between 2-chloro-1,3-di nitro-5-triflouro methyl benzene and 4-amino-6-methyl-5-one-3-thion-1,2,4-Triazine through two methods (1-reflux & 2-microwave) in the presence of suitable solvents Using Nano-catalyst MgO under microwave conditions have been reported. The MAOS method is more effective in synthesizing these compounds than the conventional method regarding to the higher chemical yields of products (54% to 96%) and the shorter reaction times (7 to 10 minutes). The 1H-NMR and other methods like FT-IR and Mass spectroscopy have determined all of the compounds. Obtained results of synthesized compounds showed that reactions were carried out with suitable speed and high confusion.

Keywords: Microwave Assisted Organic Synthesis, Conventional method, 1H NMR, 1, 2, 4-Triazine, 2-chloro-1, 3-di nitro-5-triflouro methyl benzene, Nano MgO.

Introduction

Triazine derivatives are of great importance because they exhibit significant biological and pharmacological activities including Anti-microbial, anti-viral, Herbicides strong and anti-inflammatory [1, 2]. The aim of this work is to synthesize some 4-[(tri fluorine methyl)-2, 6-di nitro phenyl amino]-4, 3-di hydro-6-methyl-3-thioxo-1, 2, 4-Triazine-5-ones derivatives via the novel method in an organic system under microwave irradiation by Nano MgO catalyst [3, 4]. It is included from the results of this study that the Microwave Assisted Organic Synthesis (MAOS) method by Nano MgO catalyst results in higher chemical yields of the products with shorter reaction time than the conventional (reflux) method [5, 6].

Result and Discussion

MgO is typical wide band gap (7.2eV) semiconductor, represents an important class of functional metal oxides with a broad range of properties. In order to study the morphology and particle size of MgO nanoparticles, scanning electron microscopy (SEM) image of MgO NPs is presented in **Fig 1.** The XRD patterns of functionalized MgO NPs are shown in **Fig 2.**

The diffraction of the MgO Nanoparticles observed in the peaks at 2θ = 37.153, 43.945, 63.595, 75.125 and 79.185 in **Fig 2.** These data are in good agreement with that of MgO nanoparticles reported before. The crystalline nature of the synthesized MgO NPs sample was further verified by X-ray diffraction pattern (XRD). The crystallite size diameter (D) of the MgO NPs has been calculated by the Debye–Scherrer equation (D = Kλ/βcosθ). The results show that MgO NPs, were gained with an average diameter of 18 nm **(Fig 2.)**. With this catalyst synthesis time in the microwave method than reflux method was very short and very high value products. FTIR was carried out with the range of 400 - 4000 cm^{-1} using IR Spectrophotometer Perkin-Elmer 783.
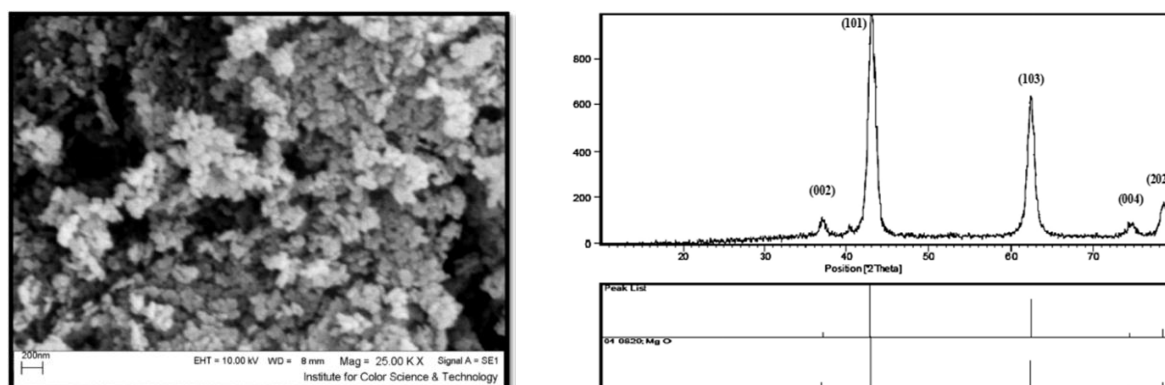
Fig 1, 2. SEM image and XRD scattering patterns of the MgO nanoparticles.

Conclusion

This technology opens up new fortuities to the synthetic chemist, and especially for reactions that are not possible using conventional heating, improved reaction yields, decreased reaction times and even solvent free reaction conditions. The results show that the reaction does not took place in 5-30 min microwave irradiation at same power. Similarly by conventional thermal heating also the reaction do not complete in 9 h.

References

[1] Neumann R.E; Lovelette C.A. *J. Hetero. Chem*, **1980**, 17, 823-824.

[2] Dornow A; Menzel H; and Marx P. *Chem. Ber.*, **1964**, 57, 2173-2178.

[3] Zaher H.A; Mohammady R. *J. Hetero. Chem*, **1984**, 21, 905-907.

[4] Asundaria S.T; Patel P.R; and Patel K.C. *Int. J. Polym*, *Mat*, **2009**, 58: 692-705.

[5] Choudhary R.B; Anand O.N; and Tyagi O.S. *J. Chem. Sci*, **2009**, 121, 353-360.

[6] Ashraf S.M; Sharif A; and Riaz U. *A. Lab. Manual. Polym*, **2009**, 1, 98-114.

Sonogashira-Hagihara cross coupling reaction catalyzed by Pd^0 nanoparticles supported on mixture of pectin/gum arabic under copper free conditions

Sadegh Rahmati*
Department of Chemistry, Payame Noor University (PNU), P.O. Box 19395-3697, Tehran, Iran
Email address: rahmati61@yahoo.com

Introduction
The Sonogashira-Hagihara C-C coupling reaction is the most powerful method in organic synthesis and often used as a key step in the sp-sp^2 carbon-carbon bond forming reactions from terminal alkynes and aryl halides directly [1]. Commonly this reaction is performed in the presence of catalytic amounts of a palladium complex and copper (I) iodide in the presence of a base [2]. In last few years, immobilization of the palladium nanoparticles on solid supports to prepare active and stable catalytic systems is an interesting topic, and different supports have been used to stabilize the nanoparticles [3-7].

Experimentals:
Catalyst Synthesis procedure: Pectin (0.5 g) and Gum Arabic (0.5 g) were dissolved in water (100 mL). To this solution was added a solution of PdCl$_2$ (100 mL, 1 mM) and diluted with water (100 mL). The reaction mixture was refluxed at 100 $^\circ$C for 5h. Then the mixture was cooled down to room temperature and the solvent was evaporated.

Sonogashira-Hagihara reaction procedure: Into a flask, a mixture of catalyst (0.05 g), aryl halide (1 mmol), terminal acetylene (2 mmol), KOAc (1.5 mmol) and DMF (2 mL) were stirred at 100 °C under aerobic conditions. After completion of the reaction, water (10 mL) and ethylacetate (10 mL) was added to the reaction mixture and decanted. After evaporation of the solvent, the products were purified by column chromatography.

Results and Discussion:
It is of current interest to develop a new catalytic system which meets the goals of simple operation procedure, low catalyst loading, and high activity toward aryl halides. So we report that palladium nanoparticles stabilized by a mixture of pectin and gum arabic can be successfully used in the Sonogashira- Hagihara reaction between aryl halides and acetylene under copper free conditions (Figure 1 and 2). These nanoparticles have been characterized by UV-Vis, XRD and EDX spectra
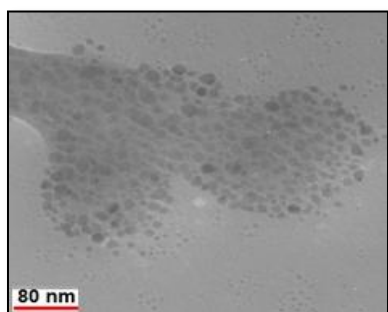

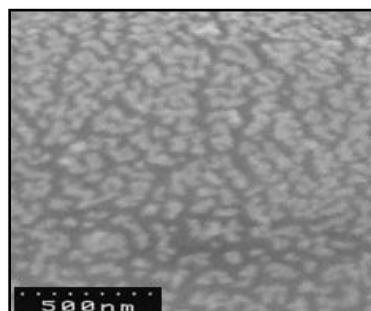Fig. 1. TEM image of the catalyst

Fig. 2. SEM image of the catalyst

as well as SEM and TEM images. The Sonogashira reaction was studied in the presence of various bases and temperatures. The results showed that KOAc in 110 ^{0}C was more effective for this coupling (scheme 1). The result of reaction table showed that the relative reactivity of organic halides in palladium catalyzed reactions is R-Cl < R-Br < R-I. These results reflect the reactivity toward oxidative addition.
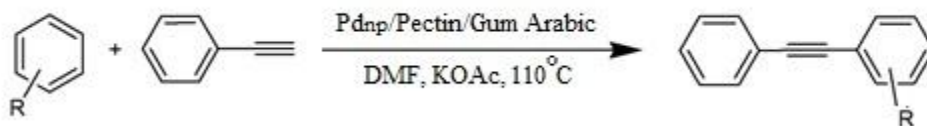
Scheme 1. Sonogashira-Hagihara reaction

The reusability of catalyst were also tested upon the reaction of iodobenzene with phenylacetylene in presence of KOAc as base. The results show that the Pd nanoparticles could be reused five times without decrease in the product yield.

Conclusion:
In conclusion a novel environmentally friendly one-step method to synthesize stable Pd_{np} is reported here. Pd_{np}/gum Arabic/pectin as a new category of nano-composite were obtained easily under green conditions without addition of any external reducing agent. This system exhibited high catalytic efficiency in the Sonogashira coupling reaction. Also the catalyst could be easily separated from the products and reused for several successive runs without significant loss in the catalytic activity.

References:

[1] K. Sonogashira, *in Comprehensive Organic Synthesis* (Eds.: B. M. Trost, I. Fleming, G. Pattenden), Vol. 3, Pergamon Press, Oxford **1991**, 521-549.

[2] K. Sonogashira, Y. Tohda, N. Hagihara, *Tetrahedron Lett.* **1975**, 4467-4470

[3] A. Balanta, C. Godard, C. Claver, *Chem. Soc. Rev.* **2011**, 40, 4973-4985.

[4] B. Tamami, S. Ghasemi, *J. Mol. Catal. A: Chem.* **2010**, 322, 98-105

[5] U.R. Pillai, E. Sahle-Demessite, A. Baiker, *Green Chem.* **2004**, 6,161-165.

[6] H. Firouzabadi, N. Iranpoor, A. Ghaderi, *J. Mol. Catal. A: Chem.* **2011**, 347, 38-45.

[7] R. Bernini, S. Cacchi, G. Fabrizi, G. Forte, F. Petrucci, A. Prastaro, S. Niembro, A. Shafir, A. Vallribera, *Green Chem.* **2010,**12, 150-158.

Facile and Environmentally Friendly Electrophilic Sulfenylation of Benzimidazole Using Bunte Salt

Babak Mokhtari,* **Alireza Kiasat, Javid Monjezi**

Chemistry Department, Faculty of Science, Shahid Chamran University of Ahvaz, Ahvaz 61357-43169, Iran

bmokhtari@scu.ac.ir

Introduction: Organic sulfides are widely present in nature, many natural products and drugs possess sulfide function. Sulfoxides, sulfones and sulfoximines can be easily prepared by the oxidation of sulfide functions.[1] On the other hand , benzimidazole is also an privileged structure in drug discovery, several drugs possessing this moiety have important biological activities, therefore, much effort has been addressed to the synthesis of its derivatives.[2]

Experimentals: To a solution of the benzimidazole in 50/50 water/ethanol the Bunte salts was added. The mixture was allowed to react at 70 °C for the required time. The mixture was then cooled to room temperature and the solvent was evaporated and the residue was washed with water), then dried and concentrated in vacuo. The product was further purified by a short flash chromatography.

Results and Discussion: The reaction procedure is very simple and the desired products were prepared in appropriate time. The proposed mechanism was depicted in Scheme 2 and the results are summarized in Table 1.
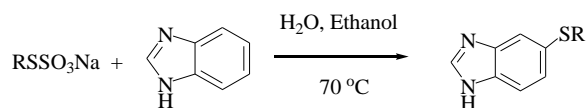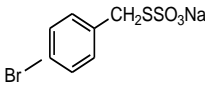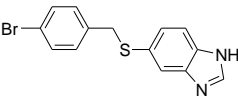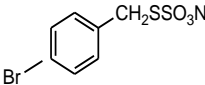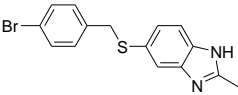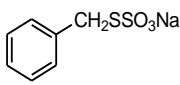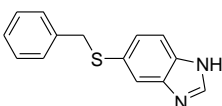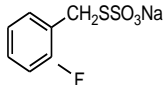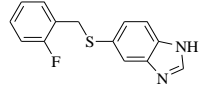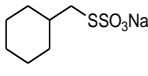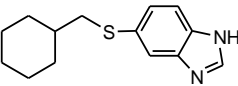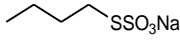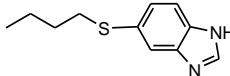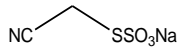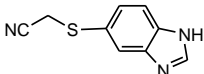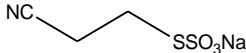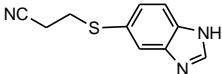

Scheme 1
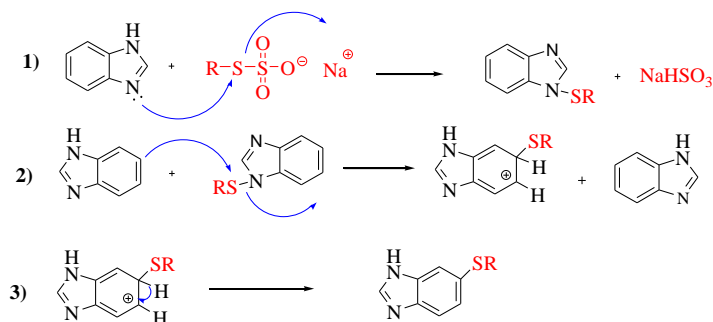
Scheme 2

Table 1: The results for Facile and Environmentally Friendly Electrophilic Sulfenylation of Benzimidazole using Bunte Salt

Entry	Bunte salt	product	Yields (%)
1			98
2			98
3			97
4			90
5			84
6			86
7			82
8			87

Conclusion: In summary, we have designed and successfully developed an efficient catalytic method for the synthesis of 3-thioindoles. This protocol displays attractive features including using odorless, stable, readily available and environment-friendly Bunte salts as the sulfenylating agents, using iodine as nonmetallic catalyst, employing water and ethanol as the solvent.

References

[1] Bang-Andersen, T. Ruhland, M. Jorgensen, G. Smith, K. Frederiksen, K. G. Jensen, H. Zhong, S. M. Nielsen, S. Hogg, A. Mork and T. B. Stensbol, *J. Med. Chem*., **2011**, *54*, 3206.

[2] Selvaraju, M. Dhole S. Sun, C-M. *J. Org. Chem*., **2016**, *81*, 8867-8875.

Synthesis and characterization of plate-like $(BiO)_2CO_3$ nanostructures by hydrothermal method

Saeed Farhadi[*], Narges Ghaderipour

[a]Department of Chemistry, Lorestan University, Khoramabad 68151-433, Iran

E-mail: sfarhadi1348@yahoo.com

****

Introduction: The nanostructured materials have attracted intensive attention in recent years due to their unique architecture dependent performance [1]. $(BiO)_2CO_3$ (BOC) is a suitable candidate for various fields, example healthcare, photocatalysis, humidity sensor, nonlinear optical application and supercapacitors [2,3]. BOC is composed of $Bi_2O_2^{2+}$ and CO_3^{2-} layers, and the plane of the CO_3^{2-} group is orthogonal to the plane of $Bi_2O_2^{2+}$ layer [4]. BOC compounds have been prepared with one-dimensional (1D) nano-structure (nanotubes and nanoparticles), two-dimensional (2D) structure (nanosheets and nanoplates), and threedimensional (3D) microstructure (flower, persimmon-like).

Fabrication of $(BiO)_2CO_3$: In a typical fabrication, a mixture of bismuth citrate and sodium carbonate in H_2O was added into an autoclave and heated at 200℃ for 24 h.The product synthesized by hydrothermal method was collected by filtration, washed four times with distilled water, ethanol, dried at 60℃ and characterized by XRD, FT-IR, SEM, UV,…

Results and Discussion: Fig. 1 shows XRD of the $(BiO)_2CO_3$ sample fabricated by one hydrothermal treatment at 200℃. All the diffraction peaks appelaed can match with the standard card of $(BiO)_2CO_3$. No peaks from other phases can be observed, indicating the high purity of the product. SEM images in Fig 2 shows that the product was formed from the flower-like and pinon-like spheres which composed of $(BiO)_2CO_3$ nanoplates.
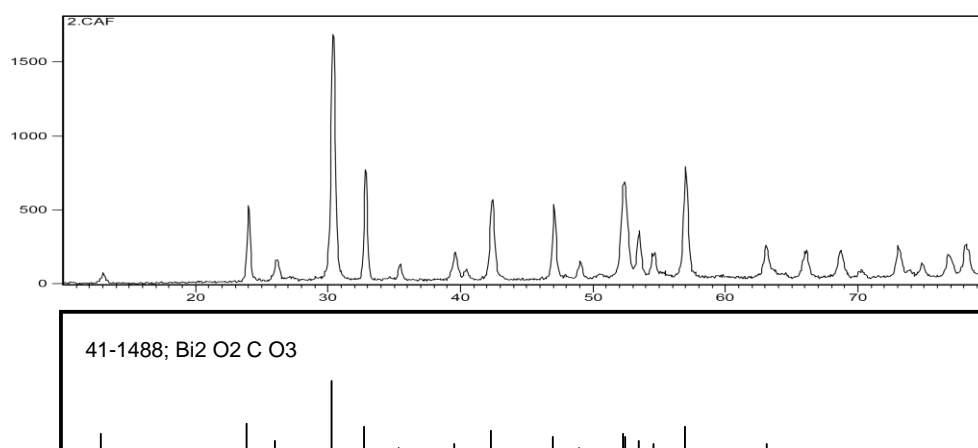
Fig. 1 XRD patterns of the as-prepared $(BiO)_2CO_3$ samples

1
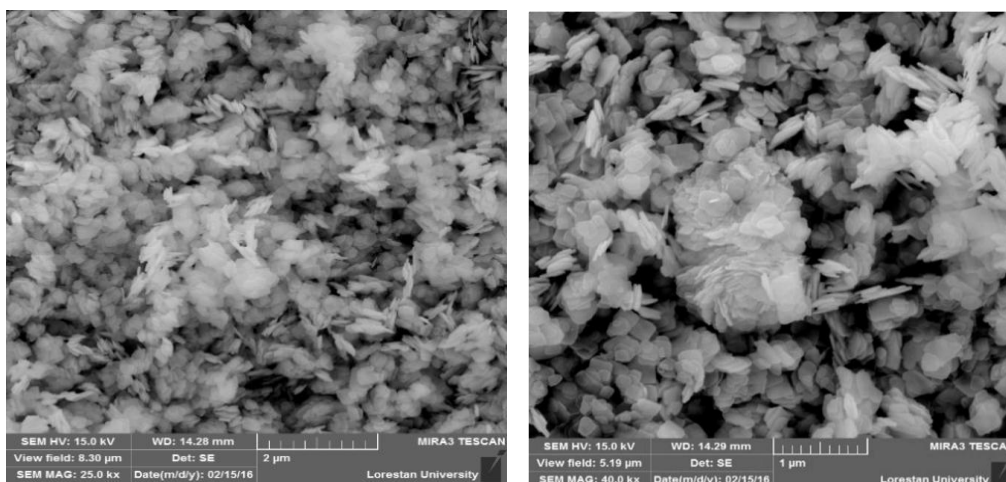
Fig. 2 SEM images of the as-prepared flower-like BOC with different scales

Fig. 3 shows the FT-IR of BOC product. The bands at 1380 and 1465 are related to CO_3^{-2} groupes.
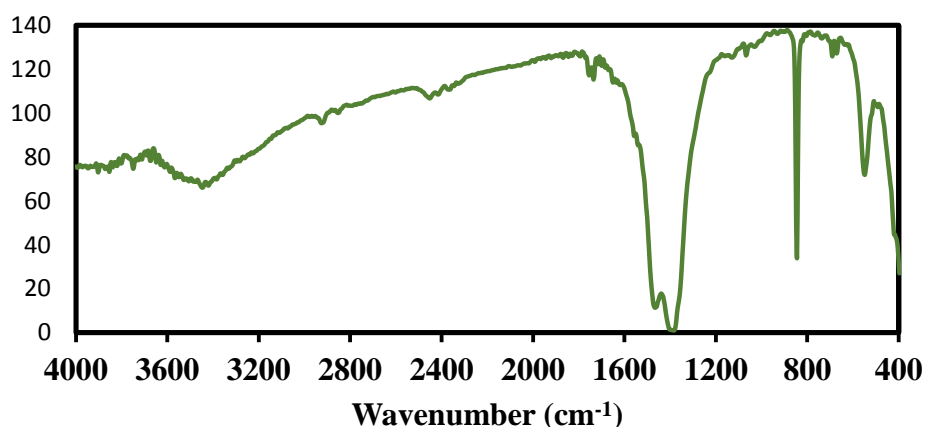
Fig. 3 FT-IR spectra of $(BiO)_2CO_3$ product

Conclusion: In the present work, we fabricated a novel nanostructure $(BiO)_2CO$ by hydrothermal method of aqueous mixture of bismuth citrate and sodium carbonate.

References

[1] X. Wang; S. Blechert; M. Antonietti. *Acs Catalysis*, **2012**, *2*, 1596-1606.

[2] Y. Zhou; H.Y. Wang; M. Sheng; Q. Zhang; Z.Y. Zhao; Y.H. Lin; H.F. Liu. *Sens. Actuators B: Chem*, **2013**, *188*, 1312–1318.

[3] J.J. Ma; S.J. Zhu; Q.Y. Shan; S.F. Liu; Y.X. Zhang; F. Dong; H.D. Liu. *Electrochim. Acta*, **2015**, *168*, 97–103.

[4] R.A. He; S.W. Cao; P. Zhou; J.G. Yu. *Chin. J. Catal*. **2014**, *35*, 989–1007.

Synthesis and Characterization of New Diorganotin(IV) Complexes with a Hydrazone Bearing Benzimidazole

Zeinab Saeedavi, Tahereh Sedaghat[*], Zeinab Ansari-asl

Department of Chemistry, College of Sciences, Shahid Chamran University of Ahvaz, Ahvaz, Iran

Email: tsedaghat@scu.ac.ir

****

Introduction: Hydrazone organotin(IV) complexes are of interest for both biological and structural reasons [1-3]. On the other hand, benzimidazole derivatives play an important role in medicinal field with many biological and pharmacological activities [4]. Therefore the synthesis of hydrazones containing benzimidazoles and their organotin(IV) complexes are the potential area of research [5,6]. In this research work, the new organotin complexes R_2SnL (R = Me, Ph) with a hydrazone bearing benzimidazole (Scheme 1) have been synthesized and investigated.

Scheme 1
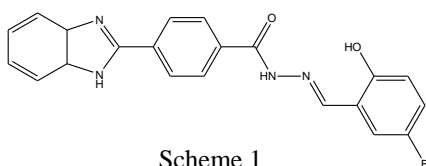
Experimental: The hydrazone (H_2L) was prepared by condensation of 4-(1H-benzimidazole-2-yl)benzoic acid hydrazide with 5-bromo-2-hydroxybenzaldehyde. Then the organotin(IV) complexes have been synthesized by reaction of R_2SnCl_2 (R = Me or Ph) with H_2L in the presence of triethylamine. All compounds were investigated by elemental analysis, FT-IR, ^{1}H and ^{119}Sn NMR spectroscopy.

Results and Discussion: The infrared spectra of the free ligand display the characteristic bands associated with the N-H and C=O bonds of the amide functionality. The absence of $\nu(C=O)$ in the complexes confirms that the ligand coordinate with tin in the enol form. The $\nu(C=N)$ band of the ligand (1621 cm^{-1}) shifts to a lower wavenumber in the spectra of complexes. These shifts support the participation of the azomethine group of the ligands in binding to the tin atom. In the IR and ^{1}HNMR spectra of the complexes, the disappearance of bands attributed to $\nu(O-H)$ and $\nu(N-H)$ in the free ligand shows complete deprotonation of the hydrazone ligand and their subsequent coordination to the tin atom. ^{119}SnNMR data confirms the coordination number of five for tin in both complexes. The appearance of new bands in the IR spectra of the synthesized complexes assigned to $\nu(Sn-N)$ and $\nu(Sn-O)$ supports the bonding of nitrogen and oxygen atoms to the tin atom.

Conclusion: The newly synthesized hydrazone are completely deprotonated and coordinate to tin(IV) as tridentate ligand through imine nitrogen, and phenolic and enolic oxygen atoms, and the coordination number of the tin atom is five.

References

[1] E. L.Torres; F. Zani; M. A. Mendiola. *J. Inorg. Biochem.* **2011**, *105***,** 600.

[2] T. Sedaghat; L. Tahmasbi; H. Motamedi; R.R. Martinez; D.M. Morales. *J. Coord. Chem.* **2013**, *66,* 712-724.

[3] T. Sedaghat; M. Aminian; H. Amiri Rudbari; G. Bruno. *J. Organomet. Chem.* **2014**, *754*, 26-31.

[4] Y. Bansal; O. Silakari. *Bioorg. Med. Chem.* **2012**, *20*, 6208-6236.

[5] M. Nath; P. K. Saini; A. Kumar. *Appl. Organomet. Chem.* **2009**, *23*, 434-445.

[6] F. Arjmand; F. Sayeed; S. Parveen. *J. Organomet. Chem.* **2011**, *696*, 3836-3845.

Click reaction on starch attached to the graphene through covalent modification with antibacterial ability

Khadijeh Soleimani, Abbas Dadkhah Tehrani*, Shabnam Sattari, Mohsen Adeli

Department of Chemistry, Faculty of Science, University of Lorestan, Khoram abad

a_dadkhahtehrani@yahoo.com

Introduction:

Graphene, a flattish monolayer of carbon atoms tightly packed into a dense honeycomb lattice, has attracted considerable attention during recent years. [1] The functionalization of graphene can be performed by covalent and noncovalent modification techniques. "Click" reaction can be performed under mild reaction conditions, shows high yields and has a good tolerance toward a wide range of functional groups and leading to the formation of 1,2,3 triazole ring. [2] The [2 + 1] cycloaddition of nitrenes is a significant addition reaction and has successfully been exploited to functionalize graphene under very simple conditions demonstrating its excellent efficiency. Furthermore, antibacterial activities of functionalized graphene oxide were investigated via bacterial studies. [3]

Methods / Experimentals:

GO was prepared using natural graphite powder by Hummer's method. [4] The terminal hydroxylic groups of polyethylene glycol were converted to terminal alkynes groups with some modifications. First, poly(ethylene glycol) was dissolved in dry dichloromethane and pyridine and toluene-4-sulphonyl chloride were added to the solution dropwise within 30 min and the reaction mixture was then allowed to stir at room temperature for 24 h under nitrogen and subsequently washed with cold distilled water twice. The residue was dissolved in dichloromethane, precipitated by addition of diethyl ether. Click coupling between propargylated PEG and azido-starch attached to graphene oxide was performed in DMF solvent. First, azido-starch attached to graphene oxide and propargylated PEG and sodium bicarbonate and ascorbic acid and copper sulfate pentahydrate left to react under continuous stirring at 90°C for 12 h, then it was washed with distilled water.

Results and Discussion:

The results revealed that, the formation of 1,2,3 triazole ring is main factor in creation anti-bacterial property. FT-IR analysis was used for characterization of all synthesized products. In all of spectrums the % of transmittance is plotted as a function of wavenumber (cm^{-1}). In the FT-IR spectra of starch, a broad peak at 3400 cm^{-1} is due to the stretching vibrations of O–H, the bands at 1356, 2902 cm^{-1} are assigned to C–O, C–H stretching, respectively (Fig. 1a) . The pristine GO, presents some characteristic absorption peaks are observed at 3369, 2916, 1715, 1640, 1337 and 1023 cm^{-1} (Fig. 1b). The appearance of a narrow band at 3325 and at 2113 cm^{-1}

indicates the functionalization of PEG with alkyne (Fig. 1c). After alkyne–azide click reaction, the peak at 2109 cm−1corresponds to the azide stretching vibrations of starch–N_3, disappeared. Furthermore, the appearance of the new peaks at 1647 and 1458 cm−1, is due to the formation of triazole ring, clearly indicate the success of this click reaction. The raman spectrum of GO and functionalized graphene oxide (Fig. 2) showed an increment in I_D/I_G ratio from 1.18 to 1.24 attributed to the enhancement in defect concentration due to functionalization and conversion of π-bonded c-sp^2 carbons to c-sp^3 ones. Moreover, the recorded trend of values reflects the increased disorder due to the formation of covalent bonds induced by the addition of nitrene to the double bonds.
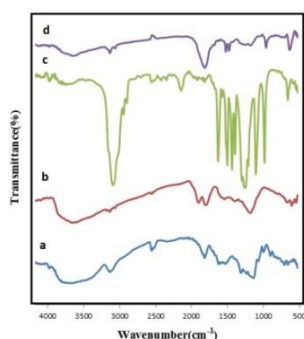
Fig. 1. FT_IR spectra of (*a*) Starch, (b) GO, (c) propargyl PEG, (d) click product.   Fig 2. Raman spectra of GO (a) and click product (b).
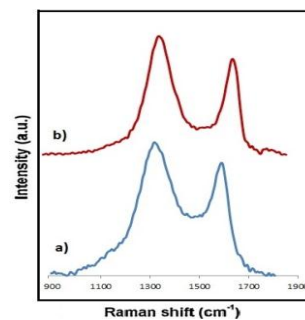
To determine the antibacterial attachment properties of the material, Gram-positive S. aureus and Gram-negative E. coli were respectively cultured for 24 h at 37◦C.

Conclusion:

In this study, we designed an Anti-bacterial material based on graphene oxide via click coupling. Here, starch was covalently attached to graphene using nitrene chemistry and then click reaction between propargylated PEG and azido-starch was performed. The results exhibited that functionalized graphene oxide with starch and poly ethylene glycol has significant antibacterial properties. The functionalized GO was subsequently verified by using FT-IR and Raman.

References

[1]. Allen MJ; Tung VC; Kaner RB. *Chemical reviews*, **2009**, 110(1), 132-45.

[2]. M. Parsamanesh; A. Dadkhah Tehrani. *Carbohydrate Polymers*, **2016**, 136, 1323–1331.

[3]. Qin Tua ; Chang Tianb; Tongtong Maa. *Colloids and Surfaces B: Biointerfaces,***2016**, 141, 196–205.

[4]. Hummers Jr WS; Offeman RE. *American Chemical Society*, **1958**, 80(6),1339.

Removal of pollutant from wastewater by graphene oxide

Sara Kaveh[a,*]

[a]Islamic Azad University of Shahr-e-Qods

Email address: skaveh٧٣@gmail.com

١. Introduction

Harmful chemical compounds containing heavy metals and dyes that should be removed from water recourses, because some of these compounds are toxic for human health and environment [١]. Heavy metals have been used by humans for thousands of years, although several adverse health effects of these metals have been known for a long time. Heavy metals effect on human livers and kidney and may eventually lead to cancer. Inhalation of Cadmium fumes or particle can be threatening, and although acute pulmonary effects and death uncommon. Cadmium exposure may cause kidney damage [٢]. MB can effect on human too like eye irritation, heart beat, asthma. Adsorption is one of the most widely techniques for removalharmful chemical compounds. GO has high adsorption power and effective economically. GO is a new type of carbon materials [٣]. The goal of this review is to explain adsorption data and some tips for the preparation of GO [٤].

٢. Experimental

٢.١ Preparation of GO:

GO is synthesized by chemical oxidation using either the Brodie, Staudenmaier, or Hummers method By treating graphite with a mixture of potassium chlorate and fuming nitric acid .Adsorption experiments were carried out in ٢٥٠ ml erlenmeyer flasks by agitating pre-weighed amount of GO with ٥٠ ml of aqueous pollutant (heavy metal or MB) solution. After adsorption, the mixture was filtered through Whatman No-١ filter paper. For isotherm analysis, adsorption experiments were conducted by varying the initial metal ion concentration from ٢٥-٢٠٠ mg/l and equilibrated for ٦ h.

٣. Results and discussion

The presence of flakey structure together with needle-like shaped morphology can clearly be seen in the images recorded at a higher magnification. Morphologically vein graphite is different from other forms of graphite. [٥].

(a)   (b)
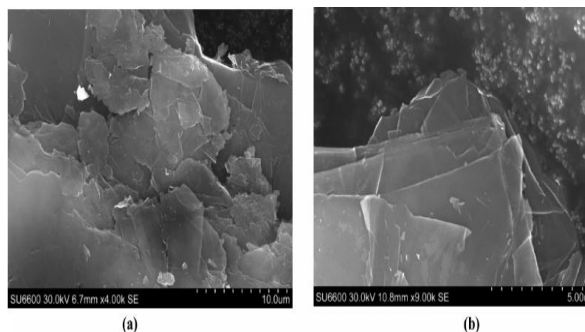
Fig.٢ SEM of the vein graphite and multilayer GO membrane

Isotherm analysis of $Cd^{٢+}$ were investigated (Fig.٣). The maximum capacity for $Cd^{٢+}$ adsorbed effectively by GO was reported as up to ٢٤٦ mg/g with a Langmuir adsorption equilibrium constant of ٥.٧ L/g (at ٢٠ °C).
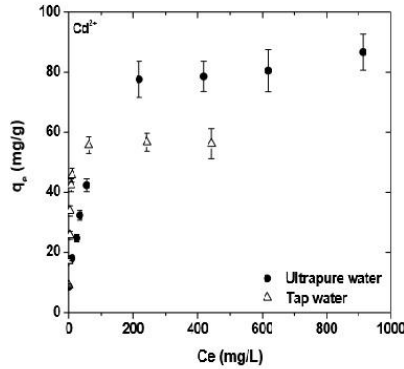
Fig.٣ Adsorption curves for cadmium (pH ٦, contact time ٢٤ h, adsorbent dosage ١ g/L).

٤. Conclusion

In this paper, the GO was prepared and used as an adsorbent to remove pollutants. The GO was characterized using SEM. The adsorption kinetics was followed by the pseudo second-order model and it showed that adsorption of dyes conform to Langmuir isotherm. The magnetic separation of the loaded adsorbent could also contribute to a convenient solid-liquid separation, required downstream. More research should be carried out.

References

[١] E. J. Granite and H. W. Pennline, " Photochemical removal of mercury from flue gas," Industrial & Engineering Chemistry Research, ٢٠٠٢, vol. ٤١, no. ٢٢, pp. ٥٤٧٠-٥٤٧٦.

[٢] L. Järup, "Hazards of heavy metal contamination," British medical bulletin, ٢٠٠٣, vol. ٦٨, no. ١, pp. ١٦٧-١٨٢.

[٣] H. kolivand, A. shahbaz and H. hashemi, "Hazf methylene blue az mahlool haye abi ba estefadeh az nano safahate graphene oxide :Kinetics and isotherms," omran modares, ١٣٩٤, vol. ١٥, pp. ١٩١-١٩٨.

[٤] G. z. Kyzas, E. A. Deliyanni and K. A. Matis, "Graphene oxide and its application as an adsorbent for wastewater treatment," Journal of Chemical Technology and Biotechnology, ٢٠١٤, vol. ٨٩, no. ٢, pp. ١٩٦-٢٠٥.

[٥] A. R. Kumarasinghe and et al, "Self-assembled multilayer graphene oxide membrane and carbon nanotubes synthesized using a rare form of natural graphite," The Journal of Physical Chemistry C, ٢٠١٣, vol. ١١٧, no. ١٨, pp. ٩٥٠٧-٩٥١٩.

A Green One-Pot Three-Component Synthesis Of Spiro [Chromeno[2, 3-C]Pyrazole-4, 3'-Indoline]-Diones Derivatives By Using Fe_3O_4@Sio_2-Imid-PMA^n Magnetic Nanocatalyst

Ali Reza Sardarian[*], <u>Milad Kazemnejadi</u>, Mohsen Esmaeilpour, Hassan Eslahi

Chemistry Department, College of Sciences, Shiraz University, Shiraz 71946 84795 (Iran)
[*]Corresponding author: sardarian@susc.ac.ir
<u>presenting author</u>: miladkazemnejadi@shirazu.ac.ir; miladkazemnejad@yahoo.com

****

Introduction: Recently, several attempts have also been made for the construction of spirooxindoles via one-pot four-component reactions of isatin, hydrazine hydrate, ethyl acetoacetate, and a compound such as dimedone or malononitrile in the presence of an acid catalyst such as meglumine [1], *p*-toluene sulfonic acid [2], 4-DMAP [3] and piperidine [4]. However, most of the reported methodologies suffer from various disadvantages, therefore, in the present research, we wish to describe a convenient procedure for the synthesis of spiro [chromeno[2, 3-c]pyrazole-4, 3'-indoline]-diones in the presence of Fe_3O_4@SiO_2-imid-PMA^n magnetic nanocatalyst under green conditions (Scheme1).
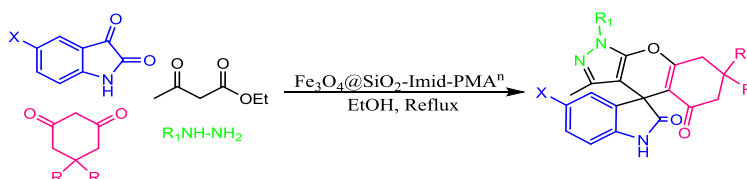
Scheme.1 One-pot synthesis of spirooxindole derivatives using the Fe_3O_4@SiO_2-imid-PMA^n catalyst.

Methods or Experimental: *2.1. Preparation of Fe_3O_4@SiO_2-imid-PMA^n*

Fe_3O_4@SiO_2-Imid-PMA^n nanoparticles were prepared in our previous work [5].

General procedure for the synthesis of spiro [chromeno [2, 3-c] pyrazole-4, 3'-indoline]-diones derivatives

A mixture of isatin (1 mmol), dimedone (1 mmol), ethyl acetoacetate (1.1 mmol), hydrazine hydrate (1.1 mmol), and Fe_3O_4@SiO_2-Imid-PMA^n (0.01 g) nanoparticles was heated in EtOH under reflux conditions for appropriate time. After reaction completion as monitored by TLC and separation of catalyst by magnetic field, the filtrate mixture was recrystallized twice in EtOAc/n-hexane (3:1).

Results and Discussion: Due to ability of Fe_3O_4@SiO_2-Imid-PMA^n as a mild and efficient acid catalyst, we decided to apply this catalyst for synthesis of spiro [chromeno[2, 3-c]pyrazole-4, 3'-indoline]-diones derivatives. After optimizing the reaction conditions (Catalyst (0.01 g), EtOH, reflux, 1:1:1.1:1.1 ratios of isatin, dimedone, ethyl acetoacetate and hydrazine hydrate) the generality of this catalytic system was confirmed by the employment

of a series of isatin, dimedone, ethyl acetoacetate and hydrazine hydrate to obtain desired products under the optimized conditions. As can be seen, the yields were good to excellent without the formation of any side products and the reaction times are very low.

Table 1. One-pot synthesis of spiro [chromeno [2, 3-c] pyrazole-4, 30-indoline]-diones catalyzed by Fe_3O_4@SiO_2-Imid-PMA[n].

Entry	R	R_1	X	Time (min)	Yield (%)	m.p. (^{o}C) Found	Reported
1	Me	Ph	H	30	93	244-245	243 [6]
2	Me	Ph	Br	30	88	242-243	244 [6]
3	Me	Ph	NO_2	25	90	307-308	307 [7]
4	Me	H	H	30	95	219-221	220 [7]
5	Me	H	Me	45	82	196-197	195 [7]
6	Me	H	Br	30	87	183-185	185 [7]
7	Me	H	Cl	30	94	214-216	215 [7]
8	Me	H	NO_2	25	92	200-202	200 [7]
9	H	Ph	H	40	85	310-311	312 [6]
10	H	Ph	NO_2	30	87	308-309	310 [6]

In order to confirm the reusability and stability of this magnetic catalyst it was recovered by applying a magnetic field and the catalyst reused for subsequent reactions at least 7 times without any activation process.

Conclusion: In conclusion, considering the importance of this catalyst, we have developed a potentially efficient, safe and eco-friendly procedure for the one-pot synthesis of spirooxindole containing chromene ring fragments via a four-component condensation reaction of isatin derivatives, dimedone, ethyl acetoacetate and hydrazine hydrate using Fe3O4@SiO2-imid-PMAn as a powerful and green catalyst. This new procedure has notable advantages such as excellent yields, short reaction time, operational simplicity, avoids the use of dry and toxic solvents, and absence of any tedious workup or purification.

References

[1] Guo, R.; An, Z.; Mo, L.; Yang, S.; Wang, S.; Zhang, Z.; *Tetrahedron*, **2013**, *69*, 9931-9938.

[2] Ghahremanzadeh, R.; Fereshtehnejad, F.; Yasaei, Z.; Amanpour, T.; Bazgir, A.; *J. Heterocycl. Chem.,* **2010**, *47*, 967-972.

[3] Feng, J.; Ablajan, K.; Sali, A.; *Tetrahedron,* **2014**, *70*, 484-489.

[4] Zou, Y.; Hu, Y.; Liu, H.; Shi, D.; *ACS Comb. Sci.,* **2012**, *14*, 38-43.

[5] Esmaeilpour, M.; Javidi, J.; Zandi, M.; *Materials Research Bulletin,* **2014**, *55*, 78-87.

[6] Ghahremanzadeh, R.; Fereshtehnejad, F.; Yasaei, Z.; Amanpour, T.; Bazgir, A.; *J. Heterocycl. Chem.,* **2010**, *47*, 967-972.

[7] Alemi-Tameh, F.; Safaei-Ghomi; J.; Mahmoudi-Hashemi, M.; Teymuri, M.; *Res Chem. Intermed.,* **2016**, *42*, 6391-6406.

Effect of Electron-Donating and Electron-Withdrawing Groups on AlN and AlP Nanotubes

Batoul Makiabadi[a,*], Sareh Sardouie Nasab[b]

[a]*Department of Chemical Engineering, Sirjan University of Technology, P.O. Box: 7813733385, Sirjan, Iran*

[b]*Department of Chemistry, Payame Noor University, Tehran, Iran*

Email: bmakiabadi@yahoo.com

Introduction

Many studies on non-carbon based nanotubes with properties independent of tube diameter and chirality demonstrated that the counterparts of groups III and V of elements are proper materials [1]. These alternative materials could be an important candidate for future electronics and optoelectronics applications as a wide gap semiconductor [2]. Aluminum nitride nanotubes have some exclusive properties such as superior mechanical strength, high thermal conductivity, and a high piezoelectric response [3]. Recently, the properties of aluminum phosphide nanotubes have been investigated by quantum chemical calculations of chemical shielding parameters [4]. The aim of this work is to compare the effect of NH_3, NH_2CH_3, $NH_2CH_2OCH_3$ and NH_2CH_2COOH adsorption on AlN and AlP nanotubes, with an equal number of atoms, same diameter and length.

Methods

The electronic properties of AlN and AlP nanotubes with NH_3, NH_2CH_3, NH_2COOH and NH_2COCH_3 molecules were studied by using B3LYP method using 6-31G(d) basis set. We have selected a zigzag nanotube consisting of 20 Al atoms and 20 N(P) atoms in which open ends have been saturated by hydrogen atoms for avoiding boundary effects. For investigation of the effect of interaction of these molecules on the electronic properties of nanotubes, the HOMO–LUMO gap, electronic chemical potential, hardness and softness were investigated for nanotubes and different complexes.

Results and Discussion

In this work, DFT studies were performed for the interaction of single-walled AlN and AlP nanotubes with NH_3, NH_2CH_3, NH_2COOH and $NH_2CH_2COCH_3$ molecules (See figure 1). In NH_2CH_3, NH_2COOH and $NH_2CH_2COCH_3$ molecules, $-CH_3$ electron-donating group, $-COOH$ and $-OCH_3$ electron-withdrawing groups replaced with one of the hydrogen atoms of NH_3, respectively. Four minima structures on the potential energy surface were found.
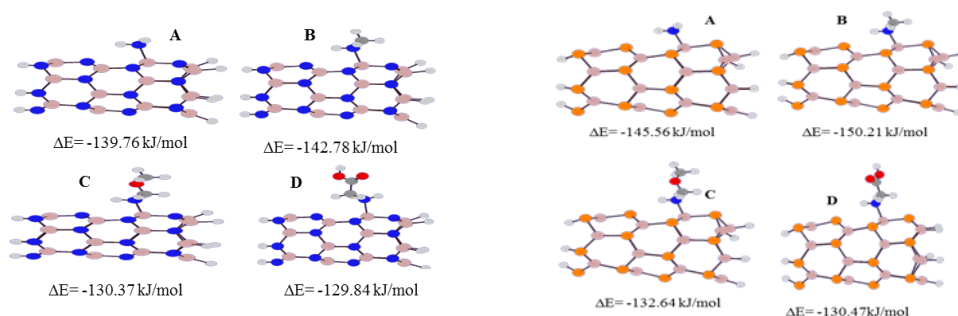
Figure 1. Optimized structural parameters for AlN and AlP complexes.

These molecules can be chemically adsorbed on the top of the aluminum atom of AlNNTs and AlPNTs. Also, the AlP nanotubes are the most energetically favorable candidates for adsorption of these molecules. The results show that in the interaction of these molecules with nanotubes, the electronic properties of the nanotubes will be changed. The band gap energies, dipole moment, chemical potential, chemical hardness and softness, electrophilicity index for complexes have been calculated. In general, the band gap, chemical hardness, decreases and chemical softness increases as well as chemical potential upon complexation. Both types of complexes have negative solvation Gibbs free energies, signifying easy dissolution in water. Based on the NBO analysis, in all complexes charge transfer occurs from these molecules to nanotubes and change the hybridization of the Al atom from sp^2 to sp^3. The Al… N interaction has a partial covalent nature. Also, this interaction in the AlP complexes is stronger than that in the AlN complexes.

Conclusions

Calculations indicated that these molecules can be chemically interacted with the Al atom of AlN and AlP nanotubes. It was found that AlPNTs could be a better candidate for adsorption of these molecules. The interaction these molecules with nanotubes results in changes in the electronic properties of NTs. In all complexes charge transfer occurs from these molecules to nanotubes. In both types of complexes, the results obtained for complexes containing electron-donating molecules are better than complexes containing electron-withdrawing ones.

References

[1] Chen, X; Ma, J; Hu, Z; Wu, Q; Chen, Y. *J. Am. Chem. Soc*. **2005**, *127*, 17144-17145.
[2] Vurgaftman, I; Meyer, J. R. *J. Appl. Phys*. **2003**, *94*, 3575.
[3] Wu, C; Kahn, A. *Appl. Surf. Sci*. **2000**, *162*, 250-255.
[4] Mirzaei, M; Mirzaei, M. *J. Mol. Struct*. **2010**, *951*, 69-71.

Silica Iodide as a New Heterogeneous Catalyst for the Efficient Acetylation of Aromatics

Efat Ejraee[*], Ebrahim Shamsi , Farajolah Mohanazadeh

Faculty of Chemical Engineering Iranian Research Organisation for Science and Technology (IROST), Tehran, Iran

e.ejraei@yahoo.com

Introduction: Friedel Crafts acylation is one of the fundamental foundation of synthetic organic chemistry at industrial groundwork and the academic level. The aromatic ketones are produced with this manner are fundamental intermediates in the pharmaceutical, agrochemical industries , ect . Until now this reaction catalyzed by Lewis acids (such as $ZnCl_2$, $AlCl_3$, $FeCl_3$,…) or strong protic acids (such as HF and H_2SO_4).Using these catalysts have several problems such as the strong complex formed between the ketone product and the metal halide or the use of more than stoichiometric amounts of catalyst[1]. In recent years, the use of catalysts supported on solid supports has received much attention, Silica gel is one of the most extensively used surface material supports for different chemical transformations in organic synthesis [2]. For example, silica chloride was synthesized and used in different reactions such as alkylation of Electron-rich Aromatics [3]. We prepared a new heterogeneous catalyst, SiO_2-I, as effective catalyst for acylation of aromatics in CCl_4 at 60 ℃ in high yield.

Methods / Experimentals : Silica iodide is as a new heterogeneous catalyst that we prepared it from reaction of silica gel with Triphenylphosphine and I_2 in DCM. To acylation of aromatics, Silica iodide (10% mmol) added to an aromatic (1mmol) and acetic anhydride (2 mmol) in CCl_4 at 60 ℃, after completion of the reaction, products was determined by GC and NMR .
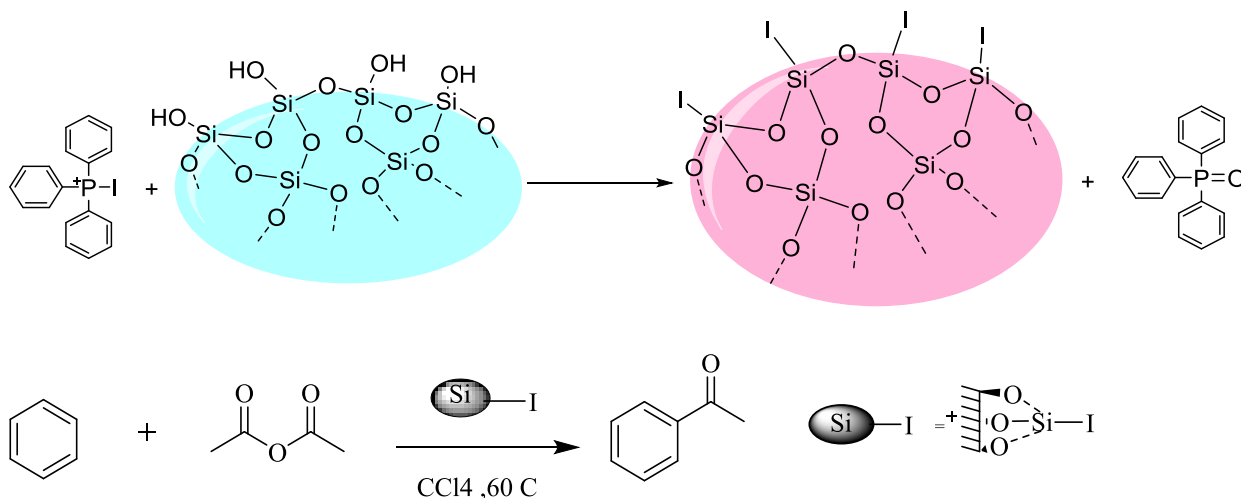
Results and Discussion: A new heterogeneous catalyst, SiO_2-I, as simple, mild and effective catalyst for acetylation of aromatics in CCl_4 at 60 ℃.

Conclusion: Results have shown that Silica iodide can be used as a new and efficient catalyst for acetylation of aromatics.

References

[1] G. Sartori, R. Maggi, *Chem. Rev*. **2006**, *Vol.106*, 1077.

[2] P. Mehtab, M. A. Mohammed, A. L. I. Akhtar, M. Parveen, A. M. Malla, A. Ali, M. Alam, and M. F. Mustafa, *Chem. Res*. **2014**., *Vol. 30*, 55.

[3] F. Mohanazadeh, H. Amini. *Bull. Korean Chem. Soc*. **2010**, *Vol. 31*,3038.

Nanomagnetic Fe$_3$O$_4$@SiO$_2$-Propyl-Pip-SO$_3$H: A green and recyclable catalyst for the synthesis of barbituric and thiobarbituric acid derivatives in aqueous media

Monireh Pourghasemi-Lati , Farhad Shirini*, Mokhtar Alinia*

Introduction: Pyrimidine derivatives are important biological compounds, due to their important properties such as antitumor, analgesic, antibacterial, and fungicidal activities. 5-Arylidine barbituric and thiobarbituric acids are synthesized *via* Knoevenagel condensation reaction between barbituric acid and its derivatives with aldehydes [1,2]. In recent years, more attention has been paid to the supported Fe$_3$O$_4$ MNPs catalysts in many different fields due to their unique properties such as high surface area, low toxicity, superparamagnetic behavior, and biocompatibility. Particularly, the Fe$_3$O$_4$ nanoparticles are easily synthesized and can be easily separated from the reaction mixture by external magnetic field and reused [3].

Methods / Experimentals: In this procedure, aldehyde (1.0 mmol), barbituric or thiobarbituric acid (1.0 mmol) and Fe$_3$O$_4$@SiO$_2$-Propyl-Pip-SO$_3$H (25 mg) were taken in a 25 mL round bottomed flask and 5 mL water was added. The mixture was stirred at 60 ^{o}C till completion of the reaction. Completion of the reaction was indicated by TLC using *n*-hexane : ethylacetate (7 : 3). After evaporation of water, ethanol (15 mL) was added to the reaction mixture. The catalyst was separated by an external magnet.

Results and Discussion: On the basis of the obtained information about the structure of Fe$_3$O$_4$@SiO$_2$-Propyl-Pip-SO$_3$H the catalytic ability of this reagent in the promotion of the synthesis of 5- arylidine barbituric and thiobarbituric acids was investigated under the conditions shown in Scheme 1. The obtained results clarified that this reagent is efficiently able to catalyze the synthesis of the requested products under mild and green conditions. All the products are obtained in high yields during very short reaction times.
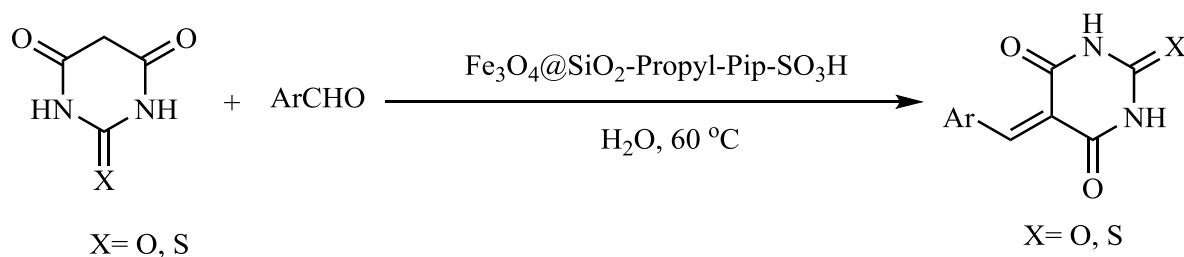
Scheme 1

Conclusion: In summary, we have represented a new and simple method for synthesis of 5-arylidine barbituric and thiobarbituric acid using Fe$_3$O$_4$@SiO$_2$-Propyl-Pip-SO$_3$H as an efficient catalyst. The Most important advantages of these methods are including

the simplicity in the preparation procedure, easy work-up, high reaction rates excellent yields, recyclability of the catalysts and eco-friendly procedure. Further work to utilize these catalysts in other organic synthesis and transformations is in progress.

References

[1] S. Mashkouri ; M. R. Naimi-Jamal. *Molecules*, **2009**, *14*, 474-479.

[2] N. Seyyedi; F. Shirini; M. Safarpoor Nikoo Langarudi. *RSC Adv*., **2016**, *6*, 44630-44640.

[3] Y. H. Leng; K. Sato; Y. G. Shi; J. G. Li; T. Ishigaki; T. Yoshida; H. Kamiya . *J Phys Chem C,* **2009**, *113*, 16681 −16685.

Removal of Heavy Metal ions from Water Sample using Nitrogen Functionalized Mesoporous Silica Coated Magnetic Nanoparticles as Adsorbent in Solid Phase Extraction

Abdolraoof Samadi-Maybodi[a], Malihe Samadi-Kazemi*[b], Zoha Hosseini[a]

[a] Analytical Division, Faculty of Chemistry, University of Mazandaran, Postal Code 47416-95447, Babolsar, Iran

[b] Department faculty of sciences, Bojnourd branch, Islamic Azad University, Bojnourd, Iran

E-Mail address: samadi24243@yahoo.com

Introduction: Today pollution of water resources is a fundamental problem. The heavy metal ions are the most important polluters existing in water that threatens human health. In this research, nitrogen functionalized mesoporous silica coated magnetic nanoparticles was used as an adsorbent for solid phase extraction and the determination of trace amounts of Cu^{2+}, Zn^{2+}, Ag^+ and Pb^{2+} from water sample using atomic adsorption spectrometry.

Methods/ Experimental: A series of sample solutions containing the M^{n+} ($M^{n+} = Cu^{2+}$, Zn^{2+}, Ag^+ and Pb^{2+}) metal ions were transferred into a beaker. The pH of the solution was adjusted to 6.0 using 0.01–0.1 mol L^{-1} HCl and/or NaOH solutions. Then, 0.15 g of the adsorbent was added to the solution and the mixtures were dispersed at room temperature by ultrasonication for 10 min. The adsorbent was washed with deionized water, the Cu^{2+}, Zn^{2+}, Ag^+ and Pb^{2+} metal ions were desorbed from the adsorbent surface with 10 mL of 1.0 mol L^{-1} HNO_3 and the concentration of the studied metal ions in the eluent was then determined by FAAS.

Results and Discussion: The effect of various parameters such as pH, adsorbent amount, contact time, type and concentration of eluent and volume of sample solution were investigated. Calibration curves were constructed for determination of metal ions according to the extraction procedure. Linearity was maintained between 0.03 µg L^{-1} to 0.50 mg L^{-1} for copper; 6.53 µg L^{-1} to 1.0 mg L^{-1} for zinc; 0.03 µgL^{-1} to 1.0 mg L^{-1} for silver and 8.43 µg L^{-1} to 0.50 mg L^{-1} for lead. The LOD was calculated as LOD= k Sb/m, where k is equal to 3 according to the desired confidence level (95%), Sb is the standard deviation of the blank signal and m is the slope of the analytical curve (n = 3).Also, the detection limits for Cu^{2+}, Zn^{2+}, Ag^+ and Pb^{2+} metal ions were obtained 8.67, 2, 8.44 and 2.53 (µg L^{-1}), respectively. The relative standard deviation (RSD) was determined by the three replicate experiments at a concentration of 0.05 mg L^{-1} from Ag^+, Zn^{2+} and 0.1 mg L^{-1} from Cu^{2+} and Pb^{2+} metal ions. RSDs were lower than 6.0% (Ag^+: 2.04 %; Cu^{2+}: 1.77 %; Pb^{2+}: 5.10 %; Zn^{2+}: 4.43%.

The proposed method was applied to the determination of Cu^{2+}, Zn^{2+}, Ag^+ and Pb^{2+} metal ions in water samples. Tap water (collected from Bojnourd, Iran) and wastewater (collected from village water and wastewater company, Esfarayen, Iran) was immediately filtered through Millipore cellulose membrane filters (0.45 μm pore size), acidified to pH 2 with HNO_3 and stored in precleaned polyethylene. Then, in extraction conditions, the amounts of were determined. Results are shown in Table 1. As can be seen from this Table, the metal ions were quantitatively recovered from the water sample by the proposed procedure.

Table 1. Determination of metal cations in water samples on optimum conditions.

	The initial concentration (μg L^{-1}) n=3	Added (μg L^{-1})	Found (μg L^{-1}) n=3	Extraction (%)
Tap water				
Ag+	ND[a]	30.00	29.12±0.45[b]	97.06
Cu^{2+}	10.34±0.14	10.00	19.87±0.29	97.68
Pb^{2+}	ND	30.00	30.56±0.30	101.87
Zn^{2+}	53.67±0.43	10.00	63.14±0.32	99.17
Wastewater				
Ag+	ND	30.00	27.67±0.12	92.33
Cu^{2+}	31.27±0.98	10.00	42.12±0.22	102.06
Pb^{2+}	51.24±0.43	30.00	80.09±0.32	98.58
Zn^{2+}	27.64±0.56	10.00	39.43±0.11	104.76

[a] Not detected.
[b] Relative standard deviation (RSD).

Conclusion: High adsorption affinity for Cu^{2+}, Zn^{2+}, Ag^+ and Pb^{2+} metal ions was achieved through the complexation of metal ions by amino groups grafted on the silica-coated magnetite anoparticles. Also, the recoveries for the studied metal ions were quantitative (>94%).

Reference

[1] Sung, Y.H; Huang, S.D. *Anal.Chim. Acta*., **2003**, 495, 165–176.

Monitoring Environmental Contamination by Modified Graphene Nanoflakes

Akbar Omidvar[*], **Afshan Mohajeri**

Department of Chemistry, College of Sciences, Shiraz University, Shiraz, Iran

Akbar.omidvar.64@gmail.com

Introduction

The amount of toxic gases released into the atmosphere has enormously increased since the industrial development, improvement of quality of life, and transit mobility in the past decades which have dramatic consequences for both the environment and the public health [1]. Nitrogen oxide (NO) and nitrogen dioxide (NO_2) are common air pollutants that play major roles in the formation of ozone and acid rain [2]. The huge amounts of NO_2 released into the atmosphere everyday can cause fatal problems not only to human beings but also to animals and plants [3]. In this context, many researchers have focused on the development of sensor capable of monitoring these toxic gases [4,5]. The current study is devoted to explore the feasibility of using modified graphene nanoflakes (GNFs) for monitoring toxic gases.

Computational Methods

The model GNF used in our calculation is finite rectangular flake which is constructed of 60 C and 22 H atoms. All electronic structure calculations were performed at B3LYP/6-31+G(d) level using GAUSSIAN 09 suite of programs [6]. We considered the adsorptions of NO and NO_2 molecule on the pristine, edge-functionalized, doped and decorated GNFs. All possible configurations were considered and the most energetically stable one was identified in the light of adsorption energies.

Results and Discussion

In view of the interesting properties of graphene and the possibilities of tuning their electronic structures by various means for a host of applications, several chemical modification schemes have been proposed to enhance the device applicability of the graphene. In this work, besides the pristine GNF, we consider edge functionalization of GNF by -COOH and -OH functional groups, B-doping, N-doping, and also alkali metal decoration of GNF. It was found that NO and NO_2 adsorptions on the pristine GNFs are exothermic and favorable. Nonetheless, functionalized

GNF become more reactive toward NO_2 and greater energy is released upon adsorption process. In particular, hydroxyl functional group prompts both sensitivity and reactivity of the GNF. We have presented the density of states (DOS) curves to understand the type of interaction between gas molecules and functionalized GNFs. As obvious from Figure 1, the strong interactions cause dramatic changes in the DOS on both sides near the Fermi level (dotted lines). The shift of valence and conduction bands to lower and higher energies results considerable band gap opening.
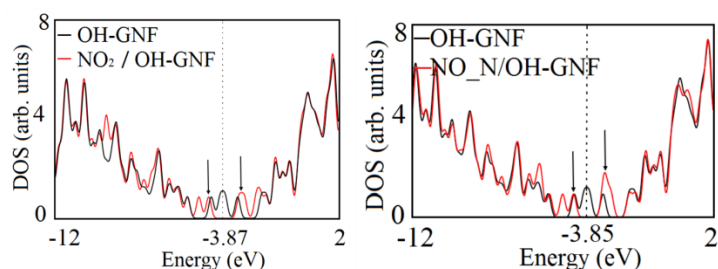
Figure 1. DOSs for the adsorption of NO_2 and NO on the GNF functionalized by hydroxyl group (black curves) and bare OH-GNF systems (red curves).

Significant enhancement of the gap between HOMO and LUMO sheet's which in turn suggests smaller electrical conductivity at a given temperature demonstrate high sensitivity of the electronic properties of functionalized GNF.

Conclusions

Chemical modification of graphene nanoflakes provides a promising route to improve their reactivity and sensitivity toward molecular adsorption as well as modify their electronic properties. Accordingly, the present work is devoted to investigate the effect of chemical doping and functionalization and metal decoration on the modification of electronic properties of GNF for adsorbing the toxic molecules such as NO and NO_2.

References

[1] A. M. Andringa; C. Piliego; I. Katsouras; P. W. M. Blom; D. M. Leeuw, *Chem. Mater.* **2014**, *26*, 773–785.
[2] D. Zhang; Z. Liu; C. Li; T. Tang; X. Liu; S. Han; B. Lei; C. Zhou, *Nano Lett.* **2004,** *4* 1919-1924.
[3] A. M. Andringaa; E. S. P. Smitsc; J. H. Klootwijkb; D. M. Leeuw, *Sensor Actuat. B-Chem.* **2013,** *181*, 668-673.
[4] A. Omidvar; A. Mohajeri, *Sensor Actuat. B-Chem.* **2014,** *202*, 622-630.
[5] A. Omidvar; A. Mohajeri, *RSC Advances,* **2015**, *5*, 54535-54543.
[6] M.J. Frisch; G.W. Trucks; H.B. Schlegel; G.E. Scuseria; M.A. Robb; J.R. Cheeseman; G. Scalmani, et al. Gaussian 09, Revision A.01, Gaussian, Inc., Wallingford CT,2009.

A link between the Net Analyte Signal and Duality

H. Abdollahi[a]*, N. Omidikia[a].S. Khalili Ali Abad[a],

[a]Department of Chemistry, Institute for Advanced Studies in Basic Sciences, Zanjan, 45195-1159, Iran
*abd@iasbs.ac.ir

Introduction

The well-known concept of the duality was introduced to chemometrics by Henry [1] and later it was generalized by Rajko for SMCR [2]. The duality concept provides a rigorous mathematical relationship between two spaces of a given bilinear data matrix, rows and column spaces.Net Analyte Signal (NAS) for a component is the part of its spectrum which is orthogonal to the subspace of interferences [3]. NAS divides data matrix to two parts; analyte and interferent(s) subspaces. Several methods were introduced for NAS calculation based on spectral or concentration information [4, 5]. In general, there are two main approaches to calculate NAS; Lorber and Schechter methods. In this contribution, analyte and interference subspaces were calculated equivalently based on NAS and duality. Finally, we link between NAS and duality concept. As duality bridges between rows and columns subspaces, NAS calculations can be implemented in terms of duality.

Methods

Let's suppose $R_{I, J}$ a bilinear data matrix. Singular-value decomposition resulted in:

$$\mathbf{R_{I \times J}} = \mathbf{U_{I \times F} D_{F \times F} V_{F \times J}^T} = \mathbf{X_{I \times F} V_{F \times J}^T} = \mathbf{U_{I \times F} Y_{F \times J}^T} \tag{1}$$

Where F is number of factors and $\mathbf{U}_{I, F}$ and $\mathbf{V}_{J, F}$ are left and right Eigen-vectors and $\mathbf{D}_{F, F}$ contains singular vectors. Duality between points in one space and hyper-planes in another space can be summarized as:

$$\text{V-space:} \quad \mathbf{X_{I \times F}} \text{ points} \qquad \mathbf{Y_{J \times F} D_{F \times F}^{-1} z_{F \times 1}} = \mathbf{V_{J \times F} z_{F \times 1}} \geq \mathbf{0_{J \times F}} \text{ hyperplanes} \tag{2}$$

$$\text{U-space:} \quad \mathbf{Y_{J \times F}} \text{ points} \qquad \mathbf{X_{I \times F} D_{F \times F}^{-1} z_{F \times 1}} = \mathbf{U_{I \times F} z_{F \times 1}} \geq \mathbf{0_{I \times F}} \text{ hyperplanes} \tag{3}$$

And $\mathbf{z_{f,1}}$ is a general variable.

For considered data, calculate subspace of analyte and interferent(s) by NAS algorithms as follows:

$$R_{I \times J} = R^k_{I \times J} + R^{-k}_{I \times J} = y_k s_k^T + R^{-k}_{I \times J} \tag{4}$$

$$R_{I \times J} \times F_{NAS} = F_{NAS} \times y_k s_k^T + F_{NAS} \times R^{-k}_{I \times J} \tag{5}$$

$$R^*_{I \times J} = y_k s^{*T}_k + 0 \tag{6}$$

Where $R^k_{I \times J}$ and $R^{-k}_{I \times J}$ are contribution of interest component and contribution of other component rather than interest component, F_{NAS} is filtering matrix and $R^*_{I \times J}$ and s^{*T}_k are NAS of data matrix and interest component, respectively. In both introduced main algorithm for NAS approaches, at first it is necessary to be available or obtain interferent(s) subspace and then NAS provides according NAS calculate procedure.

Experimental

Real data consist of three component system including three amino acids such as tryptophan, tyrosine and phenylalanine where subjected to NAS calculation for tryptophan's analyte with existing methods such as Lorber's and Schechter's approaches, and new introduced approach based on duality.

Results and Discussion

Subspace of interferents and NAS of interest component were calculated for real data by Lorber, Schechter's and duality approaches. Computed subspace of interferents based on Lorber's and Schechter's algorithm is exactly the same as subspace calculated based on duality. In Lorber's approach, spectra of tyrosine and phenylalanine utilized to calculate interferents subspace and then NAS of interest component evaluated by proposed algorithm. NAS matrix includes information about concentration of tryptophan analyte. Based on duality, pure spectra of interferents define a hyper-plane in U-space with coefficients equal to tryptophan's concentration coordination. Schechter's approach, interferents subspace calculated with concentration profile of tryptophan. After that, NAS evaluated by obtained interferents subspace. In similar manner, duality employed for data matrix to calculate interferents subspace with tryptophan concentrations. Coordinate of tryptophan concentration is the coefficients of a hyper-plane involving interferent subspace.

Conclusion

NAS based methods can be properly interpreted based on duality concept as a geometrical tool. In other words, duality is equivalence with NAS and both of these concepts try to separate analyte and interferents sub-spaces. Interferents subspace can easily obtain by duality with homologically required information in each method.

References

[1] R. C. Henry, "Duality in multivariate receptor models", Chemom. Intell. Lab. Syst. 2005, 77, 59– 63.

[2] R. Rajko, "Natural duality in minimal constrained self modeling curve resolution" *J. Chemom.* 2006, 20,164–169.

[3] A. Lorber, "Error Propagation and Figures of Merit for Quantification by Solving Matrix Equations", *Anal. Chem.* 1988, 58, 1167-1172

[4] A. Lorber, K. Faber., B. R. Kowalski. "Net Analyte Signal Calculation in Multivariate Calibration", *Anal. Chem*. 1997**,** 69, 1620-1626.

[5] I. Schechter; L. Xu. "A Calibration Method Free of Optimum Factor Number Selection for Automated Multivariate Analysis. Experimental and Theoretical Study", *Anal. Chem.* 1997**,** 69, 3722-3730.

Selective and sensitive determination of ultra-trace amounts of chromium (VI) by graphite furnace atomic absorption spectrometry after surfactant-assisted dispersive liquid-liquid microextraction based on the solidification of floating organic drop (SA-DLLME-SFO)

Ehsan Rostami* [a], Marzieh Sadeghi [a],
[a] Department of Chemistry, Razi University, Kermanshah, Iran
Corresponding author: Email: erostami1989@gmail.com

Introduction

Cr (VI) known as a carcinogenic and mutagenic substance for humans [1]. Therefore, there is a great need for reliable, selective, and sensitive procedures for chromium determination in biological but also industrial and environmental samples [2]. Dispersive liquid liquid microextraction (DLLME) belongs to one of the best liquid phase microextraction methods. Recently, surfactant-assisted DLLME (SA-DLLME) has been developed as a novel method for extraction of inorganic compounds from water samples [3]. In this work the possibility of implementation of SA-DLLME-SFO for trace metal determination was developed. The applicability of the approach was demonstrated for trace determination of chromium in water and food samples, with satisfactory results.

Extraction procedure

The optimum concentration of diethyl-dithiophosphate (DDTP as chelating agent) was added into the metal solution. Then the optimal amounts of surfactant (Triton X-114) were added into the solution and 45 µL of extractant (1-undecanol) was injected quickly into the solution by using a syringe and a cloudy solution was formed. The mixture was then centrifuged and dispersed fine droplets of the extraction phase were collected on the top of the conical test tube. Finally 10 µL of extraction solvent was analyzed by GFAAS.

Results and discussion

It was essential to examine the effect of all parameters that can probably influence the efficiency of extraction. Effects of the five factors (concentration of DDTP: Fig.1, Type and volume of 1-undecanol: Fig.2 and Fig.3, concentration of Triton X-114 and pH) on the extraction recovery of Chromium ions were examined.

a) **Effect of concentration of chelating agent**: Based on the results in Fig.1, a concentration of 0.03 % (v/v) DDTP was selected as the best choice to prevent any interference. **b) Effect of type and volume of extraction solvent:** The first step in the development of the SA-DLLME-SFO method was to select a proper extraction solvent. The results (Fig.2) show that 1-undecanol has the highest extraction recovery among the examined solvents. Therefore, 1-undecanol was chosen for further experiments. In order to study the effect of the volume of the extraction solvent on the performance of the presented SA-DLLME-SFO procedure, the volume of selected extraction solvent (1-undecanol) was varied in the range of 20–80 µL. As shown in Fig.3, 50 µL of 1-undecanol were used for further study. **c) Effect of Triton X-114**

and pH: Optimization of concentration of Triton X-114 and effect of pH were also investigated and optimums were used for further experiments.

Fig. 1 The effect of concentration of DDTP on the extraction recovery of Cr^{6+}. Extraction conditions: (sample solution, 5 mL of 1µg L^{-1} of Cr^{6+}; pH: 1; extraction solvent, 1-undecanol; extraction solvent volume, 50 µL; surfactant, Triton X-114; centrifugation time, 3 min at 5000 rpm)
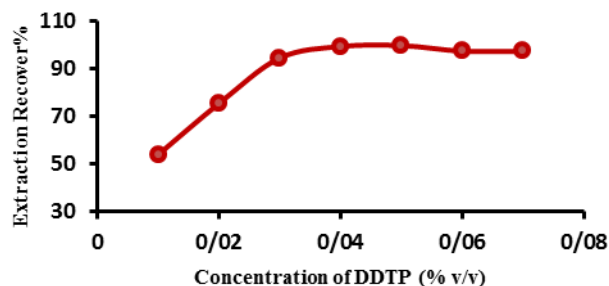
Fig. 2 The effect of organic solvent type on the extraction recovery of Cr^{6+}. Extraction conditions: (sample solution, 5 mL of 1 µg L^{-1} of Cr^{6+} the; pH: 1; surfactant, Triton X-114, 0.02 mmol L^{-1}; extraction solvent volume, 50µL; centrifugation time, 3 min at 5000 rpm).
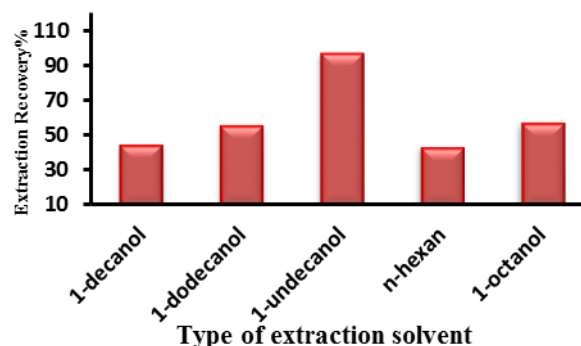
Fig. 3 The effect of volume of organic solvent on the extraction recovery of Cr^{6+}. Extraction conditions: (sample solution, 5 mL of 1 µg L^{-1} of Cr^{6+} the; pH: 1; extraction solvent, 1-undecanol; surfactant, Triton X-114, 0.02 mmol L^{-1}; centrifugation time, 3 min at 5000 rpm)
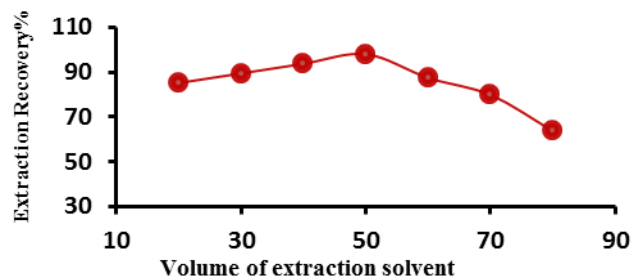
Conclusions

In this work, SA-DLLME-SFO has been described for the preconcentration analysis of Cr (VI) in water samples at sub-µg L^{-1} level. Generally the main advantages of this method are its simplicity of operation, low cost, high extraction recovery and environmental friendly, due to non-toxic and biodegradability of the surfactant solution used instead of the organic extraction solvents. The method has also good repeatability and reproducibility with low LODs.

Reference

[1]. Susan Sadeghi*, Ali Zeraatkar Moghaddam. RSC Adv., **2015**, 5, 60621–60629

[2]. Seyedeh Mahboobeh Yousefi, Farzaneh Shemirani*. Journal of Hazardous Materials, **2013**, 254–255, 134–140.

[3]. Mei-I. Leong, Ming-Ren Fuh, Shang-Da Huang*. Journal of Chromatography A, **2014**, 1335, 2–14.

Highly Efficient and Selective Protocol for the Direct Conversion of Alcohols into Azides using Ph_3P/I_2/[bmim]N_3

Somayeh Behrouz*

Department of Chemistry, Shiraz University of Technology, Shiraz 71555-313, Iran

E mail: behrouz@sutech.ac.ir

****

Introduction: Azides are versatile substrates in organic chemistry. They are useful precursors for the preparation of nitrenes, amines, and *N*-heterocyclic compounds [1, 2]. In the light of wide diversity, readily availability, ease of handling, and lower toxicity of alcohols in comparison with alkyl halides, the direct synthesis of alkyl azides from alcohols seems to be a suitable and attractive strategy. In this context, methods based on Mitsunobu conditions are widely used [3, 4]. To reduce the problems encountered in this methods, we wish to report a simple and highly efficient method for the direct conversion of alcohols into azides using Ph_3P/I_2 in the presence of [bmim]N_3 as a green source of azide and solvent (Scheme 1).

$$R-OH \xrightarrow[\text{r.t.}]{Ph_3P/I_2/[bmim]N_3} R-N_3$$
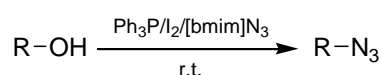
R= 1°, 2° and 3° alkyl
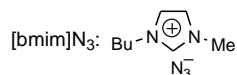
[bmim]N_3:

Scheme 1

Experimental: In a round bottom flask, it was added a mixture of Ph_3P, I_2 and alcohol in [bmim]N_3. The mixture was stirred at room temperature until TLC monitoring indicated no further improvement in the conversion. The reaction mixture was then dissolved in $CHCl_3$ and washed with water. The organic layer was dried and evaporated. The crude product was purified by short column chromatography on silica gel eluting with a mixture of *n*-hexane/EtOAc.

Results and Discussion: To optimize the reaction conditions, we chose the reaction of 2-phenylethanol with Ph_3P, I_2, and [bmim]N_3 at room temperature as a sample reaction. Initially, the effect of common organic solvents as well as several ionic liquids was studied on the sample reaction. The best results was acquired when the sample reaction was achieved in [bmim]N_3 as the green source of azide and solvent. Then, we investigated the influence of several reagents as positive-halogen sources in combination with triphenylphosphine. Thus, the use of Ph_3P/I_2 was found to be the most suitable reagent for this conversion.

With optimized reaction conditions in hand, we then explored the scope and versatility of the present protocol for the direct conversion of various structurally diverse alcohols into the corresponding azides. Various alcohols including primary, secondary and tertiary alcohols were efficiently converted into their alkyl azides in good to excellent yields. The generality of the method was confirmed with respect to allylic, benzylic, aliphatic, alicyclic and other alcohols containing *N*-heterocycles.

The selectivity of this method was demonstrated via a competitive reaction in a binary mixture of 2-phenylethanol and 1-phenylethanol under the optimized conditions. High selectivity for azidation of the primary alcohol rather than the secondary analogue was observed.

Conclusion: We have described a selective, convenient, and highly efficient protocol for the direct conversion of structurally diverse alcohols into the corresponding alkyl azides using $Ph_3P/I_2/[bmim]N_3$ at room temperature. The use of $[bmim]N_3$ as the green and safe source of azide and solvent, mild reaction conditions, ease of operation, and good to excellent yields of the product make this method attractive for the synthesis of structurally diverse alkyl azides.

References

[1] Bräse, S.; Gil, C.; Knepper, K.; Zimmermann, V. *Angew. Chem., Int. Ed.*, **2005**, *44*, 5188-5240.

[2] Scriven, E. F. V.; Turnbull, K. *Chem. Rev.*, **1988**, *88*, 297-368.

[3] Mitsunobu, O.; Wada, M.; Sano, T. *J. Am. Chem. Soc.*, **1972**, *94*, 679-680.

[4] Lee, S.-H.; Yoon, J.; Chung, S.-H.; Lee, Y.-S. *Tetrahedron*, **2001**, *57*, 2139-2145.

Synthesis and biological investigation of novel bis-Azo compounds

A. Sheykhi Estalkhjani[a], A. Yahyazadeh [b],[*], N. O. Mahmoodi [c],[*], M. Pasandideh[d]

[a] Department of Organic Chemistry, University of Guilan, PO Box 41335-1914, Rasht, Iran
chem8590@gmail.com

****

 Introduction: dye is used to impart color to materials of which it becomes an integral part of human life. The colour of dyes depends on their ability to absorb light in the visible range of electromagnetic radiation (400-700 nm). Azo dyes are the largest class of synthetic aromatic dyes composed with one or more (N=N) groups. Azo dyes account for the major produced synthetic dyestuffs because they are extensively used in the textile, leather, pharmaceutical and cosmetics industries, pose a threat for all life forms.

As a part of our ongoing investigation concerning the synthesis of some new bis-azo compounds. here we describe synthesis of some novel bis-azo derivatives under reflux condition in high yields.

Methods / Experimentals: In this procedure, A mixture of azo compound (2 mmol), Adipic acid dihydrazide (1 mmol) and p-TsOH as catalyst was solved in EtOH and The reaction mixture was heated under reflux for 10–15 h . progress of the reaction was monitored by TLC using n-hexane : ethylacetate (6 : 3). After completion of reaction, the precipitate formed was filtered and purified by column chromatography using petroleum ether and ethyl acetate as an eluant.

Results and Discussion: In continuous to our previous works in synthesis of azo compounds, here in we report one-pot synthesis of substituted bis-azo compounds in ethanol as solvent and p-TsOH as catalyst under reflux condition in high yields . In order to obtain optimum conditions of the reaction first , the reaction was performed without catalyst. Then the reaction was performed in the presence of p-TsOH , KSF, K10, and $ZnCl_2$ as catalyst and the best result obtained in the presence of 10 %mol of p-TsOH . H_2O, Ethanol,Chloroform and DMF were used as solvent , the results showed that Ethanol was an efficient solvent . All the synthesized compounds were characterized by TLC, Melting point and IR. Analysis indicated by the symbols of the elements is very close to the theoretical values.

Conclusion: Many synthetic processes are known for the production of Azo and its derivatives. In summary, This article has presented comprehensive details about synthesis of some new bis-Azo analogues in high yields. The Most important advantages of these methods are including the simplicity in the preparation procedure, easy work-up, excellent yields and eco-friendly procedure.

References
[1] N. O. Mahmoodi ; M. Pasandideh Nadamani; T. Behzadi. Journal of Molecular Liquids, 2013, 187, 43-48.
 [2] D. Xua ; Z. Lia ; Y.Penga ; J. Genga ; H.Qianb ; W. Huanga. Dyes and Pigments, 2016,133, 143-152.

Nickel-Catalyzed Oxidative Sterification of Formamides with 1,3-Dicarbonyl Compounds Under Mild Reaction Conditions

Dariush Saberi∗

Fisheries and Aquaculture Department, College of Agriculture and Natural Resources, Persian Gulf University, Bushehr 75169, Iran; E-mail: saberi_d@pgu.ac.ir.

Introduction: Cross-dehydrogenative coupling (CDC) reactions are a new version of coupling reactions in which two nucleophiles are combined together. These reactions are able to synthesize molecular complexity from simpler and safer precursors. In recent years, we witness a remarkable progress in applying CDC reactions in C–C and C–X bond formation [1-2]. Synthesis of enol carbamates via copper-catalyzed CDC reaction of formamides with β-dicarbonyl compounds have been previously reported [3-4]. We found out that Ni can be effective catalyst for this transformation (Scheme 1). When $NiCl_2$, a cheap and readily available salt, was used as catalyst, the above-mentioned reaction was performed under milder reaction conditions than copper.
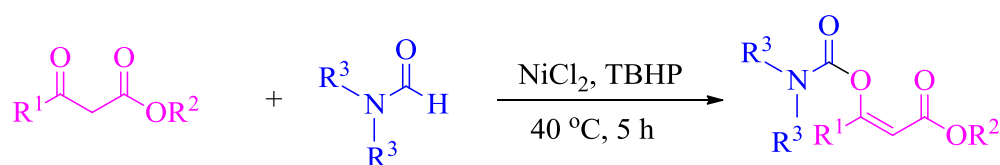
Scheme 1: Ni-catalyzed synthesis of enol carbamates

Methods / Experimentals: General procedure: TBHP (70 wt% in water, 4 equiv) was added dropwise to a mixture of 1,3-dicarbonyl compounds (1 mmol), $NiCl_2 \cdot 6H_2O$ (24 mg, 10 mol%) and formamide (2 mL) at 40 °C. After stirring for five hours, the reaction mixture was extracted with ethyl acetate and dried over anhydrous Na_2SO_4. Removal of the solvent under vacuum afforded the crude product, which was purified by plate chromatography to afford the desired product. All products were identified by recording IR, [1] H NMR, and ^{13}C NMR spectra.

Results and Discussion: Ethyl acetoacetate and DMF was selected as the model substrates to achieve the optimum reaction conditions. After screening the various parameters such as Ni salts, Oxidant, and temperature, optimum conditions was obtained as follows: 1,3-dicarbonyls (1 mmol), formamides (2 mL), TBHP (4 equiv) as oxidant, at 40 ºC under air atmosphere. In order to establish the scope of the procedure, a wide range of 1,3-dicarbonyl compounds were subjected to the reaction conditions. The results are shown in Figure 1.
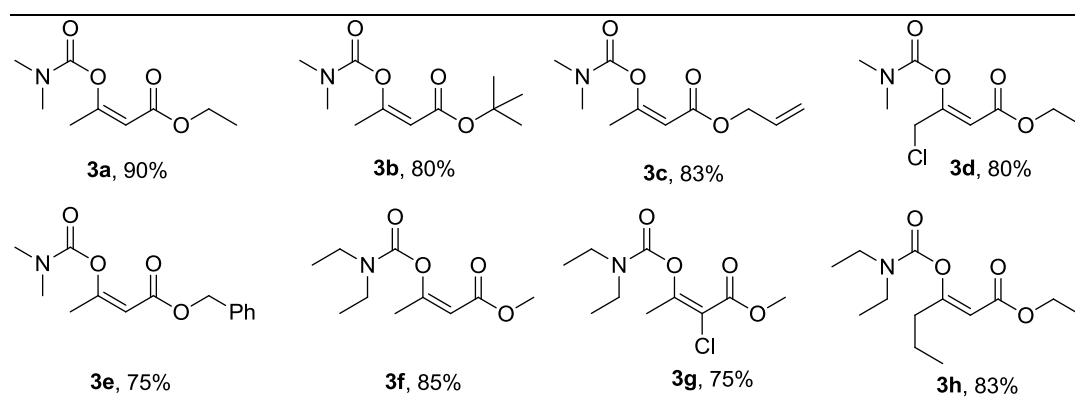
Figure 1: The structures of some synthesized enol carbamate

Generally speaking, the desired enol carbamates were obtained in high yields and the nature of the 1,3-dicarbonyl compounds and dialkyl formamides did not have any profound influence on the reactivity.

Conclusion: In summary we have developed a green protocol based on Ni-catalyzed oxidative sterification of 1,3-dicarbonyl compounds with formamides toward synthesis of enol carbamates under mild conditions. $NiCl_2$ was used as an effective, cheep, and readily available catalyst for this transformation. Various enol carbamates were synthesis in good to excellent yields.

 References

[1] J. A. Ashenhurst. *Chem. Soc. Rev.,* **2010**, *39*, 540-548.

[2] J. Miao; H. Ge, *Eur. J. Org. Chem.,* **2015**, 7859-7868.

[3] G. S. Kumar; C. U. Maheswari; R. A. Kumar; M. L. Kantam; K. R. Reddy. *Angew. Chem. Int. Ed.* **2011**, *50*, 11748-11751.

[4] B. D. Barve; Y.-C. Wu; M. El-Shazly; D.-W. Chuang; Y.-M. Chung; Y.-S. Tsai; S.-F. Wu; M. Korinek; Y.-C. Du; C.-T. Hsieh; J.-J. Wang; F.-R. Chang. *Eur. J. Org. Chem.,* **2012**, 6760-6766.

Synthesis and characterization of $ZnAl_2O_4$ and $ZnMn_2O_4$ nanoparticles as catalyst in the thermal decomposition of ammonium perchlorate

Nafise Modanlou Juibari, **Abbas Eslami**

Department of Inorganic Chemistry, Faculty of Chemistry, University of Mazandaran,
P.O.Box 47416-95447, Babolsar, Iran

Email address: nafisemodanlou@gmail.com

****

Introduction

Ammonium perchlorate (AP) is known as the most important oxidizer in solid composite propellants and its thermal decomposition plays an important role in the burning behavior of composite propellants [1]. Thermal decomposition of AP is very sensitive to various additives such as metal oxides, mixed metal oxides spinels [2] and other types of nanomaterials. In recent years, spinel nanostructures have attracted much attention for their use as catalyst in the thermal decomposition of ammonium perchlorate [3]. $ZnAl_2O_4$ nanoparticles have high chemical and thermal resistance, high mechanical stability, and low surface acidity [4], which make it suitable candidate for a variety of applications [5]. Zinc manganite ($ZnMn_2O_4$) is known as the most attractive spinel due to its low potential of oxidation and low material cost [6]. Studies on the optical and catalytic properties of zinc aluminate and zinc manganite nanoparticles were carried out by many researchers, but to the best of our knowledge there is no report, so far, on their catalytic effect on thermal decomposition of ammonium perchlorate

Experimental

$ZnAl_2O_4$: Zinc nitrate was dissolved in water and added into aqueous solution of aluminum nitrate. Then, aqueous solution of ammonia (25 wt. %) was added to the resulting solution, and the mixture was stirred until complete precipitation occurs at pH value of about 8.5. the powders then filtered, washed with distilled water, dried and calcined at 700 °C for 2h.

$ZnMn_2O_4$**:** $MnCl_2$ was added to 5.25 g citric acid which dissolved in 50 ml deionized water. Then, 1 g ZnO was added to above solution and heated at 80°C for 50 min. The colorless solution cooled to room temperature and subsequently 80 mL ethanol 96% was added to take precipitation. The suspension was filtered, washed with deionized water and ethanol, and dried at

1

80°C in an electric oven and calcined at 800°C for 2h. The synthesized nano powders mixed with AP at mass ratio of 97:3 to prepare the target samples for thermal analysis.

Results and discussions

The XRD pattern of $ZnAl_2O_4$ and $ZnMn_2O_4$ nanoparticles showed that all correspond to $ZnAl_2O_4$ (JCPDS Card No. 071-0968) and $ZnMn_2O_4$ (JCPDS file No.77–0470), respectively. The average particle size estimated by Debye-Scherrer equation was about 48 and 58 nm for $ZnAl_2O_4$ and $ZnMn_2O_4$, respectively. The catalytic effect of the synthesized spinel on thermal decomposition of AP was investigated by DSC and TGA analyses. The thermal decomposition of pure AP occurs through three sequential processes. Initially, an endothermic process takes place at around 250 °C which is assigned to the solid state phase transition from the orthorhombic phase to the cubic one. Then, a partial decomposition occurs exothermically at the temperatures around 300-330 °C. Finally, the last event, which is also an exothermic process and happens at the temperatures higher than 350 °C, is attributed to the complete decomposition of the intermediate product into volatile products. $ZnAl_2O_4$ nanoparticles have little effect on thermal decomposition of AP, but addition of nano zinc manganite has significant effect on both reduction of HTD temperature and increasing of released heat. Table 1 summarized the results of catalytic properties of synthesized samples.

Table. 1. The synthesis conditions and catalytic properties of prepared samples.

Sample	Additive	Metal/AP ratio	LTD/°C	HTD/°C	Released heat/Jg^{-1}
Pure AP	-	-	298	420	400
AP1	$ZnAl_2O_4$	3:100	294	405	736
AP2	$ZnMn_2O_4$	3:100	299	350	1130

Conclusion

In summary, two nano spinels of zinc were synthesized by co-precipitation method and have been examined as a catalyst for thermal decomposition of ammonium perchlorate. The catalysts were mixed with AP in 97:3 ratios and examined via DSC and TGA techniques. The DSC results showed that $ZnMn_2O_4$ nanoparticles have better catalytic effect than $ZnAl_2O_4$ nanoparticles.

References:
[1]   Boldyrev VV.Thermochim. Acta. 2006; 443(1):1-36.
[2]   Zhao S, Ma D, J. Nanomater. 2010; 2010:48.
[3]   Liu T, Wang L, Yang P, Hu B. Mater. Lett. 2008; 62(24):4056-58.
[4]   Nilsson M, Jansson K, Jozsa P, Pettersson LJ. Appl. Catal. B: Environ. 2009; 86(1):18-26.
[5]   Tzing WS, Tuan WH, J. Mater. Sci. Lett. 1996;15(16):1395-96.
[6]   Courtel FM, Duncan H, Abu-Lebdeh Y, Davidson IJ. J. Mater. Chem. 2011, 21(27):10206-18.

Determination of hesperidin in lemon juice samples by high performance liquid chromatography in order to detect adulteration

Zahra shafiei ,Afshin rajabi khorrami[*]

Department of chemistry, Karaj branch, Islamic Azad University, Karaj, Iran

Email address: chemafshin@gmail.com

****

Introduction: Lemon juice is one of those foods which has been cheated in its production from long times ago. For instance, the producers may mix rough straw with warm water and use of its essence, adding citric acid to watery lemon juice, or adding mineral acid and etc. are some ways of adulteration. Most of these adulterations is happening in the primary materials of foodstuff factories, and can make many problems for the controllers [1]. Flavonoids are a group of polyphenolic compounds with health related properties [2]. In general, flavonoids may contribute to fruit and juice quality in many ways, influencing the appearance, the taste and the nutritional value of the product from the plant [3].The aim of this research is to develop a reliable method to determine hesperidin in lemon juice samples as an indicator of adulteration.

Methods/Experimental: In this research, hesperidin extracted and purified by Soxhlet system from orange peels. Then it was identified and characterized by melting point, H^1 NMR and IR spectroscopy. The extracted hesperidin was used as standard for the next measurements. The chromatographic conditions were as follows: ODS column (250mm × 4.6mm), wavelength 280 nm, mobile phase composition $H_2O:CH_3CN:CH_3COOH$ (78:21:1, v/v) and a flow rate of 0.8 ml min^{-1}.

Result and Discussion: The concentration of hesperidin in lemon juice samples were determined by 5 replicate measurements using standard addition method (n=5). According to the Iran National Standard, the lemon juice should contain at least 80 mg per 1000 ml of hesperidin. Representative chromatograms after standard addition of standards to lemon juice are shown in Fig. 1. A typical calibration curve based on peak height of hesperidin is plotted by extrapolation method and is shown in Fig. 2. Six different commercial lemon juice samples from various brands and one natural sample of lemon juice were analyzed. Table 1 shows the concentration of hesperidin in the samples.
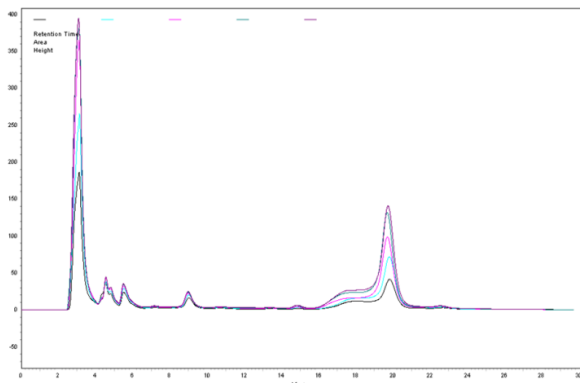
Fig. 1. Chromatograms of standard addition of hesperidin to a typical lemon juice
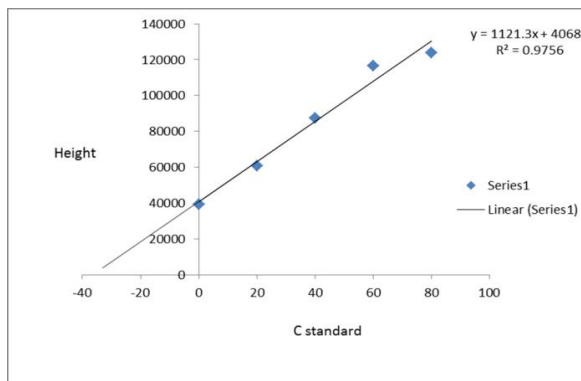
Fig. 2. Calibration curve of standard addition

Table 1. Hesperidin content in different lemon juice samples.

Samples	Equation	Concentration (mg per 1000 ml)
Lemon juice (natural)	y = 1121.3x + 40683	181.4585
Brand A (commercial)	y = 1129.2x + 26061	109.9048
Brand B (commercial)	y = 1470.9x + 4020	13.6735
Brand C (commercial)	y = 1583.2x + 3710.6	11.7183
Brand D (commercial)	y = 1049.9x + 8684.4	41.3918
Brand E (commercial)	No peak of hesperidin	N.D.
Brand F (commercial)	No peak of hesperidin	N.D.

N.D.: not detected

Conclusion: Flavonoids determination including hesperidin by HPLC and UV detection is a powerful technique to detect lemon juice adulterations. It can play a unique role as an easy and reliable detection tool for legal administrative/quality control laboratories. According to the obtained results, within six different commercial lemon juice samples one of them pass the limits of hesperidin compared to Iran National Standard. Thus, it seems a widespread adulteration in lemon juice production.

References

[1] P. Helmseresht, E. Delpishe, The principles of nutrition and food hygiene.The second edition, Tehran: print center Chehr Publishing, 1995: pages 231-229.

[2] M. Sato, N. Ramarathnam, Y. Suzuki, T. Ohkubo, M. Takeuchi, H. Ochi, Varietal Differences in the phenolic content and superoxide radical scavenging potential of wines from different sources, J. Agric. Food Chem. 44 (1996) 37–41.

[3] S. Mizrahi,; Z. Berk. Physio-chemical characteristics of orange juice cloud. J. Sci. Food Agric. 1970, 21, 250–253.

Tautomerization and intramolecular hydrogen bond strength of 1-(4-Chlorophenyl)-4,4,4-trifluorobutane-1,3-dione by quantum calculations and experimental spectroscopy

Vahidreza Darugar[a*] , Mohammad Vakili[a] , Raheleh Afzali[a]
[a]Department of Chemistry, Ferdowsi University of Mashhad, Mashhad 91775-1436, Iran
E-mail address: Vahidrezadarugar@stu.um.ac.ir (Vr. Darugar)   Tel.: +989352225197

****

Introduction : It is well known that the cis-enol forms of β-dicarbonyles are characterized by a strong intramolecular hydrogen bond (IHB)[1]. The molecular structure and IHB strength of 1-(4-Chlorophenyl)-4,4,4-trifluorobutane-1,3-dione (p-Cl-TFBA), an asymmetric β-diketone, have been investigated by quantum calculations and experimental methods such as vibrational spectroscopy and ^{1}HNMR spectroscopy. The theoretical results are compared with the experimental data. The obtained theoretical and experimental results will be compared with those for 4,4,4-trifluoro-1-phenyl-1,3-butanedione (TFBA) molecule.

Method / Exprimental : All quantum calculations have been done by Gaussian 09W[2] and AIM2000 [3] softwares.The molecular structure, IHB strength, and the zero point vibrational energy,ZPE, corrections of titled molecule have been investigated by (DFT) calculations at the B3LYP/6-311++G** level [4,5].
The Far-IR spectra in the 500–200 cm^{-1} region were collected employing a Thermo Nicolet NEXUS 870 FT-IR spectrometer. The spectra were collected with a resolution of 2 cm^{-1} by averaging the results of about 60 scans.

Result and Discussion : Two stable cis-enol forms can be drawn for p-Cl-TFBA and TFBA, the structure and their relative stabilities, calculated at B3LYP/6-311++G** level of theory, are show in Fig.1. The relative stabilities for the cis-enol forms of TFBA is a little more than that in p-Cl-TFBA. The theoretical and experimental parameters related to IHB strength for p-Cl-TFBA and TFBA are listed in Table 1. According to this table the IHB strength of p-Cl-TFBA is about the TFBA.
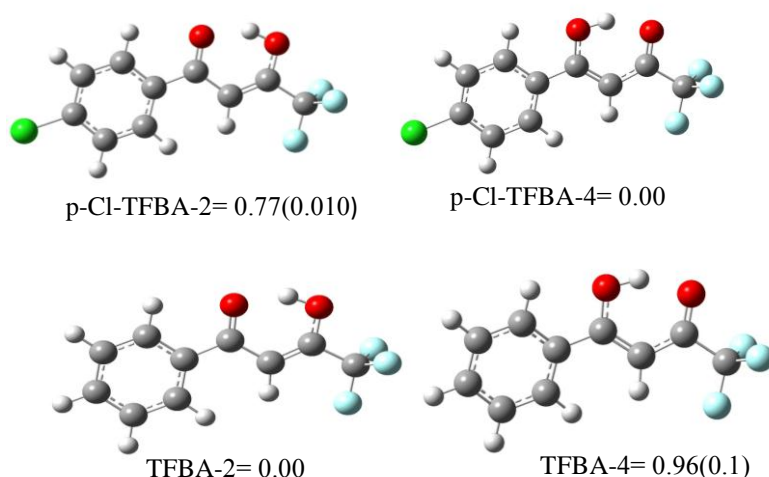

p-Cl-TFBA-2= 0.77(0.010)   p-Cl-TFBA-4= 0.00

TFBA-2= 0.00   TFBA-4= 0.96(0.1)

Fig.1: Two stable cis-enol forms of p-Cl-TFBA and TFBA and their relative stabilities.

Table 1: Comparison between several properties related to the hydrogen bond strength for TFBA and p-Cl-TFBA.[a]

	p-Cl-TFBA			TFBA		
	p-Cl-TFBA-2	p-Cl-TFBA-4	Avg(Exp.)	TFBA-2	TFBA-4	Avg(Exp.)
δOH(in ppm)	15.96	15.88	15.92(15.00 [b])	16.06	15.83	15.94(15.06 [c])
ϑOH (in cm^{-1})	3050	3072	3061	3037	3051	3044(2870)
γOH(in cm^{-1})	926	918	922(894)	929	937	933(895)
RO...O (in Å)	2.526	2.538	2.532	2.525	2.540	2.530
RO...H (in Å)	1.624	1.628	1.626	1.621	1.630	1.625
R−OH (in Å)	1.004	1.001	1.002	1.006	1.001	1.004
<OHO (in °)	146.9	148.7	147.8	147.0	148.8	147.9
E_{HB} (in kcal/mol)[d]	18.7	18.2	18.4	19.0	18.1	18.5
ρ_{BCP}(in au^{-3}.)	0.058	0.057	0.058	0.059	0.057	0.058
$\nabla^2\rho_{BCP}$(in au^{-5}.)	-0.1483	-0.1485	-0.1484	-0.1488	-0.1481	-0.1484

[a] All calculated at the B3LYP/6-311++G**level, the experimental values are in parenthesis.
[b]Data from Ref. [6].
[c] Data from Ref. [7].
[d]E_{HB} is the IHB energy in kcal/mol, according to Espinosa et al. suggestion [7].

Conclusion : The Cl substitution in the para position decreses the relative energy between two stable cis-enol forms. According to the theoretical calculations and spectroscopic results, the hydrogen bond strength of p-Cl-TFBA do not significantly change compared with that in TFBA. Also the following trend in IHB strength for two cis-enol forms of p-Cl-TFBA is: p-Cl-TFBA-2 > p-Cl-TFBA-4

References
[1] S.F.Tayyari; M.Vakili; A.R.Nekoei; H.Rahemi; Y.A.Wang.SpectrochimicaActa Part A, **2007**, 66, 626–636.
[2] FrischMJ et al. 2009 Gaussian 09, Revision A.02-SMP,Gaussian, Inc., Wallingford CT.
[3] Biegler-König F and Schönbohm J AIM2000 Version 2.0.
[4]A.D. Becke, J. Chem. Phys. **1993**, 98, 5648–5652.
[5]C. Lee, W. Yang, R.G. Parr, Phys. Rev. **1988**, 37B, 785–789.
[6] A.E.Cotman, D. Cahard, B. Mohar, Angewandte Chemie International Edition, **2016**, 55, 17, 5294-5298.
[7]E. Espinosa, E. Molins, C. Lecomte, Chem. Phys. Lett. **1998**, 285, 170–173.

Immobilized Lanthanum (III) triflate on graphene oxide as a novel multifunctional heterogeneous catalyst for a tandem reaction

Sara Sobhani,* Farzaneh Zarifi

Department of Chemistry, College of Sciences, University of Birjand, Birjand

ssobhani@birjand.ac.ir, sobhanisara@yahoo.com

Introduction: The combination of acid and base catalysts for tandem reactions is known as the most attractive approach in organic synthesis [1]. Apparently, the coexistence of acidic and basic functions in a homogeneous system is impossible due to the neutralization reaction that forms inactive salts. Fascinatingly, a heterogeneous multifunctional catalyst could address this challenge by spatially isolated incompatible active organic groups, avoiding their mutual deactivation in so-called "wolf-and-lamb" reactions [2]. Hosting of both acids and bases on solid surfaces often requires complicated synthetic methods including tedious protection-deprotection [3]. Therefore, design of a simple synthetic approach for the preparation of multifunctional catalysts is a challenge in organic catalysis.

Methods/Experimental:

La(OTf)$_3$ was added to the dispersed Schiff base supported on amine grafted GO in acetonitrile and stirred at room temperature for 24 h. The solid was centrifuged, washed with acetonitrile and dried to give La(OTf)$_2$-grafted-GO.

A mixture of La(OTf)$_2$-grafted-GO (0.5 mol%), ethyl acetoacetate (2 mmol) and phenyl hydrazine (2 mmol) was stirred at 100 °C for 5 min. Then aldehyde (1 mmol) was added to the reaction mixture and stirred for the appropriate reaction time. EtOH was added to the reaction mixture and the catalyst was separated by centrifugation. Then water was added to the organic solution and the precipitated product was separated by filtration in high purity.

Results and Discussion: Immobilized Lanthanum (III) triflate on graphene oxide as a new multifunctional heterogeneouse catalyst was synthesized by a simple procedure. At first, the condensation of salicylaldehyde with amine grafted GO produced a Schiff base supported on amine grafted GO (Schiff base-GO). Then the reaction of lanthanum (III) triflate [La(OTf)$_3$] with Schiff base-GO in dry acetonitrile led to the formation of La(OTf)$_2$-grafted-GO. The chemical nature of immobilized Lanthanum (III) triflate on amine grafted graphene oxide [La(OTf)$_2$-grafted-GO] was revealed by FT-IR, XPS and solid-state MAS NMR (Figure 1a). The morphology and distribution of elements on La(OTf)$_2$-grafted-GO was determined by FESEM, TEM and EDS images. The amount of anchored lanthanum on 1.0 g of La(OTf)$_2$-grafted-GO was determined by ICP analysis. La(OTf)$_2$-grafted-GO employed as the first reusable multifunctional catalyst for the efficient one-pot five-component condensation reaction of

phenylhydrazine, ethyl acetoacetate and arylaldehydes. Due to the homogeneous distribution of the active sites along with the crumpling structure of the catalyst, reactants and products can easily access or leave the active sites on both sides of the two-dimensional catalyst with limited mass transfer resistance. These properties increase the catalytic activity of La(OTf)$_2$-grafted-GO. Meanwhile, it could be easily recycled and reused repetitively. The morphology and structure of La(OTf)$_2$- grafted-GO remained intact after five recoveries according to the FT-IR spectrum and TEM image of the used catalyst (Figure 1b and c).
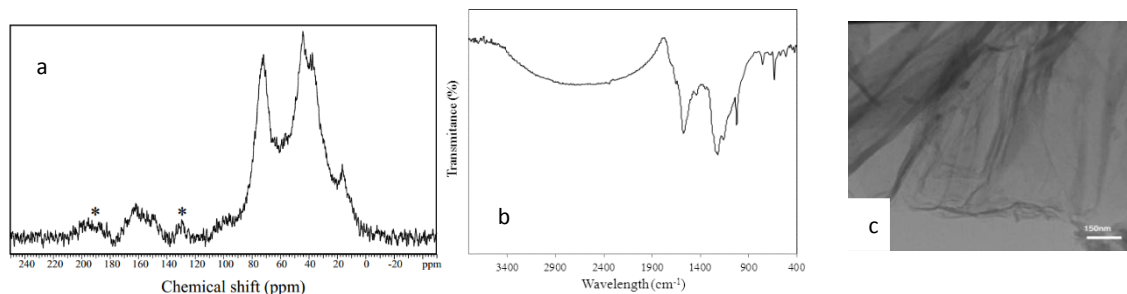
Figure 1. a) ^{13}C CP MAS NMR spectra of La(OTf)$_2$-grafted-GO, b) FT-IR spectrum and c) TEM image of La(OTf)$_2$-grafted-GO after five times reuse.

Conclusion: In this work, immobilized Lanthanum (III) triflate on graphene oxide as a new multifunctional heterogeneous catalyst was synthesized. Systematic characterizations demonstrated that active sites were readily introduced on the surface of graphene oxides with homogeneous distribution. Notably, the synthesized multifunctional catalyst showed superior catalytic performance and synergistic catalytic effects in the one-pot five-component condensation reaction of phenylhydrazine, ethyl acetoacetate and arylaldehydes as a tandem reaction. It was easily recycled and reused repetitively.

References

[1] (a) Ma, J.-A.; Cahard, D. *Angew. Chem.* **2004**, *116*, 4666-4683; *Angew. Chem. Int. Ed.* **2004**, *43*, 4566-4583. (b) Wang, Y.; Li, H.; Wang, Y.-Q.; Liu, Y.; Foxman, B. M.; Deng, L. *J. Am. Chem. Soc.* **2007**, *129*, 6364-6365.

[2] Gelman, F.; Blum, J.; Avnir, D. *J. Am. Chem. Soc.* **2002**, *124*, 14460-14463.

[3] (a) Huang, Y. L.; Xu, S.; Lin, V. S. *Angew. Chem., Int. Ed.* **2011**, *50*, 661-664. (b) Motokura, K.; Tada, M.; Iwasawa, Y.J. *Am. Chem. Soc*. **2007**, *129*, 9540-9541.

Synthesis of Novel Nanostructured Pyrazine Molten Salt and its Application in the Synthesis of Pyridine derivatives

Mohammad Ali Zolfigol[a]*, Maliheh Safaiee[b]*, Bahar Ebrahimghasri[a], Saeed Baghery[a], Saied Alaie[a], Mahya Kiafar[a], Avat (Arman) Taherpour[c,d], Yadollah Bayat[e], Asiye Asgari[e]

a Department of Organic Chemistry, Faculty of Chemistry, Bu-Ali Sina University, Hamedan 6517838683, Iran
b Department of Medicinal Plants Production, Nahavand University, Nahavand, 6593139565, Iran.
c Department of Organic Chemistry, Razi University, Kermanshah, P.O. Box: 67149-67346, Iran.
d Medical Biology Research Center, Kermanshah University of Medical Sciences, Kermanshah, Iran.
e Faculty of Chemistry and chemical Engineering, Malek Ashtar University of Technology, Tehran, Iran

E-mail: *zolfi@basu.ac.ir, mzolfigol@yahoo.com (M.A. Zolfigol) and azalia_s@yahoo.com (M. Safaiee).*

****

Introduction:

Molten salts and ionic liquids are both liquids mainly composed of ions. ILs and MSs are defined as those fused salts with a melting point less than 100 °C, with salts with higher melting points mentioned to as molten salts [1]. Also, the anomeric effect is a fundamental concept, which includes an interaction between the lone pair electrons of heteroatom and the anti-bonding orbitals of adjacent bonds and can control reaction mechanism. In this regard, a new term "anomeric based oxidation" is introduced for unusual hydride releasing from crabon [2], [3]. Therefore we decided to design and synthesize a novel, task-specific MSs for synthesis of 2-Amino-3,5-dicarbonitrile-6-sulfanylpyridine derivatives *via* Anomeric Based of Oxidation mechanism.

Methods/experimaentals: In the first step, nano pyrazine molten salt catalyst was synthesized. Then the pyridine derivatives were prepared using this catalyst. The progress of the reaction was monitored by TLC and after completion of the reaction, the catalyst was separated from the reaction mixture to be used again for another reaction. The products were washed and then recrystallized from an appropriate solvent. Finally the synthesized catalyst and products were characterized by different analysis.

Results and discussion: In continuation of our previous investigation related to the knowledge-based development of task-specific nanostructured ionic liquids (NILs), molten salts (NMSs) and their applications in multi component reactions (MCRs)[4], we wish to report the synthesis of a novel task-specific nanostructured pyrazine molten salt (NPMS) .The catalytic application of the described NPMS in the synthesis of 2-amino-3,5-dicarbonitrile-6-sulfanylpyridines *via* the one-pot condensation reaction between aromatic aldehydes, malononitrile and benzyl mercaptan at room temperature and solvent-free conditions were examined.
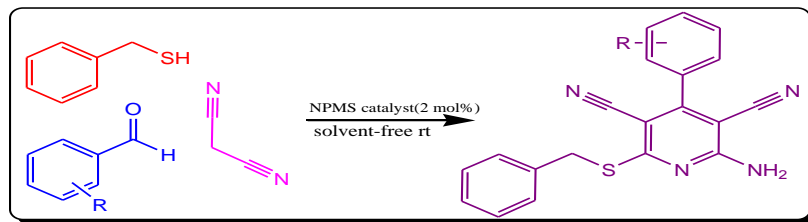
Scheme 1: Synthesis of 2-amino-3,5-dicarbonitrile-6-sulfanylpyridines using NPMS as a catalyst
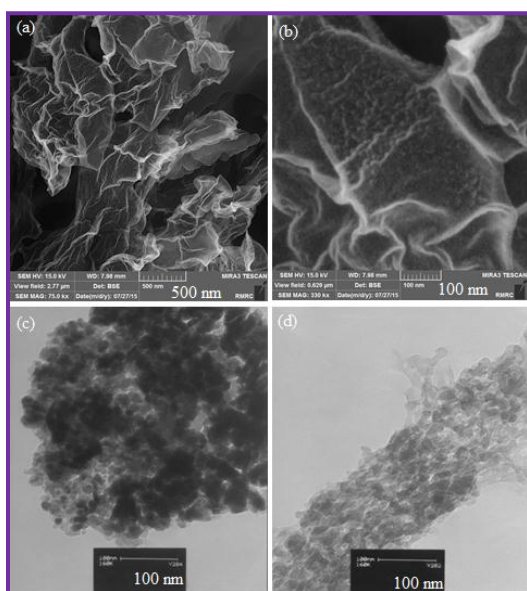

Figure 1: Scanning electron microscopy (SEM) (a and b) and transmission electron microscopy (TEM) (c and d) of the catalyst

Conclusion: A task-specific nanostructured molten salt was designed and characterized. Its catalytic application was investigated in the synthesis of 2-amino-3,5-dicarbonitrile-6-sulfanylpyridines. Numerous advantages of this study are relatively cleaner reaction profile, simplicity of product isolation, low cost, high yield, short reaction time, reusability of the NMS catalyst and agreement with the green chemistry disciplines.

References

[1] T.L. Greaves, C.J. Drummond, *Chem. Rev.* **2008**, *108*, 206-237.

[2] Zolfigol, M. A; Afsharnadery, F; Baghery, S; Salehzadeh, S; Maleki, F. *RSC Adv*, **2015**, 5, 75555-75568.

[3] Zolfigol, M. A; Safaiee, M; Afsharnadery, F; Bahrami-Nejad, N; Baghery, S; Salehzadeh, S; Maleki, F. *RSC Adv*, **2015**, 5, 100546- 100559.

[4] (a) Moosavi-Zare, A. R; Zolfigol, M. A; Khakyzadeh, V; Böttcher, C; Beyzavi, M. H; Zare, A; Hasaninejad, A; Luque, R. *J. Mater. Chem. A*, **2014**, 2, 770-777. (b) Zolfigol, M. A; Baghery, S; Moosavi-Zare, A. R; Vahdat, S. M, *RSC Adv*. **2015**, 5, 32933- 32940. (c) Zolfigol, M. A; Baghery, S; Moosavi-Zare, A. R; Vahdat, S. M; Alinezhad, H; Norouzi, M. *RSC Adv*, **2015**, 5, 45027-45037. (d) Zolfigol, M. A; Baghery, S; Moosavi-Zare, A. R; Vahdat, S. M; Alinezhad, H.; Norouzi, M. *RSC. Adv*, **2014**, 4, 57662-57670. (e) Ghorbani, M; Noura, S; Oftadeh, M; Gholami, E; Zolfigol, M. A. *RSC Adv*, **2015**, 5, 55303-55312; (f) Zolfigol, M. A; Baghery, S; Moosavi-Zare, A. R; Vahdat, S. M. *J. Mol. Catal. A. Chem*, **2015**, 409, 216-226.

One-Pot Synthesis of Polyhydroquinoline Derivatives Using Cross-linked Poly(4-vinylpyeidine) Supported Ferric Chloride

Mohammad Ali Karimi Zarchi[a *], Hormoz pourtaher[a]

[a] Department *of Chemistry, College of Science, Yazd University, P. O. Box 89195-741, Yazd, Iran.*

• Corresponding authors: Tel: +98-351-8211670-9; FAX: +98-351-8210644, *E-mail address*:
makarimi@yazd.ac.ir

****

Introduction:
1,4-Dihydropyridines were synthesized more than a century ago by Hantzsch by heating a mixture of an aldehyde, a β-ketoester and ammonia in ethanol under reflux conditions for several hours [1]. Recently, much attention has been directed toward the multicomponent synthesis of 1,4-dihydropyridyl compounds because of a variety of biological activities such as Ca^{2+} channel blockers [2].

In recent years heterogeneous catalysts have attracted a great attention due to efficiency, economic and environmental considerations, cross-linked Poly(4-vinylpyeidine) supported catalyst is an important heterogeneous catalyst used in various chemical transformations, such as cross-linked Poly(4-vinylpyeidine) supported copper sulfate/sodium ascorbate for one-pot three-component synthesis of 1,4-disubstituted 1H-1,2,3-triazoles [3]. In continuation of our work [3,4] on the applications of heterogeneous catalysts on organic transformations we report here a convenient and efficient method for the synthesis of polyhydroquinoline (containing 1, 4-dihydropyridine moiety) using cross-linked poly(4-vinylpyeidine) supported ferric chloride as a reusable heterogeneous catalyst.

Methods/Experimental:
All chemical reagents were purchased from Fluka, Aldrich, or Merck (Germany) chemical But, $[P_4\text{-VP}]\text{-FeCl}_3$ was prepared in our laboratory. The progress of the reaction was monitored by thin-layer chromatography (TLC) with silica gel PolyGram SIL G/UV 254 plates. All of the products were characterized by Fourier transform infrared (FT-IR) and nuclear magnetic resonance (NMR).

A mixture of an aromatic aldehyde (1mmol), ethyl acetoacetate (1mmol), ammonium acetate (1.5 mmol), dimedone (1mmol), $[P_4\text{-VP}]\text{-Fecl}_3$ (0.10 g) in ethanol (5 ml) was heated under reflux conditions. The progress of the reaction was monitored by TLC. After completion the reaction, the mixture was fi1tered and the catalyst was recovered from the residue by washing with EtOH (3 × 5 mL). Then, the reaction mixture was cooled to room temperature and scratched. The solid product was appeared and then filtered and recrystallized from ethanol to give polyhydroquinolines in good to high yields (88-95%).

Results and Discussion:
$[P_4\text{-VP}]\text{-FeCl}_3$ was easily prepared according our procedure and used as an efficient and reusable catalyst for synthesis of polyhydroquinolines (Scheme 1).
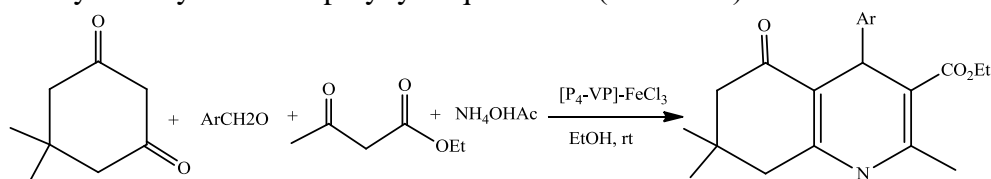
Scheme 1

In order to be able to carry out such a reaction in a more efficient way, 4-chlorobenzaldehyde (1mmol), ethyl acetoacetate (1mmol), ammonium acetate (1.5 mmol), dimedone (1mmol), as the model substrates and some experimentation regarding reaction time, reaction temperature, the amount of catalyst and possible solvents were run and the results are summarized in Table 1.

Table1: Optimization of the reaction conditions for the model reaction

Entry	Temp	Solvent	Cat. Amount (g)	Time (min)	Yield (%)[a]
1	80	EtOH	0.10	150	95
2	80	$CHCl_3$	0.10	380	60
3	80	MeOH	0.10	220	75
4	80	CH_3CN	0.10	190	55
5	80	CH_2Cl_2	0.10	370	55
6	60	EtOH	0.10	200	82
7	70	EtOH	0.10	170	89
8	80	EtOH	010	150	95
9	90	EtOH	0.10	150	94
10	80	EtOH	0.08	250	70
11	80	EtOH	0.09	180	89
12	80	EtOH	0.10	150	95
13	80	EtOH	0.110	150	95

[a] Isolated yield

Under optimized reaction conditions, different aromatic aldehydes were investigated and the results are summarized in Table 2.

Table 2: One-pot synthesis of polyhydroquinolines using $[P_4\text{-VP}]\text{-FeCl}_3$

Entry	Aldehyde	Reaction time (min)	Yield (%)
1	Ph	140	90
2	$O\text{-}NO_2C_6H_4$	150	22
3	$P\text{-}NO_2C6H_4$	155	95
4	$O\text{-}ClC_6H_4$	140	94
5	$O\text{-}OmeC_6H_4$	145	88

Conclusion:
In conclusion, we have demonstrated a simple and efficient procedure for the synthesis of polyhydroquinolines using $[P_4\text{-VP}]\text{-Fecl}_3$ as a reusable catalyst. The main advantages of this method over other reported methods are: (a) operational simplicity, (b) short reaction times, (c) high yields of products, and (d) the use of relatively non-toxic and reusable catalyst and solvents.

References:
[1] Hantzsch, A. *Ann. Chem.*, **l882**, *215*, 1-82.
[2] Mannhold, R; Jablonka, B; Voigdt, W; Schoenafinger, K; Schravan, K. *Eur. J. Med. Chem.* **1992**, *27*, 229-235.
[3] Karimi Zarchi, M. A; Nazem, F. *J. Iran. Chem. Soc.*, **2014**, *11*, 1731–1742.
[4] Karimi Zarchi, M. A;Banihashemi, R. *J. Sulfur Chem.* **2016**, *37*, 282-295.

Synthesis of 3-(4-Aroyl-3-bromo-4,5-dihydroisoxazol-5-yl)-4*H*-chromen-4-ones *via* Nitrile Oxide Cycloaddition

Reza Rezaiyehrad[a], Atefeh Roosta[a], Abdolali Alizadeh[a],*

[a]Department of Chemistry, Tarbiat Modares University, P.O. Box 14115-175, Tehran, Iran

aalizadeh@modares.ac.ir

Introduction:

The 4*H*-chromen-4-one scaffold and the isoxazole ring are structure a privileged parts that found in an important class of oxygen-containing heterocycles. These compounds have shown a variety of biological and pharmaceutical activities such as antitumor, anti-inflammatory, anticonvulsant, antituberculosis, antiviral, antihepatotoxic, antioxidant, antispasmolytic, and antibacterial activities [1-3].

Herein, we report a suitable method for synthesis of 3-(4-aroyl-3-bromo-4,5-dihydroisoxazol-5-yl)-4*H*-chromen-4-ones **5** *via* 1,3-dipolar cycloaddition and wittig reaction.

Methods / Experimentals:

Chemicals were purchased from Merck and Aldrich chemical companies and were used without further purification. Melting points were determined using an Electrothermal 9100 apparatus. The IR spectra were performed with a NICOLET FT-IR 100 spectrometer. Mass spectra were recorded on Agilent technologies 5975C spectrophotometer. The NMR spectra were obtained using Bruker Advance DRX-500 in CDCl$_3$.

Results and Discussion:

3-(4-aroyl-3-bromo-4,5-dihydroisoxazol-5-yl)-4*H*-chromen-4-ones **5** were synthesized by reaction between nitrile oxide **4** and (*E*)-3-(3-oxo-3-arylprop-1-en-1-yl)-4*H*-chromen-4-ones **3** that were obtained from treatment of 3-formyl-4*H*-chromen-4-ones **1** with wittig reagents **2**, at roomtemperature in DCM (Scheme 1).
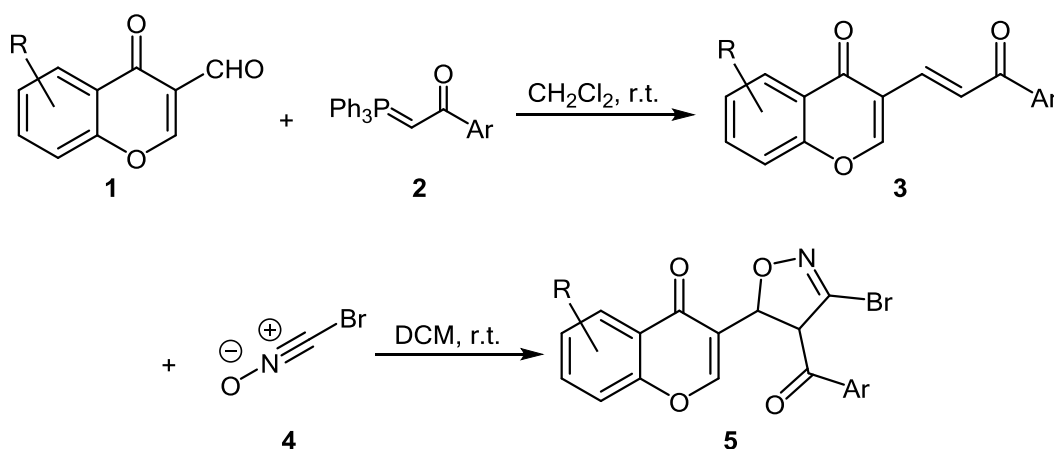
Scheme 1.

The products were purified by column chromatography with nHexane/EtOAc (4/1). The melting point of the product **5a** (R=H, Ar=Ph) was 142-144 °C. The mass spectra showed the molecular ion in 398 m/z. the ^{1}H NMR spectrum of **5a** exhibited one doublet and one doublet of doublet (δ= 5.42 and 6.04 ppm, J= 7.5, and 7.5 and 1.1 Hz, respectively) for the hydrogens of isoxazole ring. The protons of the 4H-chromen-4-one scaffold were appeared in the range of 7.42-8.24 ppm. The ^{13}C NMR spectrum of **5a** showed characteristic signals at 192.9 and 176.5 (the carbonyl groups), at 64.2, 84.2 and 134.5 (the carbon atoms of isoxazole ring), at 129.1, 129.5, 134.5 (for the phenyl ring), and the eight peak at 118.5, 121.1, 123.8, 125.8, 129.5, 134.5, 135.5, 135.8, 153.8, 156.6 (for the 4H-chromen-4-one moiety) ppm (Scheme 2).
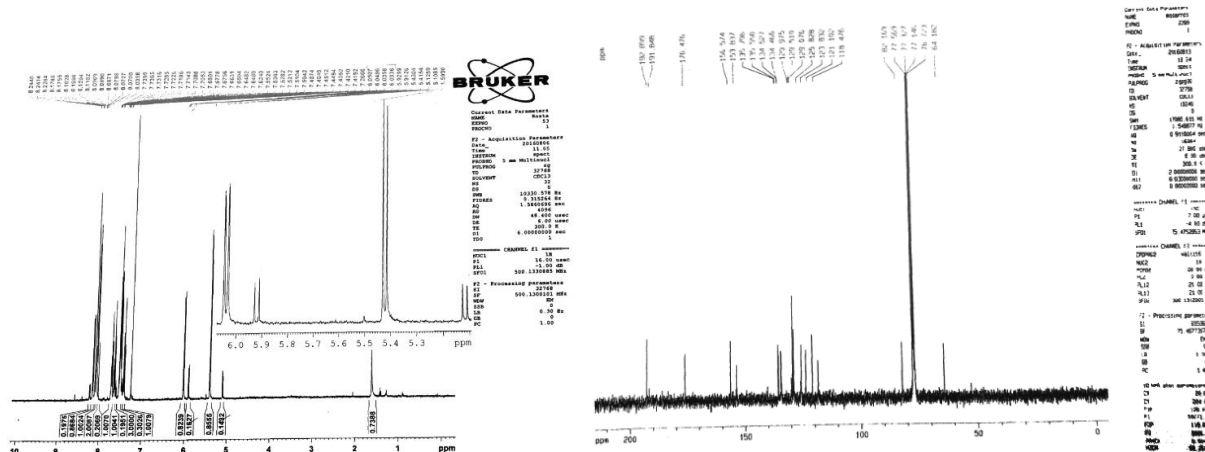
Scheme 2.

Conclusion:

In summary, we introduced a suitable synthesis method for the preparation of 3-(4-aroyl-3-bromo-4,5-dihydroisoxazol-5-yl)-4H-chromen-4-ones in excellent yields. The mild condition of the reaction and the simple operation are the main advantages of this reaction.

References

[1]. Magdy, A. I.; Tarik, E. A.; Youssef, A. A.; Yassin, A. G. *ARKIVOC*, **2010**, *(i)*, 98-135.

[2]. Ahad, A.; Farooqui, M. *Iranian Journal of Organic Chemistry*, **2016**, *8*, 1685-1691.

[3]. Kesornpun, C.; Aree, T.; Mahidol, C.; Ruchirawat, S.; Kittakoop, P. *Angewandte Chemie International Edition*, **2016**, *55*, 3997–4001.

Sulfur Doping on the Edge of Graphdiyne: Theoretical Prediction

Afshan Mohajeri[*]**, Azin Shahsavar**

Department of Chemistry, College of Sciences, Shiraz University, Shiraz, Iran

E-mail: amohajeri@shirazu.ac.ir.

Introduction

Graphdiyne a new carbon allotrope first time was discovered on 1997 and successfully synthesized by Baughman on copper surface that suggested as tremendous carrier for batteries. To achieve higher capacity, surface modification such as functionalization and doping, especially on reactive atoms on edges, has been introduced. In a recent publication, we have suggested edge oxygenated graphyne and graphdiyne as promising candidates for storage and sensors application [1].Yun et al proposed sulfur doped graphene to gain extra capacity into Li batteries [2]. With the aim of proposing new and efficient hydrogen carrier, we have modified graphdiyne by S-doping on the edges.

Methods

Our model graphdiyne (GDY) contains 90 carbon atoms which terminated by hydrogen on the edges to prevent boundary effect as shown in Figure 1. All calculations were carried out at PBE/6-31G(d) level as implemented in Gussian09 suit of programs [3]. Cohesive energies were calculated by $E_{coh} = (E_{tot} - \sum_i n_i E_i)/N$ where E_{tot}, n, i and N are the total energy of isosurfaces, number of each specific atom (C, H and S) and total number of atoms on surface respectively.

Results and Discussion

Considering verified effectiveness of sulfur doping on carbonic surfaces, we study effect of S-dopant concentration on the graphdiyne edges. Zhou and coworkers proved thionc S on the edges of graphene leads to higher efficiency for Li-S batteries [4]. Accordingly we studied doping with thionic S and varied the concentration of dopant from 5.5% to 33.3%. Calculated cohesive energy shows negligible increment trend on stability of isosurfces in higher level of sulfur. Along increasing the dopant concentration shifts the Fermi energy to lower energy and p-type semiconductors produced. This leads to energy gap reduction that is essential to achieve higher reactivity. In order to get clear insight into electronic structures the project density of state (PDOS) and total density of state (TDOS) for S-doped GDY illustrated on

Figure 2. The sulfur introduces states is in range of ~ -4.5_-5.5 eV on the valance region and leads to slightly down shift of Fermi energy level as indicated by dashed line.

Conclusion

In the current work, edge engineering surfaces by varying the concentration of S-dopant on the graphdiyne nanoflake has been explored. The result indicates better efficiency of system at higher S-dopant levels which is obvious from the energy gap reduction from 1.49 eV for GDY to 0.59 eV for S-doped GDY(33.3%) (see Table 1). The modified surfaces can be introduced as capable host for hydrogen storage devices.
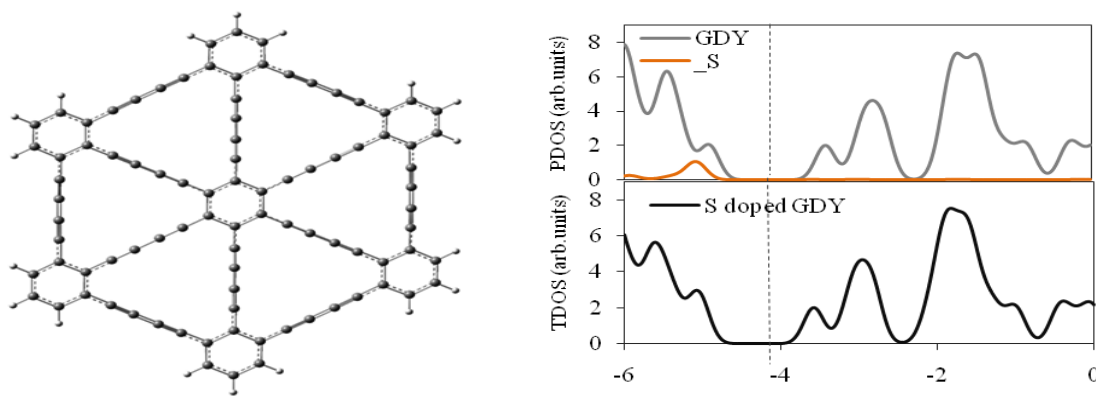
Figure 1. The structure of GDY model.   Figure 2. TDOS and PDOS of S-doped GDY.

Table 1. Electronic properties of S-doped GDY surfaces (eV).

	E_{HOMO}	E_F	E_{LUMO}	E_g	%|ΔE_g|
GDY	-4.91	-4.16	-3.41	1.49	-
S-doped GDY(5.5%)	-4.88	-4.18	-3.47	1.41	9
S-doped GDY(11.1%)	-4.84	-5.31	-5.78	0.94	56
S-doped GDY(16.6%)	-4.92	-5.31	-5.71	0.79	71
S-doped GDY(22.2%)	-4.96	-5.39	-5.82	0.86	64
S-doped GDY(27.7%)	-5.18	-5.56	-5.95	0.77	73
S-doped GDY(33.3%)	-5.35	-5.64	-5.93	0.59	91

References

[1] Afshan Mohajeri; Azin Shahsavar. *Computational Material Science*, **2016**, *115*, 51-59.

 [2] Young Soo Yun; Viet-Duc Le; Hyoung-Joon Jin. *Journal of Power Sources*, **2014**, *262*, 79-85.

[3] Mike Frisch; Gary Trucks; Berny Schlegel; Gustavo Scuseria; Mike Robb; et al. Gaussian 09, revision A.02; Gaussian, Inc.: Wallingford CT, **2009**.

[4] Guangmin Zhou; Eunsu Peak; Arumugam Manthiram. *Nature Communications*, **2015**, *6*, 7760-1_7760-11.

One-pot Route to Highly Substituted [1,8]Naphthyridin-1-phenyl-1-ethanone Derivatives *via* Four-component Reaction

Atefeh Roosta[a], Abdolali Alizadeh[a]*

Department of Chemistry, Tarbiat Modares University, P.O. Box 14115-175, Tehran, Iran

aalizadeh@modares.ac.ir

Introduction:

Heterocyclic compounds are notably important structural units and have constituted one of the fascinating areas of research for producing synthetic organic molecules of natural products [1]. Various naphthyridine derivatives have gained wide interest over the past years due to their exceptionally broad spectrum of biological activities [2] and they are frequently obtained from marine sources. Substituted [1,8]naphthyridine derivatives are attractive synthetic targets for the reason that they have a broad spectrum of biological activities [3].

As part of our continued research in the synthesis of *N*-heterocyclic compounds *via* MCRs, we report herein a novel one-pot procedure for the synthesis of substituted [1,8]naphthyridin-1-phenyl-1-ethanone derivatives **3**.

Methods / Experimentals:

Chemicals were purchased from Merck and Aldrich chemical companies and were used without further purification. Melting points were determined using an Electrothermal 9100 apparatus. The IR spectra were performed with a NICOLET FT-IR 100 spectrometer. Mass spectra were recorded on Agilent technologies 5975C spectrophotometer. The NMR spectra were obtained using Bruker Advance DRX-500 in CDCl$_3$ and DMSO.

Resultsand Discussion:

[1,8]naphthyridin-1-phenyl-1-ethanone derivatives **3** were synthesized *via* a one-pot protocol including a four-component condensation reaction of 2-chloroquinolin-3-carbaldehyde and 1-phenyl-2-(1,1,1-triphenyl-λ^5-phosphanylidene)ethan-1-one, 1,1-bis(methylthio)-2-nitroethylene or ketene *N,S*-acetals **1**, and aliphatic amine or diamines **2** under catalyst free and mild reaction conditions and in excellent yields at reflux temperature in EtOH (Scheme 1).
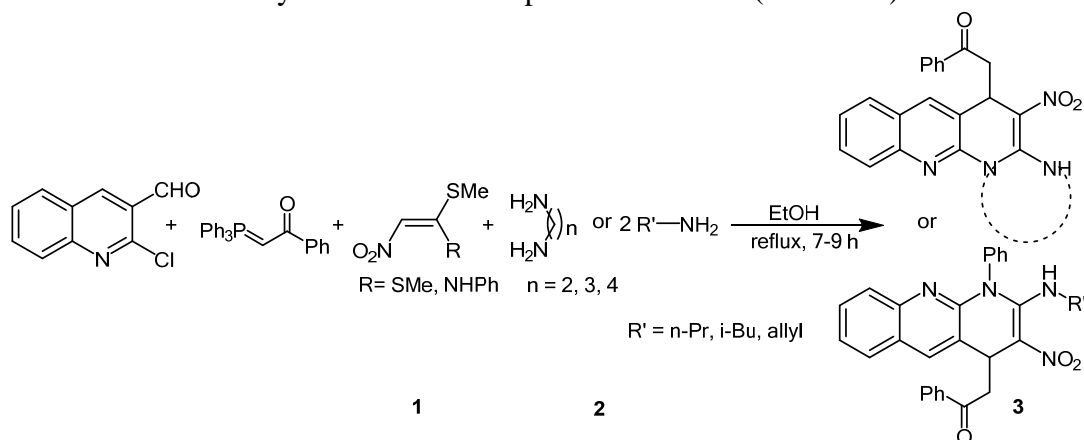
Scheme 1. Synthesis of substituted 1,4-dihydrobenzo[b][1,8]naphthyridin-4-yl)-1-phenylethanones **3**

The products were purified by crysrallisation with solvents. The melting point of the product **3a** was 224 °C. The stretching bands for CO and NO_2 groups were appeared respectively at 1674, 1542 and 1338 cm^{-1} in the IR spectrum. The ^1H NMR spectrum of **3a** exhibited one singlet at 11.67 ppm and one singlet at 5.06 and 3 multiplets at 3.29-3.34, 3.42-3.65 and 4.09-4.20 ppm and some aromatic peaks for the aromatic hydrogens. The ^{13}C NMR spectrum of **3a** showed characteristic signals at 19.3, 34.0, 38.3, 42.1, 43.5, 106.0, 121.2, 125.3, 125.5, 127.3, 127.4, 127.9, 128.6, 129.8, 133.2, 136.1, 136.5, 144.9, 147.8, 152.0, 198.2 ppm.

Conclusion:

In conclusion, we have developed a procedure for the facile synthesis of various potentially biologically active [1,8]naphthyridin-1-phenyl-1-ethanone derivatives, based on a novel four-component domino reaction. Using this method, a diverse collection of naphthyridine derivatives were rapidly constructed with excellent yields in short reaction times by simply heating a mixture of 2-chloroquinolin-3-carbaldehyde and 1-phenyl-2-(1,1,1-triphenyl-λ^5-phosphanylidene)ethan-1-one, 1,1-bis(methylthio)-2-nitroethylene or ketene *N*,*S*-acetals, and aromatic/aliphatic amine or diamines in EtOH, without any catalyst and base at reflux conditions.

References

[1]. Majumdar, K. C., Chattopadhyay, S. K. Heterocycles in Natural Product Synthesis Eds.; Wiley-VCH: Weinheim, Germany, **2011**.

[2]. Hussein, I.; El, S.; Suhair, M. A. Z.; Mona, A. M.; Farid, B.; Abdulrahman, M. A. O. *J. Med. Chem.* **2000**, *43*, 2915-2921.

[3]. (a) Kumar, V.; Jaggi, M.; Singh, A. T.; Madaan, A.; Sanna, V.; Singh, P.; Sharma, P. K.; Irchhaiya, R.; Burman, A. *Eur. J. Med. Chem.* **2009**, *44*, 3356-3362.

An Imidazole Based Brønsted Acidic Ionic Liquid as a Mild and Efficient Catalyst for the Preparation of Indazolo[2,1-*b*]Phthalazine-trione Derivatives

Farhad Shirini,* Hasan Tajik,* <u>Maryam Shirzad</u>, Mitra Nasiri, Nader Daneshvar

Department of Chemistry, College of Sciences, University of Guilan, 41335, Rasht,Iran.; Fax: +98 131 3233262; Tel: +981313233262
E-mail: shirini@guilan.ac.ir, tajik@guilan.ac.ir

Intorduction: Nitrogen heterocycles containing a phthalazine moiety are important because they show biological and pharmacological activities such as anticonvulsant, cardiotonic, and vasorelaxant, and also unique electrical and optical properties [1]. Ionic liquids have received considerable interest as eco-friendly solvents, catalysts and reagents in green synthesis. This interest can be attributed to their unique properties such as negligible vapor pressure, nonflammability, nomiscibility with nonpolar solvents, reasonable thermal and chemical stability and reusability for many times without considerable decrease in their activity [2]. Among these types of compounds, acidic ionic liquids are the most important ones which have been successfully used in different types of organic transformations [3].

Methods / Experimentals: In a 10 mL round-bottomed flask a mixture of aldehyde (1.0 mmol), phthalhydrazide (1.0 mmol), 1,3-cyclodicarbonyl compound (1 mmol) and the catalyst (7.5 mol%) was heated at 90°C under solvent free conditions for the appropriated time. After the compilation which was monitored by TLC, 5 mL of water was added and stirred for 2 minutes. The product was separated by filtration. The separated product was washed with few drops of cold ethanol. After drying, the pure product was obtained in high yields (Scheme 1).
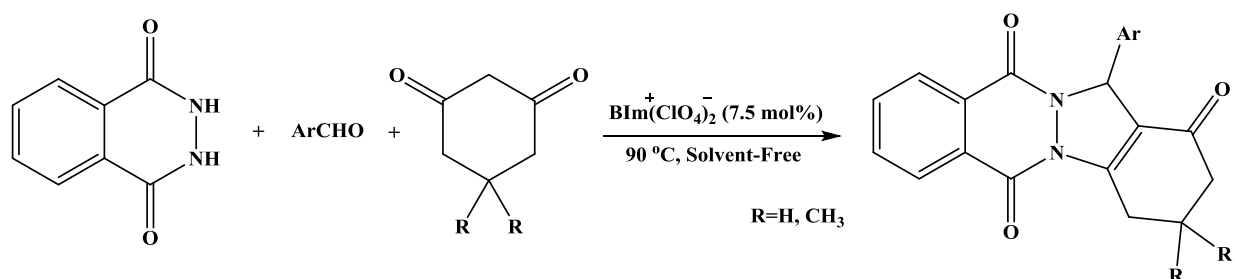
Scheme1. Prepration of indazolo[2,1-*b*]phthalazine-trione derivatives

Results and Discussion: $BIm^+(ClO_4)^-_2$ was prepared during a simple procedure and was characterized using different types of methods including FT-IR, ^1H NMR, ^{13}C NMR and mass spectroscopy. After characterization of the catalyst and optimization of the reaction, series of aromatic aldehydes containing either-electron-donating or electron-withdrawing substituents successfully reacted in 15-40 minute and yielded the products in 80-92% yield under the selected conditions. The nature and electronic properties of the substituents had no obvious effect on the rate and reaction yields. Meanwhile the catalyst showed good reusability for this reaction.

Conclusion: In this work, we have used a homogeneous brønested ionic liquid based on imidazole (BIm$^+$(ClO$_4$)$^-_2$) as the catalyst for the efficient synthesis of indazolo[2,1-*b*]phthalazine-triones with good to excellent yields during short reaction times and also the reusability of the catalyst was good.

References:

[1] F. W. Lichtenthaler, *Acc. Chem. Res.,* **2002**, *35*, 728–737.

[2] (a) A. K. Chakraborti, S. R. J. Roy. *Am. Chem. Soc.,* **2009**, *131*, 6902-6903; (b) A. K. Chakraborti, R. R. Sudipta, K. Dinesh Kumar, C. Pradeep. *Green Chem*., **2008**, *10,* 1111-1118.

[3] H. G. O. Alvim, T. B. de Lima, H. C. B. de Oliveira, F. C. Gozzo, J. L. de Macedo, P. V. Abdelnur, W. A. Silva, B. A. D. Neto. *ACS Catal.,* **2013**, *3*, 1420-1430.

Introduction of an efficient organo-catalyst for the preparation of 2-amino-3-carbonirile-4*H*-pyran derivatives

**Farhad Shirini**[a,b*]**, Fariba Hasanzadeh**[b]

[a]*Department of Chemistry, College of Sciences, University of Guilan, 41335, Rasht,Iran. Fax: +98 131 3233262; Tel: +981313233262.*
[b]*Department of Chemistry, College of Sciences, University of Guilan, university campus 2, Islamic Republic of Iran.*
E-mail: shirini@guilan.ac.ir

Introduction: The synthesis of tetrahydrobenzo[*b*]pyran derivatives are important due to their significant anti-coagulant, diuretic, spasmolytic, anti-cancer, and anti-anaphylactic properties [1]. Several methods have been introduced for the preparation of tetrahydro-4*H*-benzopyran derivatives [2]. Organocatalysis uses small organic molecules predominantly composed of C, H, O, N, S and P to accelerate chemical reactions. The advantages of organocatalysts include their lack of sensitivity to moisture and oxygen, their ready availability, low cost, and low toxicity, which confers a huge direct benefit in the production of pharmaceutical intermediates when compared with (transition) metal catalysts [3].

Methods / Experimental: In a10 ml round-bottomed flask a mixture of aldehyde (1.0 mmol), malononitrile (1.1 mmol), 1,3-cyclodicarbonyl compound (1.0 mmol) and the catalyst (20 mol%) was heated at 80 ^{o}C in H_2O/EtOH (1:1) as the solvent for the appropriated time. After the compilation which was monitored by TLC, 5ml of water was added and stirred for 2 minutes. The product was separated by filtration. The separated product was washed several times with water. After drying, the pure product was obtained.
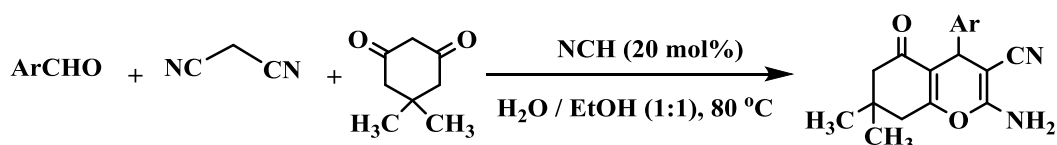
Scheme1. Multicomponent synthesis of 2-amino-3-carbonirile-4*H*-pyran derivatives

Results and Discussion: After the optimization of the condition and amount of the catalyst, Series of aromatic aldehydes with electron-donating and electron-withdrawing groups reacted successfully in this reaction. No difference was observed to be attributed to the group effect. The purity and yields of the achieved products were excellent even without recrystallization and reaction time was good. Also the reusability of the catalyst was excellent.

Conclusion: In this work, we have used a nitrogen containing heterocycle as a catalyst for the synthesis of 2-amino-3-carbonitrile-4*H*-pyran derivatives.

Refrences:

[1] L. Bonsignore; G. Loy; D.Secci; A.Calignano. *Eur. J. Med. Chem.* **1993**, *28*, 517-520.

[2] S. Abdolmohammadi, S. Balalaie, *Tetrahedron Lett*., **2007**, *48*, 3299-3303.

[3] A. Berkessel; H. Gröger. *Asymmetric Organocatalysis,* 1st ed, WILEY-VCH Verlag GmbH & Co.KGaA, **2005**. Ch 1.

Hirshfeld surface analysis of co-crystal P(O)(NHC$_6$H$_{11}$)$_3$(C$_6$H$_{11}$NH$_3$)$^+$(CH$_3$COO)$^-$ and proton transfer [C$_6$H$_{11}$NH$_2$CH$_3$]$^+$[4-CH$_3$C$_6$H$_4$S(O)$_2$NP(O)[N(CH$_3$)(C$_6$H$_{11}$)]$_2$]$^-$

Atekeh Tarahhomi[a],*

[a]*Department of Chemistry, Semnan University, Semnan 35351-19111, Iran*

Email address: tarahhomi.at@semnan.ac.ir

****

Introduction: Recently, the graphical representations based on Hirshfeld surfaces (HSs) [1] and two-dimensional fingerprint plots (FPs) [2] have received great attention as the valuable and useful tools for the visualization and quantification of the intermolecular interactions involved in crystal packing. Such studies allow easy comparison of intermolecular contacts relative to van der Waals radii by a strategy based on a simple coloring scheme.

In this work, we present the 3D HSs and 2D FPs of the previously reported structures: [P(O)(NHC$_6$H$_{11}$)$_3$][C$_6$H$_{11}$NH$_3$]$^+$[CH$_3$C(O)O]$^-$ co-crystal (**1**) [3] and [C$_6$H$_{11}$NH$_2$CH$_3$]$^+$[4-CH$_3$C$_6$H$_4$S(O)$_2$NP(O)[N(CH$_3$)(C$_6$H$_{11}$)]$_2$]$^-$ proton transfer (**2**) [4], for detailed discussion on close intermolecular contacts in the crystal packing such as H...H, O...H/H...O and C...H/H...C.

Experimental: Syntheses and X-ray structures of **1** [3] and **2** [4] were previously reported by Pourayoubi *et al.*.

Hirshfeld surface analysis: The d_{norm} Hirshfeld surfaces of the components of **1** and **2** were generated using *CrystalExplorer 3.1* [5] basing on results of X-ray studies in CIF format. Bond lengths to hydrogen atoms were set to standard neutron values during calculations. In these d_{norm} HSs, a red-blue-white color scheme represents contacts shorter, longer and close to sum of van der Waals radii, respectively. The Hirshfeld surface fingerprint plots (FPs) [2] were plotted on an evenly spaced grid formed by (d_e, d_i) pairs (the distances of the nearest atoms outside, d_e, and inside, d_i, from the HS) for each individual surface spot.

Result and discussion: Table 1 summarizes the percentage contributions of various intermolecular contacts for the different components of **1** and **2**, introducing the characteristic contacts as red spots on HSs. The d_{norm} HSs plotted on the molecule, cation and anion components of **1** are presented in Fig. 1.

In **1**, the red spots on the related HSs are assigned to the charged hydrogen bonds N–H…$^-$OC(O)CH$_3$, between the N–H unit of the phosphoric triamide molecule and the O atoms of the CH$_3$C(O)O$^-$ anion, H$_2$N$^+$–H…$^-$OC(O)CH$_3$, between the cationic [C$_6$H$_{11}$NH$_3$]$^+$ and anionic [CH$_3$C(O)O]$^-$ components and H$_2$N$^+$–H…O=P, between the NH$_3$$^+$ group of the cation and the P=O group of the molecule P(O)(NHC$_6$H$_{11}$)$_3$, and the non-charged hydrogen bond N–H…O=P, between the N–H and P=O groups of two adjacent molecules phosphoric triamide, reflecting stronger interactions relative to the other ones.

In **2**, the red spots on the related HSs are corresponded to the charged hydrogen bonds HN$^+$–H…O=P, between the NH$_2$$^+$ group of cation [C$_6$H$_{11}$NH$_2$CH$_3$]$^+$ and the P=O group of anion [4-CH$_3$C$_6$H$_4$S(O)$_2$NP(O)[N(CH$_3$)(C$_6$H$_{11}$)]$_2$]$^-$, and HN$^+$–H…O=S, between the mentioned cationic and anionic components. There are also seen the small red spots on HSs of cation and anion which reflect the H…H contacts.

By considering FPs, they have asymmetric shapes for the cationic and anionic components of **1** and **2**, while a nearly symmetric shape appears for the phosphoric triamide molecule of **1**. The highest proportions of interactions are observed for H…H contacts in all components of **1** and **2**.

For **1**, the O…H/H…O contacts are viewed as two sharp spikes in the phosphoric triamide molecule. The H…O contacts in cation $C_6H_{11}NH_3^+$ and the O…H contacts in anion $CH_3C(O)O^-$ are appeared as the sharp spikes (Fig. 1). For **2**, the O…H (of anionic) and H…O (of cationic component) contacts are identified as the sharp spikes. The H…H contacts in the cationic component are also displayed as a short spike. Moreover, the C…H and H…C contacts are represented the points in the regions of bottom right ($d_e < d_i$, C…H) and top left ($d_e > d_i$, H…C) of the related plots which in the anion FP of **2** are visible as a pair of wings. Apart from the discussed contacts, the N…H/H…N contacts in the molecular and cationic components of **1** and in the components of **2** are displayed by FPs which only comprise the minor proportions of the HSs (Table 1).

Table 1. Summary of the percentage contributions of intermolecular contacts for the components of **1** and **2**.

	H…H[†]	O...H/H…O	C…H/H…C	N…H/H…N		H…H[†]	O...H/H…O	C…H/H…C	H…N/N…H
Molecule of **1**	88.3	4.1/6.4 (RS[‡])	0/0.4	0.5/0.2	Cation of **2**	75.3	0/18.9 (RS)	0/4.2	1.6/0
Cation of **1**	84.5	0/14.4 (RS)	0/0.4	0/0.8	Anion of **2**	82.2	8.8/0.6 (RS)	5.4/2.3	0/0.7
Anion of **1**	50.1	45.6/0.7 (RS)	3.5/0	—					

[†]Some H…H contacts are appeared as light red spots on HSs.
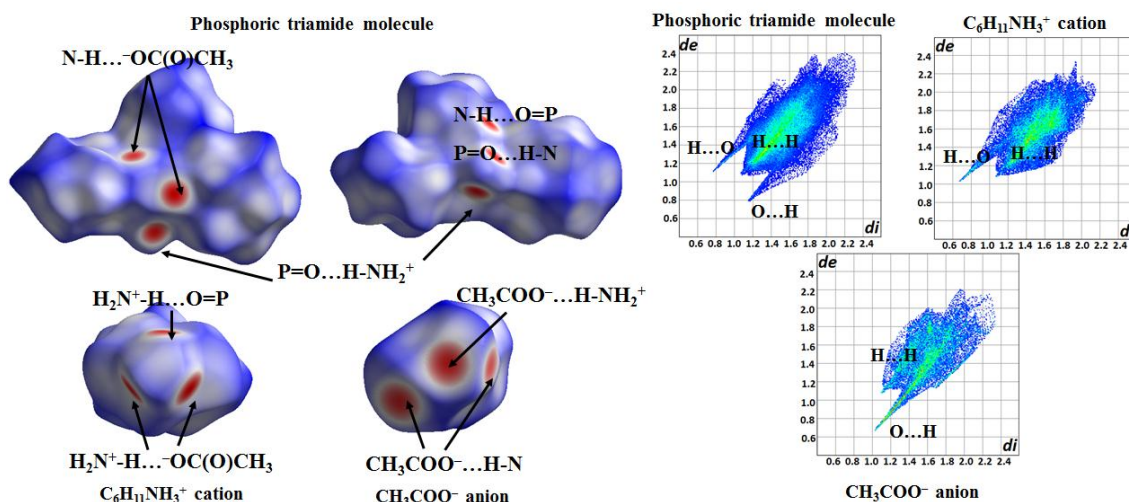[‡]RS refers to red spot on HSs.

Fig. 1. Views of d_{norm} Hirshfeld surfaces (left) and fingerprint plots (right) for the components of structure **1**.

Conclusion: In this study, 3D Hirshfeld surfaces and 2D Fingerprint plots were employed to obtain the visual identification of various interactions within the structures of **1** and **2**. The contacts H...H, O...H/H...O, C...H/H...C and N...H/H...N were recognized in the studied structures, exhibiting both symmetric (for molecule of **1**) and asymmetric (for cationic and anionic components of **1** and **2**) shapes for the full FPs. The characteristic contacts are of type O...H/H...O.

References

[1] M. A. Spackman; D. Jayatilaka. *CrystEngComm*, **2009**, 11, 19 – 32.

[2] J. J. McKinnon; M. A. Spackman; A. S. Mitchell. *Acta Crystallogr.*, **2004**, B60, 627 – 668.

[3] M. Pourayoubi; M. Keikha; A. L. Rheingold; J. A. Golen. *Acta Crystallogr.*, **2012**, E68, o2266.

[4] M. Pourayoubi; H. Fadaei; A. Tarahhomi; M. Parvez. *Acta Crystallogr.*, **2011**, E67, o2795.

[5] S. K. Wolff; D. J. Grimwood; J. J. McKinnon; M. J. Turner; D. Jayatilaka; M. A. Spackman. *CrystalExplorer 3.1*, University of Western Australia, Crawley, Australia, **2013**.

[6] M. A. Spackman; J. J. McKinnon. *CrystEngComm*, **2002**, 4, 378 – 392.

Novel hybrid material of Intercalated Orange G dye into Zn/Al-Layered double hydroxide

S. Samuei[a], Z. Rezvani[b]*

[a] Department of basic science, University of Azarbayjan shahid madani, Tabriz, Iran e-mail: SaraSamuei1411@gmail.com

[b] Department of basic science, University of Azarbayjan shahid madani, Tabriz, Iran *e-mail: zrezvani @azaruniv. ac.ir

Introduction: Organic-inorganic hybrid composites have attracted significant interest due to their thermal, optical, and physicochemical properties that lead to the potential applications of these compounds in photophysical and photostable fields [1] .Layered double hydroxide (LDH) materials, also called hydrotalcite like compounds, and represent an alternative class of clay-type materials [2]. These materials can be described with the general formula: $[M^{2+}_{1-x}M^{3+}_x(OH)_2]^{x+}(A_n^-)_{x/n} \cdot mH_2O$, where M^{2+} and M^{3+} are di- and trivalent cations respectively and A_n^- is an exchangeable anion, and x is defined as the ratio of $M^{3+}/(M^{2+} + M^{3+})$.The layer charge will depend on the M^{2+}/M^{3+} ratio [3,4]. Various anionic species have been intercalated into the gallery domain of LDHs, e.g., organic dyes, inorganic acids, amino acids, anionic polymers, and etc. [5, 6]. These layered LDH solids based upon the alternation of inorganic and organic interlayer species have received considerable attention, since they can be applied to change the chemical, electronic, optical, and magnetic properties of a host lattice. The intercalation chemistry of LDH hosts is very extensive. The dimensions and functional groups of the guest molecule are critical in determining the separation between the layers. The number (monolayer, bilayer), size, orientation of the guest as well as the interactions between the negatively charged guest and positively charged host are all critical factors [7].

Methods/ Experimentals: All the used chemicals were of analytical grade and obtained from Merck manufacture and steps of synthesis were conducted using bi distilled water. The pH values were adjusted by combining different amounts of 0.1 M solutions of NaOH and 0.1 M solution of HCl. All solutions had been previously decarbonated by saturating with N_2. For intercalation of dye in to Mg/Al LDH, aqueous solution of Zn $(NO_3)_2 \cdot 6H_2O$ and Al $(NO_3)_3 \cdot 9H2O$ were continuously dropwise mixed by dye solution and the pH was maintained at 9.5 by addition of NaOH solution under the protection of an N_2 stream [8]. The resulting suspension was aged at 80 °C for 24 h.

Results and Discussion: The XRD patterns for the Mg-Al layered double hydroxides and the dye intercalated layered double hydroxide are shown in Fig. 1. Representative XRD patterns of samples exhibit the characteristic reflections of LDH materials. It can be seen that the samples show symmetric reflections for (003), (006), (110) and (113) planes and broad asymmetric peaks for (009), (015) and (018) planes, which are characteristic as the hydrotalcite-like compounds [9, 10]. Study on the XRD patterns for this intercalated layered double hydroxide revealed a broadening and shifting of some basic reflections. These results shows that the organic guest anions replaced and expanded interlayer distance fit well within the interlayer galleries of Zn-Al layered double hydroxide.
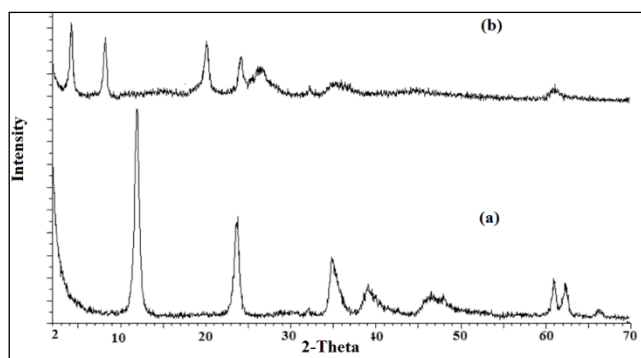
Fig. 1. (a) Zn/Al-LDH, (b) Zn/Al-Orange G-LDH

The thermogravimetric analysis for Zn-Al layered double hydroxide and Orange G intercalated ZnAl layered double hydroxide were shown in Fig. 3. LDHs commonly show three decomposition stages. The first step, in the range of 50-180°C is ascribed to the water releases from the surface and interlayer of LDH. The second step observed in the ranges of 180–350 °C is due to the dehydroxylation of the brucite-like octahedral layers and the final stage in the range of 270–500 °C is attributed to the decomposition of the interlayer anions. The DTG curves show two distinct peaks for all samples and one shoulder. The first peak around 110 °C is related to the removal of water. The small peak in the DTG curve arises from the dehydration of LDH layers. The Zn-Al layered double hydroxide intercalated with Orange G show three weight losses at 383-513, 533-553 and 713-793 K. The first two weight losses were due to loss of hydrocarbons of the aromatic moiety present in the azo dye. The second weight loss is due to the breaking of dye linkages. The third weight at slightly higher temperature was due the loss of sulphate anions. The comparison of the TGA pattern with that of pristine LDH indicate that intercalation enhances the thermal stability of this azo dye.

Fig. 2. (a) Zn/Al-LDH, (b) Zn/Al-Orange G-LDH
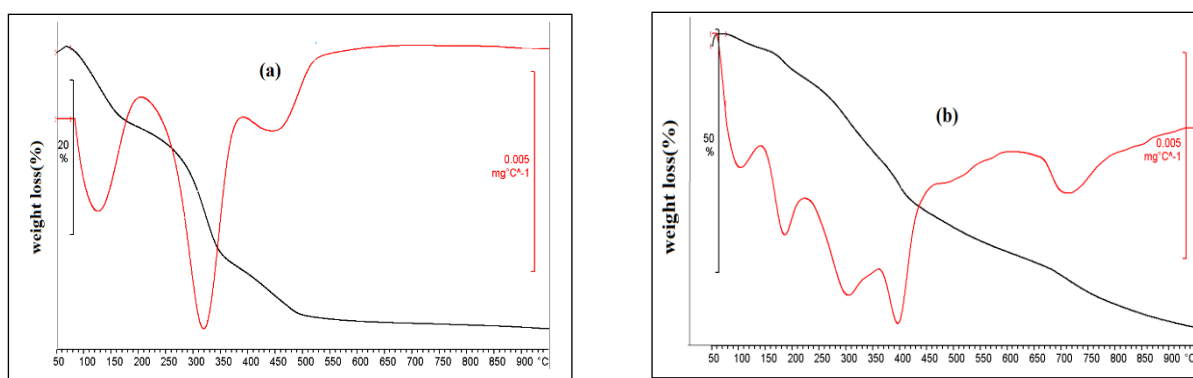
Conclusions: We have successfully prepared intercalated Orange G azo dye in to Zn/Al layered double hydroxide via coprecipitation process. Intercalation of ZnAl layered double hydroxide with this dye shows increasment in the basal spacing as evidenced by PXRD and Intercalation has led to the increase in the thermal and optical stability of these dyes.

References

[1] Chakraborty Ch., Dana K, Malik S., *Journal of physical chemistry*, **2011**, 115,1996-2004.

[2] Rives V. (Ed.), *Nova Science Publishers*, New York, **2001**.

[3] Ai L, Jiang J, *Chemical Engineering Journal*, **2012**,192, 156-163.

[4] Yan H, Zhang W, Kan X, Dong L, Jiang Z, Li H, Yang H, Cheng R, *Colloids and Surfaces A: Physicochemical and Engineering Aspects*, **2011**, 380, 143-151.

[5] You Y, Zhao H, Vance G.F, *Applied Clay Science*, **2002**, 21, 217-226.

[6]Wei M, Shi S, Wang J, Li Y, Duan X, *Journal of Solid State Chemistry*, **2004**, 177, 2534-2541.

[7] Khan A.I., O'Hare D, *Journal of Materials Chemistry*, **2002**, 12, 3191-3198.

[8] Zhao Y, Li F, Zhang R, Evans D.G, Duan X, *Chemistry of materials*, **2002**, 14, 4286-4291.

[9] Guo Y, Zhu Z, Qiu Y, Zhao J, *Journal of hazardous materials*, **2012**, 239, 279-288.

[10] Nejati K, Rezvani Z, Mansurfar M, Mirzaee A, Mahkam M, *Zeitschrift für anorganische und allgemeine Chemie*, **2011**, 637, 1573-1579.

An Imidazole Based Brønsted Acidic Ionic liquid as a Mild and Efficient Catalyst for the Preparation of Pyrano[2,3-*d*]pyrimidines Derivatives

Farhad Shirini,* Hasan Tajik,* Mitra Nasiri, Maryam Shirzad, Nader Daneshvar

Department of Chemistry, College of Sciences, University of Guilan, 41335, Rasht,Iran.; Fax: +98 131 3233262; Tel: +981313233262
E-mail: shirini@guilan.ac.ir, tajik@guilan.ac.ir

Introduction: Pyran derivatives are ordinary structural subunits in a variety of important natural products, including carbohydrates, alkaloids, polyether antibiotics, pheromones and iridoids [1]. Ionic liquids (ILs) have become powerful alternatives to conventional molecular organic solvents and catalysts, due to their particular properties, such as undetectable vapor pressure, ability to dissolve many organic and inorganic substances, recyclability and tunable character to specific tasks [2]. Brønsted acidic ionic liquids (BAILs) have attracted special attention as efficient catalysts for the synthesis of valuable chemicals. The current review deals with the applications of BAILs as clean and versatile replacements for the traditional mineral homogeneous acids [3].

Methods / Experimentals: In a 10 mL round-bottomed flask a mixture of aldehyde (1.0 mmol), Barbituric acid (1.0 mmol), Malononitril (1.1 mmol) and the catalyst (6.0 mol%) was refluxed in water for the appropriated time. After the compilation which was monitored by TLC, 5 mL of water was added and stirred for 2 minutes. The product was separated by filtration. The separated product was washed with few drops of cold ethanol. After drying, the pure product was obtained in high yields (Scheme 1).
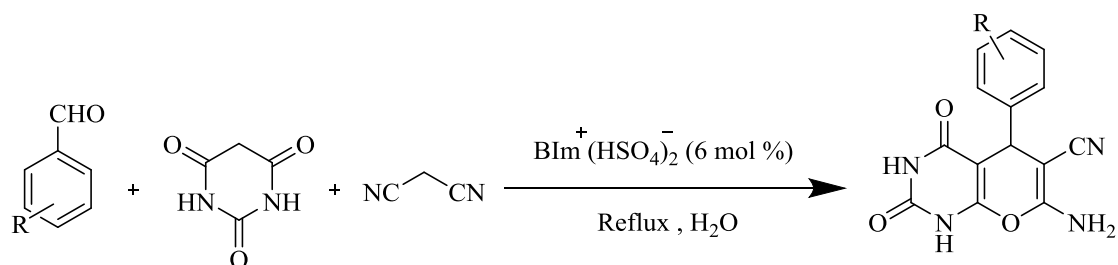
Scheme 1. Preparation of Pyrano[2,3-*d*]pyrimidines derivatives

Results and Discussion: $BIm^+(HSO_4)^-_2$ was prepared during a simple procedure and was characterized using different types of methods including FT-IR, ^1H NMR, ^{13}C NMR and mass spectroscopy. After optimization of the condition and amount of the catalyst, series of aromatic aldehydes containing either-electron-donating or electron-withdrawing substituents successfully reacted during very short reaction times in high yields under the selected conditions. The nature and electronic properties of the substituents had no obvious effect on the rate and reaction yields. Meanwhile catalyst showed good reusability for this reaction.

Conclusion: In this work, we have used a homogeneous brønseted ionic liquid based on imidazole $BIm^+(HSO_4)^-_2$ as the catalyst for the efficient synthesis of Pyrano[2,3-*d*]pyrimidines derivatives with good to excellent yields during short reaction times.

References:

[1] L. Tietze, G. Kettschau. In Topics in Current Chemistry,Volume 189. Ed. Berlin: Springer **1997**, 1–120.

[2] P. Wassercheid, T. Welton, Ionic Liquids in Synthesis, 2nd ed., Wiley-VCH,Weinheim, 2007.

[3] M. Vafaeezadeh; H. Alinezhad. *J. Mol. Liq*.**, 2016**, 218, 95–105.

Theoretical Studies of Method Using
MWCNT to Concentrate (E)-Citral Component in Essential Oil of Melissa *officinalis* L.

Rojin Kariminya[a,*] , **Ako Yari**[b] and **Avat (Arman) Taherpour**[b,c,*]

[a] *Department of Nano Chemistry, Faculty of Chemistry, Razi University, Kermanshah, Iran*
[b]*Department of Organic Chemistry, Faculty of Chemistry, Razi University, Kermanshah, Iran*
[c] *Medical Biology Research Center, Kermanshah University of Medical Sciences, Kermanshah, Iran*

*Corresponding authors; Email: **avatarman.taherpour@gmail.com** and **roj.k1990@gmail.com**
****

Introduction: The main component of Melissa *officinalis* L. from the Kurdistan province of Iran is (E)-citral. (E)-citral have among the highest percentage(37.2%) [1]. Citral, or 3,7-dimethyl-2,6-octadienal or lemonal, is either a pair, or a mixture of terpenoids with the molecular formula $C10H_{16}O$. The two compounds are double bond isomers. The E-isomer is known as geranial or citral A. The Z-isomer is known as neral or citral B. Geranial has a strong lemon odor. Neral's lemon odor is less intense, but sweeter. Citral is therefore an aroma compound used in perfumery for its citrus effect. Citral is also used as a flavor and for fortifying lemon oil. It also has strong antimicrobial qualities, and pheromonal effects in insects. Citral is used in the synthesis of vitamin A, ionone, and methylionone, to mask the smell of smoke [2].

Methods: The molecular quantum (QM) and molecular mechanics (MM) calculations were carried out by the *Spartan '10* package [3]. Two layers of Nano tubes were separately modeled and optimized using molecular mechanic (MM) methods. The smaller SWCNT pipe has been located inside the other, and by using molecular mechanic method MMFFaq the double wall CNT was optimized. The ends of the two pipes of CNT were closed. The different modes of essential oil optimized components on carbon Nano tube were evaluated and calculated by QM-MM method. The ideal states were obtained by making thermo-dynamical calculation and comparison of sustainable energy. The optimum states (with the lowest energy) were obtained.

Result and Discussion: Carbon Nano materials have attracted the attention of many researchers [4]. Especially, sp^2 carbon Nano materials, such as carbon nanotubes (CNTs) and graphene have lots of significant applications in many various fields. CNTs, which are considered to be extremely superior adsorbents due to their high specific surface area and large micro pore volume, have been utilized for the sorption of a number of organic and inorganic compounds and pollutants [5]. The absorption of (E)-Citral component on MWCNT was modeled. For (E)-Citral component nine different states have been investigated (See Figure 1) and the energies for those modes were calculated and compared. In Figure 1 was shown the different location forms of (E)-Citral in the proximity of MWCNT and the calculated energies of the different states of (E)-Citral in proximity of the modeled MWCNT. These states were used for final consideration, and studying the interactions of all states with the outer wall of carbon Nano tubes interactions (Vander Waals or π-π interactions between CNTs and the guest molecule). The optimum state (with the lowest energy) was obtained. Due to energies of these states, the most stable state has the lowest energy. Acording to the Table 1 state A is the lowest form. Form Figure 1A is the most stable form and Figure 1H is the most unstable proximity on (E)-Citral with MWCNT. The most stable mode was determined based on obtained energy. This state should be the best state for the vander Waals or π-π interactions between CNTs and (E)-Citral. It shows stronger interaction between (E)-Citral and MWCNT.

Table 1: The calculated energies of the different states of (E)-Citral in proximity of the modeled MWCNT.

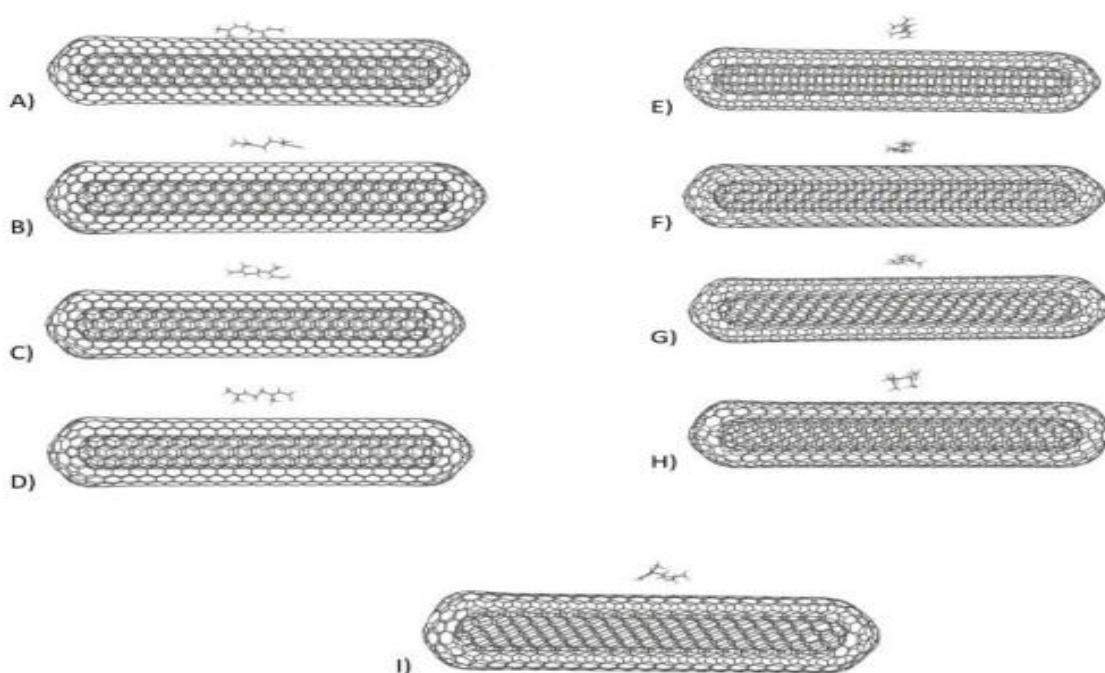| States	Equilibrium Geometry of States in KJmol^{-1}
A	۵۴۷۴۱.۰۶
B	۵۴۷۴۱.۴۶
C	۵۴۷۴۵.۵۲
D	۵۴۷۵۶.۶۳
E	۵۴۷۶۰.۰۶
F	۵۴۷۴۹.۸۸
G	۵۴۷۴۵.۶۵
H	۵۴۷۶۰.۸۱
I	۵۴۷۴۹.۹۰

Figure 1: The different location forms of (E)-Citral in the vicinity of MWCNT

Conclusion: The theoretical studies confirms that the vander Waals and/or π-π interactions between MWCNT and state A of (E)-Citral has stronger tendency to the absorption on MWCNT among the other components of the essential oil of Melissa *officinalis* L.. The result of this method could utilize to increase the concentrations of some components in the extracted essential oil of this herb.

References
[1] Taherpour,AA; Maroofi,H; Rafie,Z; Larijani,K. *Natural Product Research*, **2012**, *26:2*, 152-160.
[2] https://pubchem.ncbi.nlm.nih.gov/compound/Citral
[3] Spatran '10-Quantum Mechanics Program: (PC/x86)-1.1.0v4.2011, Wavefunction Inc USA.
[4] Beg,S; Rizwan,M; Sheikh,AM; Hasnain,MS; Anwer, K; Kohli, K. *J Pharm Pharmacol*, **2011**, *63(2)*, 141-63.
[5] Wu,CH. *J Hazard Mater*, **2007**, *144*, 93–100

Fabrication and electrochemical investigation of potentiodynamic electropolymerized PANI-nanofiber on graphite electrode

Mohsen Babaiee [a*], Abbas Bagheri [b], Mahmood Pakshir [c], Babak Hashemi [d]

[a] **Institute of Mechanics, Iranian Space Research Center, Shiraz ٧١٥٥٥-٤١٤, Iran.**
[b] **College of Sciences, Chemistry Department, Shiraz University.**
[d,c] **Material Science Engineering, Shiraz University.**

Email address: Babaiee.mohsen@gmail.com

****

Introduction: Conducting polymers are modern materials with various applications [١]. Among numerous known electroconducting polymers, polyaniline is the most investigated because of their unique properties [١,٢]. It is clear that the morphology of produced polymer affects its properties to a large extent. Among different morphologies that may be obtained from the polymerization of PANI, the formation of fibrous morphology has various important applications due to effective increase in its surface area. It is found that cyclic voltammetry is a preferred method in producing controlled nanofibers with excellent electrochemical properties [٣-٦]. The aim of the present study is to investigate the electrochemical characteristics of PANI nanofibers prepared by potentiodynamic method.

Methods / Experimentals: Electrochemical deposition and investigation of PANI was dealt with, using potintiostat instrument with a three-electrode cell assembly. Electropolymerization reactions were carried out in ٠.٧٥ M HNO_3 + ٠.٢٥ M H_2SO_4 + ٠.١ M Aniline solution in a nitrogenous atmosphere, employing the cyclic voltammetry technique by potential sweep between -٠.٢ and ١ V for different scan rates of ١٢.٥, ٢٥, ٥٠, ٧٥ and ١٠٠ mV s^{-1}. Electrochemical behavior of PANI was assessed using a CV of -٠.٢ to ٠.٨ V, scan rate of ٥٠ mV s^{-1} in electropolymerization solution without the aniline monomer.

Results and Discussion: Typical CV responses of such films that were gathered at various potential sweep rates are illustrated in Fig. ١. As can be seen, the CV responses are characterized by predominate oxidation and reduction peaks (A–A´). Peak A is the characteristic peak of PANI corresponding to the conversion of fully reduced states of leucoemeraldine form to the ٥٠٪-oxidized emeraldine form resulting in an increase in the conductivity of polymer [٣٠]. Hence through characterizing this peak (A) in each condition one can investigate the electrochemical properties of electropolymerized polymer. The results of Q in Table ١ show that by increasing the scan rate from ١٢.٥ to ٢٥ mV s^{-1}, the charge (Q) increases and by further increasing SR, this value decreases. It can also be noticed that the maximum value for Q is related to the electropolymerization at the scan rate of ٢٥ mV s^{-1}, which indicates the maximum amount of electroactivity. The effects of different scan rates on the morphology of nanofibers were also investigated (Fig. ٢.). The results showed that electropolymerization of aniline at the scan rate ٢٥ mV s^{-1} causing the formation of aniline nanofibers with diameters ranging from ٦٥ to ٧٠ nm and having good electroactive properties.

Fig. ١. Cyclic voltammetry test on polyaniline, performed in different electro-polymerization conditions: effect of different scan rates.
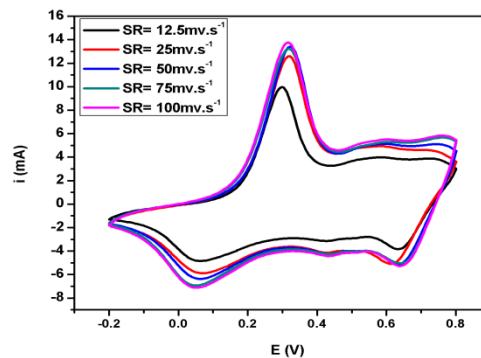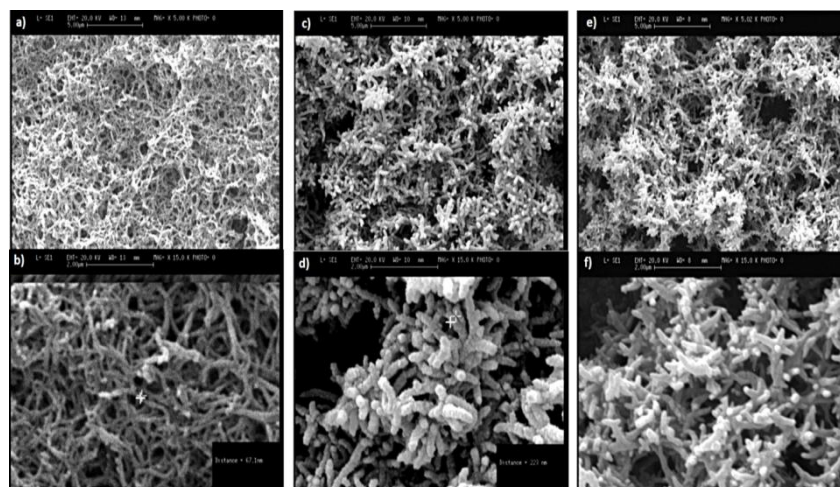
Table ١. Values of parameters obtained from cyclic voltammetry test performed on electropolymerized PANI in different conditions.

Polymerization condition	Q_a(C)	Q_c(C)	Q_{cv}(C)	$E_{p(A)}$(V)	$I_{p(A)}$ (A)	Q(C)
SR= ١٢.٥ mV.s⁻¹	٦.٠٢E-٠٢	٥.٩٠E-٠٢	٠.٠٥٩٦	٠.٣٠٠	٧.٩٧٦E-٠٣	١.٨٩E-٠٢
SR= ٢٥ mV.s⁻¹	٧.٦٦E-٠٢	٧.٥٣E-٠٢	٠.٠٧٥٩	٠.٣٢٠	٩.٨٢٩E-٠٣	٢.٨٦E-٠٢
SR= ٥٠ mV.s⁻¹	٨.٠٩E-٠٢	٧.٨٨E-٠٢	٠.٠٧٩٨	٠.٣٢٠	١.٠٦٢E-٠٢	٢.٨٤E-٠٢
SR= ٧٥ mV.s⁻¹	٨.٥٣E-٠٢	٨.٢٩E-٠٢	٠.٠٨٤١	٠.٣٢٠	١.٠٣٧E-٠٢	٢.٨٢E-٠٢
SR= ١٠٠ mV.s⁻¹	٨.٨٤E-٠٢	٨.٦١E-٠٢	٠.٠٨٧٢	٠.٣١٠	١.٠٧٩E-٠٢	٢.٨٠E-٠٢

Fig. ٢. SEM micrograph at two magnifications for electro-polymerized aniline at different scan rate: a) ٢٥mV.s⁻¹; ٥٠٠٠X, b) ٢٥mV.s⁻¹; ١٥٠٠٠X, c) ١٢.٥mV.s⁻¹; ٥٠٠٠X, d) ١٢.٥mV.s⁻¹; ١٥٠٠٠X, e) ١٠٠mV.s⁻¹; ٥٠٠٠X, f) ١٠٠mV.s⁻¹; ١٥٠٠٠X.

Conclusion: Aniline nanofibers were fabricated through cyclic voltammetry electropolymerization and the effect of different scan rates on the electroactivity and the morphology of nanofibers were also investigated. The results showed that aniline fibers with excellent stability and conductivity could be produced at condition where the scan rate is ٢٥ mV s⁻¹ that causing the formation of aniline nanofibers. With electropolymerization at scan rates lower than ٢٥ mV s⁻¹ the obtained fiber is thick while at higher scan rates, the produced PANI has a dendrites' morphology.

Reference:
[١] H.S. Nalwa (Ed.), Handbook of Organic Conductive Molecules and Polymers, Wiley, New York, ١٩٩٧.
[٢] A.A Syed, M.K Dinesan, Polyaniline A novel polymeric material, Talanta, ٣٨ (١٩٩١) ٨١٥-٨٣٧, DOI: ١٠.١٠١٦/٠٠٣٩-٩١٤٠(٩١)٨٠٢٦١-W.
[٣] C. Dalmolin, S. C. Canobre, S. R. Biaggio, R. C. Rocha-Filho, N. Bocchi, Electropolymerization of polyaniline on high surface area carbon substrates, J. Electroanal. Chem. ٥٧٨ (٢٠٠٥) ٩–١٥, DOI: ١٠.١٠١٦/j.jelechem.٢٠٠٤.١٢.٠١١.
[٤] J.-C Lacroixa, J.-L Camaleta, S. Aeiyacha, K.I. Chane-Chinga, J. Petitjeanb, E. Chauveaub, P.-C Lacazea, Aniline electropolymerization on mild steel and zinc in a two-step process, J. Electroanal. Chem., ٤٨١ (٢٠٠٠) ٧٦-٨١, DOI: ١٠.١٠١٦/S٠٠٢٢-٠٧٢٨(٩٩)٠٠٤٩٠-٨.
[٥] M.J Giz, S.L de Albuquerque Maranhão, R.M Torresi, AFM morphological study of electropolymerized polyaniline films modified by sufractant and large anions, Electrochem. Commun., ٢ (٢٠٠٠) ٣٧٧-٣٨١, DOI: ١٠.١٠١٦/S١٣٨٨-٢٤٨١(٠٠)٠٠٠٤١-٢.
[٦] A. Pron, P. Rannou, Processible conjugated polymers: from organic semiconductors to organic metals and superconductors, Prog. Polym. Sci., ٢٧ (٢٠٠٢) ١٣٥-١٩٠, DOI: ١٠.١٠١٦/S٠٠٧٩-٦٧٠٠(٠١)٠٠٠٤٣-٠.

Preparation and Characterization of MoO$_3$ nanoparticles on the Surface of Carbon Nanotube for Supercapacitor Application

Samaneh Bayatpour[a], Maryam Afsharpour[a],*, Zahra Dini[a]

[a] *Department of Inorganic Chemistry, Chemistry &Chemical Engineering Research Center of Iran, Tehran, Iran*

Email address: afsharpour@ccerci.ac.ir

*********************

Introduction: Because of the ever increasing demand for energy, researchers have been encouraged to find more new materials and processes to improve energy storage devices. Among energy storage system, supercapacitors have drawn abundant attention due to their fast charge-discharge characteristics, excellent cycle stability, and high power density compared to battery [1]. The overall performance of supercapacitors is close related to properties of both the electrode and the electrolyte materials. Among the materials used in supercapacitors, the noble/transition metal oxides are considered to be the most appropriate materials for the next generation of SCs due to their high pseudocapacitances. However, toxicity and high price of this material have restricted its extensive use. Molybdenum, a metal with a wide range of oxidation states from $+2$ to $+7$, possesses variety of oxides and other compounds, of which MoO$_2$ and MoO$_3$ have drawn considerable attention for using in supercapacitors, due to a high electrochemical activity, low cost, and eco- friendly nature. Moreover, carbon nanotube (CNT) functionalized with oxygen can enhance the energy density of carbon electrodes because of surface redox reactions between the oxygen groups and electrolyte ions. Recently, conducting substrates such as various carbon materials, and Ni foam have been added to poor electronic conductor to form composites as supercapacitor materials [2].

In this study, we have used carboxylated carbon nanotube CNT/MoO$_3$ as SC electrode material. The CNT/MoO$_3$ was stuck on Ni foam as a current collector without binder. Then the electrochemical behavior of supercapacitors was investigated.

Experimental: First, the MWNTs were functionalized by oxidation with nitric acid and sulfuric acid at 120°C for 3h, and the treated MWNTs were then rinsed and dried at 60°C. Then the MWNTs (100 mg) were added to the solution of molybdenum oxide in hydrogen peroxide and refluxed at 100°C. The solution was cooled at room temperature and the product was centrifuged, washed several times with distilled water and dried in an air oven.

Results and Discussion: In the IR spectrum of CNT/MoO₃, the new strong peaks at ١٦٦٧ and ١٧٢٩ cm⁻¹ in the IR spectrum apparently corresponds to the stretching modes of the carbonyl groups on the MWNTs and very broad bands that appeared in the ٢٩٠٠-٣٣٠٠ cm⁻¹ range are identified to O-H stretching modes. Also, there are sharp peaks at ٩٨٥ and ٩١٨ cm⁻¹ can be assigned to the formation of the Mo-O and the sharp peak at ٦١٧cm⁻¹ shows the presence of Mo-O-Mo bonds. These results show that molybdenum center is supported to MWNTs. Fig. ١ shows XRD patterns of synthesized CNT/MoO₃ sample. The reflections at ٢θ = ١٢.٧٧, ٢٣.٤١, ٢٧.٣٣, ٣٣.٧٣, ٤٥.٨٩, ٤٩.٢٥° values indicate the presence of MoO₃ that correspond to the (٠٢٠), (١١٠), (٠٢١), (١٣٠), (١١١), (٠٤١) planes of orthorhombic molybdenum oxide (JCPDS=٣٥-٠٦٠٩) and ٢θ = ٢٥.٧٣, ٣٩.٠١° indicate the presence of MWNTs that corresponded to the (٠٠٢) and (١٠٠) planes (JCPDS No. ٤١-١٤٨٧). TEM images of CNT/MoO₃ sample, which reveal that the hollow cavities of MWNTs are filled with MoO₃ nanoparticles at the entire length.

The pseudocapacitive properties of these electrodes were investigated in aqueous KOH solution by cyclic voltammetry (CV), chronopotentiometry (CP) and AC impendence. Fig. ٢ displays the typical CV curves of the pure Ni foam and Ni/CNTMoO₃ electrode at a scan rate of ٥ mV/s. Impressively, the Ni /CNT/MoO₃ electrode typically exhibits a greatly increased CV integrated area with respect to that of pure Ni foam, indicating the much higher specific capacitance of the synthesized electrode. This fact is also supported by the galvanostatic charge-discharge curves. The specific capacitance of the Ni/CNTMoO₃ was ٥٧٥ F/g. in the current density of ١A/g.
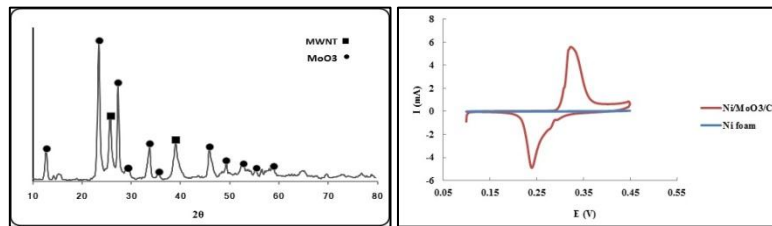
Conclusion: The simple method to synthesize these electrodes and the outstanding electrochemical performance is attributed to the three-dimensional (٣D) and interconnected networks of Ni foam/CNT/MoO₃ that can effectively reduce resistant pathways for ion diffusion in the pores as well as provide a large accessible surface area for ion transport.

References

[١] T. Brezesinski; J. Wang; S.H. Tolbert; B. Dunn. *Nat. Mater.* ٢٠١٠, ٩, ١٤٦–١٥١.

[٢] Shakir; M. Shahid; H.W. Yang; D.J. Kang. *Electrochim Acta*, ٢٠١٠, ٥٦, ٣٧٦–٣٨٠.

Optimization the Test Method of Average Molecular Weight of LABS

Mohammad Fazel Abedini[a], Mohammad Baghdadi[b], Seyedeh Fatameh Mashhadi[c]*

a: manager of Paknam co. laboratory

b: expert of Paknam co. laboratory

c: head of Paknam co. labratory

Email address: saeedeh.mashhadi@gmail.com

Introduction: Linear alkyl benzene ($C_6H_5C_nH_{2n+1}$) is an organic compound. Typically, n situation between ١٠ and ١٦, although generally supplied as a tighter cut, such as $C_{١٠}$-$C_{١٣}$. They are mainly produced as intermediate in the production of surfactants, for use in detergent. Since the ١٩٦٠s, chains of LAB have emerged as the dominant precursor of biodegradable detergents. The aim of this study was optimized the method for measuring average molecular weight (Av.Mw) of sulfonated linear alkyl benzene (LABS). The References were used and investigated in this study including handbook of surfactant analysis [١], SANS No: ١١٧٠:٢٠١٠ [٢] and ISIRI No: ١٤٤٤٨ [٣].

Methods / Experimentals: In this method was used the special glass set calling the desulfonation apparatus of Osburn [١], the desulfonating process of LABS performed in the presence of acid at ٢٦٠±٥°C for ٩٠ minutes [١, ٢]. Then, the desulfonated product was neutralized and extraction process was done by the organic solvent. Organic phase injected into the gas chromatography according to the isothermal temperature program, CP-Sil٢٤CB column and FID detector. Distribution of carbon chain was assessed and average molecular weight was calculated.

Results and discussion: This study performed base on available methods for desulfonation of LABS.

Standard method of South African No. ١١٧٠:٢٠١٠ [٢] due to lack full desulfonating of LABS and the longtime of extraction process is not appropriate.

The Method of ISIRI ١٤٤٤٨:١٣٩٠ [٣] is not appropriate because of a) the dangerous condition due to the safety valve on reaction tube during experiment, b) working with oil bath which is in direct contact with the atmosphere and influence toxic gas during the experiment, c) hazard due to using oxygen-gas flame, d) being longtime

test and e) getting high error due to less weight of sample (less than ٠.١g) and liquid- liquid extraction process.

In this study, we optimized temperature, type of extraction solvent and extracting process according to standard method of South African No. ١١٧٠:٢٠١٠ [٣] and obtained results were shown in Table (١).

Table (١): The results of analysis

Test method	ISIRI ١٤٤٤٨:١٣٩٠	SANS ١١٧٠:٢٠١٠	Optimized method
Repeat١ (g/mol)	٢٤٠.٢٨	٢٤٠.٩٠	٢٤٠.٨٩
Repeat٢ (g/mol)	٢٣٩.٨٩	٢٤٠.٣٥	٢٤٠.٨٤
Repeat٣ (g/mol)	٢٤٠.٢٨	٢٤٠.٥٧	٢٤٠.٦٦
Average (g/mol)	٢٤٠.١٥	٢٤٠.٦١	٢٤٠.٨٠
Standard deviation	٠.٢٢٥	٠.٢٧٦	٠.١٢١

Conclusion:

Optimization method of desulfonation LABS was done to assess the Av.Mw by optimized temperature, replacing ٢-methyl butane with acetone and direct injection of extracted solution to GC. The advantages of the optimized method are reducing environmental pollution, increasing its safety with equal or higher accuracy (T-Test) and precision (F-Test). Comparison between Av.Mw of LABS was prepared from LAB (٢٤٠.٨٠g/mol) with Av.Mw of LAB (٢٤٠.٧٧g/mol) was shown a good conformity.

References:

[١] Dietrich O.Hummel. Handbook of surfactant analysis, ٢٠٠٠, ١٥٧-١٦٠

[٢] Standard South African: SANS No. ١١٧٠:٢٠١٠, edition ١.٤

[٣] National Standard of Iran: ISIRI No. ١٤٤٤٨:١٣٩٠

Synthesis and Investigation of a Novel Seven Coordinate Organotin(IV) Complex

Zeinab Ansari-Asl[a,*], **Tahereh Sedaghat**[a], **Abbas Tarassoli**[a], **Hadi Amiri Rudbari**[b]

[a] *Department of Chemistry, Faculty of Science, Shahid Chamran University of Ahvaz, Ahvaz, Iran*

[b] *Department of Chemistry, Faculty of Science, University of Isfahan, Isfahan, Iran*

****

Introduction: Organotin*(IV)* compounds containing electronegative atoms show Lewis acidic character and the tin(IV) can increase its coordination number from four to five or six or rarely seven by addition of donor ligands [١-٣]. The study of organotin complexes with hydrazones continues to be of interest owing to their remarkable chemical and structural characteristics and potential pharmacological applications [٤, ٥]. During the last few years, metal complexes with water-soluble ionic hydrazones derived from Girard's reagents represent an interesting research subject [٦, ٧]. In this research, We reports a novel organotin(IV) complex with an ionic hydrazone, (BrH₂SalGP)Cl.

Experimental: The hydrazone ligand, (BrH₂SalGP)Cl, was prepared by condensation of Girard-P with ٥-bromo-٢-hydroxybenzaldehyde. Then The organotin(IV) complex was synthesized by reaction of Ph₂SnCl₂ with (٥-BrH₂SalGP)Cl in the presence of triethylamine. The synthesized complex was investigated by elemental analysis, FT-IR, ¹H and ¹¹⁹Sn NMR spectroscopy. Recrystallization in dimethyl sulfoxide in presence of a trace acetate ion gives yellow needle single crystals suitable for X-ray crystallography.

Results and Discussion: In the IR spectrum of complex the ν(C=N) band appeared at ١٦٢٠ cm⁻¹ in the spectra of ligands is shifted towards lower frequency (١٦٠٦ cm⁻¹) indicating coordination of the azomethine nitrogen to the tin. In the ¹HNMR spectra of complex the absence of signals assigned to two acidic hydrogens suggests deprotonation and coordination of phenolic and enolic oxygens to tin. In addition, the proton of CH=N gave resonance signal in the down field region with ³J(¹¹⁹Sn-¹H) coupling constant value of ٣١ Hz due to the coordination of nitrogen with tin(IV). The ¹¹⁹Sn{¹H}NMR spectrum of complex shows one sharp singlet at -٤٦٥.٣٣ ppm. This chemical shift is significantly at lower frequency than those of the original SnPh₂Cl₂ (-٣٢ ppm) indicates an increasing in coordination number of tin. The molecular structure of synthesized complex is shown in Figure ١. The hydrazone coordinates *via* the nitrogen from the imine and the two oxygen atoms from the phenolate and enolate. The coordination sphere is completed by two phenyl and one bidentate acetate groups. Therefore the tin environment is seven coordinate

with a distorted pentagonal bipyramidal geometry and phenyl groups are in axial positions. **Conclusion:** In this research, we have synthesized and characterized a diorganotin(IV) complex with ionic Schiff base derived from Girard-P reagent. On the basis of spectroscopic and structural data the hydrazone behaves as ONO tridentate dibasic ligand and coordinates though phenolate and enolate oxygens and imine nitrogen. This complex is structurally interesting because the coordination number of tin(IV) is seven.

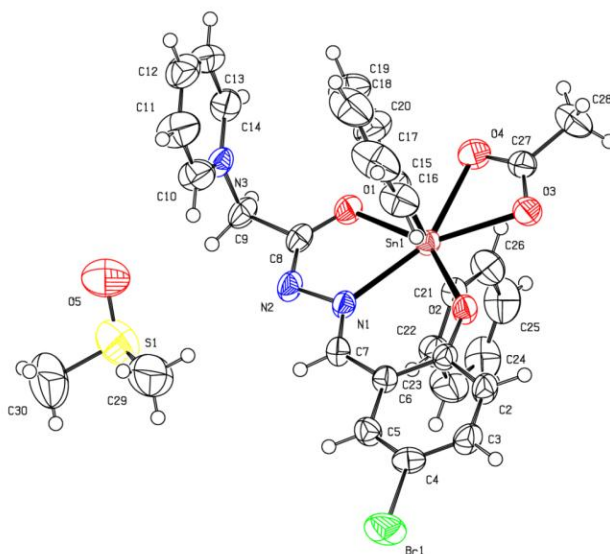**Keywords:** Organotin(IV), Schiff Base, Girard-P, Crystal Structure

Fig. ١. Crystal structure of organotin(IV) complex

References

١. C. Ma; Q. Wang; R. Zhang. *Heteroat. Chem.* ٢٠٠٨, ١٩, ٥٨٣-٥٩١.

٢. T. Sedaghat; M. Naseh; H. R. Khavasi; H. Motamedi. *Polyhedron,* ٢٠١٢, ٣٣, ٤٣٥-٤٤٠.

٣. A. Ramirez-Jimenez; E. Gomez; S. Hernandez. *J. Organomet. Chem.* ٢٠٠٩, ٦٩٤, ٢٩٦٥-٢٩٧٥.

٤. S. Alexander; V. Udayakumar; V. Gayathri. *J. Mol. Catal. A: Chem.* ٢٠٠٩, ٣١٤, ٢١-٢٧.

٥. S. Hazra; A. Paul; G. Sharma; B. Koch, B; M.F.C. Guedes da Silva; A.J.L. Pombeiro. *J. Inorg. Biochem.* ٢٠١٦ (in press).

٦. O. V. Palamarciuc; P. N. Bourosh; M. D. Revenco; J. Lipkowski; Y. A. Simonov; R. Clérac. *Inorg. Chim. Acta* ٢٠١٠, ٣٦٣, ٢٥٦١-٢٥٦٦.

٧. L. S.Vojinovic-Jesic; V. I. Cesljevic; G. A. Bogdanovic; V. M. Leovac; K. Meszaros Szecsenyi; V. Divjakovic; M. D. Joksovic. *Inorg. Chem. Commun.* ٢٠١٠, ١٣, ١٠٨٥-١٠٨٨.

Preparation, modification and charactrization of biocompatible nanoparticles through covalent and supramolecularintractions as drug delivery system.

Hosseini M , Dadkhah A[*]
Department of Chemistry, Faculty of Science, Lorestan University, Khoramabad, Iran.
a_dadkhahtehrani@yahoo.com

Introduction

Dendrosomes are a type of supramolecular systems that formed by molecular self-assembly of amphiphilic block copolymers in aqueous solutions. These supramolecular systems are able to encapsulate and deliver hydrophobic and hydrophilic therapeutic agents and small guest molecules. [1-5].

Here in we report *a* dendrosomes consisting a Yellow Anilline (YA) graft to polycaprolactone and hyperbranched poly glycidol(PG) with α-cyclodextrin core as linear and hyperbranched blocks respectively. Linear and hyperbrached blocks were associated together by host-guest interactions. Self-assembly of *α-CD-g-PG block YA-g- CL* in aqueous solutions led to fully supramolecular dendrosomes with a high capacity to encapsulate and transfer drugs.this dendrosome were sensitive to the best regions of pH and temperature[6-9].

Experimental

Preparation of α-CD-g-PG

glycidol (6.17 ml, 92 mmol) was added to the deprotonated *α-CD*(0.5 g, 0.5 mmol) gradually at 100 °C for 2 h. Mixture was stirred at 120 ºC for 12 h. Then it was dissolved in methanol and precipitated into acetone .

Preparation of YellowAnilline-g- polycaprolactone (YA-g-CL) :

YA (0.5 g) was added to a polymerization ampoule equipped with a magnetic stirrer and vacuum inlet. Then ε-caprolactone (2.82 ml) was added to polymerization ampule and mixture was stirred for 12h at 120 °C.

Preparation of α-CD-g-PG block YA-g- CL:

Host-guest interactions between *YA-g-CL* and cyclodextrin core of *α-CD*-g-PG were led to *α-CD-g-PG block YA-g- CL*. Solutions of *α-CD*-g-PG (2.3×10^{-2} M in water) were added to *YA-g-CL*(0.03 mmol) dispersed in water, and then mixture was sonicated for 2h at room temperature.

### Examination of the pH-Sensitivity of Dendrosomes

In order to study the stability of *α-CD-g-PG block YA-g- CL* in the different pHs, solutions of *α-CD-g-PG block YA-g- CL* (1.3×10^{-3} mol/L) in phosphate buffer with pH 7.4, 6.5, 6 and 5.5 was prepared and UV-vis spectra of these solutions was recorded at ambient conditions.

Results and discussion

α-CD-g-PG was synthesized via an anionic ring opening polymerization according to reported method in literature [18]. In the IR spectrum of *α-CD* -g-PG, three absorbance bands corresponded to the O-H, C-O-C and C-H groups are exhibited at 3380, 1116 and 2921 cm^{-1}, respectively.

In the ^{1}H NMR spectrum of *α-CD* -g-PG signals for protons of cyclodextrin and polyglycerol are overlapped at 4.3-3.6 ppm area. In this spectrum a small signal at 5.2 ppm is assigned to the anomeric protons of cyclodextrin. In the IR spectrum of YA-g-CL, three absorbance bands corresponded to the O-H, N=N and N-H groups are exhibited at 3380, 1598 and 3450 cm^{-1}, respectively.

Formation of Host-Guest (scheme 1) could be understand visually, because YA-g-CL insoluble in H$_2$O dissolved upon addition of *α-CD* -g-PG. However host-guest interactions between YA-g-CL and *α-CD* -g-PG leading to α-CD-g-PG block YA-g- C**L** were investigated by UV-vis spectroscopy methods.
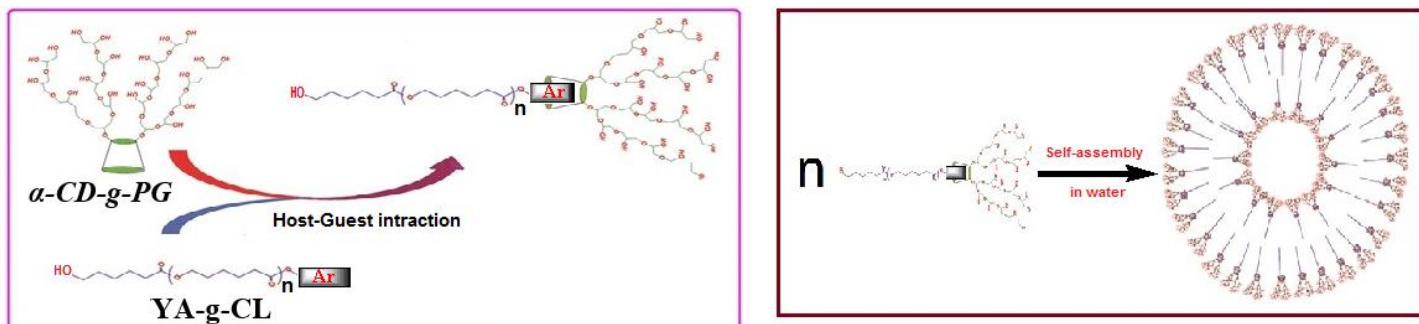
Scheme 1. Host-guest interactions between YA-g-CL and *α*-CD-g-PG.   **Scheme 2.** Self-assembly of Host-Guest nanopolymer in aqueous solutions .

Dendrosomes(scheme2) were able to encapsulate drugs such as paclitaxel with a high loading capacity. Drug loading content and drug loading efficiency of dendrosomes was evaluated using UV-vis spectroscopy.

Conclusion

 In this work we successfully developed a novel type of supramolecular Dendrosomes whit core_shell_corona structures upshot self-assembled from supramolecular amphiphilic block copolymer *α-CD* -g-PG: YA-g-CL. This study demonstrates that supramolecular Dendrosomes have highly stability in the aqueous environments, extremely high drug-loading capacity and good biocompatible. Hence, such supramolecular Dendrosomes are very promising candidates for improvements in drug delivery systems.

References:

[1] Movassaghian, S.; Moghimi, H R.; Shirazi, F H.; Torchilin, V P. *Journal of Drug Targeting*. **2011**, 19, 925.

[2] Zarrabi, A.; Adeli, M.; Vossoughi, M.; Shokrgozar, M. A. *Macromol. Biosci*. **2011**, 11, 383.

[3] Hassan Namazi, Abbas Dadkhah, *Journal of polymer* , 2012, 20, 794-800

[4] Kesharwani, P.; Gajbhiye, V.; Jain, N.K. *Biomaterials.***2012**, 33, 7138.

[5] Sun, S.; Du, J. *Polymer*. **2012**, 53, 2068.

[6] Lee, J.S.; Feijen, J. *Journal of Controlled Release.***2011**.

[7] Felber, A.E.; Dufresne, M.H.; Leroux, J.C. *Advanced Drug Delivery Reviews.***2012**.

[8] Chen, W.; Meng, F.; Cheng, R.; Zhong, Z. *Journal of Controlled Release.***2010**, 142, 40.

[9] Fleige, E.; Quadir, M.Q.; Haag, R. *Advanced Drug Delivery Reviews*. **2012**, 64, 866.
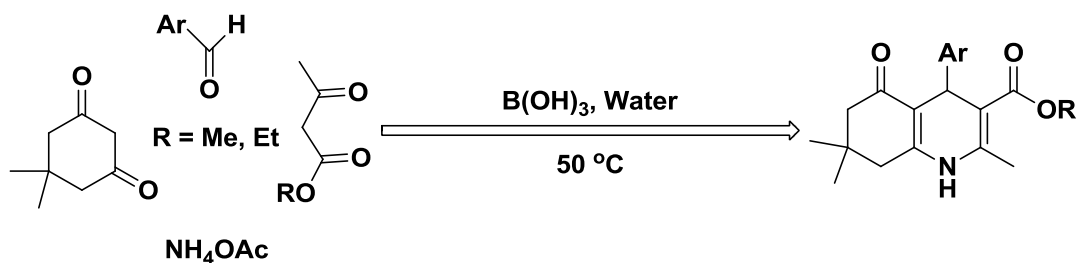
The synthesis of hexahydroquinolines using boric acid aqueous solution system

Ahmad Reza Moosavi-Zare,* Hamid Goudarziafshar,* Hadis Afshar-Hezarkhani

Sayyed Jamaleddin Asadabadi University, Asadabad, 6541835583, I. R. Iran.

Email address: moosavizare@yahoo.com & hamid_gafshar@yahoo.com.

Introduction: Quinolines with a 1,4-dihydropyridine structure are promising scaffolds because of their pharmacological activities. This part of quinoline derivatives has very utilizations in medicinal chemistry and used as antiasthamatic, antibacterial antihypertensive, anti-inflammatory, antimalarial, and tyrosine kinase inhibiting compounds[1-3]. One of the important classes of DHPs with a modified structural scaffold is hexahydroquinolines (HHQs) which could be prepared by the Hantzsch synthesis by the reaction of various aromatic aldehydes, dimedone, *β*-ketoesters and ammonium acetate *via* the one-pot four-component condensation reaction in the persence of various catalysts [4].

Scheme 1. The one-pot four-component preparation of hexahydroquinolines catalyzed by boric acid.

Experimental:

Procedure for the synthesis of hexahydroquinolines.

To a mixture of dimedone (1 mmol), arylaldehyde (1 mmol), ethyl acetoacetate (1 mmol) and ammonium acetate (1.2 mmol) in a 10 mL round-bottomed flask connected to a reflux condenser, was added boric acid (10 mol%) and a few drops of water, and the resulting mixture was stirred at 50 ℃. After completion of the reaction, the reaction mixture was cooled to room temperature. The crude product was purified by recrystallization from ethanol (95%).

Results and discussion:

To investigate the efficacy and the generality of the catalyst, dimedone was reacted with various aromatic aldehydes, ethylacetoacetate and ammomium acetate under the optimized reaction conditions. All reactions proceeded efficiently to give the desired hexahydroquinoline derivatives in high yields and in short reaction times. Therefore, boric acid aqueous solution system was a highly efficient and general catalyst for the preparation of HHQs.

Conclusion: In this work, we have reported the preparation of hexahydroquinolines using boric acid, at 50 °C under aqueous conditions.

References:

[1] R. Simsek, U. B. Ismailoglu, C. Safak, I. Sahin-Erdemli, *Farmaco*, **2000**, *55*, 665-668.

[2] R. D. Larsen, E. G. Corley, A. O. King, J. D. Carrol, P. Davis, T. R. Verhoeven, P. J. Reider, M. Labelle, J. Y. Gauthier, Y. B. Xiang, R. Zamboni. *J. Org. Chem.* **1996**, *61*, 3398-3405.

[3] Y. L. Chen, K. C. Fang, J. Y. Sheu, S. L. Hsu, C. C. Tzeng. *J. Med. Chem.* **2001**, *44*, 2374-2377.

[4] M. P. Maguire, K. R. Sheets, K. Mcvety, A. P. Spada, A. Ziberstein, *J. Med. Chem.*, **1994**, *37*, 2129-2137.

Investigation [4+2] Cycloaddition Reaction by Using Bismaleimides Derivative Functionalized with Magnetic Nanoparticles

Farzaneh Hamani[a], Zahra Hassani*[b], Mohamad Mahani[a]

[a] Department of Chemistry, Faculty of Sciences & Modern Technologies, Graduate University of Advanced Technology, P.O.Box: 76315-117, Kerman, Iran.
[b] Department of New Materials, Institute of Science, High Technology and Environmental Sciences, Graduate University of Advanced Technology, P.O.Box: 76315-117, Kerman, Iran.
*E-mail: hassanizahra@yahoo.com

Introduction: Iron oxide nanoparticles have been interested, due to unique properties, such as suitable surface chemistry and superparamagnetic properties [1]. Applications of nanoparticles can be mentioned in the catalysis fields, drug or gene delivery and its performance study in organic reactions [2] such as Micheal addition, Diels Alder and etc. DA reaction is a [4 + 2] cycloaddition between a diene and a dienophile leading to that formed a six membered ring [3] an adduct which dissociates under thermic treatment to turn back into the previous diene and dienophile compounds. The key point of the reaction, DA adducts are cleaved with heat as they undergo the opposite retro-Diels–Alder (rDA) that lead to changes in the properties of these materials and its application in various systems such as self-healing systems, thermoreversible materials, or materials having a controlled cross-linking reaction[4].

Methods / Experimentals: In this research, the Fe_3O_4 magnetic nanoparticles (MNPs) were synthesized by co-precipitation method and then functionalized with 3-amino propyl triethoxy silane (APTES) to create a suitable substrate. At the follow, synthesized bismaleimide derivatives as good dienophiles by condensation of maleic anhydride with various diamine [5]. The Micheal addition reaction has carried between an amine group in the surface of MNPs and carbon-carbon double bond of bismaleimide [6]. Diene separately was connected to functionalized nanoparticles with silane and finally Diels-Alder reaction performed between furan and bismaleimide.

Results and Discussion: The chemical structure of bismaleimide was confirmed using Fourier Transform Infrared spectroscopy (FT-IR) and measurement melting point. The FTIR spectra of bismaleimide showed the carbonyl characteristic peak in the range around of 1690-1700 cm^{-1} regarding amide group and 3101 cm^{-1} (=C–H); 1408, 1124 cm^{-1} (C-N-C). The DA reaction indicated by FTIR, which shows the increased wavelength of the carbonyl group in the area 1705-1715 cm^{-1} and the new peak appeared at 1271 cm^{-1} that shows the C–O–C ether peak of furan ring. The results of nuclear magnetic resonance spectroscopy (NMR) confirmed that the

Diels-Alder reaction performed between diene and bismaleimide. The absence of signal at the rigon130-136 ppm due to C=C maleimide and the appearance of new peak at 36-38 ppm corresponding to the new C-C bond, show that the synthesis was carried out successfully.

Conclusion: In this study a series of bismaleimides with structures and different amide groups were synthesized and characterized by FTIR and melting point. BMIs used in thermoset polymer, high performance application from military industry and aviation equipment. BMIs functionalized Fe_3O_4/APTES nanoparticles combined with diene by Diels Alder reaction. The product obtained from DA reaction can be used in the preparation of self-healing polymer to composite material and cross-linked network.

References

[1]. Jadhav, N.V., et al. "*Synthesis of oleic acid functionalized Fe_3O_4 magnetic nanoparticles and studying their interaction with tumor cells for potential hyperthermia applications*", Colloids and Surfaces B: Biointerfaces, **2013**, 108, 158-168.

[2]. Jain, T.K., et al. "*Magnetic nanoparticles with dual functional properties: drug delivery and magnetic resonance imaging*", Biomaterials, **2008**, 29, 4012-4021.

[3]. Knot-Tso, M.E., Schmart, I. M. "*endo- vs. exo-selectivity in diels alder reaction of maleic anhydride*", Chem, Ed, **2004**, 81, 1633-1636.

[4]. Dolci, E. et al. "*Remendable thermosetting polymers for isocyanate-free adhesives: a preliminary study*", Polym. Chem, **2015**, 6, 7851-7861.

[5]. Kumar, A., et al. "*Preparation and characterization of siliconized epoxy-1, 2-bis (maleimido) ethane intercrosslinked matrix materials*", Appl Polym Sci, **2003**, 89, 3808–3817.

[6]. Peterson, A.M., Jensen, R.E., and Palmese, G.R."*Thermo reversible and remendable glass–polymer interface for fiber-reinforced composites*", Composites Science and Technology, **2011**, 71, 586-592.

Application of methyl phenyl silicon as Adsorbent for Detection of Butachlor pesticide Using Quartz Crystal Nano balance

Abdolreza Mirmohseni[a,*], Khalil Farhadi [b] , Shim jahangiri[c]

[a]Polymer Research Technology Laboratory, Applied Chemistry Department, University of Tabriz, Tabriz, Iran

[b]Department of chemistry, faculty of science, Urmia University
[c]Department of chemistry, faculty of science, Urmia University

Email address:mirmohseni@yahoo.com

Introduction:

Butachlor is an organochlorine herbicide of the acetanilide class. It is used as a selective pre-emergent herbicide. It is extensively used in the form of granules in rice as post emergence herbicide.During the last few years, in solid phase micro extraction technique, polydimethylsiloxane, silica fibers, and polydimethylsiloxane coated silica fibers have frequently been used as a selective polymer layer for extraction of chlorinated hydrocarbons and organochlorine pesticides (OCPs) [1–4].Despite high sensitivity and reliability of common procedures used to analyze pesticides (GC[5–7], high-performance liquid chromatography (HPLC)[8–9], GC–MS with chemical ionization-selected ion monitoring (CI-SIM)[10] and GC–spectrometry (MS)[11]), these techniques suffer from practical limitations, such as: instrumental complexity, sample manipulation, specialist operator mplementation and requiring preconcentration step.In recent years, due to some advantages including low cost, portability and easy on-line analysis, much attention has been paid to use quartz crystal nanobalance based sensors for various pesticides monitoring. Sensors based on quartz crystal nanobalance have been developed for detection and determination of telone [12], imidacloprid and thiacloprid [13], carbaryl insecticide and 3,5,6-trichloro-2-pyridinol,organophosphorus and carbamate.[14, 15]Therefore, the purpose of this work is to study of high selectivity from the piezoelectric microgravimetry using selective methyl phenyl silicon films technique and high sensitivity from quartz crystal nanobalance detection to develop a simple, sensitive, and reproducible sensor based on quartz crystal nanobalance for the determination of Butachlor in aqueous solutions.

Methods / Experimentals:

The quartz electrode was coated using 5 μL of methyl phenyl silicon in chloroform (0.5 % w/v) solution. Solvent evaporated for 24 h and a thin layer of adsorbent was formed on the surface of the electrode. All measurements were carried out in a glass cell with an internal volume of 15 mL. First 10 mL of distillated water was added to the cell then certain volumes of analyte were injected into the water by Hamilton micro liter syringes and the frequency shift of crystal was recorded. In order to recover the modified quartz electrode after a measurement had been made it was exposed to N_2 gas. All measurements were carried out at room temperature (25°C).

Results and Discussion:

The calibration curve was constructed by plotting the frequency shifts versus the concentrations of Butachlor solutions (Fig. 1). The frequency shifts were recorded after 45 min exposing samples to the modified electrode. According to the calibration curve, there is a linear relationship between the Butachlor concentration and the magnitude of the response obtained. The correlation coefficient of R2= 0.97 was obtained for coated electrode**.** A response obtained by a sensor should be linear against the concentration of analyte. This property was evaluated by exposing the selective coating electrode to various concentrations of Butachlor solutions ranging from 1 to 30 mg L^{-1} . It is obvious from these results that the value of the frequency shift increases monotonically with increasing Butachlor concentration. This result suggests the possibility of fabrication a Butachlor sensor using selective coated electrode. To investigate the reproducibility of the results, the coated quartz crystal nanobalance was alternatively exposed to 20 mg L$_{-1}$ of Butachlor and the change in the frequency of the quartz crystal was recorded. indicates that the sensors perform in a rather reproducible manner (Fig. 2). In order to recover the modified quartz electrode after ameasurement, it was exposed to N$_2$ gas. The frequency of the crystal were back-shifted to its initial, indicating full desorption of analyte from the electrode surface (Fig. 3).

Conclusions:

An inexpensive method was developed for simple and quantitative determination of Butachlor levels in the aqueous solutions. A selective coating for the selective determination of Butachlor was constructed on a quartz crystal nanobalance electrode. Frequency shifts versus concentration changes of analytes exhibited satisfactory linear correlation. Results showed that the sensor is sensitive enough to detect the Butachlor.

References

[1] s. Magdic; J.B. Pawliszyn. , *Journal of Chromatography A*, **1996**, *723*, 111–122.*.*

[2] J.L.R. Junior; N. Re-Poppi. *Talanta*, **2007**, *72*, 1833–1841.

[3] C. Dong; Z. Zeng. *Water Res*, **2005**, *39*, 4204–4210.

[4] J. Zeng; J. Chen; Z. Lin. *Anal. Chim. Acta*, **2008**, *619*, 59–66.*.*

[5] W. Driskell; D. Groce. *Journal of Analytical Toxicology*, **1991**, *15*, 339–340.

[6] M.Araki.; K.Yonemitsu; T.Kambe. *J. Leg. Med*, **1982**, *36*, 584–588.

[7] J.Ikebuch; S.Kotoku; T.Nishigaki. *J. Leg. Med*. **1983**, *37*, 421–427.

[8] A.Tsatsakis; E.Michalodimitrakis; A.Tsakalof. *Bull. Int. Assoc. Forensic Toxicol*. **1992**, *22*, 23–26.

 [9] G.Wei.; Y.Li; X.Wang. *J Sep Sci*. **2007**, *30*, 3262–3267.

[10]T. Miyazaki; M.Yashiki;T. Kojima*. Forensic Sci. Int*. **1989**, *42*, 263–270.

[11]S. Bogialli; R.Curini; A.Corcia. *Journal of Chromatography A*. **2004**, *1054*, 351–357.

[12] A.Mirmohseni; M.Rastgouy Houjaghan. *Journal of Environmental Science and Health, Part B*. **2012**, *47*, 677–686.
[13] X.Bi; K.Yang.*Anal. Chem*. **2009**, *81*, 527–532.
[14] C.March; J.Manclus. *Talanta* **2009**, *78*, 827–833.
[15]N. Karousos.; S.Aouabdi; A.Way. *Analytica Chimica Acta*. **2002**, *469*(2), 189–196.

Preparation of MnO$_x$/γ-alumina Nanocatalysts by homogeneous deposition precipitation; It's NH$_3$-SCR efficiency

Seyed Mahdi Mousavi [a,*], **Parvaneh Nakhostin Panahi** [b]

[a] *Faculty of Chemistry, University of Kashan, Kashan, Iran*

[b] *Department of Chemistry, Faculty of Science, University of Zanjan, Zanjan, Iran*

Email address: mousavi.smahdi@kashanu.ac.ir

****

Introduction: The selective catalytic reduction of NO$_x$ using NH$_3$ (NH$_3$-SCR) is a highly efficient technology for NO$_x$ emissions control [1]. Different groups of catalytic systems, including transition, noble and rare earth metal have been studied for NH$_3$-SCR of NO$_x$ [2,3]. Among the transition metal oxides, Manganese oxide is the most studied due to their low volatility (various types of loosely bound oxygen species) [4]. The aim of the present work is to develop the MnO$_x$/γ-alumina nanocatalysts for NH$_3$-SCR of NO$_x$. MnO$_x$/γ-alumina nanocatalysts were prepared by homogeneous deposition precipitation (HDP) and were characterized by XRD, H$_2$-TPR, N$_2$ adsorption and TEM.

Methods: The MnO$_x$/γ-alumina nanocatalysts were prepared by HDP using urea as the precipitating agent. The NH$_3$-SCR activity of catalysts was measured in a fixed bed reactor. A feed containing 1000ppm NO, 1000ppm NH$_3$, 5% O$_2$ and Ar as balance was passed over 0.2 g catalysts (at temperature range of 100 to 400 °C with a step of 50 °C). The concentrations of NO, NO$_2$, N$_2$ and N$_2$O were monitored by a flue gas analyzer and gas Chromatograph.

Results and discussion: According to the XRD patterns of MnO$_x$/γ-alumina (Fig.1), the original structure of γ-alumina is not destroyed during preparation of nanocatalysts. There is no diffraction peak related to MnO$_x$ phases, suggesting that the well-dispersed nanosized MnO$_x$ phases were formed on the γ-alumina structure, which is justified by the TEM images (Fig.2). Form the H$_2$-TPR (Figure not shown), The shift of the reduction peaks to lower temperatures could be due to the dispersion of Mn species on the support and/or the synergistic effect between the Mn species and support [7, 10]. The NH$_3$-SCR activity of MnO$_x$/γ-alumina with different Mn loading in term of NO$_x$ conversion (%) and N$_2$ selectivity (%) as function of reaction temperature is
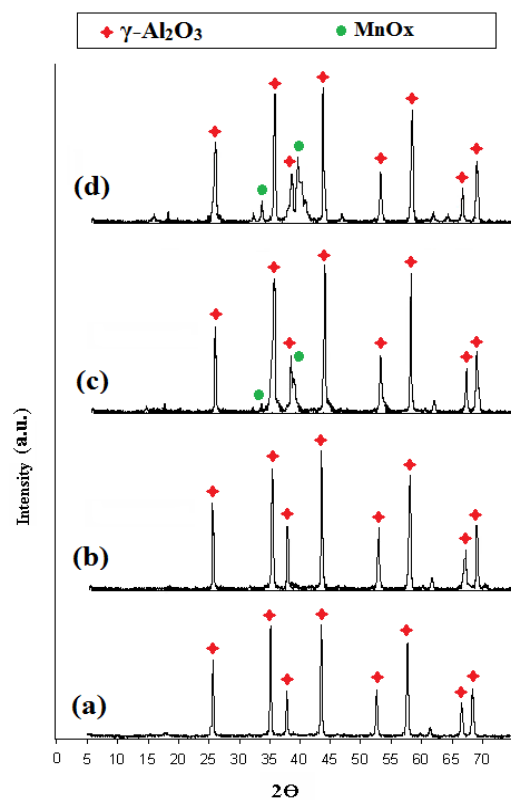

Fig. 1: X-ray diffraction patterns of; (a) γ-alumina, (b) 1 wt. % MnO$_x$/γ-alumina (c) 5 wt. % MnO$_x$/γ-alumina, (d) 9 wt. % MnO$_x$/γ-alumina

presented in Figure 3. NO conversion significantly increases with increasing the Mn loading and shows a maximum at loading of 5 wt. %. A further increase in the Mn loading does not result in a further increase in NO conversion.
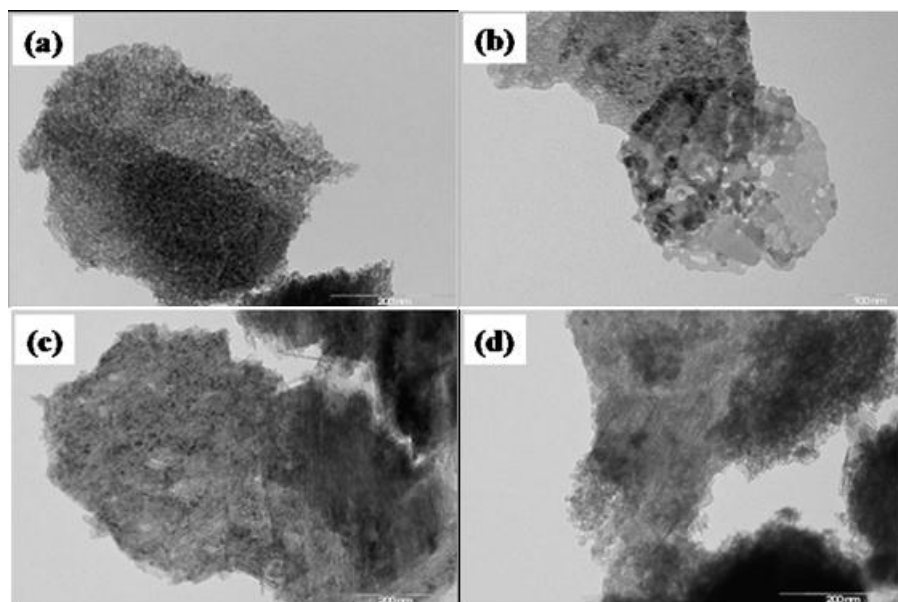

Fig. 2: TEM images of; (a) γ-alumina, (b) 1 wt. % MnO_x/γ-alumina, (c) 5 wt. % MnO_x/γ-alumina and (d) 9 wt. % MnO_x/γ-alumina
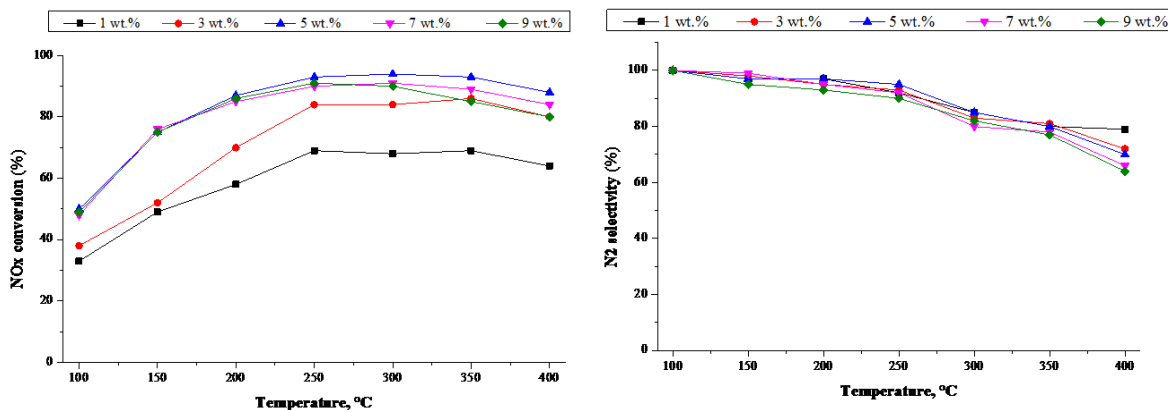

Fig. 3: NO_x conversion and N_2 selectivity MnO_x/γ-alumina nanocatalysts with different Mn loading as function of temperature

References

[1] Liu Z, Woo SI. *Cat Rev Sci Eng,* **2006**, 48, 43-89.
[2] Nakhostin Panahi P, Salari D, Niaei A, Mousavi SM. *J Ind Eng Chem,* **2013,** 19, 1793-1799.
[3] Mousavi SM, Niaei A, Illán Gómez MJ, Salari D, Nakhostin Panahi P, Abaladejo-Fuentes V. *Mater Chem Phys,* **2014**, 143, 921-928.
[4] Mousavi SM, Niaei A, Salari D, Panahi PN, Samandari M. *Environ Technol,* **2013,** 34, 1377–1384.

Synthesis of Substituted Pyrazoles *via* Three Component Reaction

Kaveh Amir Ashjei Asalemi[a], Abdolali Alizadeh[a,b]*

[a]Department of Chemistry, Tarbiat Modares University, P.O. Box 14115-175, Tehran, Iran

[b]aalizadeh@modares.ac.ir

Introduction:

The pyrazole moiety is present in a wide variety of biologically active compounds [1,2]. Numerous compounds containing pyrazole moiety have been shown to exhibit antihyperglycemic, analgesic, anti-inflammatory, antipyretic, antibacterial, hypoglycemic, sedative-hypnotic activity. Thus, many efforts have been devoted to the development of more synthetic methodologies to this class of compounds [3-5].

In our attempt to synthesis of pyrazoles, we succeeded to synthesis of substituted pyrazoles *via* three component reaction using ketene dithioacetal.

Methods / Experimentals:

Chemicals were purchased from Merck and Aldrich chemical companies and were used without further purification. Melting points were determined using an electro thermal 9100 apparatus. The IR spectra were performed with a NICOLET FT-IR 100 spectrometer. Mass spectra were recorded on Agilent technologies 5975C spectrophotometer. The NMR spectra were obtained using Bruker Advance DRX-500 in DMSO.

Results and Discussion:

1-Phenyl-2-(5-phenyl-1*H*-pyrazol-3-yl)ethan-1-one were synthesized *via* a three component reaction between 3,3-bis(methylthio)-1-phenylprop-2-en-1-one **1**, acetophenone **2** and hydrazine at room temperature in THF (Scheme 1). The ketene dithioacetal **1** was obtained from treatment of acetophenone with CS_2. All products were precipitated in solvent and purified by washing with cold Ethanol.
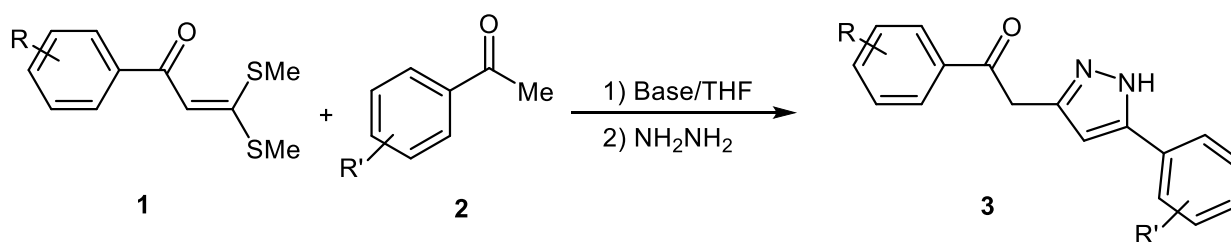
Scheme 1. Synthesis of 1-aryl-2-(5-aryl-1*H*-pyrazol-3-yl)ethan-1-ones **3**

The melting point of product **5a** (R = H, R' = H) was 153-154 °C. The IR spectrum of **5a** shows a sharp peak at 1670 cm^{-1} that belongs to carbonyl group and a sharp peak at 3390 cm^{-1} that shows the NH group. The ^{1}H NMR spectrum of **5a** show two singlet peaks for NH hydrogen (δ = 12.7 ppm and δ = 13.11 ppm). Two singlet peaks belong to existence of two isomers in reaction pot (Scheme 2). Signal of methylene group appeared in 4.3 ppm and a signal of the aromatic hydrogen's appeared in 6.55-8 ppm.
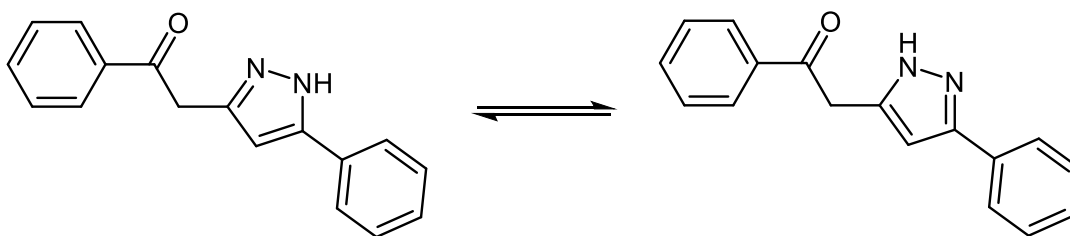
Scheme 2.

Conclusion:

We introduced a facile way for synthesis of 1-phenyl-2-(5-phenyl-1*H*-pyrazol-3-yl)ethan-1-one in moderate yield and mild condition. The most advantage of this reaction was that all the product compounds were purified simply.

References

[1] Elguero, J. *Karitzyky, AR* **1984**, 167-303.

[2] Genin, M. J.; Biles, C.; Keiser, B. J.; Poppe, S. M.; Swaney, S. M.; Tarpley, W. G.; Yagi, Y.; Romero, D. L. *Journal of Medicinal Chemistry* **2000**, *43*, 1034-1040.

[3] Lyga, J. W.; Patera, R. M.; Plummer, M. J.; Halling, B. P.; Yuhas, D. A. *Pesticide science* **1994**, *42*, 29-36.

[4] Babinski, D. J.; Aguilar, H. R.; Still, R.; Frantz, D. E. *The Journal of Organic Chemistry* **2011**, *76*, 5915-5923.

[5] Huang, Y. R.; Katzenellenbogen, J. A. *Organic Lett.* **2000**, *2*, 2833-2836.

Preparation of pyrano[2,3-d]pyrimidines using SPSA as novel reusable catalysts

Zahra khazaei poul,* Masoud Mohammadi zeydi

Department of Chemistry, College of Science, University of Guilan, Rasht, 41335-19141, Iran

Email: Zahrakhazaei69@gmail.com

****

Introduction: The pyranopyrimidines and its derivatives have attracted attention due to their wide variety of biological activities including antitumor [1], antibacterial and antifungal [2], anti-inflammatory [3], anticancer [4], antimicrobial [5]. There are some methods for the synthesis of pyranopyrimidines using different catalysts, such as SBA-Pr-SO$_3$H [6], dibutylamine (DBA) [7], 1,2-dimethyl-*N*-butanesulfonic acid imidazolium hydrogen sulfate ([DMBSI]HSO$_4$) Bronsted-acidic [8], *L*-Proline [9], diammonium hydrogen phosphate [(NH$_4$)$_2$HPO$_4$] (DAHP) [10]. Many of these methods involve expensive reagents, long reaction times, low yields, use of excess of reagents catalysts and use of toxic organic solvents. Therefore, to avoid these limitations we here report that solvent-free condensation of aromatic aldehyde barbituric acid with malononitrile using SPSA, as heterogeneous acid catalyst quickly prepared the pyranopyrimidine derivatives in good yields.

Methods/Experimentals: Melting points were recorded on an electrothermal type 9100 melting points apparatus. The IR spectra were obtained using a 4300 Shimadzu spectrophotometer as KBr disks. ^{1}H NMR (500 MHz) spectra were recorded with Bruker DRX500 spectrometers.

To a mixture of barbituric acid (1 mmol), malononitrile (1 mmol) and aryl aldehydes (1 mmol) was added SPSA (5 mol%) and the reaction mixture was stirred mechanically at 100 °C. The progress of reaction was monitored by TLC, after completion of the reaction, the reaction mixture was diluted with hot ethanol, residue was dissolved in ethanol, the solid catalyst was filtered off, and the fairly pure crystals of products obtained from the recrystallized in ethanol.
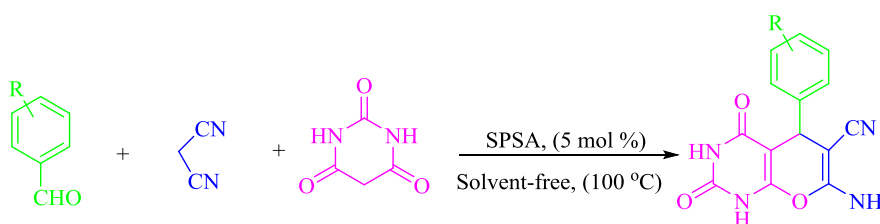
Scheme 1. Synthesis of pyranopyrimidine derivatives

Results and Discussion: Following our continued studies in the development of new methods for the synthesis of pyranopyrimidine derivatives, we have described the preparation of SPSA, and its use as an efficient catalyst for synthesis of pyranopyrimidine derivatives of condensation reaction of various aromatic aldehydes, barbituric acid with malonnonitrile in solvent- free reaction conditions. We initiated our survey with producing SPSA by addition of amount of cholorosulfonic acid to SP. The reaction is easy and clean and needs no special workup procedure. In the following, to find the best reaction conditions, we studied the

synthesis of (4-chlorophenyl)pyranopyeimidine as a model reaction in the presence of different amounts of SPSA under different conditions.
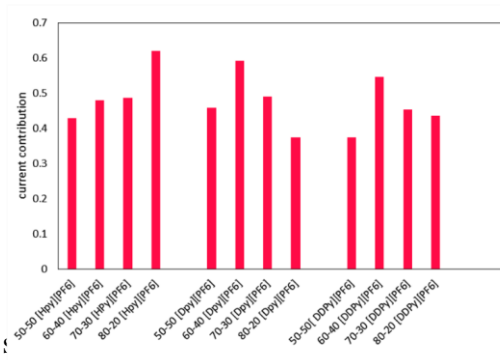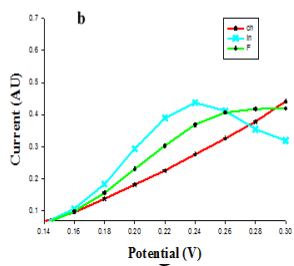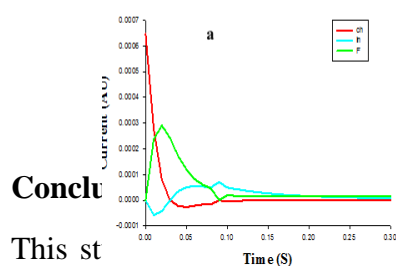
Raise the quantity of the catalyst increased the yield of the product. The optimal amount of the catalyst was 5 mol%, the higher amount of the catalyst beyond this value did not increase the yield noticeably. Based on the result, this procedure was then extended to variety of aldehyde derivatives at the optimized system. The reactions of aromatic aldehydes having electron withdrawing groups were somewhat faster than electron donating groups. The reusability of the catalyst was checked via the same model reaction under optimized conditions. The catalyst could be reused at least five times with only little reduction in the catalytic activity of the catalyst.

Conclusion: In conclusion, we have successfully developed a very efficient, simple, and mild methodology for the preparation of a wide variety of pyranopirimidines through reaction of aromatic aldehyde, barbituric acid and malononitrile employing SPSA as the recyclable solid acid catalyst under solvent-free conditions for the first time. Other advantages of this protocol are excellent yields, ease of preparation of the catalyst, simplicity, short reaction time, easy work-up.

References

[1] Jamal R.B.; Rajendra S.D.; Rupali S.S. *J. Pharm. Biosci*, **2014**, *5*, 422-430.

[2] Bhat A.R; Shalla A.H; Dongre R. S. *J. Adv. Res*, **2015**, *6*, 941-948.

[3] El-Gazzar A.B.A.; Hafez H.N. *Bioorg. Med. Chem. Lett,* **2009**, *19*, 3392-3397.

[4] Srivastava A.; Pandeya S.N. *Int. J. Curr. Pharm. Rev. Res.* **2011**, *4*, 5-8.

[5] Patel, N.B.; Agravat, S.N. *Chem. Heterocycl. Compd,* **2009**, *45*, 1343-1353.

[6] Ziarani, G.M.; Faramarzi, S.; Asadi, S.; Badiei, A.; Bazl, R.; Amanlou M. *J. Pharm. Sci.* **2013**, *21*, 1-13.

[7] Bhata A.R.; Shalla A.H.; Dongrea R.S. *J. Taibah Uni. Sci*, **2016**, *10*, 9-18.

[8] Hossein N.R.; Mamaghani M.; Tabatabaeian K.H.; Shirini F.; Rassa M. *Acta Chim. Slov.* **2013,** *60,* 889–895.

[9] Bararjanian M.; Balalaie S.; Movassagh B.; Amani A.M.; *J. Iran. Chem. Soc,* **2009**, *6*, 436-442.

[10] Abdolmohammadi S.; Balalaie S. *J. Org. Chem*, **2012**, *2*, 7-14.

A Comparative Study on the Effect of Ionic Liquid Composition on the Contributions of Faradic Current in Ionic Liquid Carbon Paste Electrodes by Chemometrics Method

B. Hemmateenejad*, J. Tashkhourian*, S. Ahmadpour, E.Talebanpour Bayat

hemmatb@sums.ac.ir (B. Hemmateenejad), Tashkhourian@susc.ac.ir (J. Tashkhourian)

Introduction

Chemical modification of electrode surfaces has been one of the most active research areas in electrochemistry [1]. In this way ionic liquids are one of the modifiers that used .One of the most important electrochemical applications of IL is the replacement of a non-conductive organic binder with a conductive IL in fabricating carbon paste electrodes (CPEs). [2] Achieving the highest possible faradaic current, is one of the main goals of applying modifiers in electrochemical systems. However, non-faradaic processes are the major interference with such measurement [3].and by using some methods we can minimize this interference. One of these methods is chemometrics method that resolve total current into the net faradaic current, and charging current. The main focus of this work is on the effect of the molecular structure of ionic liquid and it's weighting percent in the electrode.

Experimental

After preparation of different electrodes. The electrochemical behavior of K_4 [Fe (CN) $_6$] was studied by that electrodes using chronoamperometry   with the sampling time of 0.01 s at different potential steps. Analyzing of data were done with MCR-ALS experiment and the programs that written in MATLAB software.

Results and Discussion

In this work, potential step-chronoamperometry technique was used as an electrochemical method for testing different electrodes, figure 1 shows the sample of recorded potential step-chronoamperograms.

After calculating significant principal components in the system by different methods. MCR-ALS analysis was employed on the system and the resolved voltammograms and chronoamperograms were achieved as shown on of this sample in Fi

chronoamperograms and voltammograms, the relative contributions of each type of current in total current were calculated for all the studied electrode as the contribution of faradic current is shown in fig 3.

Conclu

This st

responses.The contribution of the relative faradaic current varies in the range of   **Fig.3**   67%
whereas the contribution of the charging current is much higher.

Fig.2

References

[1] R.C. Alkire, D.M. Kolb, J. Lipkowski, P.N. Ross, Chemically modified electrodes, John Wiley & Sons2009.

[2] N. Maleki, A. Safavi, F. Tajabadi, Analytical Chemistry, 2006, 78, 3820-3826.

[3] J. Tu, W. Cai, X. Shao, Analyst, 2014, 139, 1016-1022.

Synthesis of aminoclay decorated with Cu(II) picolinic acid complex via ionic interaction as a novel efficient heterogeneous phosphine-free catalyst for amination of aryl and heteroaryl iodides and bromides with alkylamines and N(H)-heterocycles

Nafiseh Fahimi[a], Ali Reza Sardarian[a],*

[a]Department of Chemistry, College of Sciences, Shiraz University, Shiraz 71946- 84795, Iran.

*Corresponding author: E-mail: sardarian@shirazu.ac.ir; Tel: +98 71 3613 7109; Fax: +98 71 3646 0788

Introduction: In the past decades, the transition metal catalyzed formation of C-heteroatom bonds has been obtained much attentions due to their high efficiency, economic viability, and stability in air [1]. There are many reports in the literature based on using palladium [2], molybdenum [3], nickel [4], iron [5], cobalt [6], and copper [7] in the C-X (X=O, N, S) couplings. The copper mediated processes, such as Ullmann reaction has become one of the general methods for C-C, C-N, and C-O bond formations in aryl couplings [8]. Copper is less expensive and the complexes of copper are heterogeneous in organic solvents [7]. *N*-arylamines are vital biologically active natural products and pharmaceuticals which have many applications in materials research [6]. In continuation of these efforts, we decided to design a novel heterogeneous phosphine-free aminoclay@ Cu (II) complex via surface functionalization of the aminoclay and then to consider its efficiency against C-N coupling reaction.

Experimentals: *Preparation of Aminoclay Immobilized Cu(II) Complex Catalyst.* The aminoclay was prepared by the method reported in literature [9]. Then the ligand was anchored on aminoclay. After that Cu salt was added and the resultant mixture was stirred for appropriate time. The catalyst was centrifuged and washed thoroughly with ethanol until the washing was colorless. The catalyst was dried overnight in air and then in oven at 120 °C. Finally a blue uniform powder was obtained. *General procedure for N-arylation of N(H)-heterocycles and amines with various aryl halides.* Aryl iodide (1 mmol), amine (1.2 mmol), Cs_2CO_3 (2 mmol), and Cu(II)- catalyst (0.01 g) were added to DMF (3 ml) and according to amine type, stirred for 4 to 8 hours at 100 °C. The reaction progress was controlled by TLC analysis and after reaction quenching, Cu-based catalyst was isolated from crude by filtering. Then, the crude was poured in ice water to extract product. The flash column has been finally applied for finding pure product.
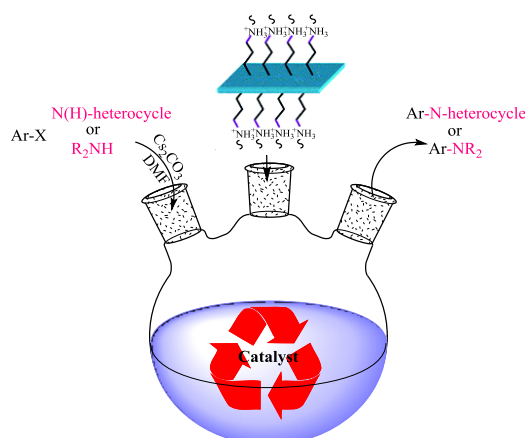
Result and Discussion: A new Cu(II) picolinic acid complex supported on aminoclay was synthesized and completely characterized by ICP, IR, XRD, TGA, EDX and UV-visible techniques. The reaction condition were optimized to find the best condition for any special coupling reaction. Various bases including Cs_2CO_3, K_2CO_3, NaOH, t-BuONa, NaOAc, and K_3PO_4 were firstly examined to find the best one in reaction. Then for solvent optimization, there were used protic and aprotic solvents. DMF was firstly studied as the solvent and other solvent that have also been investigated were EtOH, acetonitrile, water, and toluene with different bases, respectively. According to our investigation, the best reaction condition was found using (0.01 g) in the presence of DMF and Cs_2CO_3 as solvent and base respectively, at 100 °C. In the following, we examine the ability of catalyst in the Cu based catalyzed Ullmann coupling reaction of different aryl halides with amines and N(H)-heterocycles such as Imidazole, Benzimidazole, Indoles, Pyrrole, Piperazine, and Phenylpiperazine. In the case of aryl halides, electron-withdrawing groups have derived the reaction to more yields and less reaction times. In addition, aryl iodides were more reactive than aryl bromides and caused satisfactory yields. The N(H)-heterocycle type changed nothing in coupling reaction; but the amine type in notable. The reactions contain aliphatic amines presents somehow less yields.

Conclusion: In this paper, a novel and efficient heterogeneous Cu-based catalyst was synthesized and investigated in C-N coupling reaction. We applied ICP analysis to find the amount of catalyst leaching and there has been observed permissible results after 7 runs. The synthesized catalyst efficiently advanced the Ullmann type C-N coupling reaction at low catalytic and reaction time in which good yields were obtained.

Refrences

[1] Miao D; Shi X; He G; et al. *Tetrahedron*, **2015**, *71*, 431-435.

[2] Yang Q; Quan Z; Wu S; et al. *Tetrahedron*, **2015**, *71*, 6124-6134.

[3] Zwettler N; Dupe A; Schachner JA; et al. *Inorg. Chem.* **2015**, *54*, 11969-11976.

[4] Montgomery, J; *Acc. Chem. Res.* **2000**, *33*, 467-473.

[5] Sherry BD; Fürstner, A. *Acc. Chem. Res.* **2008**, *41*, 1500-1511.

[6] Amatore M; Gosmini C; *Angew. Chem. Int. Ed.* **2008**, *47*, 2089-2092.

[7] Zhang J; Jia R-P; Wang D-H; et al. *Tetrahedron Lett*. **2016**, *57*, 3604–3607.

[8] Damkaci F; Alawaed A; Vik E; et al. *Tetrahedron Lett*. **2016**, *57*, 2197–2200.

[9] Patil AJ; Muthusamy E; et al. *Angew. Chem. Int. Ed.* **2004**, *43*, 4928-4933.

Comparison of conventional and microwave-assisted synthesis of perphenazine magnetic molecularly imprinted polymer

Zahra Ramezani [a, b], Mehdi Safdarian [a,*]

[a] Nanotechnology Research Centre, Ahvaz Jundishapur University of Medical Sciences, Ahvaz, Iran

[b] Medicinal Chemistry Department, Faculty of Pharmacy, Ahvaz Jundishapur University of Medical Sciences, Ahvaz, Iran

Email address: Msafdaryan@yahoo.com

****

Introduction: Microwave energy, in contrast to heating reactions with traditional equipment, such as oil baths, is introduced into the chemical reactor remotely and passes through the walls of the reaction vessel, heating the reactants and solvents directly. The use of microwave energy instead of conventional heating often results in good yields in a short time [1, 2]. In this work microwave-assisted synthesis of magnetic molecularly imprinted polymer (MMIP) for perphenazine are introduced and compared with conventional perphenazine MMIPs [3] in preconcentration of perphenazine (PPZ) from human urine and plasma samples.

Methods / Experiments: At first, nano absorbent synthesize from two methods, conventional and/or microwave heating (MH), were characterization with TEM and FESEM microscopic image, FTIR, VSM and BET. Secondly, experimental conditions were optimized for each adsorbate pre-concentration of PPZ. Finally, analytical performance of absorbents in extraction and pre-concentration of PPZ from biological fluids were investigated.

Results and discussions: MMIPs which were synthesized through MH have shown narrow distribution smaller size particles with more uniform spherical morphology, fig. 1.B. Instead, conventional heating results in more amorphous particles with 150 nm in size (fig. 1.A). Adsorbate capacity of microwave synthesized particles and particles prepared by conventional methods for perphenazine were 80 and 50 mg g^{-1}, respectively. While Polymerization time were deduced from 90 min to 30 min from conventional to microwave assisted synthesis for perphenazine.

At optimum condition 5 mL of standard or real samples adjust to pH 6 and 5 mg of absorbent was added and vortexed for 1 min. The resulting solution was decanted by applying the magnetic field. After washing absorbent by appropriate solution, PPZ was finally extracted from MMIPs shell by eluting the adsorbent twice with 200 µL of MeOH:HOAc (9:1, v/v) followed by sonication for about 1 min. Extraction time for both absorbent is 1 min and desorption time is 2 min.
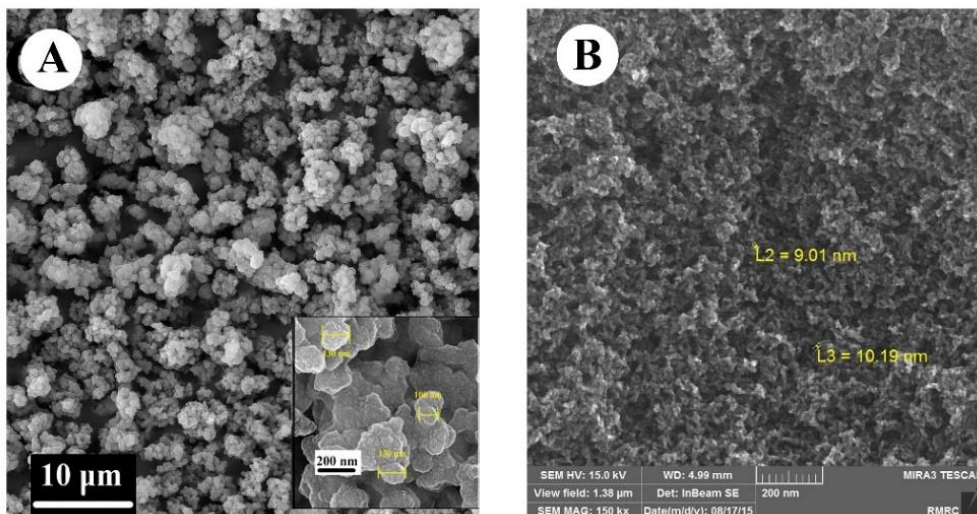
Fig. 1: FESEM image of final absorbents synthesize with A) conventional heating B) microwave assisted heating

Conclusion: To sum up, MH is more efficient for perphenazine MMIP syntheses compared to conventional heating system. MH produce more uniform particles with smaller size and good capacity. About 67% decrease in polymerization time was observed while using MH for MMIP synthesis. Absorbent synthesized by both methodology have shown the same analytical performance in HPLC analysis of human urine and plasma. It indicates that differences in physical properties of perphenazine MMIPs doesn't affect the analytical performances.

References

[1] M. Seifi, M. Hassanpour Moghadam, F. Hadizadeh, S. Ali-Asgari, J. Aboli, S.A. Mohajeri, Int J Pharm, 471 (2014) 37-44.
[2] Y. Zhang, R. Liu, Y. Hu, G. Li, Analytical Chemistry, 81 (2009) 967-976.
[3] M. Safdarian, Z. Ramezani, A.A. Ghadiri, J Chromatogr A, 1455 (2016) 28-36.

Fe₃O₄@SiO₂@La nanocomposite: An efficient and recyclable catalyst for the one-pot synthesis of 5-substituted-1H-tetrazoles

Fatemeh Pourhassan [a], Hossein Eshghi [a,*]

[a] Department of Chemistry, Faculty of Science, Ferdowsi University of Mashhad, Mashhad, Iran. E-mail: heshghi@um.ac.ir

****

Introduction: Tetrazoles are important and useful class of heterocycles with wide range of applications in medicinal chemistry, coordination chemistry and material science. Due to the harsh conditions and harmful side products of the acid-catalyzed procedures for the synthesis of 5-substituted-1H-tetrazoles, new metal-based catalysts have been reported. Among them Cu, Cd, Fe, Zn, Ag, and In-based homogeneous catalyst have been investigated for production of tetrazoles via a [3+2] cycloaddition reaction between azide ion and organic nitriles. In this work, new magnetically recoverable lanthanum-based heterogeneous catalyst has been studied for the synthesis of tetrazoles for the first time [1].

Methods / Experimental:

The Stöber method was utilized for the synthesis of core-shell Fe₃O₄@SiO₂ MNPs [2]. An aqueous dispersion of Fe₃O₄ were dissolved into a mixture of ethanol/deionized water. Ammonia solution was then added and tetraethyl orthosilicate was dropped into the mixture. Finally, aqueous solution of LaCl₃ was dropped into the suspension of Fe₃O₄@SiO₂ under stirring and were heated at 723K. Catalyst was then separated with an external magnet and washed with ethanol and dried at 80 °C.

Results and Discussion:

The TEM micrographs and size distributions (70 and 68 nm) of nanocatalyst are shown in Fig. **1a** and Fig. **1b**. TEM images indicated that the most of the prepared nanoparticles are rod shaped and have sized 60-70 nm (Fig.**1a**). The energy dispersive spectrum (EDS) indicated the presence of Fe, O, Si and La elements (Fig. **1c**). This analysis confirms that La is supported on catalyst. The magnetic saturation value of the Fe₃O₄ and Fe₃O₄@SiO₂@La is 64.99 and 35.13 emu/g, respectively, demonstrating that the composite particles possess magnetic properties (Fig. **1d**).
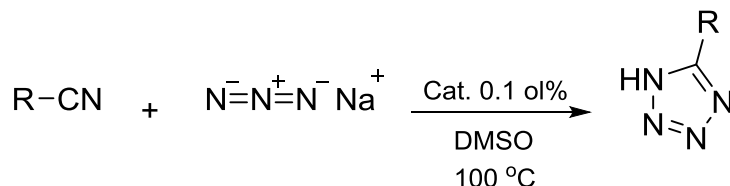
Scheme 1. Synthesis of tetrazoles.

Only 40% addition product is obtained when the reaction is carried out without catalyst in DMSO at 100 ºC, despite of prolonged reaction time. At the same reaction condition, 100% conversion was obtained after 30 min in the presence of Fe₃O₄@SiO₂@La. This result highlights the specific role of our catalyst in [3+2] cycloaddition reaction of benzonitrile with sodium azide

(Scheme 1). Among the different tested solvents, DMSO was found to be the solvent of choice for the synthesis of tetrazoles. Increasing the catalyst loading than 0.1 mol% did not lead to higher conversion, while lower catalyst loading has lessened the reaction yield even after longer reaction time.
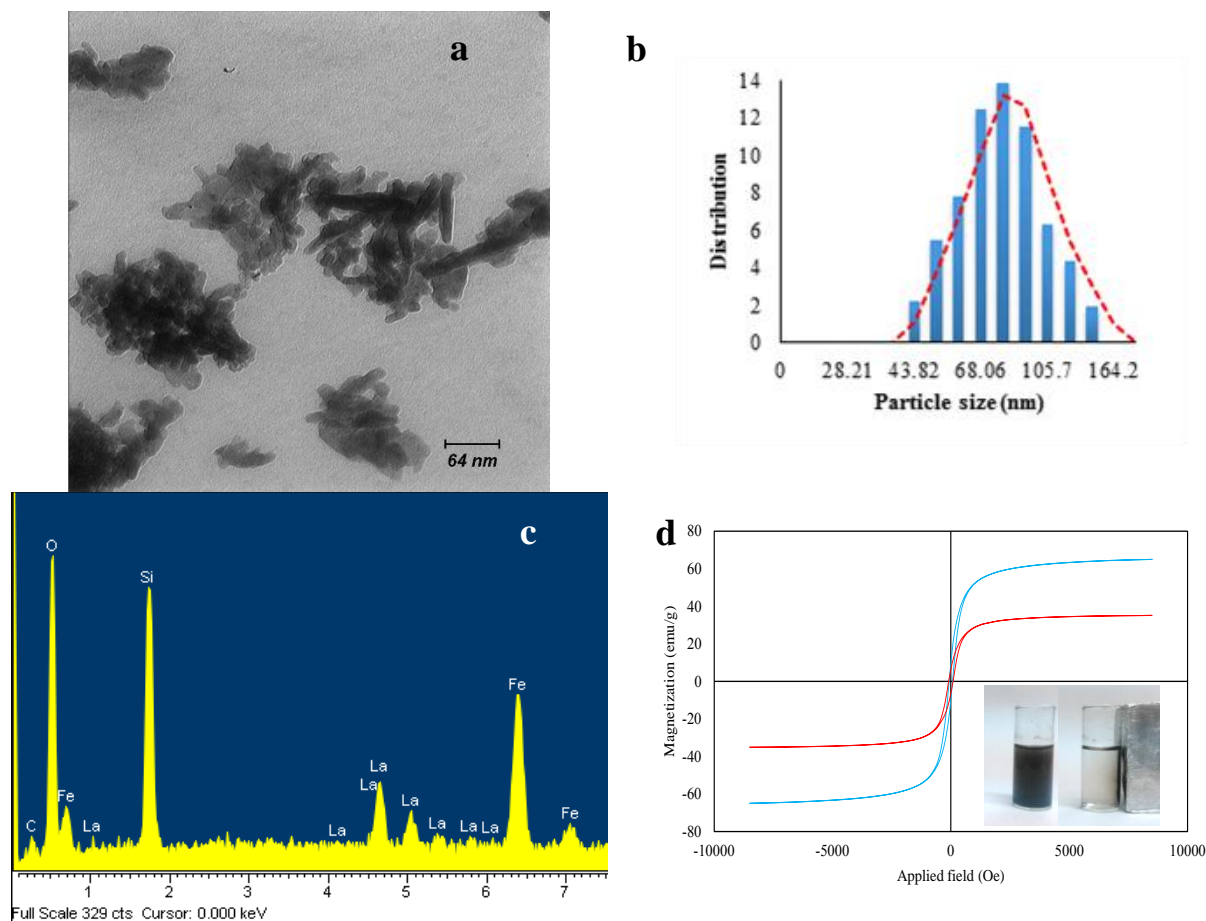

Fig. 1. a) TEM image, b) Particle size histogram, c) EDS analyze, d) VSM of $Fe_3O_4@SiO_2@La$.

Conclusion:

In conclusion, a simple and effective method for the synthesis of 5-substituted-1H-tetrazoles from nitriles and sodium azide has been developed using $Fe_3O_4@SiO_2@La$. This nano sized heterogeneous catalyst is easily prepared and stable to air which shows excellent catalytic performance for various nitriles.

References:

[1] a) L. Bosch and J. Vilarrasa, *Angew. Chem.*, **2007**, *46*, 3926; b) G. Venkateshwarlu, A. Premalatha, K. C. Rajanna and P. K. Saiprakash, *Synth. Commun.*, **2009**, *39*, 4479; c) J. Bonnamour and C. Bolm, *Chem.–Eur. J.*, **2009**, *15*, 4543; d) D. J. Carini, J. V. Duncia, P. E. Aldrich, A. T. Chiu, A. L. Johnson, M. E. Pierce, W. A. Price, J. B. Santella and G. J. Wells, *J. Med. Chem.*, **1991**, *34*, 2525; e) P. Mani, A. K. Singh and S. K. Awasthi, *Tetrahedron Lett.*,

2014, *55*, 1879; f) V. S. Patil, K. P. Nandre, A. U. Borse and S. V. Bhosale, *E-J. Chem.*, **2012**, *9*, 1145.

[2] S. Shylesh, V. Schünemann, W. R. Thiel, *Angew. Chem. Int. Ed.* **2010**, *49*, 3428.

Synthesis and Characterization of Organopalladium(IV) Complexes and Their C–C Bond Formation Reactivity

Marzieh Daryanavard [a,*]

[a] Estahban Higher Educational Center, Ghaem Boulevard, Estahban, Fars 74519-44655, Iran

E-mail address: m.daryanavard@ch.iut.ac.ir

****

Introduction: The award of the 2010 Nobel Prize in chemistry to Heck, Negishi, and Suzuki for their studies on the palladium catalyzed cross coupling reactions has recognized the important role of palladium in organic synthesis [1]. Although the common Pd oxidation states involved in the catalytic cycles are Pd(0) and Pd(II) [2], Pd(III) and Pd(IV) species are also proposed as reactive intermediates [3,4], that much less is known about them. Since the pioneering work of Canty *et al.* in 1986 [5], Pd(IV) chemistry has grown extensively [4,6]. Since reductive elimination readily occurs at or below room temperature, the presence of the strong donor ligands including bidentate or tripodal ligands with C-σ-donor and/or N-σ-donor atoms, is essential to stabilize Pd(IV) complexes. Also, the high redox potential of the oxidants is important for the oxidation of Pd(II) to Pd(IV) complexes. For the first time, we used the aryldiazonium salts as the oxidant, in this respect.

Experimental:
A solid sample of [(COD)PdMe$_2$] was placed into an cooled air-free flask. A solution of potassium hydridotris-(3,5-dimethylpyrazolyl)borate was then added and the reaction mixture was stirred under Ar at -5 °C for 1 h. The resulting solution was evaporated to give yellow solid. The precipitate was redissolved in acetone; aryldiazonium salt including 4-methoxybenzenediazonium tetrafluoroborate or 4-bromobenzenediazonium tetrafluoroborate was added at room temperature immediately resulted in a rapid color change. The solvent was removed by evaporation and the resulting solid was transferred to the glove box, extracted with diethyl ether, filtered, and evaporated to dryness to give an orange solid of Pd(IV) aryldiazenido complexes.

Results and Discussion:
The synthesized organopalladium(IV) aryldiazenido complexes, [Me$_2$Pd(Tp*)(mbd)] (**1**) and [Me$_2$Pd(Tp*)(bbd)] (**2**) (mbd = 4-methoxybenzenediazenido and bbd = 4-bromobenzenediazenido), were characterized by X-ray crystallography, elemental analysis, and ^{1}H, ^{13}C{H} and ^{15}N-^{1}H gHMBC NMR spectroscopies. Characterization of both **1** and **2** revealed that their structures are the same. The ^{1}H and ^{13}C{H} NMR spectra are in accord with the occurrence of two pyrazole ring environments in 2:1 ratio for both **1** and **2**.

We next investigated the transformation and reactivity of **1** toward the C–C bond-forming reductive elimination. Thermolysis of **1** at 70 °C in C$_6$D$_6$ for 1 h leads to formation of one soluble organometallic product and one major soluble organic product (4,4'-dimethoxybiphenyl), as determined by ^{1}H NMR spectroscopy, along with formation of a dark, insoluble precipitate. The organometallic product was identified as [(Tp*)PdMe$_3$] (**3**). It is easily identifiable by NMR spectroscopy due to its high symmetry. Compound **3** was also isolated by recrystallization from Et$_2$O solution at -35 °C, and characterized by elemental

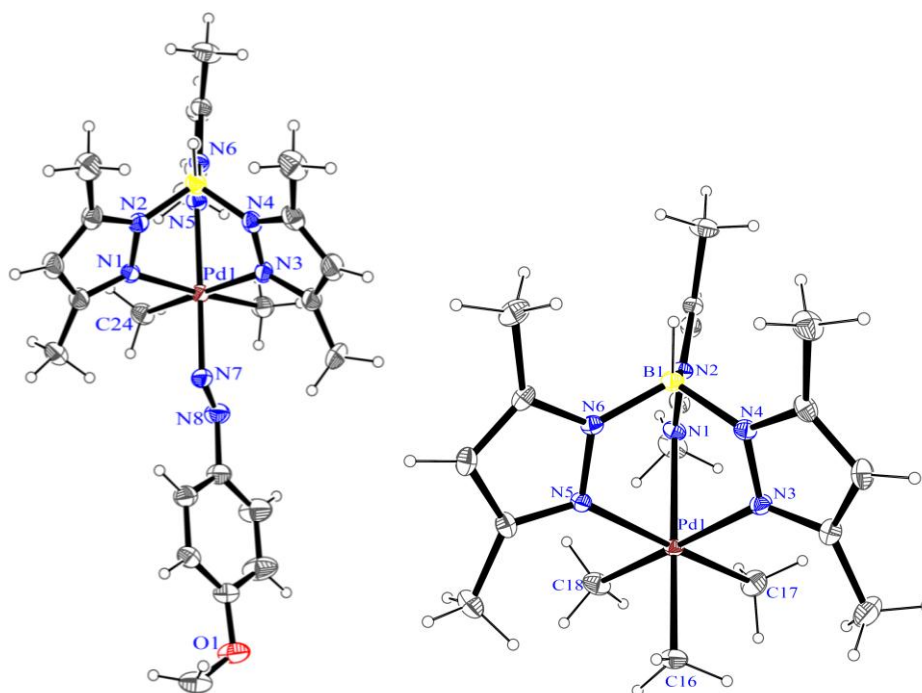analysis and X-ray crystallography. The ORTEP view of these Pd(IV) complexes are shown in Fig 1.

Fig. 1. ORTEP representation (50% probability ellipsoids) of **1** and **3.**

Conclusion: In summary, we have demonstrated the synthesis and characterization of the first remarkable stable organopalladium(IV) complexes, using aryldiazonium salts to oxidize Pd(II) to Pd(IV). Moreover, reported here is the observation of a new Pd(IV) complex formation upon thermolysis of another Pd(IV) complex, that we have been able to isolate and characterize it. These Pd(IV) complexes can selectively undergo C–C bond-forming and ethane reductive elimination at elevated temperatures.

References:
[1] http://nobelprize.org/nobel-prizes/chemistry/laureates/**2010**/.
[2] Hartwig, J. F. *Organotransition Metal Chemistry: From Bonding to Catalysis*; University Science Books: Sausalito, CA, **2010**.
[3] Luo, J.; Rath, N. P.; Mirica, L. M. *Organometallics,* **2013**, *32*, 3343-3353.
[4] Bonney, K. J.; Schoenebeck, F. *Chem. Soc. Rev.,* **2014**, *43*, 6609-6638.
[5] Byers, P. K.; Canty, A. J.; Skelton, B. W.; White, A. H. *J. Chem. Soc., Chem. Commun.,* **1986**, 1722-1724.
[6] Sehnal, P.; Taylor R. J. K.; Fairlamb, I. J. S. *Chem. Rev.* **2010**, *110*, 824-889.

Design, Characterization and Use of Fe_3o_4@Nano-cellulose/Ticl as a Magnetically Recoverable Nano-catalyst for Synthesis of Tetrahydropyridines

Sara Azad[a], Bi Bi Fatemeh Mirjalili[a],*, Abdolhamid Bamoniri[b]

[a]Department of Chemistry, College of Science, Yazd University, Yazd, 89195-741, I. R. Iran

[b]*Department of Organic Chemistry, Faculty of Chemistry, University of Kashan, Kashan, I. R. Iran*

*Email: fmirjalili@yazd.ac.ir

Introduction

Recently, polysaccharides as natural polymers have been used to prevent magnetite nanoparticles from aggregating, and represent an attractive choice for preparation of functional materials [1-3]. Among polysaccharides, the nano structure of the cellulose is particularly appealing duo to combining important properties of cellulose with amazing features of nano-scale materials [4]. Hence, one of the main goals of the present work is preparation of nano-cellulose by sulfuric acid hydrolysis of cotton and using it for the synthesis of Fe_3O_4@nano-cellulose/TiCl (Fe_3O_4@NCs/TiCl) as magnetic nano-catalyst for the synthesis of tetrahydropyridines *via* multi-component reaction of *p*-substituted anilines, *p*-substituted aldehydes and alkyl acetoacetate.

Experimental

To a stirring solution of para-substituted anilines (2 mmol), ethyl acetoacetate (1 mmol) and Fe_3O_4@NCs/TiCl (0.03 g) in 5 mL EtOH, para-substituted benzaldehydes (2 mmol) was added and the reaction mixture was refluxed for an appropriate time. After completion of the reaction, the catalyst was separated by using an external magnet and the reaction mixture was decanted. Subsequently by adding water to the decanted solution, the product was appeared as a pure solid in high yields.

Result and discussion

Fe_3O_4@NCs/TiCl was prepared and characterized by FT-IR spectroscopy, Field emission scanning electron microscopy, transmission electron microscopy, X-ray diffraction, X-ray fluorescence, vibrating sample magnetometry and thermogravimetric analysis [5].

The catalytic activity of Fe_3O_4@NCs/TiCl was investigated for the synthesis of highly functionalized tetrahydropyridines via five-component condensation reaction of p-substituted anilines, aldehydes and ethyl acetoacetate. The best reaction condition for this transformation is the use of 0.03 g of the catalyst in EtOH as solvent under reflux condition. Based on the optimized reaction conditions, a range of THP derivatives were synthesized (Table 1).

Table 1. Synthesis of highly functionalized tetrahydropyridines (IV_{a-n}) in the presence of Fe_3O_4@NCs/TiCl under reflux condition in EtOH.
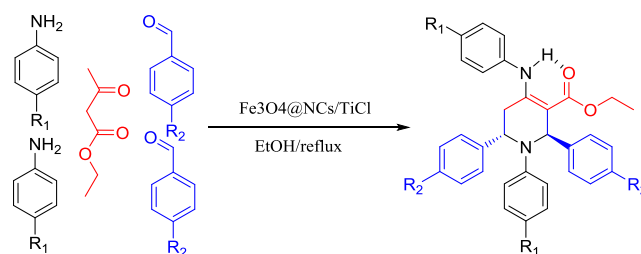
Entry	R^1	R^2	Product	Time (h)	Yield (%)	M.P. [Ref]
1	H	Br	IV_a	1	86	218-220 [6]
2	Me	H	IV_b	1	90	193-194 [7]
3	Me	Br	IV_c	2	89	215-217 -
4	Et	Cl	IV_d	3	92	209-211 -
5	Cl	H	IV_e	1	93	202-204 [8]
6	Cl	Cl	IV_f	2	92	214-215 [9]
7	Br	Cl	IV_g	3	89	193-195 [6]
8	Br	OMe	IV_h	1	92	217-219 [10]
9	H	Me	IV_i	2	82	228-230 [10]
10	H	Cl	IV_j	2	80	202-204 [6]

Conclusions

In summary, we have demonstrated the preparation and characterization of Fe_3O_4@NCs/TiCl as efficient, magnetically recyclable bio-based heterogeneous catalyst. The catalytic activity of the prepared catalyst was investigated in the synthesis of highly functionalized tetrahydropyridines through one-pot five-component reaction of p-substituted anilines, aldehydes and ethyl acetoacetate under reflux condition in EtOH. This protocol offers the advantages of mild reaction conditions, excellent yields, easy work-up procedure, magnetic separation and reusability of nano-catalyst.

References

[1]   Feng, G., Hu, D., Yang, L., Cui, Y., Cui, X. A., & Li, H. *Sep. Purif. Technol.,* **2010**, 74, 253-260.
[2]   Di Carlo, G., Curulli, A., Toro, R. G., Bianchini, C., De Caro, T., Padeletti, G., Zane, D., & Ingo, G. M. *Langmuir,* **2012**, 28, 5471-5479.
[3]   Primo, A., & Quignard, F. *Chem. Commun.,* **2010**, 46, 5593-5595.
[4]   Brown, R. M., & Saxena, I. M. Cellulose: molecular and structural biology: selected articles on the synthesis, structure, and applications of cellulose: Springer, **2007**.
[5]   Azad, S., Mirjalili B.F. *RSC Adv.,* **2016**, 6, 96928-96934.
[6]   Mukhopadhyay, C., Rana, S., Butcher, R. J., & Schmiedekamp, A. M. *Tetrahedron Lett*., **2011**, 52, 5835-5840.
[7]   Hazeri, N., Maghsoodlou, M. T., Habibi-Khorassani, S. M., Aboonajmi, J., & Sajadikhah, S. S. *J. Chin. Chem. Soc.,* **2013**, 60, 355-358.
[8]   Sajadikhah, S. S., Maghsoodlou, M. T., Hazeri, N., Habibi-Khorassani, S. M., & Shams-Najafi, S. J. *Monatsh. Chem.,* **2012**, 143, 939-945.
[9]   Safaei-Ghomi, J., & Ziarati, A. *J. Iran. Chem. Soc.,* **2013**, 10, 135-139.
[10]   Harichandran, G., Amalraj, S. D., & Shanmugam, P. *J. Heterocyclic Chem.,* **2013**, 50, 539-543.

TiO$_2$ Nanoparticles Coated with Iron Ascorbic acid Complex as an Effective Heterogeneous Photocatalyst for Aerobic Oxidation of Benzylic alcohols

Fahimeh Feizpour, Maasoumeh Jafarpour*, Abdolreza Rezaeifard*

Catalysis Research Laboratory, Department of Chemistry, Faculty of Science, University of Birjand, Birjand, Iran

E-mail address: mjafarpour@birjand.ac.ir; rrezaeifard@birjand.ac.ir

****

Introduction: Alcohol oxidation is one of the most important transformations in organic chemistry that is also widely used in industry. Typically, stoichiometric oxidants having transition metals are used to effect this oxidation in high yields and selectivities [1]. However, transition metal oxidants generate considerable amounts of wastes that are undesirable from the environmental point of view. For this reason, there has been a strong move toward the development of catalytic reactions using benign oxidizing reagents [2-4]. In this context, the direct use of oxygen as an oxidizing reagent is a very desirable feature for modern synthetic methods.

In this work a titania-based nanocatalyst containing iron-ascorbic acid complex (TiO$_2$/AA/Fe) as a reusable and effective photocatalyst for aerobic oxidation of benzyl alcohols, under green conditions is presented (Figure 1).
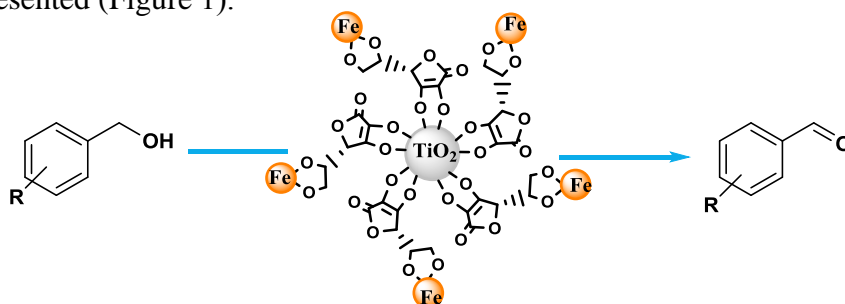

Figure 1.

Methods: Titanium oxide nanoparticles was synthesized by a modified polymerized complex derived sol–gel method followed by coating with ascorbic acid (AA) to modify its surface. The reaction with Fecl$_3$. 6H$_2$O under ultrasonic agitation yielded the TiO$_2$/AA/Fe nanohybrid. The structure of prepared catalyst was confirmed by different techniques such as FT-IR, UV-Vis spectra, TGA, XPS and TEM images.

Results and Discussion: In this work, a novel heterogeneous titania-based nanocatalyst with enhanced visible light photocatalytic activity has been prepared by simple incorporating of FeCl$_3$ to ascorbic acid-coated TiO$_2$ nanoparticles (Scheme 1). Benzylic C-H oxidation of alcohols enhanced significantly under photocatalytic influence of title nanocatalyst induced by visible-light irradiation in ethyl acetate as a safe solvent (Fig. 1). The efficiency, selectivity and

oxidative stability of catalyst well documented. A synergistic effect of iron ascorbic acid complex and TiO_2 nanoparticles on the visible-light photocatalytic activity well demonstrated. The UV-Vis and FT-IR spectra along with ICP analysis confirmed that TiO_2/AA/Fe catalyst maintain its structural integrity under the photocatalytic oxidation conditions.
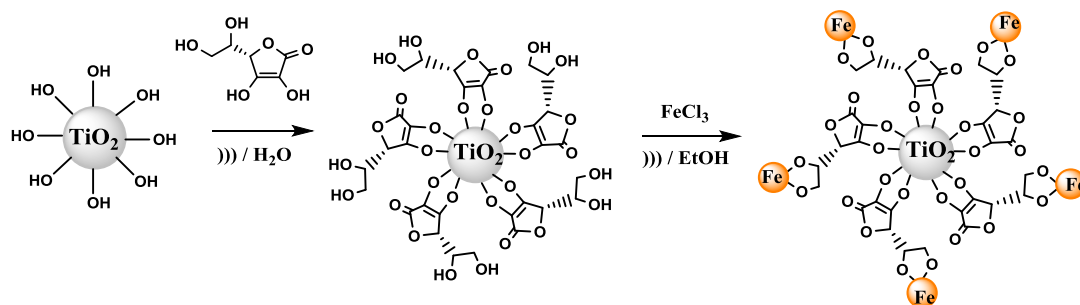
Scheme 1

Conclusion: In conclusion, the nanocrystalline TiO_2 surface modified with iron ascorbic acid complex under ultrasonic agitation produced a novel low band-gap photocatalyst (TiO_2/AA/Fe) with size ranging between 18-25 nm. Enhanced visible light photocatalytic activity was observed towards aerobic benzylic C-H oxidation of benzylic alcohols. The use of air as oxygen source, visible light as energy source, ethyl acetate as a safe reaction media as well as reusing of catalyst with very low catalyst loading providing the scalability of the methods are the strengths of the presented work. Thus, our method is cost effective which enable the industrially important reactions to be carried out efficiently under aerobic and practically attainable conditions.

References:

[1] Lenoir, D. *Angew. Chem. Int. Ed*. **2006**, *45*, 3206-3210.

[2] Corma, A.; Garcia, H. *Chem. Soc. Rev*. **2008**, *37*, 2096-2126.

[3] Sheldon, R. A. *Chem. Soc. Rev*. **2012**, *41*, 1437-1451

[4] Piera, j.; Bäckvall, j. E. *Angew. Chem. Int. Ed*. **2008**, *47*, 3506-3523.

Theoretical Study of Dynamic Flow and Diffusion of anti cancer medicines through Single wall Armchair (10, 10) Carbon Nanotubes

Azar Hassani Daramroodi[a,*], Avat (Arman) Taherpour[b,c,*]
[a] *Department of Nano Chemistry, Faculty of Chemistry, Razi University, Kermanshah, Iran*
[b] *Department of Organic Chemistry, Faculty of Chemistry, Razi University, Kermanshah, Iran*
[c] *Medical Biology Research Center, Kermanshah University of Medical Sciences, Kermanshah, Iran*

* Corresponding author;   **E-mail: avatarman.taherpour@gmail.com** and
s.hassani70.sh@gmail.com

****

Introduction: Cancer is one of the most challenging diseases of modern times because its therapy involves distinguishing normal healthy cells from affected cells. Carbon nanotubes (CNTs) were discovered in 1991[1] and shown to have certain unique physicochemical properties, attracting considerable interest in their application in drug delivery. Reducing toxicity of therapeutic materials is the main aim of developing drug-delivery systems that is achieved using carbon nanotubes (CNTs) [2, 3]. The intense interest in CNTs is due to the capability of absorbing or conjugating with a wide variety of medicinal molecules [4]. The delivery potential of anticancer drugs might be ascribed to their needle-like shapes, which enable them to insert into the target cancer cells and thereby potentially reducing the drug side effects by preserving the non cancerous tissues of the patients [5, 6].

Methods: Theoretically, this study elaborates on the dynamic flow and diffusion of anti cancer medicines (ACs) through the single wall armchair (10, 10) carbon nanotubes as nanocarrier. To investigate the movement of the polyatomic molecular species through carbon nanotubes, the dynamic and diffusive flow of the selected anti cancer medicines (Carmustine (1), Lomustine(2), Ifosfamide(3), Azathioprine(4), Gemcitabine(5), Procarbazine(6) and Methotrexate(7); 1-7) molecules were modeled through single-walled carbon nanotubes (Armchair (10, 10)) while in this modeling, the study of the dynamic flow is done with the nanometer-scale analogue of macroscopic scale fluid flow through pipes. The selected method was Semi- empirical/PM6 to optimize the structures of the selected anti cancer medicines (1-7) and to investigate the dynamic flow of them through the SWCNTs (Armchair (10, 10)) the MMFF94 method (molecular mechanics) was utilized in this modeling.

Result and discussion: The behavior nature of the dynamic flow and diffusion of the selected anti cancer medicines (1-7) would be changed by different the angles of dipole moments of the anti cancer medicines "ACs" with the dipole moment or "ACs" diffusion and dynamic flow of the nanotubes (or flow pathway) "θ_T" (0º, 90º and 180º). Figure-1 shows the energy diagrams of Carmustine (1.Car.) flow through Armchair (10, 10) nanotube. The different forms of the interactions between "Car." with Armchair (10, 10) nanotube were calculated by the MMFF94 method. The calculated results demonstrated that the most stable interactions between "Car." with Armchair (10, 10) nanotube belongs to the state that the angle of dipole moment of "Car." with the nanotube (or flow pathway) "θ_T" is 90º. The MMFF94 calculations show the energy gaps of the flow diagram of the processes. The

biggest energy gaps of the flow diagram of the processes 1-3 were: 2098.82, 52.02 and 2573.4 kj.mol^{-1}.

As Figure-1 shows, the abundance of the stability points are in θ_T =90° and it is more than "θ_T" 0° and 180°. As Figure-1(θ_T =90°) demonstrate the most stable energy point exists in Stage-9. In this stage the distance of "Car" with the other side of Armchair (10, 10) nanotube is 13.30Å (θ_T =90°). In accordance with the results, the better flow pathway for Carmustine (1) in Armchair (10, 10) nanotube is related to the θ_T =90° than "θ_T" 0° and 180°.

The calculated results show that there were almost similar patterns in the flow of other molecules through Armchair (10, 10) nanotube and this method was reapeated for all selected anti cancer medicines (1-7). Table 1 were shows the collections of the best "θ_T" for flow process of the selected anti cancer medicines (1-7) inside of the selected nanotube (*i.e* Armchair(10,10)). It should be noted that due to radius size limitations of Armchair (10, 10) nanotubes and Methotrexate and Procarbazine molecules, it is possible, the state of the angles of dipole moment of "Mtx." and "Pro." with the nanotube (or flow pathway) "θ_T" is 90°.

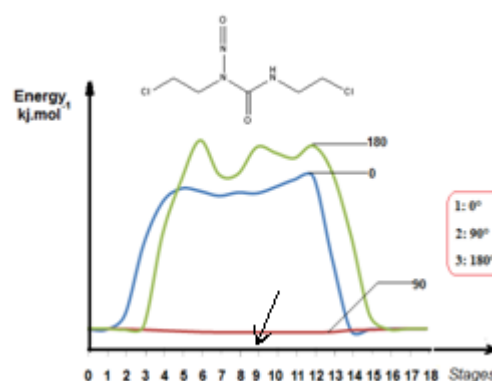| Medicines	Armchair(10,10) Nanotube		
	θ_T (°)		
	0	90	180
Carmustine		●	
Lomustine	●		●
Ifosfamide		●	
Azathioprine	●		●
Gemcitabine		●	
Procarbazine		●	
Mehotrexate		●	

Table 1   Figure 1

Conclusion:

Theoretically, this study elaborates the dynamic flow and diffusion of the selected anti cancer medicine (1-7) through the Armchair (10, 10) carbon nanotube. The selected method was Semi- empirical/PM6 to optimize the selected anti cancer medicines (1-7) and MM-methods (molecular mechanics) to optimize the selected carbon nanotube in this modeling**.**

The results demonstrate that the best probability of the flow of the anti cancer medicines in Armchair (10, 10) nanotube is when θ_T is 90° in the flow process. So, It is possible to perform better purification of Lomustine and Azathioprine (1, 4) from others by Armchair(10,10) nanotubes due to the best probability of the flow of them are $\theta_T = 0°$, 180°.

Refrences:

[1] IIJIMA, S. *Nature*, **1991**, *354*, 56–58.

[2] Chen, Q; Wang, Q; Liu, Y. C; Wu, T; Kang, Y; Moore, J. D; Gubbins, K. E. *J. Chem. Phys*. **2009**, *131*, 15101.

[3] Park, K. *ACS Nano*, **2013**, *7*, 7442.

[4] Pantarotto, D; Briand, J. P; Prato, M; Bianco, A. *Chem. Commun*, **2004**, *10*, 16.

[5] Wong, B. S; Yoong, S. L; Jagusiak, A; Panczyk, T; Ho, H. K; Ang, W. H; Pastorin, G; *Adv. Drug Delivery Rev*, **2013**, *13*, 188.

[6] Liu, P. *Ind. Eng. Chem. Res*, **2013**, *52*, 13517.

Efficient Catalytic Reduction of Nitroaromatic Compounds Using Silver Nanoparticles

Bahareh Ghorbannezhad[a], Alireza Khorshidi[a],*

[a] *Department of Chemistry, Faculty of Sciences, University of Guilan, P. O. Box: 41335-1914, Iran*

Email address: khorshidi@guilan.ac.ir

****

Introduction:

Nitroaromatic compounds are widely used in the industry and pollution caused by them has been a widespread environmental concern. Till now, a vast variety of reagents have been used for reduction of nitroaromatic compounds to corresponding anilines. Among them metal nanoparticles (NPs) especially Ag nanoparticles have gained much attention as catalysts used for rapid conversion of nitro compounds into their respective amines in aqueous medium [1]. However, metal nanoparticles are highly unstable in nano range due to aggregation among themselves rapidly to reduce their surface area [2]. Thus, their catalytic activity is reduced. The best way to address this issue is to use different stabilizing agents.

Silver nanoparticles are used in a large number of processes because of their high catalytic activity at room temperature [3]. The performance of silver nanoparticles in most of applications could be significantly enhanced by controlling dimensions and uniformity. Therefore, many approaches have been invented to fabricate silver nanoparticles [4]. Hereby, we report silver nanoflowers as effective reducing catalysts in reduction of Nitroaromatic compounds.

Experimental:

Silver nanoflowers were prepared according to the literature [5]. The obtained nanoparticles were characterized by SEM, XRD and EDS techniques. Nitrobenzene was selected as a pollutant model and reduction reaction was monitored by UV-VIS absorption at 268 nm. Various factors affecting the catalytic reduction such as PH, temperature and catalyst dose were investigated.

Result and discussion:

Fig 1 (left) shows SEM image of the synthesized Ag nanoflowers and Fig 1 (right) shows the corresponding XRD difractogram, and both confirmed that the desired product was obtained.
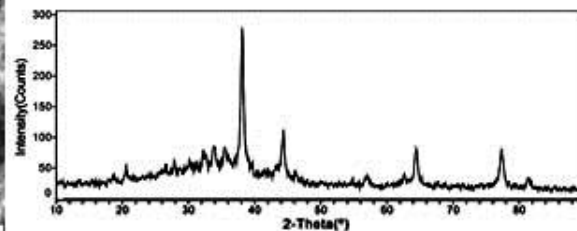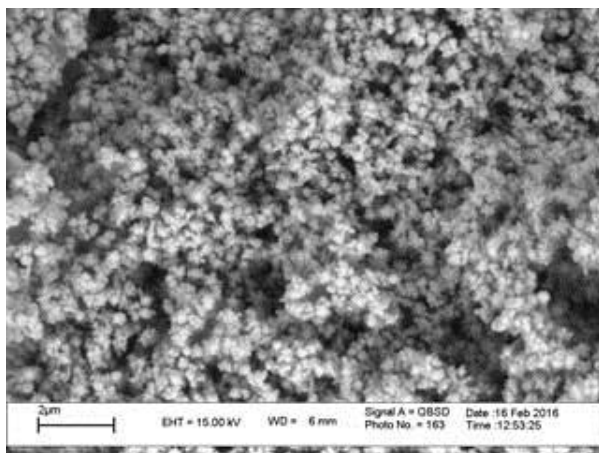
Fig 1. SEM (left), and XRD of the synthesized silver nanoflowers

It is clear that the formed silver nanoflowers have a flower-like morphology with the fcc crystal structure (card No. 04-0873).

After optimization of the reduction reaction conditions with regard to time, catalyst loading, temperature, PH, etc, the conversion of nitrobenzene as a function of time is shown in figure 2. As it is illustrated, 75% of nitrobenzene at room temperature was successfully reduced to corresponding amine within 40 min.
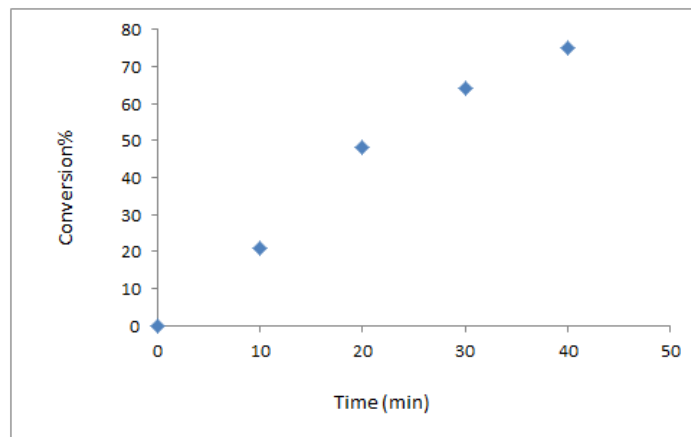
Fig 2. Trend of nitrobenzene reduction in presence of silver nanoflowers under optimized conditions

Conclusion:

To conclude, we have introduced a new efficient catalyst for reduction of nitrobenzene as a model nitroaromatic compound, by employing $NaBH_4$ in aqueous solution as the reducing agent. The results showed that reduction proceed with low amount of $NaBH_4$ in rather short time under mild conditions.

[1] Pogorelić I; Filipan-Litvić M; Merkaš S; Ljubić G; Cepanec I; Litvić M; Journal of Molecular Catalysis A: Chemical, **2007**, 274, 202-207.

[2] Khan S R; Farooqi Z H; Ali A; Begum R; Kanwal F; Materials Chemistry and Physics, **2016**, 171, 318-327.

[3] Li Z; Xu X; Jiang X; Li Y; Yu Z; RSC Advances, **2015**, 5, 30062-30066.

[4] Perez D P; *Silver nanoparticles*, In-Teh, Vukovar, Croatia, 2010.

[5] Liang H; Li Z; Wang W; Wu Y; Xu H; Advanced Materials, **2009,** 21, 4614-4618.

Kinetic and mechanistic studies of the Fischer-Tropsch synthesis over iron–nickel–manganese (ternary) nano catalyst

Somayeh Golestan[a]*, Ali Akbar Mirzaei[a]*, Hossien Atashi[b]

[a]Department of Chemistry, Faculty of Sciences, University of Sistan and Baluchestan, P.O. Box: 98135-674,Zahedan,Iran.

[b]Department of Chemical Engineering, Faculty of Engineering, University of Sistan and Baluchestan, P.O. Box 98164-161, Zahedan, Iran.

*Corresponding author. Tel.: +98 541 8056246; fax: +98 541 2447231.

E-mail: golestan_somayeh@yahoo.com (S. Golestan).

****

1. Introduction

The Fischer-Tropsch synthesis (FTS) reaction is one of the most attractive ways of diesel production, which involves the catalytic synthesis of hydrocarbons and oxygenates from coal-derived synthesis gas (syngas) and natural gas [1, 2]. Kinetic study and kinetic description of the FTS process are extremely important for the development of catalyst and the industrial FTS practices [3]. The complexity of the FTS mechanism and the large number of product species and surface intermediates, however, make the kinetic expressions of the reaction quite hard to be accurately described [4]. In this work, we illustrate the intrinsic kinetics and reaction mechanism over the unsupported iron–nickel–manganese nano catalyst for hydrocarbon formation based on Langmuir-Hinshelwood-Hougen-Watson (LHHW) rate expressions. This nano catalyst was prepared by the solvothermal procedure in presence of oleylamine.

2. Experimental
2.1. Catalyst testing

The FTS reaction rates were measured in a fixed-bed tubular micro reactor [5, 6] wherein inlet feed gases were passed through pressurized stainless steel cylinders using the mass-flow controllers. The gases were mixed in a container and then fed into the reactor-bed. The reactor tube was placed inside a tubular furnace and the temperatures of different zones of the reactor were monitored using three separate thermocouples. The sample was placed in the middle of reactor tube and reduced in the P=1 bar under a flow of pure hydrogen (30 ml/min) for 24 h at 400 °C.

3. Results and discussion
3.1. Experimental results

In each experiment, 1.0 g of the catalyst sample (d_p< 250 μm) was powdered and diluted with a glass wool to get a more uniform bed temperature. The FT reaction tests were carried out at different operating conditions in the following ranges: T = 270–340 °C, P = 1.2–7.0 bar, H_2/CO feed ratio of 0.5–2.0 and GHSV = 4200 h^{-1}. In this research, all rate data within the reactor were obtained at low conversions of CO (7–20%) and were calculated assuming differential reactor conditions.

3.2. Kinetic study
3.2.1. Reaction rate equations

The rate equations are based on LHHW and Eley–Rideal methodologies. According to the mentioned assumptions in our previous literatures [5-7], we offered thirty five different rate equations basis of various possibilities for the syngas

adsorption and chain initiator intermediates. All the equations were fitted separately, against experimental data. According to the obtained results, the model including the dissociative adsorption of CO and associative adsorption of H_2 was chosen as the best fitted model. The reaction rate of the rate-determining step for the best model can be written as below:

$$-r_{CO} = k_p \theta_C \theta_O \theta_{H_2} \tag{1}$$

By substituting of the surface coverage fraction of C, O and H_2 into the rate equation of RDS, Eq. (1), the final rate expression is obtained as:

$$-r_{co} = \frac{kP_{CO}P_{H_2}}{\left(1 + 2(b_{co}P_{CO})^{0.5} + b_{H_2}P_{H_2}\right)^3} \tag{2}$$

where $k = k_p b_{H_2} b_{CO}$. As shown, Eq. (2) indicates the best fit to the experimental data in this work. The activation energy, kinetic parameters and statistical tests results obtained for the best model are summarized in Table 1.

Table 1: Values of kinetic parameters of best model.

Parameter	Value	Dimension
*k_0	0.027E-02	$mol.min^{-1}.gr^{-1}$
k_{0p}	1.030E+08	$mol.min^{-1}.gr^{-1}$
E_a	70.433	$kj.mol^{-1}$
ΔH_{H_2}	-11.520	$kj.mol^{-1}$
ΔH_{CO}	-57.720	$kj.mol^{-1}$
b_{0H_2}	0.015	$mol.min^{-1}.gr^{-1}$
b_{0CO}	1.740E-10	$mol.min^{-1}.gr^{-1}$
R^2	0.970	-
R_{msd}	6.602E-06	-
MARR (%)	14.180	-
Variance	1.553E-09	-

*k_0=$k_{0p}b_{0H2}b_{0CO}$

4. Conclusion

The kinetic experiments for FT reaction were carried out on the iron–nickel–manganese nano catalyst prepared by solvothermal procedure. Using the nonlinear regression method and statistical tests, the model of $-r_{CO} = \frac{kP_{CO}P_{H_2}}{\left(1 + 2(b_{co}P_{CO})^{0.5} + b_{H_2}P_{H_2}\right)^3}$

was chosen as the best model. This model shows that the rate-determining step proceeds via reaction dissociative adsorbed CO and associative adsorbed H_2. The values of the apparent activation energy and adsorption enthalpies of CO and H_2 were 70.43, −57.72 and −11.52 kJ/mol, respectively.

References

1. R Guettel; T. Turek. *Chemical Engineering Science*, **2009**, 64, 955-964.
2. A Tavasoli; A Khodadadi; Y Mortazavi; K Sadaghiani; M Ahangari. *Fuel processing technology*, **2006**, 87, 641-647.
3. B T Teng; J Chang; C H Zhang; D B Cao; J Yang; Y Liu; X H Guo; H W Xiang; Y W Li. *Applied Catalysis A: General*, **2006**, 301, 39-50.
4. B Todic; T Bhatelia; G F Froment; W Ma; G Jacobs; B H Davis; D B Bukur. *Industrial & Engineering Chemistry Research*, **2013**, 52, 669-679.
5. A Eshraghi; A A Mirzaei; H Atashi. *Journal of Natural Gas Science and Engineering*, **2015**, 26, 940-947.
6. M Arsalanfar; A Mirzaei; H Atashi; H Bozorgzadeh; S Vahid; A Zare. *Fuel processing technology,* **2012**, 96, 150-159.
7. A Mirzaei; A Pourdolat; M Arsalanfar; H Atashi; A Samimi. *Journal of Industrial and Engineering Chemistry,* **2013**, 19, 1144-1152.

DNA Interaction of new Anticancer Oxalipalladium Analogue with Glycine Derivative as a Ligand

Sara Hadian Rasanani[1], **Mahboube Eslami Moghadam[2,*]**, **Esmaeil Soleimani[1]**, **Ali Akbar Tarlani[2]**

[1] *Faculty of Chemistry, Shahrood University of Technology, Shahrood, Iran*

[2] *Chemistry & Chemical Engineering Research Center of Iran, Tehran, Iran*

E-mail: eslami_moghadam@yahoo.com

Introduction:

Deoxyribonucleic acid (DNA) is an important genetic substance in the organism and is quite often the main molecular target for anticancer agents [1]. Among anticancer drugs transition metals based molecules are biologically active due to their binding capacities with important biological entities such as DNA. Probably, it is due to the presence of vacant d-orbitals and positive charge on metal ions, which act as binding sites [2]. Platinum-based anticancer agents such as cisplatin, carboplatin, and oxaliplatin are known as world-wide anticancer metallodrugs, but their remarkable side-effects have prompted a search for other metal-based antitumour agents [3]. Several water soluble palladium complexes with bidentate essential amino acids have been reported .These complexes exhibited a noticeable *in vitro* cytotoxic activity; comparable to standard platinum-based drugs [4]. Since among amino acids, glycine significantly improve cellular uptake of biologically active alkylating agents, in this work the interaction $[Pd(DACH)(R\text{-}gly)]NO_3$, were studied with calf thymus DNA via UV–visible (UV–vis), and circular dichroism (CD), where dach is (1R,2R)-cyclohexane-1,2-diamine and R is isopentyl.

Methods / Experimental:

DNA-denaturation

This experiment was done by looking at the changes in the UV absorption spectrum of DNA solution at 260 nm upon addition of palladium complex at two temperatures of 27 °C and 37 °C. The concentration of metal complex at midpoint of transition, $[L]_{1/2}$ was determined. Also, thermodynamic parameters were found out using Pace method [4].

Circular dichroism (CD) measurement

The CD measurements of the interaction between Pd complex and DNA were recorded, while the concentration of DNA was kept constant (120 µM) and the Pd (II) complexes were varied from 0 to 0.99 mM (r_i = [com]/[DNA] = 0.0, 2, 4.1,6.2 and 8.3). Each sample was scanned at a wavelength range of 200–320 nm at room temperature. Finally, changes in CD spectrum indicated DNA structure changing during adding the metal complex.

Results and Discussion:

The profile of DNA denaturation by $[Pd(DACH)(isopentylgly)]NO_3$ complex (Figure 1) indicates, that the concentration of palladium complex in the midpoint of transition, $[L]_{1/2}$, is 0.31 mM and 0.26 mM at 27 °C and 37 °C, respectively, and by increasing temperature the stability of the DNA system is decreased.
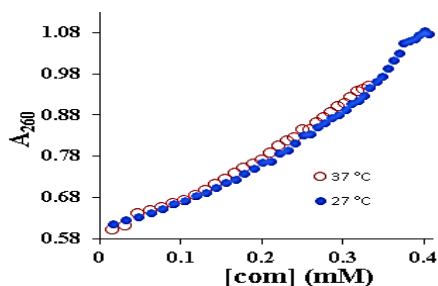
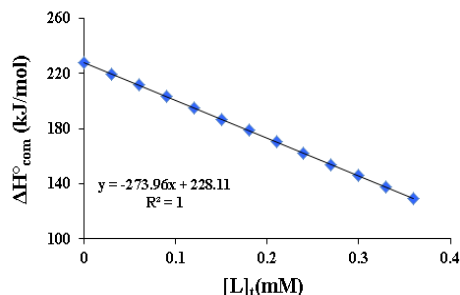**Figure 1:** The changes of absorbance of DNA (λmax = 260 nm due to increasing the total concentration of [Pd(DACH)(isopentylgly)]NO$_3$

Figure 2: Plot of the molar enthalpies of DNA denaturation in the interaction with [Pd(DACH)(isopentylgly)]NO$_3$

Using the DNA denaturation plot and Pace method, the value of $\Delta H°_{H2O}$, molar enthalpy of DNA denaturation in the absence of complex in the range of 27 °C to 37 °C is 228 kj/mol (Figure 2). The descending enthalpy plot indicates that the interaction of Pd complex with DNA is exothermic and spontaneous reaction.

CD signals are exactly sensitive to the mode of DNA interaction with drug molecules. The observed CD spectrum of natural calf thymus DNA consists of a positive band at 275nm due to base stacking and a negative band at 245nm due to helicity, which is characteristic of DNA in right-handed B form. The intensities of both of the negative and positive bands significantly decrease (shifting to zero levels) with increasing concentration of Pd complex. This observed data suggest that DNA binding with drug molecule induces conformational changes, the conversion form of B-like to C-like. (Figure 3) These changes in DNA conformation are increase possibility of groove binding of pd complex [5].
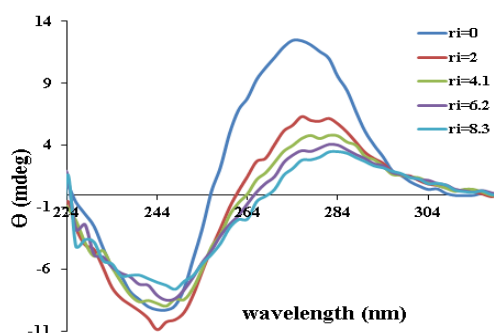

Figure 3: CD spectra of CT-DNA (120 μM) in the absence and presence of [Pd(DACH)(isopentylgly)]NO$_3$ r$_i$:[Complex]/[DNA] = 0.0, 2, 4.1, 6.2 and 8.3 in Tris–HCl buffer at 25 °C.

Conclusion:

This synthesized complex can denature DNA at low concentration. Thus, if this complex is used as anticancer agent, low doses will be needed, so this may have fewer side effects. CD results showed deep conformational changes in the DNA double helix upon groove binding with the palladium complex can occurred.

References

[1] Saeidifar Maryam; Mansouri-Torshizi Hassan; Palizdar .Y; Eslami-Moghaddam. M; Divsalar Adeleh; Saboury Ali Akbar. *Acta Chim. Slov.* **2014,** 61, 126‑136.

[2] Imran Ali; Waseem A. Wani; Kishwar Saleem; Ashanul Haque. *Anticancer Agents Med Chem*. **2013,** 13, 296-306.

[3] Kantoury, Mahshid; Eslami Moghadam, Mahboube; Tarlani, Ali Akbar; Divsalar, Adeleh. *Chem Biol Drug Des*. **2016**, 88, 76–87.

[4] Eslami Moghadam, Mahboube; Saidifar, Maryam; Divsalar, Adeleh; Mansouri-Torshizi, Hassan; Saboury, Ali Akbar; Farhangian, Hossein; Ghadamgahi, Maryam. *J Biomol Struct Dyn*. **2015**, 34, 206-222.

[5] Shahabadi, Nahid; Maghsudi, Maryam; Mahdavi, Maryam; Pourfoulad, Mehdi. *DNA Cell Biol.* **2012**, 31,122-127.

Design and facile synthesis of some 2-[4-(1-Benzyl-1H-[1,2,3]triazol-4-ylmethoxy)-phenylamino]-[1,4]naphthoquinone derivatives via "click" reaction as chemotherapeutic agents

Maryam Gholampour[1]*, Najmeh Edraki[2], Mehdi Khoshneviszadeh[1,2]

[1]Department of Medicinal Chemistry, School of Pharmacy, Shiraz University of Medical Sciences, Shiraz, Iran.
[2]Medicinal and Natural Products Chemistry Research Center, Shiraz University of Medical Sciences, Shiraz, Iran.
Email address: mary.gholampoor@gmail.com

****

Introduction: 1,4-naphthoquinones are important natural substances that are commonly found throughout many areas of chemistry and biology, being renowned for their extremely rich pharmacological properties such as remarkable antineoplastic activity. [1]

Herein we present the synthesis of 1,4-disubstituted 1,2,3-triazole linkages between the 2-amino-1,4-naphthalenedione system and benzylic derivatives using a "click" reaction. These triazole derivatives are of interest for medicinal chemistry and material science. [2,3]

Thorough our efforts to design molecular scaffolds using hybridization protocol, the aim of this work consists in design and synthesis of new molecular scaffolds using hybridization protocol with enhanced anticancer activity.
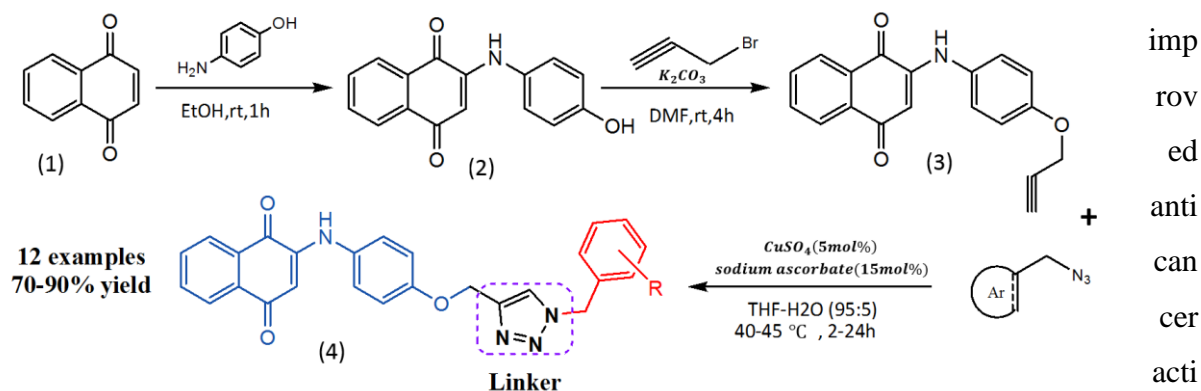
Methods: To the best of our knowledge it is the first time that 2-(4-Hydroxy-phenylamino)-1,4-naphtho-quinone was prepared in excellent yield without using any catalyst.

The corresponding 1,4-disubstituted 1,2,3-triazole derivatives were obtained by a copper-catalyzed azide-alkyne 1,3-dipolar cycloaddition, "click" reaction. Compounds were prepared without the need of chromatographic purification, at room temperature and using our optimized and general reaction conditions.

Results and discussion: Applying this protocol, it was possible to prepare 12 derivatives in moderate to high yield. This protocol for the preparation of synthetically, biologically and pharmaceutically relevant derivatives of 1,4-Naphthoquinone bearing 1,2,3-Triazole moieties, includes some important aspects like the easy work-up procedure, high yield and mild reaction conditions.

New compounds were fully characterized by Melting point, IR, ^{1}H NMR, ^{13}C NMR and mass spectral analysis, also further

According to the idea of rational drug design, these novel conjugated compounds supposed to afford improved anticancer activity comparing to the individual scaffolds.

Conclusion: The results from this research may provide valuable insight for further structural modifications of the mentioned compounds aimed at developing selective agents disturbing cancer cell pathways.

References

[1] Wellington KW. *RSC Advances*, *2015, 5*, 20309-20338.

[2] Sandip G. Agalave, Suleman R. Maujan. *Chemistry, an Asian journal*, *2011, 6*, 2696-2718.

[3] da Cruz EH, Hussene CM, Dias GG. *Bioorganic and Medicinal Chemistry*, *2014, 22*, 1608-1619.

Automated preconcentration and analysis of medical compounds by fully automated on chip electromembrane extraction coupled with high performance liquid chromatography

Y. Abdossalami Asl, Y. Yamini[*]

Department of Chemistry, Tarbiat Modares University, Tehran, Iran

*E-mail: yyamini@modares.ac.ir

****

Intoduction: Sample preparation step has essensial role in the analysis of various biological, enviromental and food samples, which involves an extraction procedure for the separation and preconcentration of target analytes from sample matrix. In the recent years, an important challenge in the microextraction methods in analytical laboratories is the automation of these techniques. Over the past decade, several automation method have been introduced for microectraction methods such as LPME, DLLME, and SPME.

Methods / Experimentals: In the present research, for the first time, we describe the first automated instrument based on on-chip electromembrane microextraction (CEME) coupled with high performance liquid chromatography (HPLC), for the preconcentration and determination of Nortriptyline and Amitriptyline as model analytes in biological matrices. Using an automated syringe pump for loading the supported liquid membrane (SLM) and acceptor solvent, a syringe pump for sample delivery to the chip device, a chip device for electromembrane extraction, a sampling loop for on-line injection of the extract to HPLC, along with an electronic board with an AVR microcontroller for storage of data and instrument programs, a sample preparation-HPLC method was developed that allowed sample extraction and extract injection to be carried out completely automatically. The chip device was composed of two microfabricated polymethyl methacrylate (PMMA) plates with a microporous membrane sandwiched between them in order to separate the sample solution and acceptor phase channels.

Results and Discussion: Efficient parameters on fully automated on chip electromembrane extraction of the model analytes were optimized using one variable at a time method. Under the optimized conditions, the new setup offered a good linearity in the range of 10.0–500.0 µg L^{-1} with coefficient of determination (R^2) higher than 0.9909. The relative standard deviation (RSD %) and LOD values were less than 6.5% based on four replicate measurements and 5.0 µg L^{-1} for the model analytes, respectively. The preconcentration factors higher than 18.8-fold were obtained.

Conclusion: The proposed method was successfully applied for determination and quantification of the model analytes in urine and plasma samples.

Keywords: Fully automated on chip electromembrane extraction; Chip-based liquid phase microextraction; Nortriptyline; Amitriptyline; Microextraction.

References:

[1] N. Petersen and S. Pedersen-Bjergaard, Microfluid Nanofluidics, 2010, 9, 881-888.

[2] S. Seidi, M. Rezazadeh, Y. Yamini and S. Esmaili, Analyst, 2014, 139, 5531-5537.

[3] A. Esrafili, Y. Yamini, M. Ghambarian and B. Ebrahimpour, J. Chromatogr. A, 2012, 1262, 27–33.

One-pot Nano-catalyst Synthesis of Thiohydantoin Derivatives under Solvent-free Conditions

Morteza Nemati[a] and Mohammad Mehdi Ghanbari[b],*

[a]Department of Chemistry, Marvdasht Branch, Islamic Azad University, Marvdasht, Iran

[b]Department of Chemistry, Sarvestan Branch, Islamic Azad University, Sarvestan, Iran

Email address: m.mehdi.ghanbari@gmail.com

Introduction: The 2-thioxoimidazolidin-4-one (thiohydantoin) is a common 5-membered ring containing a reactive cyclic 2-thioxoimidazolidin-4-one (thiohydantoin) are a common 5-membered ring containing a reactive cyclic thiourea core. They have a number of biological activities as antiarrhythmic, anti-inflammatory, antitumor, and antidiabetic properties, as well as herbicidal and fungicidal activity [1]. In recent years, considerable efforts have been devoted to the development of novel and more efficient methods for the preparation of hydantoin and thiohydantoin derivatives. Besides conventional multi-step methods, one-pot, solid-phase and microwave-assisted approaches have been published [2]. As part of our current studies on the development of new routes in heterocyclic synthesis [3-4]. We now report here a novel and efficient method for the solid-phase synthesis of thiohydantoin **3**. Scheme 1 illustrates the synthesis of thiohydantoins **3**. All these facts prompted me to find a new ecofriendly method and to employ grinding for the synthesis of the of thiohydantoins 3a–y in a solvent-free environment.

Results and Discussion: The synthesis of a number of thiohydantoins **3** has been reported [3-4]. The compounds of type **3** have been prepared by reacting benzils **1** with thiourea derivatives **2** in the presence of nano-catalyst base in solvent under reflux or solvent-free under microwave irradiation. The reaction proceeded spontaneously under Solvent-Free Conditions, and was completed within a few minutes (Scheme 1).
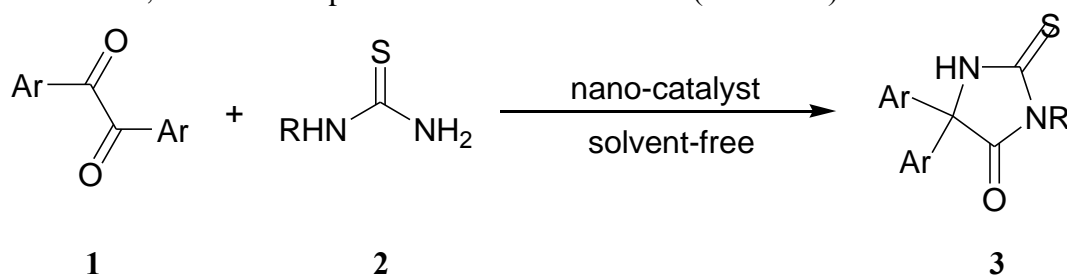
Scheme 1. Synthesis of compounds **3**.

Conclusion: In conclusion, we have developed a simple, rapid, efficient and ''green'' synthesis of thiohydantoins in solvent-free conditions. Nano-catalysts have been applied to the reaction mixtures containing benzils and thiourea derivatives, which allowed me to achieve thiohydantoin derivatives in a good yield, low cost, simple workup, easy purification and short reaction time. This convenient procedure will allow a further increase of the diversity within the thiohydantoin family.

General procedure for the preparation of 3: A mixture of 1 mmol of **1** and **2** mmol of thioureas were placed into a mortar, 0.080 g (2 mmol) of nano-catalyst was added, and the mixture was thoroughly mixed in by grinding or MW irradiation until the completion of

reaction as indicated by thin-layer condensation (TLC). The hot mixture was then poured into ice water, and the precipitate was filtered off. The filtrate was acidified with concentrated hydrochloric acid, and the precipitate of **3** was filtered off, dried for 2 days in a desiccator over calcium chloride, and recrystallized from ethanol.

[1] Colacino E; Lamaty F; Martinez J; Parrot I. *Tetrahedron Letters,* **2007,** *48*, 5317.

[2] Safari, J.; Naeimi, H.; Ghanbari, M. M.; Sabzi-Fini, O. *Russ. J. Org. Chem*, **2009**, *45* 477.

[3] Ghanbari, M M; Mahdavinia G H; Safari J; Naeimi H; Zare M. *Synth Commun,* **2010**, *41*, 2414-2417.

[4] Ghanbari, M M. *Chem Month,* **2011**, *142*, 794-797.

Determination of diazinon in environmental samples using modified multi-walled carbon nanotubes as pipette-tip solid phase extraction sorbent

Mohammad Reza Rezaei Kahkha*[1], **Massoud Kaykhaii**[2], **Mahdi Shafiee Afarani**[3]

[1]Departement of Environmental Health Engineering, Faculty of Health, Zabol University of Medical Sciences, Zabol, Iran.

[2]Departement of Chemistry, University of Sistan and Baluchestan, Zahedan, Iran.

[3]-Departement of Material Engineering, University of Sistan and Baluchestan, Zahedan, Iran.

Corresponding author; email: m.r.rezaei.k@gmail.com.

****

Introduction: Diazinon is an organophosphorus compound often used in agriculture as a soil pesticide [1]. Several methodologies have been reported for determining diazinon residues in aqueous samples preceded by different preconcentration procedures, including, solid phase microextraction (SPME) [2], Reserved dispersive-solid phase extraction [3], dispersive liquid–liquid microextraction (DLLME) [4] and other techniques based on microextraction principles [5].

Methods / Experiments: A suspensions of CNTs were prepared by dispersing 100 mg of CNT powder in 100 mL absolute ethanol under ultrasonication for 10 min. Ethylene glycol (EG) as an surface modifier was added to the CNTs suspensions in this step to make the surface of CNTs ready for absorption of ZnS:Mn nanoparticles. Then, 0.4 g sodium sulfide hydrate was added to the suspension during mixing (suspension A). In the second step, the cationic solution was prepared by dissolution of 1.124 g zinc acetate and 8.63 ml manganese acetate solution (0.04 g.L^{-1}) in 100 ml deionized water (solution B). In the third step, solution B was added drop wise to suspension A for 30 min. The nanocomposites were dried in an electric oven at 60 °C for 24 h and used without further purification for pipette tip extraction

Results and Discussions:

1- **Optimization of procedure**

Best extraction recovery obtained as pH, ٣.٥, when ٧٠ mg of ZnS-CNTs as adsorbent was used. ٣٠µl of Acetonitrille as eluting solvent was applied to desorb ٣٠٠٠ µl of ١٠ mg. l^{-1} diazinon solution. LOD, RSD and Enrichment Factor of this method were ٠.٠٣µg l^{-1}, ٣.٧٨٪ and ١٠٠, respectively. Proposed methods were applied successfully for analysis of diazinon in one soil samples as shown in bellow figure.
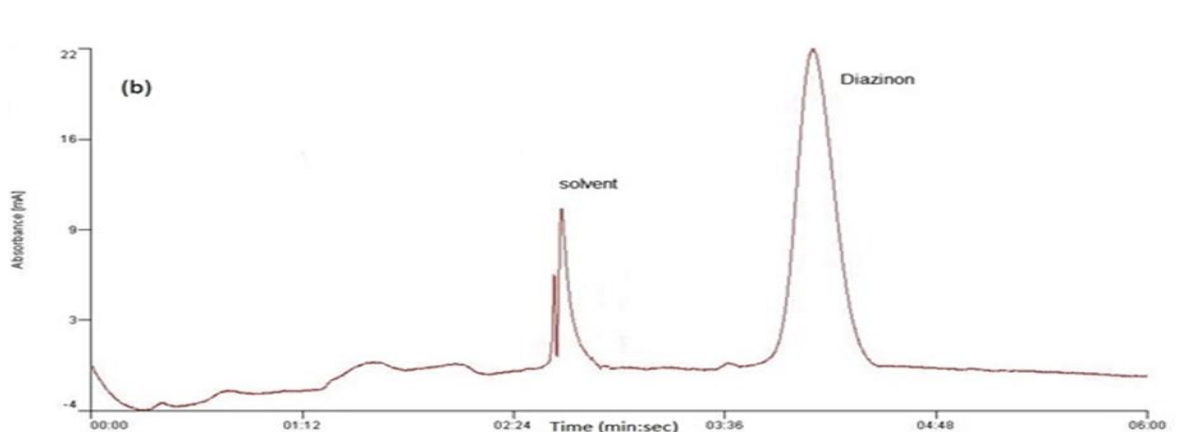
HPLC chromatograms obtained from extraction of (a) water sample and (b) soil sample spiked by ٢٥ µg.L^{-1} of diazinon

Conclusion

In this study, pipette-tip solid phase extraction with a novel sorbent based on CNT–ZnS nano particles followed by high performance liquid chromatography has been developed for the determination of diazinon in water and soil samples.

References

١- M. R. Sohrabi, S. Jamshidi, A. Esmaeilifar. *Chemom. Intell. Lab*., Syst.١١٠ (٢٠١٢); ٤٩–٥٤.

٢- C. Padrn Sanz, R. Halko, Z. Sosa Ferrera, J. J. Santana Rodriguez, *Anal. Chim. Acta,* ٥٢٤(٢٠٠٤): ٢٦٥–٢٧٠.

٣- C. Aprea, C. Colosio, T. Mammone, C. Minoia, M. Maroni. *J. Chromatogr. B*, ٧٦٩(٢٠٠٢): ١٩١–٢١٩.

٤- H. Bagheri, A. Es'haghi, N. Mesbahi. *Anal. Chim. Acta*,٧٤٠(٢٠١٢):٣٦–٤٢.

٥- B. Albero, C. Sa nchez-Brunete, J. L. Tadeo. Multiresidue. *Talanta*, ٦٦ (٢٠٠٥): ٩١٧–٩٢٤.

٦- W. Guan, Z. Li, H. Zhang, H. Hong, N. Rebeyev, Y. Ye, Y. Ma. . *J. Chromatogr. A,* ١٢٨٦ (٢٠١٣): ١–٨.

A New Dendrimer Containing the Copper Nanoparticles: Synthesis, Characterization, and Its Application for the Catalytic Reduction of 4-Nitrophenol

Parastoo Keshtiara[a], Negin Mousavi[a], Marzieh Daryanavard[b], Hassan Hadadzadeh[a,*]

[a] Department of Chemistry, Isfahan University of Technology, Isfahan 84156-83111, Iran

[b] Estahban Higher Educational Center, Ghaem Boulevard, Estahban, Fars 74519-44655, Iran

E-mail address: hadad@cc.iut.ac.ir

****

Introduction: Dendrimers are highly branched, monodisperse, three-dimensional macromolecules synthesized by a divergent or convergent method [1]. Due to their unique structure and chemical versatility, dendrimers can be applied in various fields such as catalysis, drug delivery, energy transfer, and molecular recognition [2,3].The cavities inside a dendrimer have the ability to trap guest molecules such as transition metal ions. It has been found that transition metal ions, including Cu^+, Ag^+, Pt^+, Pd^+, Ru^+, and Ni^+ partition into the interior of poly amido amin (PAMAM) dendrimers [4]. The objective of this study was to synthetize and characterize dendrimer-encapsulated copper nanoparticles (Cu-DENPs), and to investigate the catalytic activity of Cu-DENPs for the reduction of 4-nitrophenol to 4-aminophenol.

Experimental: The synthesis of Cu-DENPs was completed in 3 steps:

Step 1: Hexakis(bromo methyl)benzene, Vanillin, and K_2CO_3 were dissolved in acetonitrile, and the mixture was refluxed. The white precipitate was obtained and collected by filtration.

Step 2: The obtained product and *para*-aminobenzoic acid were dissolved in 2-methoxyethanol, and followed by the addition of one drop of acetic acid glacial. The mixture was then refluxed for 10 h.

Step 3: $CuCl_2 \cdot 3H_2O$, AgTFA, and the resulting product of the second step were dissolved in 2-methoxyethanol, and refluxed.

Then, the catalytic activity of Cu-DENPs for the reduction of 4-nitrophenol to 4-aminophenol was monitored by UV-Vis spectroscopy.

Results and Discussion: In order to determine the morphology and distribution of the copper particles in the dendrimer structure, field emission scanning electron microscope (FE-SEM) was used. These images illustrate uniform distribution of copper nanoparticles in dendrimer structure (Fig. 1).
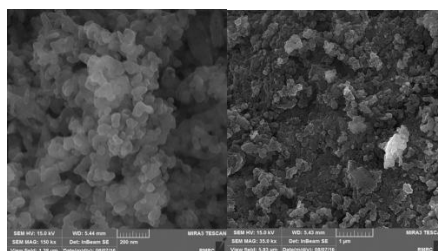

Fig. 1. The FE-SEM images of Cu-DENPs.

Also, the high-resolution transmission electron microscope (HRTEM) was used for determination of the size of copper nanoparticles encapsulated within the dendrimer. Fig. 2

shows the images with different scales. These results confirmed that the size of copper particles were achieved about 4-10 nm.
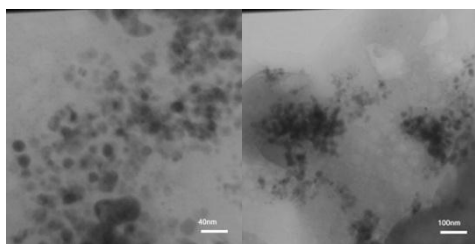

Fig. 2. The HRTEM images of Cu-DENPs.

The surface area, volume and pore diameter of dendrimer containing copper nanoparticles were investigated using BET technique. The obtained results are presented in table 1.

Table 1. The obtained results using BET technique.

BET surface area (m^2/g)	9.193
Mean volume of cavities (cm^3/g)	0.085
Mean diameter of cavities (nm)	37.0

Conclusion: The dendrimer-encapsulated copper nanometals were synthesized and fully characterized by FT-IR, ICP, FE-SEM, TEM, BET, and XRD. The metallic nanoparticles of copper were applied as the catalyst for the reduction of 4-nitrophenol to 4-amionphenol in the presence of $NaBH_4$. The reaction progress was monitored by UV–Vis spectroscopy. This prepared catalyst was found to exhibit good activity for this reduction reaction.

References:
[1] B. Klajnert; M. Bryszewska. *Acta Biochimica Polonica*, **2001**, *48*, 199-208.
[2] Y. Niu; R. M. Crooks. *Comptes Rendus Chimie*, **2003**, *6*, 1049-1059.
[3] M. Nemanashi; R. Meijboom. *Journal of Colloid and Interface Science*, **2013**, *389*, 260-267.
[4] M. Zhao; R. M. Crooks. *Advanced Materials,* **1999**, *11*, 217-220.

One-pot three-component synthesis of 4*H*-pyran derivatives using an acidic ionic liquid based on DABCO in aqueous media

Nazanin Nabinia, Farhad Shirini*, Hasan Tajik, Maryam Mashhadinezhad

Department of Chemistry, Faculty of Science, University of Guilan, Rasht, Iran

E-mail: shirini@guilan.ac.ir

Introduction:

4*H*-Chromenes have recently attracted attention as an important class of heterocyclic scaffolds in the field of drugs and pharmaceuticals. These compounds are widely used as anti-coagulant, diuretic and anti-cancer agents [1-3].

The development of multi-component reactions (MCRs) in the presence of task-specific ionic liquids (ILs), used not only as environmentally benign reaction media,but also as catalysts, is a new approach that meet with the requirements of sustainable chemistry[4].

In this study, an efficient and environmentally benign procedure for the synthesis of tetrahydrobenzo [b]pyran derivatives has been developed in the presence of an acidic ionic liquid based on DABCO as catalyst in aqueous media.

Experimentals:

A mixture of aromatic aldehydes (1mmol), malononitril (1mmol), dimedone (1mmol) and catalyst (30 mg), in a mixture of water and ethanol (1:1) was refluxed for approprated time. The progress of the reaction was monitored by TLC. Upon completion of the reaction, the mixture was cooled to room temperature, the crude product was filtered off and washed with H_2O. The crude products were purified by recrystallization from ethanol.

Results and Discussion:

Different types of aldehydes were examined under the determined conditions (Scheme 1). A series of aromatic aldehydes containing either electron-donating or electron-withdrawing substituents successfully reacted and afforded high to excellent yields of the pure products under the selected conditions. Moreover, the heterocyclic aryl aldehyde also could be successfully converted to the corresponding compounds.

R=H, CH$_3$
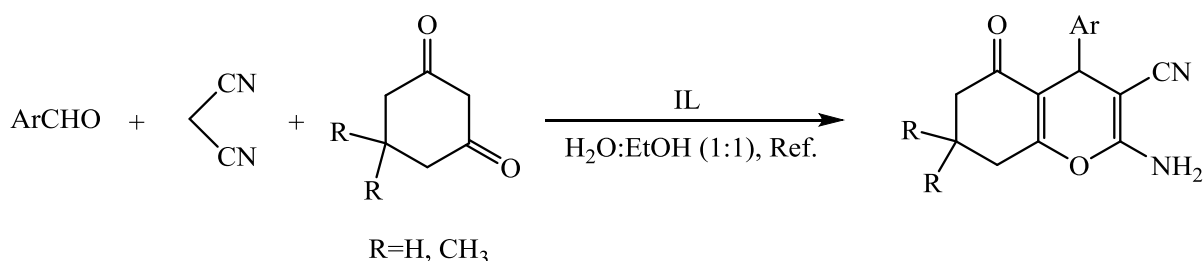
Scheme 1

Conclusion:

We have developed an efficient methodology for the synthesis of tetrahydrobenzo[b]pyran derivative *via* one-pot three-component reactions by using an acidic ionic liquid based on

DABCO as a green, efficient and safe catalyst. Short reaction times, easy work-up and high yields of the products are significant advantages of this method. Also, this ionic liquid could be successfully recovered and recycled at least for four runs without significant loss in its activity.

References

[1] Bonsignore, L.; Loy, G.; Secci, D.; Calignano, A.; *Eur. J. Med. Chem*. **1993**, *28*, 517-520.

[2] Singh, K.; Singh, J.; Singh, H.; *Tetrahedron*, **1996**, *52*, 14273–14280.

[3] Green, G. R.; Evans, J. M.; Vong, A. K.,*Comprehensive heterocyclic chemistry II*, **1995**, 469–500.

[4] Isambert, N.; del Mar Sanchez Duque, M.; Plaquevent*, J., Chem. Soc. Rev.,* **2011**, *40*, 1347–1357.

Graphene-Benzimidazole Supported Palladium Complex as a Novel Catalyst for the Aqueous-Phase Suzuki-Miyaure Reaction

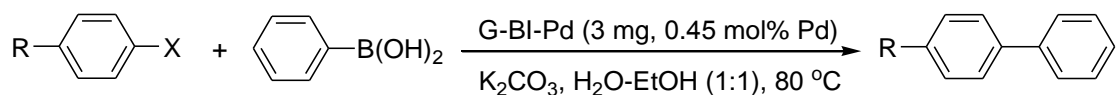**Roya Azadi**[*], **Mosayeb Sarvestani**

Chemistry Department, College of Science, Shahid Chamran University of Ahvaz, Ahvaz 61357-43169, Iran

E-mail address: razadi@scu.ac.i r

Introduction: Biaryl compounds are versatile building blocks in the field of pharmaceuticals, herbicides, polymers, liquid crystals, natural products, ligands for catalysis, and advanced materials. The palladium-catalyzed Suzuki cross coupling reaction between an aryl halide and a phenyl boronic acid has been among the most powerful tools for the preparation of biaryls in organic synthesis.[1-2] Usually, the cross-coupling reactions were performed under homogeneous situation using soluble palladium organic complex as the catalyst.[3] In this regard, heterogeneous catalysis appears particularly well suited since the palladium catalyst immobilized on a support could be easily separated from the product without losing catalytic activity.[4-5] Up to this point, recently a few quality papers using graphene or graphene oxide (GO) or functionalized graphene-based materials serving as a solid support for palladium nanoparticles catalyst have been reported for carbon-carbon cross coupling reactions. [6]

Experimentals: In this report, we demonstrate graphene functionalized with benzimidazole and its complex with palladium chloride (G-BI-Pd) for the aqueous phase Suzuki-Miyaura cross-coupling reaction. GO was synthesized from graphite by a modified Hummers' method.[7] G-BI was synthesized by polyphosphoric acid catalyzed cyclization reaction of carboxylic acid group of GO with *o*-phenylenediamine. For the preparation of G-BI-Pd, the G-BI was dispersed in ethanol. Subsequently, $PdCl_2$ was added and the mixture was subjected to sonication for 5 min, then stirred for 24 h at room temperature. After the reaction, the compound G-BI-Pd was isolated by centrifugation and washed with distilled water for five times. The obtained catalyst was air-dried.

Results and Discussion: Graphene oxide was functionalized with benzimidazole for palladium immobilization. The resultant graphene-benzimidazole supported Pd composite (G-BI-Pd) was characterized by Infrared spectroscopy, Raman spectroscopy, Transmission Electron Microscopy (TEM), and Energy Dispersive X-ray Spectroscopy (EDS). It was demonstrated that the G-BI-Pd showed excellent catalytic activity and fast reaction kinetics in the aqueous-phase Suzuki-Miyaura reaction of aryl iodides and bromides with phenylboronic acid at relatively mild conditions (5-25 min, 80 ^{o}C). The catalyst can be used several times without any significant loss of its catalytic activity.

$$R-\text{C}_6\text{H}_4-X + \text{C}_6\text{H}_5-B(OH)_2 \xrightarrow[\text{K}_2\text{CO}_3,\ \text{H}_2\text{O-EtOH (1:1), 80 °C}]{\text{G-BI-Pd (3 mg, 0.45 mol\% Pd)}} R-\text{C}_6\text{H}_4-\text{C}_6\text{H}_5$$

○ = Pd nanoparticles

G-BI-Pd
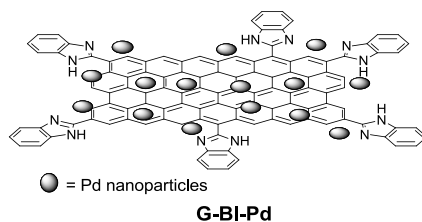
Conclusion: In summary, we successfully developed a new and practical graphene-supported Pd complex catalyst. This novel heterogeneous catalyst is easy to prepare and handle as it is stable in air. The catalytic activity of this catalyst was investigated towards aqueous-phase Suzuki-Miyaura reaction. The catalyst exhibited high stability and reusability up to five cycles.

References

[1]   (a) N. Miyaura, A. Suzuki, *Chem. Rev*. **1995**, *95*, 2457-2483; (b) A. Suzuki, *J. Organomet. Chem.* **1999**, *576*, 147-168.

[2]   H. Li, C. C. C. Johansson Seechurn, T. J. Colacot, *ACS Catal.* **2012**, *2*, 1147-1164.

[3]   R. Martin, S.L. Buchwald, *Acc. Chem. Res.* **2008**, *41*, 1461-1473.

[4]   K. Okumura, T. Mushiake, Y. Matsui, A. Ishii, *Chem. Phys. Chem.* **2015**, *16*, 1719-1726.

[5]   Q. Zhang, H. Su, J. Luo, Y. Wei, *Tetrahedron* **2013**, *69*, 447-454.

[6]   (a) V. Sharavath, S. Ghosh, *RSC Adv.* **2014**, *4*, 48322-48330; (b) J. H. Park, F. Raza, S. J. Jeon, H. I. Kim, T. W. Kang, D. Yim, J. H. Kim, *Tetrahedron Lett.* **2014**, *55*, 3426-3430.

[7]   W. S. Hummers, R. E. Offemann, *J. Am. Chem. Soc.* **1958**, *80,* 1339-1339.

Synthesis of Novel Derivatives of Pyrazolo[5,1-b]purine: A Straightforward Approach

Seddigheh Sheikhi-Mohammareh, Ali Shiri[*]

Department of Chemistry, Faculty of Science, Ferdowsi University of Mashhad, 91775-1436 Mashhad, Iran.

Email address: alishiri@um.ac.ir

Introduction: Purine is a privileged nitrogen-containing heterocycle which exists in various bioactive compounds. The biological importance of purines has led to an interest in synthesis of them with pharmaceutical properties such as antiviral [1], antibacterial [2], anticancer [3] and anti-inflammatory activities.[4] They also have agrochemical properties including herbicidal and soil fungicidal activity.[5]
On the other hand, pyrazoles are a motif found in a number of small molecules that possess a wide range of agricultural and pharmaceutical activities such as herbicidal, fungicidal, insecticidal and anti-inflammatory properties [6-10]. Also they have applications in polymer chemistry as ligands for transition metal-catalyzed reactions.[11]

Methods/Experimentals: The heterocyclization of compound (1) with thiourea (2) in refluxing CH_3CN in the presence of Et_3N gave compound (3). The latter compound subsequently underwent N-alkylation via reaction with appropriate alkyl halide in KOH/DMF at 80°C to obtain novel pyrazolo[5,1-b]purine derivatives in good yields.

Results and Discussion: Our approach is based on using compound (1) as starting material that was obtained via the reaction of 2-(ethylthio)-5-methyl-7-oxo-6,7-dihydropyrazolo[1,5-a]pyrimidine-3-carbonitrile with bromine in acetic acid at room temperature [12]. In order to synthesize a novel heterocyclic system, compound (1) was reacted with thiourea (2) as a dinucleophile in the presence of Et_3N in CH_3CN to give product (3) with either structure (A) or (B). (Scheme 1) The ^{1}H NMR and ^{13}C NMR spectra both revealed the formation of only one product. The IR spectrum did not exactly demonstrate the formation of either structure (A) or (B). Also, the observation of the molecular ion peak at *m/z* 290 in the mass spectrum together with the elemental analysis confirms the occurrence of heterocyclization through path (A) or (B).
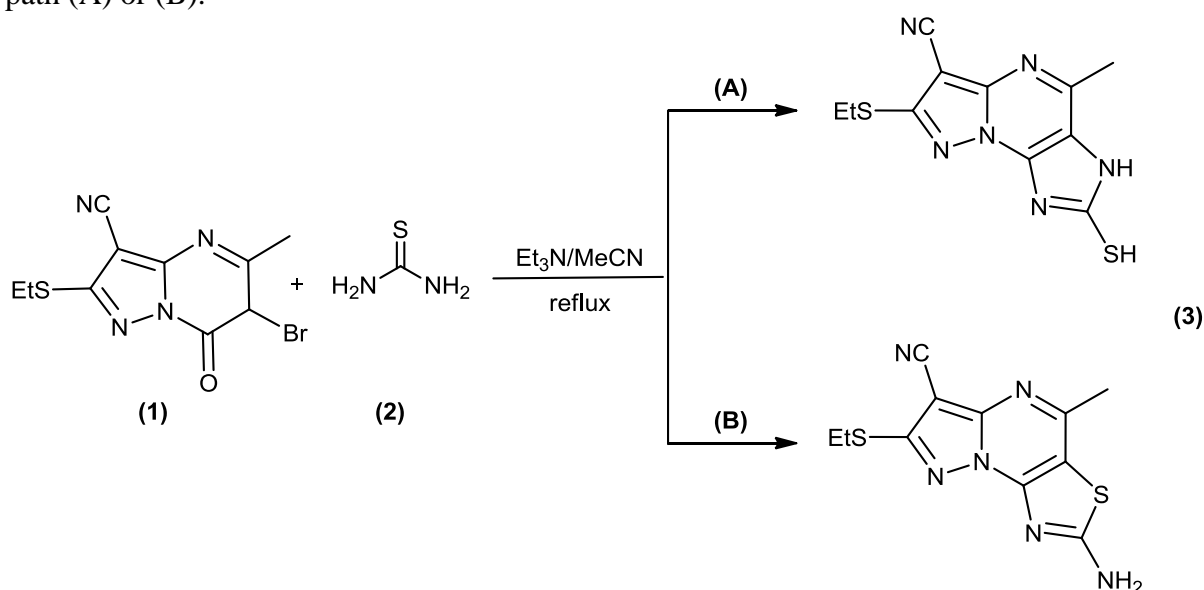
Scheme 1

Eventually, the N-alkylation of compound (3) with several alkyl halides in KOH/DMF gave the desired new derivatives of products (4a–e) quantitatively. (Scheme 2) An unequivocal establishment of the true structure (A) came from a 2D-NOESY analysis on the newly synthesized derivative (4a).

R= Me, Et, n-Pr, n-Bu, Bn
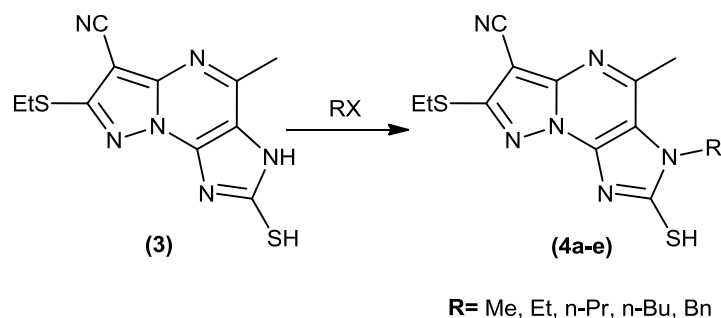
Scheme 2

Conclusion: We have reported a protocol for the synthesis of new derivatives of novel heterocyclic system of pyrazolo[5,1-b]purine. These potential pharmacologically active compounds were prepared through the cyclocondensation of compound (1) with thiourea (2) to obtain compound (3) as the novel heterocyclic system. Alkylation of compound (3) with various alkyl halides in KOH/DMF gave the desired alkylated new products (4a–e).

References

[1]   Gazivoda, T.; Plevnik, M.; Plavec, J.; Kraljevic, S.; Kralj, M.; Pavelic, K.; Balzarini, J.; De Clercq, E.; Mintas, M.; Raic-Malic, S. *Bioorg. Med. Chem.*, **2005**, 13, 131–139.
[2]   Hirokawa, Y.; Kinoshita, H.; Tanaka, T.; Nakamura, T.; Fujimoto, K.; Kashimoto, S.; Kojima, T.; Kato, S. *Bioorg. Med. Chem. Lett.*, **2009**, 19, 170–174.
[3]   Montgomery, J.A.; Carroll Jr., T. *J. Am. Chem. Soc.*, **1957**, 79, 5238–5242.
[4]   Wang, Y.; Yang, X.; Zheng, X.; Li, J.; Ye, C.; Song, X. *Fitoterapia*, **2010**, 81, 627–631.
[5]   Dhivya Vadhana, M.S.; Cinzia, N.; Rosita, G. *Cardiovasc. Toxicol.*, **2010**, 10, 199–207.
[6]   Lahm, G. P.; Cordova, D.; Barry, J. D. *Bioorg. Med. Chem.*, **2009**, 17, 4127-4133.
[7]   Fustero, S.; Roman, R.; Sanz-Cervera, J. F.; Simon-Fuentes, A.; Bueno, J.; Villanova, S. *J. Org. Chem.*, **2008**, 73, 8545-8552.
[8]   Lamberth, C. *Heterocycles*, **2007**, 71, 1467-1502.
[9]   De Paulis, T.; Hemstapat, K.; Chen, Y.; Zhang, Y.; Saleh, S.; Alagille, D.; Baldwin, R. M.; Tamagnan, G. D.; Conn, P. J. *J. Med. Chem.*, **2006**, 49, 3332-3344.
[10]   Bekhit, A. A.; Abdel-Aziem, T. *Bioorg. Med. Chem.*, **2004**, 12, 1935-1945.
[11]   Halcrow, M. A. *Dalton Trans.*, **2009**, 2059-2073.
[12]   Sheikhi-Mohammareh, S.; Shiri, A.; Bakavoli, M.; Mague, J. *J. Heterocycl. Chem.*, **2016**, 53, 1231-1235.

LABLE-FREE FLUOROMETRIC DETECTION OF ADENOSINE TRIPHOSPHATE AND CYTOCHROME C BY USING DNA-STABILIZED SILVER NANOCLUSTERS/ GRAPHENE OXIDE

Karam Molaei[a], Mojtaba Shamsipur[b*], Fatemeh Molaabasi[a]

[a] *Department of Chemistry, Tarbiat Modares University, Tehran, Iran*
[b] *Department of Chemistry, Razi University, Kermanshah, Iran*
mshamsipur@yahoo.com (M. Shamsipur)

****

Introduction: metal nanoclusters (NCs) have drawn attention due to their fascinating properties such as, high photostability, ease of synthesis, great biocompatibility, low toxicity and high quantum yield [1-4]. Graphene oxide (GO), the water-dispersible derivative of graphene, attracts great interest recently owing to its innovative electronic and optical properties [6]. GO has been widely investigated as an electron and energy acceptor. In this regard, GO was proposed as a universal highly efficient long-range quencher in sensor designing [5]. Herein, we designed four label free DNA-encapsulated fluorescent Ag NCs/GO nanoassemblies as sensitive fluorescent probes for detection of ATP and Cyt *c*.

Methods / Experimental: Ag NCs was prepared by reacting the C-bases of DNA with the Ag^+, and after that reducing of the Ag^+ ions in the presence of $NaBH_4$ as the reducing agent.GO was prepared from graphite powder using modified Hummer's method and Offeman [6]. The graphite powder was first oxidized into graphite oxide by use of $H_2SO_4/KMnO_4$, and after that the graphite oxide was exfoliated into GO sheets by sonication in water.

Results and Discussion:

On the basis of the fact that the single strand DNA (ssDNA) can be adsorbed onto GO through hydrophobic interaction and π–π stacking, many sensing strategies have been designed. The DNA-AgNCs can be adsorbed to GO surface by the aim of ssDNA that elongated with them. Desorption of AgNCs from GO surface allows reliable quantification of ATP and Cyt *c*. It was found that the fluorescence intensity of AgNCs (**1**)/GO and AgNCs (**3**)/GO nanoassemblies decreased linearity proportional concentration of ATP and Cyt *c* (Fig. 1a, b). A linear correlation was obtained from 1–200 nM and 5-200 nM based on a linear decrease of fluorescence intensity with regression value (R^2) more than of 0.990. The very low detection limit for analyzing ATP and Cyt c were achieved corresponding to 0.42 and 2.3 nM, which is similar to or even better than earlier published reports on ATP and Cyt c detection. Moreover, the binding assay specificity of AgNCs (**1**)/GO and AgNCs (**3**)/GO nanoassemblies were evaluated with structurally related molecules to ATP and Cyt c. As illustrated in Fig. 1c, d, these compounds did not cause remarkable fluorescence change, because of inherent specificity of the DNA aptamer toward its target.
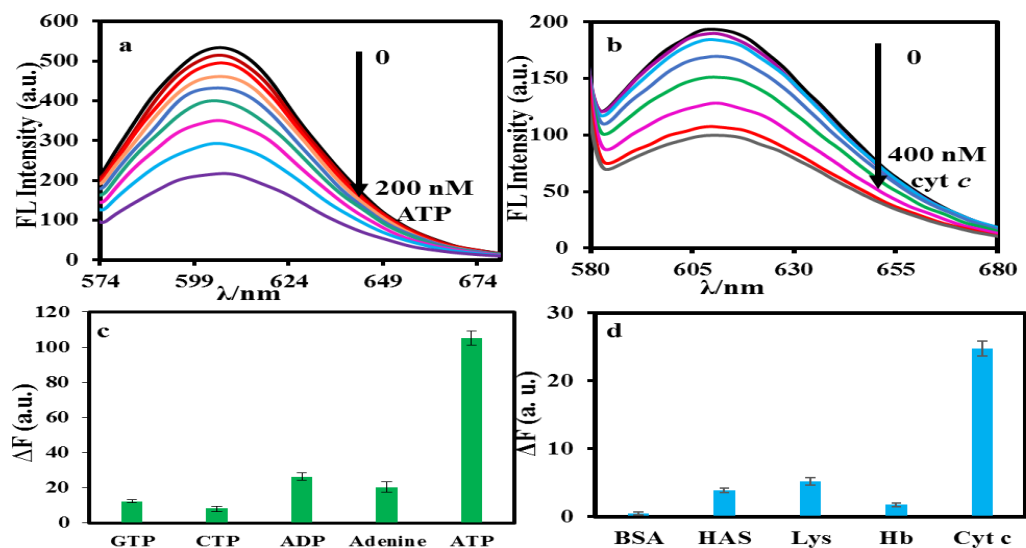
Figure 1.

Conclusion:

In summarize, we have designed sensitive fluorescent probes for the detection of ATP and Cyt *c* in biological samples based on AgNCs/GO nanoassemblies. The length of oligonucleotides affected photophysical of DNA-stabilized Ag NCs. The experimental data show, when nanoclusters contact with GO surface, depending on length of sequence of Ag NCs and different behavior of fluorescence can be observed.

References

[1] Petty J. T.; Zheng J.; Hud N. V.; Dickson R. M. *Journal of the American Chemical Society* **2004**, 126 (16), 5207-5212

[2] Molaabasi F.; Hosseinkhani S.; Moosavi-Movahedi AA.; Shamsipur M. *RSC Advances*, **2015**, 5, 33123-35.

[3] Zhou Q.; Lin Y.; Xu M.; Gao Z.; Yang H.; Tang D. *Analytical Chemistry*, **2016**, 8, 8886-92.

[4] Del Bonis-O'Donnell JT.; Pennathur S.; Fygenson DK. *Langmuir*, **2016**, 6, 569-76.

[5] Obliosca J. M.; Liu C.; Yeh H.-C. *Nanoscale*, **2013**, 5, 8443-8461.

[5] Dreyer D. R.; Todd A. D.; Bielawski C. W. *Chemical Society Reviews,* **2014**, 43, 5288-5301.

 [6] Kovtyukhova, N. I.; Ollivier, P. J.; Martin, B. R.; Mallouk, T. E.; Chizhik, S. A.; Buzaneva, E. V.; Gorchinskiy, A. D. *Chemistry of Materials,* **1999**, 11, 771-778.

Determination of Furanic Compounds in Various Food Products by Headspace Solid Phase Microextraction using graphene/PES Nanocomposite Coated Fiber Coupled to GC-FID

Hatam Amanzadeh, Yadollah Yamini *

*Department of Chemistry, Tarbiat Modares University, P.O. Box 14115-175, Tehran, Iran*

*yyamini@modares.ac.ir

Introduction: In SPME, the type and properties of the coating material is the most important key to improving its extraction efficiency (i.e., sensitivity, selectivity, repeatability, and reproducibility). Recent efforts in SPME are focused on the development and evaluation of novel materials as sorbent coatings, able to provide high extraction efficiency as well as high selectivity while maintaining high mechanical and chemical stability [1]. In this study, the composite coating involving graphene and polyethersulfone (PES) was prepared on the stainless steel wire and it was applied for the extraction of furanic compounds from various food products.

Experimental: To perform the extraction of furanic compounds, sample solution (10 mL) containing 3 g NaCl was added into a 15-mL glass vial equipped with a Teflon-coated magnetic stirrer bar and covered with a cap. The nanocomposite coated SPME fiber was exposed to the headspace above sample solution. After 30 min extraction, the fiber was removed from the vial and immediately transferred into the GC injection port for thermal desorption at 250 $^\circ$C in the splitless mode for 6 min.

Results and Discussion: Desorption parameters were optimized using the one-variable-at-a-time (OVAT) process. It was observed that a desorption time of 4 min at 250 $^\circ$C was sufficient to avoid carryover effects. The optimization of the extraction conditions of HS-SPME analysis was carried out by the multivariate approach of "Experimental design" (Fig. 1). A full factorial central composite design was employed to determine the optimal conditions for above-mentioned four factors. Based on the obtained results, an extraction temperature equal to 60 ± 1 °C, an extraction time of 35 min, salt addition of 20 % w/v and a stirring rate equal to 1200 rpm were chosen for further experiments. Under the optimized conditions, a series of experiments with regard to the linearity, limits of detection (LODs), single fiber repeatability and fiber-to-

fiber reproducibility were evaluated to validation the developed HS-SPME-GC-FID method. The LODs and LOQs for the tested analytes ranged from 0.01 to 0.05 µg L^{-1} and 0.03 to 0.15 µg L^{-1} based on the signal-to-noise ratio of 3 and 10, respectively. Finally, to test the applicability of the established method, it was successfully applied to the determination of furanic compounds in various food products.
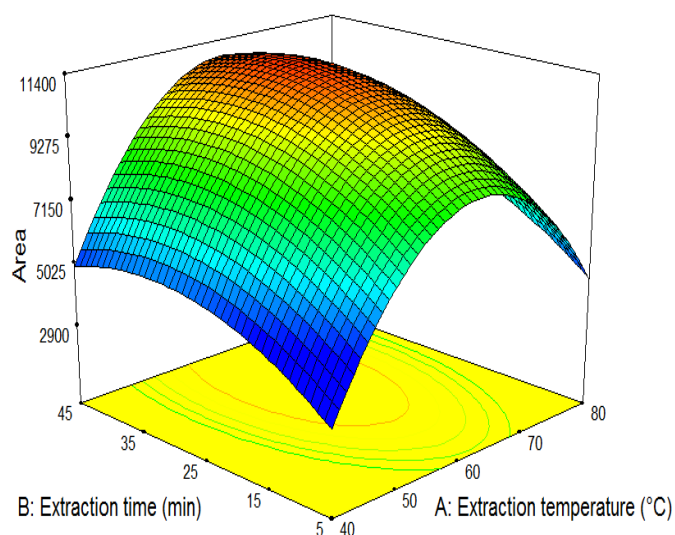
Conclusions: The coated fiber showed high stability and reusability and could be used for more than 100 replicate extractions without measurable performance loss. The developed HS-SPME method with the innovatively prepared fiber showed satisfactory reproducibility, wide linear range, and low LODs for the determination of furanic compounds under optimized conditions, and it was successfully used in analyzing various food products.

References

[1] A. Spietelun, A. Kloskowski, W. Chrzanowski, J. Namieśnik, Chem. Rev., **2013**, 113, 1667-1685.

Miniaturization of DLLME Technique on a Centrifugal Microfluidic Device

Monireh Karami, Yadollah Yamini *, Yousef Abdossalami Asl

Department of Chemistry, Tarbiat Modares University, P.O. Box ١٤١١٥-١٧٥, Tehran, Iran

*yyamini@modares.ac.ir

****

Introduction: Dispersive liquid-liquid microextraction (DLLME) which is a rapid, inexpensive and easy to operate method has gotten much attention since its introduction in ٢٠٠٦ by Assadi [١]. Despite of the advantages of DLLME, the method has some drawbacks including a great amount of sample needed and a centrifuge device is applied for phase separation. By emerging microfluidic systems, which is capable to integrate a number of functions on a small device, miniaturization has complied lots of interest in the field of analytical chemistry. Centrifugal microfluidic device (CMD) has become a dominant trend in making commercialized and portable devices [٢].

Methods / Experimentals: The CMD was designed and carved on a Poly(methyl methacrylate) sheet by a CNC milling machine including two analysis units. Each analysis unit consists of an analyte and an organic solvent champers, mixing channels and an extraction chamber at the end of the unit. Length of each unit is ٧ centimeters and centrifugal pumping force is used to transfer liquids.

Results and discussion: In the present work an on-chip DLLME using a centrifugal microfluidic devise followed by HPLC-UV was employed to determine cimetidine as model analyte. To obtain the optimal conditions, two series of conditions should be investigated: first, conditions related to spinning program of CMD and second, DLLME conditions. According to the high surface-to-volume ratio in any microfluidic system, analytes and solvents are in direct contact with the substance which the devise is made from. Thus the substance can affect the DLLME effective parameters such as choosing dispersive and extracting solvent. Also chemical resistance of the substance should be noticed. Finally, the optimal conditions of proposed device were applied for extraction and quantification of cimetidine in waste water sample. The suggested method offers satisfactory repeatability (RSD %< ٣.٢) and acceptable limits of detection and linearity.

Conclusion: In this work a new device based on centrifugal microfluidic platform was designed and successfully applied for miniaturization of one of the popular conventional methods of microextraction, DLLME. The proposed device is capable to be automated and portable therefore could solve one of the main problems on the way of conventional DLLME.

 References

[١] M. Rezaee; Y. Assadi. Journal of Chromatography A, ٢٠٠٦,١١١٦, ١-٩.

[٢] O. Strohmeier; M. Keller. Chemical Society Reviews, ٢٠١٥, ٤٤, ٦١٨٧-٦٢٢٩.

On-chip electromembrane extraction of ephedrine and clonidine from human urine and plasma samples

Mahroo Baharfar[a], Yadollah Yamini[a],*, Shahram Seidi[b], Monireh Karami[a]

[a] Department of Chemistry, Tarbiat Modares University, P.O. Box 14115-175, Tehran, Iran

[b] Department of Analytical Chemistry, K.N. Toosi University of Technology, Tehran, Iran

yyamini@modares.ac.ir

****

Introduction: In the recent years, the advent of lab on a chip systems has addressed so many necessities in sample preparation. In these systems, analysis can be performed on a small sample size and be accelerated due to the small dimensions and the short diffusion distances [1-3]. Electromembrane extraction has advantages over other similar techniques comprising: rapid extractions, efficient sample clean up and dispense with sample pretreatment [4]. In this work the advantages of electromembrane extraction and an on-chip system have been combined for the extraction and preconcentration of ephedrine and clonidine from biological fluids.

Methods/ Experimentals: Two polymethylmethacrylate plates were exploited at each a long channel was carved by a CNC milling machine. The upper plate acted as acceptor phase channel and the other one mounted underneath was dedicated for donor phase flow pass. Three individual holes were drilled on each plate for embedding the platinum electrodes and providing the inlet and the outlet tubes. A polypropylene sheet which was impregnated by an organic solvent was located between two plates and fixed by bolts and nuts.

Results and Discussion: The influential parameters on extraction procedure were identified and optimized. The supported liquid membrane (SLM) composition was optimized by one variable at a time method and the rest of parameters by a central composite design model. The results showed that 10% di-(2-ethylhexyl) phosphate in 2-nitrophenyl octyl ether has the best extraction efficiency and the rest optimized values were 74 volts for applied voltage, 28 µL min^{-1} and 0.2 for flow rate and ion balance respectively. Under the optimal conditions, the calibration curves were linear in the range of 30-500 µg L^{-1} with coefficient of determinations (r^2) greater than 0.9914 in plasma and 0.9950 in urine samples. The LODs were less than 9 µg L^{-1} and 5 µg L^{-1} in plasma and urine respectively. Relative standard deviations (RSDs%) less than 6.9% were observed for both analytes.

Conclusion: In this work a chip based electromembrane extraction was developed for the analysis of trace amount of ephedrine and clonidine in biological fluids. The effective parameters on the extraction procedure were optimized and under the optimal conditions low LODs and efficient sample clean-up were attained. This technique showed good extraction efficiency due to the increase of surface to volume ratio and exploitation of electrical field along with the whole channel.

References

[1] Bin Li; Nickolaj Jacob Petersen; María D. Ramos Payán; Steen Honoré Hansen; Stig Pedersen-Bjergaard. *Talanta*, **2014**, 120, 224-229.

[2] Yousef Abdossalami Asl; Yadollah Yamini; Shahram Seidi; Behnam Ebrahimpour. *Analytica Chimica Acta*, **2015**, 898, 42-49.

[3] María D. Ramos Payán; Henrik Jensen; Nickolaj Jacob Petersen; Steen Honoré Hansen; Stig Pedersen-Bjergaard. *Analytica chimica acta*, **2012**, 735, 46-53.

[4] Yadollah Yamini; Shahram Seidi; Maryam Rezazadeh. *Analytica chimica acta*, **2014**, 814, 1-22.

Magnetic FeNi$_3$/SiO$_2$ Nanocomposite Catalyzed Epoxidation of Olefins

Samaneh Ghiami, Mohammad Ali Nasseri*, Ali Allahresani

Department of Chemistry, Faculty of Sciences, University of Birjand, P. O. Box 97175-615, Birjand, Iran

E-mail: manaseri@birjand.ac.ir

****

Introduction: Selective epoxidation of alkenes with different catalyst such as transition metal oxides (NiO, CoO, MoO$_3$, CuO, TiO$_2$–SiO$_2$, Au/SiO$_2$, CuO$_x$/SiO$_2$) into valuable chemicals is of great attention in chemical and pharmaceutical industries [1-7]. From an economic point of view, the separation of ultra-scaled and nano-sized catalysts from the reaction system via routine methods such as free sedimentation, centrifuging, is time-consuming and costly.

Magnetic nanoparticles which can be easily separated with external magnet without any significant loss of activity put forward a solution to this problem. In this study, epoxidation of alkenes was investigated using FeNi$_3$/SiO$_2$ as a magnetic nanocomposite.

Experimental: In a typical procedure, an appropriate amount of catalyst (0.04 gr) was dispersed in 3 mL dichloromethane for 30 min. Then, alkene (1 mmol) was added to the mixture followed by addition of oxidant (2 mmol). The mixture was stirred for 1.5 h. after completion of the reaction, the catalyst was separated by external magnet and the solution was worked up. Finally, the conversion of the products was determined by GC. The catalyst was washed twice with ethanol and reused.

Results and discussion: In this study, FeNi$_3$/SiO$_2$ was tested to catalyze the selective oxidation of alkenes using *m*-CPBA as an oxidant at room temperature in dichloromethane (Fig. 1).
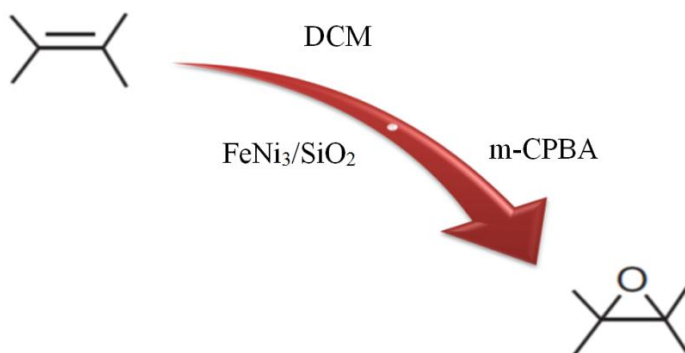

Fig. 1 Epoxidation of alkenes with *m*-CPBA catalyzed by FeNi$_3$/SiO$_2$ in dichloromethane media.

To optimize the amount of catalyst, the reaction was carried out in the presence of different amount of FeNi$_3$/SiO$_2$ (0.01–0.06 gr) at room temperature. It was found that, 0.04 g of FeNi$_3$/SiO$_2$ was sufficient enough to afford styrene oxide with 97 % isolated yield. To explore

the effect of solvent on the reaction, the same reactions were performed in different solvents. The best conversion was observed when the reaction was performed in DCM (97 %). The effect of various oxidants such as $NaIO_4$, *m*-chloroperbenzoic acid, Urea Hydrogen Peroxide, H_2O_2, Oxone, PhIO, $PhI(OAC)_2$ and *t*-butylhydroperoxide was investigated in the epoxidation of styrene and m-CPBA was selected as the best oxidant. The effect of different temperature was also investigated on the conversion of the substrate and the results showed that the best conversion and selectivity were obtained at ambient temperature.

Conclusion: In summary, we developed a facile, highly efficient, and eco-friendly procedure for the epoxidation of olefins in the presence of $FeNi_3/SiO_2$ as a heterogeneous catalyst. This catalyst is highly reactive in the epoxidation of a wide range of alkenes such as linear and cyclic ones. Moreover, easy preparation, handling and recovery, reusability and long-term stability of the catalyst, as well as excellent yields are some advantages of this heterogeneous catalyst.

References:

[1] Cui HT; Zhang Y; Qiu ZG; Zhao LF; Zhu YL. *Applied Catal. B* **2010**, *101*, 45–53.
[2] Choudhary VR; Jha R; Jana P. *Catal. Commun*, **2008**, *10*, 205–207.
[3] Choudhary VR; Jha R; Jana P. *Green Chem*, **2006**, *8*, 689–690.
[4] Choudhary VR; Jha R; Chaudhari NK; Jana P. *Catal. Commun.* **2007**, *8*, 1556–1560.
[5] Khouw CB; Dartt CB; Labinger JA; Davis ME. *J Catal*, **1994** *149*, 195–205.
[6] Xie J; Wang Y; Li Y; Wei Y. *React Kinet Mech Cat*, **2011**, *102*, 143–154.
[7] He J; Zhai Q; Zhang Q; Deng W; Wang Y. *J Catal*, **2013**, *299*, 53–66.

An electrochemical ceruloplasmin nanoaptasensor using a glassy carbon electrode modified by diazonium-functionalized multiwalled carbon nanotubes

Esmaeel Haghshenas[a], Tayyebeh Madrakian[a,*] , Abbas Afkhami[a], Haidar Saify Nabiabad[b]

[a]Faculty of Chemistry, Bu-Ali Sina University, Hamedan, Iran

[b]Department of Biotechnology, College of Agriculture, Bu-Ali Sina University, Hamadan, Iran

***Email address**: madrakian@basu.ac.ir, madrakian@gmail.com

****

Introduction: Low levels and high levels of ceruloplasmin (Cp) in serum cause several diseases such as Wilson's disease [1, 2], so its accurate determination in human fluids is much essential. To date, numerous DNA or RNA aptamers have been identified for various targets with high affinity that have been applied in various fields, such as therapeutics, diagnostics and biosensors [3, 4]. Aptamer-based biosensors have exceptional adequate, compared to the natural receptors, such as enzymes and antibodies. The intrinsic properties of aptamers, such as high flexibility of structure, and convenience in the design of their structure, enable to develop the various novel aptasensors.

Experimentals: The proposed nanoaptasensor was based on a glassy carbon electrode modified with diazonium-functional multiwall carbon nanotubes. The aptamer was linked onto the electrode surface, via electrochemical approach, followed by chemical immobilization of aminated-aptamer. Each fabrication steps was accompanied by changes to the electrochemical parameters. The binding of Cp to aptamer was monitored using CV, DPV, and EIS. While detecting Cp with the aptamer-based biosensor, EIS and DPV of $[Fe(CN)_6]^{3-/4-}$ was used to quantify the response of the aptamer–Cp interaction.

Results and Discussion: The different stages of the nanoaptasensor preparation were investigated by recording CV, DPV and EIS of a modified electrode in the presence of the reversible $[Fe(CN)_6]^{4-/3-}$ redox system. At the next step, the experimental parameters such as aptamer concentration, incubation time and pH in the solution was optimized. 2.0 µmol L^{-1}

aptamer solution, pH of 7.4, and 20 min for incubation time were selected as optimized values for Cp sensing.

Under the optimal condition, the proposed nanoaptasensor was employed for the determination of Cp using DPV and EIS. The calibration curve for Cp concentration was linear at 0.02 to 80.0 ng mL^{-1} with detection limit (signal-to-noise ratio of 3) of 1.7 pg mL^{-1}. Then, selectivity, reproducibility and stability of the nanoaptasensor were investigated. The results were shown that the nanoaptasensor has good selectivity, reproducibility and stability. In order to investigate the ability of the nanoaptasensor for the determination of Cp in real samples, the nanoaptasensor was applied to the analysis of Cp in serum sample. The detection results showed that the recoveries were from 97.5% to 104.0% indicating the suitability of the developed nanoaptasensor for Cp detection in clinical applications.

Conclusion: The nanoaptasensor was fabricated after Cp aptamer immobilized on MWCNTs/GCE. Compared with other reported electrochemical sensor for Cp, the present sensor is superior in its ease of operation, broad response range of 0.02–80 ng mL^{-1} and an extremely low detection limit (1.7 pg mL^{-1}). The nanoaptasensor showed acceptable specificity, reproducibility and stability. The proposed nanoaptasensor is a potential candidate for routine analysis of Cp in real samples.

References

[1] Somani, B.L., Ambade, V., *Clinical Biochemistry,* **2007**, 40, 571-574.

[2] Korman, J.D., Volenberg, I., Balko, J., Webster, J., Schiodt, F.V., Squires, R.H., Fontana, R.J., Lee, W.M., Schilsky, M.L., Pediatric, *Adult Acute Liver Failure Study, G.,* **2008**, 48(4), 1167-1174.

[3] Liu, X., Cheng, Z., Fan, H., Ai, S., Han, R., *Electrochimica Acta,* **2011**, 56, 6266-6270.

[4] Seok Kim, Y., Ahmad Raston, N.H., Bock Gu, M., *Biosensors and Bioelectronics,* **2016**, 76, 2-19.

New vanadium (IV) complex with water soluble tridentate Schiff base ligand based on ionic liquid: Synthesis, characterization and investigation of its catalytic activity for oxidation reactions.

Somayeh Azizi Talouki[a], Gholamhossein Grivani[b,*]

[a,b]Department of chemistry, University of Damghan, Damghan, Iran

E-mail: Grivani@du.ac.ir

Abstract. Water-soluble ligands and their metal complexes based on ionic liquid have emerged as a synthetic strategy for homogeneous catalysis. In this research, vanadium (IV) Schiff base complex namely VO(acac)L obtained by reaction between tridentate Schiff base ligand derivated from salicylaldehyde with ionic liquid base (Triphenylphosphin) and vanadin (IV)-oxid-acetylacetonate in 1:1 stochiometery. This water soluble complex has been characterized by IR, ^{1}HNMR, UV-Vis spectroscopy and mass spectrometry, as well as elemental analysis. This complex has ability to catalyze the epoxidation of cyclooctene by using tert-butyl hydroperoxide (TBHP) as an oxidant in good yield (98%). Also it has been used as a catalyst for the oxidation of methyl phenyl sulfide to sulfoxide with good yield in 4 minutes.

Keywords: Vanadium (IV) complex, Schiff base ligand, Ionic liquid, Oxidation reaction.

1   Introduction

Schiff base complexes can be widely employed as catalysts, i.e. in the epoxidation of alkenes [1], or the enantioselective oxidation of organic sulfides [2]. Also the ionic liquids can also have widely been promoted as "green solvents". Water-soluble ligands and their metal complexes containing ionic liquid fragment have emerged as a synthetic strategy for homogeneous catalysis. In this research, we describe the synthesis of the task-specific ionic liquid Schiff base ligand and its vanadyl complex named as VO(acac)L.

2   Experimental

2.1   Synthesis of task-specific ionic liquid vanadyl Schiff base complex of VO(acac)L

VO(acac)$_2$ and prepared L Schiff base ligand (mixing by salicylaldehyde with triphenylphosphin) was dissolved in methanol as 1:1 for 4 h in reflux condition. By evaporation of solvent the product was obtained. Then anionic exchange are carried with 1:1 stochiometry between complex and KPF$_6$ in water that leads to complex VO(acac)L with anion PF$_6^-$ instead of Cl$^-$. By evaporation of solvent and drying in vacuum the solid was obtained. (Fig. 1)
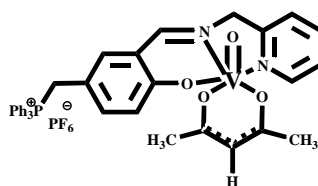

Fig. 1. Schematic of complex VO(acac)L

3 Result and discussion

For ligand L, the IR spectra showed on ν(O–H)$_{phenolic}$, 3355-3382; ν(C=N), 1635; ν(P-F) 842; and ^{1}HNMR data (δ, ppm; CDCl$_3$): 13.39 (1H, H^a); 7.18 (1H, H^b); 7.23 (1H, H^c); 7.27(1H, H^d); 8.42-8.44 (1H, H^e); 5.24-5.28 (2H, H^f); 7.52-7.67 (15H, H^g); 4.74 (2H, H^h); 6.78- 6.81 (1H, H^i); 7.08-7.12 (1H, H^j); 6.52-6.55 (1H, H^k); 8.24 (1H, H^l); UV-Vis (nm): 269, 321. Fig. 2 showed the ligand L and ^{1}HNMR spectra of ligand.
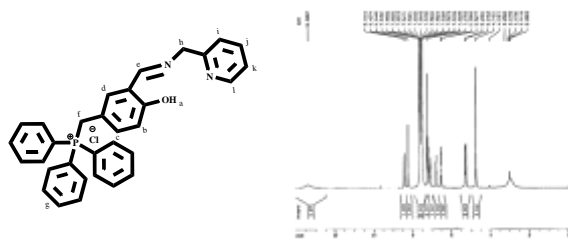
Fig. 2. Schematic of ligand L and its ^{1}HNMR spectra

And also in complex VO(acac)L the IR spectra are in ν(C=N), 1635; ν(V=O), 951; ν(P-F), 840 . Mass (M/Z): 795 (M$^+$), 410, 262, 259, 230, 203, 183, 164, 152, 115, 107, 105, 89, 85, 79, 77, 63, 51, 49, 43 and 41 (M$^+$), UV-Vis (nm): 271, 382, 549 (d-d).

4 Catalytic activity

The catalytic activity of complex VO(acac)L in epoxidation reactions was carried by cyclooctene as a model substrate and different reaction parameters, such as solvent, oxidant, alkene/oxidant ratio and the amount of the catalyst [3]. For this reaction TBHP was chose as an oxidant. According to the optimal condition of 1:3 ratio of cyclooctene/oxidant and 0.01mmol of the catalyst, the yield was 98% in 140 minutes. And also the catalytic activity of complex in the oxidation of sulfides (thioethers) to sulfoxides and sulfones was surveid [4,5]. The optimum condition was using by 4 mmol of MeSPh, 4.4 mmol of TBHP and 0.024 mmol of catalyst led to the 82% yield with TOF=161 in 4 min in solvent free condition [6].

5 Conclusion

In summary, task-specific ionic liquid Schiff base complex of vanadium (IV) had been synthesized and characterized. The spectroscopic studies showed the six coordinated vanadium (IV) structure in solid state. This complex VO(acac)L is quite water soluble and also in other organic solvents. This task-specific ionic liquid Schiff base complex showed high activity in epoxidation of cyclooctene and oxidation of methyl phenyl sulfide in optimized conditions as a catalyst.

References

[1] Pisk. J; Daran . J. C; Poli. R; Agustin. D. J. Mol Catal A: Chem, **2015**, 403, 52-63.

[2] Hsieh.S. H; Kuo. Y. P; Gau. H. M. Dalton Trans. **2007,** 97.

[3] Conte. V; Coletti. A; Floris. B; Licini. G; Zonta. C. Coord. Chem. Rev, **2011**, 255, 2165.

[4] Ligtenbarg. A. G. J; Hage. R; Feringa. B. L. Coord. Chem. Rev, **2003**, 237, 89-101.

[5] Adao. P; Costa Pessoa. J; Henriques. R.T. Inorg. Chem, **2009**, 48, 3542- 3561.

[6] M.R. Maurya; M. Bisht. Journal of Molecular Catalysis A: Chemical, **2011**, 344, 18.

Effect of different precipitating agents upon textural properties of γ-Al$_2$O$_3$

P. Moghimpour Bijani[a],* , **F. Yaripour[a] and M. Mahboubie[a]**

[a] Catalyst Research Group, Petrochemical Research and Technology Company, National Petrochemical Company, Tehran, Iran.
p.bijani@gmail.com

Introduction

Among the different transition aluminas known, γ-Al$_2$O$_3$ is perhaps the most important with direct application as a catalyst [1]. γ-Al$_2$O$_3$ could be prepared by different methods including sol–gel, hydrothermal processing and precipitation of various precursors such as aluminum salts, alkoxides and metallic powders. The preparation of γ-Al$_2$O$_3$ has been largely based on the precipitation method with a great quality, i.e., controlled chemistry, morphology and textural properties [2]. The present research deals with synthesis of mesoporous γ-Al$_2$O$_3$ samples prepared precipitation method. Different precipitating agents comprising sodium carbonate, ammonium bicarbonate and sodium hydroxide have been used in this research.

Methods

The precipitation was carried out by simultaneous addition of the aluminum nitrate solution and aqueous precipitating agent in the precipitating vessel under vigorous stirring at 50 ℃. The pH of this solution was adjusted to 7.5 ± 0.5 during precipitation. After aging, the white precipitate was dried at 110 ℃. The final solid was then calcined at 550 ℃ for 6 h. BET surface area, total pore volume and average pore diameter were determined by N$_2$ adsorption–desorption isotherm at -196 ℃.

Results and Discussion

Results of sample characterization showed that the textural characteristics vary significantly from one sample to another. Among the studied samples, S3 exhibits the highest specific surface area (SSA) and the lowest average pore diameter (Table 1). The nitrogen adsorption/desorption isotherms of all samples shown in Fig. 1. For the samples, the classical type IV isotherm can be observed, typical for mesoporous solids. The type H1 hysteresis loop indicates uniform cylindrical shape but pore size distribution significantly vary for the different samples.

---

* Corresponding author Email: p.bijani@gmail.com

Table 1. Textural characteristics of the γ-Al$_2$O$_3$ samples.

Sample	precipitating agent	Phase (from XRD)	SSA (m^2/g)	Total pore volume (ml/g)	Average pore radius (Å)
S1	sodium carbonate	Al(OH)$_3$, (Bayerite& Nordstrandite), Na$_2$CO$_3$, NaHCO$_3$, NaAlCO$_3$(OH)$_2$	76.29	0.529	138.8
S2	ammonium bicarbonate	γ-Al$_2$O$_3$	268.84	1.101	81.95
S3	sodium hydroxide	γ-Al$_2$O$_3$	311.1	0.757	48.65

The hysteresis loop operating at higher relative pressure indicates larger mesopores. Thus S2 have larger mesopores than S3. Fig.1 b confirms this. Also it can be seen that S2 have some macropores in their structures.
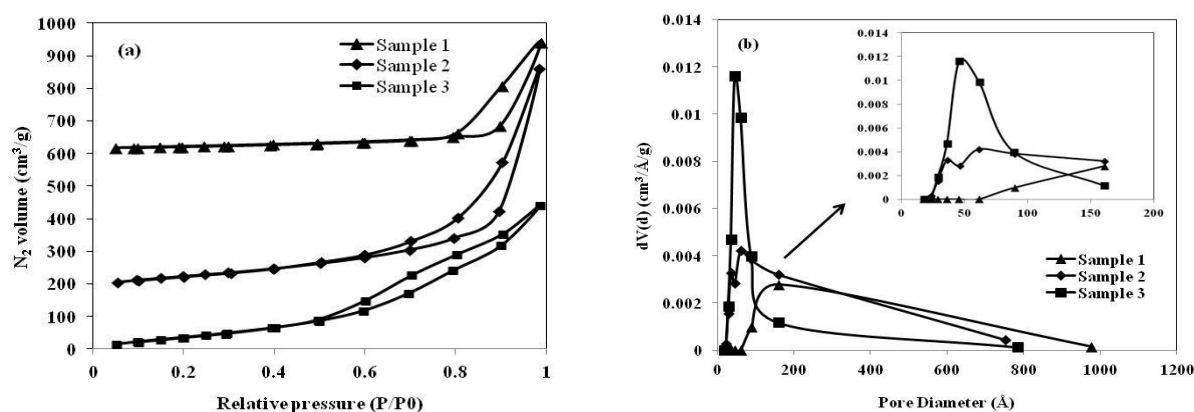
Fig. 1. The N$_2$ adsorption/desorption isotherms (a) and pore size distribution (b) of the studied samples.

Conclusion

A precipitation method was successfully utilized to produce γ-Al$_2$O$_3$ samples with different textural properties. For this purpose, three precipitating agents were used to precipitate aluminum cations and produce γ-Al$_2$O$_3$. The γ-Al$_2$O$_3$ prepared by sodium hydroxide (⊙S3) had the highest surface area and lowest pore radius.

References

[1] M. Trueba; S. P. Trasatti. *European Journal of Inorganic Chemistry*, **2005**, 3393-3403.

[2] S. Y. Hosseini; M. R. Khosravi Nikou. *Journal of Industrial and Engineering Chemistry*, **2014**, *20*, 4421-4428.

A study on preparation of curcumin complexes of niobium(V)

ZariNozari[a], AlirezaKhorshidi[a],*

[a]*Department of Chemistry, Faculty of Sciences, University of Guilan, P. O. Box: 41335-1914, Iran*

Email address: khorshidi@guilan.ac.ir

****

Introduction:

Curcumin is the main ingredient of turmeric obtained from curcuma longa [1,2]. Curcumin was first isolated in 1815 when Vogel and Pelletier reported the isolation of a "yellow coloring-substance" from the rhizomes of turmeric and named it curcumin [3].

Curcumin has been used historically in medicine[4]. Its potential medicinal properties however, are an area of active investigation [5].

Niobium, on the other hand, has physical and chemical properties similar to those of tantalum, but its complexes with curcumin have not been investigated yet. We decided to investigate complexation of curcumin with niobium and the results were surprising.

Experimental:

All of the chemicals were purchased from Mecrk and was used without further purification. The products were characterized by using different techniques such as ^1H and ^{13}C NMR spectroscopy, FTIR spectroscopy, TGA analysis etc.

Result and discussion:

Upon treatment of curcumin (2.0 mmol) with niobium(V) in methanolic solution, a brown precipitate was formed which was further purified by recrystallization form H_2O/CH_3OH. The obtained product was formed as needle like crystals (Fig. 1), and its NMR spectra revealed a *trans*- geometry with D_{2h} symmetry (Fig. 2)

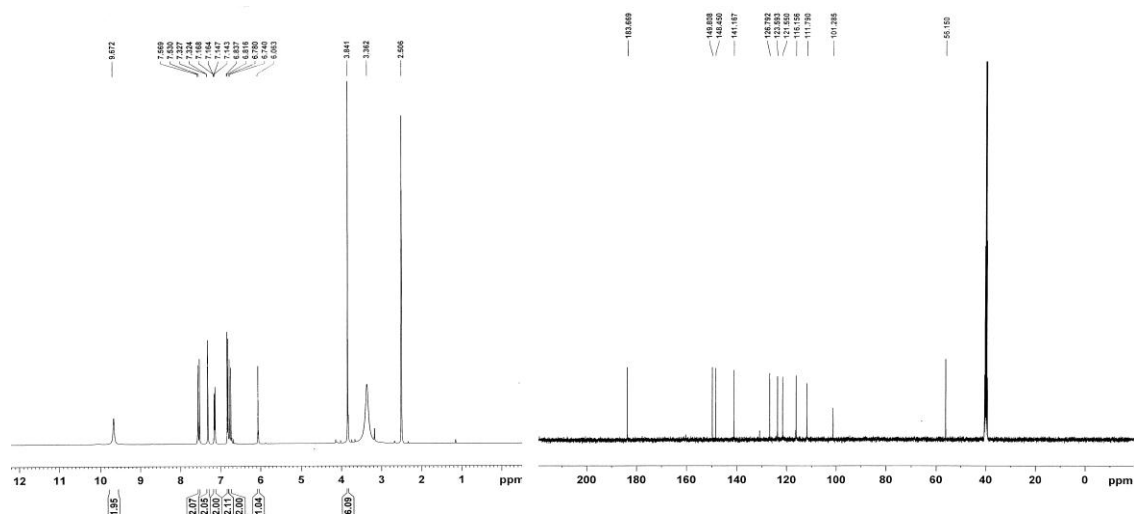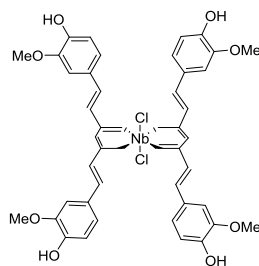Fig. 1. Crystals of the obtained complex under optical microscope

Fig. 2. ^{1}H and ^{13}C NMR spectra of the obtained complex

Based on these data and other related analyses, the following structure is proposed for this compound.

Conclusion:

To conclude, we have introduced a new complex of niobium(V) with curcumin, which is expected to have interesting biological properties. Further study on this complex is currently under way in our laboratory.

References:

1. Shaheen, M. (2015). "The State of the Curcumin Market".Natural Products Insider.
2. DeFoe, D., &Gambrill, E. (2014) Site navigation.
3. Vogel, H. A., & Pelletier, J. (1815). Curcumin-biological and medicinal properties. J. Pharma, 2, 50.
4. Wilken, Reason, et al. (2011)"Curcumin: A review of anti-cancer properties and therapeutic activity in head and neck squamous cell carcinoma." Molecular cancer 10.1: 1.
5. Jacobson, J. S., Workman, S. B., &Kronenberg, F. (2000). Research on complementary/alternative medicine for patients with breast cancer: a review of the biomedical literature. Journal of Clinical Oncology, 18(3), 668-668.

One-Pot Synthesis of Pyrano[2,3-d]pyrimidinone Derivatives Catalyzed by Fe$_3$O$_4$@SiO$_2$-Imid-PMA^n in Aqueous Media

Ali Reza Sardarian[a],*, Hassan Eslahi[a], Mohsen Esmaeilpour[a], Milad kazemnezhad[a]

[a]*Department of Chemistry, College of Sciences, Shiraz University, Shiraz 71946- 84795, Iran.*

*Corresponding author: E-mail: sardarian@shirazu.ac.ir; Tel: +98 71 3613 7109; Fax: +98 71 3646 0788

Introduction: Multicomponent reactions (MCRs) have been considered in modern medicinal chemistry [1]. Pyrano[2,3-d]pyrimidine structures have a wide range of biological activities such as anticancer, antiallergic, anticoagulant, anticoagulant, antitumor, diuretic, spasmolytic, and antianaphylactic activity [2]. Synthesis of pyrano[2,3-d]pyrimidines has been achieved by many methods, including ultrasonic irradiation [3], microwave condition [4], alum [5], Zn[(L)proline]$_2$ [6], and ionic liquids [6]. Reported methods appearing in literature usually involve forcing conditions, waste creation, long reaction time and involvement of organic solvents. So, due to environmental concerns associated with aspects of organic solvents, development of aqueous-phase synthesis of pyrano[2,3-d]pyrimidines is of considerable interest. We have been interested in development of the efficient and environmentally benign synthetic methodologies using economical and ecofriendly catalysts [7]. Therefore, herein, we report the synthesis of pyrano[2,3-d]pyrimidine derivatives from a three-component, one-pot condensation of benzaldehyde derivatives, malononitrile, and barbituric acid in the presence of Fe$_3$O$_4$@SiO$_2$-Imid-PMA^n as catalyst (Scheme1).
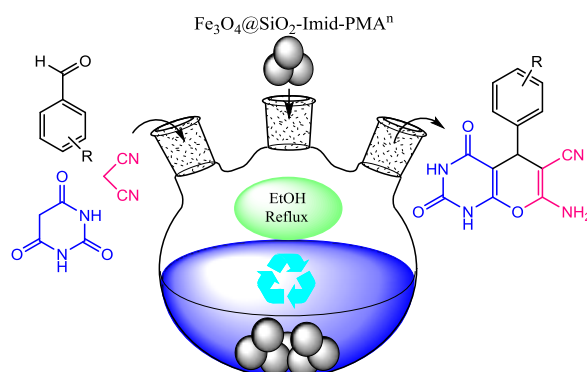
Scheme 1. Synthesis of pyrano[2,3-d]pyrimidine derivatives.

Experimentals: *Preparation of Fe$_3$O$_4$@SiO$_2$-imid-PMA^n:* Fe$_3$O$_4$@SiO$_2$-Imid-PMA^n nanoparticles were prepared in our previous work [7]. *General procedure for synthesis of pyrano[2,3-d]pyrimidinone derivatives:* Substituted aromatic aldehydes (1 mmol), malononitrile (1 mmol), barbituric acid (1 mmol), and Fe$_3$O$_4$@SiO$_2$-Imid-PMA^n (15 mg) in EtOH (5 mL) was stirred at reflux conditions for appropriate time. After reaction completion as monitored by TLC and separation of catalyst by magnetic field, the filtrate mixture was recrystallized to provide pure crystals of pyrano[2,3-d]pyrimidinone derivatives with excellent yields.

Result and Discussion: Due to ability of Fe$_3$O$_4$@SiO$_2$-Imid-PMA^n as a mild and efficient acid catalyst, we decided to apply this catalyst for synthesis of pyrano[2,3-d]pyrimidinone derivatives. At the first stage, to obtain the best reaction conditions, the reaction of benzaldehyde, malononitrile and barbituric acid as a model reaction was chosen. The best result was obtained with 1:1:1 ratios of benzaldehyde, malononitrile and barbituric acid in the

presence of 0.015 g of $Fe_3O_4@SiO_2$-Imid-PMA^n magnetic catalyst in ethanol under reflux conditions. Following the obtained results, other derivatives of pyrano[2,3-d]pyrimidinone were synthesised using different types of aldehydes under the optimized conditions. A series of aromatic aldehydes carrying either electron-releasing or electron-withdrawing substituents afforded high yields of products.

Entry	R	Time (min)	Yield(%)	m.p. (^{o}C)	
				Found	Reported
1	H	20	94	204-205	205–207 [8]
2	4-MeO	30	92	278-280	280–284 [9]
3	3-MeO	25	90	199-201	200–202 [9]
4	4-Me	25	89	228-229	226–228 [8]
5	3-Me	20	93	223-225	224–225 [9]
6	3-OH	30	88	162-164	160–162 [9]
7	4-NO$_2$	15	96	239-240	237–240 [8]
8	3-NO$_2$	15	92	269-270	271–272 [9]
9	4-F	15	89	270-272	268–270 [9]
10	4-Br	15	90	233-234	235–236 [9]
11	4-Cl	15	95	235-237	234–235 [9]
12	3-Cl	20	92	243-245	242–244 [9]
13	2,4-Cl$_2$	15	94	240-242	239–241 [9]

Finally, the possibility of recycling the catalyst was examined using the reaction of benzaldehyde malononitrile, barbituric acid under the optimization conditions. The recycled catalyst was consecutively reused seven times with negligible loss in its activity.

Conclusions: In summary, this method is attractive, since it offers some advantages over earlier reported protocols. This new procedure has notable advantages such as avoids the use of dry and toxic solvents, operational simplicity, excellent yields, short reaction time, and absence of any tedious workup or purification. In addition, easy preparation, thermal stability and separation of the catalyst make it a good heterogeneous system.

References
[1] Weber L. *Curr. Med. Chem.* **2002**, *9*, 2085-2093.
[2] Arnoldi A; Bonsignori A; Melloni P; Merlini L; Quabri M.L; Rossi A.C; Valsecchi M. *J. Chem. Med.* **1990**, *33*, 2865-2869.
[3] Jin T.S; Liu L.B; Tu S.J; Zhao Y; Li T.S. *J. Chem. Res.* **2005**, *3*, 162-163.
[4] Gao Y; Tu S; Li T; Zhang X; Zhu S; Fang F; Shi D. *Synth. Commun.* **2004**, *34*, 1295-1299.
[5] Mobinikhaledi A; Foroughifar N; Bodaghi Fard M.A. *Synth. React. Inorg. Met. Org. Nano Met. Chem.* **2010**, *40*, 179-185.
[6] Yu J; Wang H. *Synth. Commun.* **2005**, *35*, 3133-3140.
[7] Esmaeilpour M; Javidi J; Zandi M. *Mater Res Bull.* **2014**, *55*, 78–87.
[8] Rezayati S; Abbasi Z; Nezhad E. R; Hajinasiri R; Farrokhni A; *Res. Chem. Intermed.* **2016**, *42*, 7597-7609.
[9] Mohammadi Ziarani G; Faramarzi S; Asadi S; Badiei A; Bazl R; Amanlou M; *DARU J. Pharm. Sci.* **2013**, 21, 1-13.

Design and synthesis of a novel nanostructured biopolymer and its application in the synthesis of dihydropyridine derivatives

Maliheh Safaiee*[a], Mohammad Ali Zolfigol[b], Bahar Ebrahimghasri[b], Saeed Baghery[b],

[a] *Department of Medicinal Plants Production, Nahavand University, Nahavand, 6593139565, Iran.*

[b] *Department of Organic Chemistry, Faculty of Chemistry, Bu-Ali Sina University, Hamedan 6517838683, Iran*

E-mail: azalia_s@yahoo.com

****

Introduction:

1,4-Dihydropyridin (1,4-DHPs) derivatives containing the 1,4-dihydropyridine structure include calcium antagonists, antitubercular agents, antitumours, bronchodilatings, antidiabetics, antivirals, antianginals and neuropeptide Y Y1 receptor antagonists [1].

Chitosan is actually a heteropolymer containing both glucosamine units and acetylglucosamine units. Among various biopolymers, chitosan based materials have attracted great interest as support for catalytic applications [2].

Herein, we report the utility of heterogeneous, biodegradable, and reusable nano chitosan-VO catalyst for the synthesis of 1,4-dihydropyridine derivatives.

Methods/experimaentals: In the first step, nano chitosan-VO catalyst was synthesized. Then the dihydropyridine derivatives were prepared using this catalyst. The progress of the reaction was monitored by TLC and after completion of the reaction, the catalyst was separated from the reaction mixture to be used again for another reaction. The products were washed and then recrystallized from an appropriate solvent. Finally the synthesized catalyst and products were characterized by different analysis.

Results and discussion: The first step in the accomplishment of this goal was the immobilization of vanadium oxo (VO) over chitosan. The utility of chitosan supported VO catalyst (ChVO) was then explored in synthesis of 1,4-dihydropyridines. The catalyst displayed high activity for this purpose. The separation and recovery of the catalyst is an important step in the synthesis of fine chemicals, which is generally performed either by centrifuge or by filtration with reduced efficiency. In this catalytic system, most of the time catalyst was recovered by simply decantation
or centrifuge.
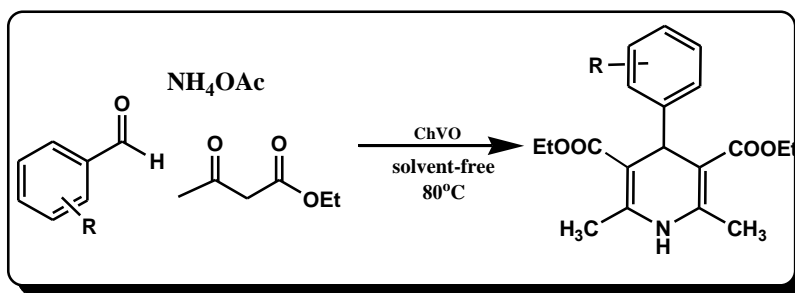
Scheme 1: Synthesis of diethyl 1,4-dihydro-2,6-dimethyl-4-arylpyridines-3,5-dicarboxylate using ChVO as a catalyst
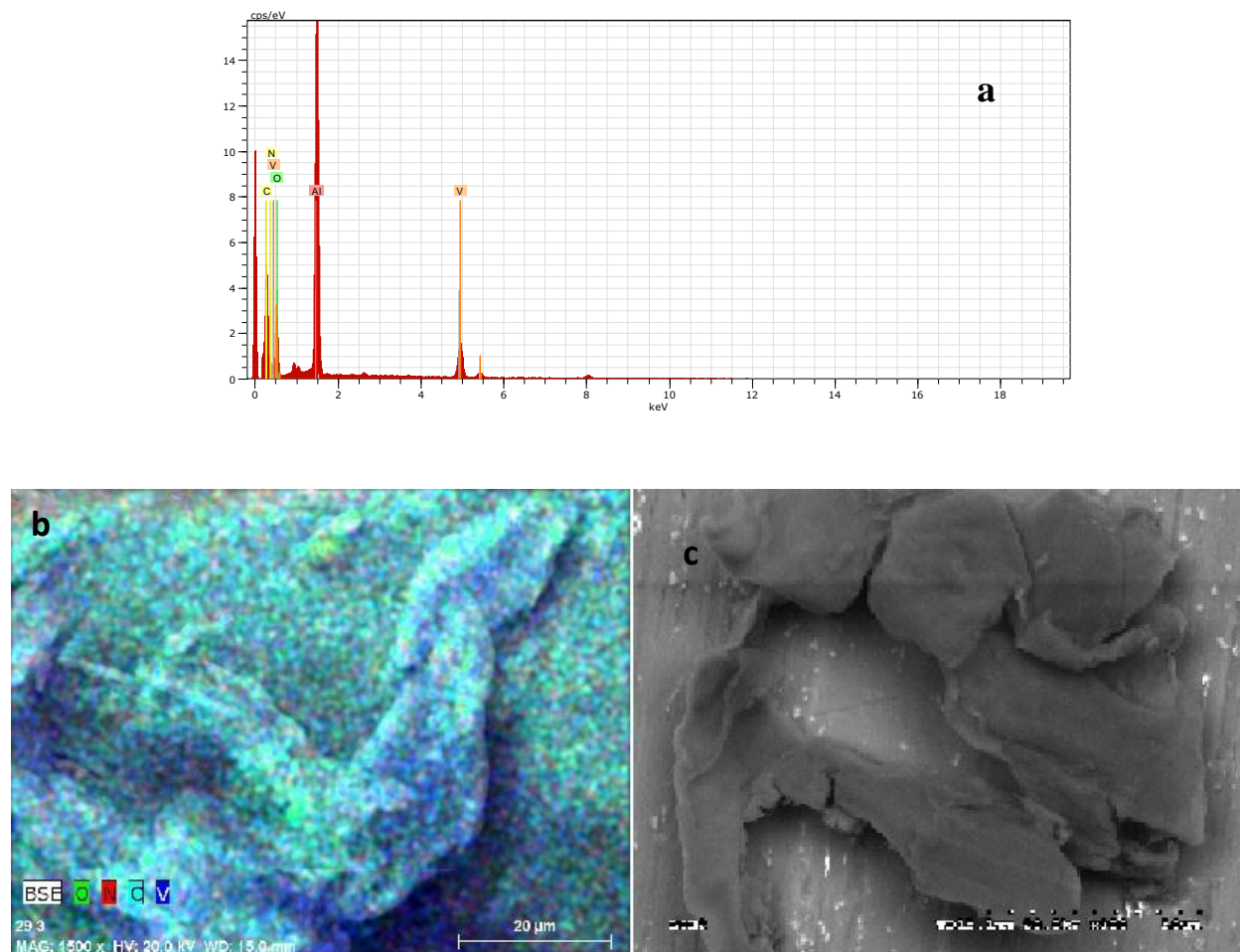

Figure1: (a) EDX analysis, **(b)** WDX analysis and **(c)** SEM image of the catalyst

Conclusion: We have developed a novel biopolymer chitosan supported vanadium oxo catalyst, which can be readily prepared in large scale at ambient condition. The Ch-VO catalyzed synthesis of 1,4-dihydropyridines in solvent free condition. After the completion of the reaction, the catalyst could be recovered and reused without affecting the reactivity.

References

[1] a) G.W. Zamponi, S.C. Stotz, R.J. Staples, T.M. Andro, J.K. Nelson, V. Hulubei, A. Blumenfeld, N.R. Natale, J. Med. Chem. 46 (2003) 87; b) S. Visentin, B. Rolando, A. Di Stilo, R. Frutterro, M. Novara, E. Carbone, C. Roussel, N. Vanthuyne, A. Gasco, J. Med. Chem. 47 (2004) 2688; c) A. Zarghi, H. Sadeghi, A. Fassihi, M. Faizi, A. Shafiee, Farmaco. 58 (2003) 1077; d) R. Peri, S. Padmanabhan, A. Rutledge, S. Singh, D.J. Triggle, J.Med. Chem. 43 (2000) 2906.

[2] a) B. R. Vaddula, A. Saha, R. S. Varma, and John Leazer, Eur. J. Org. Chem. 2012, 6707; b) M. Chtchigrovsky, A. Primo, P. Gonzalez, K. Molvinger, M. Robitzer, F. Quignard and F. Taran, Angew. Chem. Int. Ed., 2009, 48, 5916; c) D. J. Macquarrie and A. Bacheva, Green Chem., 2008, 10, 692; d) M. Bradshaw, J. Zou, L. Byrne, K. S. Iyer, S. G. Stewartc and C. L. Raston, Chem. Commun., 2011, 47, 12292; e) B. C. E. Makhubela, A. Jardine and G. S. Smith, Green Chem., 2012, 14, 338; f) D. Kuhbeck, G. Saidulu, K. R. Reddy and D. Dıaz, Green Chem., 2012, 14, 378.

Determination of Glucose by using of Carbon/Iron oxide Magnetic Nanocomposite

Shima Sadravi[a], Fatemeh Honarasa[a,*]

[a] Department of Chemistry, Shiraz Branch, Islamic Azad University, Shiraz, Iran

[*]fhonarasa@gmail.com

Introduction: Diabetes is increasing worldwide at an unprecedented pace and has become a serious health concern during the last two decades. Based on its rapidly increasing incidence, it has been declared a global epidemic by the World Health Organization. There have been continuous advances in the field of glucose monitoring during the last four decades.

Recently, nanostructures were used for colorimetric determination of glucose. In 2007, Gao et al reported the intrinsic peroxidase-like activity of magnetic nanoparticles [1]. In this way, magnetic nanoparticles were used for determination of glucose in presence of glucose oxidase [2].

Experimental: Magnetic iron oxide nanoparticles were synthesized by using partial reduction method in alkali media [3]. Then, carbon was added to the solution of magnetic nanoparticles. For glucose determination, appropriate concentration of glucose and the glucose oxidase solution (50 μL) were mixed and incubated for 1 min. Then UV-Vis spectra of each solution were recorded in the presence of 0.014 mol L^{-1} TMB and 0.27 mg mL^{-1} of nanocomposite.

Result and Discussion: It was shown that Fe_3O_4 magnetic nanoparticles exhibit an intrinsic enzyme mimetic activity similar to that found in natural peroxidases [1]. More importantly, a sensitive and selective method for glucose detection was developed using glucose oxidase (GOx) and the as-prepared Fe_3O_4 magnetic nanoparticles. Glucose detection is a common analysis in the clinic and the laboratory. Generally, glucose oxidase catalyzed the oxidation of glucose to produce gluconic acid and hydrogen peroxide in the presence of oxygen. Subsequently, the formed hydrogen peroxide was catalyzed by nanostructures and then reacted with 3,3',5,5'-tetramethylbenzidine (TMB), resulting in the development of a blue color. Therefore, the color change from the converted TMB was employed to indirectly measure glucose content.

In the present study, carbon/iron oxide magnetic nanocomposite was used for glucose determination. In fact, absorbance of solution containing carbon/iron oxide magnetic nanocomposite, TMB, glucose oxidase and glucose arises with increasing concentration of glucose. In this way, linear range of 5×10^{-8} mol L^{-1} to 5×10^{-3} mol L^{-1} was obtained with correlation coefficient equal to 0.916. Also, limit of detection was obtained as 5×10^{-8} mol L^{-1}, experimentally.

Conclusion:

It was demonstrated that carbon/iron oxide magnetic nanocomposites possess intrinsic peroxidase-like activity for determination of glucose. The catalytic activity of the carbon/iron oxide magnetic nanocomposite was higher than Fe_3O_4 magnetic nanoparticles.

References:

[1] Gao, L.; Zhuang, J.; Nie, L.; Zhang, J.; Zhang, Y.; Gu, N.; Wang, T.; Feng, J.; Yang, D.; Perrett, S.; et al. *Nat. Nanotechnol.* 2007, *2*, 577-583.

[2]. Yu, F., Huang, Y., Cole, A.J. and Yang, V.C., *Biomaterials*, 2009, *30*, 4716-4722.

[3] Zuo, X.; Peng, C.; Huang, Q.; Song, S.; Wang, L.; Li, D.; Fan, C. *Nano Res.* 2009, *2* , 617-623.

A highly efficient and environmentally friendly method for the synthesis of malonamide derivative in the presence of MCM-48/$H_5PW_{10}V_2O_{40}$ catalyst in aqueous media at room temperature

Mirzaagha Babazadeh*, Rahim Hosseinzadeh-Khanmiri

Department of Chemistry, Tabriz Branch, Islamic Azad University, Tabriz, Iran

Email address of the corresponding author. babazadeh@iaut.ac.ir

****

Introduction: Malonamide derivatives are important goals in synthetic chemistry because they display interesting properties in various fields. They have important applications such as effective liquid–liquid extractants [1], poncoments in peptidomimetic substances, excellent ionophores [2], bidentate chelates and monomers in the nylon family [3]. Novel route for the synthesis of malonamide derivatives using isocyanide-based multicomponent reactions in the absence of catalyst in CH_2Cl_2 has been reported [4]. This work reports a highly versatile, eco-friendly and efficient one-pot three-component heterogeneous protocol for the synthesis of malonamide derivative (**1**) in the presence of MCM-48/$H_5PW_{10}V_2O_{40}$ catalyst [5] in water at room temperature.

Methods/Experimentals: A mixture of cyclohexylisocyanide (1 mmol), Meldrum's acid (1 mmol), 2-amino-4-methylphenol (1 mmol) and MCM-48/$H_5PW_{10}V_2O_{40}$ (0.05 g,) was reacted in water (3 ml) as solvent at room temperature for appropriate times. After completion of reaction, as indicated by TLC (ethyl acetate–n-hexane, 1:1), ethanol (3 ml) was added to the reaction mixture which was then heated at 60°C. Catalyst was removed by filtration and the filtrate solution was crystallized to give pure crystalline compound **1** (Scheme 1).
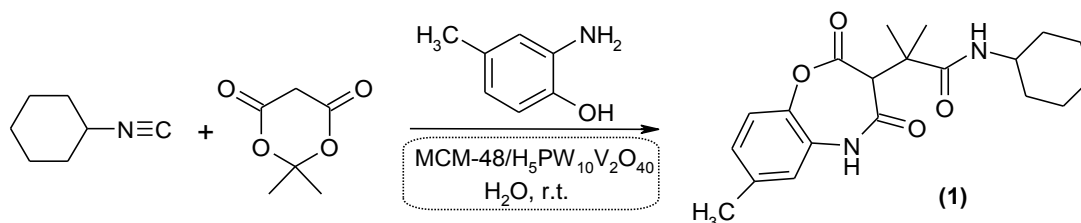
Scheme 1. Synthetic route of malonamide derivative (**1**).

Results and Discussion: The effect of solvent was examined for the reaction mentioned above, and the results indicate that the solvent has an effect on the reaction. Performing the reaction of 2-amino-4-methylphenol with cyclohexylisocyanide and Meldrum's acid in

various protic and aprotic solvents reveals that polar solvents are more efficient than nonpolar solvents, and preferentially water as the reaction solvent (Table 1). According to expectations, the catalytic efficiency should be influenced by the amount of catalyst. Thus, a set of experiments was conducted using various amounts of MCM-48/$H_5PW_{10}V_2O_{40}$. The optimum amount of catalyst was 0.05 g resulting in 86% yield of compound **1**. Lower amounts of catalyst result in a decrease in the efficacy of the reaction, while higher amounts lead to complete conversion in the same reaction time. Recovery/reuse is one of the important properties of catalysts. It is observed that the MCM-48/$H_5PW_{10}V_2O_{40}$ catalytic activity stays almost unaltered even after four recovery/reutilization cycles (Table 2). Therefore, the catalyst was recovered from the reaction by filtration.

Table 1. Influence of solvent on yield of compound **1**.

Entry	Solvent	Time (h)	Yield (%)
1	H_2O	2	86
2	CH_3CH_2OH	2	93
3	CH_3CN	2	89
4	$PhCH_3$	2	38
5	CH_2Cl_2	2	87
6	$CHCl_3$	2	85
7	THF	2	79

Table 2. Reusability of the catalyst for the synthesis of **1**.

Cycle	Time (h)	Yield (%)
0	2	86
1	2	84
2	2	82
3	2	81
4	2	79

Conclusion: Easy workup, low cost, short reaction time, easy recyclability of the catalyst with no loss in its activity and using mild reaction condition are some advantages of the method presented. The experimental procedure for this reaction is remarkably simple and requires no toxic organic solvents or inert atmosphere.

References

[1] C. Musikas, *Inorg. Chim. Acta* **1987**, *140*, 197.
[2] V. Tereshko, E. Navarro, J. Puiggali, J. A. Subirana, *Macromolecules* **1993**, *26*, 7024.
[3] P. B. Ruikar, M. S. Nagar, *Polyhedron* **1995**, *14*, 3125.
[4] A. Shaabani, H. Mofakham, A. Maleki, F. Hajishaabanha, *J. Comb. Chem.* **2010**, *12*, 630.
[5] M. Babazadeh, R. Hosseinzadeh-Khanmiri, S. Zakhireh, *Appl. Organometal. Chem.* **2016**, *30*, 514-518.

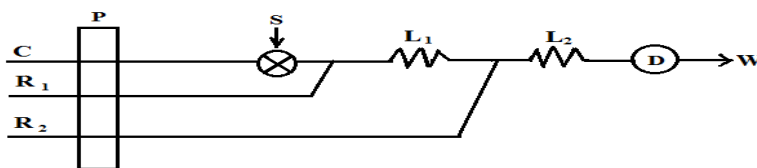# Flow Injection Determination of Hypochlorite by Graphene Quantum Dots

Somayyeh Baghi Sefidan [a], **Habibollah Eskandari** [a,*]

[a]Department of Chemistry, Faculty of Basic Sciences, University of Mohaghegh Ardabili, Ardabil

heskandari@uma.ac.ir

Introduction: Hypochlorite is widely used as a bleaching agent and disinfectant in the fabric, wood pulp, and food industries. It has been extensively used in hygienic chemical studies on tap water, treating skin cancers, disinfectant, in the milk industry, and in the determination of blood urea[1]. Hence, there is a need for a rapid and sensitive method for its determination. The polarographic [2], bromination of fluorescein [3], chemiluminescence [4], and colorimetric [5] methods are the ones most commonly used; colorimetric methods are often preferred, however, as they involve less expensive instrumentation and provide better sensitivity when the appropriate chromogenic reagents are available. In the present investigation, a simple, rapid and sensitive flow injection based spectrophotometric method has been applied for the determination of hypochlorite with a new reagent, graphene quantum dots. The crux of the method is the reaction in that 2,4-dinitrophenyl hydrazine was oxidized to its related arylamine by using hypochlorite in an acidic medium. The amine then was coupled with graphene quantum dots to form a yellow colored azo product.

Methods / Experimentals: The flow system used in this work is given in Scheme 1.

Scheme. 1: Schematic diagram of the flow-injection system used for the determination of hypochlorite.

Notations: C, carrier (H_2O); R_1, 2,4-dinitrophenyl hydrazine (2×10^{-3} mol L^{-1}) in 5×10^{-1} mol L^{-1} HCl; R_2, graphene guantum dots (4-fold diluted); P, peristaltic pump; i. d. of tubes=0.8 mm; S, sample injection unit; length of $L_{1=}$ 10 cm; length of $L_{2=}$ 40 cm; D, detector; wavelength=427 nm; W, waste.

The absorbance was measured with a Cecil model CE 1021 spectrophotometer, equipped with a flow-through cell of 20 µL inner volume and 1.0 cm optical path. A Shimadzu 1650 PC spectrophotometer with 1.0 cm matching quartz cells was used for obtaining the sample spectra. All chemicals used were of analytical reagent grade and distilled water was used for preparation of the solutions.

Results and Discussion: The colorimetric hypochlorite determination method is based on the oxidation of 2,4-dinitrophenyl hydrazine by using hypochlorite in an acidic medium, and then coupling with graphene quantum dots. The product of the azo coupling reaction gives an absorption maximum at 427 nm, as can be seen in Fig. 1
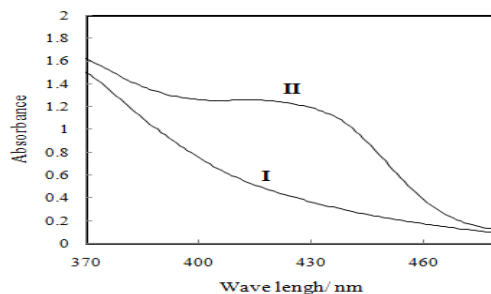
Fig. 1: (I) Absorption spectra of azo dye produced (4 µg mL^{-1} hypochlorite) against water, and (II) blank against water.

All instrumental parameters optimized with one at a time method and under these optimal conditions, the chemical parameters were optimized with central composite design method.
The optimal conditions for the established method were applied and a calibration graph was obtained at 427 nm. One linear range was observed. The calibration equation was Abs =0.0892 × C$_{Hypochlorite}$ -0.0186 (R^2 =0.9995) in the range of 0.27-12.34 µg mL^{-1}.
The selectivity of the method also was evaluated after adding different concentrations of foreign species to the solutions containing hypochlorite as 1.0 µg mL^{-1}. The obtained results showed that the method has appropriate selectivity.
For examining the suitability of the recommended method for hypochlorite determination in real samples, it was applied to various bleach, water and pool water samples. The results of the analysis of the pool water samples are given in Table 1.

Table 1: Determination of hypochlorite in the swimming pools.

Sample	Hypochlorite, µg mL^{-1}	
	Proposed method (n=6)	Standard method (n=6)
Swimming pool 1	0.446±0.014	0.464±0.011
Swimming pool 2	3.28± 0.026	3.17± 0.011

± means standard deviation.

In all cases, the t-test results illustrated that there are not statistical differences between the results of the standard method and the presented method.
Conclusions: The proposed method for the determination of hypochlorite is simple, accurate, rapid, and sensitive. The reagent is outstanding in its sensitivity and selectivity. The proposed method has been successfully applied for the determination of hypochlorite in various samples.
References
[1] Narayana, B.; Mathew, M.; Vipin, K.; Sreekumar, N.V.; Cherian, T. Journal of Analytical Chemistry, 2005, 60, 706–709.
[2] Drozdetskaya, E.P.; Ilin, K.G. Zhurnal Analiticheskoi Khimii, 1972, 27, 200-208.
[3] Zhixiang, H.; Minghui, D.; Guoxi, L.; Xiangyang, W. Applied Mechanics and Materials, 2013, 295, 475-478.
[4] MacDonald, A.; Chain, K.W.; Nieman, T.A. Analitical Chemistry, 1979, 51, 2077-2082.
[5] Saad, B.; Tatt, W.; Sariff, M.; Wan, W.; Saleh, M.; Slater, J. Analytica Chimica Acta, 2005, 537, 197–206.

A New Triazine-Functionalized PN Ligand for Copper-Catalyzed C-N Bond Formation Reaction

Sajjad Rahimi[a], Farhad Panahi[a,b], Mohammadesmaeil Moayyed[a], Nasser Iranpoor[a],*

[a] Department of Chemistry, College of Sciences, Shiraz University, Shiraz 71454, Iran

[b] Department of Polymer Engineering and Color Technology, Amirkabir University of Technology, Tehran, Iran

*Corresponding Author's E-mail: iranpoor@susc.ac.ir

Introduction

There is often an emphasis on the development of ligands that influence efficiency and selectivity in transition metal-catalysis (TMC) [1]. Heteroatomic bidentate ligands have received considerable attention in recent years due to their widespread applications in TMC [2]. More importantly, the heteroatomic bidentate P,N-ligands have revealed their superiority in activity and selectivity over other phosphorous containing ligands [3-5]. In this study, a triazine-functionalized PN ligand was employed in copper-catalyzed amination of aryl halides [6]. The TMC amination of aryl halides is an important tool for the production of aryl amines [7].

Methods / Experimentals

Synthesis of triazine-functionalized PN ligand
Into a canonical flask containing 60 mmol of (n-Pr)$_3$N, 20 mmol of cyanuric acid is added and stir for 1h at 60-80 °C. Then, 20 mmol of PCl$_3$ is added to the reaction and is stirred for 12h. The obtained crude yellow product is washed with water and EtOAc and dried in oven.

General procedure for Cu-catalyzed synthesis of aryl amines
A reaction flask was charged with aryl halide (1.0 mmol), aryl amine (1.2 mmol), CuI (5.0 mol%), NaOtBu (1.5 mmol), ligand (0.05 g) and PEG 200/H$_2$O (2 mL; 1:1) and heated to 100 °C. After completion of the reaction, the organic solution was extracted with EtOAc and was purified by chromatography using EtOAc and n-hexane as eluent.

Results and Discussion

The synthetic ligand was characterized using ^{13}C NMR, ^{31}P NMR, FT-IR, TEM and elemental analysis. There is one carbon at 149.8 ppm in ^{13}C NMR of this compound which is attributed to the carbon of triazine ring. Also, the ^{31}P NMR of this reagent show twopeaks at 1.13 and 1.25 ppm which confirm the presence of two types of phosphor in its structure. A comparison

between the FT-IR of PCl$_3$, cyanuric acid and ligand was accomplished and appearance or disappearances of some peaks demonstrate the reaction between starting materials and formation of triazine-phosphite compound. The TEM images show both the porous and sheet nature of the ligand. The sheets and the cavities are in the range of nanometers. The elemental analysis shows 23.84% of N and 29.56% of C. In order to evaluate the applicability of the PN ligand in TMC it was employed in the Cu-catalyzed cross-coupling of aryl halides and a wide range of amines. The substrates bearing different functional groups were all efficiently coupled under the optimized conditions (scheme 1) to provide the corresponding *N*-arylated products with good to excellent isolated yields. The obtained results represent that this methodology is a general and practical process for the synthesis of diverse *N*-arylamines.
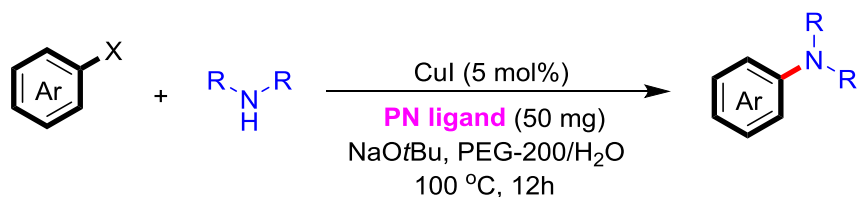
Scheme 1. Optimized conditions for amination of aryl halides using the PN ligand. Reaction conditions: aryl halides (1.0 mmol), amines (1.2 mmol), NaOtBu (1.5 mmol), PEG-200/H$_2$O (2.0 mL; 1:1).

Conclusion

In conclusion, we have introduced a new PN ligand which can be used as a reusable ligand in transition-metal catalyzed organic reactions. This ligand is a porous material possessing a sheet morphology with cavities in the range of the nanometer scale which can act as an efficient ligand in organic reactions. In this study, the synthetic ligand was used in Cu-catalyzed cross-coupling of aryl halides and a wide range of amines.

References

[1] Sipos, G.; Drinkel, E. E.; Dorta, R. *Chem. Soc. Rev.*, **2015**, 44, 3834–3860.
[2] Toma, S.; Csizmadiova, J.; Meciarova, M.; Sebesta, R. *Dalton Trans.*, **2014**, 43, 16557–16579.
[3] Fernandez, E.; Guiry, P. J.; Connole, K. P. T.; Brown, J. M. *J. Org. Chem.*, **2014**, 79, 5391–5400.
[4] Chena, X.; Zhua, H.; Wanga, T.; Lia, C.; Yana, L.; Jiang, M.; Liu, J.; Sund, X.; Jiang, Z.; Ding, Y. *J. Mol. Catal. A: Chem.*, **2016**, 414, 37–46.
[5] Yang, Z.; Yu, B.; Zhang, H.; Zhao, Y.; Chen, Y.; Ma, Z.; Ji, G.; Gao, X.; Han, B.; Liu, Z. *ACS Catal.*, **2016**, 6, 1268–1273.
[6] Ge, S.; Green, R. A.; Hartwig, J. F. *J. Am. Chem. Soc.*, **2014**, 136, 1617–1627.
[7] Ricci, A. Modern Amination Methods, Wiley-VCH, Weinheim, **2000**.

A novel tungsten(VI) complex with N_2O tridentate Schiff base ligand for oxidation of sulfides

Leyla Shariati[a], Hadi Kargar[a]*, Majid Moghadam[b], Nourollah Feizi[a]
[a]Department of Chemistry, Payame Noor University, Tehran 19395-3697, I. R. Iran
[b]Department of Chemistry, University of Isfahan, Isfahan 81746-73441, I. R. Iran
e-mail[*]: **h.kargar@pnu.ac.ir** *and* **Hadi_Kargar@yahoo.com**

Introduction:

Tungsten and molybdenum oxides are potential heterogeneous catalyst in metal-oxide-catalyzed organic oxidation [1]. Current interest in tungsten is due to the consequence of the metal as an essential trace element that participates in a number of main enzymatic reactions [2]. Oxidation of sulfides is the simplest method for the synthesis of sulfoxides and sulfones, both of which are significant as commodity chemicals and, in some cases, as pharmaceuticals. There are a few reports on preparation and catalytic activity of tungsten(VI) complexes in oxidation reactions [3 , 4].

Experimentals:

A tridentate Schiff base ligand derived from isoniazide and its tungsten(VI) complex were synthesized. The prepared ligand and also complex were characterized by FT-IR, ^{1}H NMR and ^{13}C NMR spectroscopic methods. After synthesis and characterization of Schiff base complex, their catalytic activity was investigated as homogeneous catalysts in the oxidation of sulfides (Scheme 1).
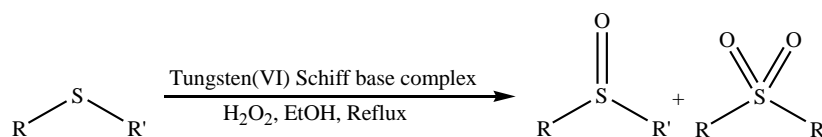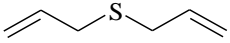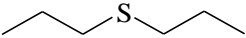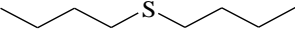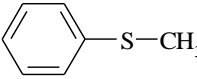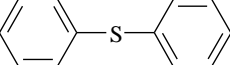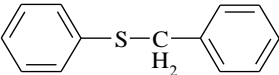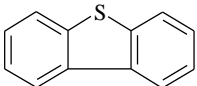

(Scheme 1)

In a 25 mL round-bottom flask equipped with a magnetic stirring bar, a solution of sulfide (1 mmol), catalyst (3 mg, 0.006 mmol) in ethanol (10 mL) was prepared. Then, H_2O_2 (2 mmol) was added to this solution and the reaction mixture was stirred under reflux conditions. The reaction progress was monitored by TLC. After the reaction was completed, the solvent was evaporated and the pure products were obtained by IR spectroscopic.

Results and Discussion:

The reaction conditions were also optimized in the oxidation of sulfides with H_2O_2 in which diphenyl sulfide was used as a model substrate. In the optimization of catalyst amount, the best results were obtained when 0.006 mmol (3 mg) of catalyst was applied with 2 mmol of H_2O_2 after 60 min. In order to choose the reaction media, different solvents were also tested and ethanol was chosen as solvent because of the higher amount of sulfoxide was produced.
This catalytic system is extremely efficient and catalyzes the oxidation of a wide range of sulfides and the sulfoxide and sulfone are produced using catalyst, substrate, and oxidant in a molar ratio of 1:125:250, respectively. The results are summarized in Table 1.

Table 1. Oxidation of various sulfides by H_2O_2 in the presence of tungsten(VI) Schiff base complex in ethanol.

Entry	Sulfide	Time(min)	Conversion	Sulfoxide(%)	Sulfone(%)
1	(diallyl sulfide)	15	100	90	10
2	(dipropyl sulfide)	15	100	90	10
3	(dibutyl sulfide)	30	100	90	10
4	(phenyl methyl sulfide) S—CH$_3$	20	100	50	50
5	(diphenyl sulfide) S	60	100	70	30
6	(benzyl phenyl sulfide) S—CH$_2$	30	100	95	5
7	(dibenzothiophene)	240	100	50	50

Reaction conditions: sulfide (1 mmol), catalyst (0.006 mmol), H_2O_2 (2 mmol), C_2H_5OH (10 mL) at 80 ℃.

Conclusion:

The prepared catalyst was used for oxidation of sulfides with aqueous hydrogen peroxide under reflux conditions. The reaction parameters such as catalyst amount, kind of solvent, oxidant amount and temperature were optimized in the oxidation of diphenyl sulfide. In comparison with the data reported in the oxidation of organic sulfides by various Schiff base complexes, our system shows the following advantages: shorter reaction times, the cheapness, easy availability and non-toxicity of oxidant.

References

[1] Davis, P.; Donald, R. T.; Harvard, N. H. *Catalyst Handbook* (Ed.: M. V. Twig), 2nd ed., Manson Publishing Ltd., London, **1996**.
[2] Maiti. S. K.; Abdul Malik. K. M.; Bhattacharyya. R. *Inorg. Chem. Commun.* **2004,** *7*, 823-828.
[3] Clark. E, Kirk-Othmer *Encyclopedia of Chemical Technology*; 4th ed.; Kroschwitz. J.I, Howe-Grant. M, Eds.; Wiley: New York, **1997**; *23*, pp 134-146.
[4] Bevers. L. E.; Hagedoorn. P. L.; Hagen. W. R. *Coord. Chem. Rev.* **2009,** *253*, 269-290.

Annulation of Internal Alkynes *via* Pd(OAc)$_2$-Catalyzed Heck Reaction for Synthesis of Pyrrolo[2,3-b]quinoxalines

Tayebeh Besharati-seidani[a], Ali Keivanloo[a]*, Babak Kaboudin[b]

[a]School of Chemistry, Shahrood University of Technology, Shahrood, 36199-95161, Iran Fax: +98-233-2395441 E-mail addresses: keivanloo@shahroodut.ac.ir & t.besharati@yahoo.com

[b]Department of Chemistry, Institute for Advanced Studies in Basic Sciences, Gava Zang, Zanjan 45137-66731, Iran, Fax: +98-241-4214949, E-mail: kaboudin@iasbs.ac.ir

Introduction:

Palladium-catalyzed Mizoroki–Heck cross-coupling reactions are extremely powerful tools for the C–C bond formations. Therefore, these reactions are widely used in the synthesis of biologically active natural products, pharmaceuticals, and fine chemicals [1]. Quinoxalines are of interest due to the fact that some natural products bear the quinoxaline unit and exhibit high biological properties such as anti-microbial, anti-inflammatory and anti-cancer activities [2-4]. Therefore, the systematic study of their reactions leading to fused quinoxaline ring systems is important. Herein we wish to report the results obtained by our team on the unprecedented synthesis of pyrrolo[2,3-b]quinoxalines.

Method/Experimental:

In this research work, 3-chloroquinoxalin-2-amines and internal alkynes were used as the starting materials. 3-chloroquinoxalin-2-amines were synthesized from 2,3-dichloroquinoxaline and primary alkyl amines according to the litterateur, and internal alkynes were prepared by the Sonogashira coupling reaction of aryl iodides and phenyl acetylene.

Results and discussion:

Herein we present an efficient strategy for the synthesis of some new pyrrolo[2,3-b]quinoxalines from 3-chloroquinoxalin-2-amines and internal alkynes thorough the palladuim-catalyzed Heck reaction. The model reaction was initially conducted in DMF at 100 °C under an N$_2$ atmosphere using 5 mol% of Pd(OAc)$_2$, as the catalyst, 10 mol% of PPh$_3$, as the ligand, and K$_2$CO$_3$, as the base, which yielded the desired product in 74% yield. All products were characterized \using IR, ^{1}H NMR, ^{13}C NMR, and mass spectroscopy. A number of synthesized compounds were screened for their in vitro anti-bacterial activity against microorganisms such as Escherichia coli (a Gram negative bacterium) and Bacillus subtilis (a Gram positive bacterium).
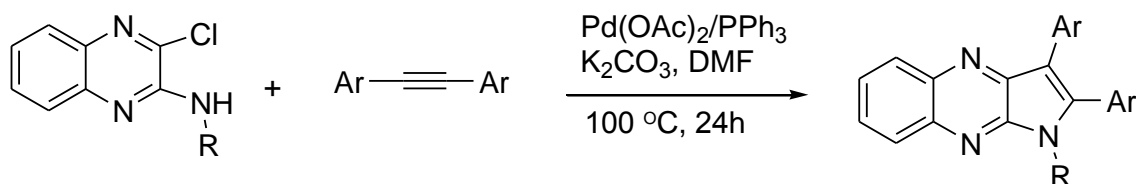
Conclusion:

We developed a one-pot annulation strategy of internal alkynes with 3-chloroquinoxalin-2-amines for the synthesis of various pyrrolo[2,3-b]quinoxaline derivatives in good-to-high yields.

References

[1] M. Waheed; N. Ahmed. *Tetrahedron Letters* **2016**, 57, 3785–3789

[2] A.Y. Ponomareva; D.G. Beresnev; N.A. Itsikson; O.N. Chupakhin; G.L. Rusinov; *Mendeleev Communications*, **2006**, 16, 16-18.

[3] D. Hadjipavlou-Litina; E. Pontiki; R. Villar; E. Vicente; B. Solano; S. Ancizu; S. Pe´rez-Silanes; I. Aldanaa; A. Monge. *Bioorganic & Medicinal Chemistry Letters*, **2007**, 17, 6439-6443.

[4] M. Waly; S. Elgogary; A. Lashien; A. Farag. *Journal of Heterocyclic Chemistry*, **2015**, 52, 411-417.

Investigation of Solvent-Solvent Miscibility in the Binary Mixtures Composed by Methanol and a Set of Different Polar and Non-polar Solvents

Roya Eftekhar i[a] , Saeed Yousefinejad [b,*]

[a]*Department of Chemistry, Shiraz Branch, Islamic Azad University, Shiraz, Iran*
[b] *Department of Occupational Health Engineering, School of Health, Shiraz University of Medical Sciences, Shiraz, Iran*
[*] Corresponding author (Email: yousefinejad.s@gmail.com; yousefisa@sums.ac.ir)

Introduction: Methanol is the simplest alcohol with a lot of applications in chemistry and analytical chemistry. On the other hand, solubility and miscibility of an alcohol like methanol is a key feature in many fields and related disciplines to chemistry and industry. As important examples, mixture of methanol with various solvents can be used in a wide range of applications such as separation, extraction, chromatography and chemical reactions [1]. Because of the importance of methanol's solubility/miscibility, in this work, focus was on the solubility of this methanol as in different solvents using a QSPR model [2,3] based theoretical and structural descriptors of solvents.

Method/experimental: In order to build QSPR model, gas-solvent partition coefficient of methanol in 41 organic solvent were used. Data set was divided into 2 set of training (about 80% of data) and test set (about 20% of data). Stepwise MLR and MLR were applied as variable selection and regression model respectively. Dragon software was utilized to calculate the structural descriptors and other statistical calculations and modeling were done in MATLAB.

Result and discussion: To select the optimum model based on stepwise multiple linear regression (SMLR), 8 linear models (contained 1 to 8 descriptors) were built. Then, to prevent overfitting and select the optimum model, the variation of squared correlation coefficient of the training set (R^2_{train}) and the squared correlation coefficient of cross-validation (Q^2_{LOO}) were followed [6]. Finally, the following four-parametric model was obtained:

$$\log L = 4.417\ (\pm 0.259) + 0.610(\pm 0.053)\text{BLTF96} + 0.143(\pm 0.022)\text{RDF050m} -$$
$$0.229(\pm 0.090)\text{MATS3p} - 1.258(\pm 0.507)\text{E1V} \qquad (1)$$

In this model, BLTF96 is the Verhaar Fish base-line toxicity from MLOGP, RDF050m is Radial Distribution Function - 050 / weighted by mass, , MATS3p is Moran autocorrelation of lag 3

weighted by polarizability and E1v is 1st component accessibility directional WHI0M index / weighted by van der Waals volume. Stability of model was evaluated using leave two-out and leave four-out cross-validation. Q^2_{L2O} and Q^2_{L4O} were calculated equal to 0.89 that indicate acceptable stability. Also, check of prediction ability with 9 solvents as external test set and values of R^2_{test} and $RMSE_{test}$ were 0.91 and 0.31 respectively which indicated good prediction proposed model. The results of evaluation with y-scrambling test or pemutation test(Q^2_{mp}=0.28) confirmed the absence of chance correlation.

Table 1 Various statistics of the developed four-parameteric QSPR model

R^2_{train} [a]	$RMSE_{train}$ [b]	Q^2_{LOO} [c]	Q^2_{L4O} [d]	$RMSE_{cv}$ [e]	R^2_{test} [f]	$RMSE_{test}$ [g]	Q^2_{mp} [h]
0.93	0.26	0.90	0.89	0.32	0.91	0.33	0.28

[a] Training correlation coefficient, [b] Train Root-mean-square-error, [c] correlation coefficient of leave-one-out cross-validation,[d] correlation coefficient of leave-four-out cross-validation,[e] Root-mean-square-error of cross-validation, [f] Test correlation coefficient, [g] Test Root-mean-square-error,[h] maximum cross-validation correlation coefficient for 30 Y-randomization test

Conclusion: in this work, a QSPR model was suggested that related structure features of solvents to their ability to dissolve methanol. This model had suitable statistical parameters in the training set, and good prediction ability based on the results of cross validation and external test set. Results revealed that solvents with higher molecular mass, lower polarazibality and lower van der Waals volume are better options for solubility of solvents. This kind of QSPR studies can be a way to obtain information about binary mixture of solvents and solvent-solvent interactions.

References

[1] Reichardt, C., Thomas W. Solvents and solvent effects in organic chemistry. John Wiley & Sons, 2011.

[2] Yousefinejad, S., & Hemmateenejad, B.. *Chemometrics and Intelligent Laboratory Systems*, **2015**. *149*, 177-204.

[3] Honarasa, F., Yousefinejad, S., Nasr, S., & Nekoeina, M. , *Journal of Molecular Liquids*, **2015**, *212*, 52-57.

In the name of Allah

Subject: Hydrogel synthesis of nano-bio-based Arabic gum and silica-coated magnetic nanoparticles of Fe-Ni bimetallic

Writing: Mahnazsadat ghezi   Master of Organic Chemistry

Abstract

can be used to achieve this goal, the synthesis was conducted multistage magnetic nanoparticles to the surface of the nanoparticles with silica sol-gel was then coated nanoparticles were deposited on the surfaces of vinyl groups. To be ready to connect to gum Arabic. Gum Arabic is also carried out reforms on bio-polymer and hydroxyl groups with groups that have replaced the vinyl monomer and initiator Khdrhzvr eventually was Vaknshytrtyb and cross-linker suitable, gum Arabic magnetic nanoparticles attached to any intrusion a synthesis steps, the product was identified by infrared spectrum analysis. The morphology of magnetic nanoparticles and the final product was evaluated Tvstmykrvskvp scanning electron field emission SEM.

١. Introduction

١- Gum Arabic and its chemical structure

Persian "Azdvtazy" and in French and in English Gomme arabiqu and Gomme Senegal Gum Arabic is called. and the central layer of wood unharmed, is obtained. In the early autumn after the rainy season and the branches and trunk of the gum of acacia trees are used. Usually at this season in Senegal called the Harmattan wind blows from the East is that the more powerful gum bleeding and the output current is more than [٣].

٢-stage synthesis

٢-١ Preparing magnetic nano-hydrogels Ni Fe٢o٤ @ SiO٢ @VTMOS

not in the acidic environment of the nanoparticles protects against acid wash. The silica coating the nanoparticles Yi improve and modify their surface by substances like silica eligible groups such as the VTMOS possible. The next step polymerization of vinyl that can provide end-to-cover silica nanoparticles connected by VTMOS be enhanced.

Figure ٢. Preparation of magnetic nano-hydrogels
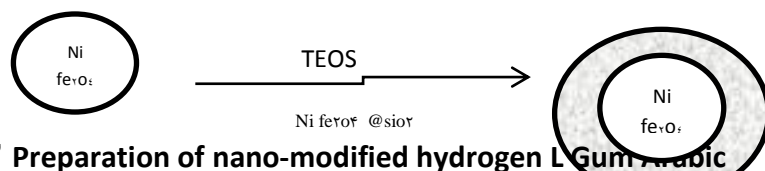
٢.٢ Preparation of nano-modified hydrogen L Gum Arabic

There are numerous hydroxyl groups Drsakhtarplymrzysty Arabic gu with these groups makes the vinyl groups on the polymer structure

picture of this process are shown in Figure ٤-٥ is the group of vinyl to create connection gum Arabic to crosslink the nanoparticle and provide at Bdysntz
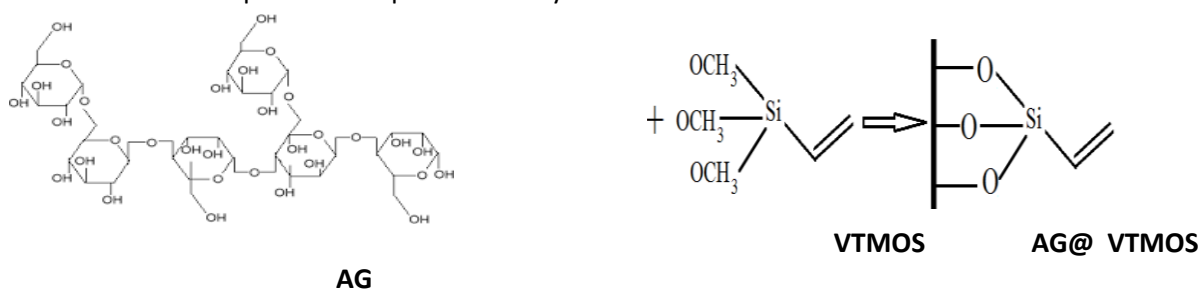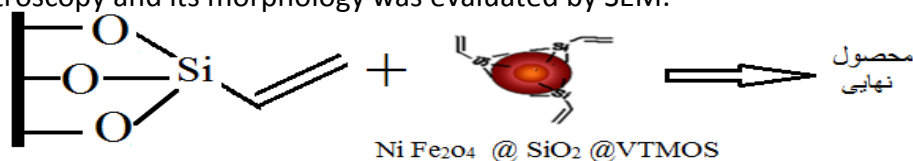

AG

VTMOS   **AG@ VTMOS**

Figure ٣. Schematic synthesis of gum Arabic and vTMOS

٣.٢ Preparation of the final product

OH and hydrogen was used connections (Figure ۴-۸). The compound was identified by FT-IR spectroscopy and its morphology was evaluated by SEM.

AG@VTMOS

$Ni Fe_2O_4$ @ SiO_2 @VTMOS

Figure ٤ - Schematic synthesis AG@VTMOS@ SiO_2@ $NiFe_2O_4$

٣ -identification

Tyf Magnetic nanoparticles prepared Ni Fe_2o_4 @ SiO_2 @VTMOS and gum Arabic VTMOS @ AG

Figure ٥. FT-IR spectra of the nanoparticles Ni Fe_2o_4 @ SiO_2 @VTMOS shows this spectrum peaks at ٥٨٠ cm-١ indicator Fe-O and Si-O-Si peak at ١٠٩٠ cm-١ is observed Shvdlavh the other indices broad range of ٢٩٠٠ to ٣٦٠٠ show that in about ٢٨٠٠ the peak of the CH stretching carbon delighted at the ١٠٠٠ peak of groups OC gum Arabic can be seen in the area of the fingerprint and the whole number ٢ in the range of ٩١٠ to ٩٩٠ peak we see about vinyl link with gum Arabic peak OC groups are together and the whole No. ٢ on the ١٦٠٠ peak of stretching is vinyl.

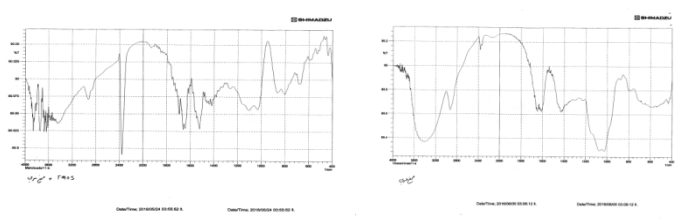Figure ٦ infrared spectrum Gum Arabic

Figure ٥-infrared spectrum $CoFe_2O_4$ @ SiO_2 @ VTMOS

٢-٣ morphology observation (morphology)

Field emission SEM images below has been prepared by scanning electron microscopy. Shkl٧-SEM image showing $NiFe_2o_4$ Dhd.hmantvr nanoparticles can be seen from most of the particles have a spherical shape and most of them have sizes below ١٠٠ nm.
SEM images of nano-bio-Shkl٨ hydrogel $NiFe_2o_4$ @ SiO_2 @ VTMOS @ AG shows can be seen as images indicate that the lump was not trying to be well prepared SEM imaging. However, the hydrogel tissue is visible.
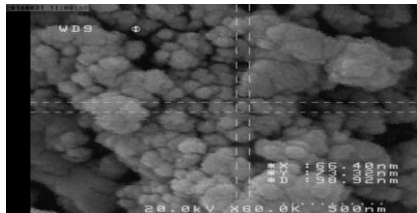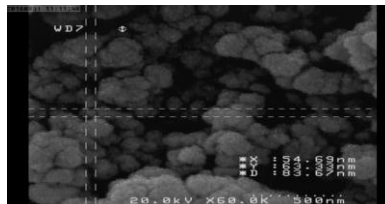
Figure ٧. SEM images of nanoparticles of $CoFe_2$ Figure ٨. SEM close-up of $CoFe_2o_4$ @ SiO_2 @ VTMOS @ AG

Green and low cost preparation of nitrogen-doped carbon dots from date kernel for label-free and sensitive assay of Zoledronic acid drug based on switching "Off - On" methodology

Niloufar Amin[a], Abbas Afkhami[a,*], Tayyebeh Madrakian[a]
[a] Faculty of Chemistry, Bu-Ali Sina University, Hamedan, Iran
afkhami @ basu.ac.ir

Introduction

Zoledronic acid, a nitrogen containing bisphosphonate compound, is an inhibitor of osteoclastic bone resorption and is clinically used for the treatment of tumor induced hypercalcemia, bone metastases arising from any cancer, and for the prevention of bone metastases associated with advanced breast cancer and prostate cancer [1-2]. Hence, quantification of Zoledronic acid in biological samples is critical to provide a daily quality control analysis.
This paper reports, for the first time, a one-step and facile preparation of the nitrogen-doped carbon quantum dots (N-CDs) from date kernel by the hydrothermal method. The synthesized N-CDs were used as a label- free platform for the determination of Zoledronic acid.

Experimental

CNDs were synthesized from kernel date. A certain amount of Fe (III) solution was added to the CDs. This caused quenching of the fluorescence of CDs. Addition of Zoledronic acid to the mixture caused restoring of the fluorescence of the system. The increased fluorescence intensity was linearly proportional with Zoledronic acid concentration in a given range.

Results and discussion

The obtained N-CDs were fully characterized by high-resolution transmission electron microscopy, X-ray diffraction spectrometry, Fourier transform infrared spectrometry, X-ray photoelectron spectroscopy, Raman spectroscopy, UV-vis absorption and photoluminescence (PL) spectroscopy. These characterizations were consistent with the previous reports [3].
The influence of pH, dosage of N-CDs and incubation time was investigated and the optimum conditions were established.
Due to the synergistic impression of the static quenching mechanism arising from the formation of a stable non-fluorescent complex between CD and Fe^{3+} [4] and inner filter effect, upon addition of ferric ions, fluorescence intensity of the N-CDs solution was gradually decreased (state Off). The CD/Fe^{3+} complex were used for the detection of Zoledronic acid by restored fluorescence intensity (state On). This phenomenon takes place due to high affinity of ferric ions to multiphosphates ligands such as Zolderonic acid. [5]

Detection limit of 40 nM for Zoledronic acid was obtained with a wide linear range of 0.1-10 μM.

The selectivity of the proposed detection method for the determination of Zoledronic acid was investigated by examining the effect of different chemical species on the analytical signal. The method was applied to the determination of Zoledronic acid in blood plasma with satisfactory results.

Conclusion

A facile method has been established to fabricate a high quantum yield (12.5%) N- CDs by a hydrothermal method. The synthesis process is very cheap and the starting material is green. These CDs were employed as a nanoprobe for the detection of Zolderonic acid by a simple off-on fluorescent method with fast response, high sensitivity and selectivity. The method was also applied to the determination of trace quantities of Fe^{3+} ions with satisfactory results.

References

[1] H. Fleisch. *Orthopade,* **2007,** *36*, 103-107.
[2] F. Legay; S. Gauron; F. Deckert. *J. Pharm. Biomed. Anal*, *2002*, *30*, 897–911.
[3] J. Liao; Z. Cheng; L. Zhou. *ACS Sustainable Chem .Eng,* **2016**, *4,* 3053–3061.
[4] H.M.R. Goncalves; A.J.Duarte; S.da. *Biosens. Bioelectron*, **2010**, *26*, 1302–1306.
[5] J.Simmons. *Water Air Soil Pollut*. **2010**, *209*, 123–132.

.

Synthesis and application of a nanocomposite contained graphene nanoribbons modified by Fe-Pt nanoparticle as a modifier with high performance for determination of ampyra drug

Pegah Hashemi[a], Abbas Afkhami[a,*], Hasan Bagheri[b], Tayyebeh Madrakian[a]

[a] Faculty of Chemistry, Bu-Ali Sina University, Hamedan, Iran

[b] Chemical Injuries Research Center, Baqiyatallah University of Medical Sciences, Tehran, Iran

afkhami@basu.ac.ir

Introduction:

Ampyra (Am) is a potassium channel blocker used in the treatment of patients with spinal cord injury (SCI) or multiple sclerosis (MS). There is evidence that Am is a drug with therapeutic value in enhancing neurological function and neurotransmission in preserved axons. It has been approved by U.S. Food and Drug Administration (FDA) for the treatment of MS on, 2010 [1]. It has been suggested that the concentration of Am in biological fluids should be monitored in clinical trials involving the use of Am because of its high toxicity [2].

Experimentals:

This work has presented a novel strategy to carry out indirect and sensitive determination of ampyra in complex matrices based on the interaction of Am with UA. For this propose Graphene oxide nanoribbon (GONR) was synthesized according to the method reported by Wei-Hung Chiang and coworkers [3]. Then FePt nanoparticles was synthesized at the GONRs. FePtGNR nanocomposites was obtained and added to uric acid (UA) solution. Obtained UA@FePtGNR nanocomposite was dropped on the screen printed carbon electrode and related DPV signal was recorded.

Results and Discussion:

Structure of synthesized nanocomposite was characterized by different techniques including Fourier transform infrared (FT-IR), X-ray powder diffraction (XRD), Transmission electron microscopy (TEM). Obtained experimental results indicated that in present of Am, oxidation peak current of uric acid was decreased. Therefor variation in oxidation current (ΔI) that arises from Am, can be applied as indicating signal for the indirect electrochemical determination of ampyra. Analytical performance of the sensor was investigation by determination of different concentration of ampyra by using differential pulse voltammetry (DPV) method under optimized condition. The relationship between ΔI and Am concentration was linear in the range 0.08 to 9 µM (see fig. 1). The limit of detection for the proposed sensor was estimated as 0.0279 µM ($3\delta_{blank}/m$).
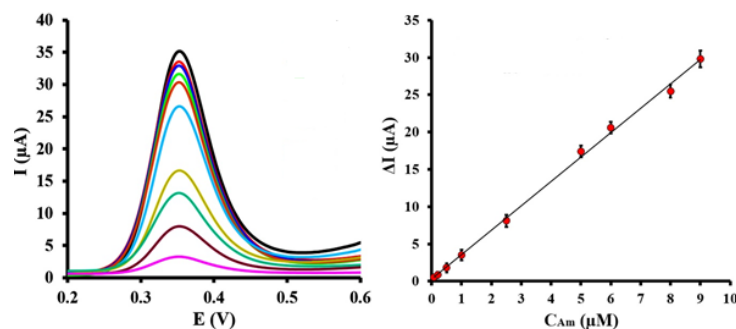
Fig. 1. DPVs for different concentrations of Am under optimum conditions and the related calibration curve.

Conclusion:

Ampyra determination by conventional electrochemical methods is not possible, because of its high redox potential. Therefore we reported a simple and inexpensive sensor for indirect determination of ampyra based on strong electrochemical methods. The fabricated sensor showed good response towards ampyra. Obtained satisfied recovery for the determination of ampyra in biological fluids and pharmaceutical samples may hold promise for fast, simple and sensitive detection of ampyra in various real samples.

References

[1] Kari V. Ahonen; Manu K. Lahtinen; Arto M. Valkonen; Martin Draˇcínsk´y; Erkki T. Kolehmainen. *Steroids*, **2011**, *76*, 261-268.

[2] Ram N. Gupta; Robert R. Hansebout b. *Journal of Chromatography B*, **1996**, *677*, 183-189.

[3] C. Wang; Y.-S. Li; J. Jiang; W.-H. Chiang. *ACS applied materials & interfaces*, **2015**, *7*, 17441-17449.

Ultra-preconcentration of benzoic acid and sorbic acid in beverage samples by magnetic-3D-Graphene based solid phase extraction followed by dispersive liquid-liquid microextraction & GC-MS

Afshin Rahimi [a,*], Mohammad Dehsaraei [a], Sadjad Bakhtiari [a]

[a] Afshin Rahimi Research Laboratory (Pardis St., Sanaat 1 Blv., 1St intrance, Rasht Industrial City, Guilan, Iran)

Email: Afshinrahimi89@yahoo.com

Introduction

Preservatives with antimicrobial properties are permitted as additives in various food products[1]. Benzoic acid inhibits bacterial development. Sorbic acid is an antifungal preservative against molds and yeasts[2]. However, the excessive use of preservatives could be harmful to human health and cause some diseases such as metabolic acidosis, convulsions, hyperpnoea and allergic reactions[3]. Therefore, developing an appropriate analytical method for the determination of benzoic and sorbic acids in wide range of concentration with acceptable accuracy is essential. The aim of this work is the coupling of MSPE and DLLME techniques for efficient pretreatment of benzoic and sorbic acids in beverage samples.

MSPE-DLLME/GC-MS procedure

At MSPE step, 50 mL of the sample solution (20 ngmL^{-1} of analytes, pH= 4) and 4% (w/v) salt was placed in a beaker. Then, 30 mg of adsorbent was added and sonicated for 2 min at room temperature. Adsorbent was isolated by using a magnet and 1 mL of elution solvent was added to it. After elution, 25 µL of extraction solvent was added for DLLME procedure. A 0.5 µL of DLLME sedimented phase was injected to GC-MS.

Results and Discussion

The prepared adsorbent (3D-G-Fe$_3$O$_4$) was characterized by FT-IR, SEM, VSM, XRD, Raman spectroscopy, BET, BJH and TEM methods (Fig.1). The effect of different parameters that affected the procedure, were carefully investigated and optimized for 50 mL of sample solution containing 20 ng mL^{-1} of each analytes. The main dtermination parameters such as amount of nanoparticles, pH, salt concentration, the type of extraction solvent in DLLME, the volume of elution solvent (disperser solvent) and extraction solvent volume were studied and optimized. Under the optimized experimental conditions, the figure of merit results showed excellent linear dynamic range (0.05-5000 ng mL^{-1}), with determination coefficients (R^2) higher than 0.994 and limits of detection (LOD) of 0.02 ng mL^{-1} (S/N=3). Intra- and inter-day relative standard deviations (RSDs) were less than 4.8 and 5.9 %, respectively (n=5). The method was successfully applied for determination of benzoic acid and sorbic acid in beverage samples and satisfactory results were obtained (RSDs < 5.4, n=5).
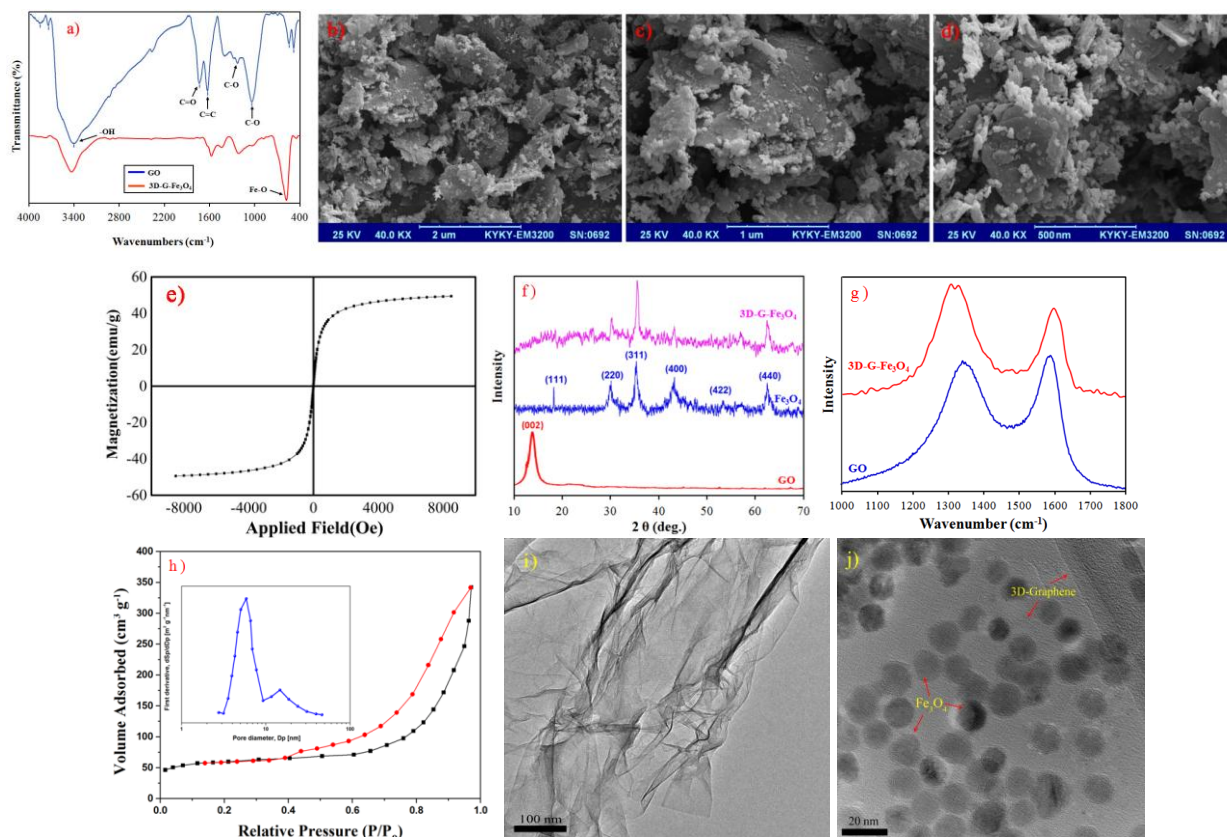
Fig.1. Characterization of 3D-G-Fe$_3$O$_4$: (a) FT-IR spectrum (b-d) low, middle and high-magnified SEM images, (e) VSM magnetization curve, (f) XRD patterns, (g) the Raman spectrums, (h) BET and BJH (i and j) TEM images.

Conclusion

A hyphenated method (MSPE-DLLME) coupled with GC-MS was used for determination of benzoic and sorbic acids in beverage samples. The 3D-G-Fe$_3$O$_4$ successfully synthesized and characterized. In order to achieve high extraction efficiency, effect of different parameters that may affect the extraction recovery was evaluated by one-variable-at-a-time approach. Results indicated the proposed method is an efficient, facile, environment-friendly, low-cost and sensitive sample preparation technique to determination of analytes in complex matrices.

References

[1] C.M. Lino, A. Pena. Food Chemistry, **2010**, 121(2), 503-508.
[2] C. Dong, W. Wang. Analytica chimica acta, **2006**, 562(1), 23-29.
[3] Y. Wen, Y. Wang, Y.Q. Feng. Analytical and bioanalytical chemistry, **2007**, 388(8), 1779-1787.

Isolation and Structure Elucidation of Two Secondary Metabolites from *Salvia lachnocalyx* Hedge.

Foroogh Mirzania[a,*], **Yaghoub Sarrafi**[a], **Mahdi Moridi Farimani**[b]

[a] *Department of Organic Chemistry, Faculty of Chemistry, University of Mazandaran, Babolsar, Iran*
Email: forooghmirzania@gmail.com
[b] *Department of Phytochemistry, Medicinal Plants and Drugs Research Institute, Shahid Beheshti University, G. C., Evin, Tehran, Iran.*

Introduction: *Salvia* is one of the most important genera of the Family Lamiaceae includes nearly 1000 species spread throughout the world. Several species of *Salvia* are used in folk medicine as antiseptics, astringents and spasmolytic. Many studies showed antimicrobial and antiviral activities of some *Salvia* species. Also many *Salvia* species and their isolated constituents possess significant antioxidant activities in enzyme-dependent and enzyme-independent systems [1]. The phytochemical analysis of *Salvia* species show the presence of many compounds belonging mainly to the group of phenolic acids, phenolic glycosides, flavonoids, anthocyanins, coumarins, polysaccharides, sterols, terpenoids and essential oils. *S. lachnocalyx* Hedge., a member of this genus, is an endemic and perennial species that grows only in too narrow region near Eghlid in Fars province. As a part of ongoing research program aimed at the isolation, structural elucidation and pharmacological evaluation of bioactive secondary metabolites from plants, we started the phytochemical analysis of *Salvia lachnocalyx* Hedge.

Experimental: The aerial parts of *Salvia lachnocalyx* Hedge. were collected from Eghlid in the Fars Province, Iran, in May 2014 and identified by Dr. A. Sonboli. The air-dried, powdered aerial parts of *S. lachnocalyx* Hedge. (5.5 kg) were extracted with chloroform by maceration at room temperature. The chloroform extract was fractionated on a silica gel column (700 g, 70-230 mesh) and eluted with n-hexane followed by a gradient of EtOAc up to 100% and then MeOH (up to 30%). Each fraction was collected at the volume of 250 mL and 168 fractions were collected totally.

Results and Discussion: Our studies led to the isolation of two secondary metabolites (**1**, **2**), together with several compounds, whose structures were secured by 1D and 2D-NMR spectroscopic studies, in particular homo-COSY and hetero-(HMQC and HMBC). Extraction of the aerial parts of *Salvia lachnocalyx* Hedge. followed by column chromatography, yielded from fraction 44, a white powder as a main constituent. The spectral data, in particular extensive homo-(COSY, NOESY) and hetero-(HMQC, HMBC) 2D NMR experiments led to the assignment of the triterpenoid **1** for this compound. This substance was isolated several years ago from *Salvia officinalis*, as a main constituent together with its corresponding compound, ursolic acid [2]. The comparison of the physical data of **1** showed the identity of the numerical values reported in reference [3] and confirmed the proposed formula. However, due to the use of more sophisticated NMR techniques which enabled the unambiguous allocation of all the protons and carbons of compound **1**, several assignments have to be revised. Also, compound **2** was isolated as yellow pure crystal. This substance extracted and purified from fractions 94 was identified on the basis of their ^{1}H-NMR spectral data and by comparing ^{1}H-NMR spectral data of this secondary metabolite with those given in literature [4].

1   2
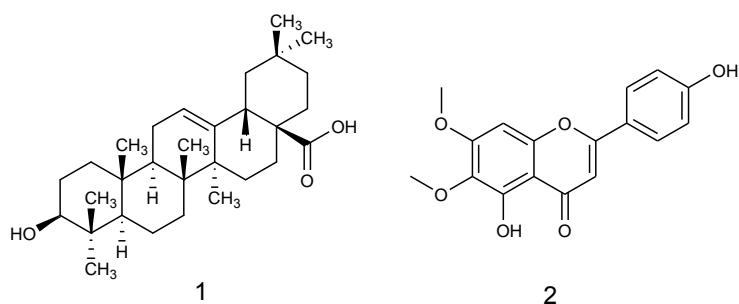
Conclusion: Traditional knowledge of Iranian peoples about medicinal plants is based on oral tradition passed through several generations and most of this information survives only in the memory of the elderly people and is now in danger of vanishing. Also, the numbers of medicinal plants that have been investigated are very few. This research illustrates the necessity of phytochemical investigations in endemic species of Iran.

References

[1] Zupkó; István;Judit Hohmann; Dóra Rédei; György Falkay; Gábor Janicsák; Imre Máthé. *Planta Medica,* **2001**, *67*, 366-368.
[2] Horiuchi; Kumiko; Sumiko Shiota; Tsutomu Hatano; Takashi Yoshida; Teruo Kuroda; Tomofusa Tsuchiya. *Biological and Pharmaceutical Bulletin*, **2007**, *30,* 1147-1149.
[3] Seebacher; Werner; Nebojsa Simic; Robert Weis; Robert Saf; Olaf Kunert. *Magnetic Resonance in Chemistry*, **2003**, *41*, 636-638.
[4] Feryal Benayache; Ahcene Boureghda; Souad Ameddah; Eric Marchioni; Fadila Benayache; Samir Benayache; *Der Pharmacia Lettre*, **2014**, *6* ,50-54.

Electrocatalytic Oxidation of Formaldehyde using green synthesized Copper oxide nanoparticles

S. Momeni[a]

[a] *Persian Gulf Marine Biotechnology Research Center, The Persian Gulf Biomedical Sciences Research Institute, Bushehr University of Medical Sciences, Bushehr 75147 Iran.*

Email address: Safieh.momeni@gmail.com

Introduction: The electrochemical oxidation of small organic molecules such as methanol, ethanol, formic acid and formaldehyde has been intensively investigated for the development of direct fuel cells due to their low toxicity, facility of storage and handling and mainly their high energy density [1]. Formaldehyde was identified as one of the main products of methanol electrooxidation. Noble metals such as Pt and Pd are initially good catalysts for the electrooxidation of formaldehyde [2]. In fuel cells, Pt catalysts are readily poisoned by CO during oxidation of fuel. In addition, the high cost of Pt and supply constraints limit its application in these types of fuel cells. Copper (II) oxide (CuO), as a cheap catalyst, has gained increasing attention with its electrochemical activity toward many compounds in alkaline or neutral medium. CuO is a promising p-type semiconductor suitable for variety of applications such as room temperature gas sensors, photocatalysts, waste water treatments and charge storage devices. It is still a challenge to develop a simple, rapid, eco-friendly, easy to control and energy-efficient method for a large scale preparation of CuO nanostructures with a designable morphology [3].

Methods/ Experimental: For synthesis of CuO nanoparticles, $CuSO_4$ and GA were added to 20 ml deionized water separately and pH of solution was reached to 8 and then stirred vigorously for 15h. The product was then washed with water and ethanol several times. The synthesized samples were characterized by different characterizations tools. A nanoscale CuO/Carbon ionic liquid electrode (CuO/CILE) was prepared by hand-mixing weighed amounts of graphite powder, ionic liquid (OPyPF6), and CuO nanoparticle (50%:45%: 5%, wt%), respectively.

Results and Discussion: Herein, we report a simple and a green chemical route to synthesize spherical CuO nanoparticles using gum Arabic (GA) and CuSO4 as the raw materials. The prepared CuO nanoparticles was used for the sensitive and selective electrochemical detection of formaldehyde in alkaline media. The morphology characterization of the as-prepared CuO was performed by FESEM (Fig. 1A), and it can be seen that the products are spherical

nanostructures. The size of the as-prepared CuO nanoparticles is about 70 nm. The powder XRD pattern (Fig. 1B) of the as-prepared products shows the typical diffraction pattern of CuO
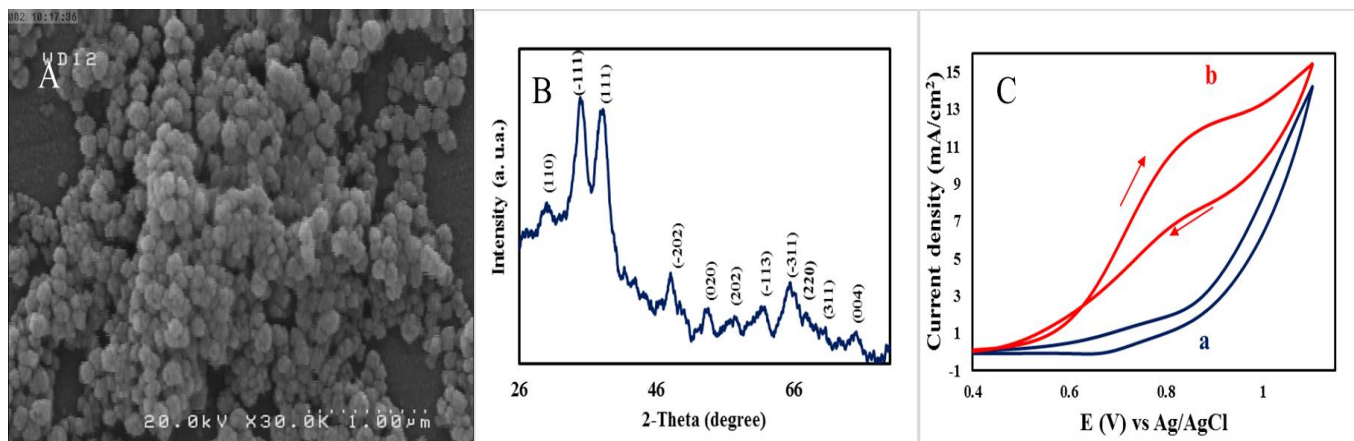
(JCPDS: no. 48-1548).

Fig.1 (A) FESEM image and (B) XRD pattern of synthesized CuO nanostructures and (C) Cyclic voltammograms of CuO/CILE in 0.1 M NaOH in the absence(a) and presence (b) of 0.05 M formaldehyde(scan rate: 50 mVs-1)

The electrocatalytic activity of the as-prepared nanoparticles for the oxidation of formaldehyde was studied using cyclic voltammetry. The as-synthesized CuO/CILE catalysts were characterized by cyclic voltammetry in an electrolyte of 0.1 M NaOH and 10 mM formaldehyde, and the resulting voltammograms are shown in Figure 1C. In the forward scan, formaldehyde oxidation produced a prominent anodic peak around 0.8 V and the anodic peak in the reverse scan was approximately absent.

Conclusion: In this report, we describe green and one-step wet chemical technique to produce large-scale CuO nanoparticles. CuO showed a good electrocatalytic activity for formaldehyde oxidation on the surface of CuO/CILE.

References

[1] H. Nonaka, Y. Matsumura, *J. Electroanal. Chem.* **2002**, *520*, 101-110.

[2] Z. Wang, Z-Z. Zhu, J. Shi, H-L. Li, *Appl. Surf. Sci.* **2007**, *253*, 8811-8817.

[3] X. Zhang, S. Sun, J. L. L. Tang, C. Kong, X. Song, Z. Yang, *J. Mater. Chem. A*, **2014**, *2*, 10073–10080.

Preparation and characterization of Fe_3O_4/SiO_2/ APTES/DTPA core-shell nanoparticles

Elham sattarzadehkhameneh[a], **Saeed Kakaei**[a], **Mostafa M. Amini**[b], **Ali Khanchi**[a]

[a]*NSTRI, Nuclear Fuel Cycle Research Institute, P.O. Box 11365/8486, Tehran, Iran*
[b]*Department of chemistry, Faculty of science, Shahid beheshti University, Tehran, Iran*
(E-mail: elham.sattarzadeh@gmail.com)

Introduction:

Superparamagnetic iron oxide nanoparticles with appropriate surface chemistry can be used for numerous *in Vivo* applications, such as MRI contrast enhancement, tissue repair, immunoassay, hyperthermia, drug delivery [1]. These applications also need peculiar surface coating of the magnetic particles, which has to be nontoxic and biocompatible. Such magnetic nanoparticles can bind to drugs, antibodies, or nucleotides and can be directed to an organ, tissue, or tumor using an external magnetic field. Magnetic drug targeting employing nanoparticles as carriers is a promising cancer treatment avoiding the side effects of conventional chemotherapy [2].

Experimental:

To begin our study, In this work, the Fe_3O_4 nanoparticles were prepared by co-precipitation of $FeCl_3 \cdot 6H_2O$ and $FeCl_2 \cdot 4H_2O$ (S1). Stober method was used for preparation of core-shell structure ($Fe_3O_4@SiO_2$) (S2). Silica-coated magnetite nanoparticles were added to a freshly prepared solution of APTES in water (2% v/v) (S3). The final product was dried at 40^oC under vacuum. The dry DTPA was activated with EDC and NHS. The colloidal solution of APTES-modified NPs was added and stirred in the dark at room temperature for 8 h (S4). The unreacted DTPA was removed by centrifugation, and the resulting DTPA-NPs were washed with PBS three times.

Results and Discussion:

In order to confirm the coating of the magnetite surface through the silanization reaction, an FTIR spectrum of the APTES-SiO_2-magnetite was obtained (Fig1). The main absorption bands of OH (3470 cm^{-1}), Fe-O-Fe (590 cm^{-1}) groups are observed. The adsorption of silane polymer onto the surface of magnetite particles was confirmed by bands at 1034 and 1125 cm^{-1} assigned to the SiO–H and Si–O–Si groups. The two broad bands at 3470 and $1632cm^{-1}$ can be ascribed to the N–H stretching vibration and NH_2 bending mode of free NH_2 group, respectively.
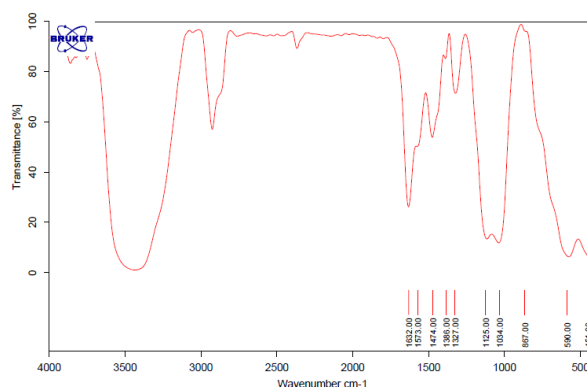

Figure1: FT-IR spectra of core shell

To confirm the bonding of the magnetite surface with DTPA, an FTIR spectrum coreshell-DTPA obtained (figure2).The two broad bands at 1629 and $1574cm^{-1}$ can be ascribed to the

C=O stretching vibration. The absorption bands of CH_2 (2800 cm^{-1}), C-O (1311 cm^{-1}), C-N (1055 cm^{-1}) groups are observed[3].
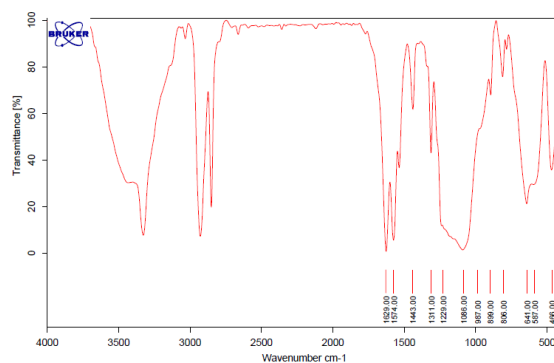

Figure2: FT-IR Spectra of Core Shell. DTPA

The X-ray diffraction (XRD) patterns Shows that standard Fe_3O_4 crystal with spinal structure has six diffraction peaks ((220), (311), (400), (422), (511), (440)) [4]. On the other hand, no peaks were detected in silica coated Fe3O4 nanoparticles which could be assignedto impurities as shown in Figure 3(b).
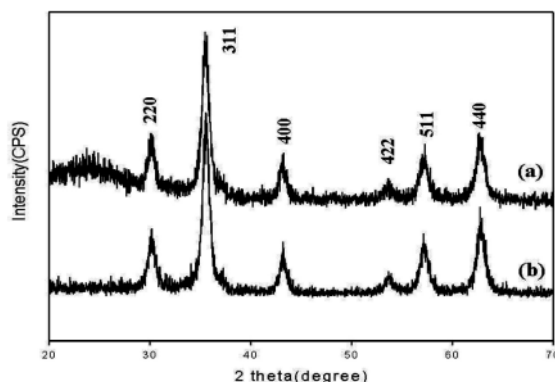

Figure3: XRD pattern of a: Fe_3O_4, b: Core Shell-DTPA.

Conclusion:

Superparamagnetic Fe_3O_4 nanocrystals of 6–7 nm diameters were synthesized by a chemical co-precipitation method, and a silica layer of about 2 nm thickness was coated on the nanocrystal surface by hydrolysis of TEOS. The thickness of the silica layer can be easily adjusted by changing the ratio of TEOS to Fe_3O_4. The amino (–NH_2) groups were successfully covalently bonded to the coated Fe_3O_4 nanocrystals and then DTPA molecules were coupled to the nanocrystal surface through the reaction of –NH_2 and –COOH, as characterized by FTIR spectra. According to the XRD observations, the present magnetic nanocrystals have a cubic spinel structure.

[1] Sophie Laurent; Delphine Forge. *Chem. Rev.* **2008,** *108,* 2064–2110.
[2] Bulte´, J. W. *Methods Mol. Med.* **2006**, *124*, 419-439.
[3] Q. Wang; R. Li2,Y. Miao1, *J. Phys. D: Appl. Phys.* **2005**, *38*, 1342–1350.
[4] Lihua. Zhang; Baifeng Liu, *J. Phys.Chem. B***2007,** *111*, 10448-10452.

Electrochemical degradation of reactive dye using nano- SnO_2/Ti anode

Farideh Nabizadeh Chianeh*[a], Jalal BasiriParsa[b]

[a]Department of Chemistry, Faculty of chemistry, University of semnan, semnan, Iran, Tel: +98 233354058.

[b] Department of Applied Chemistry, Faculty of chemistry, University of Bu-Ali Sina, Hamadan, Iran, Tel: +98 813 8282807.

Email: Nabizadeh@semnan.ac.ir

1. Introduction: Electrochemical advanced oxidation processes (EAOPs) have attracted increasing attention as one of the most promising technologies for the treatment of industrial wastewaters containing toxic or non-biodegradable compounds [1-3]. The efficiency of EAOPs depends strongly on the kinds and structure of anode materials, supporting electrolyte, and applied power (current and voltage), among which the electrode materials are the key factor in the development of electrochemical technologies. [2-4, 6]. This study has focused on surface modification and coating of the titanium electrode by nano SnO_2 particles and its application as an anode for oxidation of Reactive Orange 7 (RO7).

2. Experimental
2.1. Materials: An azo dye RO7, was selected as a model pollutant. SnO_2 nanoparticles were purchased from the Neutrino Corporation (Iran).
2.2. Electrode preparation: The nano-SnO_2 / Ti electrode was prepared by electrophoretic deposition (EPD) method.
2.3. Experimental design: To optimize the RO7 removal, a CCD model based on four input variables was used as experimental design model. The variable parameters were pH (X_1) , current density (I) (X_2), electrolyte concentration (X_3) reaction time (X_4).

3. Result and discussion
3.1. Morphology of nano-SnO_2 films on titanium surface: The FE-SEM images of SnO_2 nanoparticles on titanium surface were shown in Fig. 1 (a-b).It can be observed from the images that the SnO_2 nanoparticles were uniformly distributed on the whole titanium surface while the simple nano-SnO_2 electrode exhibited regularly packed particles and porosity and probably permeability.
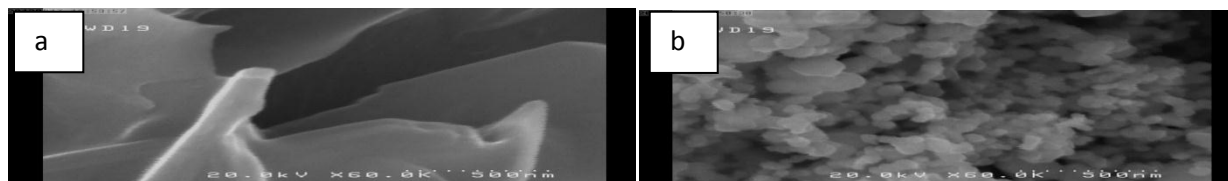

Figure 1. The FE-SEM images of (a) Ti electrode without coating, (b) nano-SnO_2/Ti electrode.

3.2. Optimization of electrochemical treatment of RO7: Based on the results, the regression equation with coded variables obtained and expressed by the following second-order polynomial equation (Eq (1)):

$$Y= 42.7571-13.0712x_1+2.8013 x_3+ 9.6912x_4- 2.4652 x_2^2-2.6215x_3^2 + 1.5969 x_1x_2-1.5056 x_1x_3-4.5156 x_1x_4 \quad (1)$$

The experimental design results were then analyzed by ANOVA to evaluate the "goodness of fit" and the significance and adequacy of the model.

3.3. Effect of operational parameters: The results of optimization showed that maximum RO7 removal efficiency was achieved at the optimum conditions: initial pH 4.4, current density 5.51 mA/cm^2, reaction time 25 min and electrolyte concentration 1.5 g/L. In optimum conditions, RO7 and TOC removal efficiency were 87.37% and 33.2%, respectively.

Conclusions: The fabrication and characterization of the nano-SnO$_2$ /Ti electrode was presented. Also, response surface methodology (RSM) using Central Composite Design (CCD) was applied to model process and to evaluate the effect of important process variables on the color removal efficiency of RO7 dye from aqueous solutions by electrochemical process. The optimum values of the pH, current density, concentration electrolyte and reaction time 4.4, 5.51 mA/cm^2, 1.5 mg/L, 25 min, respectively.

References

[1] Kim S, Choi SK, Yoon BY, Lim SK, Park H. *Appl Catal B Environ*, **2010**, 97, 135-141.
[2] Yang SY, Choo YS, Kim S, Lim SK, Lee J, Park H. *Appl Catal B Environ,* **2012**, 111, 317-325.
[3] Feng Y, Cui Y-H, Liu J, Logan BE. *J Hazard Mater,* **2010**, 178, 29-34.
[4] Du L, Wu J, Hu C. *Electrochim Acta,* **2012**, 68, 69-73.
[5] Liu Y, Liu H, Ma J, Li J. *J Hazard Mater,* **2012**, 213–214 , 222-229.
[6] Ravikumar K, Ramalingam S, Krishnan S, Balu K. *Dyes Pigments,* **2006**, 70, 18-26.

Kinetic Studies of Adduct Formation of Cobalt (ii) Tetraaza Schiff Base Complexes with Different Anions

Fatemeh Gholami, Zahra Asadi*

Department of Chemistry, College of Sciences, Shiraz University, Shiraz 71454, I.R. Iran

Email address: zasadi@shirazu.ac.ir

Introduction:

Schiff bases, as an important class of ligands and their metal complexes, have a variety of applications including biological, clinical, analytical, and industrial usage in addition to their important roles in catalytic and organic synthesis. The interest in tetradentate Schiff base complexes of the first row transition metals is to a significant extent based on the fact that they can serve as models for some biomolecules. With the development of biochemistry, the role of model compounds has been steadily increasing. Bioinorganic chemistry is no exception to this rule, its model compounds being mostly the first row transition metal complexes [1-5].

Experimentals:

Synthesis of cobalt(II) tetraaza complexes: N,N'-ethylenebis-(5-chloro-*o*-amino-α-phenyl benzylideneiminato) cobalt(II)] [Co(campen)] was prepared according to previously published procedures. A slow stream of nitrogen was passed through a vigorously stirred solution of ligand heated under reflux in methanol and a deoxygenated suspension of cobalt(II) acetate in methanol was added dropwise in a 1:1 molar ratio. A bright red solid was obtained on cooling the mixture. Kinetics of the interaction between various anions (X^-) as donor with Co(II)tetraaza complexes as acceptor were studied spectrophotometrically.

In a typical process 2.5 ml of the complex solution was transferred into the thermostated cell compartment of the UV-vis instrument, which was kept at constant temperature (10-40°C) by circulating water, and was injected with excess values of X^- in the molar ratio $\geq$ 10:1.

Result and Discussion:

The kinetics of the reaction by means of titration of the complex solution in UV−vis region at various concentrations of anions with fixed time intervals was studied. The schematic of the reaction is:

$$[Co(campen)] + X^- \longrightarrow [Co\,(campen)(X^-)]$$
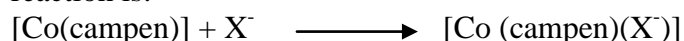
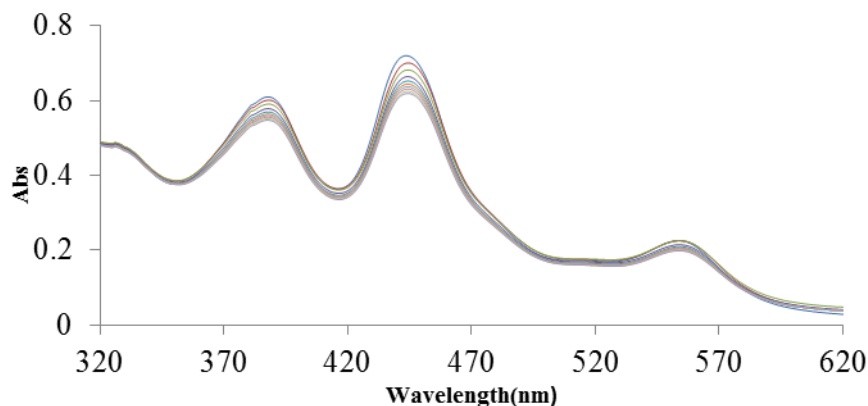UV−vis spectral changes of **[Co(compen)]** is given in Figure 1.

Figure 1. UV−vis spectra changes for [Co(campen)] (2.4×10^{-4} M) with excess [Cl$^-$] in DMF at 293 K

The calculated Pseudo-first-order rate constants (k_2) values at different temperature are given in Table 1.

Table 1. Pseudo-first-order rate constants $10^2 k_2$ ($M^{-1}s^{-1}$), $10^4 k_{obs}$ for the reaction of [Co(compen)] with Cl^- at different temperatures. [complex]= $2\times10^{-5}M$

10^2[Cl]/M	1.0	1.6	2.1	2.6	3.1	3.7	$10^2 k_2/M^{-1}s^{-1}$
10ºC	3.7(0.3)	5.2(0.1)	6.7(0.1)	7.1(0.3)	8.5(0.1)	9.4(0.1)	2.0(0.1)
20ºC	4.6(0.1)	6.7(0.5)	8.6(0.3)	10.6(0.6)	12.3(0.3)	14.6(0.6)	3.7(0.06)
30ºC	5.3(0.1)	8.0(0.7)	10.9(0.8)	13.5(2.8)	16.4(2.1)	19.3(1.2)	5.3(0.05)
40ºC	6.4(0.2)	9.2(0.6)	13(0.8)	16.8(2.3)	20.6(2.3)	24.3(1.1)	6.9(0.1)

Conclusion:

The low values of enthalpy of activation, $\Delta H^{\#}$, and the large negative values of entropy of activation, $\Delta S^{\#}$, an excellent linearity of k_{obs} versus the molar concentration of the donor, and the high span of k_2 values are compatible with our suggested mechanism. By comparing k_2 values for different halide anions I^-, Br^-, and Cl^- it is clear that the more electronegative group act as weak donor. Thus k_2 values follow the trend as: $I^->Br^->Cl^-$.

References:
[1]. M. Asadi, Z. Asadi, international journal of chemical kinetic, 39, **2007**, 137.

[2]. Connelly, N. G.Nomenclature of Inorganic Chemistry,Cambridge: RSC Publishing, **2005**, 266.

[3]. Zhang, Y. L.; Ruan, W. J.; Zhao, X. J.; Wang, H. G. and Zhu, Z. A. *Polyhedron* ,22, **2003** , 1535.

[4]. M. R. Maurya, A. Kumar, A.R. Bhat, A. Azam, C. Bader, D. Rehder, *Inorg. Chem.* , 45, (**2006**), 1260.

[5].S. Koner, S. Saha, T. Mallah, K.I. Okamoto, *Inorg. Chem*; 43, **2004**, 840.

Studying the Physicochemical Properties of ester containing Gemini surfactants at water/ethylene glycol medium

Shirin lashgari[*] **, Soheila Javadian**
Department of Chemistry, Tarbiat Modares University, Tehran, Iran
E-mail: shirin.lashgari@gmial.com

Introduction:

The aim of the present work is studying the effect of ethylene glycol (EG) and ester bond position on size and morphology of ester-containing cationic gemini surfactants, esterquat and betainate geminis in the absence and presence of KCl. The interfacial, structural properties and aggregation behavior have been studied using tensiometry, dynamic light scattering (DLS), transmission electron microscopy (TEM), and cyclic voltammetry techniques at room temperature. The critical micelle concentration (CMC) , surface excess (Γ max), mean molecular surface area (Amin), and the thermodynamic parameters of micellization were determined from the surface tension. CV measurements were done to determine the diffusion coefficients of aggregates and the interparticle interaction parameters. The mean diameters of aggregates obtained by CV can be obtained by alternative methods such as DLS and TEM as well[1, 2].

Methods/ Experimentals:

The surface tension of measurements were made with a Krüss K12 tensiometer by the ring method. Cyclic voltammetry measurements were performed at 298 K, with electro-active probe of ferrocene. Dynamic light scattering were carried out with Malvern zetasizer. Transmission electron micrographs were recorded on on a Zeiss electron microscope operated at 80 kV. Viscosity measurements were carried out using an Ubbelohde viscometer (model Semi-micro).

Results and Discussion:

The CMC values of the pure esterquat gemini and betainate gemini in water/ Ethylene glycol (EG) solutions at 298 K in the absence and presence of KCl were determined from surface tension measurements (Figures 1) as shown in Table 1. The findings indicate that an increase in EG volume percentage increases the CMC since it stabilizes the tail hydrophobic groups at water/EG medium. Since EG decreases the edielectric constant of the medium, it increases the head group repulsive interactions at water/air interface and hence decreases the excess surface concentration. The results indicate that all aggregations were formed at spherical shape in saline medium. Since the EG additive affects both micellar properties and dielectric constant, the overall effect is obtained from the resultant effect of these effects. As indicated by CV study, the dielectric constant is negligible while the effect of EG on micellar properties is significant since it results in a phase transition.

Surfactant	EG %v/v	[KCl] mM	CMC mM
Esterquat gemini	0	0	0.4000
	20	0	0.5800
	35	0	1.3200
	50	0	1.9300
	0	50	0.0030
	20	50	0.0033
	35	50	0.0040
	50	50	0.0044
Betainate gemini	0	0	0.2700
	20	0	0.5400
	35	0	1.2000
	50	0	1.7500
	0	50	0.0010
	20	50	0.0012
	35	50	0.0016
	50	50	0.0026

Table 1- Critical Micelle Concentration

Conclusion:

Addition of EG decreases the aggregation number and hydrodynamic radius since it increases the headgroup-head group repulsion at the micellar surfac The results showed that the position of ester bonds in alkyl tail and present of ethylene glycol (EG) play an important role in aggregation behavior of pure ester-containing gemini surfactants in mixed solvents in the absence and presence of KCl. Current study showed that these geminis spontaneously formed aggregates in the nanometer range, which makes them potentially applicable as drug delivery vehicles.

Reference

[1] Aghdastinat H, Javadian S, Tehrani-Bagha A, Gharibi H. Spontaneous Formation of Nanocubic Particles and Spherical Vesicles in Catanionic Mixtures of Ester-Containing Gemini Surfactants and Sodium Dodecyl Sulfate in the Presence of Electrolyte. The Journal of Physical Chemistry B. 2014;118:3063-73.

[2] Yousefi A, Javadian S, Gharibi H, Kakemam J, Rashidi-Alavijeh M. Cosolvent effects on the spontaneous formation of nanorod vesicles in catanionic mixtures in the rich cationic region. The Journal of Physical Chemistry B. 2011;115:8112-21.
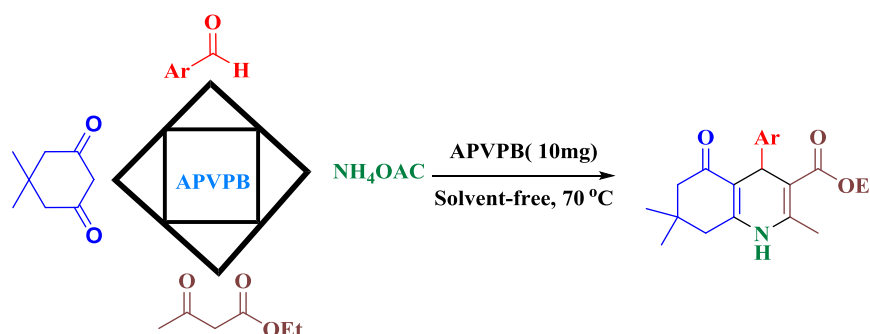
One-pot synthesis of hexahydroquinolines using acetic acid functionalized poly (4-vinylpyridinium) salt as new nono catalyst

EhsanNoroozizadeh[a], Mohammad Ali Zolfigol[a],* Ahmad Reza Moosavi-Zare[b], Mahmoud Zarei[a]

[a] *Faculty of Chemistry, Bu-Ali Sina University, Hamedan, 6517838683, I. R.Iran, mzolfigol@yahoo.com*
[b]*Sayyed Jamaleddin Asadabadi University, Asadabad, 6541835583, I. R. Iran,*
moosavizare@yahoo.com

One series of DHP derivatives with an improved structural scaffold, the hexahydro-quinoline derivatives (HHQs), can be synthesized according to a Hantzsch synthesis using aryl aldehydes, dimedone (5,5-dimethylcyclohexane-1,3-dione), ethyl acetoacetate, and ammonium acetate in a one-pot multi-component condensation reaction [1, 2]. Quinolines bearing a 1,4-dihydropyridine scaffold have been identified as promising structure in medicinal chemistry because of their many pharmacological properties, including their antibacterial antihypertensive, anti-inflammatory, antimalarial, antiasthmatic, and tyrosine kinase inhibitory activity [3–8]. In this methodology we have reported the synthesis of hexahydroquinolines using nano APVPB as reusable catalyst (**Scheme1**). The promising points for the presented methodology are efficiency, generality, high yields, very short reaction times, cleaner reaction profile and simplicity.
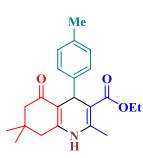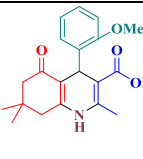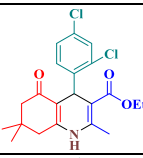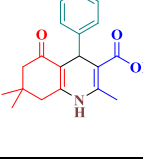

Scheme 1: The Synthesis of hexahydroquinoline derivatives (HHQs), from of dimedone, arylaldehydes, ethyl acetoacetate, and ammonium acetate.

Experimentals

To a mixture of dimedone (0.14 g, 1 mmol), arylaldehyde (1 mmol), ethyl acetoacetate (0.13 g 1 mmol) and ammonium acetate (0.0925 g, 1.2 mmol) in a 25 mL round-bottomed flask, was added APVPB (10 mg), and the resulting mixture was firstly stirred magnetically, and after solidification of the reaction mixture with a small rod, at 70 ℃. After completion of the reaction, as monitored by TLC, the reaction mixture was cooled to room temperature. Afterward, ethanol (95%) (20 mL) was added to the reaction mixture, stirred and refluxed for 3 min, and centrifuged to separate APVPB from the mixture.The solvent was evaporated, and the crude product was purified by recrystallization from ethanol (95%).

Results and Discussion

To assess the efficiency and the scope of the organic catalyst in the preparation of hexahydroquinolines, the condensation of dimedone, ethyl acetoacetate, and ammonium acetate with various arylaldehydes was examined in the presence of nono APVPB at 70 °C . The corresponding results are displayed in below.

Entry	Product	Time (min)	Yield (%)	Mp (°C) (lit)
1		20	90	258-260 (259–262) [9]
2		19	86	258-260 (257–259) [9]
3		15	92	242-244(243–245) [9]
4		16	88	210-212 (206–208) [9]
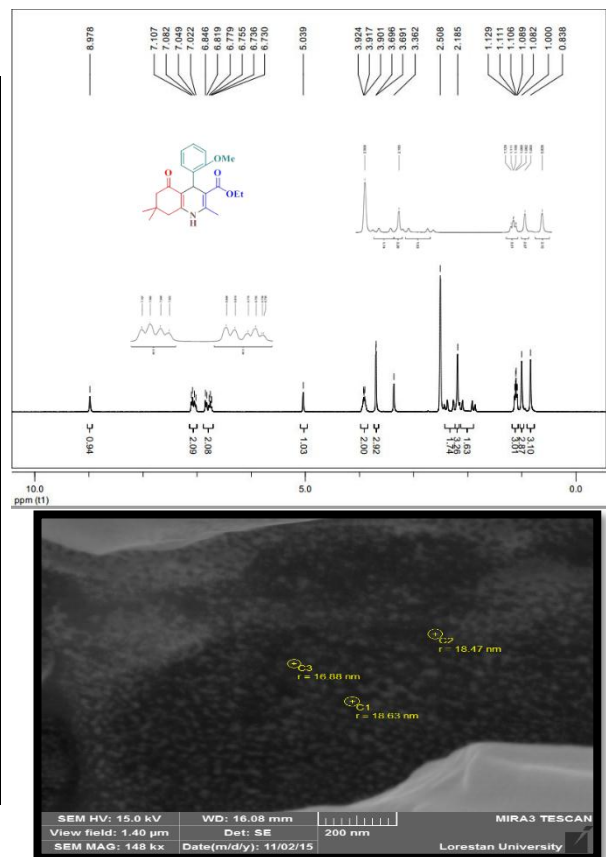
Conclusion

We have introduced the Brönsted acidic ionic liquid poly (4-vinylpyridinium) salt as a novel, highly efficient, general, and homoge-neous catalyst for the one-pot multi-component reaction of dimedone, aromatic aldehydes, ethyl acetoacetate, and ammonium acetate leading to hexahydroquinolines. The advantages of the current protocol include its efficiency, broad scope, high prod-uct yields, short reaction time, clean reaction profile, simplicity, low cost, ease of preparation, and the recyclability of the cata-lyst.

References

[1] C. Safak, I. Sahin, R. Sunal, Arzneimittel Forsch, **1990**, 40, 119-123.

[2] R. Simsek U B. Ismailoglu, C. Safak, I. Sahin-Erdemli Farmaco, **2000**,55, 665-668.

[3] R. D. Larsen, E. G. Corley, A. O. King, J. D. Carrol, P. Davis, T. R. Verhoeven, P. J. Reider, M. Labelle, J. Y. Gauthier, Y. B. Xiang, R. J. Zamboni, J Org Chem, **1996**, 61, 3398-3405.

[4] Y. L. Chen, K. C. Fang, J. Y. Sheu, S. L. Hsu, C. C. Tzeng,J Med Chem, **2001**, 44, 23742377.

[5] G. Roma, M. Di Braccio, G. Grossi, F. Mattioli, M. Chia, Eur J Med Chem, **2000**, 35,1021-1035.

[6] X. Geng, S. S. Li, X. Q. Bian, Z. Y. Xie, C. D. Wang, ARKIVOC, **2008**, 50, 297-313.

[7] M. P. Maguire, K. R. Sheets, K. McVety, A. P. Spada, A. Zilberstein, J Med Chem, **1994**, 37 2129-2137.

[8] O. Billker, V. Lindo, M. Panico, A. E. Etienne, T. Paxton, A. Dell M. Rogers,
R. E. Sinden, H. R. Morris, Nature, **1998**, 392, 289-292.

[9]. A. R. Moosavi-Zare, M. A. Zolfigol, M. Zarei, A. k. Zare, J. Afsar, **2015**, 505, 224–234.

Functionalized MWCNTs/TiO$_2$ Nanoparticles Modified Carbon Paste Electrode as a New Voltammetric Sensor for Determination of 5-Aminosalicylic acid

M.R. Baezzat *, Masoud Mahmoodi, Fatemeh Shojai, Roghiyeh Pourghobadi

of Payame Noor, university, Tehran, 19395-3697, Iran Department

*Mrbaezzat@pnu.ac.com

1. Introduction

5-aminosalicylic acid (5-ASA) is an important non-steroid anti-inflammatory drug used in the treatment of Crohn's disease and ulcerative colitis, [1]. In the recent decades, there have been several reports on the electroanalytical determination of MES [2-4].

In this work, the utilization of a new Functionalized multi-walled carbon nanotubes/TiO2 nanoparticles modified carbon paste electrode prepared by a simple and rapid procedure for the determination of 5-ASA was described. The electrochemical behaviour of 5-ASA was investigated at the surface of FMWCNT/ TiO$_2$ NPs-CPE using current methods cyclic voltammetry and differential pulse voltammetry and electrochemical impedance spectroscopy.

Keywords: Differential pulse voltammetry, 5-aminosalicylic acid (5-ASA), FMWCNT/ TiO$_2$ NPs-CPE, Electrochemical impedance spectroscopy.

2. Electrode preparations

Graphite powder 70% was hand mixed with TiO$_2$ nanoparticles20%, Functionalized MWCNTs 5%, and paraffin oil 10% w/w in a mortar and pestle to manufacture a homogenous carbon paste. The modified carbon paste was then packed into an insulin syringe. A copper wire was inserted into the carbon paste and provided an electrical contact. When essential, a new surface was obtained by pushing an excess of paste out of the syringe, which was then polished with weighing paper.

3. Results and Discussion

3.1. Voltammetric investigation

Fig. 1 shows cyclic voltammograms of 5-ASA 0.1mM at the modified and unmodified using cyclic voltammetry in 0.1 M phosphate buffer and pH 7.0. The oxidation peak current significantly increases to 8.8 µA, which is 2 times higher than that at CPE. The effect of solution pH on the response of 5-ASA was investigated by cyclic voltammetry over the pH range of 4.0–11.0. The largest anodic current appearing at pH 7.0, so this value was selected throughout the experiments. The effect of scan rates on the peak currents at the FMWCNT/ TiO$_2$ NPs-CPE in 0.1 M PBS pH 7·0 were investigated by cyclic voltammetry. The results showed that the peak current increased linearly with increasing the square root of scan rate

that ranged from 10 to 500 mV s^{-1} Fig. 2. The result shows that the electrode process is controlled under the diffusion step.
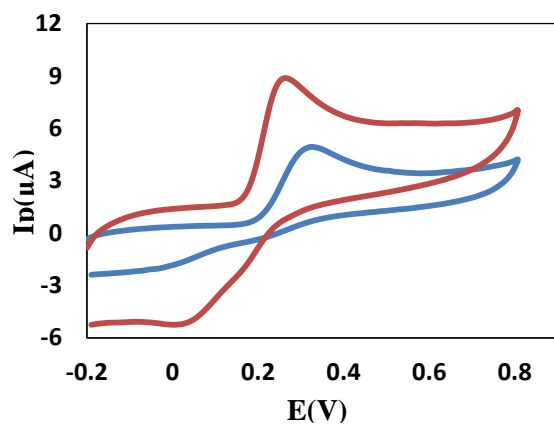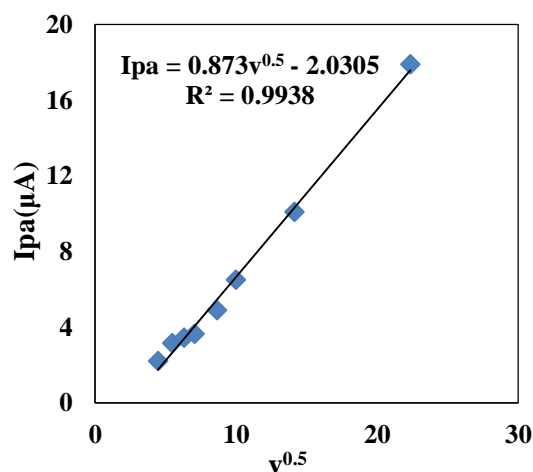

Fig. 1

Fig. 2

3.2. Determination of 5-ASA

  The electrooxidation of 5-ASA was studied in 0.1 M PBS pH 7·0at the surface of FMWCNT/ TiO$_2$ NPs-CPE using DPV technique. The results showed linear relationships between oxidation peak currents and 5-ASA concentration in linear range 1.0-400.0 μM. The detection limit (3σ) of 5-ASA was found to be 0.26 μM

4. Conclusion

  In this work, a new electrochemical sensor was fabricated based on FMWCNT/ TiO$_2$ NPs-CPE for sensitive determination of 5-ASA. SEM and EIS methods were employed to investigate characteristics of the FMWCNT/ TiO$_2$ NPs-CPE. This electrode has number of advantages, such as easy preparation, high stability, reasonable selectivity, fast response time, long-term stability and applicability over a wide pH range. Also, shows excellent stability, reproducibility, high sensitivity in real samples.

References

[1] K. Mladenovska; R. S. Raicki; E. I. Janevik; T. Ristoski; M. J. Pavlova;Z. Kavrakovski; M. G. Dodov; K. Goracinova. Int. J. Pharm, 2007, 342, 124-136.

[2] V. Carolina; U. H. Yamanaka. Quim. Nova, 201033, 33, 964-967.
[3] S. Shahrokhian; P. Hosseini; Z. Kamalzadeh. Electroanalysis, 2013, 25, 2481–2491.

[4] M. Torkashvanda; M.B. Gholivand; F. Taherkhani. Materials Science & Engineering C,

    2015, doi: 10.1016/j.msec.2015.05.031.

A Mathematical Approach for Balancing Chemical Equations

M. Bamdad[a],*, **M. Ramesh, H. Heydari, and M. Bassam.**

[a] **Department of Chemistry, Faculty of Sciences, Shahid Chamran University of Ahvaz, Ahvaz, 61357-43169, Iran.**

mbamdad@scu.ac.ir

Introduction: The first step for chemical calculations is the mass balancing of chemical reactions. Various methods have been presented in the literature for chemical balancing. It is obvious that all these methods are based on the law of conservation of mass, but approaches for chemical balancing are different for various reactions e.g. reaction in acidic or alkaline environment. However for years it has been published algebraic methods to balancing a chemical reaction, but this method is not popular yet [1].

Method: According to the conservation law of mass, for each element, the same number of atoms of the element must appear on each side of a chemical equation. Based on this reason it is possible to construct a linear systems of equations for the individual stoichiometric coefficients. Solving the equations by appreciates mathematical method led to the proper stoichiometric coefficients [2 -4]. The presented approach not only is valid for neutral chemical reaction but also applicable for ionic form of chemical equations.

Results and Discussion: Based on the law of the conservation of mass for a typical reaction such as:

$$x_1\, H^+ + x_2\, H_2O + x_3\, As_4O_6 + x_4\, MnO_4^- \longrightarrow x_5\, H_3AsO_4 + x_6\, Mn^{2+}$$

we can write linear systems of equations for each stoichiometric coefficients:

$$
\begin{array}{lll}
\text{H)} & x_1 + 2x_2 & = 3x_5 \\
\text{O)} & x_2 + 6x_3 + 4x_4 & = 4x_5 \\
\text{As)} & 4x_3 & = x_5 \\
\text{Mn)} & x_4 & = x_6 \\
\text{charges} & x_1 - x_4 & = 2x_6 \\
\text{normalize} & x_1 & = 1
\end{array}
$$

Solving the system of linear homogeneous equations by matrix methods $\mathbf{x}=\mathbf{A}^{-1}\mathbf{b}$ led to the normalized stoichiometric coefficients.

Conclusion: Solving a system of linear equations based on the concept of the law of conservation of mass is provided an excellent way for balancing chemical equations. The presented method not only appreciated for computing calculations but also is straight-forward and is applicable for ionic form of chemical equations.

References

[1] H. A. Curtis. *Science*, **1922**, LVI, 258-260.

[2] K. Wayne. SEAS short course programing in MATLAB, Tutorial 2: Numerical Algebra, **2005**, 3.0, 1-19.

[3] C. I. Gabriel; G. I. Onwuka. *Journal of Natural Sciences Research*, **2015**, 5, 29-36.

[4] S. C. Das. *International Journal of Mathematical Education in Science and Technology*, **1986**, 17, 191-200.

Synthesis, characterization and Quantum study of dinuclear copper(II) complexes with halogen bridges [LCu(μ-X)X]$_2$ (X $^-$ = F$^-$, Cl $^-$, Br $^-$)

H. Golchoubian, S. Koohzad *

Department of chemistry, University of Mazandaran, Babolsar, Iran Postal Code 47416-95447

Email address: Sara.Kohzad@gmail.com

Background: The study of dinuclear complexes of copper (II) is a very active research field in chemistry society and more than nine hundreds of such complexes have been structurally characterized [1, 2] so far. The main strategy for designing the polynuclear complexes is to use suitable bridging groups. Among the most common ligands used as bridging ligand in binuclear complexes are halide. In recent years, density functional theory (DFT) calculations have proved highly successful at predicting the structures and electronic properties of transition metal complexes. In addition, time-dependent density functional theory (TD-DFT) calculations allow chemists to probe the nature of the excited states of the complexes and facilitate a better understanding of the observed electronic absorption spectra [3, 4].

The main purpose of the present paper is syntheses, characterization and investigation of the structure of dinuclear copper (II) complexex of [(L) Cu (μ-X) X] $_2$ (where X $^-$ = F$^-$ (1), Cl $^-$ (2), Br $^-$ (3) and L = *N, N*-dimethyl, *N′*-benzyl-ethylenediamine) and assignment of their electronic absorption spectra by means of DFT and TD-DFT calculations. The calculated data is also compared with the corresponding experimental results.

Methods or Experimental:

Synthesis of complexes:

To a methanolic solution of the diamine ligand was slowly added CuX$_2$ in methanol (10 ml) with the same molar ratios. The resultant mixture was stirred for 1 h at room temperature. The desired compound precipitated off from the reaction mixture. After separation it was recrystallized from diffusion of diethyl ether into methanol solution.

Computational methods:

DFT approach (B3LYP) with the basis sets 6-31G+(d, p) for all nonmetal atoms combined with the SVP for Cu, as implemented in the GAUSSIAN 09 software package, was used to optimize geometry without any symmetry restrictions and wavenumber calculations were carried out to verify whether the optimized molecular structure corresponded to minimum energy.

Results and Discussion:

In this research, we synthesized three new dinuclear copper (II) complexes and characterized them, on the basis of elemental analysis, IR spectroscopy & X-ray crystallography. The

elemental analyses data and the infrared spectra support the expected formulation of the complexes, which was further confirmed by X-ray crystallography. The crystallographic data of complexes show distorted square pyramidal and trigonal bipyramidal geometries around the copper centers for 2 and 3, respectively (Figure 1).
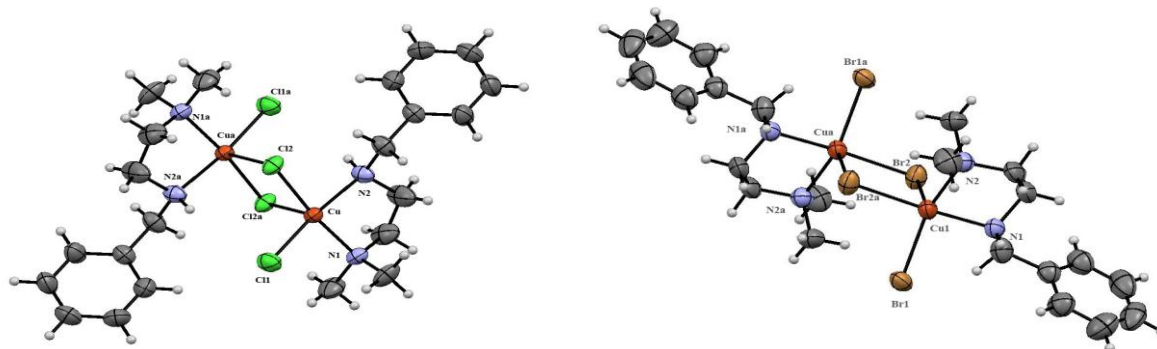

Figure 1. ORTEP view of 2, 3 with atom labeling.

In computational study, the single crystal X-ray diffraction data was used as initial input for geometries optimizations. The X-ray crystallographic structure of **2** was used as a starting coordinate to generate the possible structure for **1**. The obtained calculated geometrical parameters showed the excellent with those X-ray data.

The electronic absorption spectra have been investigated in the framework of time-dependent density functional theory (TDDFT) and polarizable continuum TDDFT (PCM-TDDFT). The complexes were further investigated by drawing a qualitative molecular orbital that include Mullikan molecular orbital percent compositions in term of fragment orbitals.

Conclusion: In summary, this work highlights the synthesis, structural characteristics and quantum study on three new binuclear Cu (II) complexes. The comparison of the calculated IR and UV-Vis spectra of the complexes with the experimental results allowed the assignation of the most characterization bands.

Keyword: copper (II), binuclear, halid, DFT, TDDFT, absorption spectra.

References

[1] F. Valach, M. Dunaj-Jurco, J. Garaj and M. Hvastijova, *Collect. Czech. Chem. Commun.*, 1974, **39**, 380-386.

[2] M.-L. Boillot, O. Kahn, C. J. O'Connor, J. Gouteron, S. Jeannin andY. Jeannin, *J. Chem. Soc., Chem. Commun.* 1985, 178-180.

[3] L. C. Xu, J. Li, S. Shi, K.C. Zheng, L. N. Ji, J. Mol. Struct. (THEOCHEM), 2008, 855, 77-81.

[4] T.F. Miao, S. Li, J. Cai, J. Mol. Struct. (THEOCHEM), 2008, 855, 45-51.

Dye-sensitized nanoTiO$_2$ as a novel efficient photocatalyst for cyclization of *N,N*-dimethylanilines with maleimides under visible light.

Mona Hosseini-Sarvari[* a], **Mehdi Koohgard** [a]

[a] **Department of Chemistry, Faculty of Science, Shiraz University, Shiraz 71454, Iran**

 **E-mail: Mehdikoohgard66@yahoo.com, Monahosseini@yahoo.com**

Introduction: Photoinduced reactions are a powerful tool in modern synthetic chemistry. They often lead to products virtually inaccessible by thermal reactions and proceed along the excited-state pathway [1]. The approach takes full advantage of visible light, which is safe, abundant, and reproducible.

Dye-sensitization on semiconductor particles has recently attracted extensive attention related to dye-sensitized solar cells (DSSCs) [2] and water splitting [3]. However, less is known about synthetically useful organic reactions catalyzed by dye-sensitized TiO$_2$ [4].
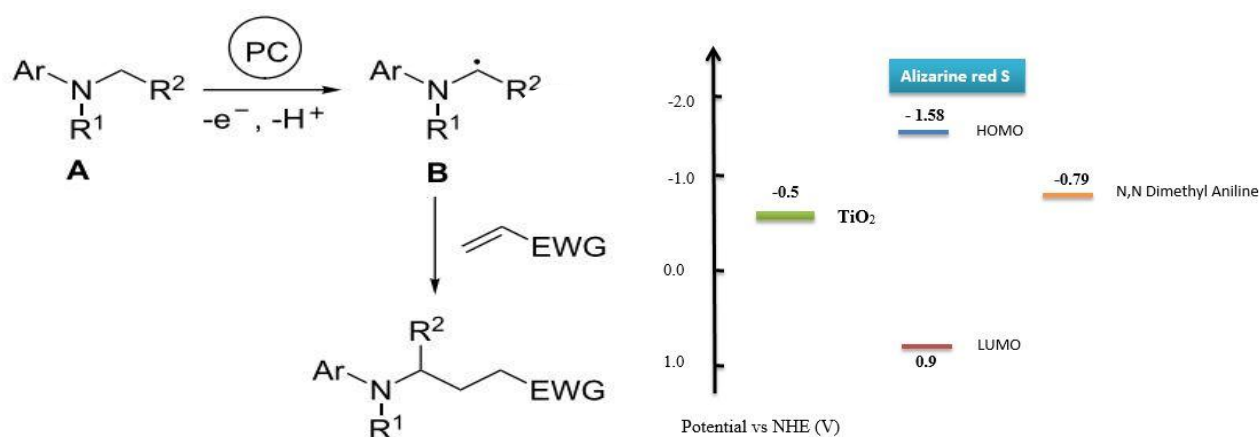
More recently, visible-light-induced sp^3 C–H bond functionalization adjacent to nitrogen atoms has been extensively studied [5]. Owing to the well-defined differences in redox potentials, the single electron transfer (SET) occurs from t-amine to excited state of phtotocatalyst / photosensitizer producing planar amine radical cation and iminium ion intermediates [6]. After generation of the intermediate it can be undergone by reaction of many nucleophiles and double bond bearing electron withdrawing groups [7].

Experimentals: To a solution of dimethyl aniline (1.5 mmol) and N-arylmaleimides (1 mmol) in CH$_3$CN (7 mL) was added dye- nanoTiO$_2$ (0.006 g). The reaction mixture was open to the air and stirred under a 14 W CFL irradiation at room temperature. After reaction completion catalyst was separated by centrifuging and the solvent removed under reduced pressure, the crude product was purified by column chromatography.

Results and Discussion: Here in, we investigated the α-aminoalkylradical route to achieve the aerobic oxidative cyclization of *N,N*-dimethylanilines with maleimides to form the corresponding tetrahydroquinoline derivatives under dye -nano TiO$_2$ catalysis. After optimization of the reaction in the air and room temperature condition, a vast variety of tetrahydroquinoline derivatives has been synthesized. According the NHE level, this reaction get started with transfer of electron form *N,N*-dimethylanilines to photoredox catalyst. After separation of H$^+$, radical intermediate add to N-arylmaleimide and in the following, cyclization of intermediade result in product (Scheme 1,2).
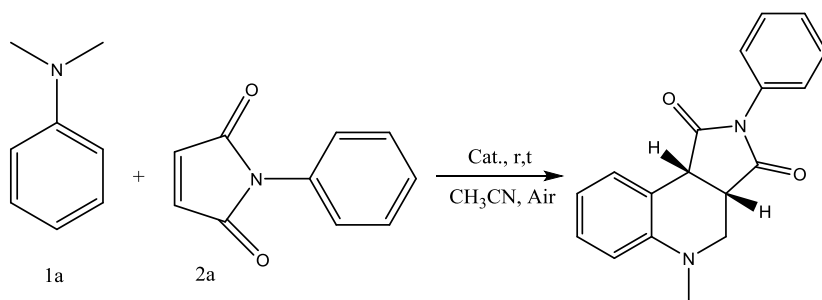
Scheme 1. Representative reagent for the reaction.

PC= photoredox catalyst, EWG= electron-withdrawing group.

Scheme 2: Plausible mechanism for the reaction of visible-light-induced sp^{3}C–H bond functionalization in accordance with NHE energy level.

Conclusion: In conclusion, we report an efficient significantly green protocol for thesynthesis of corresponding tetrahydroquinolines from *N,N* dimethylanilines and maleimides using molecular oxygen as oxidant and dye-nano TiO$_2$ as catalyst under the irradiation of visible light.

References:

1. J. Svoboda, B. Konig. Chem. Rev. 2006, 106, 5413−5430.

2. B. O'Regan, M. Grätzel. Nature, 1991, 353, 737–740.

3. R. Abe. Bull. Chem. Soc. Jpn. 2011, 84, 1000–1030.

4. S. Füldner; R. Mild; H.I. Siegmund. Green Chem. 2010, 12, 400–406.

5. J. Xie; H. Jin; P. Xu. Tetrahedron Lett. 2014, 55, 36–48.

6. Y. Miyake; K. Nakajima; Y. Nishibayashi. J. Am. Chem. Soc. 2012, 134, 3338–3341.

7. S. Zhu; A. Das; L. Bui. J. Am. Chem. Soc. 2013, 135, 1823−1829

Separation and preconcentration trace amounts of Cd(II) ions using of modified Nylon-66 nanofibers sorbent prior to FAAS determination

S. Saeedi [a]*, D. Afzali[a], H. Hashemipour[b]

[a] *Department of Chemistry, Graduate University of Advanced Technology, Kerman, Iran*

[b] *Department of Chemical Engineering, Shahid Bahonar University of Kerman, Iran*

* E-mail: saeidisamira89@yahoo.com

****

Introduction:

Diverse heavy-metal ions, which may bring long-term threat to the environment and human beings, are released into the water by human activities [1]. Several methods such as precipitation, ion exchange, electro dialysis, adsorption and membrane technology have been used for metal ions uptake from water and wastewater [2]. The electrospun nanofibers as an adsorbent showed higher potential for metal ions separation [3].

In this work, we prepared nanofibers modified nylon-66 as SPE sorbents for Separation the of cadmium ion from environmental water. Considering some factors such as a function pH, contact time and initial concentration were optimized.

Methods / Experimentals:

Synthesis of modified Nylon-66 nanofibers

Nylon-66, rhodanine solution with 12:2 wt% prepared. Then the solution was electrospun at a constant flow of 0.5 mL h^{-1}, the distance between the tip-collector are 10 cm and voltage was applied 30 kv.

Separation and preconcentration

5.0 ml of solution 1.0 ppm Cd(II) was passed through the sorbent by a peristaltic pump, then cleaned sorbent with distilled water. Afterwards, the metal ions retained on column were eluted with 2.0 M HNO_3 solution.The analytes in the elution were determined by FAAS.

Results and Discussion:

Fig1: Shows SEM image of modified nanofibers 12:2 wt% (nylon-66: rhodanine) under optimum conditions.
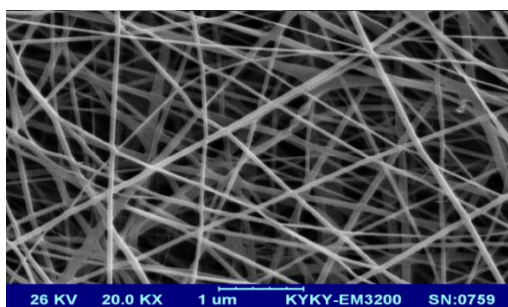

Fig1: SEM image of sorbent.

Effect of pH

Effect of pH on sorption of Cd(II) was shown in Fig 2. It can be seen that pH value plays an important role with respect to the sorption of different ions on oxide surfaces.

At pH=7-9 the metal recovery values could reach the maximum (>99%). Avoided hydrolyzing at higher pH value, pH=7 was selected as the optimum acidity.
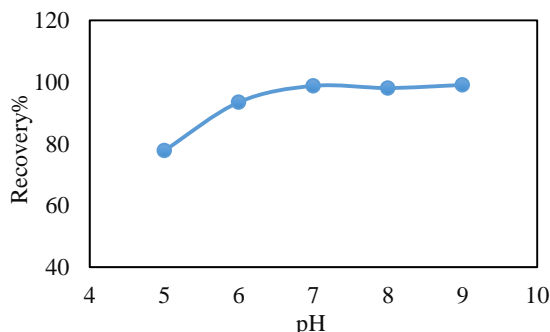

Fig 2: Effect of pH on the sorption Cd^{2+}.

Effect of sample flow rate

Sample flow rate investigated revealed that quantitative retention was achieved at a flow rate of 15 rpm as shown in Fig 3. The optimum conditions obtained for Cd^{2+} in flow rate=5-12.5 rpm maximum sorption obtained that speed 12.5 rpm was selected.
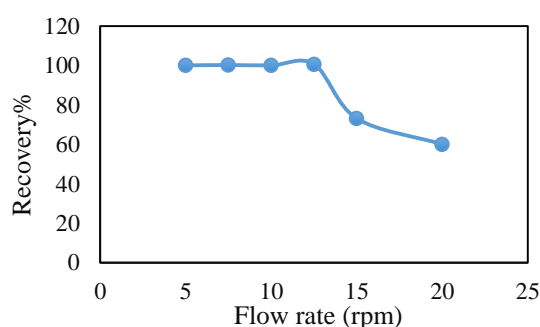

Fig3: Effect of sample flow rate

Effect of elution type

In order to choose a proper eluent for the retained Cd^{2+} ions, after its extraction from the sample solutions, the adsorbed ions were stripped with different acidic solutions such as HNO_3, HCl, and $H_2SO_4(2 \text{ mol} \cdot L^{-1})$. It was found that HNO_3 2.0 M can used as elution with most recovery%.

Conclusions

In this work, modified nanofiber was synthesized and applied as membrane for preconcentration of trace amount Cd (II). The using this method with flow injection causes decrease the time and increase speed and repeatability for separation of Cd (II). The results of the application to a real sample were satisfied.

References

[1] Järup L. British medical bulletin, 2003, 68, 167-182.

[2] Beheshti H; Irani M; Hosseini L; Rahimi A; Aliabadi M, Chemical Engineering Journal. 2016, 284, 557-564.

[3] Feng C; Khulbe KC; Matsuura T; Tabe S; Ismail AF. Separation and Purification Technology, 2013, 102, 118-135.

Correlation in ^{1}HNMR chemical shifts and hydrogen bond strength of some beta-diketones

R. Afzali*, M. Hakimi-Tabar

Department of Chemistry, Ferdowsi University of Mashhad, Mashhad 91775-1436, Iran
Email address: raheleh.afzali@yahoo.com

Introduction

β-diketones are widely used in organic and inorganic chemistry. The cis-enol form of β-diketones is characterized by a strong intramolecular hydrogen bond. The nature of intramolecular O–H···O hydrogen bond in the enol form of symmetric and asymmetric β-diketones have been the subjects of intensive studies [1,2]. NMR spectroscopy technique has been intensively used to study the hydrogen bond strength in these compounds [3,4]. On the other hand, it has been also shown that modern ab initio and density functional quantum chemical calculations can predict the strength and nature of the intramolecular hydrogen bond in β-dicarbonyl compounds extremely well [5,6]. Factors that affect the electronic structure of the chelated ring could have important influences on the IHB strength. The aim of the present paper is comparing the variations in hydrogen bond energy (E_{HB}) and theoretical and experimental chemical shifts of enolic proton in some beta-diketones with similar substitutions, acetylacetone (AA), benzoylacetone (BA), dibenzoylmethane (DBM), 5,5-dimethylhexane-2,4-dione (DMHD), 2,2,6,6-tetramethyl-3,5-heptanedione (TMHD), and 4,4-dimethyl-1-phenylpentane-1,3-dione (DMPD), by using DFT, NMR, and atoms in molecules (AIM) calculations.

Method of analysis

The computations in the present study were performed at different levels (B3LYP, X3LYP, TPSSh, and BLYP levels using 6-31G*, 6-31G**, 6-311G**, and 6-311++G** basis sets) by using Gaussian 09 software package. AIM 2000 software was applied to obtain the energy of hydrogen bond according to Bader's atoms in molecules (AIM) theory at the B3LYP/6-311G** level. NMR calculations were applied by using gauge-independent atomic orbital (GIAO) method at the different levels of theory.

Results and Discussion

The chemical shifts of mentioned beta-diketones have been calculated by means of DFT calculations at different levels of theory. The results were compared with the experimental data from literatures [7-9]. According to Table 1, the measured and calculated ^{1}HNMR chemical shifts for the stable cis-enol forms of mentioned compounds show the 6-311G** basis set in most levels of beta-diketones is in better agreement with the experimental results. So, this basis set can be a good one for calculating the chemical shifts of compounds. For finding the correlation of enolic proton chemical shifts and that of hydrogen bond strength of the compounds with similar substitutions, they compared to each other experimentally and theoretically at B3LYP/6-311G** (see Table 1). By comparing those of BA and DBM with AA, it's concluded by replacing the phenyl group instead of methy group in AA, the experimental and theoretical chemical shifts increase about 0.8 ppm and in the case of E_{HB}, it's about 1.5 Kcal/mol, which by replacing the second phenyl group, these values interestingly doubled. Also, the corresponding variations for DMHD and TMHD are about

0.3 ppm and 1.5 Kcal/mol. By substituting the second *t*-But in beta position, these variations doubled. So, good correlation have been obtained. So, it is expected for DMPD with different substituents in beta position (phenyl ring & *t*-But group), the chemical shifts increase about 1.2 ppm and E_{HB} increase about 3.00 Kcal/mol, which is in very good agreement with our results.

Table 1.
The ^{1}HNMR chemical shifts for enolic proton of some beta-diketones in different levels of theory.[a]

Calculation level	AA	BA	DBM	DMHD	TMHD	DMPD
Theo.						
B3LYP/6-31G*	14.2	14.8	15.3	15.7	14.9	15.2
B3LYP/6-31G**	15.8	16.6	17.1	16.1	16.6	17.0
B3LYP/6-311G**	15.7	16.5	17.1	16.0	16.3	16.8
B3LYP/6-311++G**	15.8	16.7	17.1	16.2	16.5	16.9
TPSSh/6-31G*	14.2	14.9	15.3	15.8	14.9	15.2
TPSSh/6-31G**	15.9	16.6	17.1	16.2	16.6	17.0
TPSSh/6-311G**	15.7	16.5	17.0	16.2	16.3	16.8
TPSSh/6-311++G**	15.8	16.7	17.1	16.2	16.5	16.9
BLYP/6-31G*	14.2	14.8	15.1	15.7	14.8	15.1
BLYP/6-31G**	15.9	16.6	17.0	16.1	16.6	16.9
BLYP/6-311G**	15.7	16.5	17.0	16.1	16.3	16.8
BLYP/6-311++G**	15.8	16.6	18.1	16.2	16.4	16.9
X3LYP/6-31G*	14.2	14.9	15.3	15.7	14.9	15.2
X3LYP/6-31G**	15.8	16.6	17.1	16.1	16.6	17.0
X3LYP/6-311G**	15.7	16.5	17.1	16.1	16.4	16.8
X3LYP/6-311++G**	15.9	16.7	17.2	16.2	16.5	17.0
Exp.	15.4	16.2	16.8	15.9	16.3	16.7
E_{HB}	18.8	20.3	22.1	20.2	21.4	22.0

[a] All chemical shifts are relative to TMS in ppm., E_{HB} is the energy of hydrogen bond in B3LYP/6-311G** level of theory.

Conclusion

The $\delta_{Theo.}$ and E_{HB} have been calculated by means of DFT calculations. For finding the correlation of chemical shifts and E_{HB}, the compounds with similar substitutions compared to each other. Good correlations on them have been obtained. The theoretical results show for most beta-diketones, the 6-311G** basis set in most levels is in better agreement with the $\delta_{Exp.}$.

References
[1] F. Jiménez-Cruz, L. Fragoza Mar, J.L. Garcia-Gutierrez, *J. Mol. Struct.* (2013), 1034, 43–50.
[2] B.K. Paul, N. Guchhait, *J. Comput. Theor*. Chem. (2013), 1012, 20–26.
[3] D.C. Nonhebel, *Tetrahedron* (1968), 24, 1869–1874.
[4] N.N. Shapet'ko, *Org. Mag. Res.* (1973), 5, 215–216.
[5] N.V. Belova, V.V. Sliznev, H. Oberhammer, G.V. Girichev, *J. Mol. Struct.* (2010), 978, 282–293.
[6] S.F. Tayyari, A.-R. Nekoei, M. Vakili, M. Hassanpour, Y.A. Wang, *J. Theor. Comput. Chem.* (2006), 5, 647–664.
[7] S.F. Tayyari, H. Rahemi, A.R. Nekoei, M. Zahedi-Tabrizi, Y.A. Wang, *Spectrochimica Acta Part A* (2007), 66, 394–404
[8] M. Vakili, S.F. Tayyari, A. Kanaani, A.-R. Nekoei, S. Salemi, H. Miremad, A.R. Berenji, R.E. Sammelson, *J. Mol. Struct.* (2011), 998, 99–109.
[9] R. Afzali, M. Vakili, S.F. Tayyari, H. Eshghi, A.-R. Nekoei, *Spectrochimica Acta Part A* (2014), 117, 284–298.

Separation and determination trace amounts of cobalt ions in natural water and food samples by use of modified magnetic nano alumina

Mohammad Reza Jamali*, **Amir Fadaifar, Reyhaneh Rahnama, Seyyed Hojjat Allah Rahimi**

Department of Chemistry, Payame Noor University, Tehran, Iran

E-mail: mr_jamali@ymail.com

Introduction

The determination of heavy metals at trace levels in the environment is one of the targets of analytical chemists, because of their significance in our life. Due to the extremely low concentration and the complexity of the environmental samples, an efficient separation and preconcentration step is usually required prior to their determinations. Among the preconcentration techniques, solid phase extraction (SPE) has received the most attention due to its simplicity, high concentration factor, and more environment friendly reagents [1]. Magnetic SPE (MSPE) has received considerable attention in recent years [2]. Magnetic nanoparticles are particularly attractive due to their unique properties such as excellent magnetic responsivity, high dispersibility, relatively large surface area and easiness of surface modification which enable them to have a wide range of potential applications in biological, environmental and food analysis [3]. In this study, an extraction method using new magnetic sorbent for separation and preconcentration trace amounts of cobalt was investigated.

Experimental

Synthesis of magnetic sorbent

The modified magnetic nano alumina was synthesized in two steps. In the first step, nano Al_2O_3 (2.0 g) were added to 50 mL of acidified ferric chloride solution ($FeCl_3$, 1.3 g and HCl, 1.0 mL) and the suspension was refluxed at 60 °C for 4 h. Then 1.1 g ferrous sulphate heptahydrate was added to the suspension. The mixture was heated at 80 °C for 15 min. After that, 100 mL of sodium hydroxide solution (1.0 mol L^{-1}) were added slowly and the mixture was sonicated for 30 min. The precipitate was isolated from the solution by applying an external magnet, washed with deionized water (200 mL, three times) and dried in vacuum oven at 50 °C. The second step was the modification of the magnetic nano alumina using sodium dodecylbenzenesulfonate and 1,2-(pyridylazo)-2-naphtol (PAN). In this case, 0.1 g of magnetic nano alumina was added to 10 mL deionized water and the pH of the mixture was adjusted to 2.5 by addition of HNO_3. Then 0.05 g sodium dodecylbenzenesulfonate and 1.0 mL of PAN solution (0.01 mol L^{-1}) were added to the suspension and mixed for 15 min. The precipitate was isolated from the solution by a magnet, and washed with deionized water (20 mL). This damped adsorbent was used for extraction step.

Extraction and determination procedure

A batch procedure was carried out for the extraction process. Firstly, a portion of sample solution containing the analyte ions was transferred into a 250 mL breaker, and adjusted to about pH 6.0. Secondly, the damped modified sorbent was added and dispersed into the solution. After 10 min the sorbent was isolated from the solution by a magnet. Thirdly, the adsorbed analytes were desorbed from the isolated adsorbent with 5 mL ethanol solution containing 0.1 mol L^{-1} HCl by ultrasonication for 10 min. Finally, the eluate was separated by magnet again and introduced into FAAS for subsequent determination.

Results and Discussion

The surface morphology and crystal structure of the sorbent were characterized by SEM and X-ray diffraction. The functionalization of modified magnetic nano alumina was demonstrated by FT-IR characterization. To attain high recovery, selectivity, and precision for the extraction and determination of cobalt (II), the influence of different parameters, which affect the extraction conditions such as the pH of sample solution, amount of the sorbent, sorption and desorption time, type and volume of eluent, sample volume and ionic strength were investigated and optimized. Under the optimized conditions, detection limit, linear range of calibration curve, preconcentration factor and relative standard deviation of the method were calculated. Table 1 shows the analytical performance and optimum conditions of the method. The procedure was successfully applied to the determination of cobalt (II) in water and food samples.

Table 1. Analytical performance and optimum conditions of the proposed method for the determination of cobalt

pH of sample solution	6.0
Amount of the sorbent (g)	0.1
Type of eluent	ethanol , 0.1 mol L^{-1} HCl
Volume of the eluent (mL)	5
Sorption time (min)	10
Desorption time (min)	10
Maximum sample volume (mL)	200
Preconcentration factor	40
LOD[a] (μg L^{-1})	0.9
LOQ[b] (μg L^{-1})	3.0
RSD[c] (%) (C_{Co}: 50 μg L^{-1}, n=10)	3.4
Linear range (μg L^{-1})	3–200

[a] Limit of detection; [b] Limit of quantification; [c] Relative standard deviation

Conclusion

The preparation of a new sorbent through the modification of nano alumina has been described and shown to be an alternative and efficient route for separation and preconcentration in the determination of cobalt (II). The method is simple, rapid and economical. This sorbent has fast adsorption and desorption kinetics. This methodology displays good accuracy, low limit of detection, excellent precision, which in turn show its potentiality in trace analysis of various samples with complicated matrix.

References

[1] M.R. Jamali, Y. Assadi, F. Shemirani, M.R. Milani-Hosseini, R. Rahnama Kozani, M. Masteri-Farahani, M. Salavati-Niasari, Anal. Chim. Acta **2006**, *579*, 68–73.

[2] M. Safarikova, I. Safarik, Magnetic solid-phase extraction, J. Magn. Magn. Mater. **1999**, *194*, 108–112.

[3] K. Aguilar-Arteaga, J.A. Rodriguez, E. Barrado, Magnetic solids in analytical chemistry: a review, Anal. Chim. Acta **2010**, *674*, 157–165.

The effect of different Substitutions on the equilibrium constant of 1-Phenyl-1,3-butanedione

Mohammad Vakili[a*], Vahidreza Darugar[a]

[a]**Department of Chemistry, Ferdowsi University of Mashhad, Mashhad 91775-1436, Iran**
E-mail address: Vakili-m@um.ac.ir (M.Vakili) Tel.: +989153215410

****

Introduction

It is well known that the cis-enol forms of β-diketones are characterized by a strong intramolecular hydrogen bond[1]. Hydrogen bonding and molecular structure of the enol forms of β-diketones have fascinated investigators for many years [2-4].

In the 1-Phenyl-1,3-butanedione (BA) and its para substitutions (p-X-BA), as an asymmetric β-diketones, the theoretical and experimental results confirm the existence equilibrium between two stable cis-enol forms of those [5-7]. The mentioned different equilibrium could be explained by considering the double minimum potential functions [7].

In the present study, we compared the experimental equilibrium constants of the titled molecules with the theoretical results in the gas phase and the solution, calculated at B3LYP level andusing different basis sets. To explore the solvent influence on the equilibrium constants, thecis-enol forms are fully optimized in three solvents, CCl_4, CH_3CN and CH_3CH_2OH, using PCM method [8].

Methods/ Exprimentals

All calculations in the present study were performed using the Gaussian 09W. The theoretical results confirm the existence equilibrium between two stable cis-enol forms for asymmetric β-diketones such as p-substituted benzoylacetone (p-X-BA) and its parent molecule (BA) at the B3LYP level with 6-311++G**, 6-31G**, 6-311G** basis sets at gas phase and CCl_4, CH_3CN, and CH_3CH_2OH solvents by using PCM method.The experimental of equilibrium constants have been obtained by using of the chelated OH proton, O^1H chemical shifts, ^{13}C chemical shifts at 227K in CH_2Cl_2solvent [7].

Result and Discussion

The structures of the stable cis-enol forms of BA and p-X-BA, X=F,Cl,CH_3,OCH_3 and their relative stabilities (calculated at the B3LYP/6-311++G**) are shown in Fig. 1. According to this Figure, the energy differences between the stable chelated enols in the gas phase are negligible (0.59-0.83 kcal/mol). So, different substituents have small effect on the stability and relative energies.

The computational calculation of equilibrium constants are obtained from Gibbs free energy calculations (equation $\Delta G^0 = - RT LnK$) at 298 K, and shows in Table.1, Which ΔG^0 is the Gibbs free energy differences between two cis-enol forms in p-X-BA. According to this table, the solvents and calculation basis sets have small effect on the equilibrium constant and the value of the equilibrium constant is near that of experiment.
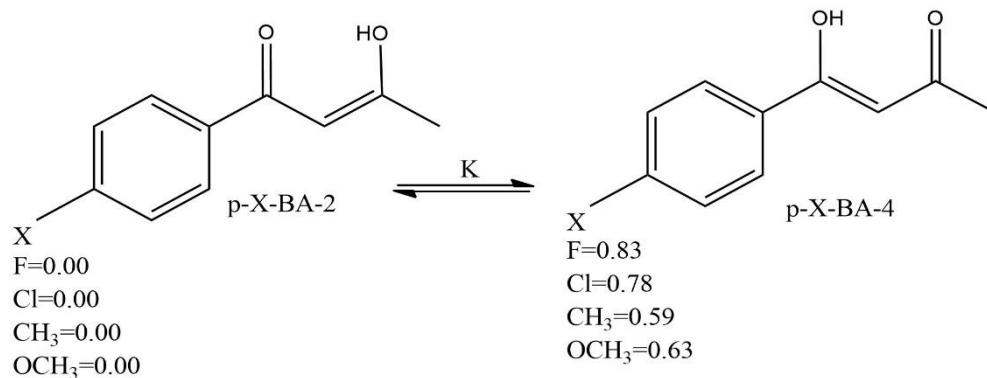
Fig.1: The equilibrium between two stable cis-enol forms in p-substituted of benzoylacetone in gas phas and relative stabilities.

Table.1: Theoretical and experimental Equilibrium constants for tautomeric equilibria stable cis-enol forms of p-substituted of benzoylacetones in various basis sets at B3LYP.

Compuond	Gas						CCl$_4$		CH$_3$CH$_2$OH		CH$_3$CN		CH$_2$Cl$_2$
	6-311++G**		6-31G**		6-311G**		6-311++G**		6-311++G**		6-311++G**		Exp.[a](227 K)
	ΔG^0	K	ΔG^0	K	ΔG^0	K	ΔG^0	K	ΔG^0	K	ΔG^0	K	K
p-F-BA	-0.0017	1.06	-0.0006	1.02	-0.0009	1.03	-0.0015	1.06	-0.0019	1.07	-0.0018	1.06	1.07
p-Cl-BA	-0.0001	1.00	-0.0011	1.04	-0.0008	1.03	-0.0001	1.00	-0.0004	1.01	-0.0005	1.02	0.93
p-CH$_3$-BA	-0.0013	1.05	-0.0014	1.05	-0.0012	1.04	-0.0012	1.05	-0.0018	1.07	-0.0018	1.07	0.96
p-OCH$_3$-BA	-0.0017	1.06	-0.0032	1.12	-0.0023	1.10	-0.0015	1.05	-0.0012	1.04	-0.0012	1.04	1.39
BA	-0.0016	1.06	-0.0014	1.05	-0.0039	1.15	-0.0012	1.04	-0.0016	1.06	-0.0017	1.06	0.89

[a] Data from Ref.[7]

Conclusion

The stability, structures, and thermodynamic parameters of the stable cis-enol forms of BA and its derivatives have been calculated at the B3LYP/6-311++G**.According to this theoretical results,the energy differences between the stable chelated enols in the gas and solution phases are negligible. The computational calculation of equilibrium constantsare obtained from standard Gibbs free energycalculations and shows that solvents and calculation levels have small effect on the equilibrium constant. The value of the equilibrium constant is near that of experiment.

References

[1] S.F. Tayyari, J.S. Emampour, M. Vakili, A.R. Nekoei, H. Eshghi,S.Salemi, M. Hassanpour, *J. Mol. Struct*, 2006, 794, 204–214.

[2] M. Vakili, A.R. Nekoei, S.F. Tayyari, A. Kanaani, N. Sanati, *J. Mol. Struct*. 2012,1021,102–111.

[3] D.C. Nonhebel, *Tetrahedron*,1968, 24 1869–1874.

[4] J. Emsley, L.Y.Y. Ma, P.A. Bates, M. Motevalli, M.B. Hursthouse, *J. Chem. Soc. Perkin Trans*. 1989, 2 527–533.

[5] M. Gorodetsky, Z. Luz, Y. Mazur, *J. Am. Chem. Soc*. 1967, 89 1183.

[6] S.F. Tayyari, J.S. Emampour, M. Vakili, A.R. Nekoei, H. Eshghi, S. Salemi, M. Hassanpour, *J. Mol. Struct*. 2006, 794 204–214.

[7] E.V. Borisov, E.V. Skorodumov, V.M. Pachevskaya, P.E. Hansen, *Magn. Reson. Chem*. 2005, 43, 992–998.

[8] J. Tomasi, M. Persico, *Chem. Rev*. 1994, 94,2027–2094.

Structure and hydrogen bond strength of the enol form of Furoylacethylacetone

M. Hakimi-Tabar*, **M. Vakili, R. Afzali**

Department of Chemistry, Ferdowsi University of Mashhad, Mashhad 91775-1436, Iran
Email address: mhakimitabar@yahoo.com

Introduction

Several theoretical and experimental data suggest that substitution at α- or β-position by electron-withdrawing groups, such as trifluoromethyl group (-CF$_3$), decreases the strength of the intramolecular hydrogen bond (IHB), whilst substitution of a π-system, such as phenyl group (-CH$_3$), increases the IHB strength [1-3]. Furoylacetylacetone (FAA), C$_4$H$_3$O-COCH$_2$CO-CH$_3$, has two β-substituted groups with different effects. Therefore, it is interesting to investigate these effects on structure and the IHB strength. However, substitution of the -CF$_3$ groups by -CH$_3$ groups declines the strength of the IHB. The aim of the this work is to predict the structure and IHB strength of four cis-enol conformers of FAA and comparison with those of furoyltrifluoroacetone (FTFA) using Atoms-In-Molecules (AIM) and Natural Bond Orbital (NBO) methods.

Method of analysis

All quantum calculations have been done by Gaussian 09W, NBO 5.0, and AIM2000 softwares. To confirm the relative stability of the cis-enol forms of FAA, the obtained stable structures were also fully optimized at the B3LYP, using 6-311G** and 6-311++G** basis sets. NBO and AIM calculations have been performed at B3LYP/ 6-311G** level of theory.

Results and Discussion

From the theoretical point of view, 32 enol forms for FAA can be drawn, which only four cis-enol conformers have the six-membered chelated ring of the intramolecular hydrogen bonding (IHB). For comparison, the calculated energies of all possible forms of FAA calculated at the B3LYP/6-311G** and B3LYP/6-311++G** level of theory (see Fig. 1 and Table 1). According to these data, in both calculations, B1 is the most stable conformation. These results can be interpreted as follows. To exist an enolated species from the diketo form, the most acidic proton first moves the C(6) atom and forms an ionic species that may change to the enolated form. Due to the less inductive effect of the -CH$_3$ group in relative to the resonance effect of the furan ring, C(7) is more positive than C(5), the negative charge on C(6) prefers to move towards C(7), and so leads to the B conformers. The averaged optimized geometrical parameters and the averaged topological parameters for FAA, and FTFA [4] molecules , calculated at the B3LYP/6-311++G** are collected in Table 2. According to this table, in FAA the averaged values of O...O distance decreases, while the OHO bond angle and O-H bond length increase in comparison with those of FTAA. By considering the electron withdrawing nature of CF$_3$ group in FTFA the C-C bond length is considerably shorter and the C=C bond length is considerably longer than those of FAA. These results confirm by the calculated wiberg bond orders. Also the electron withdrawing nature of CF$_3$ group in FTAA makes O2 positive than that in FAA and the IHB weaker in FTFA (see Table 3). Therefore, upon substitution of CF$_3$ group by CH$_3$ group, a considerable

increasing of the H-bond strength occurs. The AIM results also show the higher values for topological parameters in FAA in comparison with FTFA.
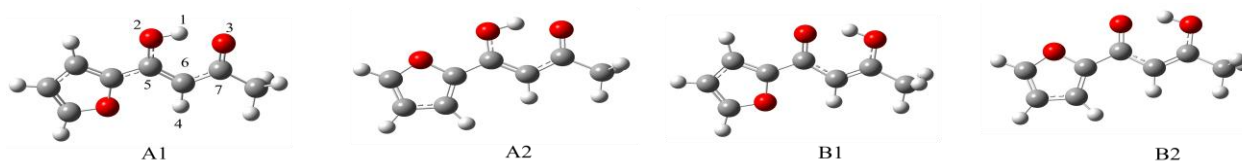

Fig. 1. The cis-enol conformers of FAA

Table 1. Calculated energies of FAA and FTFA at different levels. [a]

	FAA			
	A1	A2	B1	B2
B3lyp/6-311G**	-535.4646	-535.4599	-535.46618	-535.46202
B3lyp/6-311++G**	-535.47537	-535.47128	-535.47686	-535.47339

[a] energies are in hartrees

Table 2. Some geometrical parameters and
the AIM results for the cis-enol forms of FAA and FTFA

	FAA	FTFA
Bond distances (Å)		
C=C	1.411	1.421
C-C	1.403	1.388
O-C	1.325	1.321
O=C	1.251	1.244
O...O	2.531	2.551
O-H	1.007	1.002
Bond angles (°)		
O-H-O	149.3	148.1
AIM results		
ρ_{BCP}	0.02140	0.02075
$\nabla^2\rho_{BCP}$	0.13399	0.12990
E_{HB}	7.31	7.05

The units of AIM results are: ρ_{BCP} (e au^{-3}), $\nabla^2\rho_{BCP}$ (e au^{-5}).

Table 3. Selected natural charges of FAA and FTFA

	FAA	FTFA
C5	0.446	0.458
C6	-0.441	-0.418
C7	0.490	0.381
O3	-0.662	-0.627
O2	-0.649	-0.631
H4	0.507	0.510

Conclusion

Among 32 possible enol forms of FAA, only four forms have the chelated IHB. The B1 is more stable than others. Comparison of theoretical parameters indicates that the hydrogen bond strength of FAA is stronger than FTFA. This result is due to electron withdrawing effect of CF$_3$ group reduces the strength of the hydrogen bond in FTFA in relative to FAA. The results of AIM and NBO confirm this conclusion.

References

[1] D.J. Sardella, D.H. Heinert, B.L. Shapiro, *J. Org. Chem.* (1969), 34, 2817-2821.
[2] F. Jiménez-Cruz, L. Fragoza Mar, J.L. Garcia-Gutierrez, *J. Mol. Struct.* (2013), 1034, 43–50.
[3] S.F. Tayyari, A.R. Nekoei, M. Vakili, Y.A. Wang, *J. Theor. Comp. Chem.* (2006), 5, 647-664.
[4] S.F. Tayyari, A-R. Nekoei, H. Rahemi, *J. Mol. Struct.* (2008), 882, 153–167.

Oxidation of sulfides with hydrogen peroxide catalyzed by polystyrene-bound Mo(VI) Schiff base complex

Mehrmah Ghorbani , Hadi Kargar*
*Department of Chemistry, Payame Noor University, 19395-3697 Tehran, I. R. Iran*
e-mail[*]: **h.kargar@pnu.ac.ir** *and* **Hadi_Kargar@yahoo.com**

Introduction:

The oxidation of organic substrates by transition metal complexes has become an important research area in both organic synthesis and bioinorganic modeling of oxygen transfer metalloenzymes. Molybdenum complexes played a critical role in homogeneous industrial catalysis in the Arco and Halcon processes, involving the typical example of the industrial production of propylene oxide using alkyl hydroperoxides as oxidants, catalyzed by a homogeneous Mo(VI) [1]. Sulfoxides and sulfones have found many applications in pharmacy [2, 3] and other fields such as engineering plastics and polymers [4]. Oxidation of sulfides is the most direct approach for the synthesis of sulfoxides and sulfones [5].

Experimentals:

We synthesized a new molybdenum Schiff base complex and demonstrated its high catalytic activity in the oxidation of sulfides under heterogeneous conditions using hydrogen peroxide as the terminal oxidant (Scheme 1). The reaction parameters such as catalyst amount, kind of solvent, oxidant amount and temperature were optimized in the oxidation of diphenyl sulfide.
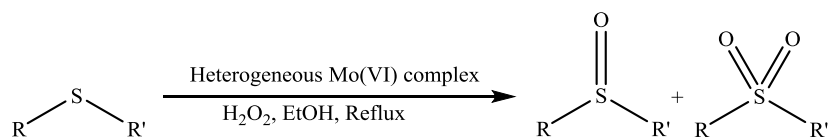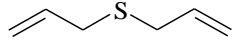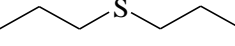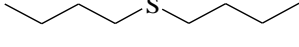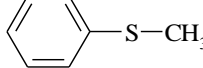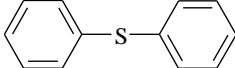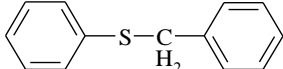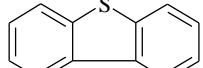

(Scheme 1)

In a 25 mL round-bottom flask equipped with a magnetic stirring bar, a solution of sulfide (1 mmol), catalyst (400 mg) in ethanol (10 mL) was prepared. Then, H_2O_2 (2 mmol) was added to this solution and the reaction mixture was stirred under reflux conditions. The reaction progress was monitored by TLC. After the reaction was completed, the solvent was evaporated and the pure products were obtained by IR spectroscopic.

Results and Discussion:

The reaction conditions were also optimized in the oxidation of sulfides with H_2O_2 in which diphenyl sulfide was used as a model substrate. In the optimization of catalyst amount, the best results were obtained when 400 mg of catalyst was applied with 2 mmol of H_2O_2 after 75 min. In order to choose the reaction media, different solvents were also tested and ethanol was chosen as solvent because of the higher amount of sulfoxide was produced.

This polystyrene bound Mo–Schiff base can be used as a robust, reusable and active heterogeneous catalyst in the oxidation of sulfides with hydrogen peroxide. The results are summarized in Table 1.

Table 1. Oxidation of various sulfides by H_2O_2 in the presence of heterogeneous Mo(VI) Schiff base complex in ethanol.

Entry	Sulfide	Time(min)	Conversion	Sulfoxide(%)	Sulfone(%)
1		30	100	100	0
2		5	100	100	0
3		25	100	100	0
4		25	100	60	40
5		75	100	65	35
6		30	100	95	5
7		210	100	50	50

Reaction conditions: sulfide (1 mmol), catalyst (400 mg), H_2O_2 (2 mmol), C_2H_5OH (10 mL) at 80 ℃.

Conclusion:

In comparison with the data reported in the oxidation of organic sulfides by various Schiff base complexes, our system shows the following advantages: simple preparation of the catalyst from commercially available materials (Schiff base and polystyrene resin) and it seems binding of Schiff base pyridyl group to polystyrene resin, nontoxicity of the catalyst, the use of supported Schiff base complex provides an easy way to recover and recycle the catalyst from the reaction media and the catalytic activity of this catalyst in the oxidation of sulfides has been found to be higher compared with corresponding non-supported molybdenum(VI) Schiff base complex.

References:

[1] J. Kolar, U.S. Pat. 3 350 422, 1967; 3 357 635, 1967; 3 507 809, 1970; 3 625 981, 1971.
[2] C.R. Craig, R.E. Stitzel, Modern Pharmacology with Clinical Applications, Lippincott Williams Wilkins, **2004**.
[3] S.A. Blum, R.G. Bergman, J.A. Ellman, *J. Org. Chem.* **2003**, *68*, 150-155.
[4] J. Fink, High Performance Polymers, William Andrew Inc., Norwich, **2008**.
[5] I. Fernandez, N. Khiar, *Chem. Rev.* **2003**, *103*, 3651-3705.

Agar–sulfuric Acid as a Bio-supported and Recyclable Solid acid Catalyst for Rapid Synthesis of 3, 4-Dihydropyrimidones *via* Biginelli Reaction

Ramin Rezaei[a,*]. Fatemeh Golshan[a]

[a]*Department of Chemistry, Firoozabad Branch, Islamic Azad University, Firoozabad, Iran*

rezaieramin@yahoo.com

****

Introduction:

The Biginelli reaction is one of the most important MCRs that offer an efficient route to produce multi-functionalized 3, 4-dihydropyridin-2(*1H*)-ones/3, 4-dihydropyridin-2(*1H*)-thiones (DHPMs) [1]. DHPMs have been receiving considerable attention because they exhibit a wide of biological and pharmacological properties [2]. The classical methods for the synthesis of 3, 4-dihydropyridin-2(1H)-ones/3, 4-dihydropyridin-2(1H)-thiones (DHPMs) is the Biginelli multicomponent synthesis between an aldehyde, ethyl acetoacetate and urea [3]. In order to improve the efficiency of Biginelli reaction, a lot of catalysts have been developed. Some of them are really fascinating from the synthetic chemist's points; however, some drawbacks still remain [4]. Agar consists of a mixture of agarose and agaropectin. Agarose, the predominant component of agar, is a linear polymer, made up of the repeating monomeric unit of agarobiose. Agaropectin is a heterogeneous mixture of smaller molecules that occur in lesser amounts, and is made up of alternating units of D-galactose and L-galactose heavily modified with acidic side-groups, such as sulfate and pyruvate [5].

Experimentals:

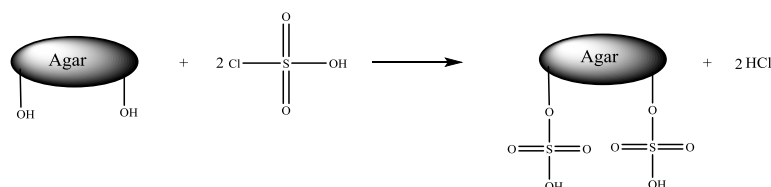*Preparation of agar–sulfuric acid [ASA]*

Chlorosulfonic acid (1.0 g, 9 mmol) was added dropwise, at 0 °C, over a period of 2 h, to a magnetically stirred mixture of 5.0 g agar in 20 ml n-hexane. HCl gas was removed from the reaction vessel immediately. When addition was complete, the mixture was stirred for 2 h. The mixture was then filtered and washed with 30 ml acetonitrile and dried at room temperature to afford 5.23 g of agar–sulfuric acid as a white powder.

General procedure for the synthesis of 3, 4- dihydropyrimidones derivatives

Agar–sulfuric acid (0.1 g) was added to a mixture of aromatic aldehyde (1mmol), ethyl acetoacetate (1 mmol), and urea (or thiourea) (1.2 mmol), and the mixture was stirred at 80 °C under solvent-free conditions. After completion of the reaction (thin-layer chromatography TLC) monitoring, EtOAc (20 mL) was added and the product was filtrated to collect the formed precipitate. The crude product was recrystallized from ethanol to yield pure 3, 4-dihydropyrimidones.

Results and Discussion:

Agar–sulfuric acid [ASA] was prepared by reaction between agar and chlorosulfonic acid (Scheme 1).

Scheme 1: Preparation of agar–sulfuric acid [ASA]

By using different starting materials such as aromatic aldehydes carrying either electron-donating or electron withdrawing substituent, different 1,3-dicarbonyls and urea/thiourea overview and possibility of this protocol were demonstrated. Moderate-to-excellent yields of the desired products under optimized reaction conditions were obtained.

X: O, S
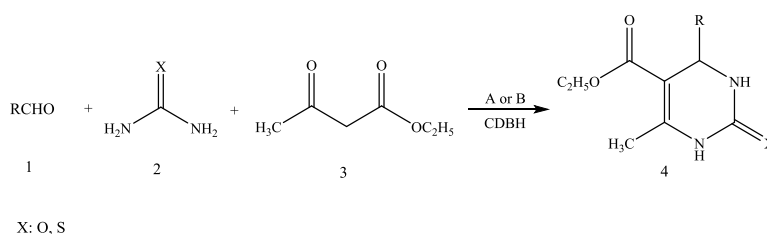
Scheme 2. Synthesized dihydropyrimidinone derivatives by using ethyl acetoacetate

Table 1 Synthesis of DHPMs derivatives by using ethyl acetoacetate catalyzed by ASA[a]

Entry	R	X	product			M.p. (°C)	
				Time (min)	Yield (%)[b]	Found	Reported
1	C_6H_5	O	**4a**	20	80	192-194	198-200
2	$2\text{-}ClC_6H_4$	O	**4b**	20	80	226-228	231–233
3	$3\text{-}O_2NC_6H_4$	O	**4c**	20	80	220-222	227–228
4	$4\text{-}CH_3C_6H_4$	O	**4d**	15	85	210-212	212-214
5	$2,4\text{-}(Cl)_2\text{-}C_6H_3$	O	**4e**	20	80	245–247	248–250
6	Ph CH=CH	O	**4f**	30	80	226-228	232-235
7	2-Furyl	O	**4g**	30	75	195-197	201-203
8	C_6H_5	S	**4h**	25	85	204-206	208-210
9	$4\text{-}ClC_6H_4$	S	**4i**	25	85	214-216	208-210
10	$4\text{-}CH_3OC_6H_4$	S	**4j**	25	90	143-145	150-152

[a] Reaction condition: Aldehydes (1 mmol), ethyl acetoacetate (1 mmol), urea or thiourea (1.2 mmol), ASA (0.1 g), 80 ℃.
[b] Isolated yield.

Conclusion:

In summary, we have synthesized Agar–sulfuric acid [ASA] and this catalyst was used for the one-pot synthesis of 3, 4-dihydropyrimidinones. The important advantages of this method are high catalytic activity, short reaction time, excellent yields, reusability of catalyst, simple work-up and mild reaction conditions.

[1] A. Domling, I. Ugi, Angew. *Chem., Int. Ed.* **2000**, *39*, 3168–3210.
[2] K.S. Atwal, B.N. Swanson, S.E. Unger, D.M. Floyed, S. Moreland, A. Hedberg, B.C. O'Reilly, *J. Med. Chem*. **1991**, 34, 806-811.
[3] P. Biginelli, *Gazz. Chim. Ital*. **1893**, *23*, 360-413.
[4] K. Kouachi, G. Lafaye, S. Pronier, L. Bennini, S. Menad, *J. Mol. Catal. A: Chem.*, **2014**, *395*, 210-216.
[5] R. Armisen, F. Galatas, *Production, Properties and Uses of Agar*. Fao.Org, **2011**.